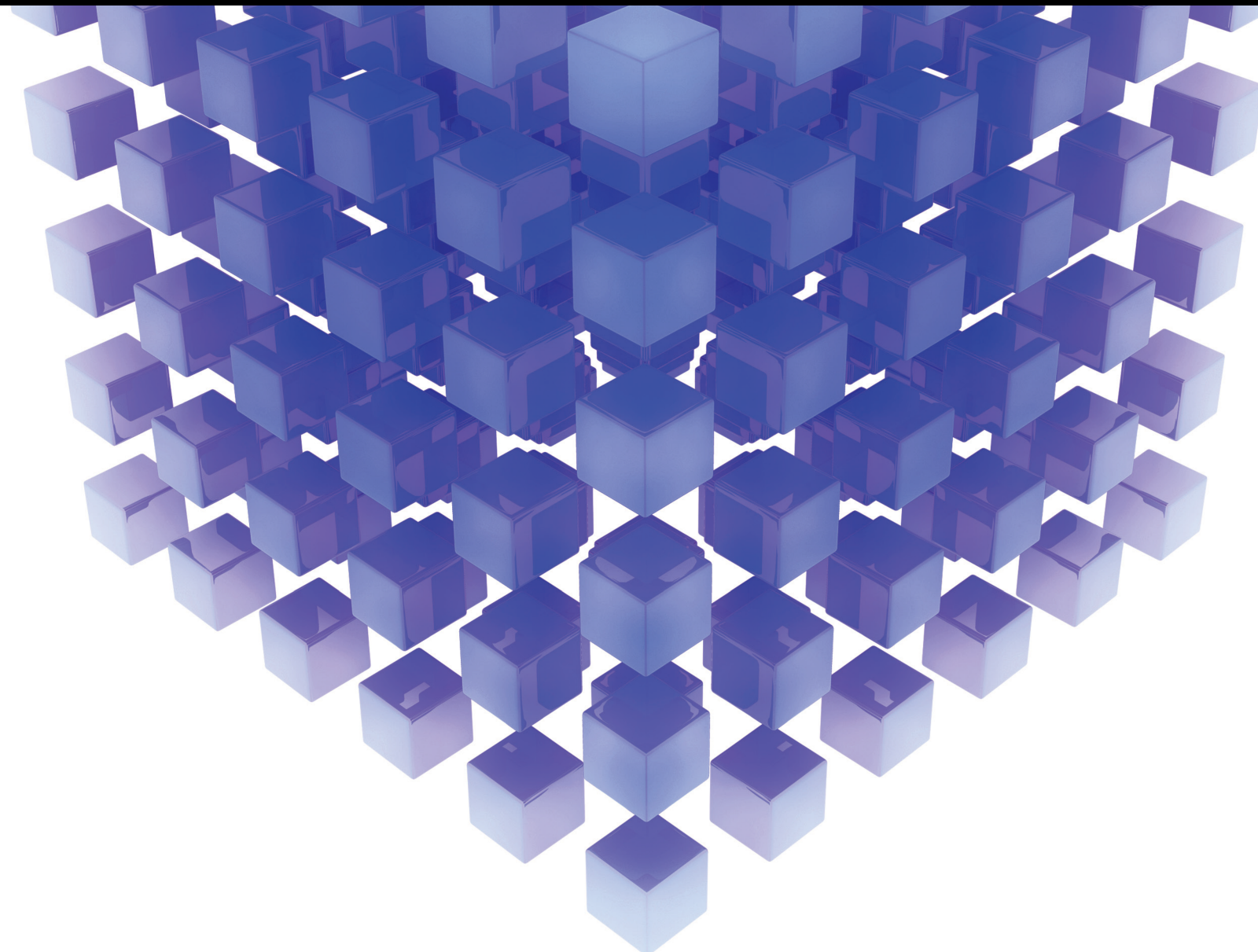


Integration and Optimization of Green Supply Chain Networks under the Epidemic Environment

Lead Guest Editor: Aijun Liu

Guest Editors: Mingbao Cheng, Yang Gao, Sang-Bing Tsai, and Xiaohang Yue





Integration and Optimization of Green Supply Chain Networks under the Epidemic Environment

Mathematical Problems in Engineering

**Integration and Optimization of Green
Supply Chain Networks under the
Epidemic Environment**

Lead Guest Editor: Aijun Liu


Guest Editors: Mingbao Cheng, Yang Gao, Sang-
Bing Tsai, and Xiaohang Yue



Copyright © 2021 Hindawi Limited. All rights reserved.

This is a special issue published in “Mathematical Problems in Engineering.” All articles are open access articles distributed under the Creative Commons Attribution License, which permits unrestricted use, distribution, and reproduction in any medium, provided the original work is properly cited.

Chief Editor

Guangming Xie , China

Academic Editors

Kumaravel A , India
Waqas Abbasi, Pakistan
Mohamed Abd El Aziz , Egypt
Mahmoud Abdel-Aty , Egypt
Mohammed S. Abdo, Yemen
Mohammad Yaghoub Abdollahzadeh
Jamalabadi , Republic of Korea
Rahib Abiyev , Turkey
Leonardo Acho , Spain
Daniela Addessi , Italy
Arooj Adeel , Pakistan
Waleed Adel , Egypt
Ramesh Agarwal , USA
Francesco Aggogeri , Italy
Ricardo Aguilar-Lopez , Mexico
Afaq Ahmad , Pakistan
Naveed Ahmed , Pakistan
Elias Aifantis , USA
Akif Akgul , Turkey
Tareq Al-shami , Yemen
Guido Ala, Italy
Andrea Alaimo , Italy
Reza Alam, USA
Osamah Albahri , Malaysia
Nicholas Alexander , United Kingdom
Salvatore Alfonzetti, Italy
Ghous Ali , Pakistan
Nouman Ali , Pakistan
Mohammad D. Aliyu , Canada
Juan A. Almendral , Spain
A.K. Alomari, Jordan
José Domingo Álvarez , Spain
Cláudio Alves , Portugal
Juan P. Amezcua-Sanchez, Mexico
Mukherjee Amitava, India
Lionel Amodeo, France
Sebastian Anita, Romania
Costanza Arico , Italy
Sabri Arik, Turkey
Fausto Arpino , Italy
Rashad Asharabi , Saudi Arabia
Farhad Aslani , Australia
Mohsen Asle Zaem , USA

Andrea Avanzini , Italy
Richard I. Avery , USA
Viktor Avrutin , Germany
Mohammed A. Awadallah , Malaysia
Francesco Aymerich , Italy
Sajad Azizi , Belgium
Michele Bacciocchi , Italy
Seungik Baek , USA
Khaled Bahlali, France
M.V.A Raju Bahubalendruni, India
Pedro Balaguer , Spain
P. Balasubramaniam, India
Stefan Balint , Romania
Ines Tejado Balsera , Spain
Alfonso Banos , Spain
Jerzy Baranowski , Poland
Tudor Barbu , Romania
Andrzej Bartoszewicz , Poland
Sergio Baselga , Spain
S. Caglar Baslamisli , Turkey
David Bassir , France
Chiara Bedon , Italy
Azeddine Beghdadi, France
Andriette Bekker , South Africa
Francisco Beltran-Carbajal , Mexico
Abdellatif Ben Makhlof , Saudi Arabia
Denis Benasciutti , Italy
Ivano Benedetti , Italy
Rosa M. Benito , Spain
Elena Benvenuti , Italy
Giovanni Berselli, Italy
Michele Betti , Italy
Pietro Bia , Italy
Carlo Bianca , France
Simone Bianco , Italy
Vincenzo Bianco, Italy
Vittorio Bianco, Italy
David Bigaud , France
Sardar Muhammad Bilal , Pakistan
Antonio Bilotta , Italy
Sylvio R. Bistafa, Brazil
Chiara Boccaletti , Italy
Rodolfo Bontempo , Italy
Alberto Borboni , Italy
Marco Bortolini, Italy

Paolo Boscariol, Italy
Daniela Boso , Italy
Guillermo Botella-Juan, Spain
Abdesselem Boulkroune , Algeria
Boulaïd Boulkroune, Belgium
Fabio Bovenga , Italy
Francesco Braghin , Italy
Ricardo Branco, Portugal
Julien Bruchon , France
Matteo Bruggi , Italy
Michele Brun , Italy
Maria Elena Bruni, Italy
Maria Angela Butturi , Italy
Bartłomiej Błachowski , Poland
Dhanamjayulu C , India
Raquel Caballero-Águila , Spain
Filippo Cacace , Italy
Salvatore Caddemi , Italy
Zuowei Cai , China
Roberto Caldelli , Italy
Francesco Cannizzaro , Italy
Maosen Cao , China
Ana Carpio, Spain
Rodrigo Carvajal , Chile
Caterina Casavola, Italy
Sara Casciati, Italy
Federica Caselli , Italy
Carmen Castillo , Spain
Inmaculada T. Castro , Spain
Miguel Castro , Portugal
Giuseppe Catalanotti , United Kingdom
Alberto Cavallo , Italy
Gabriele Cazzulani , Italy
Fatih Vehbi Celebi, Turkey
Miguel Cerrolaza , Venezuela
Gregory Chagnon , France
Ching-Ter Chang , Taiwan
Kuei-Lun Chang , Taiwan
Qing Chang , USA
Xiaoheng Chang , China
Prasenjit Chatterjee , Lithuania
Kacem Chehdi, France
Peter N. Cheimets, USA
Chih-Chiang Chen , Taiwan
He Chen , China

Kebing Chen , China
Mengxin Chen , China
Shyi-Ming Chen , Taiwan
Xizhong Chen , Ireland
Xue-Bo Chen , China
Zhiwen Chen , China
Qiang Cheng, USA
Zeyang Cheng, China
Luca Chiapponi , Italy
Francisco Chicano , Spain
Tirivanhu Chinyoka , South Africa
Adrian Chmielewski , Poland
Seongim Choi , USA
Gautam Choubey , India
Hung-Yuan Chung , Taiwan
Yusheng Ci, China
Simone Cinquemani , Italy
Roberto G. Citarella , Italy
Joaquim Ciurana , Spain
John D. Clayton , USA
Piero Colajanni , Italy
Giuseppina Colicchio, Italy
Vassilios Constantoudis , Greece
Enrico Conte, Italy
Alessandro Contento , USA
Mario Cools , Belgium
Gino Cortellessa, Italy
Carlo Cosentino , Italy
Paolo Crippa , Italy
Erik Cuevas , Mexico
Guozeng Cui , China
Mehmet Cunkas , Turkey
Giuseppe D'Aniello , Italy
Peter Dabnichki, Australia
Weizhong Dai , USA
Zhifeng Dai , China
Purushothaman Damodaran , USA
Sergey Dashkovskiy, Germany
Adiel T. De Almeida-Filho , Brazil
Fabio De Angelis , Italy
Samuele De Bartolo , Italy
Stefano De Miranda , Italy
Filippo De Monte , Italy

José António Fonseca De Oliveira
Correia , Portugal
Jose Renato De Sousa , Brazil
Michael Defoort, France
Alessandro Della Corte, Italy
Laurent Dewasme , Belgium
Sanku Dey , India
Gianpaolo Di Bona , Italy
Roberta Di Pace , Italy
Francesca Di Puccio , Italy
Ramón I. Diego , Spain
Yannis Dimakopoulos , Greece
Hasan Dinçer , Turkey
José M. Domínguez , Spain
Georgios Dounias, Greece
Bo Du , China
Emil Dumic, Croatia
Madalina Dumitriu , United Kingdom
Premraj Durairaj , India
Saeed Eftekhar Azam, USA
Said El Kafhali , Morocco
Antonio Elipe , Spain
R. Emre Erkmen, Canada
John Escobar , Colombia
Leandro F. F. Miguel , Brazil
FRANCESCO FOTI , Italy
Andrea L. Facci , Italy
Shahla Faisal , Pakistan
Giovanni Falsone , Italy
Hua Fan, China
Jianguang Fang, Australia
Nicholas Fantuzzi , Italy
Muhammad Shahid Farid , Pakistan
Hamed Faruqi, Iran
Yann Favennec, France
Fiorenzo A. Fazzolari , United Kingdom
Giuseppe Fedele , Italy
Roberto Fedele , Italy
Baowei Feng , China
Mohammad Ferdows , Bangladesh
Arturo J. Fernández , Spain
Jesus M. Fernandez Oro, Spain
Francesco Ferrise, Italy
Eric Feulvarch , France
Thierry Floquet, France

Eric Florentin , France
Gerardo Flores, Mexico
Antonio Forcina , Italy
Alessandro Formisano, Italy
Francesco Franco , Italy
Elisa Francomano , Italy
Juan Frausto-Solis, Mexico
Shujun Fu , China
Juan C. G. Prada , Spain
HECTOR GOMEZ , Chile
Matteo Gaeta , Italy
Mauro Gaggero , Italy
Zoran Gajic , USA
Jaime Gallardo-Alvarado , Mexico
Mosè Gallo , Italy
Akemi Gálvez , Spain
Maria L. Gandarias , Spain
Hao Gao , Hong Kong
Xingbao Gao , China
Yan Gao , China
Zhiwei Gao , United Kingdom
Giovanni Garcea , Italy
José García , Chile
Harish Garg , India
Alessandro Gasparetto , Italy
Stylianos Georgantzinou, Greece
Fotios Georgiades , India
Parviz Ghadimi , Iran
Ştefan Cristian Gherghina , Romania
Georgios I. Giannopoulos , Greece
Agathoklis Giaralis , United Kingdom
Anna M. Gil-Lafuente , Spain
Ivan Giorgio , Italy
Gaetano Giunta , Luxembourg
Jefferson L.M.A. Gomes , United Kingdom
Emilio Gómez-Déniz , Spain
Antonio M. Gonçalves de Lima , Brazil
Qunxi Gong , China
Chris Goodrich, USA
Rama S. R. Gorla, USA
Veena Goswami , India
Xunjie Gou , Spain
Jakub Grabski , Poland















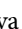








Antoine Grall , France
George A. Gravvanis , Greece
Fabrizio Greco , Italy
David Greiner , Spain
Jason Gu , Canada
Federico Guarracino , Italy
Michele Guida , Italy
Muhammet Gul , Turkey
Dong-Sheng Guo , China
Hu Guo , China
Zhaoxia Guo, China
Yusuf Gurefe, Turkey
Salim HEDDAM , Algeria
ABID HUSSANAN, China
Quang Phuc Ha, Australia
Li Haitao , China
Petr Hájek , Czech Republic
Mohamed Hamdy , Egypt
Muhammad Hamid , United Kingdom
Renke Han , United Kingdom
Weimin Han , USA
Xingsi Han, China
Zhen-Lai Han , China
Thomas Hanne , Switzerland
Xinan Hao , China
Mohammad A. Hariri-Ardebili , USA
Khalid Hattaf , Morocco
Defeng He , China
Xiao-Qiao He, China
Yanchao He, China
Yu-Ling He , China
Ramdane Hedjar , Saudi Arabia
Jude Hemanth , India
Reza Hemmati, Iran
Nicolae Herisanu , Romania
Alfredo G. Hernández-Díaz , Spain
M.I. Herreros , Spain
Eckhard Hitzer , Japan
Paul Honeine , France
Jaromir Horacek , Czech Republic
Lei Hou , China
Yingkun Hou , China
Yu-Chen Hu , Taiwan
Yunfeng Hu, China

Can Huang , China
Gordon Huang , Canada
Linsheng Huo , China
Sajid Hussain, Canada
Asier Ibeas , Spain
Orest V. Iftime , The Netherlands
Przemyslaw Ignaciuk , Poland
Giacomo Innocenti , Italy
Emilio Insfran Pelozo , Spain
Azeem Irshad, Pakistan
Alessio Ishizaka, France
Benjamin Ivorra , Spain
Breno Jacob , Brazil
Reema Jain , India
Tushar Jain , India
Amin Jajarmi , Iran
Chiranjibe Jana , India
Łukasz Jankowski , Poland
Samuel N. Jator , USA
Juan Carlos Jáuregui-Correa , Mexico
Kandasamy Jayakrishna, India
Reza Jazar, Australia
Khalide Jbilou, France
Isabel S. Jesus , Portugal
Chao Ji , China
Qing-Chao Jiang , China
Peng-fei Jiao , China
Ricardo Fabricio Escobar Jiménez , Mexico
Emilio Jiménez Macías , Spain
Maolin Jin, Republic of Korea
Zhuo Jin, Australia
Ramash Kumar K , India
BHABEN KALITA , USA
MOHAMMAD REZA KHEDMATI , Iran
Viacheslav Kalashnikov , Mexico
Mathiyalagan Kalidass , India
Tamas Kalmar-Nagy , Hungary
Rajesh Kaluri , India
Jyottheswara Reddy Kalvakurthi, India
Zhao Kang , China
Ramani Kannan , Malaysia
Tomasz Kapitaniak , Poland
Julius Kaplunov, United Kingdom
Konstantinos Karamanos, Belgium
Michal Kawulok, Poland

Irfan Kaymaz , Turkey
Vahid Kayvanfar , Qatar
Krzysztof Kecik , Poland
Mohamed Khader , Egypt
Chaudry M. Khalique , South Africa
Mukhtaj Khan , Pakistan
Shahid Khan , Pakistan
Nam-Il Kim, Republic of Korea
Philipp V. Kiryukhantsev-Korneev ,
Russia
P.V.V Kishore , India
Jan Koci , Czech Republic
Ioannis Kostavelis , Greece
Sotiris B. Kotsiantis , Greece
Frederic Kratz , France
Vamsi Krishna , India
Edyta Kucharska, Poland
Krzysztof S. Kulpa , Poland
Kamal Kumar, India
Prof. Ashwani Kumar , India
Michal Kunicki , Poland
Cedrick A. K. Kwuimy , USA
Kyandoghere Kyamakya, Austria
Ivan Kyrchei , Ukraine
Márcio J. Lacerda , Brazil
Eduardo Lalla , The Netherlands
Giovanni Lancioni , Italy
Jaroslaw Latalski , Poland
Hervé Laurent , France
Agostino Lauria , Italy
Aimé Lay-Ekuakille , Italy
Nicolas J. Leconte , France
Kun-Chou Lee , Taiwan
Dimitri Lefebvre , France
Eric Lefevre , France
Marek Lefik, Poland
Yaguo Lei , China
Kauko Leiviskä , Finland
Ervin Lenzi , Brazil
ChenFeng Li , China
Jian Li , USA
Jun Li , China
Yueyang Li , China
Zhao Li , China































Zhen Li , China
En-Qiang Lin, USA
Jian Lin , China
Qibin Lin, China
Yao-Jin Lin, China
Zhiyun Lin , China
Bin Liu , China
Bo Liu , China
Heng Liu , China
Jianxu Liu , Thailand
Lei Liu , China
Sixin Liu , China
Wanquan Liu , China
Yu Liu , China
Yuanchang Liu , United Kingdom
Bonifacio Llamazares , Spain
Alessandro Lo Schiavo , Italy
Jean Jacques Loiseau , France
Francesco Lolli , Italy
Paolo Lonetti , Italy
António M. Lopes , Portugal
Sebastian López, Spain
Luis M. López-Ochoa , Spain
Vassilios C. Loukopoulos, Greece
Gabriele Maria Lozito , Italy
Zhiguo Luo , China
Gabriel Luque , Spain
Valentin Lychagin, Norway
YUE MEI, China
Junwei Ma , China
Xuanlong Ma , China
Antonio Madeo , Italy
Alessandro Magnani , Belgium
Toqeer Mahmood , Pakistan
Fazal M. Mahomed , South Africa
Arunava Majumder , India
Sarfranz Nawaz Malik, Pakistan
Paolo Manfredi , Italy
Adnan Maqsood , Pakistan
Muazzam Maqsood, Pakistan
Giuseppe Carlo Marano , Italy
Damijan Markovic, France
Filipe J. Marques , Portugal
Luca Martinelli , Italy
Denizar Cruz Martins, Brazil

Francisco J. Martos , Spain
Elio Masciari , Italy
Paolo Massioni , France
Alessandro Mauro , Italy
Jonathan Mayo-Maldonado , Mexico
Pier Luigi Mazzeo , Italy
Laura Mazzola, Italy
Driss Mehdi , France
Zahid Mehmood , Pakistan
Roderick Melnik , Canada
Xiangyu Meng , USA
Jose Merodio , Spain
Alessio Merola , Italy
Mahmoud Mesbah , Iran
Luciano Mescia , Italy
Laurent Mevel , France
Constantine Michailides , Cyprus
Mariusz Michta , Poland
Prankul Middha, Norway
Aki Mikkola , Finland
Giovanni Minafò , Italy
Edmondo Minisci , United Kingdom
Hiroyuki Mino , Japan
Dimitrios Mitsotakis , New Zealand
Ardashir Mohammadzadeh , Iran
Francisco J. Montáns , Spain
Francesco Montefusco , Italy
Gisele Mophou , France
Rafael Morales , Spain
Marco Morandini , Italy
Javier Moreno-Valenzuela , Mexico
Simone Morganti , Italy
Caroline Mota , Brazil
Aziz Moukrim , France
Shen Mouquan , China
Dimitris Mourtzis , Greece
Emiliano Mucchi , Italy
Taseer Muhammad, Saudi Arabia
Ghulam Muhiuddin, Saudi Arabia
Amitava Mukherjee , India
Josefa Mula , Spain
Jose J. Muñoz , Spain
Giuseppe Muscolino, Italy
Marco Mussetta , Italy

Hariharan Muthusamy, India
Alessandro Naddeo , Italy
Raj Nandkeolyar, India
Keivan Navaie , United Kingdom
Soumya Nayak, India
Adrian Neagu , USA
Erivelton Geraldo Nepomuceno , Brazil
AMA Neves, Portugal
Ha Quang Thinh Ngo , Vietnam
Nhon Nguyen-Thanh, Singapore
Papakostas Nikolaos , Ireland
Jelena Nikolic , Serbia
Tatsushi Nishi, Japan
Shanzhou Niu , China
Ben T. Nohara , Japan
Mohammed Nouari , France
Mustapha Nourelfath, Canada
Kazem Nouri , Iran
Ciro Núñez-Gutiérrez , Mexico
Włodzimierz Ogryczak, Poland
Roger Ohayon, France
Krzysztof Okarma , Poland
Mitsuhiro Okayasu, Japan
Murat Olgun , Turkey
Diego Oliva, Mexico
Alberto Olivares , Spain
Enrique Onieva , Spain
Calogero Orlando , Italy
Susana Ortega-Cisneros , Mexico
Sergio Ortobelli, Italy
Naohisa Otsuka , Japan
Sid Ahmed Ould Ahmed Mahmoud , Saudi Arabia
Taoreed Owolabi , Nigeria
EUGENIA PETROPOULOU , Greece
Arturo Pagano, Italy
Madhumangal Pal, India
Pasquale Palumbo , Italy
Dragan Pamučar, Serbia
Weifeng Pan , China
Chandan Pandey, India
Rui Pang, United Kingdom
Jürgen Pannek , Germany
Elena Panteley, France
Achille Paolone, Italy

George A. Papakostas , Greece
Xosé M. Pardo , Spain
You-Jin Park, Taiwan
Manuel Pastor, Spain
Pubudu N. Pathirana , Australia
Surajit Kumar Paul , India
Luis Payá , Spain
Igor Pažanin , Croatia
Libor Pekař , Czech Republic
Francesco Pellicano , Italy
Marcello Pellicciari , Italy
Jian Peng , China
Mingshu Peng, China
Xiang Peng , China
Xindong Peng, China
Yuxing Peng, China
Marzio Pennisi , Italy
Maria Patrizia Pera , Italy
Matjaz Perc , Slovenia
A. M. Bastos Pereira , Portugal
Wesley Peres, Brazil
F. Javier Pérez-Pinal , Mexico
Michele Perrella, Italy
Francesco Pesavento , Italy
Francesco Petrini , Italy
Hoang Vu Phan, Republic of Korea
Lukasz Pieczonka , Poland
Dario Piga , Switzerland
Marco Pizzarelli , Italy
Javier Plaza , Spain
Goutam Pohit , India
Dragan Poljak , Croatia
Jorge Pomares , Spain
Hiram Ponce , Mexico
Sébastien Poncet , Canada
Volodymyr Ponomaryov , Mexico
Jean-Christophe Ponsart , France
Mauro Pontani , Italy
Sivakumar Poruran, India
Francesc Pozo , Spain
Aditya Rio Prabowo , Indonesia
Anchasa Pramuanjaroenkij , Thailand
Leonardo Primavera , Italy
B Rajanarayan Prusty, India

Krzysztof Puszynski , Poland
Chuan Qin , China
Dongdong Qin, China
Jianlong Qiu , China
Giuseppe Quaranta , Italy
DR. RITU RAJ , India
Vitomir Racic , Italy
Carlo Rainieri , Italy
Kumbakonam Ramamani Rajagopal, USA
Ali Ramazani , USA
Angel Manuel Ramos , Spain
Higinio Ramos , Spain
Muhammad Afzal Rana , Pakistan
Muhammad Rashid, Saudi Arabia
Manoj Rastogi, India
Alessandro Rasulo , Italy
S.S. Ravindran , USA
Abdolrahman Razani , Iran
Alessandro Reali , Italy
Jose A. Reinoso , Spain
Oscar Reinoso , Spain
Haijun Ren , China
Carlo Renno , Italy
Fabrizio Renno , Italy
Shahram Rezapour , Iran
Ricardo Rianza , Spain
Francesco Riganti-Fulginei , Italy
Gerasimos Rigatos , Greece
Francesco Ripamonti , Italy
Jorge Rivera , Mexico
Eugenio Roanes-Lozano , Spain
Ana Maria A. C. Rocha , Portugal
Luigi Rodino , Italy
Francisco Rodríguez , Spain
Rosana Rodríguez López, Spain
Francisco Rossomando , Argentina
Jose de Jesus Rubio , Mexico
Weiguo Rui , China
Rubén Ruiz , Spain
Ivan D. Rukhlenko , Australia
Dr. Eswaramoorthi S. , India
Weichao SHI , United Kingdom
Chaman Lal Sabharwal , USA
Andrés Sáez , Spain

Bekir Sahin, Turkey
Laxminarayan Sahoo , India
John S. Sakellariou , Greece
Michael Sakellariou , Greece
Salvatore Salamone, USA
Jose Vicente Salcedo , Spain
Alejandro Salcido , Mexico
Alejandro Salcido, Mexico
Nunzio Salerno , Italy
Rohit Salgotra , India
Miguel A. Salido , Spain
Sinan Salih , Iraq
Alessandro Salvini , Italy
Abdus Samad , India
Sovan Samanta, India
Nikolaos Samaras , Greece
Ramon Sancibrian , Spain
Giuseppe Sanfilippo , Italy
Omar-Jacobo Santos, Mexico
J Santos-Reyes , Mexico
José A. Sanz-Herrera , Spain
Musavarah Sarwar, Pakistan
Shahzad Sarwar, Saudi Arabia
Marcelo A. Savi , Brazil
Andrey V. Savkin, Australia
Tadeusz Sawik , Poland
Roberta Sburlati, Italy
Gustavo Scaglia , Argentina
Thomas Schuster , Germany
Hamid M. Sedighi , Iran
Mijanur Rahaman Seikh, India
Tapan Senapati , China
Lotfi Senhadji , France
Junwon Seo, USA
Michele Serpilli, Italy
Silvestar Šesnić , Croatia
Gerardo Severino, Italy
Ruben Sevilla , United Kingdom
Stefano Sfarra , Italy
Dr. Ismail Shah , Pakistan
Leonid Shaikhet , Israel
Vimal Shanmuganathan , India
Prayas Sharma, India
Bo Shen , Germany
Hang Shen, China

Xin Pu Shen, China
Dimitri O. Shepelsky, Ukraine
Jian Shi , China
Amin Shokrollahi, Australia
Suzanne M. Shontz , USA
Babak Shotorban , USA
Zhan Shu , Canada
Angelo Sifaleras , Greece
Nuno Simões , Portugal
Mehakpreet Singh , Ireland
Piyush Pratap Singh , India
Rajiv Singh, India
Seralathan Sivamani , India
S. Sivasankaran , Malaysia
Christos H. Skiadas, Greece
Konstantina Skouri , Greece
Neale R. Smith , Mexico
Bogdan Smolka, Poland
Delfim Soares Jr. , Brazil
Alba Sofi , Italy
Francesco Soldovieri , Italy
Raffaele Solimene , Italy
Yang Song , Norway
Jussi Sopanen , Finland
Marco Spadini , Italy
Paolo Spagnolo , Italy
Ruben Specogna , Italy
Vasilios Spitas , Greece
Ivanka Stamova , USA
Rafał Stanisławski , Poland
Miladin Stefanović , Serbia
Salvatore Strano , Italy
Yakov Strelniker, Israel
Kangkang Sun , China
Qiuqin Sun , China
Shuaishuai Sun, Australia
Yanchao Sun , China
Zong-Yao Sun , China
Kumarasamy Suresh , India
Sergey A. Suslov , Australia
D.L. Suthar, Ethiopia
D.L. Suthar , Ethiopia
Andrzej Swierniak, Poland
Andras Szekrenyes , Hungary
Kumar K. Tamma, USA


Yong (Aaron) Tan, United Kingdom
Marco Antonio Taneco-Hernández , Mexico
Lu Tang , China
Tianyou Tao, China
Hafez Tari , USA
Alessandro Tasora , Italy
Sergio Teggi , Italy
Adriana del Carmen Téllez-Anguiano , Mexico
Ana C. Teodoro , Portugal
Efstathios E. Theotokoglou , Greece
Jing-Feng Tian, China
Alexander Timokha , Norway
Stefania Tomasiello , Italy
Gisella Tomasini , Italy
Isabella Torcicollo , Italy
Francesco Tornabene , Italy
Mariano Torrisi , Italy
Thang nguyen Trung, Vietnam
George Tsiatas , Greece
Le Anh Tuan , Vietnam
Nerio Tullini , Italy
Emilio Turco , Italy
Ilhan Tuzcu , USA
Efstratios Tzirtzilakis , Greece
FRANCISCO UREÑA , Spain
Filippo Ubertini , Italy
Mohammad Uddin , Australia
Mohammad Safi Ullah , Bangladesh
Serdar Ulubeyli , Turkey
Mati Ur Rahman , Pakistan
Panayiotis Vafeas , Greece
Giuseppe Vairo , Italy
Jesus Valdez-Resendiz , Mexico
Eusebio Valero, Spain
Stefano Valvano , Italy
Carlos-Renato Vázquez , Mexico
Martin Velasco Villa , Mexico
Franck J. Vernerey, USA
Georgios Veronis , USA
Vincenzo Vespri , Italy
Renato Vidoni , Italy
Venkatesh Vijayaraghavan, Australia

Anna Vila, Spain
Francisco R. Villatoro , Spain
Francesca Vipiana , Italy
Stanislav Vitek , Czech Republic
Jan Vorel , Czech Republic
Michael Vynnycky , Sweden
Mohammad W. Alomari, Jordan
Roman Wan-Wendner , Austria
Bingchang Wang, China
C. H. Wang , Taiwan
Dagang Wang, China
Guoqiang Wang , China
Huaiyu Wang, China
Hui Wang , China
J.G. Wang, China
Ji Wang , China
Kang-Jia Wang , China
Lei Wang , China
Qiang Wang, China
Qingling Wang , China
Weiwei Wang , China
Xinyu Wang , China
Yong Wang , China
Yung-Chung Wang , Taiwan
Zhenbo Wang , USA
Zhibo Wang, China
Waldemar T. Wójcik, Poland
Chi Wu , Australia
Qihong Wu, China
Yuqiang Wu, China
Zhibin Wu , China
Zhizheng Wu , China
Michalis Xenos , Greece
Hao Xiao , China
Xiao Ping Xie , China
Qingzheng Xu , China
Binghan Xue , China
Yi Xue , China
Joseph J. Yame , France
Chuanliang Yan , China
Xinggang Yan , United Kingdom
Hongtai Yang , China
Jixiang Yang , China
Mijia Yang, USA
Ray-Yeng Yang, Taiwan

Zaoli Yang , China
Jun Ye , China
Min Ye , China
Luis J. Yebra , Spain
Peng-Yeng Yin , Taiwan
Muhammad Haroon Yousaf , Pakistan
Yuan Yuan, United Kingdom
Qin Yuming, China
Elena Zaitseva , Slovakia
Arkadiusz Zak , Poland
Mohammad Zakwan , India
Ernesto Zambrano-Serrano , Mexico
Francesco Zammori , Italy
Jessica Zangari , Italy
Rafal Zdunek , Poland
Ibrahim Zeid, USA
Nianyin Zeng , China
Junyong Zhai , China
Hao Zhang , China
Haopeng Zhang , USA
Jian Zhang , China
Kai Zhang, China
Lingfan Zhang , China
Mingjie Zhang , Norway
Qian Zhang , China
Tianwei Zhang , China
Tongqian Zhang , China
Wenyu Zhang , China
Xianming Zhang , Australia
Xuping Zhang , Denmark
Yinyan Zhang, China
Yifan Zhao , United Kingdom
Debao Zhou, USA
Heng Zhou , China
Jian G. Zhou , United Kingdom
Junyong Zhou , China
Xueqian Zhou , United Kingdom
Zhe Zhou , China
Wu-Le Zhu, China
Gaetano Zizzo , Italy
Mingcheng Zuo, China


Contents

Action Mechanism and Model of Cross-Border E-Commerce Green Supply Chain Based on Customer Behavior

Xiaheng Zhang and Sukun Liu 


Research Article (11 pages), Article ID 6670308, Volume 2021 (2021)

Sports Sequence Images Based on Convolutional Neural Network

Yonghao Chen 






Research Article (14 pages), Article ID 3326847, Volume 2021 (2021)

Improvement of Support Vector Machine Algorithm in Big Data Background

Babacar Gaye , Dezheng Zhang, and Aziguli Wulamu

Research Article (9 pages), Article ID 5594899, Volume 2021 (2021)

A Traceability Public Service Cloud Platform Incorporating IDcode System and Colorful QR Code Technology for Important Product

Shaqing Zhang , Jinhui Liao , Shuangcheng Wu , Junrui Zhong , and Xiaoping Xue 

Research Article (15 pages), Article ID 5535535, Volume 2021 (2021)

Evaluation Model of Cable Insulation Life Based on Improved Fuzzy Analytic Hierarchy Process

Lei Li , Xian Min Ma, and Wei Guo 


Research Article (11 pages), Article ID 6638258, Volume 2021 (2021)

The Integration of Blockchain Technology and Smart Grid: Framework and Application

Xiaomin Du , Ying Qi , Beibei Chen , Biaoan Shan , and Xinyu Liu 


Research Article (12 pages), Article ID 9956385, Volume 2021 (2021)

Optimal Service Commission Contract Design of OTA to Create O2O Model by Cooperation with TTA under Asymmetric Information

Pingping Shi, Yaogang Hu , and Yongfeng Wang





Research Article (17 pages), Article ID 9934726, Volume 2021 (2021)

Intelligent Recognition of Safety Risk in Metro Engineering Construction Based on BP Neural Network

Mengchu Li and Jingchun Wang 





Research Article (10 pages), Article ID 5587027, Volume 2021 (2021)

Incentive Contract Design for Supply Chain Enterprise's Pollution Abatement with Carbon Tax

Jing Yu , Chi Zhou , Yixin Wang , and Zhibing Liu 


Research Article (14 pages), Article ID 5556796, Volume 2021 (2021)

The Level of Regional Economic Development, Green Image, and Enterprise Environmental Protection Investment: Empirical Evidence from China

Quanxin Gan , Liu Yang , Jin Liu , Xiaofan Cheng , Han Qin , Jiafu Su , and Weiyi Xia 

Research Article (12 pages), Article ID 5522351, Volume 2021 (2021)

Competitive Analysis of Operation Mode of Enterprise Value Chain under the Background of Green Economy

Peng Fan , Yifeng Wang, and Yuwei Dong


Research Article (11 pages), Article ID 6681545, Volume 2021 (2021)

Risk Aversion of Public Service Marketization Based on Fuzzy Analytic Hierarchy Process

Shoubin Qi and Junwen Feng 




Research Article (9 pages), Article ID 6668516, Volume 2021 (2021)

Construction of Control Rights Allocation Index of Listed Companies Based on Neural Network and Machine Learning

Tao Zhang and Yuxiang Peng 



Research Article (13 pages), Article ID 6628916, Volume 2021 (2021)

Particle Swarm Optimization Algorithm in Numerical Simulation of Saturated Rock Slope Slip

Bowen Liu , Zhenwei Wang , and Xiaoyong Zhong 


Research Article (11 pages), Article ID 6682659, Volume 2021 (2021)

Evolutionary Game Research on the Impact of Environmental Regulation on Overcapacity in Coal Industry

Bo Fan, Tingting Guo , Ruzhi Xu , and Wenquan Dong

Research Article (19 pages), Article ID 5558112, Volume 2021 (2021)

Application of Computer Technology in Optimal Design of Overall Structure of Special Machinery

Caiping Guo 

Research Article (9 pages), Article ID 6619485, Volume 2021 (2021)

Parallel Processing Method of Inertial Aerobics Multisensor Data Fusion

Hongda Zhang  and Ting Zhang


Research Article (11 pages), Article ID 6657362, Volume 2021 (2021)

Decision-Making Behavior of Fertilizer Application of Grain Growers in Heilongjiang Province from the Perspective of Risk Preference and Risk Perception

Xin Li and Jie Shang 


Research Article (8 pages), Article ID 6667558, Volume 2021 (2021)

Neural Network Optimization Method and Its Application in Information Processing

Pin Wang, Peng Wang , and En Fan

Research Article (10 pages), Article ID 6665703, Volume 2021 (2021)


Offline and Online Channel Selection of Low-Carbon Supply Chain under Carbon Trading Market

Qiang Han , Zhenlong Yang, Zheng Zhang, and Liang Shen

Research Article (17 pages), Article ID 6627937, Volume 2021 (2021)

Contents


Decisions of E-Commerce Supply Chain under Consumer Returns and Different Power Structures

Liang Shen, Runjie Fan, and Yuyan Wang 

Research Article (21 pages), Article ID 8884963, Volume 2020 (2020)

Research Article

Action Mechanism and Model of Cross-Border E-Commerce Green Supply Chain Based on Customer Behavior

Xiaheng Zhang^{1,2} and Sukun Liu ³

¹School of Economics and Management, Chuzhou University, Chuzhou 239000, Anhui, China

²College of Business and Trade, Nanchang Institute of Science and Technology, Nanchang 330108, China

³School of Economic and Management, Dalian Ocean University, Dalian 116001, Liaoning, China

Correspondence should be addressed to Sukun Liu; liusukun@dlou.edu.cn

Received 25 December 2020; Revised 12 May 2021; Accepted 25 June 2021; Published 8 July 2021

Academic Editor: Aijun Liu

Copyright © 2021 Xiaheng Zhang and Sukun Liu. This is an open access article distributed under the Creative Commons Attribution License, which permits unrestricted use, distribution, and reproduction in any medium, provided the original work is properly cited.

In recent years, China's cross-border e-commerce has flourished, and the transaction volume has increased year by year. Cross-border e-commerce has become a favorable breakthrough point for China's foreign trade. This article mainly studies the action mechanism and model of cross-border e-commerce green supply chain based on customer behavior. Green supply chain partners select 24 secondary indicators of the evaluation system as the input vector. The historical data of each index is collected by field investigation as sample data and brought into the neural network for training. The output vector of the only output layer of the network is used as the evaluation result of the supplier. This paper divides the operation mode of green supply chain into four stages and puts forward improvement tools for the functional modules in each stage. Enterprises can use the tools in the modules to improve the operation efficiency of green supply chain. According to the green level evaluation demand of green supply chain, this paper uses the hierarchical method to evaluate it. According to the survey results, this paper uses arithmetic average method to deal with the operation and establishes a secondary index after decomposition. Finally, this paper uses confirmatory factor analysis to test the measurement model and further uses analysis of variance to test the relationship between the two types of social cues and behavioral willingness. The data shows that the orderly fluctuation range of the east, middle, and west cross-border logistics subsystems basically remains at around 0.2 to 0.6. The results show that the establishment of the green supply chain model has a very positive significance for the implementation and development of the green supply chain in China's manufacturing industry. Through the research of profit and profit distribution in the green supply chain, it provides guidance for the green supply chain to effectively select the supply chain members to cooperate and calculate and distribute the profit reasonably, so that the green supply chain management can be widely used in reality.

1. Introduction

In recent years, China's economy has been under great downward pressure, and the cost of manufacturing industry is rising. The traditional foreign trade mode and large cross-border trade have been greatly impacted [1]. Compared with traditional foreign trade, at present, China's Internet economy is in the leading position in the world, and the cross-border e-commerce industry is developing rapidly. Online retailing, especially small cross-border transactions, shows great competitive advantages. Simultaneously, the national policies continue to be

favorable to support the development of cross-border e-commerce [2].

It is a general trend that Chinese goods are sold to consumers all over the world through e-commerce and will gradually replace traditional trading methods. In this context, it has become more and more difficult to realize the development of enterprises only relying on cost-effective products [3, 4]. Only by making breakthroughs on the product side, channel side, brand building, and supply chain building at the same time can they have a foothold in the fierce competition [5]. Through the research of this article, we provide selection criteria and basis for the platform's

overseas warehouse construction model. This has important practical significance for the improvement and innovation of the existing cross-border logistics model, improvement of logistics links, and promotion of China's foreign trade structure adjustment and power conversion [6].

The development of the green supply chain has greatly enhanced the competitiveness of Chinese enterprises. The motivation of Kang's research is to activate recent poverty alleviation practices in the green supply chain. He examined the individual behaviors and cooperative behaviors of supply chain participants in the "green poverty alleviation" supply chain; that is, manufacturers initiate product "greening" and provide microcredit to alleviate the poverty of poor raw material suppliers. By establishing a series of supply chain game models, he analyzed the impact of cooperation mechanisms on green levels, prices, and profits and examined the impact of consumers' green sensitivity and small loan interest rates. On this basis, he proposed an optimal cooperation mechanism based on a two-part tariff contract. He also proposed to improve the economic and environmental performance of the supply chain "green poverty alleviation" through cooperation [7]. Rezaee proposed a two-stage stochastic planning model to design a green supply chain in a carbon trading environment. The model solves the discrete location problem and determines the optimal material flow and carbon credits/subsidies for transactions. He has contributed to the development of the supply chain by incorporating the uncertainty of carbon prices and product demand. He applied the model to actual case studies and carefully analyzed and explained the numerical results. Although his research has certain positive significance, it is not very innovative [8]. Wu believes that although people pay more and more attention to sustainable development and green innovation, in the context of supply chain relations, especially in emerging countries like China, few empirical efforts have been made to explore the factors affecting the performance of green innovation. In order to solve this research gap, he studied the role of specific investment in green supply chain innovation from the perspective of specific investment. He proposed that knowledge transfer plays a mediating role in the relationship. According to stakeholder participation theory, he believes that the social responsibility of partners plays a moderate role in not only specific investment (green supply chain innovation performance linkage) but also knowledge transfer and performance linkage. He tested the proposed relationship with a sample of 331 questionnaires and verified the responses from 187 high-tech companies in China. The external factors considered in his research are not comprehensive [9]. Pourjavad believes that the qualitative criteria for evaluating the performance of green supply chain management (GSCM) are affected by uncertainty, which is mainly due to the inherent ambiguity in the evaluation of qualitative factors. He aims to reduce the uncertainty caused by human judgment in the GSCM performance evaluation process using language terms and membership. He proposed a fuzzy set theory method to deal with the imprecision of language and the ambiguity of human judgment. His research lacks necessary experimental data [10]. Yun believes

that, with the development of economic globalization, the quality competition among enterprises has been extended to the supply chain. In order to achieve sustainable development, enterprises must change the traditional closed "vertical integration" mode. He studied the multiattribute decision-making problem and used binary linguistic information to estimate the performance of green supply chain in the low-carbon agricultural economic environment. Then, he proposed the 2-tuple power Einstein weighted geometric operator to summarize the 2-tuple linguistic information and then used the 2tpewg operator to evaluate the performance of the green supply chain in the low-carbon agricultural economic environment by using the 2-tuple linguistic information. His research is not accurate enough [11]. Miret studied the multiobjective optimization problem from the perspectives of economy, environment, and society. He quantified the environmental dimension through the life cycle assessment, especially the ecological cost method. For the latter, he proposed a new method based on financial accounting analysis to estimate direct, indirect, and induced job creation. Once the superstructure is described, the optimization problem is described as a mixed integer linear programming, which considers the seasonality of biomass, geographical availability, biomass degradation, process conversion technology, and final product requirements. Although his method for solving multiobjective optimization problems has a certain optimization effect, it lacks specific steps [12].

With the establishment of a central database between distributed computer units, an information sharing environment within the organization has emerged. Now, every unit of the organization can get all kinds of information needed from the database at any time and process it in its own unit. Simultaneously, the transaction processing system within the organization and the customer support system outside the organization are gradually connected, and a unified EDI standard compatible with various industries has been established, thus forming a supply chain process management system [13]. Each actor becomes the knowledge node in the internal supply chain of the organization, and the competitiveness of each technical link in the organization depends on the innovation power of these knowledge nodes [14]. These knowledge nodes are connected together to form a powerful internal supply chain system of the organization. The more competitive each knowledge node in the organization is, the more capable the organization will be to expand its internal supply chain, which in turn promotes the expansion of the enterprise scale [15]. In the industrial cluster or the supply chain governance environment, the network characteristics of the organization are more obvious [16]. Any subject can ingest property rights from network relational capital and expand the boundary of its information and decision-making capabilities [17, 18]. Large enterprises embed their databases and system software on the Internet, which can enhance the functions of their system software and reduce their operating costs. Small businesses or individual actors have a greater flexibility in using network capital [19]. In most cases, the network relationship of industrial clusters or supply chain governance

is always conducive to the externalization of enterprise production links or knowledge nodes. The emergence of virtual organizations is based on information sharing, organizational transparency, and independent information capabilities of actors. Each of the actors throughout the supply chain can flexibly extract the fruits of related industrial links with their own core advantages. In this environment, the formal form of organization becomes redundant, and the informal teamwork becomes extremely competitive [20]. This flexible organizational form liberates the individual core capabilities of the actors from the rigid formal organization and combines these core advantages with the help of network relationships and electronic connections and further integrates the entire body on a larger scale [21, 22]. The core competitiveness of each knowledge node of the supply chain is connected, so that the competition between enterprises becomes the competition between supply chains.

The main research sequence of this paper is as follows: Section 1 is an introduction, including the research background, significance, literature review, and main innovation mentioned in this paper. Section 2 mainly introduces customer behavior, cross-border e-commerce, and green supply chain. Section 3 mainly introduces the cross-border e-commerce green supply chain action mechanism and model simulation experience, including data acquisition, data preprocessing, model establishment, and supply chain evaluation weight. Section 4 mainly discusses and analyzes the experimental results. Section 5 is the summary of the whole research.

This article deconstructs the total factor efficiency of green supply chain companies into the total factor management efficiency of green supply chain companies and the full factor environmental efficiency of green supply chain companies from the two-dimensional level of management and environment and deeply explores the root causes of inefficiency of green supply chain companies. The internal and external environments provide a reliable basis for seeking a path to improve the efficiency of all elements. Simultaneously, the relevant theories of the green supply chain are researched, to construct a green supply chain operation model and analyze the model's process design and index system construction. This paper extracts transportation cost reliability, transportation timeliness reliability, and transportation safety and reliability. It has certain reference significance for the improvement of the theory of transportation mode choice influence.

2. Customer Behavior and Green Supply Chain

2.1. Customer Behavior. Customer demand is the primary link of service design. The ability to accurately obtain customer needs will directly affect the quality of the entire service design and is related to the ability to design products or services that satisfy customers. The determination of customer needs is mainly done by the service designer. The information obtained in a short period of time cannot guarantee accuracy and completeness, so it will take a long time to complete. In addition, it is necessary to ensure that

the accuracy of obtaining customer demand information is very important and determines the success or failure of service design. Forecast is the first part of income management, soul of income management, and important foundation of the other three parts of income management. In reality, market-related departments of most companies will predict and analyze the market demand for their products. The more accurate the market forecast, the more targeted the company's market strategies, such as pricing [23].

With the development of service enterprises and changes of business environment, customer loyalty can make enterprises occupy a favorable position in the market competition, have greater pricing space and market advantages, and have a great impact on the profitability and competitive strategies of service enterprises. Loyal customers can save the cost of developing new customers and reduce the transaction and service costs of customers. Simultaneously, it also brings higher premium income to the enterprise, which is mainly reflected in the basic profit and the profit brought by the increase of purchase quantity. Moreover, in most industries, loyal customers are less price-sensitive and have higher tolerance. They are willing to buy products and services of the enterprise at full price instead of waiting for a discount and price reduction, which makes loyal customers pay more than new customers, while enterprises sell more products at a full price and obtain a premium income [24].

2.2. Cross-Border E-Commerce. The cross-border e-commerce supply chain process is shown in Figure 1. With the increasing trade exchanges among countries in the world, the future trade will be presented in front of the world in a new way and channel of cooperation, and the development of cross-border e-commerce will appear as a new trend of a larger market, with more profits, better products, and being closer to the consumers. Under the environment of market economy, the development of an organization is not only constrained by its own resources but is also directly or indirectly influenced by the external environment. In the era of Internet and globalization, the developmental activities of organizations are increasingly closely related to the external environment. Therefore, if an organization can make full use of the external macroenvironment to "follow the trend," it will greatly promote the development of the organization; otherwise, it will bring many obstacles to the development of the organization. Therefore, it is of great significance for the development of the organization to analyze the macroenvironment faced by the organization [25].

In the Internet era, the network connects the world as a whole, and the characteristics of globalization and decentralization are increasingly obvious. In particular, the development of cross-border e-commerce is not constrained by time and space. Internet users can purchase and trade products from any country in any place at any time through the Internet with the help of cross-border e-commerce platforms, so as to realize "global trading" in a real sense and promote the flow of global capital, products, and other elements across the world [26].

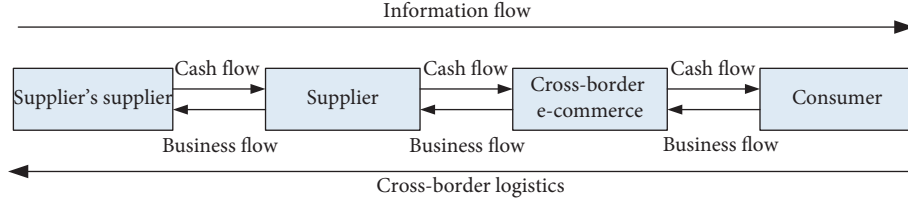


FIGURE 1: Cross-border e-commerce supply chain process.

2.3. Green Supply Chain. According to the theory of green supply chain management, the objects of green supply chain management include raw material suppliers, sellers, logistics providers, and so on. In the process of implementing green supply chain management, the green requirements of each link in the supply chain must be clear. Only when every link is “green” can we promote the development of green supply chain from inside to outside and also promote the formation of green procurement market system. To distinguish common products from green products, product green degree is born. It represents the coordination degree between green products and environment and is an evaluation index. Generally speaking, the greener a product is, the more environmentally friendly it is [27].

The output vector of the hidden layer of BP neural network is

$$Y = f_1 \left(\sum_i w_{ij} x_i + b_i \right). \quad (1)$$

The output vector of the output layer is

$$Z = f_2 \left(\sum_j w_{j1} x_j + b_1 \right). \quad (2)$$

Here, x_i is the input layer input vector and x_j is the hidden layer input vector.

The modified value of the connection weight from the output layer to the hidden layer is

$$\Delta w_{ij} = -\eta \frac{\partial \varepsilon}{\partial w_{ij}}. \quad (3)$$

The modified value of the connection weight from the hidden layer to the output layer is

$$\Delta w_{j1} = -\eta \frac{\partial \varepsilon}{\partial w_{j1}}. \quad (4)$$

Here, η is the learning rate of the BP neural network model, and the general value range is the interval (0, 1).

For each factory i and product p , the purchase of raw materials plus the production of products should equal the amount of products shipped from the factory to the warehouse plus the amount of raw materials consumed [28]:

$$PU_{jpt} + \sum_{i \in \text{OUT}(P)} W_{ijpt} = \sum_k Q_{jkpt}^{\text{PL}} + \sum_{i \in \text{IN}(P)} W_{ijpt}. \quad (5)$$

Here, PU_{jpt} represents the amount of raw materials purchased by factory j in the production of product p at

period t and W_{ijpt} represents the input or output of product p in plant j at period t under equipment i .

The following material conversion relationship exists for equipment i of plant j :

$$W_{ijpt} = \mu_{ip} + W_{ijp't}. \quad (6)$$

Here, μ_{ip} represents the material conversion coefficient.

The original inventory plus the transportation volume from the factory to the warehouse equals the flow from the warehouse to the market plus the final inventory, which is written as follows:

$$\text{INV}_{kpt-1} + \sum_j Q_{jkpt}^{\text{PL}} = \sum_l Q_{klpt}^{\text{WH}} + \text{INV}_{kpt}. \quad (7)$$

The sales volume of products on the market depends on the quantity allocated by the warehouse, which is written as follows:

$$\sum_k Q_{klpt}^{\text{WH}} = \text{SA}_{lpt}. \quad (8)$$

The relationship between the environmental impact factors of product storage and the geographic location of the facility is not obvious, but the material flow in different regions will be different. Therefore, the emissions at this stage are only affected by the material flow as follows:

$$\begin{aligned} I_{ps} &= f_{ps} \sum_g F_{ps,g}, \\ \sum_g F_{ps,g} &= \sum_k \sum_p \sum_t \text{INV}_{k,p,t}, \\ I_{ps} &= f_{ps,k} \sum_k \sum_p \sum_t \text{INV}_{k,p,t}. \end{aligned} \quad (9)$$

As it is assumed that the technical equipment and processes of the company's branches are basically the same, the impact factors are not regionally dependent, so GHG emissions and production have a certain proportional relationship as follows:

$$I_{pp} = \sum_g f_{pp} F_{pp,g}, \quad (10)$$

$$F_{pp,g} = W_{ijpt}.$$

NPV is obtained by converting the cash flows generated in each period and then adding them up as follows:

$$\text{NPV} = \sum_t \frac{\text{CF}_t}{(1+i_r)^{t-1}}. \quad (11)$$

Here, i_r represents the interest rate.

In the coordination relationship of green supply chain of large-scale catering enterprises, the evaluation and selection of green suppliers are the primary problems to be solved. Different from the traditional supplier evaluation and selection, green supply chain management requires large-scale catering enterprises not only to consider the economic performance of the enterprise but also to pay attention to the environmental performance objectives. Due to the large number of raw materials in large-scale catering enterprises, through the different impact of raw materials on the economic and environmental performance of enterprises and the influence of large-scale catering enterprises on raw material suppliers, the procurement objectives of raw materials are determined, targeted supplier evaluation standards are established, and the green practice of suppliers is influenced, so as to improve the environmental performance of the whole supply chain [29].

3. Cross-Border E-Commerce Green Supply Chain Action Mechanism and Model Simulation Experiment

3.1. Data Acquisition. Customer behavior analysis is based on positioning and consumption information. Therefore, this paper mainly obtains the required data from location and client databases. Simultaneously, to encourage customers to purchase using cards, to ensure the effectiveness of data collection, customers who carry membership cards can enjoy a certain discount [30].

- (1) Customer information: the information in this part comes from the client's database, which mainly includes the customer's name, age, corresponding tag number, income, education level, occupation and hobbies.
- (2) Record of consumption behavior: the consumption behavior records that need to be collected in this part mainly include the serial number of the entertainment facility, consumption price of each facility, area and category of the entertainment facility, and consumption amount of customers in each area.
- (3) Record of customer activity scope: the record of customer activity range mainly includes the time when customers enter and exit, time that customers stay in each area of the venue, number of times customers appear in each area, and number of people included in each area in a certain period of time [31].

3.2. Data Preprocessing. Green supply chain partners choose 24 secondary indicators of the evaluation system as input vectors. The historical data under each index are collected by field investigation and brought into the neural network for training. The output vector of the network's only output layer is used as the evaluation result of suppliers. The first part is to train the established BP neural network. First, normalize the sample data, set the appropriate training parameters, and bring the sample data into the BP neural network for trial calculation until the output is less than the

allowable error value. In the second part, the test data is brought into the trained BP neural network to get the output value, that is, the final output value. After the final output result is obtained, it is necessary to use the function to inverse-normalize the operation result, so as to facilitate the selection of multiple evaluation objects and select suppliers that meet the requirements through comparison.

3.3. Model Establishment. The green supply chain model is shown in Figure 2. This paper divides the operation mode of green supply chain into four stages and puts forward improvement tools for the functional modules in each stage. Each enterprise can use the tools in the module to improve the green supply chain, so as to improve the operation efficiency of the enterprise green supply chain. The initial formation of the operation mode of green supply chain is a comprehensive, modern, and circular development management mode initially formed by the influence of value holding and value driving factors, which determines the value goal of implementing green supply chain and comprehensively considers the internal and external obstacles and advantages.

The green supply chain of core enterprises in the supply chain is a supply chain mode with the manufacturer as the core to promote and pull, which fully considers the whole life cycle of products and the needs of final customers. The operation results and evaluation of the green supply chain operation mode are mainly composed of value creation and value acquisition. According to the value objectives of the mode operation and path selection and implementation of the mode operation, the composition structure of the main benefits of all parties can be determined. Simultaneously, with the support of system support and technological innovation, it is possible to provide value acquisition for stakeholders in the supply chain [32].

3.4. Supply Chain Evaluation Weight. The evaluation scale set refers to the scale for evaluating each indicator, which can be expressed in a variety of ways such as grades and scores, and varies with different evaluation needs. According to the green level evaluation requirements of the green supply chain, this article uses a graded approach to evaluate it. The construction of the judgment matrix is to compare the elements in the element set at each level and then determine the relative importance of the two elements and assign a certain value. Based on the results of the interview survey, this paper uses the arithmetic average method for operation and processing and establishes a secondary index after decomposition.

3.5. Model Checking. First, according to the two-stage method, confirmatory factor analysis was used to test the measurement model. The reliability of the questionnaire is evaluated using Cronbach's α coefficient and composite reliability. This article uses a two-factor analysis of variance to test the relationship between the two types of social cues and the participants' social presence. The relationship

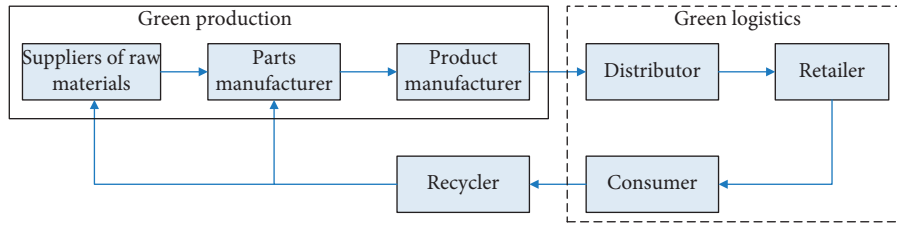


FIGURE 2: Green supply chain model.

between the two types of social cues and behavioral willingness was further tested through analysis of variance. After verifying the relationship between social cues and social presence, the structural equation model was further used to test the relationship between social presence and subsequent variables [33].

4. Model Simulation Results

4.1. Customer Behavior Analysis. The demand density faced by the two manufacturers is shown in Table 1. Assuming that the initial inventory quantity of two manufacturers is 100, simulate the optimal price sequence and equilibrium price of the two manufacturers when the initial inventory quantity is the same. It can be seen that both manufacturers will adopt low prices at the beginning of the sales period. When the initial inventory is the same, the price conversion time of manufacturer 2 is faster than that of manufacturer 1. This is because the calculation example assumes that the demand density faced by manufacturer 1 is higher than that of manufacturer 2. Therefore, manufacturer 2 must “first move” to make itself in strive for more revenue in the competition [34].

Keep other parameters unchanged, when the simulated initial inventory quantity is the same. The change of conversion time under different α values is shown in Table 2. It can be seen from the table that obviously as α increases, the time for manufacturers to use high prices decreases, and the time to use low prices increases. This is because, under the circumstance that the total demand remains unchanged, the larger the α , the smaller the proportion of the second category of customers and the relative reduction in the demand faced by the two manufacturers during dynamic pricing, which increases the risk of surplus inventory at the end of the period, so the price must be adjusted downward in hope of increasing the probability that customers are willing to buy and reducing the possibility of surplus inventory [35].

Using the factor analysis results output by SPSS software, we can get the objective weight result of the evaluation of innovation ability of import cross-border e-commerce platform, which makes the comprehensive evaluation of each platform objective and accurate. The analysis results show that the service innovation of import cross-border e-commerce platform needs to consider both internal and external factors. The internal factors include the staff's culture and quality, platform's own network technology level, and so on, and the external factors include the change of consumer demand brought by social progress [36]. The comprehensive score of service innovation ability of each import cross-border e-commerce platform is shown in

TABLE 1: Demand density faced by the two vendors.

$P1 = 100$	0.49	0.38	0.53	0.30	0.59	0.26	0.64	0.23
$P2 = 120$	0.39	0.44	0.44	0.35	0.47	0.28	0.51	0.25
$P3 = 140$	0.27	0.48	0.37	0.40	0.39	0.32	0.43	0.29
$P4 = 160$	0.24	0.53	0.31	0.43	0.35	0.36	0.38	0.33

TABLE 2: Price conversion time under different α values.

$\alpha = 0.1$	112	623	795	961	94	583	767	914
$\alpha = 0.2$	145	587	774	923	121	545	758	865
$\alpha = 0.3$	172	567	732	861	150	509	714	831
$\alpha = 0.4$	212	554	713	858	209	527	685	818
$\alpha = 0.5$	284	548	689	822	258	494	637	783
$\alpha = 0.6$	335	527	653	804	314	501	628	766
$\alpha = 0.7$	362	503	627	773	345	492	596	738
$\alpha = 0.8$	384	473	606	739	365	457	572	690
$\alpha = 0.9$	406	458	582	711	385	437	559	671

Figure 3. The scores of various import cross-border e-commerce platforms in the market are quite different, which indicates that there is a big gap between the strengths and weaknesses of service innovation ability. Among them, the comprehensive score of platform A is the highest, which is 3.67; the score of platform B and platform C is not much different, which is 0.79 and 0.72, respectively; the score of platform D is -0.47 , ranking the fourth; the score of platforms E and F is significantly different from those of the previous platforms, which are -1.46 and -2.39 , respectively. The service innovation ability needs to be strengthened [37].

The change of customer status with time and parameters is shown in Figure 4. When the utility of social preference increases, the curve of buy increases as a whole, so hesitant customers are more willing to buy goods than give up. When all the parameters are reduced, the number of customers who buy decreases significantly and the number of customers who give up buying increases significantly. When the contact between customers is closer, compared with discount, social preference utility plays a greater role, and customers trust more the recommendation of friends and the reputation of sellers. When the utility of time to customers with deposit becomes smaller, more customers are willing to wait, and the number of customers with deposit increases more rapidly and the curve is steeper [38].

4.2. Evaluation Index Analysis. The degree of collaboration between cross-border e-commerce and logistics in different regions is shown in Table 3 and Figure 5. From the table, we

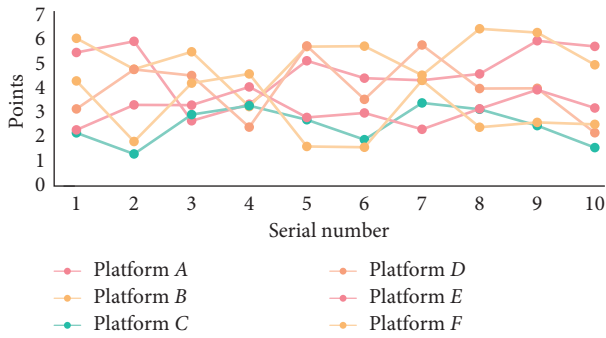


FIGURE 3: Comprehensive scores of service innovation capabilities of various imported cross-border e-commerce platforms.



FIGURE 4: Customer status changes with time and parameters.

can see that the order degree of the east, middle, and west cross-border logistics subsystems is increasing as a whole, and the numerical difference is not big, and the fluctuation range basically remains at about 0.2~0.6. Relatively speaking, the order of the cross-border logistics subsystem in the central region is slightly higher than that of the east and west, reaching 0.653 in 2018. In recent years, the logistics industry of China’s cross-border e-commerce has developed rapidly, and the construction of related logistics infrastructure has been continuously improved, which has also laid a solid foundation for the further development of the cross-border logistics industry [39].

The optimal decisions for the green efficiency of different products are shown in Table 4 and Figure 6. In the process of collaboration between cross-border e-commerce enterprise think tanks and cross-border e-commerce information service related platform institutions, factors such as synergy benefits, synergy costs, and speculative returns affect the collaboration of cross-border e-commerce enterprise think tanks and related platforms. However, because of the different modes and contents of information services, cross-border e-commerce enterprise think tanks will be affected by other factors in the process of collaboration with different platforms. Strengthening the connection between cross-border e-commerce enterprise think tanks and cross-border e-commerce information service related platforms is of great significance for the effective integration of information resources and the transformation of resources from decentralization to aggregation [40].

The result of index weight calculation is shown in Figure 7. In the evaluation index system of B2C cross-border

TABLE 3: Cross-border e-commerce and logistics collaboration in different regions.

Years	East	Central	West
2014	0.048	0.036	0.089
2015	0.059	0.059	0.098
2016	0.079	0.076	0.182
2017	0.108	0.136	0.104
2018	0.217	0.148	0.143

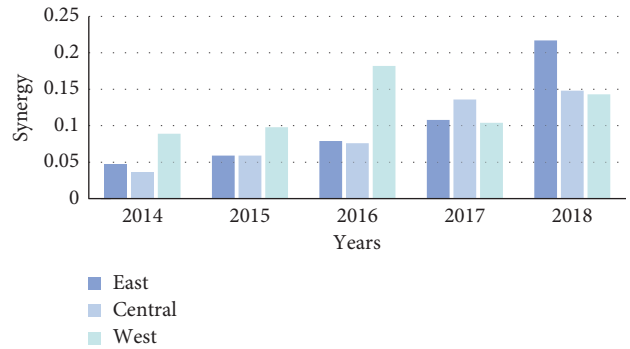


FIGURE 5: Cross-border e-commerce and logistics collaboration in different regions.

e-commerce overseas warehouse construction mode selection, the weights of service quality, market competition environment, platform characteristics, and supporting environment are 0.4335, 0.3049, 0.1615, and 0.1001, respectively. The market competition environment includes three specific indicators, namely, the proportion of online shopping consumers, e-commerce penetration rate, and Internet penetration rate. According to the calculation results of Yaahp software, the weights of the three are 0.0835, 0.2037, and 0.7128 respectively, and the test coefficient $CR = 0.0300 < 0.1$, passing the consistency test. The order of consideration is the Internet penetration rate, e-commerce penetration rate, and proportion of online shopping consumers. This is mainly because the Internet is the basis for the survival of cross-border e-commerce. The Internet penetration rate of the target country market has the greatest impact on people’s online shopping demand, and it is also important for B2C cross-border e-commerce to choose overseas warehouse.

4.3. Model Test Results. Through software analysis, the corresponding cross-border e-commerce company supply chain risk index layer and the weight value of each index corresponding to the total index are obtained, as shown in Table 5. According to the weight data table, it can be determined that the transaction risk has the greatest impact on the risk level of the cross-border e-commerce company supply chain risk, with a corresponding weight value of 0.42; that is, if the cross-border e-commerce company supply chain has a risk, the risk that is most likely to occur is transaction risk, which can also be understood as the probability of transaction risk occurring at 42%. The second is the environmental risk, with a corresponding weight value

TABLE 4: The optimal decision of green efficiency of different products.

Centralized decision		Decentralized decision-making	
Pr	Pd	Pr1	Pd1
50.97	58.11	58.38	57.76
54.38	61.53	62.16	60.67
58.62	65.76	66.69	64.15
63.93	71.07	72.13	68.34
70.51	77.65	78.52	73.26
79.28	86.42	86.51	79.4
91.97	99.11	97.1	87.55
111.64	118.7	111.5	98.68
143.1	150.2	130.8	113.5

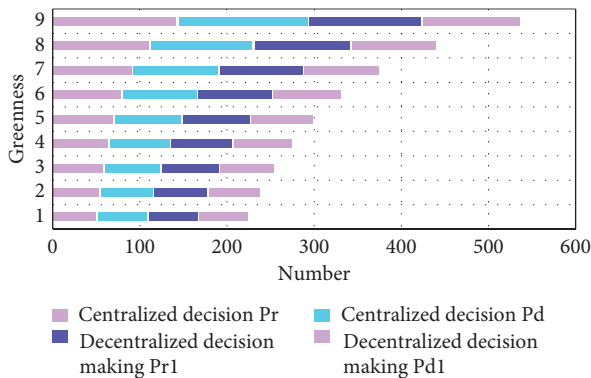


FIGURE 6: Optimal decisions for green efficiency of different products.

TABLE 5: Weight value of each indicator.

First level indicator	Weights	Comprehensive weight
Cross-border logistics risk (0.22)	0.76 0.24	0.17 0.05
Transaction risk (0.42)	0.94 0.06	0.39 0.03
Internet marketing risk (0.05)	0.80 0.20	0.04 0.01
	0.45 0.15	0.14 0.05
Environmental risk (0.31)	0.37 0.03	0.11 0.003

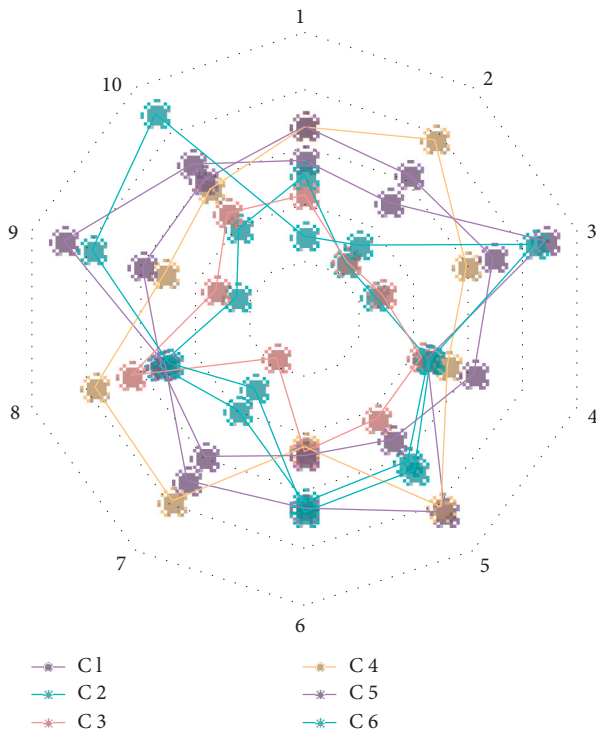


FIGURE 7: Result of index weight calculation.

of 0.31, which can also be understood as the probability of environmental risk occurring at 31%. The third is the cross-border logistics risk, with a corresponding weight value of

0.22, which can also be understood as the probability of cross-border logistics risk occurring at 22%. The fourth is the network marketing risk, with a corresponding weight value of 0.05; that is, the probability of network marketing risk occurrence is relatively low, less than 0.1. The risks of online marketing can be ignored in this article. From the overall perspective of cross-border e-commerce company supply chain risks, the most obvious impact is credit risk, with an overall weight value of 0.39. The second is the logistics itself risk, with an overall weight value of 0.17. The third is legal and regulatory risk, with an overall weight value of 0.14. The fourth is the industry environmental risk, with an overall weight value of 0.11.

The effect of information sharing cost coefficient on profit is shown in Figure 8. When the cost coefficient of information sharing between the two sides continues to decline over time, the products of cross-border export enterprises can create greater market demand and sell on the platform e-commerce platform at a higher price. The degree of information sharing in the supply chain will also be improved, and the overall supply chain will enter a virtuous cycle. If the cost coefficient of information sharing in the supply chain gradually decreases, the profits of platform providers and cross-border export enterprises and the total profits of the supply chain will be improved, and the competitiveness of the supply chain will be enhanced. In this process, the profits of the platform providers will increase faster than those of the cross-border export enterprises, and the platform enterprises will get more benefits by reducing the information sharing degree in the supply chain.

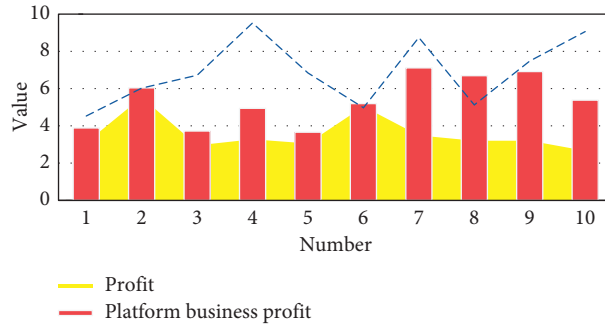


FIGURE 8: The impact of information sharing cost coefficient on profit.

TABLE 6: GSETFE value of green supply chain companies.

Enterprise	2014	2015	2016	2017	2018	Average value
Weichai Power	0.788	0.842	0.709	0.761	0.818	0.784
Goldwind Technology	0.787	0.864	0.935	0.896	0.936	0.884
Snowman shares	0.835	0.638	0.786	0.352	0.695	0.661
Sany heavy industry	0.817	0.748	0.637	0.707	0.889	0.760
TBEA	0.850	0.781	0.693	0.716	0.773	0.763
Zhenhua heavy industry	0.604	0.553	0.423	0.396	0.472	0.490
Haier Zhijia	0.971	0.774	0.787	0.767	0.869	0.834
Sichuan Changhong	0.704	0.595	0.653	0.733	0.796	0.696
Average value	0.836	0.779	0.762	0.733	0.825	0.787

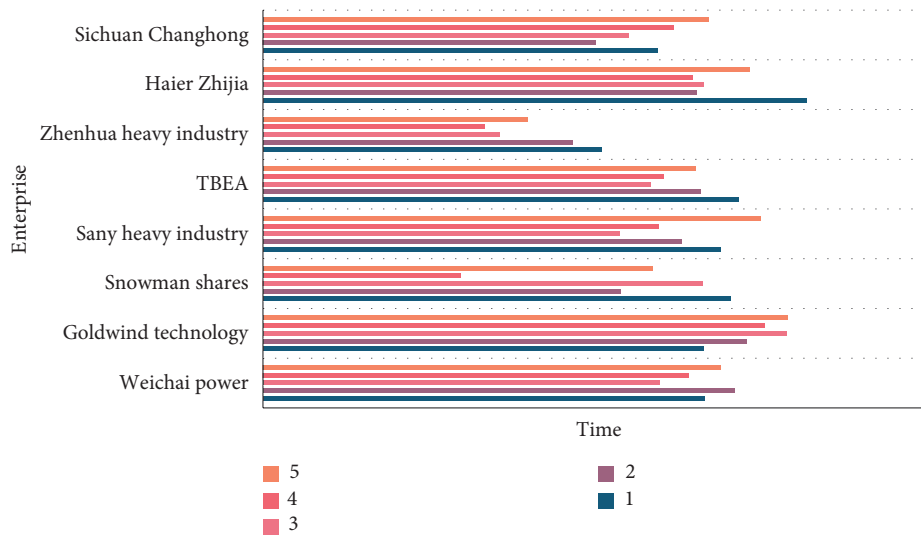


FIGURE 9: GSETFE value of green supply chain companies.

GSETFE values of green supply chain enterprises are shown in Table 6 and Figure 9. From the sample average level, without considering the influence of external environmental factors, the total factor efficiency of green supply chain enterprises in China is between 0.73 and 0.85, and there is still 15%–27% room for improvement, which shows that the development potential of green supply chain enterprises in China is huge.

5. Conclusions

The supply chain management of cross-border e-commerce should take the ultimate goal of improving the sensitivity of

the supply chain system, enhancing the competitive advantage of the enterprise supply chain, and reducing the operating cost of the enterprise supply chain and consider the construction factors, such as reasonable logistics grid and customer value. Major cross-border e-commerce companies rely on the professionalism of third-party logistics resources. The layout of cross-border logistics networks should be based on their own product characteristics and service requirements and use logistics service outsourcing resources, especially for the delivery services of the destination country of commodity delivery. It is difficult to penetrate overseas countries, and logistics outsourcing can improve the efficiency of distribution and reduce the cost at the same time.

Now, large enterprises are facing more brutal competition. In order to highlight their main business and develop their core competitiveness, many large enterprises are also forced to get rid of some of the branches and industrial links that they are not good at and cannot afford to lose. In some new industrial areas or industrial cluster areas, this situation becomes particularly clear. Therefore, if a region wants to obtain a sustainable competitive advantage, it must adopt two strategies at the same time. One is to optimize the geographical environment and give play to the advantages of industrial clusters; the other is to participate in or create a network alliance of global supply chains, reduce logistics costs, and share.

This paper uses evolutionary game theory and mathematical modeling analysis tools to construct an evolutionary game model of core enterprises and their upstream SMEs in the supply chain based on core enterprise guarantee strategies and uses numerical simulation analysis to prove that core enterprises take guaranteed actions to promote green supply in my country. The implementation of chain finance strategy is of great significance. Through the research of profit and profit distribution in the green supply chain, it provides guidance for the green supply chain to effectively select the supply chain members to cooperate and calculate and distribute the profit reasonably, so that the green supply chain management can be widely used in reality.

The construction of reasonable power mechanism, sharing mechanism, negotiation mechanism, and trust mechanism can ensure the efficient and steady operation of the green supply chain, improve the overall competitiveness of the supply chain, and achieve the win-win goal of the whole and part. Through the construction of mechanism and model, it can be concluded that when enterprises implement green supply chain operation and if node enterprises can share knowledge, negotiate, and trust with each other, then the overall revenue of the supply chain will be greatly improved, and the overall competitiveness of the supply chain will be enhanced. Due to the authors' limited knowledge level and time, it is difficult to form a systematic and complete theoretical system in a short time. There are still many limitations in this paper. For example, the analysis of the impact of customer behavior on the operation of green supply chain is not deep enough, and the combination of behavior theory and enterprise supply chain management will be the direction of further research.

Data Availability

No data were used to support this study.

Conflicts of Interest

The authors declare that they have no conflicts of interest.

Acknowledgments

This work was supported by Nanchang Institute of Technology Introduced Personnel Research Start-Up Project

Research on the Whole Industry Chain Agglomeration of Cross-Border E-Commerce (NGRCZX-20-11) and 2020 Scientific Research Fund Project of Education Department of Liaoning Province (QW202001)

References

- [1] C.-H. Wu and S.-B. Tsai, "Using DEMATEL-based ANP model to measure the successful factors of E-commerce," *Journal of Global Information Management*, vol. 26, no. 1, pp. 120–135, 2018.
- [2] K. Choudhary and K. S. Sangwan, "Benchmarking Indian ceramic enterprises based on green supply chain management pressures, practices and performance," *Benchmarking: An International Journal*, vol. 25, no. 9, pp. 3628–3653, 2018.
- [3] Y.-C. Huang, C.-H. Huang, and M.-L. Yang, "Drivers of green supply chain initiatives and performance," *International Journal of Physical Distribution & Logistics Management*, vol. 47, no. 9, pp. 796–819, 2017.
- [4] Y. S. Fabio, G. C. D. Oliveira Neto, F. C. Silva, and E. C. Pompone, "Corporate profile, performance and green supply chain management: a research agenda," *Ram Revista De Administração Mackenzie*, vol. 18, no. 3, pp. 117–146, 2017.
- [5] S. Luthra, D. Garg, and A. Haleem, "The impacts of critical success factors for implementing green supply chain management towards sustainability: an empirical investigation of Indian automobile industry," *Journal of Cleaner Production*, vol. 121, no. 5, pp. 142–158, 2016.
- [6] C. Mahesh, B. Neha, and S. Rajesh kumar, "ANP-MOORA-based approach for the analysis of selected issues of green supply chain management," *Benchmarking*, vol. 25, no. 2, pp. 642–659, 2018.
- [7] K. Kang, Y. Zhao, Y. Ma, and Z. Li, "Green supply chain poverty alleviation through microfinance game model and cooperative analysis," *Journal of Cleaner Production*, vol. 226, no. 7, pp. 1022–1041, 2019.
- [8] A. Rezaee, F. Dehghanian, B. Fahimnia, and B. Beamon, "Green supply chain network design with stochastic demand and carbon price," *Annals of Operations Research*, vol. 250, no. 2, pp. 463–485, 2017.
- [9] A. Wu and T. Li, "Gaining sustainable development by green supply chain innovation: perspectives of specific investments and stakeholder engagement," *Business Strategy and the Environment*, vol. 29, no. 3, pp. 962–975, 2020.
- [10] E. Pourjavad and A. Shahin, "The application of mamdani fuzzy inference system in evaluating green supply chain management performance," *International Journal of Fuzzy Systems*, vol. 20, no. 3, pp. 901–912, 2018.
- [11] T. Yun, "Model for evaluating the green supply chain performance under low-carbon agricultural economy environment with 2-tuple linguistic information," *Journal of Intelligent and Fuzzy Systems*, vol. 32, no. 3, pp. 2717–2723, 2017.
- [12] C. Miret, P. Chazara, L. Montastruc, S. Negny, and S. Domenech, "Design of bioethanol green supply chain: comparison between first and second generation biomass concerning economic, environmental and social criteria," *Computers and Chemical Engineering*, vol. 85, no. 2, pp. 16–35, 2016.
- [13] H.-K. Liu, D. Chen, H. Jin et al., "A survey of non-volatile main memory technologies: state-of-the-arts, practices, and future directions," *Journal of Computer Science and Technology*, vol. 36, no. 1, pp. 4–32, 2021.

- [14] S. Nathaniel and S. Abdul, "The nexus between urbanization, renewable energy, trade, and ecological footprint in ASEAN countries," *Journal of Cleaner Production*, vol. 272, 2020.
- [15] S. A. Rehman Khan, A. Sharif, H. Golpra, and A. Kumar, "A green ideology in asian emerging economies: from environmental policy and sustainable development," *Sustainable Development*, vol. 27, no. 2, pp. 1063–1075, 2019.
- [16] Z. A. Yu, B. Sark, C. Ak et al., "Is tourism really affected by logistical operations and environmental degradation? An empirical study from the perspective of Thailand," *Journal of Cleaner Production*, vol. 227, no. 1, pp. 158–166, 2019.
- [17] S. A. R. Khan, C. Jian, Y. Zhang, H. Golpıra, A. Kumar, and A. Sharif, "Environmental, social and economic growth indicators spur logistics performance: from the perspective of south asian association for regional cooperation countries," *Journal of Cleaner Production*, vol. 214, pp. 1011–1023, 2019.
- [18] S. A. Rehman Khan, Y. Zhang, M. Anees, H. Golpıra, A. Lahmar, and D. Qianli, "Green supply chain management, economic growth and environment: a GMM based evidence," *Journal of Cleaner Production*, vol. 185, pp. 588–599, 2018.
- [19] S. A. R. Khan and D. Qianli, "Impact of green supply chain management practices on firms' performance: an empirical study from the perspective of Pakistan," *Environmental Science and Pollution Research*, vol. 24, no. 20, pp. 16829–16844, 2017.
- [20] Y. Zhang and S. Khan, "Evolutionary game analysis of green agricultural product supply chain financing system: COVID-19 pandemic," *International Journal of Logistics*, no. 4, pp. 1–21, 2021.
- [21] S. Khan, K. Zkik, A. Belhadi, and S. Kamble, "Evaluating barriers and solutions for social sustainability adoption in multi-tier supply chains," *International Journal of Production Research*, vol. 59, no. 9, pp. 1–20, 2021.
- [22] Y. Zhang and R. K. Syed Abdul, "Green supply chain network optimization under random and fuzzy environment," *International Journal of Fuzzy Systems*, vol. 92, no. 5, 2021.
- [23] A. Longoni and R. Cagliano, "Inclusive environmental disclosure practices and firm performance," *International Journal of Operations and Production Management*, vol. 38, no. 9, pp. 1815–1835, 2018.
- [24] V. K. Sharma, P. Chandna, and A. Bhardwaj, "Green supply chain management related performance indicators in agro industry: a review," *Journal of Cleaner Production*, vol. 141, no. 1, pp. 1194–1208, 2017.
- [25] A. A. Teixeira, C. J. C. Jabbour, A. B. L. de Sousa Jabbour, H. Latan, and J. H. C. de Oliveira, "Green training and green supply chain management: evidence from Brazilian firms," *Journal of Cleaner Production*, vol. 116, no. 3, pp. 170–176, 2016.
- [26] K. S. Abdallah, A. M. Fathollahi-Fard, and M. Hajiaghaei-Keshteli, "A collaborative stochastic closed-loop supply chain network design for tire industry," *International Journal of Engineering Research*, vol. 31, no. 10, pp. 1715–1722, 2018.
- [27] F. Gholian-Jouybari, M. M. Paydar, M. Hajiaghaei-Keshteli, and A. M. Fathollahi-Fard, "A Bi-objective stochastic closed-loop supply chain network design problem considering downside risk," *Industrial Engineering and Management Systems*, vol. 16, no. 3, pp. 342–362, 2017.
- [28] A. Cheraghalipour, M. Hajiaghaei-Keshteli, and M. M. Paydar, "Tree Growth Algorithm (TGA): a novel approach for solving optimization problems," *Engineering Applications of Artificial Intelligence*, vol. 72, no. 6, pp. 393–414, 2018.
- [29] V. Hajipour, R. Z. Farahani, and P. Fattahi, "Bi-objective vibration damping optimization for congested location-pricing problem," *Computers & Operations Research*, vol. 70, no. 6, pp. 87–100, 2016.
- [30] S. Rezapour, R. Z. Farahani, D. Zhang, and F. Mohammaddust, "Strategic design of a competing supply chain network for markets with deterministic demands," *IMA Journal of Management Mathematics*, vol. 27, no. 2, pp. 109–141, 2016.
- [31] Ö. Uygun and A. Dede, "Performance evaluation of green supply chain management using integrated fuzzy multi-criteria decision making techniques," *Computers & Industrial Engineering*, vol. 102, no. 12, pp. 502–511, 2016.
- [32] Q. Zhang, W. Tang, and J. Zhang, "Green supply chain performance with cost learning and operational inefficiency effects," *Journal of Cleaner Production*, vol. 112, no. 1, pp. 3267–3284, 2016.
- [33] A. Gurtu, C. Searcy, and M. Y. Jaber, "An analysis of keywords used in the literature on green supply chain management," *Management Research Review*, vol. 38, no. 2, pp. 166–194, 2016.
- [34] J. F. Kirchoff, W. L. Tate, and D. A. Mollenkopf, "The impact of strategic organizational orientations on green supply chain management and firm performance," *International Journal of Physical Distribution and Logistics Management*, vol. 46, no. 3, pp. 269–292, 2016.
- [35] M.-L. Tseng, K. Tan, and A. S. F. Chiu, "Identifying the competitive determinants of firms' green supply chain capabilities under uncertainty," *Clean Technologies and Environmental Policy*, vol. 18, no. 5, pp. 1247–1262, 2016.
- [36] M. Sawadogo and D. Anciaux, "Intermodal transportation within the green supply chain: an approach based on ELECTRE method," *International Journal of Business Performance and Supply Chain Modelling*, vol. 3, no. 1, pp. 43–65, 2018.
- [37] K. T. Shibin, A. Gunasekaran, T. Papadopoulos, R. Dubey, M. Singh, and S. F. Wamba, "Enablers and barriers of flexible green supply chain management: a total interpretive structural modeling approach," *Global Journal of Flexible Systems Management*, vol. 17, no. 2, pp. 171–188, 2016.
- [38] H. Younis, B. Sundarakani, and P. Vel, "The impact of implementing green supply chain management practices on corporate performance," *Competitiveness Review*, vol. 26, no. 3, pp. 216–245, 2016.
- [39] M. A. Miranda-Ackerman, C. Azzaro-Pantel, and A. A. Aguilar-Lasserre, "A green supply chain network design framework for the processed food industry: application to the orange juice agrofood cluster," *Computers and Industrial Engineering*, vol. 109, no. 7, pp. 369–389, 2017.
- [40] Y. Chen, W. Zheng, W. Li, and Y. Huang, "The robustness and sustainability of port logistics systems for emergency supplies from overseas," *Journal of Advanced Transportation*, vol. 2020, Article ID 8868533, 2020.

Research Article

Sports Sequence Images Based on Convolutional Neural Network

Yonghao Chen 

Sports Department, Xi'an Medical University, Xi'an 710021, Shaanxi, China

Correspondence should be addressed to Yonghao Chen; chenyonghao@xjtu.edu.cn

Received 27 April 2021; Revised 28 May 2021; Accepted 4 June 2021; Published 24 June 2021

Academic Editor: Ming Bao Cheng

Copyright © 2021 Yonghao Chen. This is an open access article distributed under the Creative Commons Attribution License, which permits unrestricted use, distribution, and reproduction in any medium, provided the original work is properly cited.

Convolution neural network has become a hot research topic in the field of computer vision because of its superior performance in image classification. Based on the above background, the purpose of this paper is to analyze sports sequence images based on convolutional neural network. In view of the low detection rate of single-frame and the complexity of multiframe detection algorithms, this paper proposes a new algorithm combining single-frame detection and multiframe detection, so as to improve the detection rate of small targets and reduce the detection time. Based on the traditional residual network, an improved, multiscale, residual network is proposed in this paper. The network structure enables the convolution layer to “observe” data from different scales and obtain more abundant input features. Moreover, the depth of the network is reduced, the gradient vanishing problem is effectively suppressed, and the training difficulty is reduced. Finally, the ensemble learning method of relative majority voting is used to reduce the classification error rate of the network to 3.99% on CIFAR-10, and the error rate is reduced by 3% compared with the original residual neural network.

1. Introduction

Convolutional neural network is a special multilayer perceptron designed to recognize two-dimensional images that can automatically extract image features. The original image does not require a lot of preprocessing to better learn the invariance characteristics of the image. Now, the typical convolutional neural network is a multilayer trainable architecture, including input, convolutional layer (local connection layer), sampling layer, normalization layer, fully connected layer, logistic regression layer, output layer, and the like. Methods to improve the image recognition effect of convolutional neural networks, methods to find the network structure and parameter configuration that are most suitable for the data set to be recognized, and the network structure with constant compatibility for various data sets have gradually become the hotspots of current research.

Due to the importance of motion sequence image research, many research teams have begun to study motion sequence images and have achieved good results. Yang and Jiang studied the tracking theory based on the Candide3 face model and further developed the tracking process on this basis. Based on the research of face tracking, a dynamic

feature extraction method based on six parameters of face model is proposed. The facial expression feature point location and tracking algorithm based on active appearance model was introduced, and the tracking principle was studied. On the basis of the Candide3 face model, the tracking process is further developed. Dynamic time warping (DTW) technology was used to align the image sequence, and then, the feature vector was extracted [1]. In recent years, a database containing a large number of human motion patterns has appeared and is expected to be reused as a new method for recognizing motions and recovering motion patterns from videos containing monocular images. Guermazi and Roemer described the design of an action database, which is composed of action configuration, pose descriptors in silhouette images, random models coded by each pose descriptor subsequence, and the relationship between data and random models. The proposed action database is used to identify images that contain specific actions performed by performers and recover all joint angles from the images [2]. Although the current research results are relatively rich, there are still shortcomings, mainly reflected in the huge amount of data and cumbersome analysis time.

In the research of algorithm analysis, convolutional neural network is a very good method that can solve many classification problems, so it is widely used in the research of algorithm analysis. He proposed the first convolutional neural network (CNN) that provide real-time SR 1080p video on a k2gpu. To achieve this, they proposed a new CNN architecture to extract feature maps in the LR space. In addition, they also introduced an efficient subpixel convolutional layer, which learns a set of upwardly expanded filters to upgrade the final LR feature map to the HR output. By doing so, they effectively replaced the bicubic filter in the hand-made SR pipeline, trained more complex upscaling filters for each feature map, and reduced the computational complexity of the entire SR operation [3]. Dong et al. proposed an online visual tracking algorithm that uses convolutional neural network (CNN) to learn and discriminate saliency maps. Assuming that CNN is pretrained on a large-scale offline image library, their algorithm uses the output of the hidden layer of the network as a feature descriptor because they show good performance in various common visual recognition problems. These features are used for online support vector machine (SVM) to learn and recognize the target appearance model [4, 5]. Due to the effectiveness of the image analysis method, the convolutional neural network method can be applied to the analysis of sports sequence images to solve the problem of slow image analysis.

In this paper, motion sequence image target detection and tracking system based on a convolutional neural network is established. A simple convolutional neural network model is established according to the image characteristics. When selecting hardware, the software system can be used to select appropriate parameters and best parameters in combination with specific conditions. The optimal algorithm can not only reduce the burden when selecting the algorithm but also provide powerful parameters for the experimental program, without wasting too much time, and can be used to complete the image classification training process and display the classification results.

2. Convolutional Neural Network and Sequence Image

2.1. Convolution Neural Network Learning Algorithm

2.1.1. The Training Process of Network. The training process of convolutional neural network is similar to the traditional BP algorithm, including four steps, which is divided into two stages:

The first stage: forward propagation process:

- (1) Take a sample from the sample set and input it into the network
- (2) Calculate the corresponding actual output

In this stage, the input information will be transformed according to the hierarchy and output to the output layer. In the calculation process through the network, in order to obtain the final output result, a little deviation is added in the weight column of input and each output.

The second stage: the process of back propagation:

- (1) Calculate the difference between the actual output and the expected output
- (2) The weight matrix is propagated and adjusted according to the error minimization method

The network training process includes net propagation and antipropagation [6, 7]. The forward wave mainly includes the feature extraction and classification calculation. The inverse wave is the wrong inverse feedback and updates calculation of weight value. After inputting images, all output must be initialized. Exhibition and sampling realize the extraction and mapping of image features, multiple exhibition and sampling processes can be used here [8]. The multilayer extraction process can extract useful information from the image. After feature extraction, the extracted features will be conveyed to the fully connected hierarchy again. There are several hidden layers in the fully connected layer. The results are fed back to the output layer through the conversion and calculation of the data information in the hidden layer. The output layer makes some calculations and gets the test results. Compare the test results with the expected results, and output the classified results if they are consistent [9, 10].

In backpropagation, for a training sample (x, y) , the loss function is defined as shown in

$$S(w, b, x, y) = \frac{1}{2} \|g_{w,b}(x) - y\|^2, \quad (1)$$

where y is the real result and g is the predicted output of the neural network. For training data containing n samples, the overall loss function is shown in

$$S(w, b) = \frac{1}{n} \sum_{i=1}^n S(w, b, x^{(i)}, y^{(i)}). \quad (2)$$

Generally speaking, the loss function of a neural network is a nonconvex function and often converges to a local minimum. The gradient descent method can be used to update the parameters. The main goal is to find the partial derivative of the objective function with respect to the parameter vector. The solution formula is shown in

$$w_{i,j}^{(l)} = w_{i,j}^{(l)} - \varepsilon \frac{\partial}{\partial w_{i,j}^{(l)}} J(w, b), \quad (3)$$

$$b_i^{(l)} = b_i^{(l)} - \varepsilon \frac{\partial}{\partial b_i^{(l)}} J(w, b), \quad (4)$$

where ε is the learning rate.

If the test result is not consistent with the expected result, the weight value and deviation should be propagated again from the output layer to the fully connected layer and layering, until each output has its own gradients and then carries out weight updating work to start a new training process [11, 12]:

- (1) *Convolution and Sampling Process.* The convolution process is the process of using a template to perform a template operation on an image. The template can also be a filter or a convolution kernel [13, 14]. The template calculation formula is shown in

$$F(x, y) * W(g, h) = \sum_{i=c}^c \sum_{j=d}^d w(i, j) f(x + i, y + j). \quad (5)$$

Among them, $*$ is the convolution operator, $F(x, y)$, $f(x, y)$, respectively, represent the domain image and the pixel value centered on the pixel point (x, y) . $W(g, h)$, $w(g, h)$ represent the template matrix and the weight in the matrix, respectively.

The specific process of the first integration process: first input image, then feature extraction process. The process of feature extraction is to integrate the filters, which can learn the input image, and then add bias. The protocol layer is generated after feature extraction. Then, the adjacent regions of the conformity layer are maximized or averaged [15]. In this process, the corresponding weight value and deviation need to be added, and the output can be obtained by activating the function. The results generate a sampled function map. In the later convolution process, the input of convolution level becomes the output of sampling layer in the previous convolution process [16, 17]. Commonly used activation functions include Sigmoid function, Tanh function, and Relu function. The formulas are as shown in

$$f(x) = \frac{1}{1 + e^{-x}}, \quad (6)$$

$$f(x) = \frac{e^x - e^{-x}}{e^x + e^{-x}}, \quad (7)$$

$$f(x) = \max(0, x). \quad (8)$$

In order to prevent the difference between adjacent features in the same channel of the feature image from being too large, the network will normalize the features when extracting the features. The normalized formula is

$$g_{x,y}^i = \frac{h_{x,y}^i}{\left(r + \alpha \sum_{j=\max(0, i-n/2)}^{\min(N-1, i+n/2)} (h_{x,y}^j)^2\right)^\beta}. \quad (9)$$

Among them, $g_{x,y}^i$, $h_{x,y}^i$ are the original activation and new activation of the convolution kernel, respectively; N, n are the number of current network layer convolution kernels and the number of channels of the feature image, respectively.

- (2) *Normalization Process.* The main function of normalization layer is to extract features after sampling layer. Local normalization is divided into local normalization and local contrast normalization in

different functional maps [18]. In the process of feature extraction in the first stage, the local normalization on the same feature graph is added between convolution and subsampling. In the second stage, local normalization between different features and graphs is added. This layer is very useful when we use unbounded neuronal activation functions [19, 20]. Because it makes neurons produce larger response, local areas allow the detection of high-frequency characteristics, resulting in fierce competition of local neurons.

2.1.2. Neuron Input and Output. In convolutional neural networks, neurons can be used in both the convolutional layer and the sampling layer. In a convolution and sampling process, only one layer of the convolutional layer and the sampling layer uses neurons, and you can freely decide which layer to use:

- (1) *Neuron Input and Output of the Convolutional Layer.*

In the forward propagation process of neural network, it generally includes multiple convolutional layers. Each convolutional layer takes the result of the previous convolutional layer as input [21, 22], and outputs its own output result to the next convolutional layer. There are many neurons on each convolutional layer.

The input and output process of the i -th neuron in the n th convolutional layer is as follows: this neuron takes the output of all neurons connected to the previous convolutional layer as the input and adds a deviation b . The output of the previous layer of neurons is represented by the variable x , and the input of the i -th neuron is multiplied by the weight corresponding to each neuron [23, 24]. Then, add up all the outputs, and we use the variable y to represent this activation value. The output x of this neuron is calculated by the activation function. The activation function is represented by F . The calculation process of the output value of the convolutional layer neuron is shown in

$$X_n^i = F(y_n^i) = F\left(\sum_{e=0}^{C_{n-1}} (W_n^{ie} X_{n-1}^e + b)\right). \quad (10)$$

In the convolution layer, the convolution kernel can be used to fold the feature map of the upper layer, and the output feature map can be obtained by activating the function. Each output feature map may be the result of folding the values of multiple input characteristic graphs. Each feature graph has an offset b , and the deviation of each layer is different [25, 26].

- (2) *Input and Output of Neurons in Sampling Layer.* In the forward propagation process, the operation of neurons in the sampling layer is actually a down-sampling process. The number of feature graphs output by this algorithm is the same as that of the

previous convolution layer, but the size of each feature graph is reduced. The calculation formula of neuron output is

$$X_j^e = f(\beta_j^e \text{down}(X_j^{e-1}) + b_j^e). \quad (11)$$

The difference from the calculation of the convolutional layer neuron is that a downsampling function down and a multiplicative deviation β are used. Assuming that the sampling factor is n , the values of all pixels in different $n*n$ regions in the feature map are weighted and summed. Two methods of operation can be used here, the average value or the maximum value. In this way, the image is reduced to $1/n$ in both the horizontal and vertical directions. In this way, a downsampling operation

process is completed, and the features of the local area of the image are collected.

2.1.3. Normalization Algorithm. The process of normalization is used to further extract features. It is divided into normalization within the same feature map and normalization within different feature maps [27–29]. First, let us talk about normalization on the same feature map. For normalization on the same feature map, we still need to perform convolution first and then correct the linearity through an activation function. The normalization is performed in a certain area through the normalization function. Therefore, we must first define a parameter to declare the size of the normalized area. The normalized calculation function is

$$f(u_f^{x,y}) = \frac{u_f^{x,y}}{\left(1 + a/N^2 \sum_{x'=\max(0,x-[N/2])}^{\min(S,x-[N/2]+N)} \sum_{y'=\max(0,y-[N/2])}^{\min(S,y-[N/2]+N)} (u_f^{x',y'})^2\right)^{\beta}} \quad (12)$$

where $u_f^{x,y}$ represents the mapping position (x, y) of f before the activation function is normalized; S represents the pixel value of the image; and N is the size of the area used for normalization.

The normalization on different feature maps is similar to the normalization on the same feature map. The difference is that each activation unit can only be assigned by other activation units at the same location but on different feature maps. If we want to normalize a unit of the fifth feature map, then we must use the units of the third to seventh feature map. Its normalized calculation function is given as

$$f(u_f^{x,y}) = \frac{u_f^{x,y}}{\left(1 + a/N^2 \sum_{f'=\max(0,f-[N/2])}^{\min(F,f-[N/2]+N)} (u_f^{x',y'})^2\right)^{\beta}} \quad (13)$$

where F represents the number of feature planes.

2.2. Target Detection of Motion Sequence Images

2.2.1. Interframe Difference Statistics. Two images of the same background are extracted from the object motion sequence at different moments for comparison, and the result of the motion of the object under this background can be reflected through the change of its position. It is a simpler and faster method to find “difference” or subtract the gray values of the extracted two images and then it is easy to find the motion information of the object from the data obtained after subtraction.

In the obtained data value, the difference is zero, that is, the part where the gray level does not change, that is, the frame time when the object is stationary (most of the static background and a small part of the target). If the target gray scale is greater than the background, the front area is

negative. The back area is positive and the other parts are zero. Extract the position of the moving object on the image from the detected part, find the movement trajectory, and further narrow the search range.

Extracting the contour of the moving object can be obtained from the difference image, the positive or negative part of the difference in the image, and then the logical sum of the sequence image is directly taken, so that the basic contour of the moving object can be extracted. Because of the influence of noise, the image of the actual moving object generally does not use a simple subtraction method but is calculated by the traditional method of interframe difference statistics.

The video sequence records the movement and change information of the video object in a certain period. The ideal video segmentation method based on moving images is to use the related information between frames for a long time to compare and judge the obtained data. Based on this idea, analyze the law of each pixel point along the time axis and select appropriate points from the entire video sequence according to the statistical law and restore the background.

The object image sequence is defined here as $I(x, y, i)$, where x, y are spatial coordinates, i is the number of frames $I = (1, 2, \dots, N)$, and N is the total number of frames in the sequence. $I_L(x, y, i)$ is the brightness of the sequence, and the gray scale changes between adjacent frames are reflected by the video frame difference $C DM$:

$$C DM(x, y, i) = \begin{cases} d, & \text{if } d \geq T, \\ 0, & \text{if } d < T, \end{cases} \quad d = |I_L(x, y, i+1) - I_L(x, y, i)|. \quad (14)$$

T is a threshold value used as a limit value to remove noise. The coordinate position (x, y) is fixed, then $C DM(x, y, i)$ is a function of the number of frames i , and

what it records is the change of the pixel at the fixed position (x, y) on the time axis curve. Then, divide this curve according to whether $C DM(x, y, i)$ is greater than zero as its dividing point and then use the part of the detected static frame to set $(S, (x, y), 1 \leq j \leq M)$ meaning that among them, ST_j and EN_j , respectively, represent the start and end of S_j . Next, extract the spatial coordinates in the set (S_j) corresponding to each position (x, y) , select the longest stationary segment, and record the corresponding $M(x, y)$ in the segment frame number. Finally, the recorded point $M(x, y)$ is used to fill the corresponding position in the video background. This logic can be described by

$$M(x, y) = \frac{(ST(x, y) + EN(x, y))}{2}, \quad (15)$$

$$B(x, y) = I(x, y, M(x, y)). \quad (16)$$

Among them, the starting point and ending point of the longest static segmentation correspond to $ST(x, y)$ and $EN(x, y)$, and $B(x, y)$ is the reconstructed video background. This method is based on the ideal hypothesis that moving objects will not always stand still in a certain position but will move away in the video sequence and finally reveal the background.

2.2.2. Classic Moving Target Detection Method. The optical flow method is a classic moving target detection method, which can detect moving targets and reflect the motion feature information of moving targets. Assuming that the gray value of the point Q in the image (x, y) at time t is $H(x, y, t)$, then after the interval d_t has elapsed, the horizontal and vertical motion components of this point are shown in

$$S = \frac{d_x}{d_t}, \quad (17)$$

$$C = \frac{d_y}{d_t}. \quad (18)$$

Expanded by Taylor expansion, ignoring the second-order infinitesimal, the basic constraint equation of optical flow is shown in

$$-\frac{\partial H}{\partial T} = \frac{\partial H}{\partial x} S + \frac{\partial H}{\partial y} C = \begin{bmatrix} \frac{\partial H}{\partial x} & \frac{\partial H}{\partial y} \end{bmatrix} \begin{bmatrix} S \\ C \end{bmatrix}. \quad (19)$$

The HS algorithm is an algorithm in the optical flow method, which introduces global smoothness into the optical flow constraint equation, and realizes the combination of two-dimensional velocity field and gray scale. The calculation formula for the deviation error of smoothness is shown in

$$E_\alpha(S, C) = \iint \left[\left(\frac{\partial S}{\partial x} \right)^2 + \left(\frac{\partial S}{\partial y} \right)^2 + \left(\frac{\partial C}{\partial x} \right)^2 + \left(\frac{\partial C}{\partial y} \right)^2 \right] dx dy. \quad (20)$$

Constant brightness requires that the error of the basic constraint equation of optical flow is as small as possible. The error calculation is shown in

$$E_\beta(S, C) = \iint [I_x S + I_y C + t]^2 dx dy. \quad (21)$$

Combining formulas (20) and (21), the optical flow in the HS algorithm should satisfy the minimum value of

$$E_\alpha(S, C) = \iint \left\{ (I_x S + I_y C + t)^2 + \mu \left[\left(\frac{\partial S}{\partial x} \right)^2 + \left(\frac{\partial S}{\partial y} \right)^2 + \left(\frac{\partial C}{\partial x} \right)^2 + \left(\frac{\partial C}{\partial y} \right)^2 \right] \right\} dx dy. \quad (22)$$

Among them, μ is the smoothing control parameter. When the detection image has higher resolution and less noise, the smaller the value of μ is obtained; otherwise, it should be increased. Make

$$F(x, y, S, C, S_x, S_y, C_x, C_y) dx dy = (I_x S + I_y C + t)^2 + \mu \left[\left(\frac{\partial S}{\partial x} \right)^2 + \left(\frac{\partial S}{\partial y} \right)^2 + \left(\frac{\partial C}{\partial x} \right)^2 + \left(\frac{\partial C}{\partial y} \right)^2 \right]. \quad (23)$$

Then, there are

$$E_{HS}(S, C) = \iint F(x, y, S, C, S_x, S_y, C_x, C_y) dx dy. \quad (24)$$

The inverse function of formula (24) is equivalent to solving the following equations:

$$\begin{cases} F_S - \frac{\partial}{\partial x} F_{S_x} - \frac{\partial}{\partial y} F_{S_y} = 0, \\ F_C - \frac{\partial}{\partial x} F_{C_x} - \frac{\partial}{\partial y} F_{C_y} = 0. \end{cases} \quad (25)$$

2.2.3. Adaptive Motion Detection Method. The difference method has limitations. It is only suitable for the case where the fluctuation of the background Krata is small. When the fluctuation of the background Krata of the two-frame image is large, the simple difference method cannot be used to obtain a satisfactory solution. At present, when the signal is relatively low, the background display panel and noise can be suppressed as much as possible, and adaptive motion detection methods are used to detect unstable image signals. The signal-to-clutter ratio here refers to SCNR, that is, when there is a large background clutter, the conventional

threshold segmentation method cannot separate this moving target. The adaptive motion detection method can solve this problem well, but there is a condition as the premise that the clutter background of the current image and the referenced image must be spatially related.

The figure below is a schematic diagram of the algorithm of the adaptive filter, as shown in Figure 1, clutter + noise 1, represented by $z(n) = s(n) + v_1(n)$, clutter + noise 2, represented by $x(n) = sb(n) + v_2(n)$, which is the reference input of the filter.

This method can detect moving objects adaptively and adjust the weighting coefficient, that is, the correlation between the reference image and the background of the input image, so that the output results can eliminate the influence of correlation factors on them and further compress the background clutter and correlation noise. Only by reducing the interference caused by clutter can the target be detected easily. This method is especially effective in tracking small targets.

We define a $T(n)$, which represents the actual number of instructions executed by the program in a perfectly ideal calculator. The execution time of a program is not entirely related to the amount of input, and the quality of the algorithm will also affect it, so we can regard it as a function of the amount of input n . Here, again, we can define the maximum execution time for the input n , which is the measure of time complexity. Usually, we use O to represent this execution program, where n represents the actual number of loop executions, n_0 represents the number of predicted loop executions; $(n + l) / 6 \leq cn_3$, $n \geq n_0$, it means that the execution program is scientifically effective.

3. Experimental Analysis of Sports Sequence Images

3.1. Experimental Data Set. The experiment in this study uses the CIFAR-10 image data set. CIFAR-10 is an image data set containing 60,000 color pictures. The size of each picture is 32×32 . It is divided into 10 categories, and each category contains 6000 images. Recognize them by comparing different methods, and compare their recognition conditions under the same guarantee premise.

CIFAR-10 is divided into 5 training files and 1 test file. Each file contains 10,000 pictures. The test file is composed of 1000 pictures randomly selected from each category. The training file contains the remaining pictures. It is out of order, so although each training file contains 5000 pictures, some files may have more pictures in a certain category than other files.

3.2. Experimental Model Structure. The network structure of this research is roughly in accordance with the design. Take CIFAR-10 as an example. First, input $32 \times 32 \times 3$ image data and pass 3×3 convolution kernels. The number of convolution kernels is 16, and the output is $32 \times 32 \times 16$ data, and then through $6n$ layers of convolution, because each multiscale residual learning module has two layers of convolution, there are a total of $3n$ multiscale residual learning

module; after each n learning modules, we will divide the size by 2 and multiply the number of convolution kernels by 2. The downsampling operation here is realized by the convolution operation of stride = 2, and the pooling operation is not used. After the convolution of these $6n$ layers, there is a global average pooling layer, followed by a dropout operation, and finally a fully connected layer and Softmax. The complete network structure is shown in Figure 2, where m is the scaling parameter. We define the depth of the entire neural network as the sum of all layers with learning parameters, that is, the first $3 \times 3 \times 16$ convolutional layer, $6n$ convolutional layers, and fully connected layers, totaling $6n + 2$ layers.

3.3. Experimental Data Preprocessing. Before the image data are transmitted to the network, necessary preprocessing work can significantly improve the accuracy of the network. However, in order to facilitate the comparison with the existing experimental results, we only used conventional pretreatment methods in this study.

For the training process, this study fills each picture with 0 in four directions to make it a 36×36 picture, then randomly crops it into a 32×32 picture and then randomly flips it left and right and uses ZCA for the picture. In the training process, there will be a shuffle process, that is, the input order of each epoch picture is random.

For the test process, this study directly input the original image data without any preprocessing operations. It will not disrupt the order.

3.4. Statistics. All data analyses in this article use SPSS19.0, statistical test uses two-sided test, significance is defined as 0.05, and $p < 0.05$ is considered significant. The statistical results are displayed as mean \pm standard deviation ($x \pm SD$). When the test data obey the normal distribution, the double T test is used for comparison within the group, and the independent sample T test is used for comparison between the groups. If the regular distribution is not sufficient, two independent samples and two related samples will be used for inspection.

4. Analysis of Experimental Results of Sports Sequence Images Based on Convolutional Neural Network

4.1. Analysis of Sports Sequence Images. The motion information extraction process is based on the difference image. The difference image refers to the image composed of the absolute value of the corresponding pixel gray difference between two consecutive frames in the sequence image. Ideally, through this subtraction operation, the still part of the image will be eliminated, and only those moving parts will remain. However, in actual situations, due to environmental changes in light and shade and noise, the difference image often contains some static parts. After getting the difference image, in order to facilitate subsequent calculations, the difference image needs to be binarized. Here, an adaptive threshold (threshold) technology is adopted.

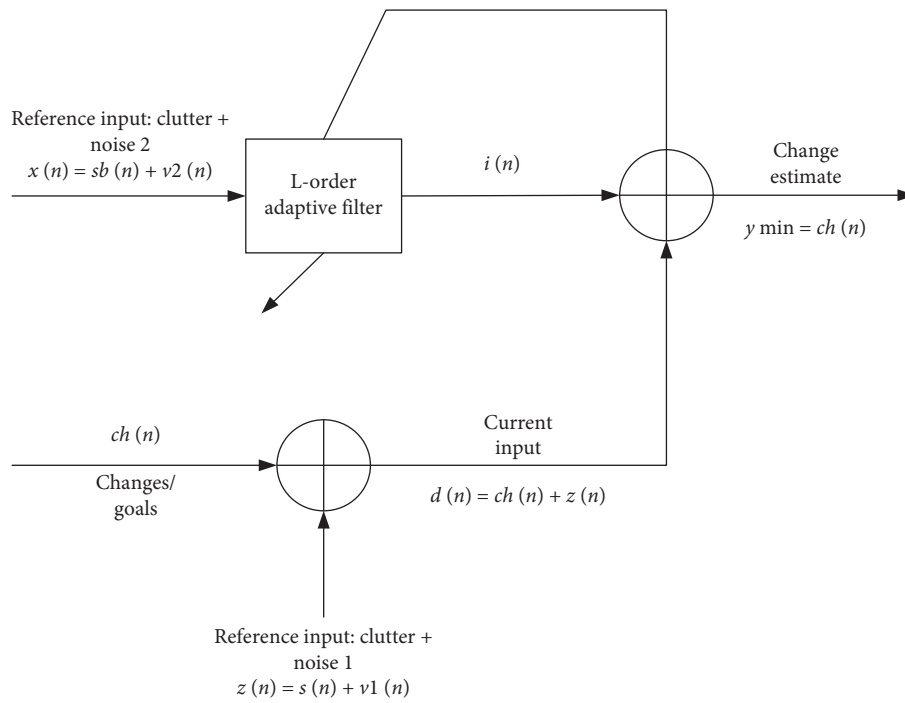


FIGURE 1: Schematic diagram of the adaptive algorithm.

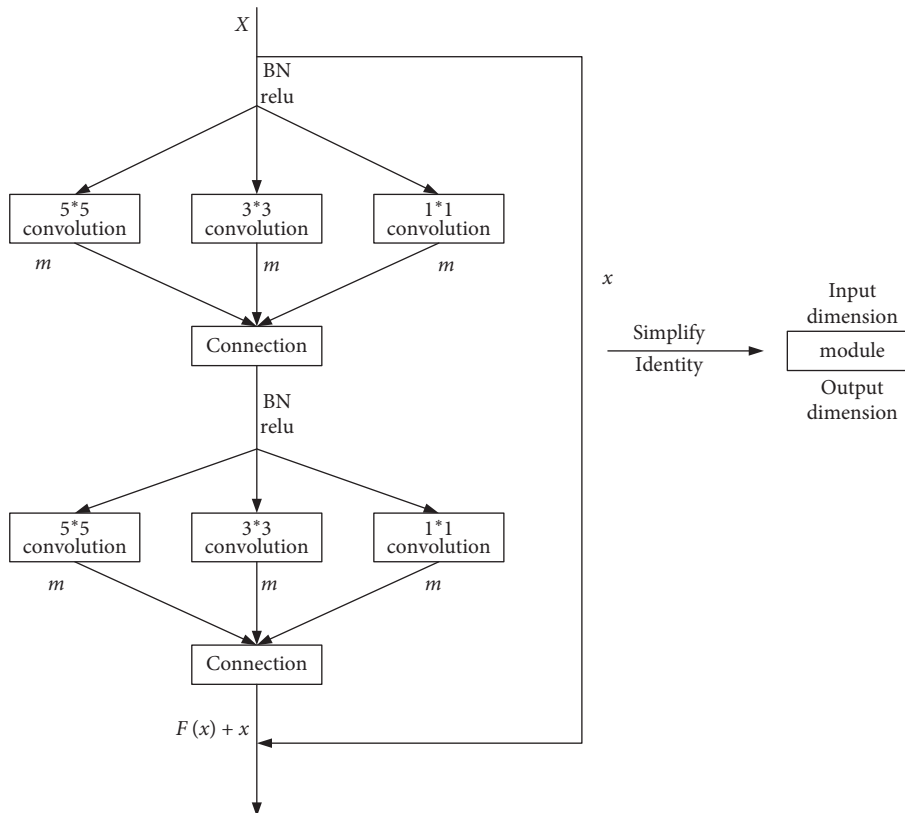


FIGURE 2: The complete network structure of the multiscale residual neural network.

First, make two assumptions: (1) The area of the still part of the image is larger than the area of the moving part. (2) For the images obtained with high-speed cameras, the

background environment changes between two consecutive frames are very small. Obviously, these two assumptions are in line with the general situation.

As shown in Figure 3, it is an example of histogram distribution of different images. Find out the positions of several troughs in the histogram distribution curve, and the area between the troughs represents the number of pixels in different regions. According to the above assumptions (1) and (2), the segmentation points of the static region and the moving region are at the trough after the area with the largest area between the troughs. In this way, the binary threshold can be dynamically selected according to different sequence images, which can achieve better results. Thus, the difference image processed by binarization contains two parts: bright spot and black spot. The black spot represents the moving part of the image, and the bright spot represents the static part of the image.

Between two consecutive images, if the joint is still, the region in the difference image is still area, which does not contain moving pixels, that is, difference, the white point in the image; if the joint moves, the joint area in the difference image contains certain motion information, including the fixed motion pixel, that is, the black spot in the difference image. In order to judge whether the joints move in the current image, the prior knowledge of the position of each joint in the previous image should be used, that is, the coordinates of each joint in the previous frame image. The position of each joint in the first frame of the sequence image needs to be marked manually. We define the joint motion weight as S . Firstly, according to the different conditions of each joint, a template with different sizes (a specific image area) is established. According to the coordinates of each joint, the corresponding coordinates in the difference image are taken as the center. Within the range of joint template size, the number of motion pixels is searched, and the appropriate threshold is selected to judge whether the joint is moving. The calculation of joint motion weight s is shown in Figure 4.

Figure 4 shows the neighboring city within the template range with a joint coordinate as the center in the difference image. The number of motion pixels (i.e., black pixels) falling within the neighborhood range is 7, so the motion weight of the joint point $S = 7$. In the real situation and high-speed sequence images, there are only a few joints that move between two consecutive frames. Through the work of this step, the scope of the next calculation is greatly reduced.

Comparing the tracking error and time of the traditional algorithm and the algorithm in this paper, the tracking error of the traditional algorithm and the algorithm in this paper are represented by $W1$ and $W2$, and the tracking time is represented by $T1$ and $T2$.

Because the environment in which motion is always changing, if the detection method of moving targets in a dynamic background continues to use the target detection method in a static background, you will find that the binary target detection result image will contain a lot of noise, and it may be severe. The tracking target is completely covered up, thus making the tracking process fail. As shown in Figure 5, we can see that motion sequence images based on convolutional neural networks can effectively avoid such problems.

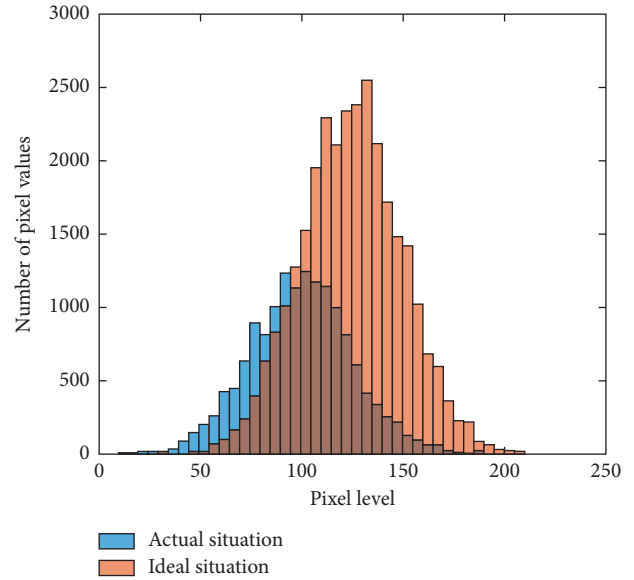


FIGURE 3: Histogram distribution of actual difference images.

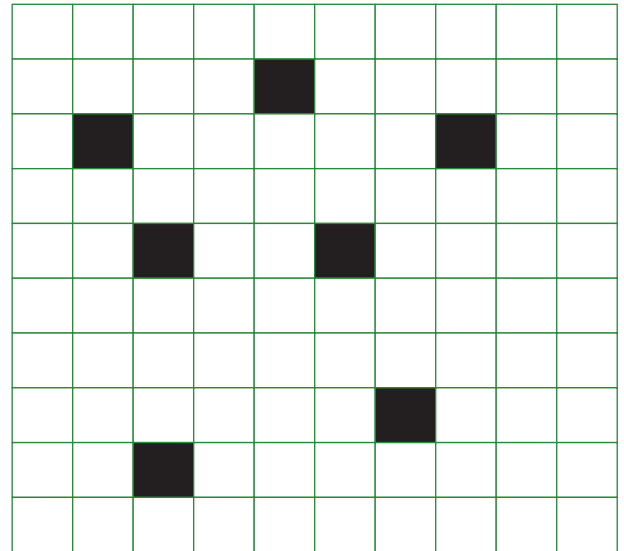


FIGURE 4: Calculation example of joint motion weight S .

4.2. Convolutional Neural Network Image Analysis. After weighing the training time, accuracy and proficiency of the convolutional neural network, its basic parameter settings are shown in Table 1:

This study gives the complete structure of the multiscale residual neural network, which includes $3n$ multiscale residual learning modules. Under the condition that each learning module has 2 layers of convolution, the entire network has $6n + 2$ layers, and each layer convolution also has a scaling parameter m . When each layer is composed of three different scale convolutions of 1×1 , 3×3 , and 5×5 , the width of our network is $3 \times m$. In order to explore the impact of different scaling parameters and depths on network performance, this study conducted multiple experiments on the CIFAR-10 data set. The results are shown in Table 2.

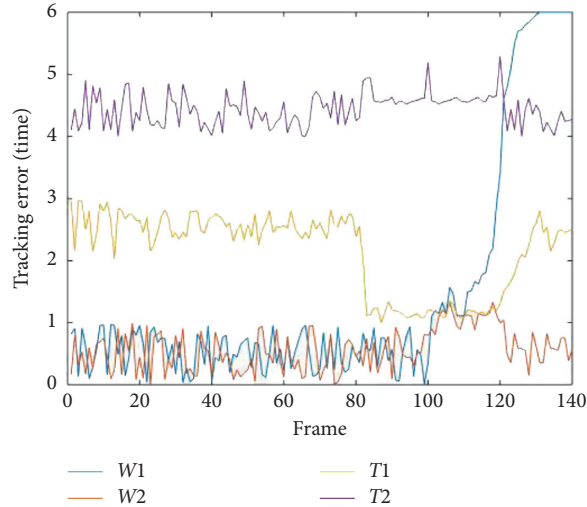


FIGURE 5: Comparison of tracking error and time between traditional algorithm and the proposed algorithm.

TABLE 1: Basic parameter settings.

Parameter	Value
Enter image size	64×64
Batch size	256
Initial learning rate	0.15
Initial learning rate decay rate	0.15
Attenuation interval	300
Dropout ratio	0.5
Weight attenuation term	$[0, 0.002]$
Maximum iteration steps	600

In order to verify the superiority of the improved weight optimization algorithm, this study selected the public CIFAR-10 data set as the experimental data set, and two different neural network models: 6-layer convolutional neural network and 16-layer convolutional neural network as the experimental model and parameters. The optimization algorithms Adagrad, RMSprop, and Adam are compared. For each algorithm, try several different initial learning rates $\{10^{-1}, 10^{-2}, 10^{-3}, 10^{-4}\}$ and several different learning rate decay coefficients $\{0, 10^{-2}, 10^{-3}, 10^{-4}\}$, finally select the pair of parameters with the highest accuracy in the test set. The convolutional neural network with several layers of convolutional layer, pooling layer, fully connected layer, and nonlinear activation function is proved to have excellent performance in real image recognition tasks. In this experiment, a 6-layer convolutional neural network is constructed, in which the first 4 layers are successively superimposed convolutional layers, and the number of filters in each layer is 32, 32, 64, 64, the first and third convolutional layers. Then, add the dropout layer with dropout rate equal to 0.25; the last two layers are fully connected layers, and the weight parameters are 1600×512 , 512×10 , respectively. The BatchNorm layer is added after the second fully connected layer; the activation function uses the ReLu function, and the pooling layer uses MaxPooling

method. The final experimental comparison results of each algorithm are shown in Figure 6.

The change trend of accuracy of different algorithms on the test set is shown in Figure 7.

As can be seen from Figure 6, although the improved algorithm in this paper lags behind the Adam algorithm in the initial convergence speed, the convergence speed gradually surpasses the Adam algorithm after the 12th round and converges to a lower loss function value. The accuracy rate change curve of the test set in Figure 7 shows that the improved algorithm in this paper finally converges to the highest accuracy rate, indicating that the improved algorithm has better parameter optimization capabilities.

4.3. Actual Application Results of the Proposed Algorithm

4.3.1. Application in Basketball Sequence Images. This algorithm is applied to the classification and goal tracking of basketball sequence images. The algorithm is used to count the number of goals and scores of team A and B in the 5 basketball games and compare them with the actual number of goals and scores.

As shown in Table 3, after statistics on the goals and scores of the two teams in 5 games, it is found that the algorithm in this paper still has some errors in actual application. In one game, the number of missed or over-remembered goals occurred, and 2 games were missed or overremembered. The specific comparison of the number of goals is as follows:

As shown in Figure 8, in the third game, the algorithm of this paper counts A team scored 25 times and actually scored 27 times, counted B team scored 30 times, and actually scored 29 times. The scores are as follows:

As shown in Figure 9, in the first game, the statistical team A scored 87 points, and the actual score was 89 points; the statistical team B score was consistent with the actual score, which was 81 points. In the third game, team A scored 49 points and the actual score was 52 points; team B scored 59 points and the actual score was 57 points.

TABLE 2: Test set error rate under different network structures.

Model number	Scaling parameters m	Network depth	Parameter	Test set error (%)
1	1	74 ($n = 12$)	13.4M	4.80
2	1	98 ($n = 16$)	17.7M	4.90
3	1	122 ($n = 20$)	22.2M	4.95
4	2	50 ($n = 5$)	34.9M	4.20
5	3	32 ($n = 6$)	48.2M	4.19
6	3	38 ($n = 4$)	58.3M	4.21
7	4	26 ($n = 3$)	67.5M	3.99

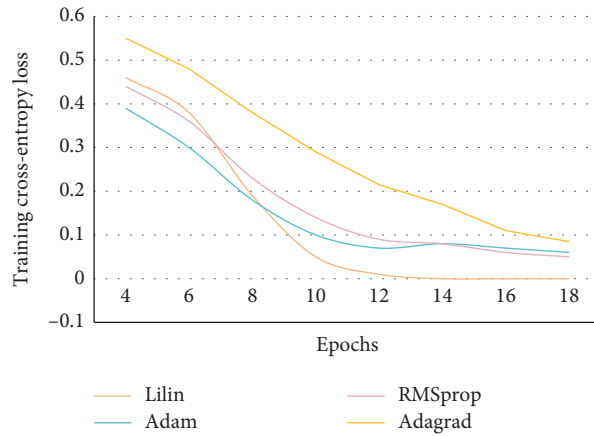


FIGURE 6: The change trend of the loss function value of different algorithms on the training set.

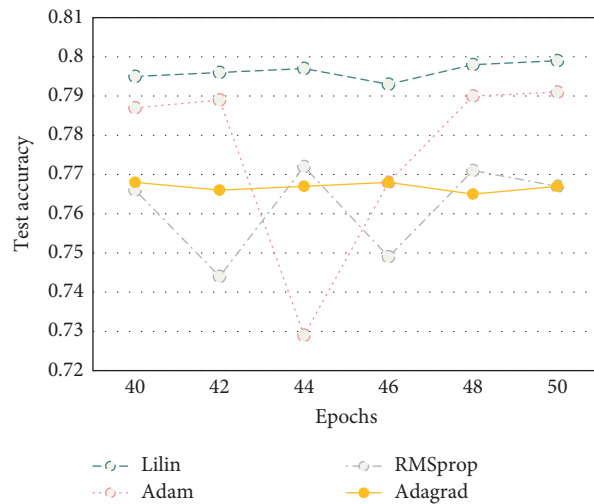


FIGURE 7: Trends of accuracy of different algorithms on the test set.

4.3.2. *Application in Sprint Motion Sequence Images.* The algorithm of this paper is applied to the classification and target tracking of sprint motion sequence images, and the situation of

a certain class of college students ($n = 42$) in the 100-m sprint physical test is tracked throughout the course. Among them, there are 18 boys and 6 in groups, which are 1–3 groups; 24 girls

TABLE 3: Number of goals and score statistics.

Sessions	Algorithm in this paper	Actual	Difference
Number of goals (A1)	36	36	0
Number of goals (B1)	32	32	0
Number of goals (A2)	21	21	0
Number of goals (B2)	24	24	0
Number of goals (A3)	25	27	2
Number of goals (B3)	30	29	-1
Number of goals (A4)	36	36	0
Number of goals (B4)	30	30	0
Number of goals (A5)	19	19	0
Number of goals (B5)	15	15	0
Total number of goals	268	269	1
Score (A1)	87	89	2
Score (B1)	81	81	0
Score (A2)	38	38	0
Score (B2)	43	43	0
Score (A3)	49	52	3
Score (B3)	59	57	-2
Score (A4)	70	70	0
Score (B4)	61	61	0
Score (A5)	45	45	0
Score (B5)	36	36	0
Total score	569	572	3

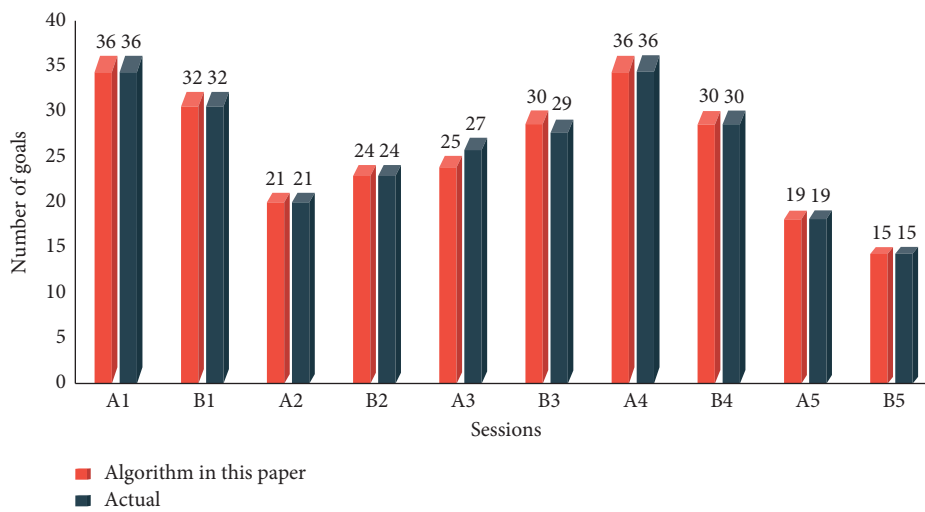


FIGURE 8: Comparison of the number of goals scored.

and 6 in groups, which are 4–7 groups. The average score of each group is calculated and compared with the actual results.

As shown in Tables 4 and 5, even if the algorithm statistics are the same as the actual highest and lowest scores, their average scores are not consistent. There are errors in the average scores of 3 out of 7 groups. The details of the average grade are as follows:

As shown in Figure 10, the algorithm statistics average score of the first group is 12.9 s, and the actual average score is 12.6s. The algorithmic statistical average score of the fourth group is 16.5 s, and the actual average score is 16.4 s. The algorithmic statistical average score of the sixth group is 16.2 s, and the actual average score is 16.7 s.

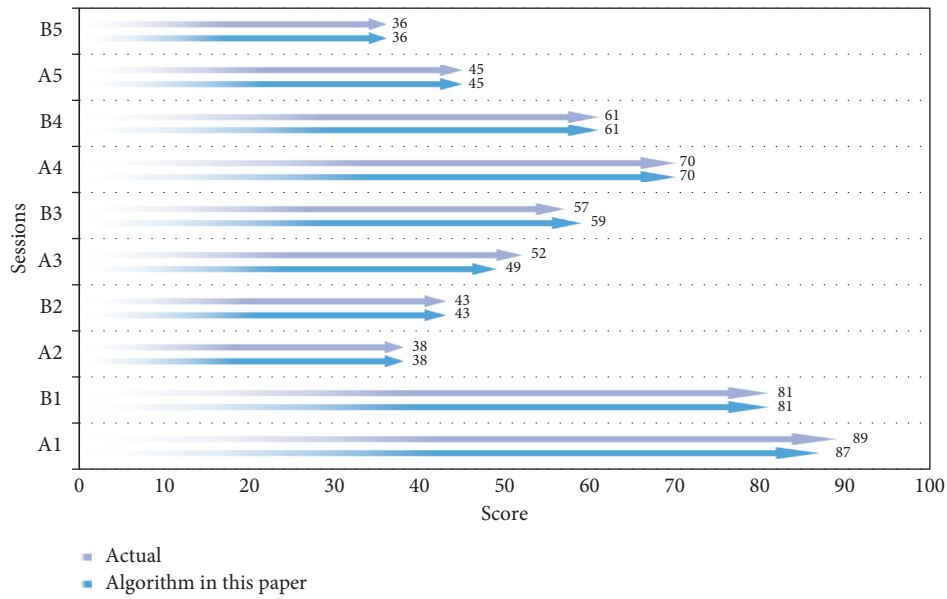


FIGURE 9: Comparison of score statistics.

TABLE 4: Algorithm to calculate the sprint performance of each group of students.

Group	Average score (s)	Highest score (s)	Minimum score (s)
1	12.9	12.5	15.1
2	13.1	12.6	15
3	12.8	12.6	14.8
4	16.5	15.7	18.1
5	16.4	15.5	18.5
6	16.2	15.5	17.9
7	16.8	15.9	19

TABLE 5: Actual sprint results of each group of students' performance.

Group	Average score (s)	Highest score (s)	Minimum score (s)
1	12.6	12.5	15.1
2	13.1	12.6	15
3	12.8	12.6	14.8
4	16.4	15.5	18.1
5	16.4	15.5	18.5
6	16.7	15.5	17.9
7	16.8	15.9	19

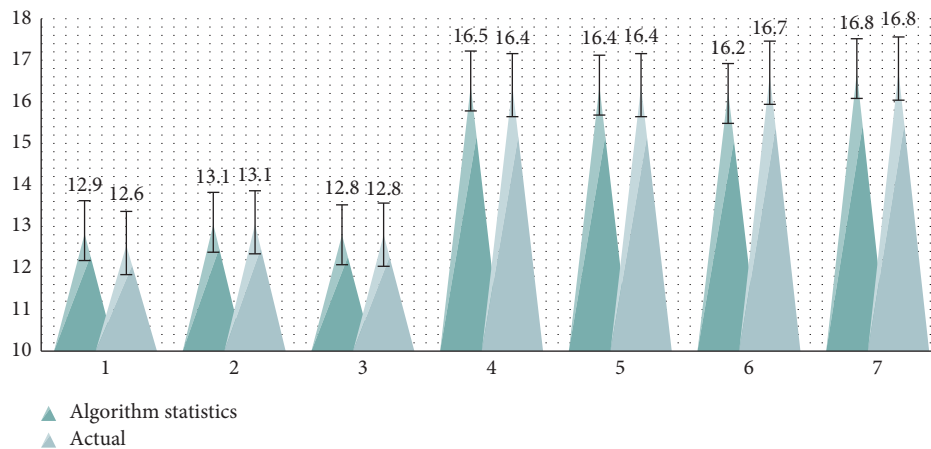


FIGURE 10: Comparison of average scores for each group.

5. Conclusion

In this paper, firstly, aiming at the problem of sports sequence image analysis in complex scenes, two improvements are made to the VGG convolutional neural network model with excellent performance. Firstly, aiming at the problems of too many parameters of the original model and the limitation of image input size, the network structure is improved to further reduce the over fitting of the model and improve the flexibility of the model; secondly, the performance of the VGG convolutional neural network is improved. Aiming at the problem that the classification accuracy of the original model is not ideal in complex scenes, the element of target detection is added to get a hybrid model with double loss function. One of the optimization objectives of the loss function is the location of the bounding box coordinate points and the length and width of the bounding box of the output target object, and the other is the correct classification of the output target object. Because the two objective functions share the weight parameters of convolution layer for feature extraction, the feature mapping biased to the coordinate region of the target object is extracted from the optimized model.

In order to further improve the optimization speed and ability of weight parameter optimization algorithm, this paper proposes an improved optimization algorithm based on Adam algorithm: in the aspect of adaptive adjustment of learning rate, an improved adaptive adjustment method of learning rate is proposed, the main content is adding a new feedback mechanism; in the aspect of learning rate annealing, a periodic annealing method is proposed, The main content is to optimize the annealing method of the improved algorithm, and integrate a periodic annealing method. The experimental results show that the improved method is superior to other optimization algorithms.

This article also has some shortcomings. The method used mainly tests the images of people in motion. But in reality, the scene often contains both people and other moving targets such as cars. The behavior of the target person may also suddenly take place in large movements. People are overcrowded in places, such as shopping malls, waiting halls, and people for a long time. The case of depth occlusion. Therefore, similar problems need further research and analysis.

Data Availability

The data underlying the results presented in the study are included within the manuscript.

Conflicts of Interest

The author declares no conflicts of interest.

Acknowledgments

This work was supported by Regular Project of Shaanxi Sports Bureau in 2020 (No. 2020105).

References

- [1] X. Yang and S. Jiang, "Research on theory and method for facial expression recognition system based on dynamic image sequence," *Open Automation & Control Systems Journal*, vol. 7, no. 1, pp. 569–579, 2015.
- [2] A. Guermazi and F. W. Roemer, "Compositional MRI assessment of cartilage: what is it and what is its potential for sports medicine?" *British Journal of Sports Medicine*, vol. 50, no. 15, pp. 896–897, 2016.
- [3] S. He, R. W. H. Lau, W. Liu, Z. Huang, and Q. Yang, "SuperCNN: a superpixelwise convolutional neural network for salient object detection," *International Journal of Computer Vision*, vol. 115, no. 3, pp. 330–344, 2015.
- [4] Z. Dong, Y. Wu, M. Pei, and Y. Jia, "Vehicle type classification using a semisupervised convolutional neural network," *IEEE Transactions on Intelligent Transportation Systems*, vol. 16, no. 4, pp. 2247–2256, 2015.
- [5] G. Xiao, R. Wang, C. Zhang, and A. Ni, "Demand prediction for a public bike sharing program based on spatio-temporal graph convolutional networks," *Multimedia Tools and Applications*, 2020.
- [6] U. R. Acharya, H. Fujita, O. S. Lih, M. Adam, J. H. Tan, and C. K. Chua, "Automated detection of coronary artery disease using different durations of ECG segments with convolutional neural network," *Knowledge-Based Systems*, vol. 132, no. 15, pp. 62–71, 2017.
- [7] S. S. M. Salehi, D. Erdogmus, and A. Gholipour, "Auto-context convolutional neural network (Auto-Net) for brain extraction in magnetic resonance imaging," *IEEE Transactions on Medical Imaging*, vol. 36, no. 11, 2017.
- [8] C. Yuan, X. Li, Q. M. J. Wu et al., "Fingerprint liveness detection from different fingerprint materials using convolutional neural network and principal component analysis," *Computers, Materials and Continua*, vol. 53, no. 4, pp. 357–371, 2017.
- [9] G. Cheng, Y. Wang, S. Xu, H. Wang, S. Xiang, and C. Pan, "Automatic road detection and centerline extraction via cascaded end-to-end convolutional neural network," *IEEE Transactions on Geoscience and Remote Sensing*, vol. 55, no. 6, pp. 3322–3337, 2017.
- [10] X. Li, Y. Wang, and G. Liu, "Structured medical pathology data hiding information association mining algorithm based on optimized convolutional neural network," *IEEE Access*, vol. 8, no. 1, pp. 1443–1452, 2020.
- [11] A. Sevastopolsky, "Optic disc and cup segmentation methods for glaucoma detection with modification of U-net convolutional neural network," *Pattern Recognition and Image Analysis*, vol. 27, no. 3, pp. 618–624, 2017.
- [12] F. C. Chen and M. R. Jahanshahi, "NB-CNN: Deep learning-based crack detection using convolutional neural network and naïve bayes data fusion," *IEEE Transactions on Industrial Electronics*, vol. 65, no. 99, pp. 4392–4400, 2018.
- [13] Z. Zhao and A. Kumar, "Accurate periocular recognition under less constrained environment using semantics-assisted convolutional neural network," *IEEE Transactions on Information Forensics & Security*, vol. 12, no. 5, 2017.
- [14] T. Hirasawa, K. Aoyama, T. Tanimoto et al., "Application of artificial intelligence using a convolutional neural network for detecting gastric cancer in endoscopic images," *Gastric Cancer Official Journal of the International Gastric Cancer Association & the Japanese Gastric Cancer Association*, vol. 87, no. 1, pp. 1–8, 2018.

- [15] M. Anthimopoulos, S. Christodoulidis, L. Ebner, A. Christe, and S. Mougiakakou, "Lung pattern classification for interstitial lung diseases using a deep convolutional neural network," *IEEE Transactions on Medical Imaging*, vol. 35, no. 5, pp. 1207–1216, 2016.
- [16] P. Chen, L. Zheng, X. Wang et al., "Moving target detection using colocated MIMO radar on multiple distributed moving platforms," *IEEE Transactions on Signal Processing*, vol. 65, no. 99, 2017.
- [17] X. Chen, J. Guan, Y. He et al., "High-resolution sparse representation and its applications in radar moving target detection," *Journal of Radars*, vol. 6, no. 3, pp. 239–251, 2017.
- [18] L. Deng and H. Zhu, "Moving point target detection based on clutter suppression using spatiotemporal local increment coding," *Electronics Letters*, vol. 51, no. 8, pp. 625–626, 2015.
- [19] G. Gao, G. Shi, L. Yang, and S. Zhou, "Moving target detection based on the spreading characteristics of SAR interferograms in the magnitude-phase plane," *Remote Sensing*, vol. 7, no. 2, pp. 1836–1854, 2015.
- [20] S. Jie, C. Fu-qing, Z. Cai-sheng, and H. You, "Experimental results of maritime moving target detection based on passive bistatic radar using non-cooperative radar illuminators," *The Journal of Engineering*, vol. 2019, no. 20, pp. 6763–6766, 2019.
- [21] E. Jaya and B. T. Krishna, "Fuzzy-based MTD," *Data Technologies and Applications*, vol. 54, no. 1, pp. 66–84, 2020.
- [22] Q. Gong and C. Wang, "Moving target detection algorithm based on sparse recovery and sample selection for airborne radar," *Xi Tong Gong Cheng Yu Dian Zi Ji Shu/Systems Engineering and Electronics*, vol. 40, no. 5, pp. 1012–1017, 2018.
- [23] L. Hai, S. Wenyu, L. Weijian et al., "Moving target detection with limited training data based on the subspace orthogonal projection," *IET Radar Sonar & Navigation*, vol. 12, no. 7, pp. 679–684, 2018.
- [24] Y. Zhao, H. Li, S. Wan et al., "Knowledge-aided convolutional neural network for small organ segmentation," *IEEE Journal of Biomedical and Health Informatics*, vol. 23, no. 4, pp. 1363–1373, 2019.
- [25] Y. Ma, H. Hong, and X. Zhu, "Multiple moving-target indication for urban sensing using change detection-based compressive sensing," *IEEE Geoscience and Remote Sensing Letters*, vol. 18, no. 99, 2020.
- [26] Z. Li, F. Santi, D. Pastina et al., "A multi-frame fractional fourier transform technique for moving target detection with space-based passive radar," *IET Radar Sonar & Navigation*, vol. 11, no. 5, pp. 822–828, 2016.
- [27] G. Zhaoming, J. Yi, and B. Shihua, "Detection probability for moving ground target of normal distribution using an imaging satellite," *Chinese Journal of Electronics*, vol. 27, no. 6, pp. 1309–1315, 2018.
- [28] M. Elhoseny and K. Shankar, "Optimal bilateral filter and convolutional neural network based denoising method of medical image measurements," *Measurement*, vol. 143, pp. 125–135, 2019.
- [29] Z. M. Zhu and X. B. Wang, "The research of ultra wide-band in searching and rescuing rader micro-moving target detection methods," *Computing Techniques for Geophysical & Geochemical Exploration*, vol. 37, no. 2, pp. 141–144, 2015.

Research Article

Improvement of Support Vector Machine Algorithm in Big Data Background

Babacar Gaye , Dezheng Zhang, and Aziguli Wulamu

School of Computer and Communication Engineering, University of Science and Technology Beijing, Beijing, China

Correspondence should be addressed to Babacar Gaye; babacargaye92@gmail.com

Received 21 February 2021; Revised 30 April 2021; Accepted 3 June 2021; Published 17 June 2021

Academic Editor: Sang-Bing Tsai

Copyright © 2021 Babacar Gaye et al. This is an open access article distributed under the Creative Commons Attribution License, which permits unrestricted use, distribution, and reproduction in any medium, provided the original work is properly cited.

With the rapid development of the Internet and the rapid development of big data analysis technology, data mining has played a positive role in promoting industry and academia. Classification is an important problem in data mining. This paper explores the background and theory of support vector machines (SVM) in data mining classification algorithms and analyzes and summarizes the research status of various improved methods of SVM. According to the scale and characteristics of the data, different solution spaces are selected, and the solution of the dual problem is transformed into the classification surface of the original space to improve the algorithm speed. *Research Process.* Incorporating fuzzy membership into multicore learning, it is found that the time complexity of the original problem is determined by the dimension, and the time complexity of the dual problem is determined by the quantity, and the dimension and quantity constitute the scale of the data, so it can be based on the scale of the data Features Choose different solution spaces. The algorithm speed can be improved by transforming the solution of the dual problem into the classification surface of the original space. *Conclusion.* By improving the calculation rate of traditional machine learning algorithms, it is concluded that the accuracy of the fitting prediction between the predicted data and the actual value is as high as 98%, which can make the traditional machine learning algorithm meet the requirements of the big data era. It can be widely used in the context of big data.

1. Introduction

The support vector machine (SVM) is a traditional machine learning method based on classification. It is derived from the idea of solving the dual form of large-dimensional problems, so that the classifier only relies on a small number of support vectors to achieve the principle of structural risk minimization. Statistical learning theory solved nonlinear and local minimum problems. The system call can use the short system frequency to convert the sequence into a call sequence with a certain length of vectors in a high-dimensional space. Therefore, anomaly detection can be performed based on support vector machines. In the context of the current big data era, it can implement multidomain applications in a big data environment. With the development of the current era, the scale of data is getting larger and larger, and the attributes of the data are also increasing. At the same time, the diversification of the values of data attributes makes it more

difficult to classify such data. However, the massive amounts of data that appear now generally have such high dimensionality and diversity, which makes it difficult for some classification algorithms to use such data to build predictive models. These difficulties are manifested in the lack of scalability of the algorithm, the long time to build the model, or the problem of dimensional disasters. Support vector machines can be well applied to high-dimensional data, and there is no limit to the value of each attribute.

In the improvement of traditional algorithms under the big data platform, the most popular framework is the Spark Framework. The Spark Big Data Framework is an iterative distributed computing framework based on memory. According to the official description of the Apache Spark Open Source Organization, Spark performs iterative calculations based on disk and compares with other frameworks and finds that its speed is more than 10 times that of other frameworks; and iterative calculation based on memory is

beyond a hundred times more. Therefore, it is very fast and efficient to build applications based on Spark's API. For example, classic traditional algorithms such as collaborative filtering algorithm and Bayesian recommendation algorithm have achieved large improvements and optimization based on this. Subsequently, finding a method to improve the support vector machine algorithm under the Spark big data framework is the problem to be solved [1, 2].

Guo proposed two multifault diagnosis methods based on the improved support vector machine (SVM), which are used for sensor fault detection and identification, respectively. First, use Online Sparse Least Squares Support Vector Machine (OSLSSVM) to detect and predict sensor failure. On this basis, Guo S. proposed a sensor fault feature extraction and online recognition method based on the combination of SVM and the Error Correction Output Code (ECOC). They used nonlinear transformation as input to the classifier to improve the separability of the initial features. Use ECOC-SVM to classify the fault status. After studying some typical faults, they found that ECOC-SVM has high recognition accuracy and can be realized in real time to meet the requirements of online fault recognition. This method can also be extended to solve other related problems [3]. Scholars such as Carrizosa found that in linear classifiers (such as support vector machines (SVM)), each feature has a score and assigns objects to classes based on a linear combination of score and feature value. Inspired by the Discrete Mental Scale (DILSVM), they proposed the Discrete Horizontal Support Vector Machine (DILSVM). The DILSVM classifier benefits from interpretability because it can be viewed as a set of Likert scales, each with one feature, where the level of consistency is scored with the positive class. In order to establish a DILSVM classifier, Carrizosa and other scholars proposed a mixed integer linear programming method and proposed a set of strategies to reduce the generation time. Our calculation experience shows that the 3-point and 5-point DILSVM classifiers have considerable accuracy and support vector machines and have a great improvement in interpretability and sparseness, thanks to the appropriate feature level selection [4].

This article introduces some basic concepts and principles of machine learning, provides necessary background support for the proposal of support vector machines, and then specifically introduces the basic ideas and specific theories and implementation algorithms of support vector machines. The solution space suitable for the scale of the data is selected, the solution of the dual space is converted into the classification surface of the original space, and it is divided into three groups for calculation. Research data shows that by improving the calculation speed of traditional machine learning algorithms, traditional machine learning algorithms can meet the requirements of the big data era. Research data shows that the improved algorithm greatly increases the time and space complexity of users. In addition, after three sets of experimental calculations, the prediction accuracy of the fitting between the predicted data and the actual value is as high as 98% (including two average tests, aptness and applicability).

2. Proposed Method

2.1. Support Vector Machine (SVM). SVM is a very classical two-classification model, and its working mechanism is to find a suitable hyperplane to segment the collected data samples. The principle of segmentation is to maximize the interval (including hard interval and soft interval), and finalize it into a special quadratic programming problem to solve. The main models are as follows: if the training sample is linearly time-sharing, use the linear separable support vector machine by maximizing the hard interval; if the training sample is approximately linearly time-sharing, use the linear support vector machine by maximizing the soft interval and selecting the appropriate kernel function; if the training sample is linearly non-time-sharing, make it possible to maximize the soft interval and select the appropriate kernel function, with a nonlinear support vector machine [5, 6]. The following is an overview of the main support vector machines.

2.1.1. Linear Separable Support Vector Machine. We first give a training sample set, the most basic idea of the so-called linear separable support vector machine is to find a suitable partition hyperplane in the sample space where the training sample set is M , separating the samples of different categories. If a linear function is able to separate samples, these data samples are called linearly separable. So specifically, what is a linear function? we generally think that a linear function is a straight line in a two-dimensional space, a plane in a three-dimensional space, and so on, if spatial dimensions are not considered; such a linear function is collectively called a hyperplane. In a two-dimensional space, for example, we look at a simple example of two-dimensional space. In the example, "O" represents positive classes and "X" refers to negative classes. Samples are linearly detachable; however, from a graphical point of view, it is clear that not only this straight line can separate samples, but also there are countless lines. The linear separable support vector machine corresponds to lines that can correctly divide the data and have the largest intervals.

Since the maximum interval is sought, it is imperative to calculate the interval in the sample space. In the sample space, we use the following linear equation to describe the division of the hyperplane:

$$W^T x + b = 0, \quad (1)$$

where W is a normal vector, which determines the direction of the hyperplane and b is a displacement, which determines the distance between the hyperplane and the origin. Assume that the hyperplane can correctly classify the training samples; that is, for the training samples, the following formula is satisfied:

$$w^t x_i + b \geq 1, y = 1, \quad (2)$$

$$w^t + b \leq -1, y = -1. \quad (3)$$

The above formula is called the maximum interval hypothesis. It indicates that the sample is a positive sample, expressed as a negative sample. In fact, the specified value of 1 or -1 here is only for the convenience of calculation, in principle can take any constant.

$$f = \left[-\frac{1}{2} \sum_{c=1}^i \sum_{d=1}^i (a_c^* - a_c)(a_c - a_c^*) Q(x_c, x_d) - \vartheta \sum_{c=1}^i (a_c^* + a_c) + \sum_{c=1}^i b_c (a_c^* + a_d) \right]. \quad (4)$$

Among them,

$$\sum_{c=1}^i a_c^* = \sum_{c=1}^i a_c \quad a_c^*, a_c \in [0, D] (c = 1, 2, 3, \dots, m), \quad (5)$$

where D is a normal number; it is called the penalty factor. If the value of D is large, it means that the penalty for fitting deviation is large. At this time, the regression function can be expressed as shown below:

$$V = \sum_{c=1}^i (a_c^* - a_c) Q(x_c, x) + s. \quad (6)$$

The selection of regression model parameters mainly includes the selection of the type of kernel function, the parameters of the kernel function, the penalty factor D , and the insensitivity coefficient. The performance characteristics of the regression machine have a great relationship with these parameters.

2.1.3. Feature Structure of the Support Vector Machine Application. SVM has good generalization ability and strong theoretical support. Scholars at home and abroad have conducted much in-depth research on support vector machine algorithms and, based on this, have optimized the algorithm, so that the performance of support vector machines is continuously improved. Support vector machines are widely used in various fields, such as face recognition, image classification, note recognition, and voice recognition, in pattern recognition and many data analysis fields such as virus detection, spam filtering, and network intrusion detection [8].

(1) *Face Recognition.* The core idea of face recognition is to use knowledge or statistical methods to model the face [9]. It is more likely that the area to be inspected matches the face model in a complex background and judges whether a face exists and separates. At present, face recognition detection technology is relatively mature and applied to various fields. Osuna first proposed to use the SVM method in face recognition technology by training a nonlinear SVM classifier to detect and classify faces and nonfaces. A basic principal component analysis (PCA) was proposed. +LDA + SVM face

2.1.2. Nonlinear Support Vector Machines. For nonlinear support vector machine regression, the basic idea is to map the data to a high-dimensional feature space (Hilbert space) through a nonlinear mapping and perform linear regression in this space so that the nonlinear problem in the low-dimensional space corresponds to the high linear regression problem of dimensional feature control [7]. The specific algorithm is as follows:

recognition improvement framework, using particle swarm optimization algorithm to optimize the two important accommodation penalty parameters and kernel functions of SVM to obtain the optimal solution, is used to train the final classifier for face recognition and obtain more high recognition accuracy [10, 11].

(2) *Image Classification.* Images have become an important means of transmitting and obtaining information in people's life and work. Quickly positioning images and properly classifying images are very important to improve the accuracy of content-based image retrieval. Literature proposes simple image and complex image classification methods based on SVM. Literature effectively combines the idea of semisupervised learning with support vector machines and proposes a small graph classification method for label mean semisupervised SVM based on mean shift. The algorithm parameter value method is improved by the mean shift result so that the image classification result can obtain higher classification accuracy and time efficiency [12, 13].

(3) *Network Intrusion Detection.* Intrusion detection technology collects and analyzes information on key nodes in computer network systems and responds to security policy violations in a timely manner [14]. The data in network intrusion detection is very large and complex. It has the characteristics of high dimensions, small samples, and linear inseparability. SVM, as a method developed on the basis of small sample machine learning, uses the principle of risk minimization to solve problems such as small samples, nonlinearity, and high dimensions, yet is able to maintain a high level of lack of prior knowledge. The classification accuracy is very suitable for network intrusion detection systems [15, 16].

2.2. Integration of Support Vector Machines with Machine Learning

2.2.1. Kernel Function. In the previous discussion, it is believed that the samples that need to be trained satisfy the condition of linear separability in the feature space, but it is often difficult to determine the appropriate kernel function in the real task to make the training set linearly separable in the feature space [17]. For nonlinear problems, the linear

separable support vector machine cannot be effectively solved, and it is necessary to use the nonlinear model in order to classify it well. Therefore, we need to introduce the concept of kernel function which refers to a symmetric function corresponding to the kernel matrix semipositive definite [18]. In other words, any kernel function implicitly defines a space called the “Regenerative Core Hilbert,” the characteristic space [7]. Samples are linearly separable within the feature space, so the quality of the feature space is crucial to the performance of support vector machines. It is particularly important to note that when we do not know the form of feature maps, we do not know what kind of kernel function is appropriate, and the kernel function only implicitly defines this feature space. Thus, kernel function selection becomes the largest variable in support vector machines. If the kernel function selection is not appropriate, it means that the sample is mapped to an inappropriate feature space, which is likely to lead to poor performance and cannot get the results we want [19].

2.2.2. Soft Spacer Support Vector Machine. Although the introduction of kernel functions plays a crucial role in dividing samples of different classes, even if such kernel functions are found to make samples linearly separable in feature space, it is difficult to judge whether it is caused by overfitting. So in order to alleviate this problem, we allow SVM to have some fault tolerance on the sample; that is, the support vector machine of “hard interval” which we want to propose is different from that of “soft interval,” which allows some samples not to meet the following constraints:

$$y_i(w^t x_i + b) \geq 1. \quad (7)$$

Naturally, this does not mean that our “error” samples are arbitrary and not limited by the number. In terms of requirements, we want as few samples as possible that do not satisfy the constraints, so we rewrite the optimization goal to

$$\min \frac{1}{2} \|w\|^2 + c \sum_{i=1}^m l_0(y_i(w^t x_i + b) - 1). \quad (8)$$

Polynomial kernel function is as follows:

$$k(x_1, x_2) = (\langle x_1, x_2 \rangle + R)^d. \quad (9)$$

Gaussian kernel function is as follows:

$$k(x_1, x_2) = \text{Exp}\left(-\frac{\|x_1, x_2\|^2}{2\sigma^2}\right). \quad (10)$$

Linear kernel function is as follows:

$$k(x_1, x_2) = \langle x_1, x_2 \rangle. \quad (11)$$

Support vector machine algorithm flow chart is shown in Figure 1.

In Figure 1, *Ht* is represented as an error sample, *Pc* is a sample that does not meet the constraints, and *ST* is an optimization goal. After the process in Figure 1, the fault tolerance of the support vector machine can be obtained.

2.3. Space-Time Complexity of Support Vector Machines. The research shows that when using support vector machines for classification, there are actually two main processes of training and classification. Therefore, the complexity of the discussion cannot be unified, and the space-time complexity of support vector machines is simplified, that is, the complexity of solving this quadratic programming problem: analytical solution, numerical solution [20].

2.3.1. Analytical Solution. An analytical solution is a theoretical solution. That is to say, as long as there is a solution to a problem, its analytical solution must exist. Of course, existence is one thing, and it can be solved, or it can be solved within a tolerable time frame, which is another matter. For SVM, the time complexity of finding the analytic solution is the worst, which is the number of support vectors. Although there is no fixed ratio, the number of support vectors is also related to the size of the training set.

2.3.2. Numerical Solution. The numerical solution is a solution that can be used, but in actual situations, it is often an approximate solution [21]. The process of finding a numerical solution is similar to the exhaustive method, and of course there must be certain rules to follow. Different algorithms have different ways of finding breakpoints, and even the stopping conditions are different. The accuracy of the resulting solutions is also different. It can be seen that the discussion of the complexity of the numerical solution cannot be separated from the specific algorithm analysis [22].

2.4. The Relationship and Development Trend of Big Data Platforms and Machine Learning. The core of big data is to use the value of data, and machine learning is just the key technology to better use the value of data. For big data platforms, machine learning is indispensable. Correspondingly, for machine learning, the greater the amount of data information, the higher the precise value for the data model [23]. Coincidentally, complex machine learning algorithms are trapped in the complexity of time and space and urgently need key technologies such as distributed computing and memory computing, and this key technology is the core of big data. Therefore, from the perspective of dialectics, big data and machine learning are mutually reinforcing and interdependent.

Although, nowadays, machine learning is closely connected with big data, it must be made clear that big data is not equivalent to machine learning. Similarly, machine learning is not equivalent to big data. This means that machine learning is a part of the big data analysis, and it is not the only analysis method under big data. There is no doubt that the close integration of machine learning and big data has produced huge benefits for the current social situation. Based on the development of machine learning

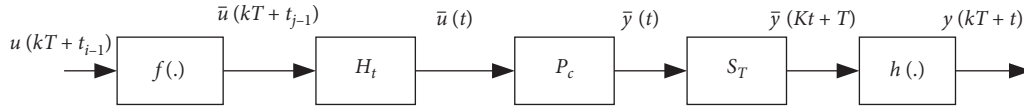


FIGURE 1: Boxplot of petal length.

technology, massive amounts of data information can be nearly “reasonably predicted.” As far as human society is concerned, especially at the stage where the Internet is popular and developing rapidly, the richer the accumulated experience, and the broader the experience, equates to more accurate projections for the future. This is relevant to the theory in the machine learning community: the more data the machine learning model has, the better the efficiency of machine learning prediction is [24].

3. Experiments

3.1. Experimental Background. Data is the raw material for machine learning models, and the current boom in machine learning is inseparable from the support of big data. In the field of machine learning, there are a large number of public datasets available, ranging from hundreds of samples to hundreds of thousands of samples. Some datasets are used for teaching, and some are used as standards for performance testing of machine learning models. These high-quality public datasets provide great convenience for us to learn and study machine learning algorithms, similar to the value of model organisms for biological experiments. In order to test the improvement and application of different algorithms on the support vector machine, this experiment selects the most classic Iris dataset as the test object.

3.2. Experimental Setup. In this paper, we find that the time complexity of the original problem is determined by the dimension of the feature space, while the time complexity of the dual problem is determined by the number of training samples. Therefore, this paper selects a suitable solution space for the data scale and converts the solution of the dual space into the classification surface of the original space and divides them into three groups for calculation.

In order to verify the above conclusions, we use MATLAB to conduct Experiment 1, write training algorithms according to the principle of SVM, customize different dimensions and different numbers of Iris datasets for training experiments, and compare training time. The featured space dimension is defined as D and the number of sample points as C , half of which are positive samples, assigned as real numbers between 0 and 100, and half as negative. Samples were assigned as real numbers between 200 and 300.

From the results of Experiment 1, it can be seen that when the dimension/number is much less than 1, the time consumed to solve the original problem is significantly less than the time consumed to solve the dual problem. Conversely, when the dimension/number is much greater than 1,

the time consumed to solve the dual problem is obviously less than the time consumed to solve the original problem.

3.3. Experimental Procedure.

- (1) Prepare experimental data: import the Iris flower dataset
- (2) Data feature analysis: multiangle feature analysis of the dataset
- (3) Visual analysis: analyze the correlation between different features in the data set, which is the core of algorithm reformation based on support vector machine
- (4) Use support vector machines for machine learning: use the correlation analysis generated in the previous experimental step to compare and test different algorithms
- (5) Analyze the experimental results

4. Discussion

4.1. Experimental Data Analysis

- (1) The Iris dataset contains 150 records in 3 categories, 50 data in each category, and each record has 4 features: calyx length, calyx width, petal length, and petal width, which can be predicted by these 4 features. Which species does the iris flower belong to? The basic discrimination basis for the three types of irises is that the seeds have 4 dimensions in the entire Iris dataset, namely, petal length, petal width, calyx length, and calyx width. After integrating the above algorithm improvements and performance optimizations, this paper draws the decision surfaces of the support vector machine classification with different kernels in these four dimensions. The decision boundaries of the two linear support vector machines are straight lines and nonlinear. The decision boundary of the kernel support vector machine (polynomial kernel and Gaussian radial basis kernel) is a nonlinear curve boundary, and 80% of users of the improved algorithm have been greatly improved in time and space complexity. It can be seen that in the era of big data, both the quantity and the dimensions of the data may be huge, and we should select the appropriate algorithm according to the scale and characteristics of the data. When the dimension is greater than the number, the dual problem is chosen to be solved; when the number is greater than the dimension, the original problem is

chosen to be solved. This will undoubtedly greatly improve the processing speed of the algorithm. Based on the big data platform, the dataset processed in this article will use more nonlinear support vector machines, and the summary analysis of the Iris dataset is shown in Table 1 and Figure 2.

- (2) Unbalanced data classification algorithms can only solve the accuracy problem. When the data size increases, the training time of the algorithm is very long; although some distributed classification algorithms can be trained for a short time, these classification algorithms are not unbalanced data classification algorithm. Describing the distribution of data, including upper and lower bounds, upper and lower quartiles, and median, you can simply view the distribution of data. Combining with the above summary analysis, if the upper and lower quartiles are far apart, they can generally be easily divided into the following categories. As shown in Figure 3 and Table 2, the following exhibits the summary statistics of each feature column of the entire dataset.

4.2. Analysis of Data Characteristics

- (1) When analyzing the relationship between features and varieties through data distribution, in order to have a deeper understanding of the dataset, this article must explore the relationship between various variables, specifically in the Iris dataset, and observe the characteristics and varieties. The relationship is shown in Figure 4. In this research, by analyzing the relationship between each feature and variety (since this is a binary variable), the linear relationship is used to analyze the relationship between the feature and the variety; then for the linear relationship, the slope relationship becomes its investigation, the core. As shown in Figure 4, the relationship between each feature and variable is compared by slope, and the relationship between each feature is analyzed. Through the above analysis, the experiment needs to perform feature analysis on all variables in the data set in order to facilitate subsequent experiments get on. The specific data is shown in Table 3 of Figure 4.
- (2) Use Andrews Curves to convert each multivariate observation to a curve and express the coefficients of the Fourier series, which is useful for detecting outliers in time series data. Andrews Curves is a method to visualize multidimensional data by mapping each observation to a function. After conducting a general analysis based on the linear regression visualization of the calyx and petals, this paper analyzes the main variables. After the above analysis, this paper finds the correlation between different features in the dataset. A high positive or negative value indicates that the features are highly correlated. This is shown in Table 4. Through the analysis of the experimental results in this paper, it is

TABLE 1: Comparison of experimental training time.

Parameter setting	Dimensions/quantity	Time spent in solving the original problem (s)	Time spent in solving dual problems (s)
$D = 50$ $C = 300$	0.15	0.4562	14.3513
$D = 100$ $C = 300$	0.26	1.1367	15.5391
$D = 200$ $C = 300$	0.53	3.2782	15.6821
$D = 300$ $C = 200$	1.40	5.1125	1.3429
$D = 300$ $C = 100$	3.00	3.2381	0.2713
$D = 300$ $C = 50$	5.00	2.1357	0.2731

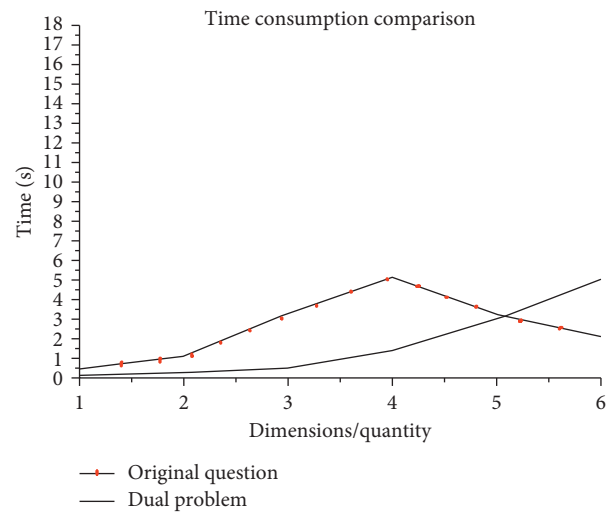


FIGURE 2: Comparison of experimental training time.

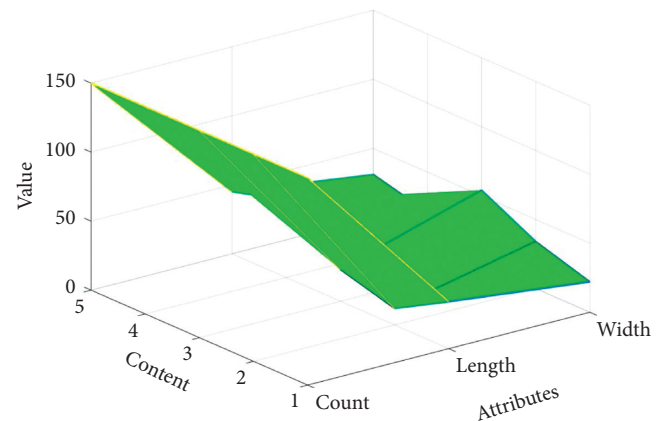


FIGURE 3: Summary information.

TABLE 2: Summary information.

Content	Count	Length	Width
Sepal length (cm)	150	34	22
Sepal width (cm)	150	12	34
Petal length (cm)	150	23	54
Petal width (cm)	150	56	21
Species	150	45	31

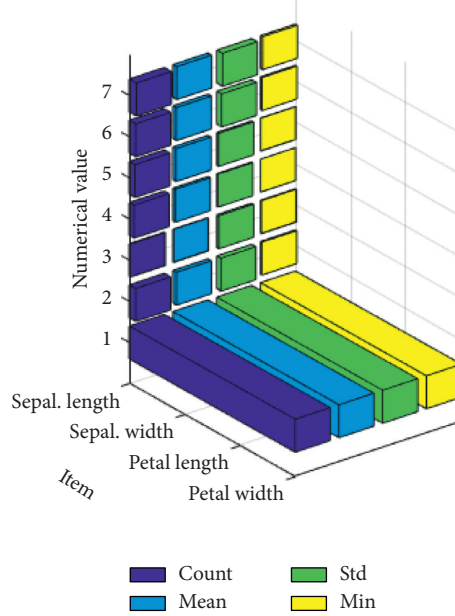


FIGURE 4: Boxplot of petal length.

TABLE 3: Feature column summary statistics.

Item	Sepal length	Sepal width	Petal length	Petal width
Count	150.000000	150.000000	150.000000	150.000000
Mean	5.843333	3.057333	3.758000	1.199333
Std	0.828066	0.435866	1.765298	0.762238
Min	4.300000	2.000000	1.000000	0.100000
25%	5.100000	2.800000	1.600000	0.300000
50%	5.800000	3.000000	4.350000	1.300000
75%	6.400000	3.300000	5.100000	1.800000
Max	7.900000	4.400000	6.900000	2.500000

TABLE 4: Data distribution analysis of the relationship between characteristics and varieties.

Vector 1	Vector 2	Vector 3
1.2	2.2	1.9
1.3	2.3	2.2
2.6	1.6	1.8
1.8	2.7	1.7
2.4	2.8	2.9

found that the length and width of the flowers are not related, and the length and length of the petals have a strong correlation. Through the above analysis, it can be found that, after three sets of calculations, the accuracy of the prediction between the predicted data and the actual value is 98% (including two average tests), indicating that the improvement of the algorithm here is for the support vector machine The rewriting is very effective. In addition to the above decision tree analysis addition, the classification method of support vector machine needs to be further improved, then as a classic traditional

clustering method KMeans cluster analysis is a very good idea analysis, this paper will experiment with the algorithm improvement results. Based on the above two-classification methods, K-means clustering and decision tree analysis, it is found through experimental results that the two can be more effectively combined to achieve algorithm optimization and process improvement in support vector machines. Such optimization results are on big data platforms which is also helpful. Figures 5 and 6 show the analysis of making a linear regression visualization.

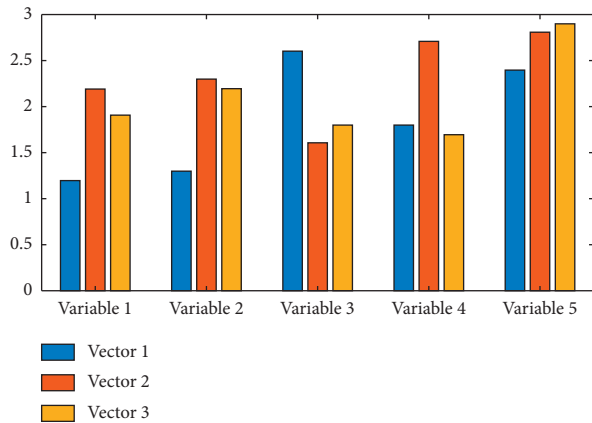


FIGURE 5: Data distribution analysis of the relationship between characteristics and varieties.

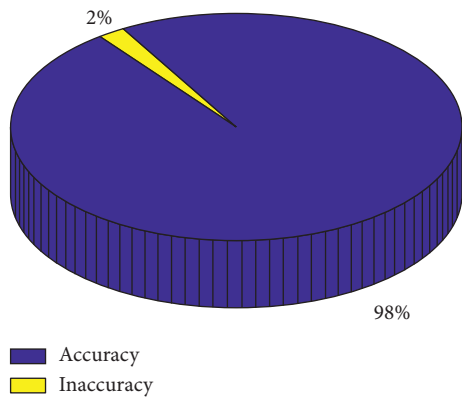


FIGURE 6: Visual analysis of linear regression based on calyx.

5. Conclusion

- (1) As a very efficient classification model in machine learning, support vector machine has many advantages such as good generalization, few parameters, and the ability to generate global optimal solutions. It is a very good choice for people to process data, analyze data, and predict data. In the context of today's big data, support vector machines, as a traditional classification method, are still applicable due to the superiority of their architecture and algorithms. However, people must improve their algorithm to get rid of the process of processing large sample data sets. This algorithm will occupy a long training time and occupy a high space-time complexity, which leads to the problem of low efficiency. Judging from the final experimental results, the problems we raised have been effectively resolved.
- (2) This article aimed to study the improvement of support vector machine algorithms in the context of big data, and the research discovered problems. This article intended to solve the problem of traditional SVM sensitive to noise points and outliers and could not solve the problem of large sample feature scale,

heterogeneous information, and feature space. We then have the problem of uneven distribution. During the research process, incorporating fuzzy membership into multicore learning, it is discovered that the time complexity of the original problem is determined by the dimension, and the time complexity of the dual problem is determined by the quantity of the data. The dimension and quantity constitute the scale of the data, so it can be based on the features we chose for different solution spaces. The algorithm speed can be improved by transforming the solution of the dual problem into the classification surface of the original space. To conclude, by improving the calculation rate of traditional machine learning algorithms, it is established that the accuracy of the fitting prediction between the predicted data and the actual value is as high as 98%, which can enable traditional machine learning algorithms to meet the requirements of the big data era in the future. It can be widely used in the context of big data.

- (3) This article used statistical learning and optimization theory to analyze the working process of support vector machines and the needs of big data platforms for support vector machines in principle, while updating and improving the kernel algorithm of support vector machines. In the experimental stage, the classic optimization dataset Iris flower dataset is used to further test the improved optimization algorithm of support vector machine. The final experimental results are a good evidence of the good fit and adaptability of researchers to improve and optimize the algorithm. In the process of improvement, it was found that many different variant models can be derived when small sample classification is performed. And the support vector machine itself also has a significant advantage as it can handle various complex operations of vector inner product in high-dimensional space through kernel functions. Therefore, it is necessary to choose a suitable solution space and a suitable kernel function for the data scale and convert the solution of the dual space into the classification surface of the original space. The final experimental results show that by further improving the calculation rate of traditional machine learning algorithms, the traditional support vector machine algorithm can meet the requirements of the era of big data. The time complexity of the original problem is determined by the dimension of the feature space, while the time complexity of the dual problem is determined by the number of training samples. Therefore, people should choose a suitable solution space for the data scale and convert the solution of the dual space into the classification surface of the original space. The final experimental results show that by improving the calculation rate of traditional machine learning algorithms, the traditional machine learning algorithms can meet the requirements

of the era of big data. Experimental data shows that 80% of users of the improved algorithm have greatly improved the complexity of time and space, showing a good fit and applicability.

Data Availability

No data were used to support this study.

Conflicts of Interest

The authors declare no potential conflicts of interest in our paper.

Authors' Contributions

All authors have seen and approved the final version of the manuscript.

References

- [1] P. Borah and D. Gupta, "Unconstrained convex minimization based implicit Lagrangian twin extreme learning machine for classification (ULTELMC)," *Applied Intelligence*, vol. 50, no. 4, pp. 1327–1344, 2020.
- [2] P. Borah and D. Gupta, "Functional iterative approaches for solving support vector classification problems based on generalized Huber loss," *Neural Computing and Applications*, vol. 32, no. 1, pp. 1135–1139, 2020.
- [3] S. Balasundaram and D. Gupta, "Knowledge-based extreme learning machines," *Neural Computing and Applications*, vol. 27, no. 6, pp. 1629–1641, 2016.
- [4] E. Carrizosa, A. Nogales-Gómez, and D. Romero Morales, "Strongly agree or strongly disagree?: rating features in support vector machines," *Information Sciences*, vol. 329, no. C, pp. 256–273, 2016.
- [5] G. Taherzadeh, Y. Zhou, A. W.-C. Liew, and Y. Yang, "Sequence-based prediction of protein-carbohydrate binding sites using support vector machines," *Journal of Chemical Information and Modeling*, vol. 56, no. 10, pp. 2115–2122, 2016.
- [6] M. Tanveer, M. A. Khan, and S.-S. Ho, "Robust energy-based least squares twin support vector machines," *Applied Intelligence*, vol. 45, no. 1, pp. 174–186, 2016.
- [7] W. Gu, W.-P. Chen, and C.-H. Ko, "Two smooth support vector machines for ϵ -insensitive regression," *Computational Optimization & Applications*, vol. 70, no. 1, pp. 1–29, 2018.
- [8] T. Tanino, R. Kawachi, and M. Akao, "Performance evaluation of multiobjective multiclass support vector machines maximizing geometric margins," *Numerical Algebra Control & Optimization*, vol. 1, no. 1, pp. 151–169, 2017.
- [9] M. Malvoni, M. G. De Giorgi, and P. M. Congedo, "Data on support vector machines (SVM) model to forecast photovoltaic power," *Data in Brief*, vol. 9, no. C, pp. 13–16, 2016.
- [10] R. Darnag, B. Minaoui, and M. Fakir, "QSAR models for prediction study of HIV protease inhibitors using support vector machines, neural networks and multiple linear regression," *Arabian Journal of Chemistry*, vol. 10, no. S1, pp. S600–S608, 2017.
- [11] J.-Y. Gotoh and S. Uryasev, "Support vector machines based on convex risk functions and general norms," *Annals of Operations Research*, vol. 249, no. 1–2, pp. 1–28, 2017.
- [12] T. Singh, F. Di Troia, and C. Aaron Visaggio, "Support vector machines and malware detection," *Journal of Computer Virology & Hacking Techniques*, vol. 41, no. 10, pp. 1–10, 2016.
- [13] J. Li, Y. Cao, and Y. Wang, "Online learning algorithms for double-weighted least squares twin bounded support vector machines," *Neural Processing Letters*, vol. 45, no. 1, pp. 1–21, 2016.
- [14] C. Ehrentraut, M. Ekholm, H. Tanushi, J. Tiedemann, and H. Dalianis, "Detecting hospital-acquired infections: a document classification approach using support vector machines and gradient tree boosting," *Health Informatics Journal*, vol. 24, no. 1, pp. 24–42, 2016.
- [15] X. Zhang, Y. Li, and X. Peng, "Brain wave recognition of word imagination based on support vector machines," *Chinese Journal of Aerospace Medicine*, vol. 14, no. 3, pp. 277–281, 2016.
- [16] J. Nalepa and M. Kawulok, "Selecting training sets for support vector machines: a review," *Artificial Intelligence Review*, vol. 52, no. 2, pp. 857–900, 2019.
- [17] A. Gangopadhyay, O. Chatterjee, and S. Chakrabarty, "Extended polynomial growth transforms for design and training of generalized support vector machines," *IEEE Transactions on Neural Networks & Learning Systems*, vol. 29, no. 5, pp. 1–14, 2018.
- [18] Y. Bai and X. Yan, "Conic relaxations for semi-supervised support vector machines," *Journal of Optimization Theory and Applications*, vol. 169, no. 1, pp. 299–313, 2016.
- [19] L. Zhang, X. Lu, and C. Lu, "National matriculation test prediction based on support vector machines," *Journal of University of Science & Technology of China*, vol. 47, no. 1, pp. 1–9, 2017.
- [20] M. Ahmer, A. Shah, S. M. Zafi S. Shah et al., "Using non-linear support vector machines for detection of activities of daily living," *Indian Journal of Science and Technology*, vol. 10, no. 36, pp. 1–8, 2017.
- [21] K. H. Yoo, Y. D. Koo, H. B. Ju, and M. G. Na, "Identification of LOCA and estimation of its break size by multiconnected support vector machines," *IEEE Transactions on Nuclear Science*, vol. 64, no. 10, p. 1, 2017.
- [22] Y. Lou, Y. Liu, J. K. Kaakinen, and X. Li, "Using support vector machines to identify literacy skills: evidence from eye movements," *Behavior Research Methods*, vol. 49, no. 3, pp. 887–895, 2017.
- [23] A. U. Mageswari and R. Vinodha, "Engine knock detection based on wavelet packet transform and sparse fuzzy least squares support vector machines (SFLS-SVM)," *IIOAB Journal*, vol. 7, no. 11, pp. 194–199, 2016.
- [24] M. Erdem, F. E. Boran, and D. Akay, "Classification of risks of occupational low back disorders with support vector machines," *Human Factors and Ergonomics in Manufacturing & Service Industries*, vol. 26, no. 5, pp. 550–558, 2016.

Research Article

A Traceability Public Service Cloud Platform Incorporating IDcode System and Colorful QR Code Technology for Important Product

Shaqing Zhang ^{1,2}, Jinhui Liao ¹, Shuangcheng Wu ¹, Junrui Zhong ³,
and Xiaoping Xue ⁴

¹School of Management, Guangdong University of Technology, Guangzhou 510520, China

²Huizhou Guangdong University of Technology IoT Cooperative Innovation Institute Co., Ltd., Huizhou 516025, China

³Information Center, The First Affiliated Hospital of Jinan University, Guangzhou 510630, China

⁴School of Information Engineering, Huizhou Economics and Polytechnic College, Huizhou 516057, China

Correspondence should be addressed to Junrui Zhong; ecis@163.com

Received 17 January 2021; Accepted 19 May 2021; Published 8 June 2021

Academic Editor: Aijun Liu

Copyright © 2021 Shaqing Zhang et al. This is an open access article distributed under the Creative Commons Attribution License, which permits unrestricted use, distribution, and reproduction in any medium, provided the original work is properly cited.

At present, the epidemic situation of COVID-19 is raging rampantly in the whole world, affecting the hearts of billions of people. The new coronavirus has been detected in many foods and agricultural products. At the same time, vaccines and medicines to prevent or treat COVID-19 are also stepping up research and development and gradually put into use. The quality and safety of foods, medicines, and agricultural products are directly related to the lives and health of people. There are many potential dangers and hidden risks of accidents in the production, sale, and transportation of dangerous goods and special equipment. Therefore, it is necessary to effectively monitor and record the workflow of the above productions or goods. In this paper, we developed an important product traceability public service cloud platform (IPTPSCP) based on batch identification and record keeping with International Two-Dimensional Code Object Identifier System (IDcode) coding rules. Through a case study of the tea factory that produces and sells Xinyang Maojian tea, a test and implementation of IPTPSCP was shown by designing a colorful QR code to prevent the traceability information from being forged in batches. Judging from the overall effect of the practical application of more than a dozen settled enterprises, IPTPSCP has improved the efficiency of data collection and monitoring by about 13%. The results show that the IPTPSCP can be considered as an effective tool to guarantee the quality and safety of products. Besides, since it is not required for the enterprise to invest much money and manpower to develop software, IPTPSCP reduces the cost of implementing product traceability by about 36%.

1. Introduction

In the current global market, product quality has increasingly become an important factor influencing the customers' purchase intention. However, there are still a large number of fake products on the market. Serious harm to the interests of consumers from product liability accidents continues to occur, such as recent outbreaks of stained milk powder and mad cow disease in the food industry [1] and incidents of problematic vaccines and bogus drugs in the pharmaceutical industry [2]. The dissemination of these hugely influential negative events through the media has caused consumers to gradually reduce their trust in the products and increased

consumers' concerns about the source of the products [3]. Thus, with the increasing public awareness of product safety, consumers' increasing demand for high-quality products has led them to pay increasing attention to and support for traceable products [4]. In the current environment where COVID-19 is raging around the world, people are particularly looking forward to high-quality, traceable, and anticounterfeit foods, medicines, vaccines, etc. However, due to the information asymmetry in the market, product adulteration and shoddy products frequently occur, triggering the outbreak of a crisis of market confidence, which may eventually lead to market failure [5, 6]. A traceability system is an efficient tool that can monitor the quality of the products and reduce the

information asymmetry of adverse selection and moral hazard in product systems. The application of a traceability system is therefore of great strategic importance to achieve continuous quality improvement [7]. And EPC (Electronic Product Code), RFID (Radio-Frequency Identification), 2D barcodes (QR, VC, and DM), and other technologies are increasingly used in traceability systems [8–11].

The frequent occurrence of various product quality and safety incidents has also aroused the concerns of the public departments of many countries and prompted them to actively implement corresponding intervention measures [12]. At present, the European Union has established the legal framework and technical support system for food safety traceability with “Regulation 178–2002” at its heart. With the Bio-Anti-Terrorism Act and the Food Safety Modernization Act as the core, the United States has also set up a food safety traceability legal system. By successively promulgating and improving the People’s Republic of China Law on Quality and Safety of Agricultural Products, the Food Safety Law of the People’s Republic of China, and other legal provisions, China has made great progress in establishing a legal system of traceability. In particular, it should be pointed out that China issued and implemented six national standards for important product traceability on October 18, 2019. These standards are primarily intended to solve the basic common requirements such as terminologies that urgently need to be standardized and system construction, as well as meet data interconnection, information collection, and other key technical requirements in the construction of traceability systems for important products including agricultural products, foods, medicines, agricultural production materials, special equipment, dangerous goods, and rare earth products. It is clear that the publication and implementation of the six national standards will effectively improve the standardization of the construction and management of important product traceability systems. Moreover, ZIIOT (Zhongguancun Industry and Information Research Institute of Two-Dimensional Code Technology) in China independently developed the IDcode coding system, which is applied to carry out the global unique two-dimensional code identification for any type of object (person, thing, and item). IDcode, which features flexible layering, good compatibility, and strong scalability, is suitable as a meta-identification mechanism for exchanging existing coding systems [13].

This paper aims to establish an important product traceability public service cloud platform (IPTPSCP) by combining IDcode coding rules and colorful QR code technology applications. The main contributions of this paper are as follows:

- (1) Using the IDcode coding system, a public service platform for traceability of important products based on the cloud computing model is developed. It can flexibly customize the process and granularity of product traceability for different products and different user needs, which reduces the cost of platform development and improves the application efficiency of the platform.
- (2) A colorful QR code is developed. Compared with ordinary black and white QR codes, it is much more

difficult for colorful QR codes to be forged in batches, thereby greatly improving the security of the traceability platform.

The remainder of the paper is structured as follows. In Section 2, a literature review is presented. In Section 3, the system analysis for IPTPSCP is elaborated. Then, in Section 4, the system design and implementation of IPTPSCP are defined in detail. Section 5 is dedicated to a case study for testing and evaluating the feasibility and effectiveness of IPTPSCP. Finally, conclusions and further research subjects are presented in Section 6.

2. Literature Review

At present, scholars from various countries have conducted a great deal of fruitful research on traceability. Different definitions of traceability can be derived from various legislations, standards, and scientific literature. Olsen and Borit analyzed and summarized many definitions of traceability. They claimed that traceability refers to the ability to access any or all information related to the information under consideration over the entire life cycle through the identification of the record [14]. Meo stated that traceability in food production can be tracked from the inside of the manufacturing plant to the whole or part of the production chain from raw materials to customers [15]. As an important subsystem of quality management, the early traceability system can work normally on the basis of pen and paper records. However, as food regulations become increasingly perfect, simple traceability mechanisms in the food industry have become growingly advanced. Traceability must be handled by the establishment of similar systems. A growing number of companies are beginning to realize the benefits of traceability systems. The application of the system forces the company to comply with mandatory regulations and promotes the company’s products to pass international standards and certification requirements. The implementation of the system can help companies to improve marketing efficiency and ensure product sources and product quality. In addition, the benefits of the system include product value-added, anticounterfeiting features, lower inventory levels, lower labor costs, improved operation plans, logistics efficiency, etc. In addition, in the face of health incidents, the systems enable enterprises to have good response capabilities [16–18]. In recent years, various regions and relevant departments in China have actively promoted the application of modern information technology, such as IoT and cloud computing, to establish traceability systems for important products such as agricultural products, foods, medicines, and rare earth. These works and outcomes have shown positive results in enhancing corporate quality management capabilities, promoting innovation in regulatory methods, and ensuring consumer safety [19].

On the one hand, from the point of view of quality management, the real-time monitoring of key environmental parameters through integrated sensors is considered an important method for the effective controlling of product quality. Wang et al. studied the mechanism and knowledge

flow of the peach export chain and built a real-time tracking and traceability framework for peaches [20]. Multiple sensors have been used to record key environmental parameters in the peach export chain. The system ensures that the quality and protection of peaches and other main links are controlled. Qi et al. used WSN as a simple network infrastructure and developed a retraceability system for aquaculture with robust decision support functions [21]. It can be deployed rapidly to obtain water temperature, salinity, dissolved oxygen, pH, etc., and to realize real-time data transmission. Alfian et al. developed a traceability system for the Korean Kimchi supply chain, which is similar to the peach traceability system proposed by Wang. Both systems used a multisensor network to collect key environmental parameters. The Kimchi traceability method uses a significant amount of data gathered for data mining to make up for missing data and implement data prediction. And RFID technology was used to record and read data to improve work efficiency [22]. Combined with the meat quality of the cold chain and the environmental information collection program, Peng et al. presented a QR code-based tracing method for a quality tracing system [23]. Gao et al. developed an Internet of Things- (IoT-) based intelligent fish farming and tracking control system that includes a forecasting method that enables automatic water quality management and supports tracking the breeding and selling of freshwater fish [24]. Hu et al. first leveraged the immutability of block-chain and the paradigm of edge computing to construct a trust framework for the organic agricultural supply chain, which makes affordable traceability solutions for those in developing countries at a low cost [25].

On the other hand, from the point of view of product supervision and traceability, information recording of key production nodes of products has become the main direction of research. Karlsen et al. proposed that the supply chain of farmed salmon should have different traceability granularities, set up different traceability granularity according to different levels within the company and between the supply chains, and used the GS1 standard for coding for traceability units with different traceability granularity [26]. The Global Trade Commodity Code (GTIN) coding framework and UML class diagrams were used to model the production, processing, and quality information of the vegetable supply chain, with which the quality traceability information and the key information framework of activity participants in the vegetable supply chain were clearly described. The model verification shows that the accuracy of data collection, quality analysis, and inventory management has been enhanced to varying degrees after the application of the traceability system [27]. Thakur and Donnelly constructed a conceptual flow chart for planting, processing, and other links in the soybean value chain and determined the information entry point through information modeling. The traceability code based on the unique identification principle in the Trace Food framework was set up, and different traceable units in different links were determined. Then, a standardized list of data elements was created for mixed operation of different batches of the same type of soybeans, and the electronic information exchange technology in the

supply chain was discussed [28]. Qian et al. designed the raw material batch code and the traceability batch code through the analysis of the wheat flour supply chain details. They associated the traceability code with the production information and used QR codes and RFID to record and read information and developed a wheat traceability system to achieve the traceability of bulk wheat flour [19]. Chen et al. developed a mobile pork products quality and safety traceability system based on batch identification and record keeping with two-dimensional codes and reduced the cost of the traceability system [29]. Liang et al. developed the food-grade grain tracers which is an identification technology for tracing from original harvest to final destination. And automatic separation and identification equipment was designed to implement online production operation for food-grade grain tracers by QR code scanning and information recording [30]. Cai et al. integrated QR code with quality data and mobile intelligent technology to develop a convenient query terminal for tracing quality in the whole industrial chain of TCM (traditional Chinese medicine) [31]. Li et al. proposed a novel two-sided matching model based on dual hesitant fuzzy preference information to solve the fuzziness and uncertainty of preference information in the matching process of complex product manufacturing tasks on the cloud manufacturing platform, which provided an effective method for supplier selection in the product traceability system [32].

In addition, some scholars study the substances contained in the product itself for traceability of products. Chemical approaches, biomolecular approaches, and isotopic approaches have been used to detect these substances. Fernandes et al. classified red meat with the aid of the study of trace factors in beef to achieve the traceability of Brazilian pork [33]. Bong et al. used a range of elements and isotopes to investigate the geographical origin of Korean beer and measured the element and isotope composition of beer to identify geographical variations [34]. Zhao et al. measured and analyzed the concentrations of 20 elements in samples of tea and soil. The findings have shown that elemental fingerprinting profiles are of obvious difference for tea leaves and provenance soils from different regions [35].

Based on the above literature review, several observations can be obtained. Firstly, the vast majority of traceability systems were developed by manufacturing companies to achieve the traceability of their specific products, and companies need to invest more capital and labor costs for this. However, for different types of products or even different products of the same kind, the key points of traceability and the traceability mechanism could be entirely different. This type of traceability system therefore has poor flexibility and scalability. Secondly, the coding systems or coding rules currently adopted in various traceability systems are different, and a unified standard has not yet been formed, which is not conducive to information sharing and dissemination. Therefore, it is of considerable significance for both academia and industry to explore and develop an IPTPSCP with the most widely used coding and identification standards in the world.

3. System Analysis

3.1. The Survey Design and Analysis. This paper adopted a variety of methods to acquire user needs, including literature collection, policy research, on-site investigation, and interviews.

Firstly, we collected information on the development and application of relevant traceability and anticounterfeiting information systems at home and abroad in recent years, analyzed the characteristics and deficiencies of these systems, and used them as a reference for the system to be developed in the future.

Secondly, we investigated the relevant policies issued by relevant Chinese government departments in the area of important product traceability and anticounterfeiting in recent years and learned that the government's attitude is to encourage third-party organizations to develop and implement important product traceability public service cloud platforms, and they have provided some specific guidance specifications, relevant standards, and requirements.

Thirdly, we have conducted on-site investigations on six enterprises that produce food, drugs, agricultural products, chemical products, dangerous goods, and clothing products in some cities in China, such as Guangzhou, Foshan, Shantou, and Xinyang, and learned about their common or specific requirements for traceability and anticounterfeiting in products.

Finally, we randomly interviewed four managers and ten production workers in the above companies. These people in different positions elaborated their perceptions of the traceability and anticounterfeiting information system and their requirements such as overall functional requirements and specific module requirements, as well as their most concerned aspects. The initial needs were formed and summarized based on these interviews.

3.2. Users' Need for IPTPSCP. Through the above research and interviews, we analyzed and summarized the basic features and key functions of IPTPSCP, as shown in Table 1.

3.3. IPTPSCP Business Flow Analysis. Following the principles of corporate self-discipline, consumer, and government supervision, the needs of different users were fully considered in IPTPSCP to improve the economic benefits and brand effect of enterprises, strengthen government supervision, ensure product quality, and protect consumer rights and interests. IPTPSCP business process analysis is shown in Figure 1.

The above business process consists of the following major steps:

- (1) The company provides its information to register in IPTPSCP, which shall be audited by the administrator and certified by a third-party certification body.
- (2) After passing the audit and certification, companies can manage basic information such as product names, categories, and specifications.

- (3) The enterprise sets up traceability units and nodes for different products and then collects and inputs complete product traceability information.
- (4) The administrator audits the authenticity and standardization of product traceability information. After approval, the company can generate product traceability code, anticounterfeiting codes, and other pieces of relevant information and then submit them to third-party certification. After being certified, the above information can be stored in the cloud database.
- (5) Consumers can browse and query the traceability and anticounterfeiting information. If problems are found, they can complain about the net and give feedback to government regulators, who will deal with it by relevant laws and regulations.

4. System Design and Implementation

4.1. IDcode Coding Rules [13]. Product coding is essential to product traceability and anticounterfeiting. In this paper, the "safe, independent, standardized, and controllable" IDcode two-dimensional code coding system was adopted for product coding. IDcode has passed GB/T 33993-2017 Commodity Two-Dimensional Code Release and is compliant with ISO/IEC 15459 Information Technology-Automatic Identification and Data Acquisition Technology-Unique Identification. As a mechanism to realize the unified management of various object identifications, IDcode is recognized by ISO, CEN, and AIM. The IDcode coding system has three characteristics:

- (1) Identity: every object (person/event/thing) can get a globally unique QR code ID.
- (2) Interconnection: a framework for mapping and linking various codes, coding systems, and application systems has been developed. Interconnections among different regions, networks, systems, and codes have been built.
- (3) Security control: IDcode coding system provides a safe mobile Internet transaction interaction environment for the public. It serves as an effective, credible information security application tool for enterprises and provides a safe QR code environment for society.

As shown in Figure 2, IDcode coding structure is a tree structure and consists of three parts:

- (1) The first part is the user root. It is made up of four nodes. The first root node identifier "MA" is a global code recognized by ISO, CEN, and AIM organizations. The second node is the area code for the region. This code can be found in ISO 3166-1:2013 Code Representation Names of Countries and Its Branches Part 1: Country Codes. The third one is the user code. It is coded by the type of user. The Government Agency User Code is 1001, Code 1002 is for Voluntary Organizations, Code 1003 is for

TABLE 1: The scientific prototype of IPTPSCP.

IPTPSCP should
(i) Allow users to flexibly set the traceability units and nodes, to meet the changes of the traceability units and nodes caused by the production of different types of products and adjustment of the production process
(ii) Adapt to the settings of different traceability units and nodes in various companies producing a variety of important products
(iii) Realize the efficient integration of hardware automatically collecting data with the software automatically processing the information via the embedded models and knowledge
(iv) Achieve the information traceability of user-defined traceability units and nodes. When product quality or safety issues occur, the smallest error subset can be found and related responsibilities can be defined
(v) Allow users to use mobile phones, computers, and other terminals to inquire information through App, WeChat Mini program, Web, etc., and report problematic companies or products
(vi) Be able to meet the need of supervision of relevant government departments and enable us to expose and punish problematic companies or products
(vii) Have certain anticounterfeiting and antichanneling functions
(viii) Reserve interfaces for future implementation of traceability, anticounterfeiting related big data analytics, and other value-added services

Scientific Research Institutes, and Code 1006 is for Certification Institutions. General enterprises and institutions adopt the administrative division codes of various countries or are coded by each country itself. The node can be extended according to the application requirements. The fourth node is the registration sequence number, arranged in order of application.

- (2) The second part is the identification object category, which is divided into two situations: general coding structure and own coding structure. The general coding structure is composed of three nodes, and the number of nodes in the own coding structure is defined by the user.
- (3) The third part is the individual code of the custom identification object. The user can customize the number of nodes and the number of bits per node according to the needs of the application.

Special note: the first part and the second part are separated by the punctuation “.” or symbol “/,” the second part and the third part are separated in the same way, and the nodes in each segment are distinguished by a “.”

In this paper, the second part (identification object category) in the IDcode coding adopts a general coding structure, for example, MA.156.441302.1184/10.29034004.0102/20201214.001, where MA.156.441302.1184 represents the root unit, 10.29034004.0102 represents the category of object, and 20201214.001 represents the individual code of the custom object.

The difference between the QR code based on IDcode coding system and the ordinary QR code is shown in Table 2.

4.2. Four-Color QR Code Generation Algorithm. Ordinary monochrome QR codes are easily forged if someone knows the link of QR code. Therefore, this paper developed a four-color QR code, which is equivalent to adding a color code to the ordinary QR code. If the color code corresponding to the QR code is not known, it cannot be forged in batches. The specific method is as follows. Firstly, the ordinary monochrome QR code is generated via the existing QR code generation algorithm. Then, we use the prebuilt color library to perform color

rendering on the upper left, lower left, upper right, and lower right of the monochrome QR code image to obtain a four-color QR code. There are 7 different colors in the color library, and each color has a color number code; see Table 3 for details. For example, the colorful QR code shown in Figure 3, which is a product anticounterfeiting code of a company in IPTPSCP, is a four-color QR code rendered by the color code sequence “1-3-7-4.” Each color QR code image requires approximately 1.12 K storage space, which takes up very little space. Compared with the black and white QR code, the color QR code is not only beautiful and safer but also does not increase the cost and difficulty of printing or spraying, which is conducive to large-scale promotion and application.

The pseudocode of the function for generating a four-color QR code is described as follows:

```
Function Generate Four Color QRCode(string)
{
  Using Google's ZXing library to generate monochrome QR codes;
  Randomly generate 4-digit color code (each digit is different from the others);
  Traverse each pixel in the monochrome QR code image
  {
    if (pixel position < image width/2 && pixel position-
    < image height/2), then set the pixel color to the color
    represented by the color code of the first digit;
    if (pixel position < image width/2 && pixel position-
    ≥ image height/2), then set the pixel color to the color
    represented by the color code of the second digit;
    if (pixel position ≥ image width/2 && pixel position-
    < image height/2), then set the pixel color to the color
    represented by the color code of the third digit;
    if (pixel position ≥ image width/2 && pixel position-
    ≥ image height/2), then set the pixel color to the color
    represented by the color code of the fourth digit.
  }
  Return to the four-color QR code image.
}
```

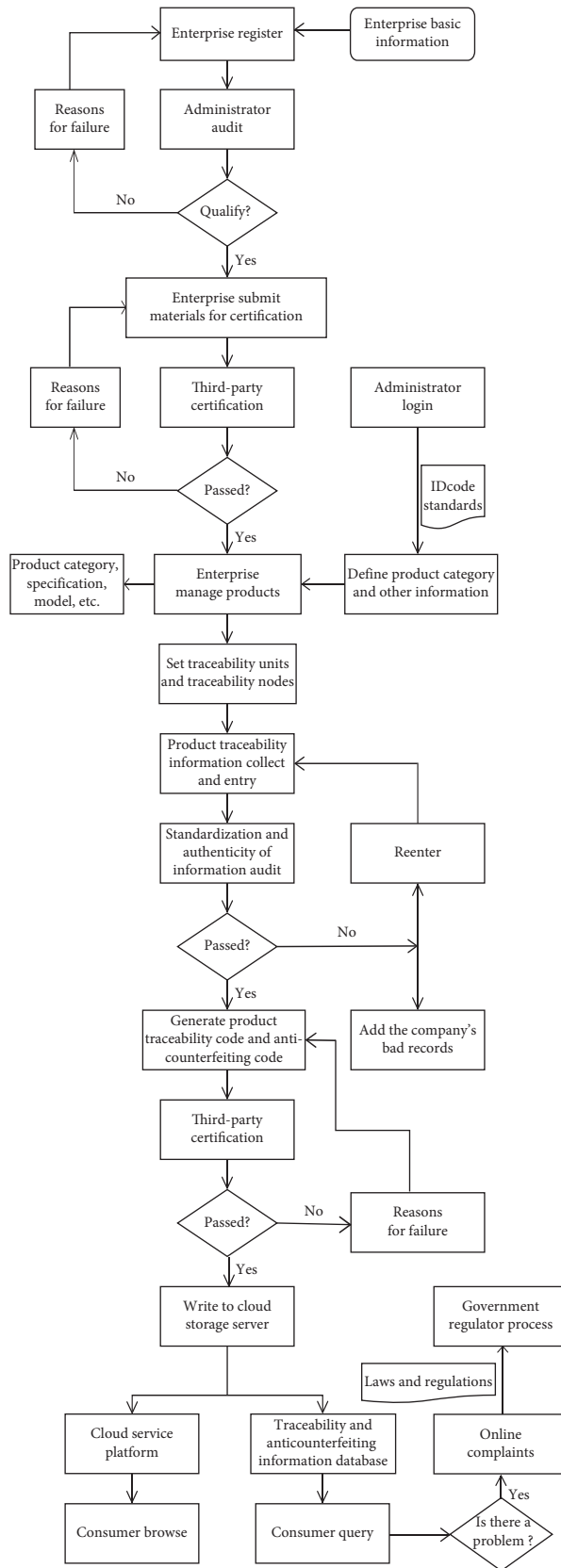



FIGURE 1: IPTPSCP business flowchart.

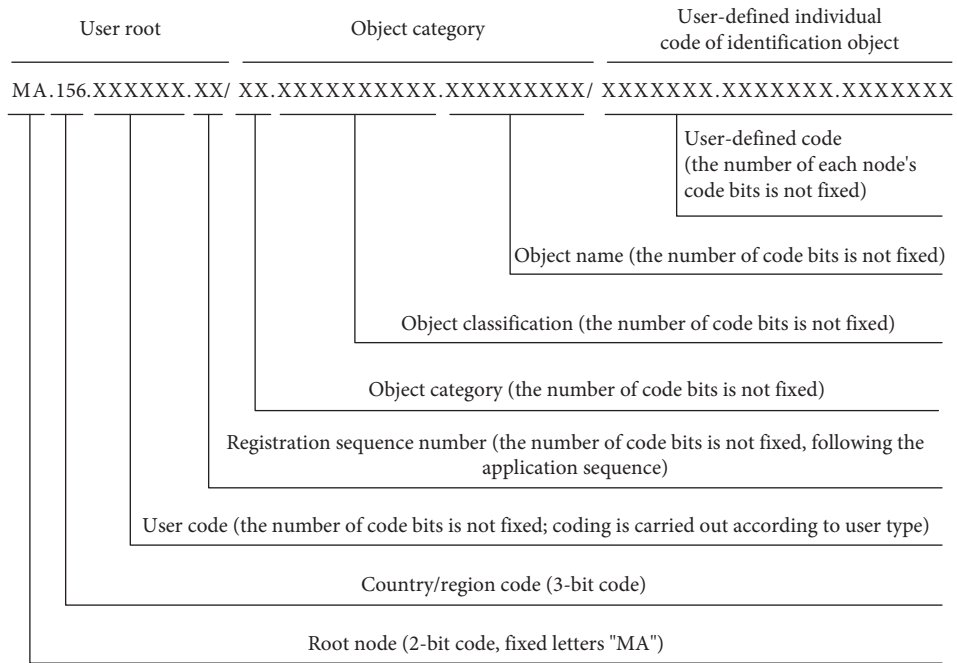


FIGURE 2: Schematic diagram of two-dimensional code identification coding data structure (general coding structure).

TABLE 2: Difference between QR code based on IDcode coding system and the ordinary QR code.

Comparison items	Ordinary QR code	QR code based on IDcode
Product identification	✓	✓
Traceability and other extended applications	✓	✓
Unified identification mechanism		✓
Compatible with multiple coding systems		✓
Safe and reliable		✓
Internationally recognized and accepted		✓
Low cost	✓	✓
Forming standards		✓

TABLE 3: Color library.

Code	Color	RGB	Template
1	Black	(0 0 0)	
2	Red	(255 0 0)	
3	Green	(0 255 0)	
4	Blue	(0 0 255)	
5	Dark red	(131 27 31)	
6	Dark green	(8 98 51)	
7	Orange	(255 165 0)	

4.3. IPTPSCP Technical Architecture. IPTPSCP clients can be divided into web client and mobile client. Consumers can query information by entering the traceability code and anticounterfeiting code string on the web client or scan the QR code image on the mobile client for product traceability and anticounterfeiting queries. The web client and the mobile client are just different in presentation, and the logic of the data layer and business layer is roughly the same. The IPTPSCP technical framework is shown in Figure 4.

4.3.1. Data Layer. The main function of the data layer is to provide storage for structured and unstructured information. The structured data was stored in the MySQL database, the unstructured data was stored in the corresponding system in the form of files, and its path was stored in the database system. For various data, different database servers were used for storage; thereby, a database service group was built. For example, a Redis cache database server was set up to improve system access speed, while a warehouse server that stores both structured and unstructured data was constructed to realize multidimensional data analysis and data mining.

4.3.2. Business Layer. The business layer is mainly composed of IPTPSCP core business logic and unified control components. The former mainly refers to the realization of related businesses, including platform management, enterprise management, and service provider management; the latter mainly refers to the realization of auxiliary functions, such as unified authority control, unified log and audit management, unified system backup and recovery, unified exception handling and alarm management, and



FIGURE 3: An example of four-color QR code.

unified external interface management. They are the basis for the safe operation of the system data and provide conditions for the function expansion of the system. What needs to be pointed out is that using the cloud snapshot service provided by Ali Cloud, a perfect data backup and recovery scheme, was built to avoid data loss caused by sudden failure, system poisoning, or human error.

4.3.3. Control Layer. The control layer is used to process the business related to the access interface; a series of advanced technologies were adopted to ensure that IPTPSCP can still operate efficiently and stably in a high concurrent access status. The purpose of caching is to improve the system access speed and increase the capacity of system processing. Degradation means that when the service has a problem or the service affects the performance of the core process, it needs to be temporarily blocked and restarted after the peak disappears or the problem is solved. Current limiting and asynchronous locking protect the system by limiting the rate and locking of concurrent access or requests, respectively. Restful API is used to achieve front and back end separation, system traffic reduction, and server performance optimization and to prevent security issues such as injection attacks.

4.3.4. Forwarding Layer. The forwarding layer realizes the clustering of application deployment through the combination of hard load and soft load processing. By setting up a backup and establishing a dynamic expansion mechanism, the service provided by the system for users is no longer restricted by the existing resources, and they can be continuously searched and expanded for service resources outside the system. Nginx acts as a proxy server (reverse proxy), forwarding requests from users to different servers, to avoid excessive pressure on the unit server. Static resource CDN acceleration refers to distributing static resources to servers located in computer rooms in multiple geographic locations to achieve nearby access to data, thereby improving access speed.

4.3.5. Application Layer. The application layer is the user GUI access interface. All kinds of users can access IPTPSCP through H5 official website, enterprise App, Platform App, enterprise WeChat Mini program, platform WeChat Mini program, PC official website, etc.

4.4. IPTPSCP Network Topology. IPTPSCP was designed using B/S architecture based on the cloud service model, as shown in Figure 5. The basic product traceability information was automatically collected or entered in the LAN of the production enterprise. After the relevant business processing of the system, the traceability and anticounterfeiting related text information and QR code image information were uploaded to the Ali Cloud database server and Qiniu Cloud storage server via the Internet. Moreover, the system was connected to the data control center of the government supervision department to provide traceability, anticounterfeiting inquiry, and management services for enterprises, consumers, the public, and system managers. The function of the firewall is mainly to discover and deal with the security risks and data transmission problems that may exist during system operation in time.

In each enterprise LAN, the integration of different data acquisition hardware equipment (or devices) with IPTPSCP is crucial. Generally, data acquisition hardware equipment is divided into three types: interface equipment, reserved standard interface equipment, and equipped with dedicated software equipment [36]. The schemes of integrating the three equipment with IPTPSCP are described as follows.

4.4.1. Interface Equipment. This type of equipment does not have any interface and usually only provides observation readings. Therefore, the simplest way to deal with this type of equipment is to provide a pure software entry interface.

4.4.2. Reserve Standard Interface Equipment. Most of these types of equipment have RS232 serial ports or parallel ports, and the parallel ports can be converted into serial ports through customized wiring. There are two mainstream methods for the integration of serial equipment: direct integration and integration by using serial ports server.

4.4.3. Equipped with Dedicated Software Equipment. The characteristic of this type of equipment is that the data has been collected and stored in the workstation, but the storage format is different, usually divided into three types: standard text file format, standard database storage format, and encrypted format. The data collection and integration of this type of equipment can generally be divided into three steps: interception, analysis, and forwarding.

5. System Application and Evaluation

5.1. Case Selection. As an example, a detailed tracking research has been made in a tea production enterprise (abbreviated as enterprise A) in Xinyang city, Henan province, China. Company A is mainly engaged in the

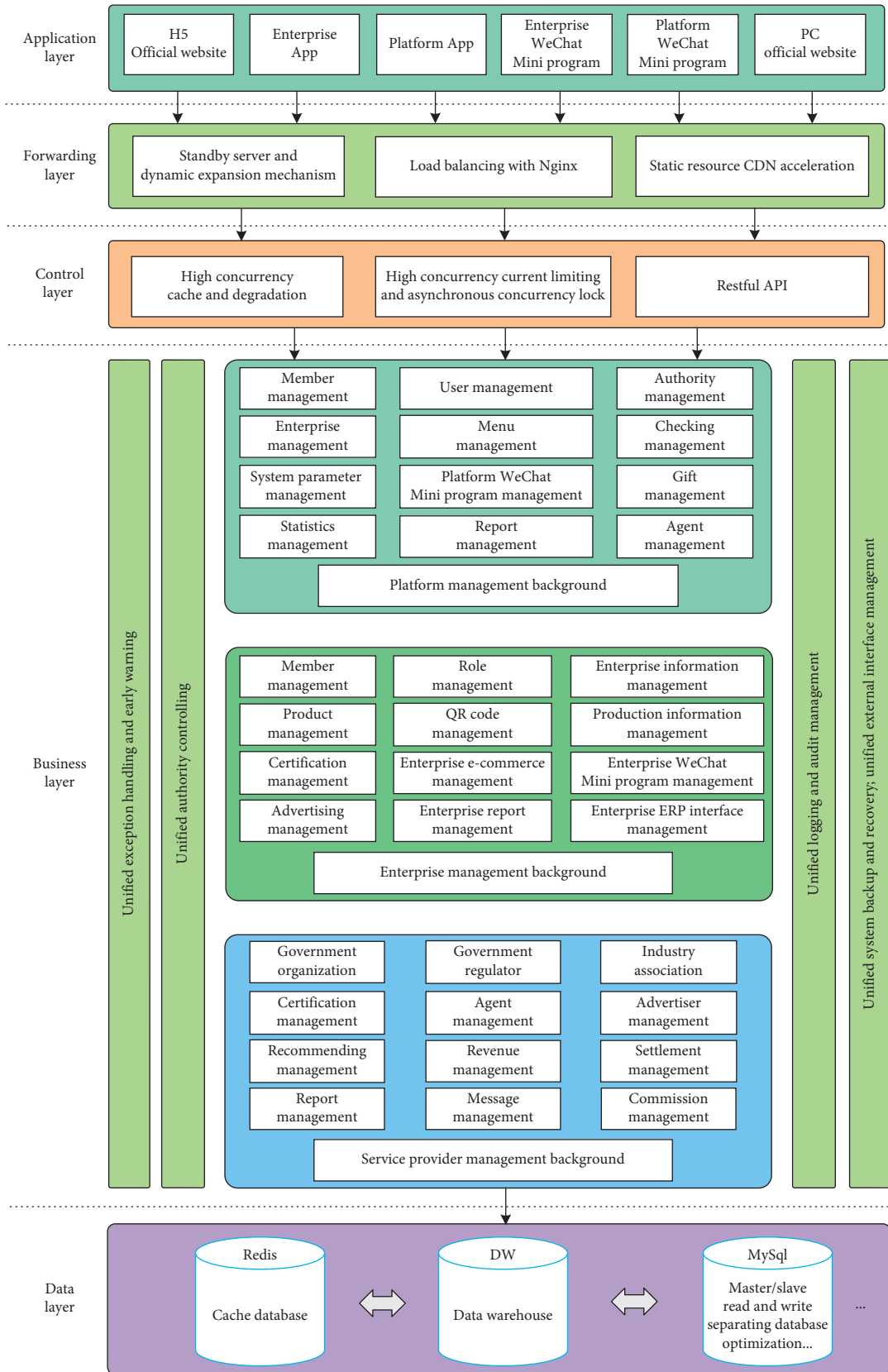


FIGURE 4: IPTPSCP technical architecture diagram.

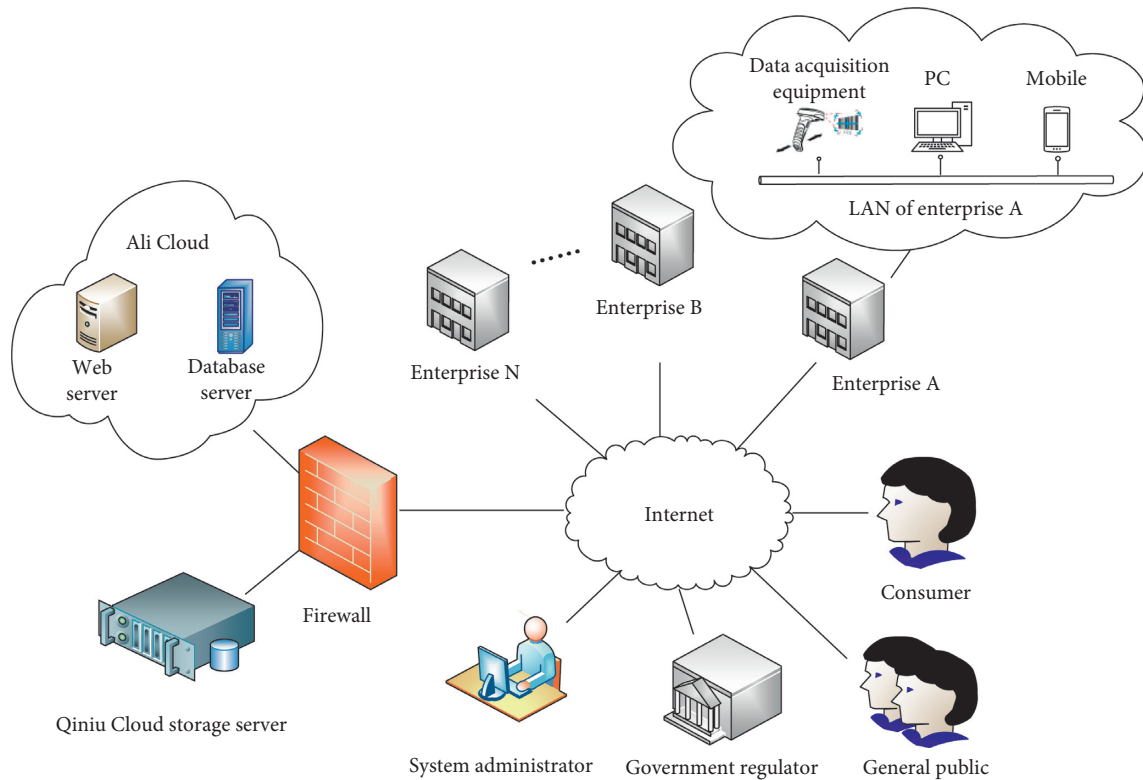


FIGURE 5: IPTPSCP network topology diagram.

processing and sales of Xinyang Maojian green tea, which is one of the top ten famous teas in China. In view of the actual processing and sales of Xinyang Maojian of company A, five traceability units of fresh leaf purchase, processing, packaging, finished product (storage), and sales were selected to record the key information of product circulation. The processing unit is a mechanized operation, which mainly includes screening, spreading, green removing, winnowing, moisture restoration, rolling, carding, and baking. Among them, the four processes of screening, green removing, carding, and baking are important processes that determine the quality and safety of tea. Therefore, after careful consideration and weighing of various influencing factors, company A set the four processes of screening, green removing, carding, and baking as the traceability nodes of the processing unit. In IPTPSCP, the smallest traceability granularity can be flexibly set according to user needs. And each item in data code design has only one code, and one code marks one item. On this basis, according to different packaging carriers, the two-level concatenated code and three-level concatenated code may be set, so as to realize the multilevel association of different packaging carriers.

5.2. System Application. After passing the registration and authentication, enterprise A becomes the IPTPSCP user.

First, the administrators of company A set the traceability units and nodes in the IPTPSCP. As shown in Figure 6, the purchase unit, packaging unit, finished product (storage) unit, and sales unit were each equipped with one traceability node, while the processing unit has four traceability nodes. Figure 7 clearly shows the logical sequence of each traceability node.

Then, the operator can automatically collect or enter the relevant information of each traceability node of the above five traceability units into the system. Taking the processing unit as an example, the information of each traceability node is shown in Figure 8.

Subsequently, the operator can generate the color traceability QR code and the anticounterfeiting QR code, as shown in Figure 9.

Figure 10 is an example of the traceability QR code and anticounterfeiting QR code of a certain specification and batch of Xinyang Maojian tea that have been issued and passed the certification. Consumers can obtain product traceability or anticounterfeiting information by scanning the QR code or inputting the traceability code or anticounterfeiting code string, as shown in Figures 11 and 12, respectively.

5.3. System Evaluation. System evaluation measures the current performance and provides the basis for future



FIGURE 6: Setting up tracing units and tracing nodes.



FIGURE 7: Logical sequence of tracing nodes.

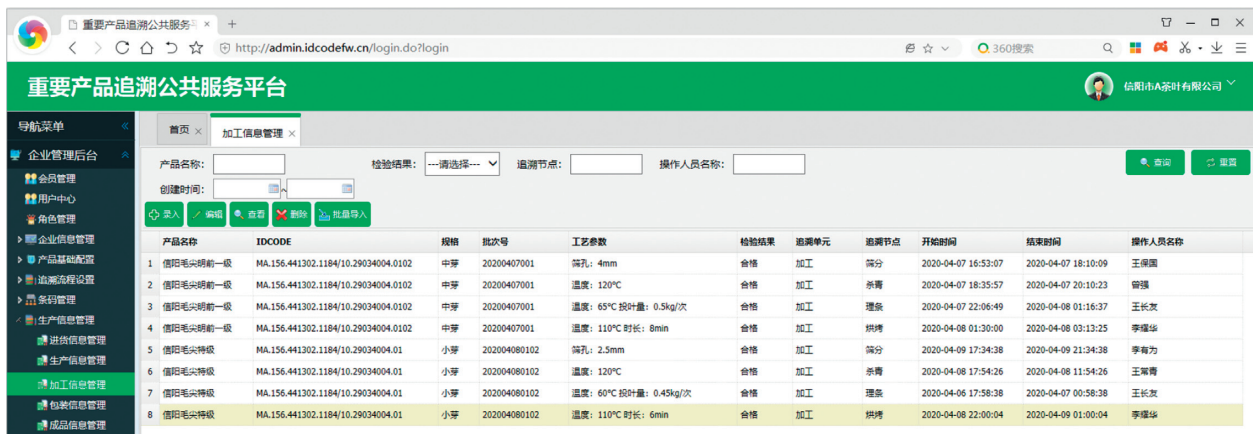


FIGURE 8: Information collection or entry for processing unit.

二级条码	是否发行	追溯码	追溯码(链接)	防伪码	防伪码(链接)	颜色编码
1 9477309941873221	是	9477309941873221	http://m.idcodew.cn/trace_detail.html?code=9477309941873221	nCpFG3C	http://m.idcodew.cn/security.html?code=nCpFG3C	7231
2	是	8491348907118348	http://m.idcodew.cn/trace_detail.html?code=8491348907118348	myIFDxE	http://m.idcodew.cn/security.html?code=myIFDxE	5241
3	是	5555051962442522	http://m.idcodew.cn/trace_detail.html?code=5555051962442522	WgkyZF90	http://m.idcodew.cn/security.html?code=WgkyZF90	5476
4	是	7326481843489412	http://m.idcodew.cn/trace_detail.html?code=7326481843489412	udKMhRah	http://m.idcodew.cn/security.html?code=udKMhRah	3214
5 4979126450373885	是	4979126450373885	http://m.idcodew.cn/trace_detail.html?code=4979126450373885	qVvH8iu	http://m.idcodew.cn/security.html?code=qVvH8iu	7216
6	是	1284442144008691	http://m.idcodew.cn/trace_detail.html?code=1284442144008691	hK0Iej2H	http://m.idcodew.cn/security.html?code=hK0Iej2H	3475
7	是	0845138231788988	http://m.idcodew.cn/trace_detail.html?code=0845138231788988	YUhhKp1	http://m.idcodew.cn/security.html?code=YUhhKp1	5163
8	是	7287042102022310	http://m.idcodew.cn/trace_detail.html?code=7287042102022310	pFcia2M	http://m.idcodew.cn/security.html?code=pFcia2M	6173
9 5236561713339440	是	5236561713339440	http://m.idcodew.cn/trace_detail.html?code=5236561713339440	acrzvbj	http://m.idcodew.cn/security.html?code=acrzvbj	7412
10	是	8938101862183658	http://m.idcodew.cn/trace_detail.html?code=8938101862183658	Lgthd12Q	http://m.idcodew.cn/security.html?code=Lgthd12Q	2573
11	是	659966165999021	http://m.idcodew.cn/trace_detail.html?code=659966165999021	fskqNCT0	http://m.idcodew.cn/security.html?code=fskqNCT0	2461
12	是	7906527849732225	http://m.idcodew.cn/trace_detail.html?code=7906527849732225	tdq5cAcR	http://m.idcodew.cn/security.html?code=tdq5cAcR	1532
13 5061236621312789	是	5061236621312789	http://m.idcodew.cn/trace_detail.html?code=5061236621312789	bhnEwJg3	http://m.idcodew.cn/security.html?code=bhnEwJg3	6413
14	是	358450209883154	http://m.idcodew.cn/trace_detail.html?code=358450209883154	wIqmFJk	http://m.idcodew.cn/security.html?code=wIqmFJk	7146
15	是	298388095688989	http://m.idcodew.cn/trace_detail.html?code=298388095688989	mHEKkuO	http://m.idcodew.cn/security.html?code=mHEKkuO	4273
16	是	507187985406403	http://m.idcodew.cn/trace_detail.html?code=507187985406403	g6HvIAz	http://m.idcodew.cn/security.html?code=g6HvIAz	5723
17 565728643109778	是	565728643109778	http://m.idcodew.cn/trace_detail.html?code=565728643109778	HGHQFIQ1	http://m.idcodew.cn/security.html?code=HGHQFIQ1	2461

FIGURE 9: Generation of tracing code and anticounterfeiting code.



FIGURE 10: Example of traceability QR code (a) and anticounterfeiting QR code (b).

improvement of the IPTPSCP. The system evaluation of IPTPSCP was implemented after it ran normally for 11 months (from March 2020 to January 2021) to estimate the technological capacity, performance, and system utilization. Three researchers from Guangdong University of Technology and five specialists from the platform settled enterprises (including enterprise A) were invited to participate in an evaluation committee in order to draw up an evaluation framework for IPTPSCP based on the views of system development and maintenance, user experience, and external influences.

System evaluation was divided into three main steps. Firstly, the evaluation content (including qualitative and quantitative indicators) was determined. Then, the

relevant data (including the data collected by the evaluators and the data automatically recorded by IPTPSCP) were organized and analyzed. Finally, the evaluators tested the platform, discussed the implementation effects of IPTPSCP, and gave the evaluation results. The effectiveness analysis before and after IPTPSCP implementation is shown in Table 4. The evaluators also analyzed and suggested some changes for IPTPSCP. The system improvement suggestions included (1) traceability information security on Web, App, and WeChat Mini program, (2) load balancing during concurrent access by multiple users, and (3) fine-tuning of the system menu and GUI interface design.



FIGURE 11: Example of traceability information (partial).



FIGURE 12: Example of anticounterfeiting information.

TABLE 4: Effectiveness analysis before and after IPTPSCP implementation.

No.	Content	Before IPTPSCP implementation	After IPTPSCP implementation
1	Management precision	Day/week	Minute/second
2	Data acquisition	Incomplete artificial collection	Automatic or semiautomatic collection
3	Traceability	Fuzzy	Precise positioning
4	Anticounterfeiting	None	Accurately identify the authenticity of goods
5	Antifleeing	None	Good prevention of fleeing goods
6	Quality analysis	Empirically with delay	Accurate, real time
7	Multidimensional statistical analysis	None	Multidimensional data analysis based on data warehouse
8	Development and deployment efficiency	None	Code reusable, mature software framework, cloud service model
9	Maintainability	None	Modularity, replaceable code, and nodes
10	User-friendliness	None	Well-designed interface, easy to use
11	Information security	Paper archives, easily damaged or lost	Database backup and recovery
12	Information sharing	Producer only	Producer, consumers, and government regulators
13	Average response time	None	<0.6 second
14	Number of concurrent users	None	≥1000
15	Queries per second	None	>2600

6. Discussion and Conclusions

IPTPSCP that utilizes QR code technology provides a significant opportunity to ensure production quality and safety. This paper analyzed the business flow of IPTPSCP and elaborated the development and implementation of IPTPSCP. Compared with the traditional system, IPTPSCP achieves a cross-communication information flow between managers, workers, consumers, and government regulators. The system test and experiment evaluation proved itself as an effective production quality management tool that leads to a flexible setting of various production workflow monitoring and recording. And now, IPTPSCP has been successfully applied in many enterprises.

To apply IPTPSCP, enterprises do not need to invest a lot of software development, deployment, and maintenance costs. Enterprises only need to invest a small amount of money to purchase or develop some hardware for data acquisition. Through the interviews and statistical analysis of the system implementation of more than 10 enterprises stationed in IPTPSCP, it can be obtained that the overall efficiency of data collection and monitoring has increased by about 13%, and the cost has been reduced by about 36%. As a result, IPTPSCP does not only increase economic benefits for enterprises but also improve consumer confidence in production quality and safety. Moreover, it also provides convenient conditions for government regulators to conduct product quality and safety supervision.

This work can be extended for future research in many directions. For example, IPTPSCP is expected to be integrated into an e-commerce system, which enables consumers to query the traceability information of the selected product in real time when shopping online. The author's team has begun preliminary work on this subject. In addition, with the evergrowing and changing data in the IPTPSCP, a big data analysis platform can be built to provide

enterprises, consumers, and government regulators with in-depth value-added services, such as product brand analysis, analysis, and mining of industry data. This will be a very meaningful thing.

Data Availability

No data were used in this study.

Conflicts of Interest

The authors declare that they have no conflicts of interest.

Acknowledgments

The authors would like to acknowledge the support from Huizhou University Scientific Research Special Fund Project (IOT Information Technology Laboratory Project, no. 20180407).

References

- [1] M. M. Aung and Y. S. Chang, "Traceability in a food supply chain: safety and quality perspectives," *Food Control*, vol. 39, pp. 172–184, 2014.
- [2] T. Kelepouris, K. Pramataris, and G. Doukidis, "RFID-enabled traceability in the food supply chain," *Industrial Management & Data Systems*, vol. 107, no. 1-2, pp. 183–200, 2007.
- [3] L. Tarjan, I. Šenk, S. Tegeltija, S. Stankovski, and G. Ostojic, "A readability analysis for QR code application in a traceability system," *Computers and Electronics in Agriculture*, vol. 109, pp. 1–11, 2014.
- [4] Y. Cao, X. Liu, C. Guan, and B. Mao, "Implementation and current status of food traceability system in Jiangsu China," *Procedia Computer Science*, vol. 122, pp. 617–621, 2017.
- [5] M. Heyder, L. Theuvsen, and T. Hollmann-Hespos, "Investments in tracking and tracing systems in the food industry: a PLS analysis," *Food Policy*, vol. 37, no. 1, pp. 102–113, 2012.

- [6] D. Paunescu, W. J. Stark, and R. N. Grass, "Particles with an identity: tracking and tracing in commodity products," *Powder Technology*, vol. 291, pp. 344–350, 2016.
- [7] T. Pizzuti and G. Mirabelli, "The global track & trace system for food: general framework and functioning principles," *Journal of Food Engineering*, vol. 159, pp. 16–35, 2015.
- [8] H. Bai, G. Zhou, Y. Hu et al., "Traceability technologies for farm animals and their products in China," *Food Control*, vol. 79, pp. 35–43, 2017.
- [9] J. Qian, X. Du, B. Zhang, B. Fan, and X. Yang, "Optimization of QR code readability in movement state using response surface methodology for implementing continuous chain traceability," *Computers and Electronics in Agriculture*, vol. 139, pp. 56–64, 2017.
- [10] B. Fan, J. Qian, X. Wu et al., "Improving continuous traceability of food stuff by using barcode-RFID bidirectional transformation equipment: two field experiments," *Food Control*, vol. 98, pp. 449–456, 2019.
- [11] S. Violino, F. Pallottino, G. Sperandio et al., "A full technological traceability system for extra virgin olive oil," *Foods*, vol. 9, no. 5, p. 624, 2020.
- [12] R. Badia-Melis, P. Mishra, and L. Ruiz-García, "Food traceability: new trends and recent advances. a review," *Food Control*, vol. 57, pp. 393–401, 2015.
- [13] ZIIOT, International Two-dimensional Code Object Identifier System (IDcode) White Papers, 2018, <http://www.ziiot.org.cn/Web/Content.aspx?c=797&m=280>.
- [14] P. Olsen and M. Borit, "How to define traceability," *Trends in Food Science & Technology*, vol. 29, no. 2, pp. 142–150, 2013.
- [15] T. Moe, "Perspectives on traceability in food manufacture," *Trends in Food Science & Technology*, vol. 9, no. 5, pp. 211–214, 1998.
- [16] F. Dabbene, P. Gay, and C. Gay, "Traceability issues in food supply chain management: a review," *Biosystems Engineering*, vol. 120, pp. 65–80, 2014.
- [17] J. A. Alfaro and L. A. Rábade, "Traceability as a strategic tool to improve inventory management: a case study in the food industry," *International Journal of Production Economics*, vol. 118, no. 1, pp. 104–110, 2009.
- [18] N. Mai, S. Gretar Bogason, S. Arason, S. Víkingur Árnason, and T. Geir Matthiasson, "Benefits of traceability in fish supply chains—case studies," *British Food Journal*, vol. 112, no. 9, pp. 976–1002, 2010.
- [19] J.-P. Qian, X.-T. Yang, X.-M. Wu, L. Zhao, B.-L. Fan, and B. Xing, "A traceability system incorporating 2 D barcode and RFID technology for wheat flour mills," *Computers and Electronics in Agriculture*, vol. 89, pp. 76–85, 2012.
- [20] X. Wang, D. Fu, G. Fruk, E. Chen, and X. Zhang, "Improving quality control and transparency in honey peach export chain by a multi-sensors-managed traceability system," *Food Control*, vol. 88, pp. 169–180, 2018.
- [21] L. Qi, J. Zhang, M. Xu, Z. Fu, W. Chen, and X. Zhang, "Developing WSN-based traceability system for recirculation aquaculture," *Mathematical and Computer Modelling*, vol. 53, no. 11–12, pp. 2162–2172, 2011.
- [22] G. Alfian, J. Rhee, H. Ahn et al., "Integration of RFID, wireless sensor networks, and data mining in an e-pedigree food traceability system," *Journal of Food Engineering*, vol. 212, pp. 65–75, 2017.
- [23] Y. Q. Peng, L. X. Zhang, Z. X. Song, J. Yan, X. X. Li, and Z. B. Li, "A QR code based tracing method for fresh pork quality in cold chain," *Journal of Food Process Engineering*, vol. 41, no. 4, Article ID e12685, 2018.
- [24] G. D. Gao, K. Xiao, and M. M. Chen, "An intelligent IoT-based control and traceability system to forecast and maintain water quality in fresh water fish farms," *Computers and Electronics in Agriculture*, vol. 166, Article ID 105013, 2019.
- [25] S. S. Hu, S. Huang, J. Huang, and J. F. Su, "Blockchain and edge computing technology enabling organic agricultural supply chain: a framework solution to trust crisis," *Computers & Industrial Engineering*, vol. 153, Article ID 107079, 2021.
- [26] K. M. Karlsen, K. A.-M. Donnelly, and P. Olsen, "Granularity and its importance for traceability in a farmed salmon supply chain," *Journal of Food Engineering*, vol. 102, no. 1, pp. 1–8, 2011.
- [27] J. Hu, X. Zhang, L. M. Moga, and M. Neculita, "Modeling and implementation of the vegetable supply chain traceability system," *Food Control*, vol. 30, no. 1, pp. 341–353, 2013.
- [28] M. Thakur and K. A.-M. Donnelly, "Modeling traceability information in soybean value chains," *Journal of Food Engineering*, vol. 99, no. 1, pp. 98–105, 2010.
- [29] T. B. Chen, K. F. Ding, S. K. Hao et al., "Batch-based traceability for pork: a mobile solution with 2D barcode technology," *Food Control*, vol. 107, Article ID 106770, 2020.
- [30] K. Liang, X. Chen, R. He et al., "Development and parameter optimization of automatic separation and identification equipment for grain tracing systems based on grain tracers with QR codes," *Computers and Electronics in Agriculture*, vol. 162, pp. 709–718, 2019.
- [31] Y. Cai, X. W. Li, R. M. Wang, Q. Yang, P. Li, and H. Hu, "Quality traceability system of traditional Chinese medicine based on two dimensional barcode using mobile intelligent technology," *PLoS One*, vol. 11, no. 10, Article ID e0165263, 2016.
- [32] B. D. Li, Y. Yang, J. F. Su, N. Zhang, and S. Wang, "Two-sided matching model for complex product manufacturing tasks based on dual hesitant fuzzy preference information," *Knowledge-Based Systems*, vol. 186, Article ID 104989, 2019.
- [33] E. A. Fernandes, G. A. Sarriés, M. A. Bacchi, Y. T. Mazola, C. L. Gonzaga, and S. R. V. Sarriés, "Trace elements and machine learning for Brazilian beef traceability," *Food Chemistry*, vol. 333, Article ID 127462, 2020.
- [34] Y.-S. Bong, J.-S. Ryu, S.-H. Choi, M.-R. La, and K.-S. Lee, "Investigation of the geographical provenance of the beer available in South Korea using multielements and isotopes," *Food Control*, vol. 60, pp. 378–381, 2016.
- [35] H. Zhao, S. Zhang, and Z. Zhang, "Relationship between multi-element composition in tea leaves and in provenance soils for geographical traceability," *Food Control*, vol. 76, pp. 82–87, 2017.
- [36] J. Tang, "Research and implementation of a data acquisition scheme for heterogeneous device interfaces," *Software Engineering*, vol. 20, no. 5, pp. 36–39, 2017.

Research Article

Evaluation Model of Cable Insulation Life Based on Improved Fuzzy Analytic Hierarchy Process

Lei Li ¹, Xian Min Ma,¹ and Wei Guo ²

¹College of Electrical and Control Engineering, Xi'an University of Science and Technology, Xi'an 710054, China

²College of Mechanical Engineering, Xi'an University of Science and Technology, Xi'an 710054, China

Correspondence should be addressed to Lei Li; liqieru@xust.edu.cn

Received 17 December 2020; Revised 17 March 2021; Accepted 5 May 2021; Published 24 May 2021

Academic Editor: Ming Bao Cheng

Copyright © 2021 Lei Li et al. This is an open access article distributed under the Creative Commons Attribution License, which permits unrestricted use, distribution, and reproduction in any medium, provided the original work is properly cited.

Since the human society entered the electrification era, people's work, life, and even the production and development of various industries in society are inseparable from the supply of electricity. The purpose of this paper is to establish a cable insulation life evaluation model based on the improved fuzzy analytic hierarchy process to test the current insulation characteristics and life of various types of cables, so as to ensure the quality of power supply and safe production of power. This paper first understands the cable insulation characteristics test process and electrical power-related knowledge through a large number of literature studies and consultation with power grid professionals. Then this paper combines the theoretical research and improvement of the fuzzy analytic hierarchy process based on the actual situation of the cable insulation characteristics, thereby constructing the cable insulation life evaluation model. In this evaluation model, this paper combines the fuzzy comprehensive evaluation method and the analytic hierarchy process as well as the actual situation of the cable characteristic test to analyze and predict the insulation life of the cable. Finally, the linear test and reliability estimation of the experimental results are carried out, and the application of this evaluation model is extended to the evaluation of insulation life of other types of cables. Based on this, this paper proposes a cable insulation life evaluation model based on the improved fuzzy analytic hierarchy process. This model combines the Weibull model and the Arrhenius model commonly used in the assessment of cable insulation aging life and the improved fuzzy analytic hierarchy process. Experiments have proved that, within a certain range, temperature factors have a significant impact on the cable insulation life. For example, when the temperature is below 55°C, the insulation life of the cable is usually 30 to 50 years. However, the evaluation model of the improved fuzzy analytic hierarchy process in this paper has much higher accuracy in evaluating cable insulation life than other life evaluation methods.

1. Introduction

1.1. Background and Significance. Electricity is the most important energy source for social production and development. Only a safe and stable electric power supply and a high-quality and reliable power supply environment can escort the vigorous development of production in various industries. The most important factor influencing power supply safety is the insulation characteristic life of the cable material. Testing the performance of the cable through scientific physical regulation and chemical reaction is a powerful measure to evaluate the life of the cable and improve the safety of the power supply [1]. Although the most important function of cables is to provide excellent conductors for power

transmission, there are huge differences in the working environment of cables in different industries. In particular, temperature, humidity, electromagnetic fields, and other environmental factors have relatively high power supply performance and insulation life [2]. Therefore, in addition to the environmental external forces and various unexpected disasters, the evaluation of the insulation performance life of the cable itself is also extremely critical in the safeguard measures for the power supply safety environment. Studies have shown that the main influencing factor of cable insulation life is the process of cable aging, which is divided into electrical aging, thermal aging, water aging, and mechanical aging [3, 4]. Because many companies often lead to overloaded operation of cables in the process of using cables for

power supply, this easily accelerates the electrical aging process of the cables and shortens the insulation life of the cables [5, 6]. In addition, changes in temperature and humidity in some special power supply production environments may also affect the thermal aging and water aging processes of the cable, which in turn affects the insulation life of the cable [7]. Therefore, this paper explores that the insulation life evaluation model of the cable should consider the insulation life test situation of the cable in various working environments as much as possible.

1.2. Related Research at Home and Abroad. Regarding the life evaluation of cable insulation aging, there have been quite in-depth studies at home and abroad, and rich research results have been obtained. For example, Santhosh performs accelerated thermal and radiation aging on control cable insulation materials used in nuclear power plants and uses oxidation induction time (OIT) and oxidation induction temperature (OITp) to evaluate the degradation of cable insulation properties due to thermal and radiation aging. Studies have found that factors such as long-term exposure and temperature rise will eventually lead to a decline in cable insulation performance [8]. In order to study the life of the cable insulation, Kim has artificially aged the samples under multiple stresses of heat and electricity. The multistress aging samples were evaluated by measuring the pulse breakdown voltage at a high temperature of 85°C. Experiments have shown that thermal aging will be regarded as one of the main factors in the life evaluation of cable insulation materials, while the effect of electrical degradation is poor [9]. However, the study did not explore the effect of humidity changes on the water aging of the cable. Seguchi et al. explain the evaluation behavior of XLPE insulation by using two popular evaluation methods, partial discharge (PD), and dielectric response (DR) measurements. For local evaluation, they proposed a comparative study of surface discharge and its characteristics under normal power frequency (50 Hz) and extremely low frequency (0.1 Hz) excitation [10]. However, the degradation of the cross-linked polyethylene (XLPE) insulated power cable material due to various factors during the experiment cannot be avoided. Hinderliter believes that the degradation of polymer sheaths and the potential for insulation of medium and low voltage power cables represent an extension of the life of nuclear power plants, and its mechanical understanding of the degradation process is essential to confidently predict the functional properties and safety margins of dielectrics. Studies have shown that the reduced exposure performance of cable sheaths and insulation materials in humid or immersed environments is due to their possible interaction with the pores in the polymer [11]. However, this study only explored the impact of medium and low voltage power on the life of cable insulation and did not make accurate assessments and corresponding improvement measures.

There are also important research conclusions on the assessment of cable insulation life in China. Studies have found that the long-term performance of cable insulation has been severely challenged by the technological advancement of high-voltage DC power lines for large-capacity long-distance

submarine or underground transmission worldwide. In order to quantify the relationship between the applied stress (electrical, thermal, and mechanical stress) and the failure time (lifetime), Zuo et al. proposed several competing life expressions based on different mechanisms and the average life data through laboratory tests. The fitting model expression can compare the different durability characteristics of insulation material candidates and study their performance in a given cable system [12]. However, this expression still has certain limitations and has not been widely adopted. Su et al. used electrical tree testing to determine the withstand voltage coefficient of solid insulating materials. In the tree test with a needle-plane electrode system, the start-up time of the tree is measured under both progressive and constant voltage, and the residual voltage method is used to determine the withstand voltage coefficient [13]. However, the measured value is affected by the test conditions, and its effectiveness still needs further proof. Zhou et al. proposed a new method of online insulation dielectric loss monitoring based on insulation layer separation as an important index test method for cable insulation health [14]. However, there are still no reports of any successful online technology for this method. Chang et al. proposed a decision tree method for judging the initial and final stages of insulation degradation of preformed power cable joints with air gaps and void defects. Using cluster theory, this decision tree method is applied to evaluate the transition of insulation status. According to the Gini coefficient and information gain of the decision tree algorithm, the insulation state diagnosis rule is derived [15].

1.3. Innovations in This Paper. This paper studies the influence of the temperature and conductivity stress coefficient of the cable insulation material on the life and reliability of the cable and conducts the evaluation experiment of the cable insulation life based on the principle of the acceleration of electric thermal aging. On the basis of the balance between the content analysis and evaluation principles of the existing cable insulation life evaluation, a cable insulation life evaluation index system was established, and the insulation life evaluation was carried out using the fuzzy analytic hierarchy process [16, 17]. Through the quantification process, the existing cable insulation characteristics are scientifically evaluated, and reference evaluation data are provided for the insulation characteristics of various types of cables under the influence of internal and external factors in different working environments [18, 19]. This paper combines the advantages of the traditional analytic hierarchy process and fuzzy analytic hierarchy process to evaluate the insulation life of the cable from various influencing factors. Finally, based on the comprehensive analysis, the evaluation and prediction of the cable insulation life are given. The experiment shows that the evaluation result of this method is more accurate than other methods [20].

2. Evaluation Model of Cable Insulation Life Based on Fuzzy Analytic Hierarchy Process

2.1. Commonly Used Cable Insulation Aging Assessment Models. In the early days when cables were used in power

supply environments, there was no standardized evaluation method for the insulation life of cables. At that time, electric power production enterprises all regulated the service life of cables based on practical experience and regular inspections. The insulation life of cables was basically the same as the service life of cables. Therefore, domestic and foreign electrical engineering scholars have carried out a large number of simulation experiments on cable insulation aging and proposed several standard cable insulation aging assessment methods. The most famous of them are the conventional evaluation method and the accelerated evaluation method. As the name suggests, the conventional evaluation method is to test the insulation aging life of conventional cables through sampling tests. However, the test cycle of this method is too long and the error is large, and it has been gradually eliminated [21]. This paper uses an accelerated assessment method and a series of cable insulation life assessment models. The commonly used insulation life assessment models for this method are the Weibull model and the Arrhenius model. The principle of the Weibull model is the theory of breaking down the weakest point of the cable insulation material to make the cable insulation failure. This theory is also called the “weakest ring principle” [22]. According to the characteristics of the cable insulation material, the Weibull model of the cable insulation breakdown can be obtained as shown in

$$P(E, t) = 1 - e^{-c(E/E_0)^\alpha (t/t_0)^\beta}. \quad (1)$$

In formula (1), P is the probability that the cable insulation material will be broken down under the action of an electric field intensity of E in time t . α and β , respectively, represent the relevant parameters of the probability density function of the cable insulation material breakdown, the breakdown electric field strength, and the action time. c is the constant coefficient in the function, and t_0 represents the minimum expected value of the cable insulation life under the action of an electric field of E_0 intensity. Assuming that the electric field breakdown probability of the same cable insulation material is the same, the insulation aging life equation can be obtained as shown in

$$\begin{aligned} C_1 &= 1 - e^{-cE^\alpha t^\beta}, \\ C_2 &= E^n t, \quad n = \frac{\alpha}{\beta}. \end{aligned} \quad (2)$$

In formula (2), C_1 and C_2 are related constants, and n represents the insulation aging life index. The value of the insulation aging life index can be calculated by simulating the relevant data of the cable insulation aging experiment, so as to obtain the evaluation value of the cable insulation life under different intensities. The above Weibull model is mainly aimed at the cable insulation life under the influence of electrical aging factors of the cable material. Another important factor affecting the aging of the cable insulation is thermal aging. The commonly used insulation life evaluation model is the Arrhenius model [23]. This model studies the relationship between temperature and the rate of chemical reaction of the cable insulation material. According to the

chemical reaction kinetic curve, the Arrhenius equation for cable aging life evaluation can be obtained as shown in

$$C(T) = k_0 e^{-E_\alpha/RT}. \quad (3)$$

In formula (3), $C(T)$ represents the chemical reaction rate constant of the cable insulation material, k_0 represents the prefactor of the chemical reaction, and E_α represents the activation energy of the chemical reaction, and its unit is kJ/mol. R and T represent gas constant and thermodynamic temperature, respectively. The unit of gas constant is J/(K·mol), and the unit of thermodynamic temperature is K. It is assumed that the cable insulation material reaches the same insulation failure standard under different thermodynamic temperatures and different chemical reaction rate constants. According to the chemical reaction kinetic curve model, the thermal aging life evaluation equation of the cable insulation chemical reaction can be obtained.

$$\begin{aligned} F(t) &= k_0 e^{-E_\alpha/RT}, \\ \ln t &= k + \frac{E_\alpha}{RT}. \end{aligned} \quad (4)$$

In formula (4), $F(t)$ is the insulation failure standard achieved by the cable insulation under different chemical reaction times t , and k is a constant coefficient related to the aging performance of the cable insulation. The Arrhenius model reflects the relationship between the aging life t of the cable insulation material and the aging temperature T and is a commonly used evaluation model in the accelerated evaluation experiment of the cable aging life evaluation.

2.2. Determine the Evaluation Index System of Cable Insulation Life. To establish a cable insulation life evaluation model based on fuzzy analytic hierarchy process, first determine the evaluation index system of cable insulation life. Then compare the relative importance of the indicators of each evaluation level of the model with the indicators of the previous level to determine the weight of the influencing factors of each level. This paper uses the judgment matrix to achieve this goal, that is, to evaluate the importance of a certain criterion level index defined in the cable insulation aging life assessment model to the target level index that needs to be analyzed and evaluated [24, 25]. This hierarchical model of message evaluation is to compare the importance of indicators at the criterion level and the target level. In this paper, the importance of factors in the standard level is measured on a scale of 1–9. The comparison of the importance of the index system in this paper is shown in Table 1. According to the defined importance evaluation rules, the element values of the matrix are listed separately to obtain the judgment matrix. The singular grades ranging from grade 1 to grade 9 in the importance evaluation grades, namely, grades 1, 3, 5, 7, and 9 respectively, indicate that the former is more and more important to the latter. Levels 2, 4, 6, and 8 represent the intermediate values of the adjacent evaluation levels corresponding to the above singular importance levels.

TABLE 1: Analytic hierarchy process importance index.

Index value	Indicator meaning (compare two indicators)
1	Have the same importance
3	The former is slightly more important than the latter
5	The former is fairly more important than the latter
7	The former is especially more important than the latter
9	The former is extremely more important than the latter
2, 4, 6, 8	The intermediate value of the above adjacent odd judgment
Reciprocal	The reciprocal of the above index indicates the importance of the latter to the former

According to the principle of the fuzzy analytic hierarchy process, this paper establishes a multilevel index system for cable insulation performance evaluation. The insulation performance of the cable is mainly reflected by the length of time the cable maintains its normal performance in the current working environment. This is also an important indicator for the evaluation of the cable insulation life. This paper divides the cable insulation performance into excellent, good, normal, poor, and so on. Combining these five levels with the quantitative index standards of cable health value and then through the mapping relationship between the indicators, the following cable insulation evaluation index set can be obtained:

$$V = (v_1, v_2, v_3, v_4, v_5) = (A, B, C, D, E). \quad (5)$$

In formula (5), V represents the cable insulation performance evaluation score set, and the five elements in the evaluation score set represent five evaluation score levels of excellent, good, normal, poor, and poor. Then the mapping relationship between the vector composed of the evaluation score set and the evaluation matrix is shown in

$$\text{CCE} = V * C^T = f(x_1, x_2, x_3, x_4, x_5). \quad (6)$$

In formula (6), CCE is the English abbreviation for comprehensive evaluation of cables and is used here to express the comprehensive evaluation of cable insulation performance. C^T represents the transposed matrix of the fuzzy comprehensive evaluation matrix. According to the fuzzy analytic hierarchy process and the evaluation matrix, the membership matrix can be further calculated. The membership degree matrix is often used in the comprehensive analysis of the indicators of the analytic hierarchy process. The maximum membership degree matrix is used to evaluate the index with higher performance as the trend of the evaluation index is larger. Conversely, the minimum membership degree matrix is used to evaluate the index with higher performance as the trend is smaller. Its evaluation principle is

$$\phi(x) = \begin{cases} 1, & x < \alpha, \\ \frac{x - \alpha}{\beta - \alpha}, & \alpha \leq x < \beta, \\ 0, & x \geq \beta. \end{cases} \quad (7)$$

According to the characteristics of cable insulation aging life, this paper chooses the principle of maximum membership degree. Obviously, the larger the comprehensive evaluation index of the cable, the higher the insulation performance and the longer the insulation life. In formula (7), $\phi(x)$ represents the maximum membership function, and α and β are the two critical levels of the comprehensive cable evaluation index.

2.3. Establish a Judgment Matrix and Calculate Indicator Weights. The evaluation of cable insulation life can start from the physical, chemical, and electrical properties of cable materials, which can extend 10 evaluation indexes of cable, such as dielectric loss, maximum internal electric field strength, impurity material, insulation resistance, insulation stress, insulation thickness, internal temperature, voltage load, external environment humidity, and elongation at break [26]. According to the evaluation index system of cable insulation life established above, a judgment matrix for the evaluation of cable insulation life is constructed.

$$M = \begin{bmatrix} Y & A & B & C & D & E \\ a & x_{11} & x_{12} & x_{13} & x_{14} & x_{15} \\ b & x_{21} & x_{22} & x_{23} & x_{24} & x_{25} \\ c & x_{31} & x_{32} & x_{33} & x_{34} & x_{35} \\ \dots & \dots & \dots & \dots & \dots & \dots \\ g & x_{n1} & x_{n2} & x_{n3} & x_{n4} & x_{n5} \end{bmatrix} \begin{bmatrix} Mi \\ m_1 \\ m_2 \\ m_3 \\ \dots \\ m_n \end{bmatrix} \begin{bmatrix} V \\ v_1 \\ v_2 \\ v_3 \\ \dots \\ v_n \end{bmatrix} \begin{bmatrix} W \\ w_1 \\ w_2 \\ w_3 \\ \dots \\ w_n \end{bmatrix}. \quad (8)$$

As shown in formula (8), matrix M represents the importance judgment value of two insulation evaluation indicators compared with each other, wherein x_{ij} represents the judgment value of the importance of the evaluation index x_i and the evaluation index x_j compared with each other. It should be noted that all elements in the judgment matrix should satisfy the condition that the sum is 1. In the above judgment matrix, the left side is the importance level evaluation matrix of the criterion layer, Mi represents the product of each row element of the importance evaluation matrix, v_i represents the value of the square root of each element in Mi according to the matrix order, and then w_i represents the value of each element in v_i . The relevant calculation formula is as follows. The calculation formula for the value Mi of each row of the judgment matrix M is shown in

$$Mi = \prod_{j=1}^n x_{ij}, \quad i = 1, \dots, 6. \quad (9)$$

In formula (8), the calculation formula for the root value v_i of each row of the target matrix is shown in formula (9), where n represents the order of the judgment matrix. Accordingly, the value w_i of each element of the weight matrix after the normalization of the target matrix can be further obtained.

$$\begin{aligned} v_i &= \sqrt[n]{Mi} = \sqrt[n]{\prod_{j=1}^n x_{ij}}, \\ w_i &= \frac{v_i}{\sum_{i=1}^n v_i}. \end{aligned} \quad (10)$$

After calculating the weight of the cable insulation life evaluation index through the judgment matrix and the weight matrix, this paper conducts CR verification on the cable insulation aging life evaluation model. The most important step of CR verification is the calculation of the consistency index CI and the consistency ratio CR. The calculation of the consistency index must first be obtained by the maximum eigenvalue of the judgment matrix. The formula for calculating the maximum characteristic value λ_{\max} is as follows:

$$\lambda_{\max} = \sum_{i=1}^n \frac{(M * W)_i}{nW_i}. \quad (11)$$

The consistency index CI of the matrix can be obtained by the maximum eigenvalue of the judgment matrix calculated in formula (11). According to the principle of consistency verification, when the consistency ratio is zero, the judgment matrix has complete consistency [27].

$$\begin{aligned} CI &= \frac{\lambda_{\max} - n}{n - 1}, \\ CR &= \frac{CI}{RI}. \end{aligned} \quad (12)$$

From the above analysis, it can be seen that there are mainly 10 judgment indicators for the assessment of cable insulation aging life. According to the survey of the average random consistency index of the same order matrix in Table 2, the average random consistency index $RI = 1.49$ of the tenth order matrix can be known, and the calculation formula of the consistency ratio CR of the evaluation matrix is shown in equation (12).

2.4. Reliability Evaluation and Life Prediction of Cable Insulation Aging. According to the cable insulation aging life evaluation model and accelerated evaluation method, the reliability evaluation and life prediction of the cable insulation aging characteristics are carried out in this paper. Studies have shown that, under the action of thermal stress, the life of the insulation material of the cable, which is the time to failure of the insulation characteristics, meets the Arrhenius equation. Combined with the study of the

TABLE 2: Average random consistency index of each order matrix.

Matrix order	1	2	3	4	5	6	7	8	9	10
RI	0	0	0.58	0.89	1.12	1.24	1.32	1.41	1.45	1.49
Matrix order	11	12	13	14	15	16	17	18	19	20
RI	1.52	1.54	1.56	1.58	1.59	1.59	1.61	1.61	1.62	1.63

influence of mechanical stress, the life equation of cable thermal aging, and mechanical aging can be obtained.

$$L(T, s) = C \cdot e^{(A/T)s^{-m}}, \quad A = \frac{E_\alpha}{R}. \quad (13)$$

In formula (13), L is the inverse power law function of cable mechanical stress. T is the thermodynamic temperature, C is the constant determined by the actual aging test, and A is the ratio parameter of the activation energy E_α of the cable aging reaction and the gas molecular constant R . s represents the stress of the insulating material. According to the above formula, the insulation failure time under different temperature and material stress can be calculated.

$$L = L_0 \left(\frac{s}{s_0} \right)^{-m} e^{(\Delta E/C) \left((1/T) - (1/T_0) \right)}. \quad (14)$$

Formula (14) expresses the cable insulation life under the conditions of temperature T_0 and material stress s_0 , where m is a constant and ΔE is the energy change in the aging reaction. According to the principle and process of cable degradation, the reliability of cable insulation materials can be evaluated through the cable insulation degradation equation.

$$X(t) = \lambda t + \mu \omega(t). \quad (15)$$

Equation (15) is the cable insulation degradation equation, where $X(t)$ represents the standard material insulation degradation process, which is regarded as a Brownian motion in chemistry, λ represents the drift factor of Brownian motion, μ represents the diffusion factor, and $\omega(t)$ represents Brownian motion movement.

3. Cable Insulation Life Evaluation Experiment

3.1. Research Objects. The research object of this experiment is the evaluation of the insulation life of commonly used cables. According to related research, this paper establishes a cable insulation life evaluation model based on the improved fuzzy analytic hierarchy process as the evaluation method of cable insulation life. According to the fuzzy analytic hierarchy process and cable insulation life evaluation analysis, this paper established a three-level cable life evaluation index system. Among them, there are two primary indicators, namely, internal factors and external factors; secondary indicators are mainly three indicators of electrical performance, thermal performance, and mechanical performance under internal factors, and no secondary indicators are set under external factors; third-level indicators mainly include 10 factors, and the specific indicators are as described in the

above analysis. According to the fuzzy analytic hierarchy process and improved, this paper will carry out analytic hierarchy through the experimental data of several life evaluation models, so as to achieve the purpose of evaluating and predicting the insulation life of cables. The index system structure of the cable insulation life assessment model is shown in Figure 1.

3.2. Experimental Design. The purpose of this experiment is to evaluate the insulation life of the cable. This paper selects the more commonly used cross-linked polyethylene (XLPE) cables and mine MYP cables for insulation aging life evaluation experiments. The experiment is mainly divided into five steps. The first step is to learn about the materials and characteristics of related types of cables through literature research and consultation with professionals to establish a cable insulation aging life evaluation index system. The second step is to build the experimental environment platform for this research in the physics laboratory, which mainly includes a vibration table, a voltage regulator, a transformer, and some temperature and humidity control devices. The third step is to simulate the actual working environment of the cable and accelerate the failure process of the cable insulation according to the electrical and thermal aging characteristics of the insulating material and record the relevant experimental data. The fourth step is to use the fuzzy analytic hierarchy process to analyze the cable insulation characteristic data recorded in the experiment to evaluate and predict the insulation life of the two types of cables. Finally, the linear test and reliability estimation of the experimental results are carried out, and the application of this evaluation model is extended to the evaluation of insulation life of other types of cables.

3.3. Test Results and Reliability Estimation. In order to analyze the performance of the cable insulation life evaluation model in this study, it is necessary to check the linearity of the data results of this experiment. The principle of the linear test is to carry out a linear test corresponding to a significant level of experimental data according to a certain confidence level of the standard confidence interval and compare the variance of the deviation from the linear regression equation with the total variance of the measured value to obtain the confidence level of the test data.

$$S^2 = \frac{[(N - m)s_1^2 + (m - 2)s_2^2]}{N - 2}, \quad (16)$$

$$F = \frac{s_2^2}{s_1^2}.$$

Formula (16) is the estimated value of the joint variance of the experimental sample population data, where s_1^2 and s_2^2 represent the variance of the deviation of the data from the regression line and the variance of the sample population, N represents the sample population, m represents the sample data used for linearity test, and F is the ratio of variance in the linearity test. Referring to the F value table of the standard

confidence in probability statistics, the t distribution value of the data can be obtained from the look-up table when the confidence is 95% and the significance level is 0.05 degrees of freedom, and the value conversion of the linear test of the data can be further calculated. Is the value t_α of the distribution of t , and the calculation formula is shown in

$$t_\alpha = \left\{ \frac{1}{t_{0.95, N-2}} - \frac{1 - (N/m)}{(N/(N+1)) + (N/2)} \right\}^{-1}. \quad (17)$$

4. Discussion on Fuzzy Analytic Hierarchy Process Evaluation Model of Cable Insulation Life

4.1. Mine MYP Cable Working Environment Detection. In order to study the insulation life of MYP cable for mine use, this paper conducted a chemical test on the environmental indicators of some mine cables. The main content of the test is the content of nitrogen, phosphorus, potassium, chlorine, calcium, and other elements. The working environment of the cable in the mine is generally buried in the soil. Therefore, it is also necessary to detect the pH value and the cation exchange capacity, that is, the hardness, humidity, and temperature in the soil. The test results are shown in Table 3. Among them, N refers to the nitrogen that can be used within a certain period of time, generally between 2 and 20 (g/kg), which is at a low level. P content refers to the content of orthophosphate in the soil, usually between 5 and 50 (g/kg), in a state of loss.

As shown in Figure 2, in the oxidation induction period curve of the cable insulation material in different working environments, the OIT of the XLPE sample after 2100 hours of electric and heating combined aging is extremely short, and the OIT of the new XLPE sample is 21 minutes. The oxidation induction period of the electric heating combined aging sample is shorter than the oxidation induction period of single thermal aging, indicating that the combined electric heating aging degree is serious, and the oxidation induction period is smaller. The OIT decreases significantly with the increase of the aging degree of the sample.

4.2. Cable Structure and Insulation Material Performance Parameter Analysis. After selecting the corresponding cable experimental sample materials, this paper investigates the insulation material properties and structural composition of the two types of cables. The results are shown in Table 4. Among them, the specific heat of the insulating layer reaches 640 J/kg°C, and the thermal conductivity is only 0.16. It can be seen that the thermal conductivity of the insulating layer is the lowest among the cable constituent materials.

The material composition structure of the two types of cables is shown in Figure 3. The XLPE cable mainly includes conductor, inner semiconducting layer, insulating layer, inner lining, steel wire armor, outer semiconducting layer, and outer sheath. Mine MYP cable is mainly composed of copper core conductor, insulation layer, impurity layer, and rubber sheath.

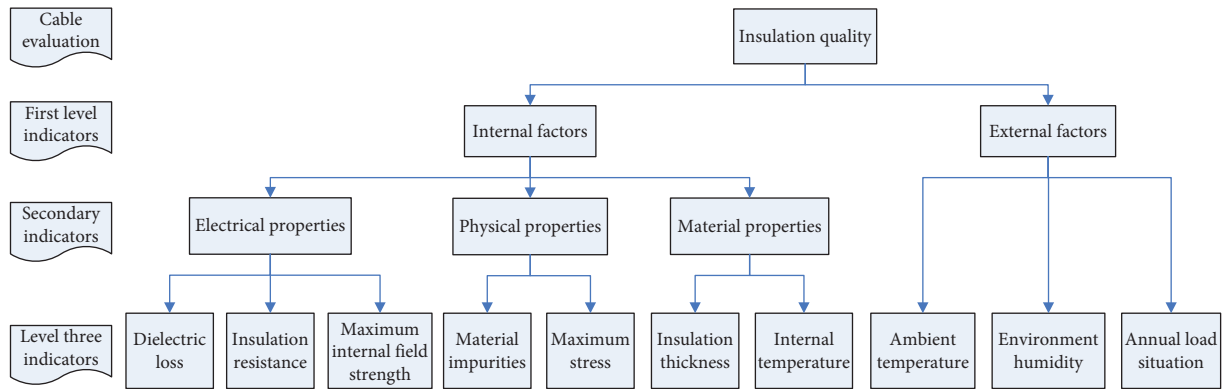


FIGURE 1: Cable insulation life evaluation system.

TABLE 3: MYP mining cable working environment chemical detection index.

Chemical index	N (g/kg)	P (g/kg)	K (g/kg)	Cl (mmol/L)	Ca (mmol/L)
Content	3.43	3.67	11.46	234.65	1.37
Chemical index	PH	Cation (cmol/kg)	Hardness (mmol/L)	Alkalinity (mmol/L)	Conductance ($\mu\text{s}/\text{cm}$)
Content	8.05	12.26	3.17	49.18	7.99

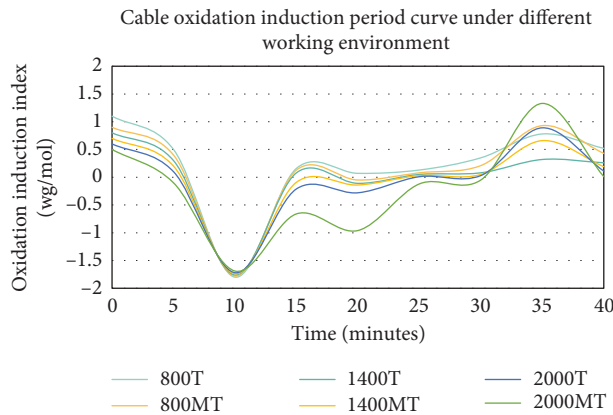


FIGURE 2: Cable oxidation induction period curve under different working environment.

TABLE 4: Cable structure and thermal performance parameters.

Cable structure	Specific heat ($\text{J}/\text{kg}^\circ\text{C}$)	Thermal conductivity	Cable radius
Large copper core	385	106	3.8
Small copper core	385	106	2.5
Neoprene sheath	490	0.25	16.0
Ethylene propylene rubber insulation	640	0.16	5.0
Other impurities	475	49.07	2.3

4.3. Aging Data Indicators of the Cable at Different Temperatures and Electric Field Strengths. The change of cable insulation aging life with temperature and working voltage field strength is shown in Table 5. ICMT represents the highest temperature inside the cable, PAT represents the

average temperature of the two phases, FMT represents the temperature of the filling material, and ICME represents the electric field strength inside the cable.

This experiment analyzes the insulation resistance and aging time under four-phase voltages, and the experimental

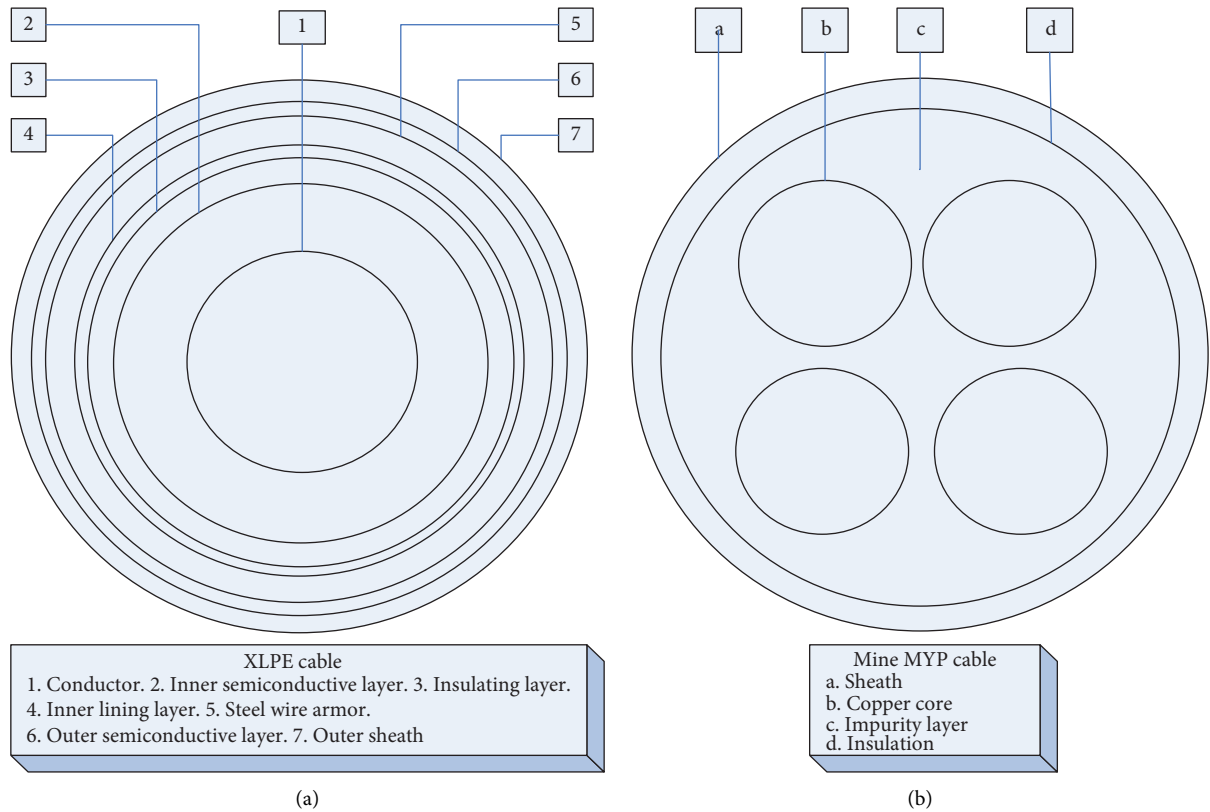


FIGURE 3: Material composition structure of (a) XLPE cable and (b) mine MYP cable.

TABLE 5: Changes of cable insulation aging temperature and electric field intensity.

Impact index	Index value	ICMT	PAT	FMT	ICME
Impurities and conductor spacing	2	51.64	47.75	43.66	5.47
	3	51.38	47.22	43.93	5.06
	4	50.49	47.16	44.17	4.65
Cable insulation performance loss	Normal	51.62	47.19	43.91	1.1476
	Loss 10%	53.44	48.07	44.07	1.2064
	Loss 20%	56.27	48.69	44.39	1.4142
	Loss 30%	58.19	49.18	44.53	1.7643
	Loss 40%	62.66	50.24	44.81	1.9065
	Loss 50%	67.49	50.68	44.89	2.1421

results are shown in Figure 4. Among them, the insulation resistance of phases A, B, and C is generally larger than that of phase D. This is because, during normal operation, the energizing current of phases A, B, and C during normal operation is much larger than that of phase D, and phase D only has a certain current flow when the cable fails and the underground power system fails.

4.4. Evaluation of Cable Insulation Aging Life under Different Temperatures and Electric Field End Levels. Table 6 shows the aging life of cable insulation at different temperatures and end levels. It can be seen from the table that the aging life of the cable can reach 106 years in theory under 60 degrees Celsius and the key level of 40% of the electric field.

However, due to various factors in actual work, the insulation life of the cable is greatly reduced. The most influential factor is electricity.

Taking different end-point levels as the abscissa and the aging life of the cable at different end-point levels as the ordinate, the SPSS software is used to perform cubic polynomial fitting, and the curve of the aging time versus performance at each temperature of the cable is obtained. Take humidification as an example, as shown in Figure 5. According to the results of the aging experiment, the insulation life of the cable under the temperature environment of 60°C and below 60°C and the electric field environment with the end level of 40% and below can reach more than 106 years, but the actual cable working environment often cannot reach this level.

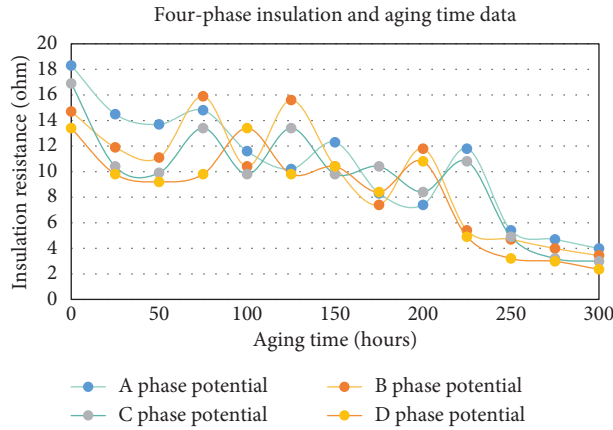


FIGURE 4: Four-phase insulation resistance and aging time data.

TABLE 6: Cable insulation aging life under different temperatures and end levels.

End level (%)	Aging life of cable insulation at different temperatures (years)								
	60°C	65°C	70°C	75°C	80°C	85°C	90°C	95°C	100°C
40	106.2	99.6	73.4	61.3	30.8	13.9	8.3	4.7	1.9
50	98.7	92.6	66.5	53.4	25.5	16.7	7.4	4.3	1.3
60	89.9	83.3	42.3	37.4	21.2	14.2	6.1	3.8	0.7
70	77.8	70.2	39.8	30.2	18.9	11.8	5.5	3.3	0.3

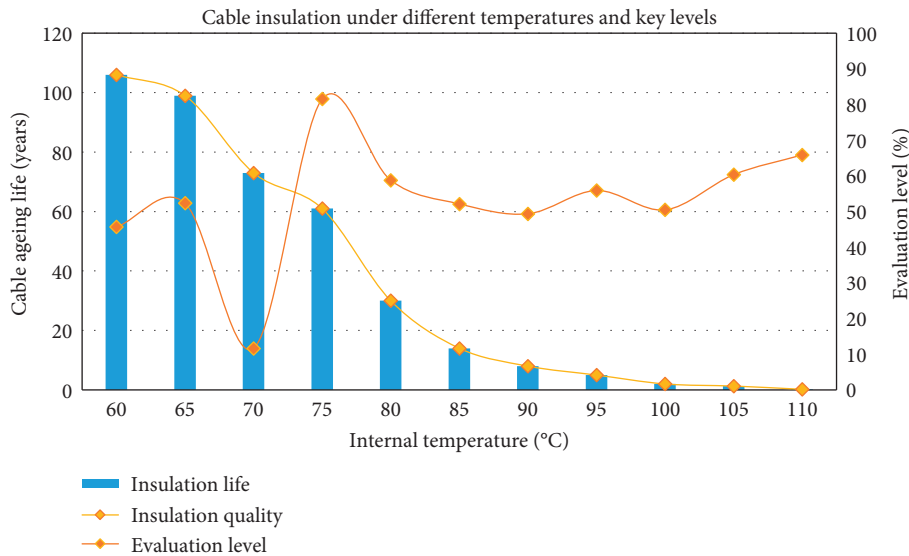


FIGURE 5: Cable insulation life under different temperatures and key levels.

5. Conclusions

This research mainly improves the fuzzy analytic hierarchy process for the evaluation of cable insulation life based on the cable insulation characteristics. In the investigation of current cable insulation aging life evaluation, this paper found that the current evaluation and prediction of cable insulation aging life are mainly evaluated by accelerated evaluation method and the principles of electrical aging and thermal aging. However, these evaluation models are highly

pertinent and strongly dependent on the working environment of the cable. Based on this, this paper proposes a cable insulation life evaluation model based on the improved fuzzy analytic hierarchy process. This model combines the Weibull model and the Arrhenius model commonly used in the assessment of cable insulation aging life and the improved fuzzy analytic hierarchy process. It can evaluate the insulation life of cables in a more in-depth and more specific manner from the perspective of various influencing factors and provide companies and individuals using cables with

more accurate cable life evaluation data, which reduces the resource consumption of power supply maintenance and improves the safety of the power supply.

The experiment in this paper adopts the accelerated thermal aging and electrical aging in the physical laboratory and the simulation experiment method of the cable working environment to conduct the insulation life of the cross-linked polyethylene cable (XLPE) and the mine mobile flexible cable (MYP) under the accelerated aging of electricity and heat. Under the influence of electrical and thermal aging, the time of cable insulation failure will be greatly shortened; that is to say, factors such as temperature and voltage will reduce the life of the cable insulation.

Due to the various types of cables, the production materials and structural specifications are different, and the performance analysis of the cable insulation life evaluation model in this study has certain limitations. It is hoped that, in the future, a more complete and better simulation effect of cable aging experiment platform can be established, and the cable insulation life evaluation model of this research can be extended to more types of cable insulation life evaluation applications.

Data Availability

No data were used to support this study.

Conflicts of Interest

The authors declare that they have no conflicts of interest.

References

- [1] B. Diban and G. Mazzanti, "The effect of temperature and stress coefficients of electrical conductivity on the life of HVDC extruded cable insulation subjected to type test conditions," *IEEE Transactions on Dielectrics and Electrical Insulation*, vol. 27, no. 4, pp. 1313–1321, 2020.
- [2] R. Hu, Z. X. Jing, Q. H. Wu, R. B. Yan, and Z. C. Cao, "Life cycle assessment of environmental impacts and total cost of power cable," *Applied Mechanics and Materials*, vol. 872, no. 9, pp. 412–419, 2017.
- [3] T. V. Santhosh, A. K. Ghosh, B. G. Fernandes, and K. A. Dubey, "Performance assessment of I&C cable insulation materials by DSC and SEM for NPP ageing management," *International Journal of System Assurance Engineering and Management*, vol. 7, no. 1, pp. 6–15, 2016.
- [4] G. Mazzanti and M. Marzintotto, "Advanced electro-thermal life and reliability model for high voltage cable systems including accessories," *IEEE Electrical Insulation Magazine*, vol. 33, no. 3, pp. 17–25, 2017.
- [5] L. Bessisa, L. Boukezzi, D. Mahi et al., "Lifetime estimation and diagnosis of XLPE used in HV insulation cables under thermal ageing: arithmetic sequences optimised by genetic algorithms approach," *IET Generation Transmission & Distribution*, vol. 11, no. 10, pp. 2429–2437, 2016.
- [6] W. Zuo, H. Yuan, Y. Shang, Y. Liu, and T. Chen, "Calculation of a health index of oil-paper transformers insulation with binary logistic regression," *Mathematical Problems in Engineering*, vol. 2016, Article ID 6069784, 9 pages, 2016.
- [7] A. N. Jahromi, P. Pattabi, J. Densley, and L. Lamarre, "Medium voltage XLPE cable condition assessment using frequency domain spectroscopy," *IEEE Electrical Insulation Magazine*, vol. 36, no. 5, pp. 9–18, 2020.
- [8] T. V. Santhosh, V. Gopika, A. K. Ghosh, B. G. Fernandes, and K. A. Dubey, "Reliability prediction of I&C cable insulation materials by DSC and Weibull theory for probabilistic safety assessment of NPPs," *Nuclear Engineering and Design*, vol. 296, no. 1, pp. 51–61, 2016.
- [9] J. Kim, W. Kim, H.-S. Park, and J.-W. Kang, "Lifetime assessment for oil-paper insulation using thermal and electrical multiple degradation," *Journal of Electrical Engineering and Technology*, vol. 12, no. 2, pp. 840–845, 2017.
- [10] T. Seguchi, K. Tamura, H. Kudoh et al., "Degradation of cable insulation material by accelerated thermal radiation combined ageing," *IEEE Transactions on Dielectrics & Electrical Insulation*, vol. 22, no. 6, pp. 3197–3206, 2016.
- [11] B. Hinderliter, E. Hill, M. Maurer-Jones et al., "Cable insulation testing for mechanistic degradation FEA modeling," *Transactions of the American Nuclear Society*, vol. 118, no. 6, pp. 595–597, 2018.
- [12] Z. Zuo, L. A. Dissado, C. Yao et al., "Modeling for life estimation of HVDC cable insulation based on small-size specimens," *IEEE Electrical Insulation Magazine*, vol. 36, no. 1, pp. 19–29, 2019.
- [13] Y. Su, Y. Liu, and L. Zhong, "Evaluation of voltage endurance characteristics for new and aged XLPE cable insulation by electrical treeing test," *IEEE Transactions on Dielectrics and Electrical Insulation*, vol. 26, no. 1, pp. 72–80, 2019.
- [14] C. Zhou, H. Yi, and X. Dong, "Review of recent research towards power cable life cycle management," *High Voltage*, vol. 2, no. 3, pp. 179–187, 2017.
- [15] C.-K. Chang, C.-S. Lai, and R.-N. Wu, "Decision tree rules for insulation condition assessment of pre-molded power cable joints with artificial defects," *IEEE Transactions on Dielectrics and Electrical Insulation*, vol. 26, no. 5, pp. 1636–1644, 2019.
- [16] T. V. Santhosh, V. Gopika, A. K. Ghosh, and B. G. Fernandes, "An approach for reliability prediction of instrumentation & control cables by artificial neural networks and Weibull theory for probabilistic safety assessment of NPPs," *Reliability Engineering & System Safety*, vol. 170, no. 2, pp. 31–44, 2018.
- [17] W.-J. Kim, S.-H. Kim, D. G. Yang, H. Lee, J.-W. Cho, and H.-J. Kim, "Mechanical bending characteristics of HTS DC cable," *IEEE Transactions on Applied Superconductivity*, vol. 26, no. 4, pp. 1–4, 2016.
- [18] J. L. Sohn, P. P. Kalbar, and M. Birkved, "Life cycle based dynamic assessment coupled with multiple criteria decision analysis: a case study of determining an optimal building insulation level," *Journal of Cleaner Production*, vol. 162, no. 9, pp. 449–457, 2017.
- [19] I. Ahmadi-Joneidi, A. A. Shayegani-Akmal, and H. Mohseni, "Lifetime prediction of 20kV field-aged silicone rubber insulators via condition assessment," *IEEE Transactions on Dielectrics and Electrical Insulation*, vol. 24, no. 6, pp. 3612–3621, 2017.
- [20] D. C. Morais, A. T. de Almeida, A. Teixeira et al., "PROM-ETHEE-ROC model for assessing the readiness of technology for generating energy," *Mathematical Problems In Engineering*, vol. 2015, Article ID 530615, 11 pages, 2015.
- [21] A. Azadeh and S. Abdolhossein Zadeh, "An integrated fuzzy analytic hierarchy process and fuzzy multiple-criteria decision-making simulation approach for maintenance policy selection," *Simulation*, vol. 92, no. 1, pp. 3–18, 2016.
- [22] M. Ashtiani and M. Abdollahi Azgomi, "Trust modeling based on a combination of fuzzy analytic hierarchy process and

- fuzzy VIKOR,” *Soft Computing*, vol. 20, no. 1, pp. 399–421, 2016.
- [23] S. Nazari, M. Fallah, H. Kazemipoor, and A. Salehipour, “A fuzzy inference-fuzzy analytic hierarchy process-based clinical decision support system for diagnosis of heart diseases,” *Expert Systems with Applications*, vol. 95, no. 4, pp. 261–271, 2018.
- [24] W. Chunsheng, L. Gaohuan, H. Chong et al., “Ecological vulnerability assessment based on fuzzy analytical method and analytic hierarchy process in yellow river delta,” *International Journal of Environmental Research and Public Health*, vol. 15, no. 5, pp. 855–859, 2018.
- [25] R. Aliyev, H. Temizkan, and R. Aliyev, “Fuzzy analytic hierarchy process-based multi-criteria decision making for universities ranking,” *Symmetry*, vol. 12, no. 8, pp. 1351–1358, 2020.
- [26] Y. A. Mowafi, T. Alaqarbeh, and R. Alazrai, “Putting context in the network access of mobile applications using fuzzy analytic hierarchy process,” *International Journal of Decision Support System Technology*, vol. 11, no. 2, pp. 13–26, 2019.
- [27] Q. Wang, W. Li, H. Yu et al., “Research on the application of evaluation method based on fuzzy analytic hierarchy process in emergency communication plans for power system,” *Dianli Xitong Baohu Yu Kongzhi/Power System Protection and Control*, vol. 46, no. 22, pp. 171–177, 2018.

Research Article

The Integration of Blockchain Technology and Smart Grid: Framework and Application

Xiaomin Du ¹, Ying Qi ¹, Beibei Chen ², Biaoan Shan ³ and Xinyu Liu ²

¹Department of Economic Management, Yingkou Institute of Technology, Yingkou 115014, China

²School of Economics and Management, Dalian University of Technology, Dalian 116024, China

³School of Management, Jilin University, Changchun 130022, China

Correspondence should be addressed to Biaoan Shan; shanbiaoan@jlu.edu.cn

Received 28 March 2021; Revised 20 April 2021; Accepted 6 May 2021; Published 17 May 2021

Academic Editor: Ming Bao Cheng

Copyright © 2021 Xiaomin Du et al. This is an open access article distributed under the Creative Commons Attribution License, which permits unrestricted use, distribution, and reproduction in any medium, provided the original work is properly cited.

Based on the diffusion of blockchain technology in the smart grid, this paper studies the framework and application of the blockchain technology in the smart grid, so as to combine the blockchain with the smart grid and establish a sustainable supply chain. However, the establishment of a sustainable supply chain is based on a layered theoretical framework. Not only should the framework take into account needless attributes and the relationship among various criteria and aspects but the application should also involve a balance of multiple stakeholders. For the above reasons, this paper uses a combination of Fuzzy-DEMATEL and ISM. The results show that (1) the hierarchical path of sustainable supply chain management of the smart grid under the blockchain starts from the social level, pays attention to system construction, grasps the technical standards, and defines the development goals of the power grid. (2) The development of green energy has become a new market growth point. (3) The control of the operation level becomes the focus of the smart grid. (4) The optimization and development of the economic structure are restricted by social factors. By integrating and optimizing the blockchain and supply chain, this paper puts forward a theoretical framework, establishes a sustainable GIP application system with multistakeholder participation at the supply chain level, and indicates the significance of the blockchain in the smart grid.

1. Introduction

The smart grid is a transparent, seamless, and instant two-way transmission of energy and information. The two-way information exchange between power grids and users is the biggest difference between smart grids and traditional power grids [1]. As another disruptive technological innovation occurring after the internet, blockchain has led to the development of distributed accounting system [2, 3], which is tamper-resistant, traceable, highly trusted, and decentralized. Blockchain can improve the security of the grid system data and help promote the realization of the reliable, effective, and trusted distributed smart grid system [4]. There have been many studies on blockchain in the energy field. In addition, blockchain technology may also subvert the supply chain [5]. This article combines the blockchain with a smart grid and establishes a grid alliance chain with the

participation of governments, enterprises, and individuals. The grid alliance chain can perform data uploads, storage, and condition queries, which promotes the further development of smart grids.

Firstly, in the entire energy industry, the construction of power grids is at the forefront of development, and the development of smart grids under the blockchain has become a focus of scholars' attention. Some scholars have explored the development of the smart grid industry under the blockchain, but this research is still in the preliminary stage and lacks systematization. Most studies on the combination of the blockchain and smart grids focus on the application of blockchain technology in a single part of the grid value chain, such as the construction of smart grid data secure storage and sharing systems based on an alliance's blockchain [6], blockchain-based distributed secure keyless signature schemes [7], distribution networks and point-to-

point energy trading platforms [8], and energy demand-side management in microgrids under blockchain technology [9]. It is not difficult to find that the development systems of smart grids under the blockchain are highly complex, but the existing research is scattered and lacks integration. Secondly, the smart grid supply chain is a system composed of organization, personnel, information, and resources [10]. Supply chains are complex by nature, and inefficient supply chains can lead to a more serious crisis of trust, thus requiring better information sharing and verifiability [5]. The blockchain will work with all the agents of smart grids at the same time in the process of application, and multiple agents will work together and affect each other. However, from the perspective of stakeholder, scholars have performed little research on the multisubject coordinated development of systems. From the perspective of sustainability, there is little research on the integration of the blockchain and smart grid, which needs to be considered from three aspects: economy, society, and environment. Thirdly, the application space of private chains is limited because it easily leads to questioning the credibility of information. In contrast to private chains, public chains have greatly improved information credibility, but they cannot ensure the privacy and security of participants [11, 12]. The aforementioned problems have increased the difficulty of the application and popularization of public chains in the real economy. Relatively speaking, alliance chains have the characteristics of “partial decentralization.” As long as a limited number of subjects are included, an alliance chain can increase security, reduce costs, and increase reliability.

Therefore, this paper has conducted the following research. Firstly, the paper systematically discusses how blockchain technology affects the development of the smart grid supply chain. Sustainability is defined by the concept of triple bottom line [5]. The paper establishes a set of sustainable development system of blockchain-based smart grids including 14 standards from three aspects. Secondly, this study analyzes the causality and sorts out the interrelationships among different levels, building an influence path of the blockchain on the smart grid sustainable development. Thirdly, we construct a smart grid sustainable supply chain based on the blockchain from the three layers: government layer, information layer, and participant layer.

We finally reached these conclusions. (1) The impact is reflected in the three aspects. However, the importance of these three aspects is different. First, the development path of smart grids under the blockchain is based on solving social problems and reflects the characteristics of national security and people’s dependence on the power industry. At the same time, transactions for renewable new energy are realized under the blockchain technology, which also shows that the blockchain has increased the trading space of new energy. (2) Control at the operation level has become the main point of smart grid construction under the blockchain, which is mainly carried out through smart contracts. In addition, the economic structure of a smart grid is restricted by social factors. The economic benefits generated by the realization of social benefits have become a potential core feature of the

power grid industry. (3) The system should be built from three levels of government, information, and participant. This study elaborates the construction path of the sustainable supply chain of the smart grid under the blockchain and promotes the combination of blockchain and smart grid. In theory, this paper makes up the research gap of the lack of systematic application of the blockchain in the smart grid field. In practice, the government-led and multiparticipatory GIP application system of the power grid alliance chain designed in this paper will contribute to the future work of the smart grid and provide an important reference for government policy update and business planning.

The rest of the paper is structured as follows. Section 2 proposes 14 criteria through the literature review. Section 3 describes the calculation steps of the method in detail. Section 4 obtains the relationship diagram and hierarchical framework among criteria. Section 5 constructs a sustainable smart grid supply chain under the blockchain based on the results. Section 6 draws the conclusion.

2. Literature Review

The concept of a smart grid integrates many aspects. Dileep [1] described a smart grid as a transparent, seamless, and instant two-way transmission of energy and information. In contrast to traditional power grids, smart grids will expand the ability to obtain grid panorama information. Smart grids can strengthen the real-time analysis, diagnosis, and optimization of power grid business flows to achieve more refined, accurate, and timely power grid operation and management. Smart grid technology is bringing innovation to the power industry and affecting all parts of the grid supply chain [13]. A supply chain consists of a number of entities related to the product and service life cycle from both upstream and downstream markets, and blockchain technology can make supply chain management data sharing safe and transparent [14]. Smart grid technology creates new challenges in terms of security and intelligence [4]. Blockchain is open and transparent and involves decentralized database technology. Effectively applying blockchain technology to the construction of smart grids has attracted widespread attention from scholars. To solve the security and intelligence problems of smart grids, many scholars have proposed solutions based on blockchain technology. Gao et al. [15] used a sovereign blockchain to automatically record and control power consumption in a power grid. In addition, Mengelkamp et al. [16] and Pop et al. [17] proposed blockchain-based smart grid solutions. By using blockchain technology, smart grid supply chain can simultaneously achieve secure transaction data storage while also stimulating the use of green energy and promoting sustainable development [18].

This paper starts from the triple bottom line theory and focuses on economic, social, and environmental aspects. We consider the cost and efficiency of the public infrastructure in the economic aspect, social welfare and top-level design issues in the social aspect, and low carbon emission and green energy in the environmental aspect.

2.1. Economy

2.1.1. Public Infrastructure Utilization Efficiency. Many scholars have used blockchain technology to solve infrastructure problems in the construction of smart grids. Blockchain technology will drive more distributed grid infrastructure and allow local producers to trade in the energy market. This will attract more resources that can invest in distributed grid technology [19]. The technical form of blockchain is highly compatible with the construction of the ubiquitous electric power [20].

2.1.2. Production Cost Management. It has been confirmed that smart grids under blockchain technology can reduce the production cost of power generation, effectively use the existing power infrastructure, and reduce carbon dioxide emissions [21]. Demand-side management under the blockchain can achieve supply and demand balance, achieve optimal production and power generation efficiency, and thus perform better in terms of production cost management [22].

2.1.3. Administration Cost Management. Smart contracts can reduce paper usage, facilitate quick discussions, and save time. At the same time, shared databases can reduce management work [23]. Blockchain can guarantee the security of the entire system through distributed accounting without having to go through a central agent or intermediary. Smart contracts stored in the blockchain can be automatically triggered in a decentralized manner, greatly saving management and service costs [24]. Blockchain technology helps smart grids use advanced power engineering and wireless communications to improve services and reduce administration costs [10].

2.1.4. Transaction Cost Management. Blockchain technology can eliminate information asymmetry by providing historical transaction records. The information cannot be changed retroactively, so the governance intermediary can be eliminated, and transaction costs can be reduced [25]. This process can lead to more short-term dynamic relationships and temporary partnerships, reducing the cost of renegotiating, drafting contracts and agreements, and implementing agreements [26]. Blockchain has features such as a decentralized database and encrypted signature protection, which can reduce the need for middlemen and transaction costs [27]. Smart contracts are usually used to realize automatic power trading and payment [14].

2.1.5. Financial Cost Management. According to the theory of information asymmetry, tax-related information is the starting point of tax collection and management. Incomplete information and information asymmetry in tax collection and management will lead to moral hazard and adverse selection, which will lead to tax loss [28]. Blockchain technology does not need to rely on any third-party transactions. Due to the characteristics of smart contracts,

blockchain can automatically achieve pairing between two parties. These characteristics allow the blockchain to automatically provide complete and accurate historical transaction records and clearing processing. This can reduce the traditional disadvantages of information asymmetry, greatly simplify the taxation process, and promote a harmonious relationship between two parties [29]. Auditing cost control has always been a major concern of national auditing departments. Processing audit data through blockchain technology can effectively control auditing costs [30].

2.2. Society

2.2.1. Security. Key management is critical to improve the security of smart grids. Blockchain is a subversive innovation of key management of the smart grid system [7]. In a blockchain system, any operation on a given block will result in a hash mismatch of all contiguous blocks, and many new applications combine distributed ledger technology with smart contracts. It is almost impossible for a third party to tamper or review private information [23]. Each participating user in a blockchain system has its own public and private keys. An exclusive public key is issued to all network users who use the same encryption or decryption algorithm, while private keys are held by only the users themselves [24].

2.2.2. Authenticity. Blockchain guarantees the authenticity of transaction information in the operation of smart grid systems with traceability and transparency. The key feature of blockchain is its ability to maintain a consistent view and consensus among participants [31], even though some of them may not be honest [32]. Information recorded by the blockchain is backed up on multiple nodes. Information updates require the joint authentication of multiple nodes. One node cannot cheat the other nodes. Therefore, the authenticity of information is enhanced [33].

2.2.3. Timeliness. By introducing blockchain technology, certain security services used by power grid operators and user agreements can be implemented in the form of smart contracts, which can save process time, reduce mistakes and improper behaviors in the sales process, and improve the timeliness and reliability of services [21]. In addition, smart contracts enable companies to develop business at a lower cost while improving service efficiency [34]. Transactions between entities in a smart grid will be more efficient as security improves.

2.2.4. Credit Evaluation System. Blockchain technology can be used to build a credit evaluation system to enhance the effectiveness of monitoring and managing smart grids [35]. Due to the provision of information on credit backgrounds, the electricity produced by green energy can be sold at a relatively high price, making green power providers profitable, and companies will be more motivated to use green renewable energy. Thus, blockchain leads to the development of a virtuous circle. In addition, through the

establishment of a blockchain-based telecommunication evaluation system for users, massive amounts of information can be automatically recorded, user's credit evaluation can be performed through the consideration of corresponding information, and certain electricity price discounts can be implemented for users with good credit. Certain punishment measures can be implemented for users who engage in bad power consumption behaviors such as stealing electricity.

2.2.5. Incentive and Punishment System. Using the blockchain, one can create a virtual currency to represent each unit of electricity. This system is very useful in the case of renewable energy produced by consumers themselves. In addition, incentive schemes can be implemented to promote renewable energy. By monitoring the transaction history in the blockchain ledger, one can select a group of peers who contributed the most to renewable energy transactions and reward them with virtual currency [36]. Pop et al. [17] proposed a smart grid monitoring system based on blockchain and smart contracts. Smart contracts set rules to identify malicious use points and can detect the malicious manipulation of usage data and enforce penalties. Smart contracts include provisions for decentralized control, the calculation of incentives or penalties, the verification of demand response protocols, and rules related to balancing grid-measured energy demand and energy production [15].

2.2.6. Power Grid Optimization. Amrollahi and Bathaee [37] studied the scale optimization of the microgrid integrating hybrid photovoltaic and wind energy systems and the impact of the demand response on scale optimization. Various model frameworks have been proposed today with the main purpose of reducing the cost of consumers using different pricing incentives [38]. A user's electricity consumption data can be obtained using a smart meter; another function of smart grids is to predict and make recommendations regarding the user's electricity consumption behavior, make full use of the distributed energy generation capacity, and reduce peak electricity use through the migration of system pressure created by electricity use to improve the operating efficiency of power systems [22].

2.2.7. Demand-Side Management. Demand-side management technology matches demand with the availability of resources in a given environment, effectively utilizing existing infrastructure in smart grids. Power demand-side management under blockchain technology is an effective tool that can be used to meet increasing demand [9]. Jabbarzadeh et al. [39] introduced how an interactive system between users and suppliers can be built using a smart grid system, which can effectively improve the poor operability of demand-side management. Smart grids can achieve two-way communication between supply and demand; however, the increased system complexity due to the introduction of demand-side management is a problem that arises when using smart grids. To solve this problem, an automatic

control system for energy consumption scheduling based on game theory was developed. This system uses intelligent algorithms instead of manual scheduling, thereby reducing the complexity of the work of the supplier system's staff [38].

2.3. Environment

2.3.1. Low Carbon Emission. Based on the use of blockchain technology and information communication technology, energy input and carbon footprint can be reduced [40]. In this process, blockchain can provide a special platform for carbon emission measurement and right certification. Blockchain can be used to register and store emission credits in a distributed database for carbon emission trading to verify renewable energy encryption credits [41]. Saberi et al. [5] proposed a framework in which the blockchain forms the basis for the detection, verification, and reporting processes in carbon trading by providing unalterable and transparent permit records.

2.3.2. Green Energy. Li et al. [21] proposed that the blockchain provides a reliable and transparent means to encourage green energy utilization and reduce energy waste in a flexible and controllable way. Specifically, blockchain can track all transactions in a network so that consumers can know the source of each unit of power and selectively use a certain type of energy, further promoting the use of green energy and reducing environmental pollution [18] (see Table 1).

3. Method

ISM and DEMATEL are appropriate techniques for establishing clear hierarchies and relationship structures. Although there are many similarities between the two approaches, ISM divides the relationships among criteria into four categories, which is used to decompose complex systems into subsystems, while DEMATEL uses a more complex assessment. It focuses more on the micro aspect, helps to determine the strength of direct and indirect relationships among criteria, and visualizes causal structures through the use of diagrams [42]. The integration of these two methods can not only obtain the hierarchy of multi-factor action in complex systems but also determine the key factors in the hierarchy, which lays a foundation for the analysis and decision-making of complex systems.

Fuzzy mathematics is a way of simulating fuzzy information processing in the human brain [43, 44]. In addition, the fuzzy concept allows the capture of human bias and uncertainty that DEMATEL cannot handle in the data, so the credibility of analysis results can be improved, and more valuable reference can be provided for managers' decision-making. Hence, this study used Fuzzy-DEMATEL for analysis.

3.1. Calculation Process: Fuzzy-DEMATEL.

Step 1: taking the research problem as the starting point, the impact factor system is constructed, which is set as F_1, F_2, \dots, F_n .

TABLE 1: Aspects and criteria.

Aspects	Criteria	Explanation
Economic	C1 Public infrastructure utilization efficiency	Uses blockchain technology to realize the sharing of public infrastructure facilities, cross-network cooperation, and scattered transactions and improve the sharing efficiency
	C2 Production cost management	Uses blockchain technology to analyze production information to achieve the optimal production and generation efficiency
	C3 Administration cost management	Reduces labor cost through automatic data upload, traceability system, and smart contract
	C4 Transaction cost management	Distributed ledger and smart contract reduce transaction cost
	C5 Financial cost management	Electronic bill management, auditing, and tax supervision
	C6 Security	Builds a secure database to ensure anonymity and privacy
	C7 Authenticity	Establishes an open, transparent, authentic, and reliable traceability system
	C8 Timeliness	Improves efficiency through the smart contract and blockchain traceability system
	C9 Credit evaluation system	Credit evaluation through the integration of information on the blockchain
Society	C10 Incentive and punishment system	Policy subsidies and illegal punishment for the behavior of blockchain participants
	C11 Power grid optimization	Microgrid regional power supply, optimal power supply, and attract more power suppliers
	C12 Demand-side management	Encourages users to upload demand information to cope with peak hours of power consumption and match energy production with demand
Environment	C13 Low carbon emission	Carbon emission trading on the chain promotes enterprises to reduce carbon emissions through technological progress
	C14 Green energy	Replaces nonrenewable energy with green energy

Step 2: the relationship among the factors in the system is determined by the expert scoring method. The semantic quantization conversion used by experts is shown in Table 2.

Step 3: use the CFCS method to obtain the n -order direct impact matrix:

(a) Normalize the triangular fuzzy number:

$$\begin{aligned}
 xa_{1ij}^k &= \frac{(a_{1ij}^k - \min a_{1ij}^k)}{\Delta_{\min}^{\max}}, \\
 xa_{2ij}^k &= \frac{(a_{2ij}^k - \min a_{1ij}^k)}{\Delta_{\min}^{\max}}, \\
 xa_{3ij}^k &= \frac{(a_{3ij}^k - \min a_{1ij}^k)}{\Delta_{\min}^{\max}},
 \end{aligned} \tag{1}$$

(b) Normalize the right and left side:

$$\begin{aligned}
 xls_{ij}^k &= \frac{xa_{2ij}^k}{(1 + xa_{2ij}^k - xa_{1ij}^k)}, \\
 xrs_{ij}^k &= \frac{xa_{3ij}^k}{(1 + xa_{3ij}^k - xa_{2ij}^k)}.
 \end{aligned} \tag{2}$$

(c) Calculate the clarity value of the score:

$$\begin{aligned}
 x_{ij}^k &= \frac{[xls_{ij}^k(1 - xls_{ij}^k) + xrs_{ij}^k xrs_{ij}^k]}{[1 - xls_{ij}^k + xrs_{ij}^k]}, \\
 z_{ij}^k &= \min a_{1ij}^k + x_{ij}^k \times \Delta_{\min}^{\max}.
 \end{aligned} \tag{3}$$

TABLE 2: Semantic transformation.

Language variable	TFN
N	(0, 0, 0.2)
VL	(0, 0.2, 0.4)
L	(0.2, 0.4, 0.6)
H	(0.4, 0.6, 0.8)
VH	(0.8, 1, 1)

(d) Calculate the average clarity value:

$$z_{ij}^k = \frac{(z_{ij}^1 + z_{ij}^2 + \dots + z_{ij}^k)}{n}. \tag{4}$$

Step 4: normalize Z.

$$\lambda = \frac{1}{\max_{1 \leq i \leq n} \sum_{j=1}^n z_{ij}}, \quad G = \lambda Z. \tag{5}$$

Step 5: in line with $T = G + G^2 + \dots + G^n$ or $T = G(E - G)^{-1}$, E is the constant matrix, then composite impact matrix T is taken.

Step 6: the degree of influence and being influenced are the values obtained by adding each row and each column of the composite impact matrix:

$$Di = \sum_{j=1}^n t_{ij} \quad (i = 1, 2, \dots, n), \tag{6}$$

$$Ri = \sum_{i=1}^n t_{ij} \quad (i = 1, 2, \dots, n). \tag{7}$$

The formulas of centrality and causality are

$$m_i = D_i + R_i \quad (i = 1, 2, \dots, n), \quad (8)$$

$$n_i = D_i - R_i \quad (i = 1, 2, \dots, n), \quad (9)$$

$$H = T_i - R_i \quad (i = 1, 2, \dots, n).$$

3.2. *Calculation Process: ISM.* ISM is an intuitive model that can transform fuzzy things into good structural relationships [45].

$$\begin{aligned} H &= T + E = h_{ij}, \\ \lambda &= \alpha + \beta. \end{aligned} \quad (10)$$

Among them, α and β are the mean and standard deviation.

Determine the reachability matrix among factors:

$$M = [m_{ij}]_{n \times n} \quad (i = 1, 2, \dots, n; j = 1, 2, \dots, n), \quad (11)$$

$$m_{ij} = \begin{cases} 1, & h \geq \lambda, \\ 0, & h \leq \lambda, \end{cases} \quad (i = 1, 2, \dots, n; j = 1, 2, \dots, n), \quad (12)$$

$$C(f_i) = L(f_i) \cap P(f_i). \quad (13)$$

According to formula (13), $L(f_i)$ is the reachable set, and $P(f_i)$ is the antecedent set. Ultimately, we can determine the composition of the ISM model.

4. Result

We select 7 experts with over 8 years of work experience in power companies to evaluate the research. Individual face-to-face interviews were used for data collection. First of all, the purpose and significance of this research are explained. Secondly, the concept involved in the questionnaire is explained. Then, the questions are answered in the process of expert scoring. Finally, the expert score sheet is recycled. After processing the data, the direct impact matrix is determined; see Table 3 for details.

Normalize the direct influence matrix, and then calculate the comprehensive influence matrix, as shown in Table 4.

From equations (6)–(9), we can get causality, centrality, influence degree, and affected degree, as shown in Table 5. Influence degree indicates the extent to which other indicators are affected. Affected degree indicates the degree of influence by other indicators. Centrality represents the position and the magnitude of its influence. Causality reflects the causal relationship among the influencing criteria.

The DEMATEL causal diagram of the factors is drawn as shown in Figure 1.

There are 6 causal factors, including authenticity (C7), power grid optimization (C11), green energy (C14), timeliness (C8), incentive and punishment system (C10), and security (C6). Among them, security (C6) is the main driver with an influence degree of 2.3556. There are 8 outcome factors, including administration cost management (C3), financial cost management (C5), production cost management (C2), public infrastructure utilization

efficiency (C1), demand-side management (C12), transaction cost management (C4), credit evaluation system (C9), and low carbon emission (C13). For centrality, the factors follow the order of security (C6), incentive and punishment system (C10), authenticity (C7), power grid optimization (C11), timeliness (C8), green energy (C14), demand-side management (C12), credit evaluation system (C9), administration cost management (C3), low carbon emission (C13), transaction cost management (C4), public infrastructure utilization efficiency (C1), financial cost management (C5), and production cost management (C2).

The overall influence matrix from equation (10) is shown in Table 6.

Table 7 is the result calculated according to formulas (11) and (12), which supports the stratification in Table 8 and Figure 1. In Table 7, the study introduces λ as a threshold to determine whether the two factors have impact.

The first-order decomposition structure is shown in Table 8.

Nq of each layer is ultimately obtained as follows: $N1 = \{C2, C3, C5\}$, primary node; $N2 = \{C1, C4, C9, C12, C13\}$, secondary node; $N3 = \{C7, C8, C11, C14\}$, third-level node; $N4 = \{C6, C10\}$, fourth-level node. According to the above analysis, based on the method of ISM, the hierarchical theoretical framework for smart grids under the blockchain technology has been shown in Figure 2.

5. Discussion

This paper tries to build the smart grid sustainable supply chain under the blockchain. This research proposes a set of smart grid development standard systems and establishes a hierarchical model.

First, the incentive and punishment system and security are at the first level of ISM and have the highest central position. Therefore, social issues are the core of promoting a whole smart grid under the blockchain. Smart grids under the blockchain are oriented to solve social problems, and they conform to the assumption that technology promotion needs to be constructed from the social problem perspective, which is consistent with social construction theory. It has been pointed out that institutions can play an important role in leading, guiding, and overall planning and then influencing and determining the bottom level. The premise of technological advancement is to take the perfect top-level design of institutions as the supporting basis and solve social problems through making technology more perfect in its application in the society, the economy, and the environment [46]. In the construction of our entire hierarchical model, the incentive and punishment system is part of the top-level system design. Security is still a social issue at the first level, reflecting the fact that the power grid industry is still part of the national security system, which concerns people's livelihood and national defense [13]. This part of the conclusion, regarding security, reflects the characteristics of grids in the smart grid industry and helps us grasp the core characteristics and potential attributes of a national pillar industry.

TABLE 3: Direct influence matrix of the blockchain on the smart grid.

	C1	C2	C3	C4	C5	C6	C7	C8	C9	C10	C11	C12	C13	C14
C1	0.0000	0.4337	0.4337	0.1616	0.1071	0.0935	0.1207	0.0935	0.1207	0.1207	0.1071	0.1071	0.1752	0.1207
C2	0.0255	0.0000	0.1480	0.1071	0.1480	0.0119	0.0799	0.1071	0.1207	0.0119	0.1207	0.2160	0.0119	0.0119
C3	0.0935	0.1752	0.0000	0.1344	0.1344	0.0527	0.0663	0.0391	0.1207	0.2160	0.0119	0.1207	0.0935	0.0799
C4	0.1071	0.0119	0.4337	0.0000	0.4337	0.1888	0.1616	0.1888	0.1888	0.2296	0.0119	0.1207	0.0119	0.0119
C5	0.0119	0.1071	0.1207	0.1071	0.0000	0.2024	0.1344	0.1071	0.1344	0.1071	0.0119	0.0799	0.0119	0.1071
C6	0.3384	0.1616	0.1616	0.3248	0.3520	0.0000	0.4881	0.4609	0.3112	0.2432	0.4881	0.2704	0.2568	0.4065
C7	0.1207	0.2840	0.3112	0.4337	0.2160	0.1071	0.0000	0.2840	0.4337	0.1616	0.2024	0.0119	0.1888	0.2160
C8	0.1616	0.1888	0.1071	0.4609	0.2160	0.2976	0.0391	0.0000	0.4337	0.2024	0.2160	0.4609	0.1752	0.1071
C9	0.2432	0.0663	0.4609	0.0663	0.4337	0.2024	0.1888	0.1071	0.0000	0.1071	0.0663	0.1207	0.1480	0.0391
C10	0.1480	0.2840	0.3112	0.2568	0.4337	0.2840	0.4337	0.1888	0.2296	0.0000	0.4609	0.3384	0.2296	0.4881
C11	0.4881	0.2024	0.1888	0.0935	0.2160	0.1207	0.2024	0.2296	0.1888	0.1207	0.0000	0.4337	0.4337	0.1752
C12	0.1752	0.1344	0.4609	0.0935	0.1071	0.1344	0.1344	0.1344	0.1207	0.1480	0.1888	0.0000	0.2840	0.1888
C13	0.1344	0.4065	0.2024	0.1071	0.0799	0.2024	0.1888	0.1071	0.1344	0.1207	0.2024	0.2160	0.0000	0.2024
C14	0.4337	0.2160	0.0391	0.1207	0.1752	0.1752	0.1752	0.1071	0.2024	0.2840	0.2160	0.2840	0.4609	0.0000

TABLE 4: Comprehensive impact matrix of the blockchain on the smart grid.

	C1	C2	C3	C4	C5	C6	C7	C8	C9	C10	C11	C12	C13	C14
C1	0.0438	0.1459	0.1583	0.0798	0.0790	0.0568	0.0688	0.0584	0.0752	0.0656	0.0625	0.0739	0.0803	0.0634
C2	0.0289	0.0263	0.0690	0.0474	0.0629	0.0234	0.0393	0.0443	0.0534	0.0236	0.0461	0.0744	0.0260	0.0216
C3	0.0489	0.0722	0.0465	0.0597	0.0695	0.0385	0.0458	0.0348	0.0597	0.0740	0.0311	0.0601	0.0494	0.0453
C4	0.0655	0.0511	0.1608	0.0514	0.1566	0.0837	0.0824	0.0827	0.0949	0.0930	0.0439	0.0758	0.0445	0.0449
C5	0.0333	0.0551	0.0691	0.0567	0.0428	0.0718	0.0617	0.0528	0.0659	0.0515	0.0325	0.0515	0.0327	0.0517
C6	0.1758	0.1439	0.1724	0.1723	0.1986	0.0877	0.2003	0.1875	0.1808	0.1389	0.1952	0.1706	0.1582	0.1733
C7	0.0900	0.1291	0.1603	0.1594	0.1338	0.0808	0.0633	0.1177	0.1674	0.0925	0.0986	0.0750	0.1016	0.0986
C8	0.1060	0.1123	0.1291	0.1676	0.1397	0.1269	0.0795	0.0644	0.1702	0.1054	0.1105	0.1781	0.1070	0.0837
C9	0.0975	0.0687	0.1682	0.0638	0.1538	0.0855	0.0883	0.0653	0.0549	0.0664	0.0560	0.0762	0.0767	0.0510
C10	0.1288	0.1619	0.1929	0.1475	0.2070	0.1401	0.1843	0.1234	0.1532	0.0824	0.1840	0.1766	0.1469	0.1868
C11	0.1733	0.1257	0.1407	0.0871	0.1252	0.0842	0.1080	0.1073	0.1145	0.0842	0.0630	0.1696	0.1638	0.0971
C12	0.0906	0.0893	0.1717	0.0713	0.0849	0.0727	0.0792	0.0730	0.0825	0.0785	0.0881	0.0599	0.1151	0.0869
C13	0.0824	0.1468	0.1163	0.0751	0.0807	0.0866	0.0920	0.0699	0.0869	0.0708	0.0931	0.1067	0.0548	0.0894
C14	0.1618	0.1275	0.1055	0.0911	0.1181	0.0957	0.1053	0.0815	0.1158	0.1179	0.1111	0.1368	0.1693	0.0627

TABLE 5: Comprehensive impact matrix analysis.

Factor	Influence degree	Affected degree	Centrality	Causality
C1	1.1116	1.3267	2.4383	-0.2151
C2	0.5867	1.4558	2.0425	-0.8691
C3	0.7355	1.8609	2.5964	-1.1254
C4	1.1311	1.3300	2.4611	-0.1989
C5	0.7292	1.6527	2.3819	-0.9235
C6	2.3556	1.1343	3.4899	1.2213
C7	1.5682	1.2981	2.8663	0.2700
C8	1.6803	1.1629	2.8432	0.5175
C9	1.1724	1.4752	2.6476	-0.3028
C10	2.2159	1.1448	3.3607	1.0710
C11	1.6436	1.2158	2.8594	0.4279
C12	1.2438	1.4852	2.7290	-0.2415
C13	1.2514	1.3265	2.5779	-0.0751
C14	1.6001	1.1563	2.7564	0.4438

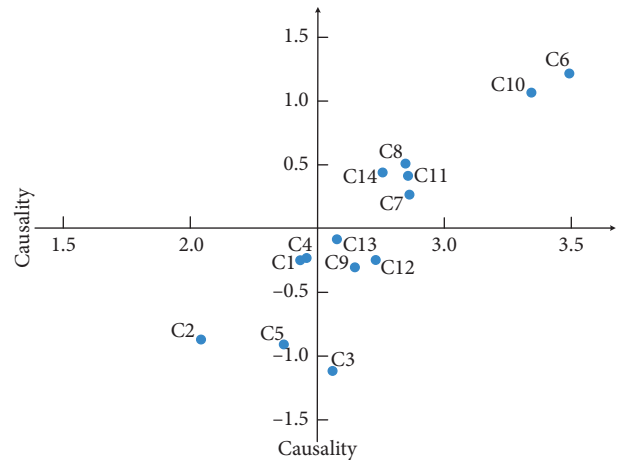


FIGURE 1: DEMATEL causal diagram.

Second, timeliness, authenticity, and power grid optimization are in the ISM's second level. The first two are characteristics of the blockchain, while power grid optimization reflects the purpose of smart grid development. In the study of the society as a whole, we divide social problems into two aspects. The first is the social welfare created by the

features of the blockchain. Social welfare is mainly considered from the two aspects of timeliness and authenticity. Every transaction record in the blockchain is bound with the information of the trader so that the transmission path of the transactions between the participants in the smart grid can

TABLE 6: Overall influence matrix of the blockchain on the smart grid.

	C1	C2	C3	C4	C5	C6	C7	C8	C9	C10	C11	C12	C13	C14
C1	1.0438	0.1459	0.1583	0.0798	0.0790	0.0568	0.0688	0.0584	0.0752	0.0656	0.0625	0.0739	0.0803	0.0634
C2	0.0289	10.0263	0.0690	0.0474	0.0629	0.0234	0.0393	0.0443	0.0534	0.0236	0.0461	0.0744	0.0260	0.0216
C3	0.0489	0.0722	10.0465	0.0597	0.0695	0.0385	0.0458	0.0348	0.0597	0.0740	0.0311	0.0601	0.0494	0.0453
C4	0.0655	0.0511	0.1608	10.0514	0.1566	0.0837	0.0824	0.0827	0.0949	0.0930	0.0439	0.0758	0.0445	0.0449
C5	0.0333	0.0551	0.0691	0.0567	10.0428	0.0718	0.0617	0.0528	0.0659	0.0515	0.0325	0.0515	0.0327	0.0517
C6	0.1758	0.1439	0.1724	0.1723	0.1986	10.0877	0.2003	0.1875	0.1808	0.1389	0.1952	0.1706	0.1582	0.1733
C7	0.0900	0.1291	0.1603	0.1594	0.1338	0.0808	10.0633	0.1177	0.1674	0.0925	0.0986	0.0750	0.1016	0.0986
C8	0.1060	0.1123	0.1291	0.1676	0.1397	0.1269	0.0795	1.0644	0.1702	0.1054	0.1105	0.1781	0.1070	0.0837
C9	0.0975	0.0687	0.1682	0.0638	0.1538	0.0855	0.0883	0.0653	1.0549	0.0664	0.0560	0.0762	0.0767	0.0510
C10	0.1288	0.1619	0.1929	0.1475	0.2070	0.1401	0.1843	0.1234	0.1532	1.0824	0.1840	0.1766	0.1469	0.1868
C11	0.1733	0.1257	0.1407	0.0871	0.1252	0.0842	0.1080	0.1073	0.1145	0.0842	10.0630	0.1696	0.1638	0.0971
C12	0.0906	0.0893	0.1717	0.0713	0.0849	0.0727	0.0792	0.0730	0.0825	0.0785	0.0881	1.0599	0.1151	0.0869
C13	0.0824	0.1468	0.1163	0.0751	0.0807	0.0866	0.0920	0.0699	0.0869	0.0708	0.0931	0.1067	1.0548	0.0894
C14	0.1618	0.1275	0.1055	0.0911	0.1181	0.0957	0.1053	0.0815	0.1158	0.1179	0.1111	0.1368	0.1693	1.0627

TABLE 7: Reachable matrix of the blockchain on the smart grid.

<i>M</i>	C1	C2	C3	C4	C5	C6	C7	C8	C9	C10	C11	C12	C13	C14
C1	1	1	1	0	0	0	0	0	0	0	0	0	0	0
C2	0	1	0	0	0	0	0	0	0	0	0	0	0	0
C3	0	0	1	0	0	0	0	0	0	0	0	0	0	0
C4	0	0	1	1	1	0	0	0	0	0	0	0	0	0
C5	0	0	0	0	1	0	0	0	0	0	0	0	0	0
C6	1	1	1	1	1	1	1	1	1	0	1	1	1	1
C7	0	0	1	1	0	0	1	0	1	0	0	0	0	0
C8	0	0	0	1	0	0	0	1	1	0	0	1	0	0
C9	0	0	1	0	1	0	0	0	1	0	0	0	0	0
C10	0	1	1	1	1	0	1	0	1	1	1	1	1	1
C11	1	0	0	0	0	0	0	0	0	0	1	1	1	0
C12	0	0	1	0	0	0	0	0	0	0	0	1	0	0
C13	0	1	0	0	0	0	0	0	0	0	0	0	1	0
C14	1	0	0	0	0	0	0	0	0	0	0	0	1	1

TABLE 8: First-order decomposition structure.

<i>i</i>	$L(f_i)$	$P(f_i)$	$C(f_i) = L(f_i) \cap P(f_i)$
C1 Public infrastructure utilization efficiency	1, 2, 3	1, 6, 11, 14	1
C2 Production cost management	2	1, 2, 6, 10, 13	2
C3 Administration cost management	3	1, 3, 4, 6, 7, 9, 10, 12	3
C4 Transaction cost management	3, 4, 5	4, 6, 7, 8, 10	4
C5 Financial cost management	5	4, 5, 6, 9, 10	5
C6 Security	1, 2, 3, 4, 5, 6, 7, 8, 9, 11, 12, 13, 14	6	6
C7 Authenticity	3, 4, 7, 9	6, 7, 10	7
C8 Timeliness	4, 8, 9, 12	6, 8	8
C9 Credit evaluation system	3, 5, 9	6, 7, 8, 9, 10	9
C10 Incentive and punishment system	2, 3, 4, 5, 7, 9, 10, 11, 12, 13, 14	10	10
C11 Power grid optimization	1, 11, 12, 13	6, 10, 11	11
C12 Demand-side management	3, 12	6, 8, 10, 11, 12	12
C13 Low carbon emission	2, 13	6, 10, 11, 13, 14	13
C14 Green energy	1, 13, 14	6, 10, 14	14

Note. *i* represents the number of criteria. $L(f_i)$ represents the factors affected by C_i . $P(f_i)$ represents the factors that affect C_i . $L(f_i) \cap P(f_i)$ represents the intersection.

be fully recorded and traced; this information cannot be destroyed or tampered with, which increases the convenience of the supervision of transactions [27]. The synergy of the blockchain’s technical features makes its features perfectly synchronous, eliminates the needless steps involved in

the current transaction settlement process [47], and makes the traceability of power products more convenient and efficient. Therefore, mastering the characteristics of the blockchain and understanding the technology and standards of the operation process of the blockchain technology are a

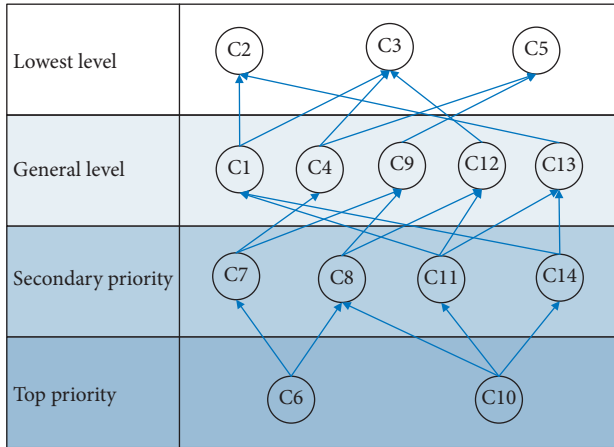


FIGURE 2: The hierarchical theoretical framework for smart grids under the blockchain technology.

prerequisite for the implementation of smart grids. We would like to emphasize the key problem of power grid optimization in smart grids. The purpose of the development of a whole smart grid is to continuously optimize the grid, which can improve the efficiency of power generation and transmission, reduce the power supply cost, and reduce the network loss rate [22]. Therefore, solving social problems is the foundation. In the whole process, new technology and industry can be combined in a way that will meet certain standards; we should pay attention to system construction, grasp technical standards, and make clear the goal of power grid development.

In the second level of the ISM, we identified a new criterion of green energy, which belongs to the environmental level. The appearance of this new criterion can indicate some new research directions. Generally, in the process of many industries' sustainable development, environmental issues are paid less attention than social and economic issues. However, in this study, green energy is seen as a new bright spot and can be explained by considering the following two aspects. First, the development of renewable energy can take advantage of blockchain technology. Because blockchain storage involves authentic and decentralized transactions, power producers can attract more small participants to engage in power generation, facilitating more private, small power generation transactions [18]. With increasing environmental concerns, power companies tend to switch from traditional generation to renewable energy, and the development of renewable energy and rapid technological innovation have become the driving forces of the grid supply chain network [47]. Blockchain technology provides more power and increases the feasibility of the development of green energy. Green energy is a target product that uses the blockchain to bring market optimization. Second, green renewable energy is a substitute for grid development for nonrenewable energy [21]. The trend is irreversible, and smart grid development is a new strategy for the future. Therefore, research conclusions on green energy highlight the promotion of energy marketization by blockchain technology and the strategic trend of new energy

industry development under blockchain technology. Our research plays a leading and guiding role in the development of the blockchain energy industry.

The third level includes the credit evaluation system and the utilization efficiency of the common infrastructure and involves low carbon emission, demand-side management, and transaction cost management. They represent three different levels of economy, society, and environment and are somewhat complicated. However, if we look at the whole third level, we can find that these five indicators are the concrete manifestation of the blockchain in the application process and the key factors of blockchain operation. The whole operation process of blockchain mainly revolves around smart contracts [48]. Smart contracts have the advantages of data irreversibility, security assurance, and full automation. The application of smart contracts to smart grids will simplify various communication processes and improve operating efficiency [14]. However, whether smart contracts can make people more active in participating requires the establishment of a sound credit evaluation system. In addition, transactions involving smart contracts increase the number of stakeholders [5]. In other words, the emergence of smart contracts will increase the common development of physical and virtual markets. In the process of market operation, smart contracts can promote the utilization efficiency of the real economy, which is mainly reflected in the utilization efficiency of public infrastructure in smart grids, while in virtual markets, it is mainly reflected in low carbon emission as a result of virtual trading and demand-side management [49]. The credit evaluation system guarantees the authenticity and visibility of the whole operation. The results of this part reveal that smart grids are enhanced by the blockchain at the operation level and present the application characteristics of smart contracts in the power grid industry.

Financial cost management, production cost management, and administration cost management are at the last level, and all belong to the economic level, which is different from other industries. For example, in the traditional manufacturing industry, economic problems are of greater concern. The construction of a national smart grid industry not only involves social issues such as people's livelihood and national defense but also shows the strength of the new energy strategy, which promotes the application of blockchain technology to social and environmental problems. Blockchain technology can reduce economic costs to a large extent, which will make it easier to control financial costs [30], reduce power generation production costs, and improve power infrastructure utilization efficiency [21].

Finally, due to the above research conclusions and stakeholder theory [50], this paper built a blockchain-based smart grid sustainable GIP application system on the supply chain level, as shown in Figure 3. It includes a government level, information level, and participant level and shows how stakeholders at all stages of the supply chain can collaborate with the blockchain. This system mainly takes the smart grid cloud platform under the blockchain as the core and spreads the information flow among the participants. The information encrypted cannot be decrypted even if it is

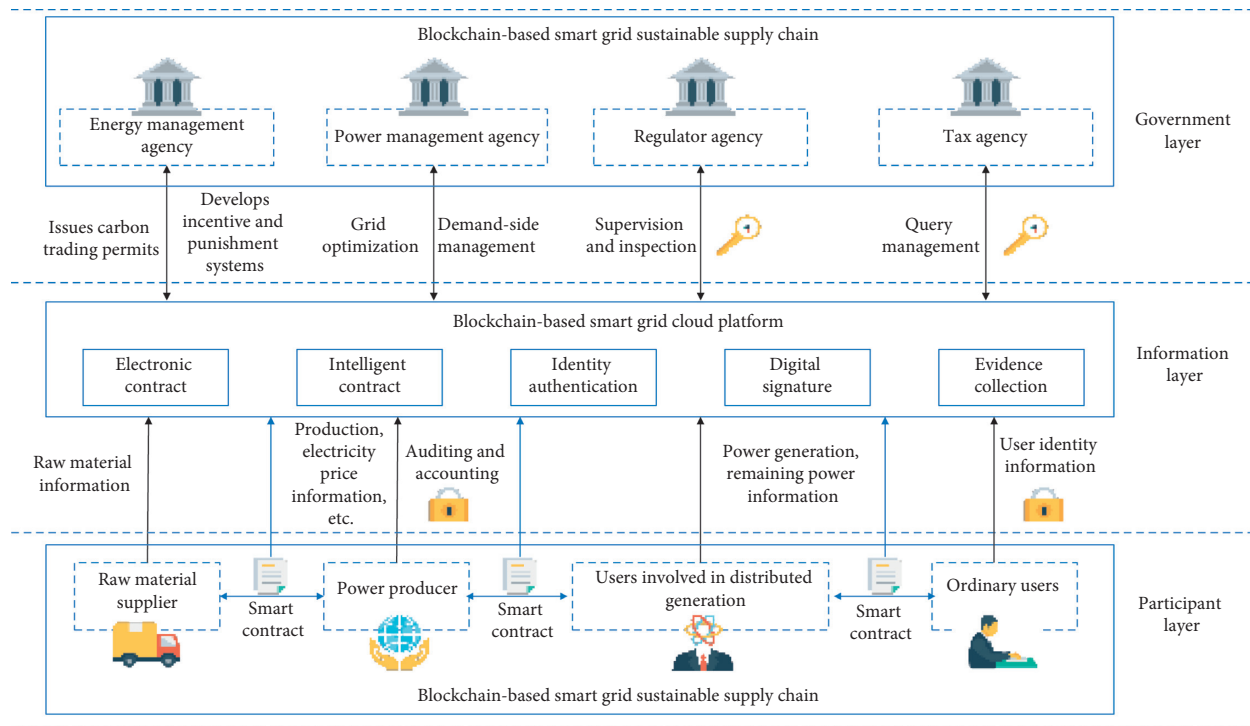


FIGURE 3: A blockchain-based smart grid sustainable GIP application system at the supply chain level.

intercepted on the internet. Blockchain can ensure the stable and efficient operation of the system.

The participation level in the system can be divided into two parts: enterprises and users. Enterprises can be divided into power producers and raw material suppliers. Asymmetric encryption technology enables all transaction information related to the enterprise to be accurately recorded in the blockchain. In addition, enterprises can upload some public information, such as production information, information on the use of raw materials, and electricity prices, to the blockchain to provide data for users' electricity transactions and allow for the supervision of government agencies. At the same time, transactions between participants will automatically generate electronic contracts and upload them to the blockchain cloud platform. Users can be divided into ordinary users and users involved in distributed generation. Ordinary users upload their real identity information that has been encrypted to the blockchain and make transaction requests with virtual identities. Users can inquire about the price of electricity, the source of raw materials for power generation, and so on. Users participating in distributed generation encrypt their real identity information and upload it to the blockchain and, at the same time, upload their power generation information to the public. The blockchain can intelligently match the remaining power generation with the corresponding ordinary users who apply for transactions.

The information level is the core link of the whole GIP application system. Through interactions and data sharing with the management and the participation layer, we can optimize power production, the use of raw materials, trading, and other links in a penetrating manner. In this way,

we can realize the whole process of trading, provide customers with dynamic product quality traceability and other services, and enable government agencies to implement management and regulation in a more reasonable and effective way.

The government level is mainly composed of relevant government management agencies. First, an energy management agency can issue carbon emission permits from the blockchain, and enterprises can trade freely. The power agency can integrate information on power grid equipment, power supply and demand, blockchain technology, and other information to make engage in more reasonable power grid planning. Regulators can conduct all-round supervision and inspection of power technology, security, quality, and market prices using keys provided by the blockchain cloud platform. In addition, tax agencies can obtain enterprises' authorization to check the enterprises' accounts, which will lead to more convenient tax management. We expect that this system can promote the sustainable supply chain development of smart grids under the blockchain technology and contribute to the development of the whole national economy.

6. Conclusion

The current literature lacks in-depth research on the sustainable supply chain development system covering the whole smart grid value chain under blockchain technology. We analyze the impact of blockchain technology on the sustainable development of smart grids from economic, social, and environmental aspects and construct a hierarchical theory framework. The sustainable GIP application

system at the supply chain level is systematic and comprehensive, which will help promote the sustainable development of the smart grid industry in the future and provide an important reference for governments and enterprises.

This study also has some limitations. In the process of using Fuzzy-DEMATEL and ISM methods to analyze the 14 influencing factors, this paper only obtains the basic structured results among the influencing factors. Future research also needs to use structural equation modeling and other methods to verify the action path of influencing factors from the operational level.

Data Availability

Data used to support the findings of this study are available upon request.

Conflicts of Interest

The authors declare that they have no conflicts of interest.

Acknowledgments

The authors would like to thank the Yingkou Institute of Technology Excellent Scientific and Technological Talents Foundation (RC201904) and the Dalian University of Technology Fundamental Research Fund (DUT19RW107).

References

- [1] G. Dileep, "A survey on smart grid technologies and applications," *Renewable Energy*, vol. 146, pp. 2589–2625, 2020.
- [2] D. Appelbaum and S. S. Smith, "Blockchain basics and hands-on guidance: taking the next step toward implementation and adoption," *The CPA Journal*, vol. 88, no. 6, pp. 28–37, 2018.
- [3] F. Hawlitschek, B. Notheisen, and T. Teubner, "The limits of trust-free systems: a literature review on blockchain technology and trust in the sharing economy," *Electronic Commerce Research and Applications*, vol. 29, pp. 50–63, 2018.
- [4] B. Bhushan, A. Khamparia, K. M. Sagayam, S. K. Sharma, M. A. Ahad, and N. C. Debnath, "Blockchain for smart cities: a review of architectures, integration trends and future research directions," *Sustainable Cities and Society*, vol. 61, Article ID 102360, 2020.
- [5] S. Saberi, M. Kouhizadeh, J. Sarkis, and L. Shen, "Blockchain technology and its relationships to sustainable supply chain management," *International Journal of Production Research*, vol. 57, no. 7, pp. 2117–2135, 2019.
- [6] K. Gai, Y. Wu, L. Zhu, M. Qiu, and M. Shen, "Privacy-preserving energy trading using consortium blockchain in smart grid," *IEEE Transactions on Industrial Informatics*, vol. 15, no. 6, pp. 3548–3558, 2019.
- [7] H. Zhang, J. Wang, and Y. Ding, "Blockchain-based decentralized and secure keyless signature scheme for smart grid," *Energy*, vol. 180, pp. 955–967, 2019.
- [8] B. P. Hayes, S. Thakur, and J. G. Breslin, "Co-simulation of electricity distribution networks and peer to peer energy trading platforms," *International Journal of Electrical Power & Energy Systems*, vol. 115, p. 105419, 2020.
- [9] S. Noor, W. Yang, M. Guo, K. H. van Dam, and X. Wang, "Energy Demand Side Management within micro-grid networks enhanced by blockchain," *Applied Energy*, vol. 228, pp. 1385–1398, 2018.
- [10] R. Azzi, R. K. Chamoun, and M. Sokhn, "The power of a blockchain-based supply chain," *Computers & Industrial Engineering*, vol. 135, pp. 582–592, 2019.
- [11] D. Bumblauskas, A. Mann, B. Dugan, and J. Rittmer, "A blockchain use case in food distribution: do you know where your food has been?" *International Journal of Information Management*, vol. 52, Article ID 102008, 2020.
- [12] V. J. Morkunas, J. Paschen, and E. Boon, "How blockchain technologies impact your business model," *Business Horizons*, vol. 62, no. 3, pp. 295–306, 2019.
- [13] J. Lukić, M. Radenković, M. Despotović-Zrakić, A. Labus, and Z. Bogdanović, "Supply chain intelligence for electricity markets: a smart grid perspective," *Information Systems Frontiers*, vol. 19, no. 1, pp. 91–107, 2017.
- [14] J. Xie, H. Tang, T. Huang et al., "A survey of blockchain technology applied to smart cities: research issues and challenges," *IEEE Communications Surveys & Tutorials*, vol. 21, no. 3, pp. 2794–2830, 2019.
- [15] J. Gao, K. O. Asamoah, E. B. Sifah et al., "Gridmonitoring: secured sovereign blockchain based monitoring on smart grid," *IEEE Access*, vol. 6, pp. 9917–9925, 2018.
- [16] E. Mengelkamp, B. Notheisen, C. Beer, D. Dauer, and C. Weinhardt, "A blockchain-based smart grid: towards sustainable local energy markets," *Computer Science-Research and Development*, vol. 33, no. 1-2, pp. 207–214, 2018.
- [17] C. Pop, T. Cioara, M. Antal, I. Anghel, I. Salomie, and M. Bertoincini, "Blockchain based decentralized management of demand response programs in smart energy grids," *Sensors*, vol. 18, no. 1, p. 162, 2018.
- [18] F. Imbault, M. Swiatek, R. De Beaufort, and R. Plana, "The green blockchain: managing decentralized energy production and consumption," in *Proceedings of the 2017 IEEE International Conference on Environment and Electrical Engineering and 2017 IEEE Industrial and Commercial Power Systems Europe (EEEIC/I&CPS Europe)*, pp. 1–5, IEEE, Milan, Italy, June 2017.
- [19] A. Wörner, A. Meeuw, L. Ableitner, F. Wortmann, S. Schopfer, and V. Tiefenbeck, "Trading solar energy within the neighborhood: field implementation of a blockchain-based electricity market," *Energy Informatics*, vol. 2, no. 1, p. 11, 2019.
- [20] Z. Dong, F. Luo, and G. Liang, "Blockchain: a secure, decentralized, trusted cyber infrastructure solution for future energy systems," *Journal of Modern Power Systems and Clean Energy*, vol. 6, no. 5, pp. 958–967, 2018.
- [21] Y. Li, R. Rahmani, N. Fouassier, P. Stenlund, and K. Ouyang, "A blockchain-based architecture for stable and trustworthy smart grid," *Procedia Computer Science*, vol. 155, pp. 410–416, 2019.
- [22] P. Samadi, A. H. Mohsenian-Rad, R. Schober, V. W. Wong, and J. Jatskevich, "Optimal real-time pricing algorithm based on utility maximization for smart grid," in *Proceedings of the 2010 First IEEE International Conference on Smart Grid Communications*, pp. 415–420, IEEE, Gaithersburg, MD, USA, October 2010.
- [23] S. Yadav and S. P. Singh, "Blockchain critical success factors for sustainable supply chain," *Resources, Conservation and Recycling*, vol. 152, p. 104505, 2020.
- [24] Z. Zheng, S. Xie, H.-N. Dai et al., "An overview on smart contracts: challenges, advances and platforms," *Future Generation Computer Systems*, vol. 105, pp. 475–491, 2020.

- [25] R. Beck, J. Stenum Czepluch, N. Lollike, and S. Malone, "Blockchain—the gateway to trust-free cryptographic transactions," *Research Papers*, vol. 153, 2016.
- [26] C. G. Schmidt and S. M. Wagner, "Blockchain and supply chain relations: a transaction cost theory perspective," *Journal of Purchasing and Supply Management*, vol. 25, no. 4, Article ID 100552, 2019.
- [27] N. Kshetri, "Will blockchain emerge as a tool to break the poverty chain in the Global South?" *Third World Quarterly*, vol. 38, no. 8, pp. 1710–1732, 2017.
- [28] S. Mann and H. Wüstemann, "Public governance of information asymmetries—The gap between reality and economic theory," *The Journal of Socio-Economics*, vol. 39, no. 2, pp. 278–285, 2010.
- [29] H. Wang, H. Qin, M. Zhao, X. Wei, H. Shen, and W. Susilo, "Blockchain-based fair payment smart contract for public cloud storage auditing," *Information Sciences*, vol. 519, pp. 348–362, 2020.
- [30] B. Putz, F. Menges, and G. Pernul, "A secure and auditable logging infrastructure based on a permissioned blockchain," *Computers & Security*, vol. 87, p. 101602, 2019.
- [31] H.-P. Lu and C.-I. Weng, "Smart manufacturing technology, market maturity analysis and technology roadmap in the computer and electronic product manufacturing industry," *Technological Forecasting and Social Change*, vol. 133, pp. 85–94, 2018.
- [32] M. Castro and B. Liskov, "Practical Byzantine fault tolerance and proactive recovery," *ACM Transactions on Computer Systems*, vol. 20, no. 4, pp. 398–461, 2002.
- [33] J. Hou, C. Wang, and S. Luo, "How to improve the competitiveness of distributed energy resources in China with blockchain technology," *Technological Forecasting and Social Change*, vol. 151, p. 119744, 2020.
- [34] Z. Li, W. M. Wang, G. Liu, L. Liu, J. He, and G. Q. Huang, "Toward open manufacturing," *Industrial Management & Data Systems*, vol. 118, no. 1, pp. 303–320, 2018.
- [35] A. Kamilaris, A. Fonts, and F. X. Prenafeta-Boldú, "The rise of blockchain technology in agriculture and food supply chains," *Trends in Food Science & Technology*, vol. 91, pp. 640–652, 2019.
- [36] T. Alladi, V. Chamola, J. J. P. C. Rodrigues, and S. A. Kozlov, "Blockchain in smart grids: a review on different use cases," *Sensors*, vol. 19, no. 22, p. 4862, 2019.
- [37] M. H. Amrollahi and S. M. T. Bathaee, "Techno-economic optimization of hybrid photovoltaic/wind generation together with energy storage system in a stand-alone micro-grid subjected to demand response," *Applied Energy*, vol. 202, pp. 66–77, 2017.
- [38] A.-H. Mohsenian-Rad, V. W. S. Wong, J. Jatskevich, R. Schober, and A. Leon-Garcia, "Autonomous demand-side management based on game-theoretic energy consumption scheduling for the future smart grid," *IEEE Transactions on Smart Grid*, vol. 1, no. 3, pp. 320–331, 2010.
- [39] A. Jabbarzadeh, B. Fahimnia, and S. Rastegar, "Green and resilient design of electricity supply chain networks: a multiobjective robust optimization approach," *IEEE Transactions on Engineering Management*, vol. 66, no. 1, pp. 52–72, 2017.
- [40] M. A. Mutchek and E. D. Williams, "Design space characterization for meeting cost and carbon reduction goals," *Journal of Industrial Ecology*, vol. 14, no. 5, pp. 727–739, 2010.
- [41] V. Brilliantova and T. W. Thurner, "Blockchain and the future of energy," *Technology in Society*, vol. 57, pp. 38–45, 2019.
- [42] G. Büyüközkan and G. Çifçi, "A novel hybrid MCDM approach based on fuzzy DEMATEL, fuzzy ANP and fuzzy TOPSIS to evaluate green suppliers," *Expert Systems with Applications*, vol. 39, no. 3, pp. 3000–3011, 2012.
- [43] S. Opricovic and G.-H. Tzeng, "Compromise solution by MCDM methods: a comparative analysis of VIKOR and TOPSIS," *European Journal of Operational Research*, vol. 156, no. 2, pp. 445–455, 2004.
- [44] W.-W. Wu and Y.-T. Lee, "Developing global managers' competencies using the fuzzy DEMATEL method," *Expert Systems with Applications*, vol. 32, no. 2, pp. 499–507, 2007.
- [45] Y. Beikhhakhian, M. Javanmardi, M. Karbasian, and B. Khayambashi, "The application of ISM model in evaluating agile suppliers selection criteria and ranking suppliers using fuzzy TOPSIS-AHP methods," *Expert Systems with Applications*, vol. 42, no. 15–16, pp. 6224–6236, 2015.
- [46] H. Liu and B. Lin, "Incorporating energy rebound effect in technological advancement and green building construction: a case study of China," *Energy and Buildings*, vol. 129, pp. 150–161, 2016.
- [47] Y.-C. Tsao and T.-L. Vu, "Power supply chain network design problem for smart grid considering differential pricing and buy-back policies," *Energy Economics*, vol. 81, pp. 493–502, 2019.
- [48] B. Scott, J. Loonam, and V. Kumar, "Exploring the rise of blockchain technology: towards distributed collaborative organizations," *Strategic Change*, vol. 26, no. 5, pp. 423–428, 2017.
- [49] S. Hall and T. J. Foxon, "Values in the Smart Grid: the co-evolving political economy of smart distribution," *Energy Policy*, vol. 74, pp. 600–609, 2014.
- [50] R. Scholz, E. Bartelsman, S. Diefenbach et al., "Unintended side effects of the digital transition: European scientists' messages from a proposition-based expert round table," *Sustainability*, vol. 10, no. 6, p. 2001, 2018.

Research Article

Optimal Service Commission Contract Design of OTA to Create O2O Model by Cooperation with TTA under Asymmetric Information

Pingping Shi,¹ Yaogang Hu ,² and Yongfeng Wang¹

¹School of Management, Chongqing University of Technology, Chongqing 400054, China

²School of Electrical and Electronic Engineering, Chongqing University of Technology, Chongqing 400054, China

Correspondence should be addressed to Yaogang Hu; 569934301@qq.com

Received 16 March 2021; Revised 19 April 2021; Accepted 21 April 2021; Published 3 May 2021

Academic Editor: Ming Bao Cheng

Copyright © 2021 Pingping Shi et al. This is an open access article distributed under the Creative Commons Attribution License, which permits unrestricted use, distribution, and reproduction in any medium, provided the original work is properly cited.

This paper studies the service commission contract of an online travel agency (OTA) to integrate the online to offline (O2O) model by cooperation with a traditional travel agency (TTA) under asymmetric information. The principal-agent models are established with symmetric and asymmetric service information, respectively. Further, the impacts of asymmetry information on the revenue of the OTA, TTA, and the whole O2O model and the properties of optimal commission contract are analyzed. The paper notes management implications: (1) OTA designs service commission contracts by weighing the fixed payment and service commission coefficient for different incentives to TTAs with different serviceabilities and (2) because the existence of asymmetric information always leads to the damage of OTA's expected revenue, OTA should encourage the TTA to disclose private service information.

1. Introduction

With the rapid development of Internet and information technology, it is a popular and convenient way for tourists to buy more diverse tourism products and services through online travel agencies (OTAs) [1–3]. However, online tourism product homogenization makes OTAs reduce the service quality to attract more tourists, such as cashback and low price, forcing consumption in the experience, which seriously increase tourists' complaints and hinder the healthy development of online tourism [4–6]. To improve competitive advantage and realize differentiation, some OTAs (e.g., Ctrip) open up offline stores to achieve online to offline (O2O) model for providing personal information and advice to tourists, and some cooperate with traditional travel agencies (TTAs), such as Uzai (<http://www.uzai.com/>) and ZhongXin TTA, Lvmama (<http://www.lvmama.com>), and JinJiang TTA [4]. In the process of cooperation between OTAs and TTAs, it is difficult for OTAs to observe TTAs' service information, which makes the cooperation and incentive problem more complicated.

Therefore, how to design the commission contract of TTAs strategically for OTAs is an urgent problem to implement O2O strategy.

The O2O model, as a new e-commerce business model, combines online trading and offline experience and has become an important strategy for the development of enterprises in recent years [7]. With the rapid development of OTAs, the online channel plays a crucial role in tourism and hospitality, and the tourism O2O model achieved by the cooperation between OTAs and hotels or airlines is a common phenomenon. Therefore, there is a growing popularity on the cooperation problem between OTAs and hotels or airlines and they have gotten some effective cooperation strategies [1, 8–11]. However, to seek better business opportunities, OTAs have to attach importance to the offline service to achieve differentiation. Although some scientific researchers have demonstrated the importance of TTAs' advice-offering and OTAs' attributes in travelers' booking, little literature in the hospitality and tourism fields has studied the service contract problem of cooperation between OTAs and TTAs.

To fill this gap and provide some suggestions for OTAs and TTAs managers on establishing the O2O model through service cooperation, this paper proposes a cooperation model to describe decision interactions of an OTA and a TTA. The OTA and TTA play a principal-agent model in which the OTA, as the principal player, determines the service commission and the TTA, as the agent, determines service effort. In addition, in the O2O model, because the OTA and TTA are relatively independent, TTA's private information is difficult to disclose and it often hides its own service information to obtain higher revenue. By comparing the case of information symmetry and asymmetry, the impacts of asymmetry information on OTA's service contract, TTA's information value, and the revenue of OTA and TTA are analyzed.

The rest of this paper is organized as follows. Section 2 reviews the related literature. Section 3 describes the service cooperation between an OTA and a TTA. Section 4 analyzes and compares equilibriums of symmetric and asymmetric information and further analyzes equilibriums when TTA's ability is continuous. Section 5 presents the results of numerical analyses. Section 6 concludes this paper by summarizing some of the managerial implications obtained.

2. Literature Review

According to the purpose of studying the service cooperation contract design of OTAs and TTAs, this section reviews three distinct of literature studies about the O2O model, service cooperation, and cooperation between tourism enterprises and OTAs.

2.1. O2O Model. Since Alex Rampel put forward the concept of the O2O model, it has attracted wide attention in academia. Although the concept and classification of the O2O model are different because of the scholars' different research perspectives, it is a business model for the effective integration of online and offline stores [4, 7]. It is believed that O2O is a new business model, which can disclose product information, change consumer brand awareness, and mitigate the adverse effects of product uncertainty on consumers' shopping decisions [12]. By using 311 respondent data from O2O e-commerce users in Greater Jakarta Area, Savila et al. showed that both multichannel integration and trust have a significant effect on both customer online loyalty and customer offline loyalty that drive customer repurchase intention [13].

According to the existing research about the O2O model, it can be divided into two categories: one is to purchase online and then experience offline, which can also be called online to offline; the other is to experience offline and then purchase online, which can also be called offline to online [14]. In the hospitality and tourism industry, because tourists have to experience tourism products offline, the O2O model achieved by the cooperation between OTAs and hotels or airlines is a common phenomenon. From the perspective of the supply chain, scholars more emphasize the sale cooperation between the OTAs and hotels or airlines

and have gotten some effective cooperation strategies [1, 8–11]. In the retail industry, as the major characteristic feature of a product is tangible, it can be touched and tried out. The O2O model, achieved by cooperating with others or opening by oneself [14, 15], becomes the main research direction. Considering that the service cost and effort information of the showroom are asymmetry, Jin et al. study the design of the commission contract of offline to online, which is considered that the showroom and online retailer have impacts on consumers' purchasing decisions, respectively [15]. In practice, online sale efforts and offline services will affect the demand for each other. Therefore, it is difficult to highlight the integrity of the online retailer and store cocreating O2O model by splitting online and offline demand.

Despite the impact of technology and the advent of online bookings, offline channels play a pivotal role in the tourism supply chain. Unlike the general retail product, the tourism product of a travel agency cannot be touched, transported, stored, or returned. The functions of offline channels are different between general retailer and travel agency. The offline channels of general retailer provide touching, trying, and even online return service for consumers. The offline channels of travel agency provide scene experience, personal and professional information, and advice to meet travelers' demands on a continuous basis by gathering and organizing information [16, 17]. The O2O model of travel agency in this paper is an integration of online and offline. Both online sale efforts and offline services will have an impact on the overall demand for the O2O model.

2.2. Service Cooperation. The existing literature on service cooperation is mostly concentrated in the supply chain field. Service cooperation not only reduces the competition between direct and retail channels but also improves supply chain revenue [18–21]. Unit service reward and service cost sharing are the main forms of service cooperation. To avoid channel conflict and improve service efficiency, Xiao, Dan, and Zhang studied after-sale service cooperation between direct channel and retailers in which direct channel pays unit service commission to retailers [18]. In the O2O retail market, the service cost sharing mechanism is introduced to coordinate conflicts and achieve a win-win strategy, thereby improving the performance of the entire O2O supply chain [19]. Due to the importance of presales services in purchasing decisions, Zhou et al. introduce that the service cost sharing contract can effectively stimulate the retailer to improve his service level while free riding occurred [20]. Considering that the retailer provides the same service level in both channels or not, Yang and Zhang compare the manufacturer's optimal profit and retailer's optimal profit under the condition of different services and the same service and provide differentiated services to enable the system to achieve the optimal profit [21]. However, the completely symmetrical assumptions in the above literature are not currently common practice. The adverse selection and moral hazard are always in the cooperation process [22].

2.3. *Cooperation between Tourism Enterprises and OTAs.* Clearly, the OTAs are an extremely important part of the tourism supply chain, recognized as an online distribution channel for hotels and airlines. A larger number of scholars have emerged to pay attention to the issue of the cooperation problem between hotels, airlines, and OTAs, such as pricing strategy, cooperation form, and coordination strategy [1, 8–11]. Koo et al. point out that the airlines are less likely to use OTA platforms if the airlines have a large loyal consumer base or if the OTA platform is highly competitive [8]. Ling et al. and Guo et al. study the optimal pricing strategy for tourism hotels when they operate their online channel by cooperation with an OTA [1, 9]. Considering the overbooking of hotels, Dong and Ling study the pricing and overbooking strategies of a hotel in the context of cooperation with multiple OTAs and analyze how these strategies influence the cooperation process [10]. The commonly used “first come first serve” form puts hotels in a disadvantageous position especially when the OTAs have much more market attractiveness than the hotels. Xu et al. propose a new form named “setting Online-Exclusive-Rooms” for a hotel to collaborate with a third-party website on room booking service [11].

To get a new business opportunity, the TTAs are increasingly aware of the need to open up online markets’ cooperation with OTAs because of the low volume of visits and lack of e-commerce operating experience of self-built website [3, 4]. Therefore, a few scholars have provided suggestions on the cooperation between TTA and OTA. Based on the resource-based view, Shi and Long analyze the complementary resources input decisions of OTAs and TTAs cocreating the O2O model, which do not propose a clear form of cooperation [3]. In a supplemental study, Long and Shi study the optimal pricing strategies of a tour operator and an OTA when they achieve the O2O business model through online sale and offline service cooperation to develop the advantage of complementary resources [4].

However, no study has addressed the problem of an OTA that wants to achieve its O2O model by cooperating with a TTA with private information. In this situation, the OTA has little information and experience regarding offline service and knows little about how to design a service contract to disclosure TTA’s real information. To enrich the scientific literature and provide some suggestions to OTA on how to pursue offline service, this paper studies the optimal service contract of OTAs under asymmetric information through the analysis of a simple O2O model composed of an OTA and a TTA.

3. Problem Description and Assumptions

In this paper, the O2O model, combining both trading and offline service, achieved by service cooperation of an OTA and a TTA is considered herein. Table 1 summarizes the main notation and its definitions used in this paper.

The OTA makes some effort to induce customers to make reservations through its website, such as ranking position. According to the literature [1], $c(e_O)$ is a convex increasing function with $dc(e_O)/de_O > 0$, $d^2c(e_O)/de_O^2 > 0$,

and $c(e_O) = 0$. The sale cost of OTA is $c(e_O) = \eta_O e_O^2/2$, where η_O is the OTA’s sale cost coefficient, which is widely used in the cost management literature [23–26].

While the TTA provides offline services for tourism products, such as the scene experience and personalized and professional travel advice, the service effort is the cost of hiring salespersons by TTA. According to the literature [4, 25, 26], a strictly convex service function $c(e_T)$ is used to depict TTA’s unit cost of service effort, $c(e_T) = \eta_T e_T^2/2$, where η_T is the TTA’s service cost coefficient, $dc(e_T)/de_T > 0$, and $d^2c(e_T)/de_T^2 > 0$.

The demand for O2O model q is influenced by OTA’s saleability s_O , sale effort e_O , TTA’s serviceability s_T , service effort e_T , market scale θ , and market random factors ξ .

$$q = f(s_O, e_O) + g(s_T, e_T) + u(\theta) + \xi, \quad (1)$$

where $f_{s_O} > 0$, $f_{s_O s_O} \leq 0$, $f_{e_O} > 0$, $f_{e_O e_O} \leq 0$, $g_{s_T} > 0$, $g_{s_T s_T} \leq 0$, $g_{e_T} > 0$, $g_{e_T e_T} \leq 0$, $u_\theta > 0$, $u_{\theta\theta} \leq 0$, and ξ follows a normal distribution $\xi \in N(0, \sigma^2)$.

In this paper, according to the literature [27], let $f(e_O) = s_O e_O$, $g(e_T) = s_T e_T$, and $u(\theta) = \theta$. Thus, the demand for O2O model is $q = s_O e_O + s_T e_T + \theta + \xi$. Assuming that the revenue of O2O model is proportional to its demand, the revenue of O2O model can be simplified into $\Pi(q) = s_O e_O + s_T e_T + \theta + \xi$. Following the studies of Jin et al. [15] and He et al. [28], OTA provides service commission (a, b) to motivate TTA to make service effort, where a represents fixed payment and b denotes service commission coefficient or the rate of revenue sharing. Therefore, given (a, b) , the service commission that OTA pays for TTA is $T(q) = a + b\Pi(q)$.

Based on the above assumptions, the OTA’s revenue function is obtained as follows:

$$\begin{aligned} \Pi_O = & \Pi(q) - T(q) - c(e_O) = (1 - b)(s_O e_O + s_T e_T + \theta + \xi) \\ & - a - \frac{\eta_O e_O^2}{2}. \end{aligned} \quad (2)$$

Assuming that OTA is risk-neutral and its utility is equal to expected revenue, the OTA’s expected revenue is

$$E\Pi_O = (1 - b)(s_O e_O + s_T e_T + \theta) - a - \frac{\eta_O e_O^2}{2}. \quad (3)$$

The TTA’s revenue is

$$\Pi_T = T(q) - c(e_T) = a + b(s_O e_O + s_T e_T + \theta + \xi) - \frac{\eta_T e_T^2}{2}. \quad (4)$$

Assuming that TTA is risk-neutral risk aversion, one form of the utility function dominant in both theoretical and applied work in areas of decision theory and finance is the exponential utility function. Following the literature [29], $U_T(\Pi_T) = -e^{-r\Pi_T}$, where r denotes TTA’s risk aversion coefficient and $r > 0$, $r = 0$, and $r < 0$ are risk aversion, risk neutrality, and risk preference, respectively. By certainty equivalence method, the revenue of TTA is obtained as follows:

TABLE 1: Notation and definitions.

Notation	Definitions
s_O	Sale ability of OTA
e_O	Sale effort of OTA
$C(e_O)$	Sale cost of OTA
η_O	Sale cost coefficient of OTA
s_T	Serviceability of TTA
e_T	Service effort of TTA
η_T	Service cost coefficient of TTA
$C(e_T)$	Unit cost of service effort of TTA
Q	The demand for O2O model
θ	Market scale
ξ	Market random factors
$T(q)$	Service commission that OTA pays for TTA
A	Fixed payment
B	Service commission coefficient or the rate of revenue sharing
$\Pi(q), \Pi_O, \Pi_T$	The revenue of O2O model, OTA, and TTA, respectively
$E\Pi_O, E\Pi_T$	The expected revenue of OTA and TTA, respectively
$U_T(E\Pi_T)$	The utility function of TTA
R	TTA's risk aversion coefficient
I	The state of TTA's serviceability, $i = H, L$
s_{Ti}	TTA's serviceability, $i = H, L$
ρ	The probability that the OTA believes that the TTA's serviceability is at a high state

Note that the superscript * denotes the optimal solutions.

$$E\Pi_T = a + b(s_O e_O + s_T e_T + \theta) - \frac{\eta_T e_T^2}{2} - \frac{r\sigma^2 b^2}{2}. \quad (5)$$

Due to the uncertainty of the O2O model market demand and equation (5), TTA's risk cost is $r\sigma^2 b^2/2$.

4. Equilibrium Solutions and Analysis

This paper mainly studies the service cooperation contract design of OTA creating O2O model by cooperating with TTA under symmetric and asymmetric information. Further, the contract model with continuous type of TTA's serviceability under information asymmetry is researched. Here, the superscripts "N," "S," and "C" represent the case of symmetric information, the discrete type, and continuous type of TTA's service capability under information asymmetry, respectively.

In the process of establishing service cooperation between an OTA and a TTA, the serviceability and effort are TTA's private information which OTA is difficult to observe. Similar to the study of Li et al. [30], it is assumed that there are two possibilities for TTA's serviceability: high serviceability s_{TH} and low serviceability s_{TL} , and $s_{TH} > s_{TL}$.

4.1. Equilibrium of Symmetric Information. In the case of symmetric information, the OTA fully knows the state of TTA's serviceability s_{Ti} ($i = H, L$). The OTA designs a service contract (a_i^N, b_i^N) and sale effort $e_{O_i}^N$ when the type of TTA's serviceability is i . Then the expected revenue of OTA $E\Pi_O(a_i^N, b_i^N)$ and TTA $E\Pi_{Ti}(a_i^N, b_i^N)$ and the optimization problem P1 is

$$\begin{cases} \max_{a_i^N, b_i^N, e_{O_i}^N} E\Pi_O = (1 - b_i^N) \left((s_O e_{O_i}^N + s_{Ti} e_{Ti}^N + \theta) - a_i^N - \frac{\eta_O e_{O_i}^{N2}}{2} \right), \\ \text{s.t. } (IR - i) a_i^N + b_i^N (s_O e_{O_i}^N + s_{Ti} e_{Ti}^N + \theta) - \frac{\eta_T e_{Ti}^{N2}}{2} - \frac{r\sigma^2 (b_i^N)^2}{2} \geq \underline{\Pi}_T, \end{cases} \quad (6)$$

where

$$e_{Ti}^N = \arg \max_{e_T} \left(a_i^N + b_i^N (s_O e_{O_i}^N + s_{Ti} e_{Ti}^N + \theta) - \frac{\eta_T e_{Ti}^{N2}}{2} - \frac{r\sigma^2 (b_i^N)^2}{2} \right). \quad (7)$$

In the above optimization problem P1, the OTA maximizes its revenue. Inequality $(IR - i)$ is individual constraints, assuring that the TTA will join the service cooperation because of exceeding the reservation revenue $\underline{\Pi}_T$. Equation

(7) denotes the TTA optimizes service effort by maximizing its revenue. The optimal decisions are found out by solving the above optimization problem P1 using the backward induction method.

Theorem 1. In the case of symmetric information, given the type of TTA's serviceability as i , the OTA's optimal service contract (a_i^{N*}, b_i^{N*}) , sale effort $e_{O_i}^{N*}$, and the TTA's optimal service effort $e_{T_i}^{N*}$ are

$$\begin{aligned} b_i^{N*} &= \frac{s_{Ti}^2}{s_{Ti}^2 + \eta_T r \sigma^2}, \\ a_i^{N*} &= \frac{\Pi_T}{\eta_O} - \left(\frac{s_O}{\eta_O} + \theta \right) b_i^{N*} + \frac{1}{2} \left(r \sigma^2 - \frac{s_{Ti}^2}{\eta_T} \right) (b_i^{N*})^2, \\ e_{O_i}^{N*} &= \frac{s_O}{\eta_O}, \\ e_{T_i}^{N*} &= \frac{s_{Ti}^3}{\eta_T (s_{Ti}^2 + \eta_T r \sigma^2)} = \frac{s_{Ti} b_i^{N*}}{\eta_T}. \end{aligned} \quad (8)$$

Theorem 1 shows that, (1) with the TTA's service cost coefficient η_T , market uncertainty σ^2 , and risk aversion coefficient r increasing, the service commission coefficient b_i^{N*} decreases; (2) when the market scale θ and OTA's sale ability decreasing s_O or OTA's sale cost coefficient η_O increasing, the OTA's fixed payment increases a_i^{N*} , so as to encourage TTA to participate in cooperation for cocreating the O2O model. In addition, s_O and η_O only affect OTA's fixed payment a_i^{N*} but have no effect on service commission coefficient b_i^{N*} ; (3) the OTA's online sales effort $e_{O_i}^{N*}$ is only related to its own saleability

s_O and cost coefficient η_O and is directly proportional to s_O and inversely proportional to η_O ; (4) with the service commission coefficient b_i^{N*} and TTA's serviceability s_{T_i} increasing or TTA's service cost coefficient η_T decreasing, the TTA's offline service effort $e_{T_i}^{N*}$ increases.

4.2. Equilibrium of Asymmetric Information. In the case of asymmetric information, the TTA surely knows which of the two serviceability states will occur, while the OTA has only a subjective assessment about the likelihood of the two serviceability states. Let ρ be the probability that the OTA believes that the TTA's serviceability is at a high state and $1-\rho$ be the probability of the low state. Due to its parsimony and tractability for analysis, this type of asymmetric information has been commonly employed in supply chain contracting [15, 27, 30]. In this paper, the OTA is an uninformed party that acts as a principal, and the TTA is an agent that holds private information about its serviceability. The service contract design problem is investigated under asymmetric serviceability information. The goal of the OTA is to design a menu of service contracts so as to maximize its expected profit based on the revelation principle.

When the state of TTA's serviceability is i and OTA gives service contract (a_i^S, b_i^S) and sale effort $e_{O_i}^S$, the revenue of OTA and TTA is $E\Pi_O(a_i^S, b_i^S)$ and $E\Pi_{T_i}(a_i^S, b_i^S)$, respectively, and then the optimization problem P2 is

$$\left\{ \begin{aligned} & \max_{a_H^S, b_H^S, e_{OH}^S, a_L^S, b_L^S, e_{OL}^S} E\Pi_O = \left\{ \rho \left((1 - b_H^S) (s_O e_{OH}^S + s_{TH} e_{TH}^S + \theta) - a_H^S - \frac{\eta_O e_{OH}^{S2}}{2} \right) + \right. \\ & \left. (1 - \rho) \left((1 - b_L^S) (s_O e_{OL}^S + s_{TL} e_{TL}^S + \theta) - a_L^S - \frac{\eta_O e_{OL}^{S2}}{2} \right) \right\} \\ & \text{s.t. (IC - H)} a_H^S + b_H^S (s_O e_{OH}^S + s_{TH} e_{TH}^S + \theta) - \frac{\eta_T e_{TH}^{S2}}{2} - \frac{r \sigma^2 b_H^2}{2} \geq \\ & a_L^S + b_L^S (s_O e_{OS}^S + s_{TH} e_{TH}^L + \theta) - \frac{\eta_T e_{TH}^{L2}}{2} - \frac{r \sigma^2 b_L^2}{2} \\ & \text{(IC - L)} a_L^S + b_L^S (s_O e_{OL}^S + s_{TL} e_{TL}^S + \theta) - \frac{\eta_T e_{TL}^{S2}}{2} - \frac{r \sigma^2 b_L^2}{2} \geq \\ & a_H^S + b_H^S (s_O e_{OH}^S + s_{TL} e_{TL}^H + \theta) - \frac{\eta_T e_{TL}^{H2}}{2} - \frac{r \sigma^2 b_H^2}{2}, \\ & \text{(IR - H)} a_H^S + b_H^S (s_O e_{OH}^S + s_{TH} e_{TH}^S + \theta) - \frac{\eta_T e_{TH}^{S2}}{2} - \frac{r \sigma^2 b_H^2}{2} \geq \underline{\Pi_T}, \\ & \text{(IR - L)} a_L^S + b_L^S (s_O e_{OL}^S + s_{TL} e_{TL}^S + \theta) - \frac{\eta_T e_{TL}^{S2}}{2} - \frac{r \sigma^2 b_L^2}{2} \geq \underline{\Pi_T}, \end{aligned} \right. \quad (9)$$

where

$$e_{TH}^S = \arg \max_e \left(a_H^S + b_H^S (s_O e_{OH}^S + s_{TH} e_{TH}^S + \theta) - \frac{\eta_T e_{TH}^{S2}}{2} - \frac{r\sigma^2 b_H^2}{2} \right), \quad (10)$$

$$e_{TL}^S = \arg \max_e \left(a_L^S + b_L^S (s_O e_{OL}^S + s_{TL} e_{TL}^S + \theta) - \frac{\eta_T e_{TL}^{S2}}{2} - \frac{r\sigma^2 b_L^2}{2} \right). \quad (11)$$

In the above optimization problem P2, the expected revenue of OTA $E\Pi_O$ is the sum of revenue under the cooperation of serviceability states of TTA. Inequalities (IC-i) are incentive compatibility constraints, assuring that the TTA does not pretend to choose the other serviceability state, where $e_{TH}^L(e_{TL}^H)$ indicates the optimal service effort level of TTA under service reward contract (a_L^S, b_L^S) ((a_H^S, b_H^S)). Inequalities (IR-i) are individual rationality constraints, assuring that the TTA will join to cocreate O2O model because of exceeding the reservation revenue Π_T . Equations (10) and (11) denote the TTA optimizes its service

effort e_{Ti}^N by maximizing its revenue according to OTA's service cooperation contract (a_i^S, b_i^S) and sale effort e_{Oi}^S . The optimal decisions are found out by solving the above optimization problem P2 using the backward induction method.

Theorem 2. *Under asymmetric information, the OTA reveals TTA's serviceability by designing separation contracts. The OTA's service commission contract, optimal sale effort, and TTA's service effort are*

$$\begin{aligned} a_H^{S*} &= \underline{\Pi_T} - \left(\frac{s_O^2}{\eta_O} + \theta \right) b_H^{S*} + \frac{1}{2} \left(r\sigma^2 - \frac{s_{TH}^2}{\eta_T} \right) (b_H^{S*})^2 + \frac{1}{2\eta_T} (s_{TH}^2 - s_{TL}^2) (b_L^{S*})^2, \\ b_H^{S*} &= \frac{s_{TH}^2}{s_{TH}^2 + \eta_T r\sigma^2}, \\ a_L^{S*} &= \underline{\Pi_T} - \left(\frac{s_O^2}{\eta_O} + \theta \right) b_L^{S*} + \frac{1}{2} \left(r\sigma^2 - \frac{s_{TL}^2}{\eta_T} \right) (b_L^{S*})^2, \\ b_L^{S*} &= \frac{(1-\rho)s_{TL}^2}{s_{TL}^2 - 2\rho s_{TL}^2 + \rho s_{TH}^2 + (1-\rho)\eta_T r\sigma^2}, \\ e_{OH}^{S*} &= e_{OL}^{S*} = \frac{s_O}{\eta_O}, \\ e_{TH}^{S*} &= \frac{s_{TH}^3}{\eta_T (s_{TH}^2 + \eta_T r\sigma^2)}, \\ e_{TL}^{S*} &= \frac{(1-\rho)s_{TL}^3}{(s_{TL}^2 - 2\rho s_{TL}^2 + \rho s_{TH}^2 + (1-\rho)\eta_T r\sigma^2)\eta_T}. \end{aligned} \quad (12)$$

Theorem 2 shows the following:

- (1) When $r \rightarrow +\infty$, $b_H^{S*} = b_L^{S*} = 0$ and $a_H^{S*} = a_L^{S*} = \underline{\Pi_T}$ can be obtained. That is, when TTA has no risk tolerance, its revenue could only be equal to its reservation revenue. When $r \rightarrow 0$, $b_H^{S*} = 1$ and $b_L^{S*} = (1/1 + \rho(s_{TH}^2 - s_{TL}^2)/(1-\rho)s_{TL}^2) < 1$. That is, when the TTA tends to be risk-neutral, TTA with high serviceability will obtain the total revenue and if the

difference between the two types of TTA's serviceability or the probability of TTA with high serviceability is greater, the OTA's service commission coefficient for TTA with low serviceability is lower. When $r > 0$, with the increase of TTA's risk aversion coefficient, the service commission coefficient decreases correspondingly, indicating that risk aversion can offset the incentive effect of the service commission coefficient.

- (2) According to $(\partial b_H^{S*} / \partial s_{TH}) \geq 0$ ($\partial b_L^{S*} / \partial s_{TL}) \geq 0$, the service commission coefficient will increase with the increasing TTA's serviceability.
- (3) The service effort of the TTA with low serviceability has no effect on the service commission coefficient the TTA with high serviceability obtains. However, the difference between service effort of TTA with high and low service will affect the service commission coefficient TTA with low serviceability obtains, and the greater the difference is, the smaller the service commission coefficient is.
- (4) According to $(\partial b_H^{S*} / \partial \rho) = 0$ ($\partial b_L^{S*} / \partial \rho) \leq 0$, the probability ρ has no effect on service commission coefficient that the TTA with high serviceability obtains. However, with the increase of ρ , the service commission coefficient that the TTA with high serviceability obtains decreases.
- (5) The relationship between service commission coefficient and TTA's service cost coefficient η_T , the degree of market uncertainty σ^2 , the degree of risk aversion r , and the relationship between fixed payment and OTA's saleability and sale cost coefficient are the same under symmetric information, which is omitted here.

Corollary 1. For TTA with different serviceability, the optimal service commission contract parameters have the relationships $b_H^{S*} \geq b_L^{S*}$ and $a_H^{S*} \leq a_L^{S*}$.

Corollary 1 shows that the motivation purpose of OTA service contract is different for TTA with different serviceability. This means that the OTA should balance the motivation cooperation and the incentive of improving service effort for TTA when designing service commission contract. If the TTA is of a low serviceability type, the OTA will give TTA a larger fixed payment to ensure TTA's initiative in cocreating the O2O model. If the TTA is of a high serviceability state, the OTA will give a larger service commission coefficient. And according to $b_H^{S*} - b_L^{S*} = ((s_{TH}^2 - s_{TL}^2) (\rho s_{TH}^2 + (1 - \rho) \eta_T r \sigma^2) / (s_{TH}^2 + \eta_T r \sigma^2) (s_{TL}^2 - 2\rho s_{TL}^2 + \rho s_{TH}^2 + (1 - \rho) \eta_T r \sigma^2)) \geq 0$, the greater the difference between service efforts of TTA with high and low service, the bigger the difference of service commission coefficient.

4.3. Comparison of Results under Symmetric and Asymmetric Information

4.3.1. Validity of Separation Service Contract. By introducing the results of Theorem 2 into incentive compatibility constraints (IC-i) and comparing the TTA's revenue of TTA false and truthfulness reporting serviceability, it is obtained as

$$E\Pi_{TH}(a_H^{S*}, b_H^{S*}) - E\Pi_{TH}(a_L^{S*}, b_L^{S*}) = 0, \tag{13}$$

$$E\Pi_{TL}(a_L^{S*}, b_L^{S*}) - E\Pi_{TL}(a_H^{S*}, b_H^{S*}) = \frac{(b_H^{S*} - b_L^{S*})(b_H^{S*} + b_L^{S*})(s_{TH} + s_{TL})}{2\eta_T} > 0.$$

When the TTA with low serviceability pretends to be the TTA with high serviceability, the revenue is strictly lower than that when TTA truthfully reports serviceability ($E\Pi_{TL}(a_H^{S*}, b_H^{S*}) < E\Pi_{TL}(a_L^{S*}, b_L^{S*})$). Therefore, the TTA with low serviceability has no motivation to disguise the TTA with high serviceability. In addition, if the TTA is of a high serviceability type, its false report will not affect its revenue ($E\Pi_{TH}(a_H^{S*}, b_H^{S*}) = E\Pi_{TH}(a_L^{S*}, b_L^{S*})$). Therefore, the TTA with high serviceability has no motivation to disguise TTA with low serviceability. It can be seen that separation of service contract has the characteristics of "self-selection" in the OTA and TTA cocreating O2O model. That is, the TTA with high or low serviceability needs to choose the service contract corresponding to its serviceability type.

Corollary 2. By comparing the expected revenue and the reservation revenue with different serviceability types, it is obtained as

$$E\Pi_T(s_{TL}) = \underline{\Pi}_T, \tag{14}$$

$$E\Pi_T(s_{TH}) = \underline{\Pi}_T + \frac{(s_{TH}^2 - s_{TL}^2)}{2\eta_T} b_L^{S*2}.$$

Corollary 2 shows that when the TTA is of a low serviceability type, TTA's revenue is reservation revenue after accepting the service commission contract. However, when the revenue of TTA with high serviceability is greater than reservation revenue, the difference $((s_{TH}^2 - s_{TL}^2)/2\eta_T) b_L^{S*2}$ shows that, in order to obtain private information of TTA's serviceability, the OTA needs to pay TTA information sharing fees. If the OTA does not pay the information fee, TTA may lie about its serviceability and damage the OTA's expected revenue.

4.3.2. The Impact of Information Asymmetric on Service Contract and Expected Revenue. According to Theorems 1 and 2, by comparing and analyzing the service contract, TTA's optimal service effort, and the revenues of the partners under symmetric and asymmetric information conditions, Theorems 3 and 4 are obtained.

Theorem 3. The optimal service contract, sale effort, and TTA optimal service effort under symmetry and asymmetry information have the following relationships:

- (1) $a_H^{S*} \geq a_H^{N*}, b_H^{N*} = b_H^{S*}$
- (2) $a_L^{S*} \geq a_L^{N*}, b_L^{S*} \leq b_L^{N*}$
- (3) $e_{TH}^{N*} = e_{TH}^{S*}, e_{TL}^{S*} < e_{TL}^{N*}$
- (4) $e_{Oi}^{N*} = e_{Oi}^{S*}$

In Theorem 3, (1) and (2) show that the OTA should pay a higher fixed payment to mobilize TTA to participate in cocreating the O2O model under asymmetric information. If the TTA is of a low serviceability type, the OTA lacks motivation to encourage TTA to provide higher service effort, and the service commission coefficient is “distorted downward.” If the TTA is of a high serviceability type, the OTA will provide a higher service commission coefficient to encourage the TTA to provide higher service effort under asymmetrical information. Here, the TTA can obtain additional information rent by “upward distorted” fixed payment. This also means that, due to the existence of asymmetric information, the service contract design of OTA needs to adjust the fixed payment and service commission coefficient to ensure that TTA can participate in cooperation and choose the appropriate level of service efforts that are beneficial to OTA. From (3), the service effort of TTA with the high serviceability is the same in symmetrical and asymmetrical information, and the service effort of TTA with the low serviceability is lower in asymmetrical information than that in symmetrical information. Therefore, the OTA is dominant in encouraging low serviceability type TTA to participate in cooperation, which will also provide incentives to participate in cooperation and service efforts to TTA with high serviceability state. (4) shows that the OTA’s optimal sale effort is the same in symmetrical and asymmetrical information. This is straightforward because the OTA knows its own saleability information.

Theorem 4. *There is the following relationship between OTA’s and TTA’s expected revenue under symmetry and asymmetry information:*

- (1) $E\Pi_{Oi}^{S*} \leq E\Pi_{Oi}^{N*}$
- (2) $E\Pi_{TH}^{S*} \geq E\Pi_{TH}^{N*}$
- (3) $E\Pi_{TL}^{S*} = E\Pi_{TL}^{N*}$

Theorem 4 shows that the information disadvantage of OTA is detrimental to its expected revenue; the information advantage of TTA does not necessarily generate information rent. When the TTA is the high serviceability type, the increase of fixed payment cost and constant service commission coefficient make OTA pay higher service commission. Therefore, the TTA with high serviceability can get additional information rent from the increased fixed payment. When the TTA is of a low serviceability type, the asymmetric information makes the service commission coefficient tilt downward and fixed payment cost rise, and the rise of fixed payment can make up for the loss of TTA caused by the decline of service commission coefficient. Therefore, the expected revenue of TTA with low serviceability remains unchanged.

4.4. Strategic Analysis When TTA’s Service Ability Is Continuous. Assuming that TTAs’ service capability is continuously distributed and satisfied $s_T \in H = [s_T^-, s_T^+]$, $F(s_T)$ and $f(s_T)$ are TTA’s cumulative distribution and distribution density function, respectively, and $f(s_T) > 0$.

Due to the fact that ξ is not related to s_T , the expected revenue of risk-neutral OTA can be obtained as

$$E\Pi_O(s_T) = \int_{s_T^-}^{s_T^+} \left\{ (1 - b^C(s_T))(s_O e_O^C(s_T) + s_T e_T^C(s_T) + \theta) - a^C(s_T) - \frac{\eta_O e_O^{C2}(s_T)}{2} \right\} f(s_T) ds_T. \quad (15)$$

The expected revenue of TTA is

$$E\Pi_T(s_T) = a^C(s_T) + b^C(s_T)(s_O e_O^C(s_T) + s_T e_T^C(s_T) + \theta) - \frac{\eta_T e_T^{C2}(s_T)}{2} - \frac{r\sigma^2 b^{C2}(s_T)}{2}. \quad (16)$$

Firstly, determine the service effort level of TTA $e_T^C(s_T)$; that is, $\forall s_T \in H$, $e_T^C(s_T) = \operatorname{argmax}_e E\Pi_T(s_T) = (s_T^C b^C(s_T) / \eta_T)$.

Bringing $e_T^C(s_T)$ to equation (16), it is obtained as

$$E\Pi_T(s_T) = a^C(s_T) + (s_O e_O^C(s_T) + \theta) b^C(s_T) + \frac{1}{2} \left(\frac{s_T^2}{\eta_T} - r\sigma^2 \right) b^{C2}(s_T). \quad (17)$$

Furthermore, when s_T is continuous, the optimization problem P3 is

$$\max_{a^C, b^C} \int_{s_T^-}^{s_T^+} \left\{ (1 - b^C(s_T))(s_O e_O^C(s_T) + s_T e_T^C(s_T) + \theta) - a^C(s_T) - \frac{\eta_O e_O^{C2}(s_T)}{2} \right\} f(s_T) ds_T \quad (18)$$

$$\text{s.t. (IC)} b^C(s_T) \geq 0,$$

$$\text{(IC)} a^C(s_T) + s_O e_O^C(s_T) b^C(s_T) + (s_O e_O^C(s_T) + \theta) b^C(s_T) + \left(\frac{s_T^2}{\eta_T} - r\sigma^2 \right) b^{C2}(s_T) = 0, \quad (19)$$

$$(IR)a^C(s_T) + (s_O e_O^C(s_T) + \theta)b^C(s_T) + \frac{1}{2} \left(\frac{s_T^2}{\eta_T} - r\sigma^2 \right) b^{C2}(s_T) \geq \underline{\Pi}_T, \tag{20}$$

where $e_T^C(s_T) = (s_T^C b^C(s_T) / \eta_T)$.

Theorem 5. When $(d/ds_T)(1 - F(s_T)/s_T f(s_T)) < 0$,

$$a^{C*}(s_T) = \underline{\Pi}_T - \left(\frac{s_O^2}{\eta_O} + \theta \right) b^{C*}(s_T) - \frac{1}{2} \left(\frac{s_T^2}{\eta_T} - r\sigma^2 \right) b^{C*2}(s_T) + \int_{\underline{s}_T}^{s_T} \frac{\omega}{\eta_T} b^{C2}(\omega) d\omega,$$

$$b^{C*}(s_T^C) = \frac{1}{1 + (\eta_T r \sigma^2 / s_T^{C2}) + (2(1 - F(s_T^C)) / s_T^C f(s_T^C))}, \tag{21}$$

$$e_O^{C*} = \frac{s_O}{\eta_O},$$

$$e_T^{C*}(s_T) = \frac{s_T^C b^{C*}(s_T)}{\eta_T}.$$

Theorem 5 shows that when the serviceability of TTA is continuous, $(d/ds_T)(1 - F(s_T)/s_T f(s_T)) < 0$ is the precondition for the existence of a service commission separation contract. At this time, $b^{C*}(s_T)$ is strictly increasing, and all TTA can choose appropriate service contracts corresponding to its serviceability type.

Corollary 3. $E\Pi_T(s_T) - \underline{\Pi}_T = \int_{\underline{s}_T}^{s_T} (\omega/\eta_T) b^{C*2}(\omega) d\omega.$

Corollary 3 shows that, apart from the TTA with the worst serviceability, all other types of TTA can get strict information rent. With the increase of TTA's serviceability, the information rent and the expected revenue of TTA increase, which is consistent with the conclusion when TTA's serviceability is discrete.

5. Numerical and Sensitivity Analysis

The impacts of the risk aversion coefficient, serviceability, and asymmetric information on OTA service contract and both TTA and OTA's revenue are analyzed so as to get more management implications. Considering that the references on cooperation between the TTA and OTA are less and numerical examples are usually hypothetical, the values of parameters are assigned according to Jin et al. [15]. A selected set of parameters is as follows: $s_O = 0.3$, $\eta_O = 0.1$, $\eta_T = 0.3$, $s_{TH} = 0.5$, $s_{TL} = 0.5$, $\rho = 0.5$, $\theta = 0$, $\sigma^2 = 4$, and $\underline{\Pi}_T = 5$. In order to study the impacts of TTA's risk aversion coefficient r and serviceability s_{Ti} on the service commission and revenue of both TTA and OTA, take s_{Ti} as the horizontal axis; that is, when $s_{TH} = 0.5$ and $s_{TL} \in (0.2, 0.5)$ or when $s_{TL} = 0.5$ and $s_{TH} \in (0.5, 1)$, fixed payment, service commission coefficient, and revenue under symmetric information and asymmetric information are plotted, respectively, with $r = 0.1$, $r = 0.5$, and $r = 0.9$. The results of numerical examples are summarized in Figures 1–3.

5.1. Analysis of the Parameters of Service Commission Contract. Figure 1 shows that (1) when TTA's serviceability s_{Ti} increases, fixed payment of a_i^{S*} and a_i^{N*} always decreases, but $a_i^{S*} > a_i^{N*}$. This is straightforward because OTA needs to give TTA more fixed payment to stimulate its initiative to cooperate and create an O2O model under asymmetric information; (2) when r takes different values, the influence of asymmetric information on fixed payment increases with the increase of the difference between TTA's serviceability, which indicates that the smaller the difference between TTA's different serviceability, the smaller the influence of asymmetric information on fixed payment; (3) no matter the serviceability type of TTA is, a_i^{S*} and a_i^{N*} increase and the distance between fixed payment curves decreases with the increase in r , indicating that r can alleviate the impact of asymmetric information on fixed payment.

Figure 2 shows that (1) when TTA's serviceability s_{Ti} increases, service commission coefficient of b_i^{S*} and b_i^{N*} always increases, and $b_H^{S*} = b_H^{N*}$ and $b_L^{S*} < b_L^{N*}$. This indicates that the existence of asymmetric information does not affect the service commission coefficient of OTA paid for TTA with high serviceability, but it will reduce the service commission coefficient of OTA paid for TTA with low serviceability; (2) no matter the serviceability type of TTA is, b_i^{S*} and b_i^{N*} decrease with the increase in r , indicating that r can offset the incentive effect of service commission coefficient on TTA; (3) Figure 2(b) shows the distance between service commission coefficient curves decreases with r or s_{TL} increases, which indicates that r can alleviate the impact of asymmetric information on service commission coefficient and the smaller the difference between TTA's different serviceability, the smaller the influence of asymmetric information on service commission coefficient.

5.2. Revenue Analysis of Both TTA and OTA. Figure 3 shows that (1) no matter the serviceability type of TTA is, there is $\Delta E\Pi_{O_i}^{SN*} < 0$, indicating that the existence of asymmetric

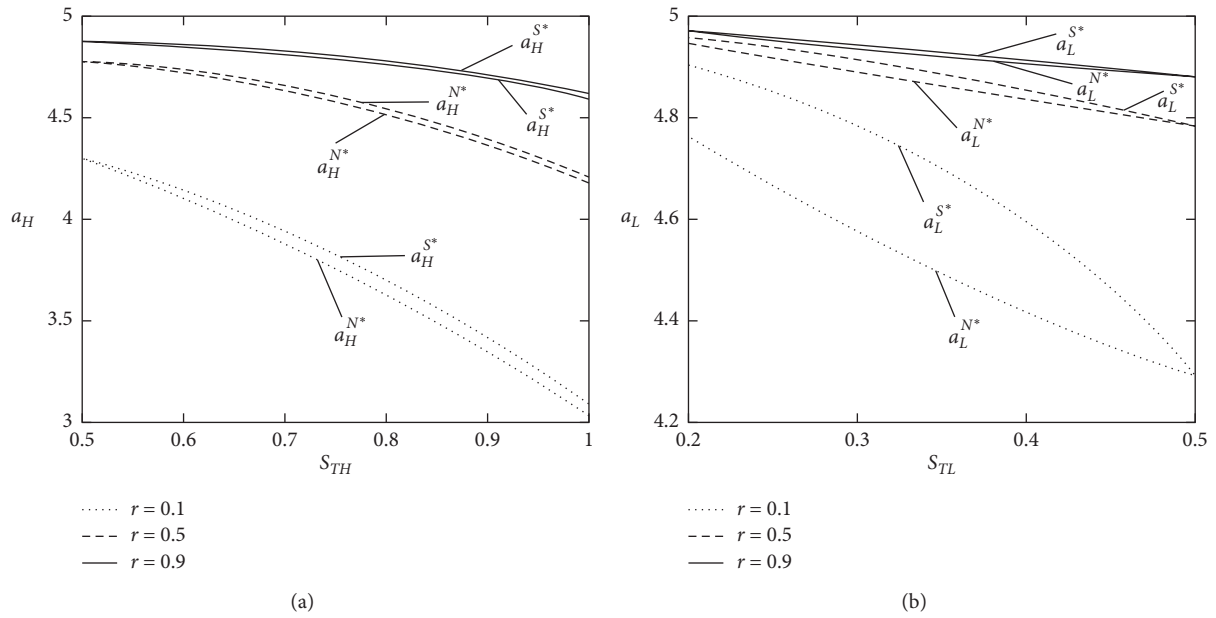


FIGURE 1: Impacts of r and s_{Ti} on fixed payment. (a) $s_{TL} = 0.5$. (b) $s_{TH} = 0.5$.

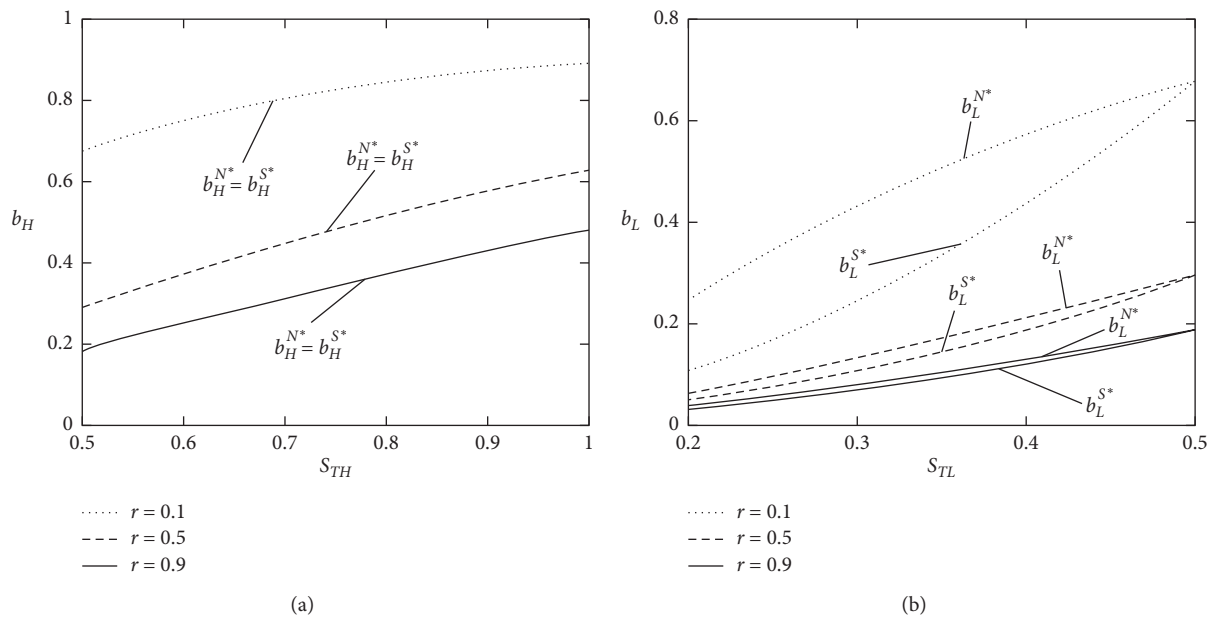


FIGURE 2: Impacts of r and s_{Ti} on service compensation coefficient. (a) $s_{TL} = 0.5$. (b) $s_{TH} = 0.5$.

information always leads to loss of OTA expected revenue. $\Delta E\Pi_{TH}^{SN^*} > 0$ and $\Delta E\Pi_{TL}^{SN^*} = 0$ show that only TTA with high serviceability can obtain additional information rent. $\Delta E\Pi_{TH}^{SN^*}$ and $\Delta E\Pi_{OH}^{SN^*}$ are symmetric with respect to the 0 value curve, which shows that, in the O2O model composed by TTA and OTA, the existence of asymmetric information transfers part of

revenue from OTA to TTA with high service capability; (2) when s_{TH} increases, $\Delta E\Pi_{Oi}^{SN^*}$ firstly decreases and then increases. The changing trend of $\Delta E\Pi_{OH}^{SN^*}$ depends on whether OTA's revenue from the improvement of TTA's serviceability can compensate for the cost of information value; (3) $|\Delta E\Pi_{Oi}^{SN^*}|$ decreases with r increases, which shows that r can alleviate the

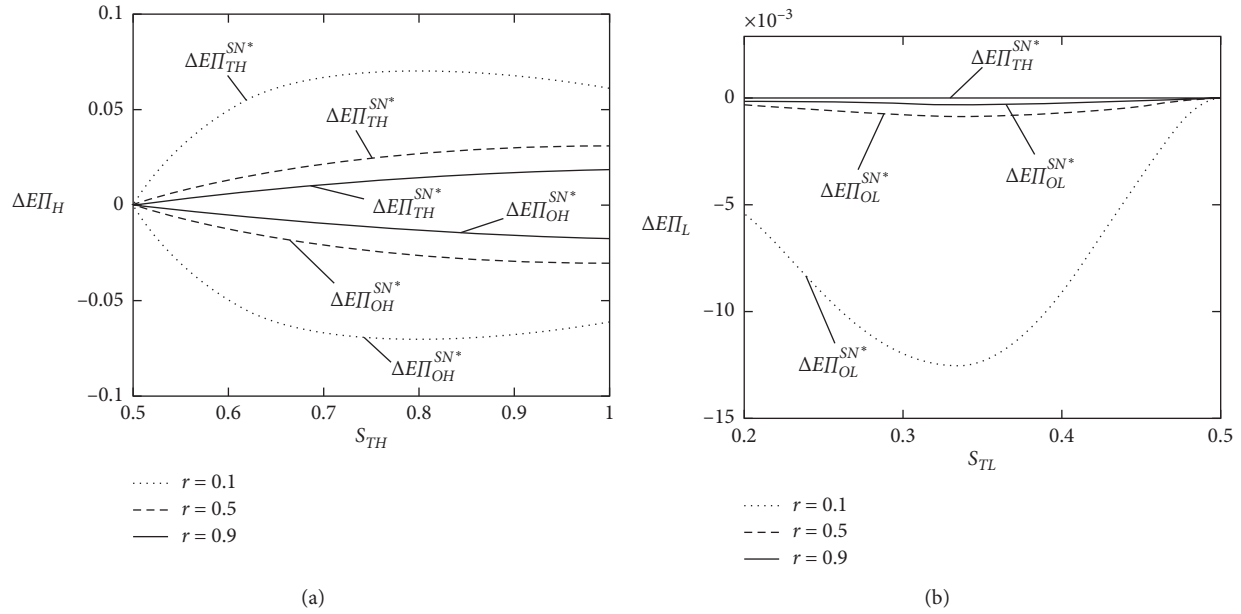


FIGURE 3: Impacts of r and s_{Ti} on $\Delta E\Pi_{Ti}^{SN^*}$ and $\Delta E\Pi_{Oi}^{SN^*}$. (a) $s_{TL} = 0.5$. (b) $s_{TH} = 0.5$.

adverse effect of OTA’s information disadvantage. $\Delta E\Pi_{TH}^{SN^*}$ decreases with r increases, which indicates that r can inhibit the information advantage of TTA with high serviceability.

6. Conclusion and Future Research

The rationality of the OTA service commission contract is an important factor to ensure the efficient operation of the O2O model in the establishment of service cooperation between OTA and TTA. Considering the serviceability information asymmetry, the OTA designs reasonable service commission contracts to differentiate TTA serviceability and motivate TTA to improve service effort level. Some suggestions for establishing a cooperation contract are provided:

- (1) When an OTA has low saleability or high sale cost, the OTA will increase the fixed payment to the TTA to support the cocreation of the O2O model. The incentive effect of the service commission coefficient can be offset by the TTA’s service effort cost coefficient, risk aversion coefficient, and the degree of market uncertainty.
- (2) When the type of TTA’s serviceability is continuous, the precondition of separation contract is $(d/ds_T)(1 - F(s_T)/s_T f(s_T)) < 0$. At this time, the TTA can choose the appropriate contract corresponding to its serviceability type.
- (3) In cocreating the O2O model, the existence of asymmetric information always results in the loss of OTA’s expected revenue. Except for TTA with the lowest serviceability, all other types of TTA can obtain strict information rent. The stronger the TTA serviceability is, the more information rent it obtains and the greater its expected revenue is.
- (4) The OTA designs service contracts by weighing the different incentives of fixed payments and service

commission coefficient to the TTA. When the TTA is a high serviceability type, the OTA sets a high service commission coefficient to encourage the TTA to make more service. When the TTA is of a low serviceability type, the OTA sets a larger fixed payment, stimulating its enthusiasm for participating in cocreating the O2O model.

Due to some of its basic assumptions, there are still some limitations of this paper. Firstly, in this paper, the service commission contract is considered as a linear form. In future research, it can be extended by other service cooperation forms, for example, service cost-sharing contract. Secondly, this study only considers that an OTA establishes service cooperation with a TTA or multiple TTAs. The next step is to extend this model, in which two or more OTAs achieve the O2O model by service cooperation with multiple TTAs. Thirdly, the optimal service commission contract is studied from a short-term perspective. However, in some cases, long-term cooperation is more conducive to the stable development of both. For example, He et al. studied sustainable tourism by using evolutionary game models [31, 32]. Although it is more complex and challenging, service cooperation could be discussed from a long-term perspective. Finally, our paper mainly utilizes an analytical approach. Thus, another future research direction is to conduct empirical research to validate our analytical findings.

Appendix

Proof of TTA’s revenue

Assuming that the random variable x follows normal distribution $x \sim N(m, n^2)$, its utility function are the same as TTA’s: $U(x) = -e^{-rx}$, and its expected utility is

$$EU(x) = \int_{-\infty}^{+\infty} -e^{-rx} \frac{1}{\sqrt{2\pi n}} e^{-((x-m)^2/2n^2)} dx = -e^{-r(m-rn^2/2)}. \quad (A.1)$$

According to certainty equivalence method $EU = U(CE)$, $-e^{-r(CE)} = -e^{-r(m-rn^2/2)}$ can be obtained and also $CE = m - (rn^2/2)$ can be get. According to $\xi \in N(0, \sigma^2)$, $E\Pi_T = a + b(s_O e_O + s_T e_T + \theta) - (\eta_T e_T^2/2)$, $\text{Var}(\Pi_T) = b^2 \sigma^2$. The TTA's revenue Π_T is regarded as a random variable x , its certainty equivalent revenue is $a + b(s_O e_O + s_T e_T + \theta) - (\eta_T e_T^2/2) - (r\sigma^2 b^2/2)$.

Proof of Theorem A.1. The optimization problem P1 is solved by using reverse induction and K-T method. The process is solved in two steps.

$$L(a_i^N, b_i^N, e_{Oi}^N) = (1 - b_i^N) \left((s_O e_{Oi}^N + s_{Ti} e_{Ti}^N + \theta) - a_i^N - \frac{\eta_O e_{Oi}^{N2}}{2} \right) + \chi \left(a_i^N + b_i^N (s_O e_{Oi}^N + s_{Ti} e_{Ti}^N + \theta) - \frac{\eta_T e_{Ti}^{N2}}{2} - \frac{r\sigma^2 (b_i^N)^2}{2} - \underline{\Pi_T} \right). \quad (A.2)$$

Let $(\partial L/\partial a_i^N) = (\partial L/\partial b_i^N) = (\partial L/\partial e_{Oi}^N) = 0$, $(\partial L/\partial \chi) \geq 0, \chi \geq 0$ and $\chi(\partial L/\partial \chi) = 0$

The only set of solutions can be obtained $(a_i^N * b_i^N * e_{Oi}^N)$. \square

Proof of Theorem A.2. The optimization problem P2 is solved by using reverse induction and K-T method. The process is solved in two steps.

- ① The TTA's response function can be obtained $e_{Ti}^S = (s_{Ti} b_i^S / \eta_T)$, with a given service contract $(a_i^S b_i^S)$, and sale effort e_{Oi}^S .

- ① The TTA's response function is $e_{Ti}^N = (s_{Ti} b_i^N / \eta_T)$, with a given service contract $(a_i^N b_i^N)$, and sale effort e_{Oi}^N .

- ② Solving OTA's optimal service contract and sale effort.

Plugging e_{Ti}^N back to optimization problem P1, it is easy to know that the OTA's expected revenue $E\Pi_O$ is linear function of a_i^N and a joint concave of b_i^N and e_{Oi}^N . Therefore, there are corner solution a_i^N and interior solution b_i^N and e_{Oi}^N under the constraint equation (IR). That is, there exists a unique optimal solution. The Lagrange function is constructed as

- ② Solving OTA's optimal service contract and sale effort.

Plugging e_{Ti}^S back to optimization problem P2, it is easy to know that the OTA's expected revenue $E\Pi_O$ is linear function of a_i^S and a joint concave of b_i^S and e_{Oi}^S . Therefore, there are corner solution a_i^S and interior solution b_i^S and e_{Oi}^S under the constraint equation (IR-i). It is easy to prove that (IC-H) and (IR-L) are tight constraints, so the above optimization problem P2 can be rewritten as follows P2'

$$\left\{ \begin{array}{l} \max_{a_H^S, b_H^S, e_{OH}^S, a_L^S, b_L^S, e_{OL}^S} E\Pi_O = \left\{ \rho \left((1 - b_H^S) \left(s_O e_{OH}^S + \frac{b_H^S s_{TH}^2}{\eta_T} + \theta \right) - a_H^S - \frac{\eta_O e_{OH}^{S2}}{2} \right) + (1 - \rho) \times \right. \\ \left. \left((1 - b_L^S) \left(s_O e_{OL}^S + \frac{b_L^S s_{TL}^2}{\eta_T} + \theta \right) - a_L^S - \frac{\eta_O e_{OL}^{S2}}{2} \right) \right\} \\ \text{s.t. (IC-H)} a_H^S + b_H^S (s_O e_{OH}^S + \theta) + \frac{(b_H^S s_{TH})^2}{2\eta_T} - \frac{r\sigma^2 b_H^2}{2} \geq \\ a_L^S + b_L^S (s_O e_{OL}^S + \theta) + \frac{(b_L^S s_{TH})^2}{2\eta_T} - \frac{r\sigma^2 b_L^2}{2} \\ \text{(IR-L)} a_L^S + b_L^S (s_O e_{OL}^S + \theta) + \frac{(b_L^S s_{TL})^2}{2\eta_T} - \frac{r\sigma^2 b_L^2}{2} \geq \underline{\Pi_T}. \end{array} \right. \quad (A.3)$$

The Lagrange function is constructed as

$$\begin{aligned}
 L(a_H, b_H, e_{OH}, a_L, b_L, e_{OL}, \chi_1, \chi_2) = & \rho \left((1 - b_H^S) \left(s_O e_{OH}^S + \frac{b_H^S s_{TH}^2}{\eta_T} + \theta \right) - a_H^S - \frac{\eta_O e_{OH}^{S2}}{2} \right) + (1 - \rho) \times \\
 & \cdot \left((1 - b_L^S) \left(s_O e_{OL}^S + \frac{b_L^S s_{TL}^2}{\eta_T} + \theta \right) - a_L^S - \frac{\eta_O e_{OL}^{S2}}{2} \right) + \chi_1 \left(a_L^S + b_L^S (s_O e_{OL}^S + \theta) + \frac{(b_L^S s_{TL})^2}{2\eta_T} - \frac{r\sigma^2 b_L^{S2}}{2} - \Pi_R \right) \\
 & + \chi_2 \left(a_H^S + b_H^S (s_O e_{OH}^S + \theta) + \frac{(b_H^S s_{TH})^2}{2\eta_T} - \frac{r\sigma^2 b_H^{S2}}{2} - a_L^S - b_L^S (s_O e_{OL}^S + \theta) - \frac{(b_L^S s_{TH})^2}{2\eta_T} + \frac{r\sigma^2 b_L^{S2}}{2} \right).
 \end{aligned} \tag{A.4}$$

The Kuhn-Tucker condition is obtained as

$$\frac{\partial L}{\partial a_i^S} = \frac{\partial L}{\partial b_i^S} = \frac{\partial L}{\partial e_{O_i}^S} = 0, \quad \frac{\partial L}{\partial \chi_1} \geq 0, \quad \frac{\partial L}{\partial \chi_2} \geq 0, \tag{A.5}$$

where $\chi_1 \geq 0$ and $\chi_1 (\partial L / \partial \chi_1) = 0$, $\chi_2 \geq 0$ and $\chi_2 (\partial L / \partial \chi_2) = 0$.

In $\chi_1 = 1, \chi_2 = \rho a_H^{S*} b_H^{S*} e_{OH}^{S*} a_L^{S*}$, b_L^{S*} and e_{OL}^{S*} can be obtained. \square

Proof of Corollary A.1.

$$\begin{aligned}
 b_H^{S*} - b_L^{S*} &= \frac{(s_{TH}^2 - s_{TL}^2)(\rho s_{TH}^2 + (1 - \rho)\eta_T r \sigma^2)}{(s_{TH}^2 + \eta_T r \sigma^2)(s_{TL}^2 - 2\rho s_{TL}^2 + \rho s_{TH}^2 + (1 - \rho)\eta_T r \sigma^2)} \geq 0, \\
 a_H^{S*} - a_L^{S*} &= \left(\left(\frac{s_O}{\eta_O} + \theta \right) - \frac{1}{2} \left(r\sigma^2 - \frac{s_{TH}^2}{\eta_T} \right) (b_L^{S*} + b_H^{S*}) \right) (b_L^{S*} - b_H^{S*}).
 \end{aligned} \tag{A.6}$$

When $r \leq 0$, it is easy to get $a_H^{S*} < a_L^{S*}$.

When $r > 0$, let

$$G(r) = \left(\frac{s_O}{\eta_O} + \theta \right) - \frac{1}{2} \left(r\sigma^2 - \frac{s_{TH}^2}{\eta_T} \right) (b_L^{S*} + b_H^{S*}) = \left(\frac{s_O}{\eta_O} + \theta \right) + \frac{s_{TH}^2}{2\eta_T} (b_L^{S*} + b_H^{S*}) - \frac{1}{2} r\sigma^2 (b_L^{S*} + b_H^{S*}), \tag{A.7}$$

where $(s_{TH}^2 / 2\eta_T) (b_L^{S*} + b_H^{S*})$ is about r monotonically decreasing.

$$\begin{aligned}
 \frac{1}{2} r\sigma^2 (b_L^{S*} + b_H^{S*}) &= \frac{1}{2} r\sigma^2 \left(\frac{s_{TH}^2}{s_{TH}^2 + \eta_T r \sigma^2} + \frac{(1 - \rho)s_{TL}^2}{s_{TL}^2 - 2\rho s_{TL}^2 + \rho s_{TH}^2 + (1 - \rho)\eta_T r \sigma^2} \right) \\
 &= \frac{1}{2\eta_T} \left(s_{TH}^2 + s_{TL}^2 - \frac{s_{TH}^4}{s_{TH}^2 + \eta_T r \sigma^2} - \frac{(1 - \rho)s_{TL}^2 (s_{TL}^2 - 2\rho s_{TL}^2 + \rho s_{TH}^2)}{s_{TL}^2 - 2\rho s_{TL}^2 + \rho s_{TH}^2 + (1 - \rho)\eta_T r \sigma^2} \right),
 \end{aligned} \tag{A.8}$$

$(1/2)r\sigma^2(b_L^{S^*} + b_H^{S^*})$ is about r monotonically increasing.

Therefore, $G(r)$ is about r monotonically decreasing, which maximizes $r \rightarrow 0$ at and minimizes at $r \rightarrow +\infty$.

$$G(+\infty) = \left(\frac{s_O^2}{\eta_O} + \theta\right),$$

$$G(0) = \left(\frac{s_O^2}{\eta_O} + \theta\right) + \frac{s_{TH}^2}{2\eta_T} \left(1 + \frac{(1-\rho)s_{TL}^2}{s_{TL}^2 - 2\rho s_{TL}^2 + \rho s_{TH}^2}\right). \quad (\text{A.9})$$

Therefore, $G(r) > 0$ and $a_L^{S^*} \geq a_H^{S^*}$, only when $r \rightarrow +\infty$, $a_L^{S^*} = a_H^{S^*}$. \square

Proof of Theorem A.3. (1)

$$a_H^{S^*} - a_L^{S^*} = (1/2\eta_T)(s_{TH}^2 - s_{TL}^2)(b_L^{S^*})^2 \geq 0;$$

$$(2) b_L^{S^*} - b_L^{N^*} = (\rho s_{TL}^2 (s_{TL}^2 - s_{TH}^2) / (s_{TL}^2 - 2\rho s_{TL}^2 + \rho s_{TH}^2 + (1-\rho)\eta_T r \sigma^2)) (s_{TL}^2 + \eta_T r \sigma^2) \leq 0;$$

$$a_L^{S^*} - a_L^{N^*} = (b_L^{N^*} - b_L^{S^*}) \left(\left(\frac{s_O^2}{\eta_O} + \theta \right) - \frac{1}{2} \left(r\sigma^2 - \frac{s_{TL}^2}{\eta_T} \right) (b_L^{N^*} + b_L^{S^*}) \right). \quad (\text{A.10})$$

The process of solving value of $(a_L^{S^*} - a_L^{N^*})$ is similar to the proof of Corollary 1.

The proofs of (3) and (4) of theorem are easy, so they are omitted. \square

Proof of Theorem A.4.

$$(1) \Delta E\Pi_{OH}^{SN^*} = E\Pi_{OH}^{S^*} - E\Pi_{OH}^{N^*} = (1/2\eta_T)(s_{TL}^2 - s_{TH}^2)(b_L^{S^*})^2 \leq 0$$

$$\begin{aligned} \Delta E\Pi_{OL}^{SN^*} &= E\Pi_{OL}^{S^*} - E\Pi_{OL}^{N^*} = (b_L^{S^*} - b_L^{N^*}) \left(\frac{s_{TL}^2}{\eta_T} - \frac{1}{2} \left(\frac{s_{TL}^2}{\eta_T} + r\sigma^2 \right) (b_L^{N^*} + b_L^{S^*}) \right) \\ &= \frac{1}{\eta_T} (b_L^{S^*} - b_L^{N^*}) \left(s_{TL}^2 - \frac{s_{TL}^2}{2b_L^{N^*}} (b_L^{N^*} + b_L^{S^*}) \right) = \frac{s_{TL}^2}{2\eta_T} (b_L^{S^*} - b_L^{N^*}) \left(1 - \frac{b_L^{S^*}}{b_L^{N^*}} \right) \\ &= -\frac{(s_{TL}^2 + \eta_T r \sigma^2)}{2\eta_T} (b_L^{S^*} - b_L^{N^*})^2 \leq 0. \end{aligned} \quad (\text{A.11})$$

$$(2) \Delta E\Pi_{TH}^{SN^*} = E\Pi_{TH}^{S^*} - E\Pi_{TH}^{N^*} = (1/2\eta_T)(s_{TH}^2 - s_{TL}^2)(b_L^{S^*})^2 \geq 0$$

$$\Delta E\Pi_{TL}^{SN^*} = E\Pi_{TL}^{S^*} - E\Pi_{TL}^{N^*} = 0. \quad (\text{A.12}) \quad \square$$

Proof of Theorem A.5. According to the display principle, when analyzing the validity of continuous variables, the analysis restriction can be displayed $\{a(\overleftrightarrow{s}_T), b(\overleftrightarrow{s}_T)\}$ directly. Therefore, $\forall (s_T, \overleftrightarrow{s}_T) \in H$, there is

$$a^C(s_T) + (s_O e_O^C(s_T) + \theta) b^C(s_T) + \frac{1}{2} \left(\frac{s_T^2}{\eta_T} - r\sigma^2 \right) b^{C2}(s_T) \geq$$

$$a^C(\overleftrightarrow{s}_T) + (s_O e_O^C(\overleftrightarrow{s}_T) + \theta) b^C(\overleftrightarrow{s}_T) + \frac{1}{2} \left(\frac{s_T^2}{\eta_T} - r\sigma^2 \right) b^{C2}(\overleftrightarrow{s}_T). \quad (\text{A.13})$$

According to In equation (A.13), there is

$$a^C(s_T) + (s_O e_O^C(s_T) + \theta) b^C(s_T) + \frac{1}{2} \left(\frac{s_T^2}{\eta_T} - r\sigma^2 \right) b^{C2}(s_T) \geq \tag{A.14}$$

$$a^C(s'_T) + (s_O e_O^C(s'_T) + \theta) b^C(s'_T) + \frac{1}{2} \left(\frac{s_T^2}{\eta_T} - r\sigma^2 \right) b^{C2}(s'_T),$$

$$a^C(s'_T) + (s_O e_O^C(s'_T) + \theta) b^C(s'_T) + \frac{1}{2} \left(\frac{s_T^2}{\eta_T} - r\sigma^2 \right) b^{C2}(s'_T) \geq \tag{A.15}$$

$$a^C(s_T) + (s_O e_O^C(s_T) + \theta) b^C(s_T) + \frac{1}{2} \left(\frac{s_T^2}{\eta_T} - r\sigma^2 \right) b^{C2}(s_T).$$

In equations (A.14) and (A.15) are added and simplified as

$$(s_T - s'_T)(b^C(s_T) - b^C(s'_T)) \geq 0. \tag{A.16}$$

So $b^C(s_T)$ is no decreasing, which shows $b^C(s_T)$ is differentiable everywhere in the interval $[s_T, \bar{s}_T]$, and $b^C(s_T) \geq 0$. In addition, the first-order condition for s_T is obtained $a^C(s_T) + s_O e_O^C(s_T) b^C(s_T) + (s_O e_O^C(s_T) + \theta) b^C(s_T) + ((s_T^2/\eta_T) - r\sigma^2) b^C(s_T) = 0$ from In equation (A.13).

According to the direct display mechanism, $\forall s_T^C \in H$ there is

$$a^C(s_T) + s_O e_O^C(s_T) b^C(s_T) + (s_O e_O^C(s_T) + \theta) b^C(s_T) + \left(\frac{s_T^2}{\eta_T} - r\sigma^2 \right) b^C(s_T) = 0. \tag{A.17}$$

In equations (18) and (19) are incentive compatibility constraints to ensure that the TTA has no motivation to deviate from the service reward contract provided by OTA. In equation (20) is the constraint condition for the TTA to participate in cooperation and cannot be lower than its reserved revenue.

Derivatives of equation (17), and further simplified according to equation (19)

$$E\Pi_T(s_T) = \frac{s_T}{\eta_T} b^{C2}(s_T). \tag{A.18}$$

Bring $E\Pi_T(s_T)$ into equation (15), the above optimization problem P3 can be rewritten as follows P3'

$$\max_{a^C, b^C} \int_{\underline{s}_T}^{\bar{s}_T} \left\{ s_O e_O^C(s_T) + \frac{s_T^2 b^C(s_T)}{\eta_T} + \theta - \frac{1}{2} \left(\frac{s_T^2}{\eta_T} + r\sigma^2 \right) b^{C2}(s_T) - E\Pi_T(s_T) - \frac{\eta_O e_O^{C2}(s_T)}{2} \right\} f(s_T) ds_T, \tag{A.19}$$

s.t. in equation (18) and (A.18), $E\Pi_T(s_T) \geq \underline{\Pi}_T$

Let $E\Pi_T(s_T) \geq \underline{\Pi}_T$, the solution of integral equation (A.18) is obtained

$$E\Pi_T(s_T) = \int_{\underline{s}_T}^{s_T} \frac{\omega}{\eta_T} b^{C2}(\omega) d\omega + \underline{\Pi}_T. \tag{A.20}$$

According to. $\int_{\underline{s}_T}^{\bar{s}_T} \left[\int_{\underline{s}_T}^{s_T} (\omega/\eta_T) b^{C2}(\omega) d\omega \right] f(s_T) ds_T = \int_{\underline{s}_T}^{\bar{s}_T} \left[\int_{\underline{s}_T}^{s_T} f(\omega) d\omega \right] (s_T/\eta_T) b^{C2}(s_T) ds_T = \int_{\underline{s}_T}^{\bar{s}_T} (1 - F(s_T)) / f(s_T) (s_T/\eta_T) b^{C2}(s_T) f(s_T) ds_T$

Then the objective function of P3 is

$$\max_{a^C, b^C} \int_{\underline{s}_T}^{\bar{s}_T} \left\{ s_O e_O^C(s_T) + \frac{s_T^2 b^C(s_T)}{\eta_T} + \theta - \frac{1}{2} \left(\frac{s_T^2}{\eta_T} + r\sigma^2 \right) b^{C2}(s_T) - \frac{1 - F(s_T)}{f(s_T)} \frac{s_T}{\eta_T} b^{C2}(s_T) - \underline{\Pi}_T - \frac{\eta_O e_O^{C2}(s_T)}{2} \right\} f(s_T) ds_T. \tag{A.21}$$

The optimal solution is

$$e_O^{C*} = \frac{s_O}{\eta_O},$$

$$b^{C*}(s_T^C) = \frac{1}{1 + (\eta_T r \sigma^2 / s_T^C) + (2(1 - F(s_T^C)) / s_T^C f(s_T^C))}, \quad (\text{A.22})$$

Where, $b^{C*}(s_T) = (1/1 + (\eta_T r \sigma^2 / s_T) + (2/ s_T f(s_T)))$, $b^{C*}(s_T) = (1/1 + (\eta_T r \sigma^2 / s_T^2))$

When $s_T = \underline{s}_T$, according to equation (16) and $E\Pi_T(s_T) = \underline{\Pi}_T$, $a^{C*}(s_T)$ can be obtained as

$$a^{C*}(s_T) = \underline{\Pi}_T - \left(\frac{s_O^2}{\eta_O} + \theta \right) b^{C*}(s_T) - \frac{1}{2} \left(\frac{s_T^2}{\eta_T} - r\sigma^2 \right) b^{C*2}(s_T). \quad (\text{A.23})$$

Bring $b^{C*}(s_T^C)$ into equation (A.20), $E\Pi_T(s_T)$ can be obtained as

$$E\Pi_T(s_T) = \int_{\underline{s}_T}^{s_T} \frac{\omega}{\eta_T} b^{C*2}(\omega) d\omega + \underline{\Pi}_T. \quad (\text{A.24})$$

Bring equation (A.24) into equation (17), $a^{C*}(s_T)$ can be obtained as

$$a^{C*}(s_T) = \underline{\Pi}_T - \left(\frac{s_O^2}{\eta_O} + \theta \right) b^{C*}(s_T) - \frac{1}{2} \left(\frac{s_T^2}{\eta_T} - r\sigma^2 \right) b^{C*2}(s_T) + \int_{\underline{s}_T}^{s_T} \frac{\omega}{\eta_T} b^{C2}(\omega) d\omega. \quad (\text{A.25})$$

□

Data Availability

The data used to support the findings of this study are included within the article.

Conflicts of Interest

The authors declare that there are no conflicts of interest.

Acknowledgments

This work was supported by the Research Fund for the Scientific Research Foundation of Chongqing University of Technology and the Humanities and Social Sciences Research Project of Chongqing Education Commission (2020CJR06).

References

- [1] L. Ling, X. Guo, and C. Yang, "Opening the online marketplace: an examination of hotel pricing and travel agency on-line distribution of rooms," *Tourism Management*, vol. 45, no. 1, pp. 234–243, 2014.
- [2] E. H. C. Wu, R. Law, and B. Jiang, "Predicting browsers and purchasers of hotel websites," *Cornell Hospitality Quarterly*, vol. 54, no. 1, pp. 38–48, 2013.
- [3] P. Shi and Y. Long, "A research on complementary resources input decision of the travel agencies co-creating the O2O model," *Tourism Science*, vol. 31, no. 2, pp. 55–68, 2017.
- [4] Y. Long and P. Shi, "Pricing strategies of tour operator and online travel agency based on cooperation to achieve O2O model," *Tourism Management*, vol. 62, pp. 302–311, 2017.
- [5] X. Guo, X. Zheng, L. Ling, and C. Yang, "Online cooperation between hotels and online travel agencies: from the perspective of cash back after stay," *Tourism Management Perspectives*, vol. 12, no. 12, pp. 104–112, 2014.
- [6] P. Shi and Y. Long, "Service quality decision-making in O2O tourism supply chains considering sharing service costs," *Tourism Tribune*, vol. 33, no. 11, pp. 90–100, 2018.
- [7] C. Lu and S. Liu, "Cultural tourism O2O business model innovation-A case study of CTrip," *Journal of Electronic Commerce in Organizations*, vol. 14, no. 2, pp. 16–31, 2016.
- [8] B. Koo, B. Mantin, and P. O'Connor, "Online distribution of airline tickets: should airlines adopt a single or a multi-channel approach?" *Tourism Management*, vol. 32, no. 1, pp. 69–74, 2011.
- [9] X. Guo, L. Ling, Y. Dong, and L. Liang, "Cooperation contract in tourism supply chains: the optimal pricing strategy of hotels for cooperative third party strategic websites," *Annals of Tourism Research*, vol. 41, pp. 20–41, 2013.
- [10] Y. Dong and L. Ling, "Hotel overbooking and cooperation with third-party websites," *Sustainability*, vol. 7, no. 9, pp. 11696–11712, 2015.
- [11] L. Xu, P. He, and Z. Hua, "A new form for a hotel to collaborate with a third-party website: setting online-exclusive-rooms," *Asia Pacific Journal of Tourism Research*, vol. 20, no. 6, pp. 1–12, 2014.
- [12] D. Bell, S. Gallino, and A. Moreno, "Showrooms and information provision in omni-channel retail," *Production and Operations Management*, vol. 24, no. 3, pp. 360–362, 2015.
- [13] I. D. Savila, R. N. Wathoni, and A. S. Santoso, "The role of multichannel integration, trust and offline-to-online customer loyalty towards repurchase intention: an empirical study in online-to-offline (O2O) e-commerce," *Procedia Computer Science*, vol. 161, pp. 859–866, 2019.
- [14] B. Swoboda and A. Winters, "Effects of the most useful offline-online and online-offline channel integration services for consumers," *Decision Support Systems*, vol. 145, Article ID 113522, 2021.
- [15] L. Jin, X. Zhang, B. Dan, and S. Li, "Commission contract design in "offline evaluation, online purchase" (O2O) supply chain in the presence of cross-selling," *Chinese Journal of Management Science*, vol. 25, no. 11, pp. 33–46, 2017.
- [16] J. K. Dong, W. G. Kim, and S. H. Jin, "A perceptual mapping of online travel agencies and preference attributes," *Tourism Management*, vol. 28, no. 2, pp. 591–603, 2007.
- [17] A. H. Walle, "Tourism and the internet," *Journal of Travel Research*, vol. 35, no. 1, pp. 72–77, 1996.
- [18] J. Xiao, B. Dan, and X. M. Zhang, "Service cooperation pricing strategy between manufactures and retailers in dual-channel supply chain," *Systems Engineering-Theory & Practice*, vol. 30, no. 12, pp. 2203–2211, 2011.
- [19] Q. Xu, G. Fu, and D. Fan, "Service sharing, profit mode and coordination mechanism in the Online-to-Offline retail market," *Economic Modelling*, vol. 91, pp. 659–669, 2020.
- [20] Y.-W. Zhou, J. Guo, and W. Zhou, "Pricing/service strategies for a dual-channel supply chain with free riding and service-cost sharing," *International Journal of Production Economics*, vol. 196, pp. 198–210, 2018.

- [21] Q. Yang and M. Zhang, "Service cooperation incentive mechanism in a dual-channel supply chain under service differentiation," *American Journal of Industrial and Business Management*, vol. 05, no. 04, pp. 226–234, 2015.
- [22] L. Zou, "Threat-based incentive mechanisms under moral hazard and adverse selection," *Journal of Comparative Economics*, vol. 16, no. 1, pp. 47–74, 1992.
- [23] F. Chen, "Salesforce incentives, market information, and production/inventory planning," *Management Science*, vol. 51, no. 1, pp. 60–75, 2005.
- [24] S.-H. Kim, M. A. Cohen, and S. Netessine, "Performance contracting in after-sales service supply chains," *Management Science*, vol. 53, no. 12, pp. 1843–1858, 2007.
- [25] Y. He, X. Zhao, L. Zhao, and J. He, "Coordinating a supply chain with effort and price dependent stochastic demand," *Applied Mathematical Modelling*, vol. 33, no. 6, pp. 2777–2790, 2009.
- [26] P. He, Y. He, C. Shi et al., "Cost-sharing contract design in a low-carbon service supply chain," *Computers & Industrial Engineering*, vol. 139, Article ID 106160, 2020.
- [27] J. Cao, C. J. Yang, P. Li, and G. Zhou, "Design of supply chain linear shared-saving contract with asymmetric information," *Journal of Management Sciences in China*, vol. 12, no. 2, pp. 19–30, 2009.
- [28] Y. He, H. Huang, and D. Li, "Inventory and pricing decisions for a dual-channel supply chain with deteriorating products," *Operational Research*, vol. 20, no. 3, pp. 1461–1503, 2020.
- [29] G. Xie, W. Yue, S. Wang, and K. K. Lai, "Quality investment and price decision in a risk-averse supply chain," *European Journal of Operational Research*, vol. 214, no. 2, pp. 403–410, 2011.
- [30] Z. Li, S. M. Gilbert, and G. Lai, "Supplier encroachment under asymmetric information," *Management Science*, vol. 60, no. 2, pp. 449–462, 2013.
- [31] Y. He, P. He, F. Xu, and C. Shi, "Sustainable tourism modeling: pricing decisions and evolutionarily stable strategies for competitive tour operators," *Tourism Economics*, vol. 25, no. 5, pp. 779–799, 2019.
- [32] P. He, Y. He, and F. Xu, "Evolutionary analysis of sustainable tourism," *Annals of Tourism Research*, vol. 69, pp. 76–89, 2018.

Research Article

Intelligent Recognition of Safety Risk in Metro Engineering Construction Based on BP Neural Network

Mengchu Li  and Jingchun Wang

School of Civil Engineering, Shijiazhuang Tiedao University, Shijiazhuang 050043, Hebei, China

Correspondence should be addressed to Jingchun Wang; wjc36295@163.com

Received 15 January 2021; Revised 6 April 2021; Accepted 13 April 2021; Published 3 May 2021

Academic Editor: Ming Bao Cheng

Copyright © 2021 Mengchu Li and Jingchun Wang. This is an open access article distributed under the Creative Commons Attribution License, which permits unrestricted use, distribution, and reproduction in any medium, provided the original work is properly cited.

With the rapid development of urban economy, the development of urban rail transit is becoming more and more rapid. As an energy-saving, land-saving, and environment-friendly green travel mode, the subway provides realistic and feasible solutions to the increasingly prominent traffic environment and other urban diseases in our country and brings a booming development in the subway construction industry with efforts to promote and build in many large cities. For a large number of subway constructions, it is particularly important to judge the construction safety status in time during the entire safety management process. Regularly conducting safety risk assessments on subway construction status can accurately predict and judge the types of accidents that occur. In order to solve the current safety risk assessment problems in the process of subway construction in our country, this paper is based on the BP neural network to intelligently identify the safety risks of subway construction, choosing from three aspects: human factors, management factors, and risk factors. We evaluate the construction safety of subway projects under construction through the model, predict the types of accidents that may occur, so that the construction unit can take corresponding preventive and improvement measures, improve the relevant safety technology of subway construction in a targeted manner, and propose corresponding reductions. We provide suggestions and measures for risk probability, to ensure that the construction unit discovers the danger in time and takes safety measures. The rectification measures provided theoretical basis and guidance.

1. Introduction

1.1. Background and Significance. With the rapid economic growth and rapid population growth, the scale of transportation and the density of people's travel have increased, and urban transportation has brought new huge overload pressure [1]. With the subway as the main mode of operation, it not only relieves the traffic and traffic congestion in the city but also changes the role of people's lifestyle and travel mode [2]. The construction of the subway has the characteristics of concealment, complexity, and uncertainty. Due to the rapid development of subway projects, the large scale of construction, and the lack of sufficient technology and management capabilities, the safe construction of subway projects has potential high safety hazards [3]. It has devastating effects on victims, property damage, and social environment. Therefore, it is very urgent to determine the

dangerous factors in subway construction and formulate appropriate countermeasures to reduce or even eliminate possible safety accidents. The purpose of this article is to establish a safety assessment prediction model, through which the safety of underground projects under construction can be evaluated and the types of possible accidents can be predicted, so that the construction unit can take appropriate preventive and remedial measures [4].

1.2. Related Work and Research. McCulloch and Pitts introduced the M.P. model in their published article. Since the birth of this model, it has pioneered the theoretical research of neural network models [5]. Yang et al. discussed methods and strategies for solving uncertainty problems and discussed appropriate assumptions for comprehensive uncertainty analysis [6]. Based on multiple examples of

engineering projects, Yang et al. started with system development, controllability, and independence and created a relatively conceptual framework based on project strategy [7]. By comparing different types of commonly used projects, the ability to predict risk and governance is improved [8, 9].

Ma of the United States applied risk analysis to tunnels and underground projects in 1970 [9]. Since then, foreign research on risk assessment methods and risk management theories has increased, and remarkable results have been achieved and widely used. He not only put forward the ideas to follow but also created a tunnel cost model based on computer simulation, the scope of which is limited to hard rock tunnels. The biggest innovation of this model is the increase of uncertainty in the project budget, so it is very suitable for actual engineering [10]. Tsai et al. have proposed an engineering risk management model for the Amsterdam North-South subway project, which is used to control the risks of technically complex underground projects [11]. It has gone through various stages of project design and construction, including project quality, duration, and cost [12].

Our country has held many informal seminars on neural networks [13]. The “First Academic Conference on Neural Networks in China” jointly organized by eight companies including our country’s computer companies and artificial intelligence companies was held in Beijing. Yiming et al. introduced the process and method of risk management combined with subway construction and explained the practicality and convenience of applying risk management methods in subway construction [14]. Han et al. analyzed the causes of domestic subway construction accidents in recent years, emphasized the importance of risk management in subway construction, summarized the characteristics of subway project risk management, and put forward suggestions on the content of subway risk management [15]. Longkang et al. introduced the risk index method in the risk assessment of mechanical tunnels, and it has been widely used in mechanical tunnels in our country [16]. Based on the system theory, Zeng et al. used dynamic control principles to study the theoretical framework of the subway project risk assessment system from the perspective of dynamic system risk assessment [17–19]. There are some shortcomings in the experimental research of the abovementioned scholars, so this paper studies the intelligent identification of safety risks in subway construction based on the BP neural network.

1.3. Innovation. This article introduces the BP neural network algorithm in the field of underground construction project risk analysis. It not only expands the scope of the BP neural network algorithm but also enriches the traditional management method system of the project management profession, which is practical. The theoretical significance and practical value of the application are studied.

This paper uses the advantages of the BP neural network in self-learning, nonlinear self-adaptation, approximation ability, etc. and, according to the subway engineering data sample, realizes the prediction of subway target risk to

quickly and effectively assess the risks of subway construction and provide solutions to the risks of subway construction.

In order to reduce the dependence on personnel in the risk identification process and realize the intelligent automatic identification of construction safety risks, this paper, based on the cloud storage and cloud sharing functions of the building information model, deeply studies the pre-construction safety risk identification, proposes a subway station construction safety risk intelligent identification model, establishes a set the safety risk identification during the construction preparation period to the safety control technology system for prevention and control, and provides reference and support for realizing the safe construction of subway stations.

This article introduces the BP neural network algorithm to use the powerful nonlinear problem processing capabilities to provide better solutions for subway project risk analysis and to obtain analysis results faster, especially when there are many indicators, evaluation, and improvement. The advantages of the BP neural network algorithm are more obvious.

This article introduces the importance of subway construction safety and current problems in the abstract section. In the second part of this article, the function of the BP neural network algorithm and its application in subway construction safety are introduced. In the third part of this article, we simulate the BP neural network algorithm in the subway construction. In the fourth part, the data are analyzed. Verification: the function of the BP neural network algorithm is verified.

2. Method of Safety Risk Identification in Metro Engineering Construction

2.1. BP Neural Network. The BP neural network structure is composed of an input layer, a hidden layer, and an output layer. The process of its learning algorithm is the forward propagation of information and the back propagation of errors [20]. Error back propagation refers to the difference between the expected value and the output value. Error: the output layer transfers it to the hidden layer according to the error gradient descent method and then passes it from the hidden layer to the input layer. The error signal is transmitted back along the original line through the network to correct the connection weight of each layer of neurons, thereby gradually approaching the goal [21]. The global minimum error is calculated, and it is determined whether the error meets the requirements. If the error is lower than the set accuracy, or if the number of training times is greater than the set maximum number of training times, the training ends; otherwise, the next learning sample is selected, and the next round is returned. Calculation: the forward propagation of information and the back propagation of errors make the weights of each layer to continuously self-adjust, and the entire network self-adaptively learns until the output error is less than the error target value or the set number of training times [22].

The working state of the BP neural network is mainly divided into two kinds of learning state and working state. The learning state is to continuously adjust the connection weights between neurons in each layer to make the network output more in line with the real situation; its working state means that the connection weights between the neurons in each layer no longer changes, and the built BP used the neural network model, input new data, and get prediction data. The BP neural network model establishes a nonlinear high-latitude functional relationship between the input factor and the output factor. This functional relationship is the result of the model training sample learning. Using this training result, new data are input outside the training sample, and we can get the correct output, that is, the prediction result, which is also the main idea of using the BP neural network to solve the problem in this article [23].

In a simple BP neural network structure, each neuron takes the output of the previous layer of neurons as input, outputs its own calculation results, and transmits it to the next layer as its input [24, 25]. The BP neural network can be single layered or multilayered [13]. The neural network has an input layer, an output layer, and a hidden layer, as shown in Figure 1.

The neuron model in the BP neural network is similar to other neurons, so the general model structure diagram can refer to the form in the figure mentioned above. The difference lies in the transmission mode. BP neurons usually use nonlinear transfer functions, such as logsig and tansig functions, both of which are sigmoid functions, and their output values will be limited to (0, 1) [26]. The standard BP network structure includes four parts: input and output, activation function, error calculation, and self-learning. The formula description is as follows:

- (1) Input output: hidden layer node and output node output model.

$$\begin{aligned} N_i &= f\left(\sum A_{ij} \times B_j - z_i\right), \\ E_k &= f\left(\sum M_{jk} \times N_j - z_k\right), \end{aligned} \quad (1)$$

where f is the nonlinear activation function; z is the threshold of the neuron.

- (2) Activation function: it mainly refers to the sigmoid function.

$$f(x) = \frac{1}{(1 + e^{-x})}. \quad (2)$$

- (3) Error calculation: in order to make the difference between the expected output of the network and the actual output meet the external expectations, the following function model can be used:

$$E_z = \frac{1}{2} \times \sum (r_{si} - n_{si})^2, \quad (3)$$

where r_{si} is the nonlinear activation function; n_{si} is the threshold of the neuron.

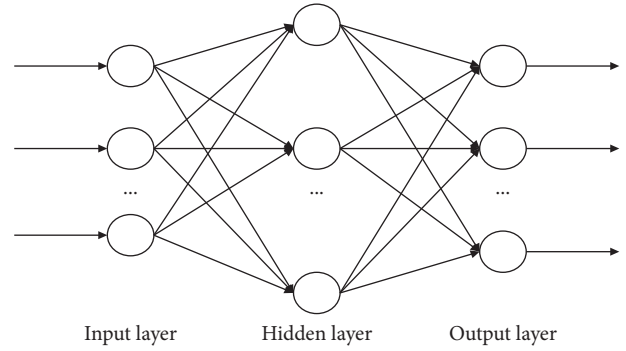


FIGURE 1: BP network model structure diagram.

The network learning process of the BP neural network can be described by Figure 2.

In the process of system risk assessment, the BP neural network has the following advantages:

- (1) The BP neural network adopts a parallel structure based on the human brain and has the characteristics of parallel processing, which can effectively overcome the influence of subjective factors and comprehensively evaluate the security status and interaction of the system. The safety in this case is multifunctional.
- (2) Using the complementarity of the BP network knowledge storage function and appropriate learning samples, we can realize the complete combination of historical experience and new knowledge and dynamically evaluate the security status of the system development process.
- (3) Using the sheep tolerance characteristics of the BP network method, it is possible to process various nondigital indicators while selecting appropriate functions and data structures to perform a fuzzy assessment of the security status of the system [27, 28].

2.2. Safety Risk and Identification of Subway Construction.

Risk is usually an abstract and relatively vague concept [29]. It includes two main factors: risk sources and risk issues. It refers to the uncertainty of hazardous events that lead to potential risk losses. This uncertainty includes objective uncertainty and subjective uncertainty [30, 31]. For objective uncertainty, one can use mathematical statistics to calculate. Subjective uncertainty is closely related to people's understanding of the risk event itself, the environment, and psychological state at the time, so the subjective risk perception of different individuals is still uncertain. The safety risk of subway construction refers to the threats that may occur during the entire process from the preparation stage of the subway project to its completion and acceptance stage [32].

From the perspective of risk uncertainty, the risk of a project can be defined as "The impact of project objectives (quality, cost, and duration) that may occur during the entire life cycle of the project and the possible interventions that

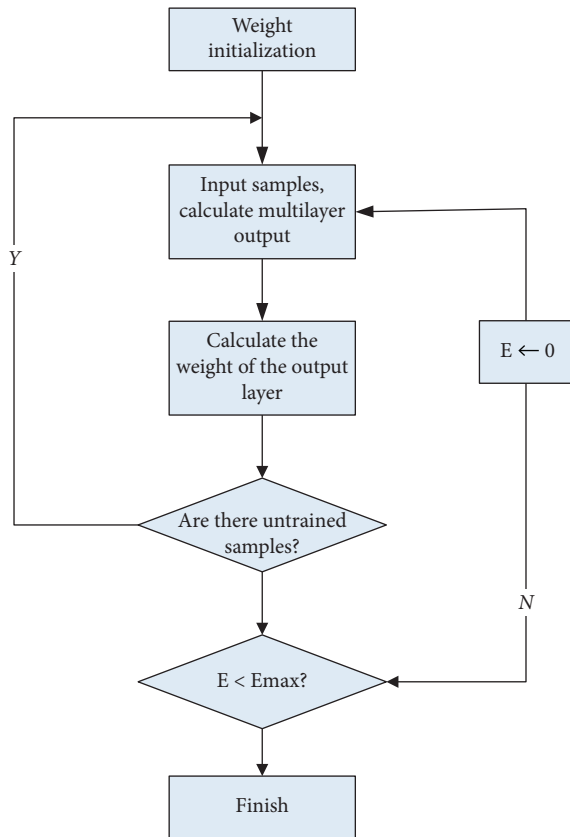


FIGURE 2: BP neural network flow chart.

may occur” in production and operations. In the process, uncertainty or the impact of events may cause damage or loss of mechanical operations [33]. The risk analysis and assessment process is shown in Figure 3.

The construction risk management of subway engineering refers to that in order to achieve the expected goals of quality, time, cost, and safety, the manager of the organization appropriately uses the basic risk management theory, including organization, design, coordination, and management. For control during the establishment of a deep foundation, the risks must be fully identified, analyzed, and evaluated, and preventive measures must be taken to reduce the possibility of risk events or reduce the adverse effects of the results [34]. Due to the objective existence of managerial subjective differences, the evaluation of objective risks and their potential impacts is unilateral. After completing the abovementioned risk identification, the risks must be analyzed and evaluated in detail. This is the whole process of risk management. An important link is also the link and bridge between risk identification and risk decision making, which is the key to risk management [35, 36].

The environment of the subway project and the construction site is complex and closely connected, interacting with and restricting each other. As an important part of the urban rescue project, it has high requirements for construction safety and construction quality. Due to the particularity of the subway construction site and the complexity of construction, the interface will contain many different

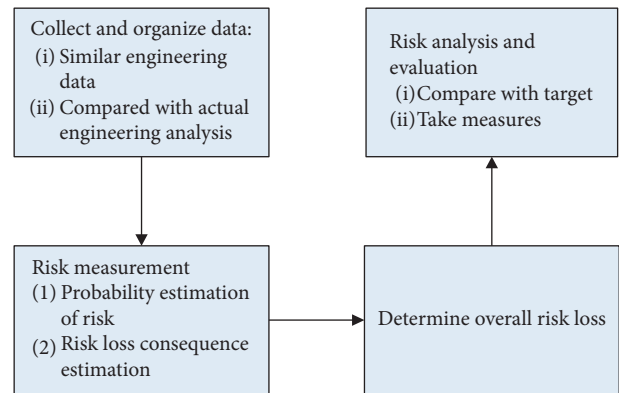


FIGURE 3: Risk analysis and estimation process.

aspects of the industry. The working area of a subway tunnel is completely different from that of buildings on the ground. The working space of the ground building is relatively wide, and the vertical and horizontal directions are combined, while the working space of the subway mechanical tunnel is mainly horizontal, and the working space is very narrow. These factors determine the longest construction period of the subway project. Urban subway is a kind of high-cost and high-cost underground transportation. There are mainly two types of overhead and underground space. The underground cost is mainly of high cost.

2.3. The Construction Safety Risk Assessment Index of Subway Engineering. Establishing a reasonable and effective risk assessment system can improve the accuracy of risk assessment and lay a good foundation for risk assessment and control.

On the basis of the existing subway project safety evaluation system, the risk factors that may affect the construction progress of the subway project are comprehensively analyzed, and the subway project construction evaluation system is established. In addition, considering the current risk factors caused by the ideas and technological innovation of each component, the innovative ideas and technological risks are taken as independent evaluation indicators to establish a risk evaluation system that best meets the requirements. In the construction of the subway, the basic principle of the index system proposed in this paper is verified through the analytic hierarchy process, which provides a theoretical basis for the next development and is more in line with the actual implementation requirements of the project [37].

In the process of risk assessment of subway project construction, not only should the identification and control of risk indicators be strengthened but also reasonable risk assessment standards should be formulated. Determining the risk level of subway construction can help decision makers familiarize themselves with the adverse effects of subway incidents and promote risk prevention. According to the literature review, this article also determines the following five risk levels in conjunction with the actual construction of the subway project, as shown in Table 1.

TABLE 1: Risk levels of subway construction.

Risk level	Interval range	Meaning
Level 1	(0, 0.2]	Acceptable and strive to control the risk within this level
Level 2	(0.2, 0.4]	Acceptable, it is allowed to occur within certain conditions without escalating the risk level
Level 3	(0.4, 0.6]	Do not want to happen; compare the adverse effects of risks and the cost of measures taken
Level 4	(0.6, 0.8]	Unacceptable; immediately formulate risk response measures
Level 5	(0.8, 1]	Completely unacceptable; eliminate or avoid risks

Establishing a project risk assessment system is an important task. The quality, rationality, and completeness of the company directly affect the results of the risk assessment. Therefore, it is very important to establish a logical, scientific, practical, and objective engineering risk assessment system. The special complexity of the subway itself, coupled with the various natural and man-made environments in which it is located, makes it even more complicated. It can be said that the risk of a subway project is a complete system, so the establishment of a risk assessment index system must also comply with this systematic principle. When selecting indicators, the factors affecting mechanical hazards should be considered as comprehensively as possible, and evaluation indicators should be considered in a stable process. Evaluation indicators must be considered systematically. In order to build an organic whole, various dynamic and static indicators should be combined for qualitative and quantitative analysis. Only in this way can the final assessment result more fully reflect the risks of the subway project [38].

3. Safety Risk Identification Experiment of Subway Construction

This article discusses the issue of subway construction safety assessment. It is easy to know that each influencing factor, namely, the safety factor index, has a different degree of influence on the safety level of the assessed item. At the same time, the construction of groundwater works in each region follows the surrounding rocks, hydrogeological sites, monasteries, political zones, and much more. In addition, expectations for the safety of an underground project should also be different.

3.1. Test Subject. This paper selects 15 existing subway projects as samples for research and determines the selection of subway projects based on the BP neural network construction method. Therefore, this paper selects 15 groups of cities under construction in A, B, C, D, and E cities. For the subway project, the study continued to invite 8 professionals in the industry who participated in the risk factor identification questionnaire to analyze and identify 12 risk evaluation index systems established for 10 projects.

3.2. Test Design. Safety management of the subway construction organization: the construction party involved in this article is the construction unit. The safety management

of the subway construction organization refers to the organization safety management of the construction unit. Organizational safety management is mainly realized through the construction unit's institutional functions, guarantee measures, and system constraints [39]. Organizational safety management restricts and guides human behavior from the management level, reduces the probability of unsafe behaviors, and standardizes construction behavior. Therefore, when evaluating indicators, the safety management indicators of subway construction organization are divided into construction site safety management, three evaluation items of safety production system, and safety management organization.

The idea of calculating the weight in this section is the number of evaluation index levels is 3 levels, first calculating the weight value of the standard level at the target level, then calculating the weight value of the index level in the corresponding standard, and finally, calculating the value of the single-layer weight combination. To obtain the total weight, we take the total weight of the index level index as the target level.

- (1) We inquire and collect knowledge about safety risks in the construction specifications of subway projects published in our country and scientific papers and documents at home and abroad
- (2) We transform risk knowledge into computer expressions
- (3) Based on cloud information technology of building information technology, we complete the construction of a knowledge base of hidden dangers in subway construction and accumulate and share the knowledge base
- (4) Based on the established knowledge base on the safety of subway structure, we intelligently extract the technical data of the BIM subway model and read the technical parameters of the various rules related to the various dangers of the subway station
- (5) use the credibility combination analysis method to formulate intelligent identification rules

The criterion layer calculates the weight of the target layer. The criterion layer is four indicators of organizational safety management, technical safety management, environmental safety management, and personnel safety management, which are represented by $T_1 T_2 T_3 T_4$ in turn and assigned values according to the importance of the target layer. Through pairwise comparison, the judgment

matrix Z of the target layer and the criterion layer is established:

$$Z = \begin{bmatrix} 1 & \frac{1}{3} & 3 & 2 \\ 3 & 1 & 4 & 2 \\ \frac{1}{3} & \frac{1}{4} & 1 & \frac{1}{3} \\ \frac{1}{2} & \frac{1}{2} & 3 & 1 \end{bmatrix}. \quad (4)$$

The consistency test is performed through the relevant formula. If the consistency ratio is less than the specified 0.10, it indicates that the consistency of the crisis matrix is good and the weight distribution of each indicator meets the requirements. Otherwise, it indicates that the distribution of the matrix is unreasonable, the degree of dispersion is large, and the crisis is not accurate. At this time, the weight of the rating index should be modified and then recalculated:

$$AM = \frac{(\alpha_{\max} - q)}{(q - 1)} = \frac{(3.112 - 3)}{(3 - 1)} = 0.056, \quad (5)$$

$$AN = \frac{(A \times M)}{(N \times M)} = \frac{0.056}{0.9} = 0.059 < 0.1.$$

3.3. Experimental Results. According to the identification results of safety hazards, potential hazards include instability of the foundation pit steel structure, instability of the foundation pit supporting structure, flowing soil and punches under the foundation pit, harmful geological conditions, and leakage and cracks. The construction team took many effective measures. Obviously, the construction of subway projects in each region depends on the surrounding rock structure soil, geological and hydrogeological conditions, management agencies, and local policy environment in different regions. The site was arranged in advance, and the entire construction work of the subway with emergency teams and various emergency equipment was safe and smooth, and good implementation results were achieved. Based on this BIM model of subway construction, the results of intelligent hazard identification using the reliability combination analysis method are given as shown in Table 2.

4. Related Analysis of Safety Risks in Subway Construction

4.1. Questionnaire for Risk Assessment of Metro Engineering Construction. We pay attention to the intersection of the two types of samples during network training because the central input of the same type of samples will cause the network to only determine the mapping relationship suitable for this type of sample during the training and determination process. When other types of samples are concentrated, the network weight value adjustment will move to the new mapping relationship, and the previous training results will be cancelled. In this article, according to the

Matlab2012a Neural Network Toolkit, it is called the BP Neural Network. Through the construction sample data of 15 subway projects in specific locations, including construction cost, pile quality, slope instability, long inspection cycle, house deformation, pipeline, and fast sand, all aspects of the data have been integrated and organized, and finally, the sample training data that have been researched and analyzed are introduced into the BP training program. The value-added evaluation and change risk curve of the mechanical deep base mirror are shown in Figure 4.

4.2. Types of Accidents in Subway Construction. Most construction accidents are not isolated, but a variety of accidents occur together, or the occurrence of other accidents due to one type of accident will eventually cause casualties to the masses and adversely affect social life. Due to limited data collection, reliable information is mainly obtained through media reports and related materials. For accidents that have no social impact but frequently occur (such as falling from a height), the device will have a certain degree of concealment, and the outside world will not be able to obtain related types of accidents. In terms of accident statistics, there were 12 collapse accidents, with the largest number of accidents, followed by collapses, pipeline damage, and mechanical accidents. These three accidents are also more common, with 6 cases, 6 cases, and 5 cases respectively. In the past four years, there have been frequent shootings and fires. The most common subway construction accidents are collapses, pipeline damage, and mechanical accidents. It seems that we should not only focus on the types of accidents that cause deaths and injuries but also ignore the types of accidents without casualties. This is incorrect because the mechanism of construction accidents is the same, but the consequences are different. Through incomplete statistics of China's subway construction accidents in the past five years, the results are shown in Figure 5.

4.3. Characteristics of Environmental Risk Factors. Due to the uncertainty of system behavior during normal subway construction, mechanical accidents may be caused, which is not conducive to subway construction. Underground engineering is a large-scale urban construction project. The construction process is very complicated and involves many risk factors. Geological hazards, environmental hazards, construction hazards, etc. are caused by the upcoming subway construction. Most subway lines pass through complex areas, such as the old city and shopping areas. There are many types of buildings along the line, such as houses, viaduct foundations, underground passages, and underground passages. The surrounding environment along the line is more complicated. According to the evaluation model and risk level standards, and when determining the weights, relevant experts and experienced technicians are first required to evaluate to determine the probability of occurrence of all risk factors and the extent of potential risks at the factor level. The estimated values are shown in Table 3.

As shown in Table 3, the risk assessment of subway construction projects can be divided into 5 levels. When the

TABLE 2: Risk intelligent identification results.

Security risk classification	Rule coding	Risk description	Credibility
Construction technology risk factors	R1-2	Quicksand	0.7
	R1-27	Unstable steel structure of foundation pit	0.49
	R1-16	Unstable foundation pit retaining structure	0.19
Project characteristics risk factors	—	—	—
Geological and hydrological risk factors	R3-02	Harmful geological conditions	0.33
Risk factors of construction environment	R4-14	Leaks and cracks in underground pipelines	0.28

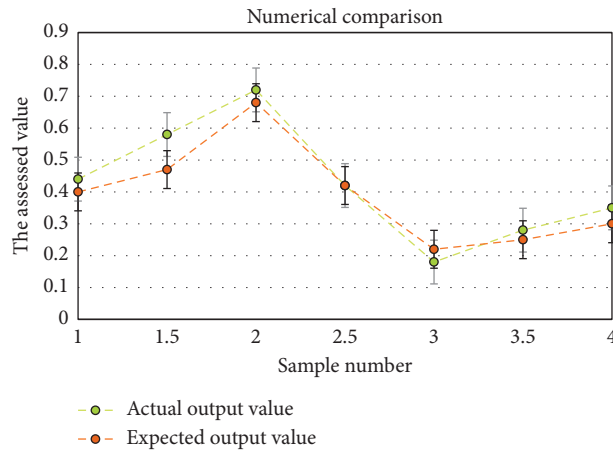


FIGURE 4: Risk assessment value of subway construction.

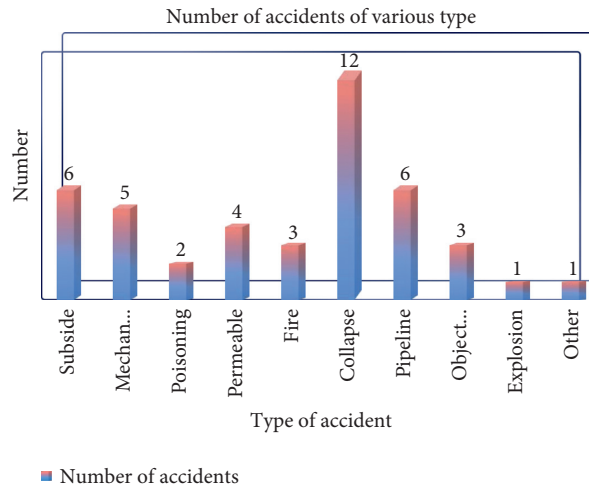


FIGURE 5: Statistics of accident types in subway construction.

TABLE 3: Classification criteria for risk level S.

Grade	Valuation S	Meaning description
Level 1	0.8–1.0	The highest level of risk, which may cause devastating disasters and heavy casualties
Level 2	0.6–0.8	The level of risk is very high, causing widespread damage or casualties
Level 3	0.4–0.6	The risk level is relatively high, which may cause damage within a certain range
Level 4	0.2–0.4	The risk level is low, and appropriate preventive measures can be taken
Level 5	0–0.2	The lowest level of risk, almost no risk

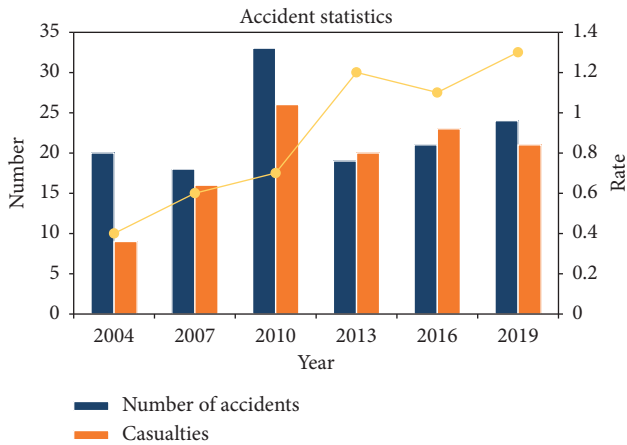


FIGURE 6: Statistics of our country's subway construction accidents from 2014 to 2019.

valuation is 0.8–1.0, the subway construction risk is the highest, and when the valuation is 0–0.2, the subway construction risk is the lowest.

4.4. Statistics of Our Country's Subway Construction Accidents in Recent Years. At present, the conduct of our country's subway is at its peak. Since the design of the subway, there have always been multiple risk factors. The construction of the subway is scattered and involves many builders. If an accident occurs, it may cause serious personal and property damage. During the subway construction process, the complexity of rocks and ground and the unpredictable state of unknown objects, the complexity of the construction process and construction equipment, the concealment of the project, the length of the construction period, and the uncertainty of the construction process risk have all increased. The total number of subway construction accidents is also increasing year by year. Therefore, the establishment of a subway construction risk assessment system can clarify the sources of danger in the subway construction process and reduce the occurrence of subway accidents. Figure 6 shows the statistical results of China's subway construction accidents from 2004 to 2019.

According to the data in Figure 6, it can be seen that, in 2004, the number of accidents was 20, with the lowest mortality rate. In 2010, the number of accidents was 33 with the highest mortality rate. In 2007, the number of accidents was the lowest with 18.

4.5. Percentage of Accidents in Each Month. According to the statistical results of domestic and foreign subway construction accidents and related research results, the subway construction process mainly includes safety accidents such as collapse, object hit, fall from height, lifting injury, and mechanical accident. In these 16 years, we can see the highest number of subway construction accidents occurred in March and May, July-August, and November; February was the lowest, and the number of adjacent months has changed greatly. From July to August, the

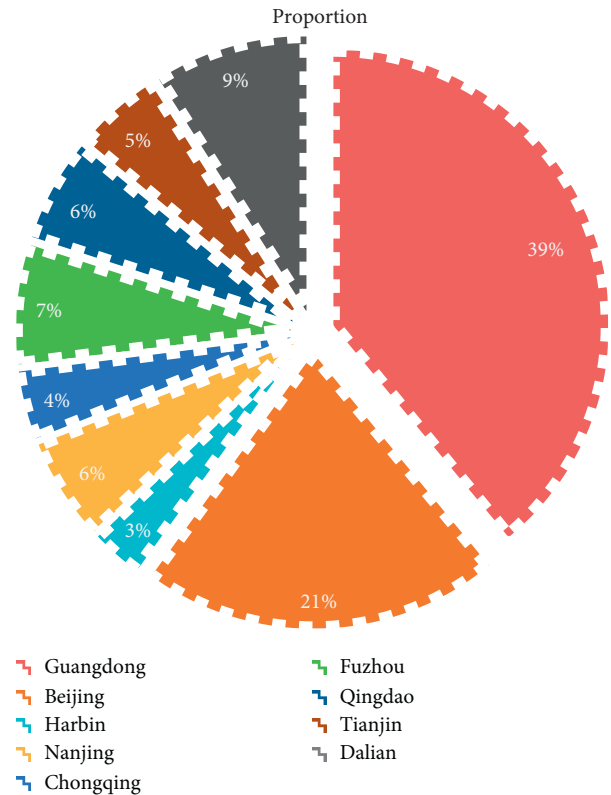


FIGURE 7: Proportion of locations where accidents occurred in March.

weather in our country is the hottest, the daytime is long, and the outdoor working environment is bad, which has become the peak of accidents. The accidents in November were mainly concentrated in cities in the middle and lower reaches of the Yangtze River. Due to weather changes, the number of rainy days exceeds 20 days, and the total number of accidents and casualties is also the highest. The Guangdong subway accidents in March mainly occurred in Guangzhou and Shenzhen, accounting for 40% of the country. The weather in Guangdong gradually warmed up in March, and the rain began to increase. There were many rivers in Guangzhou and Shenzhen, and the ground was loose, which also increased the safety risks of subway construction, as shown in Figure 7.

5. Conclusions

Safety assessment and prediction research during the subway construction stage can identify major risks in advance based on the analysis results, improve the management, and control capabilities and early warning capabilities of subway construction, thereby improving the safety level of the construction site and reducing accidents during the construction of the subway in our country. Avoiding or reducing losses and financial losses as much as possible to provide safety guarantees for the promotion of China's urban rail transit construction is of great theoretical significance for the comprehensive subway safety assessment in the future.

On the basis of summarizing the existing research results and combining the construction characteristics of subway projects, this study constructed a set of index systems consistent with the risk analysis of subway construction progress and introduced the improved BP neural network algorithm into the risk preassessment. It has theoretical research significance and practical application value, takes the risk of conceptual technological innovation as an independent evaluation index, and has established a set of progress evaluation index systems that is more in line with the characteristics of current construction projects. This will help subway construction projects to more completely and accurately identify the risk factors that may occur during the construction process and to preconfigure countermeasures to reduce the possibility of efficiency hazards and their impact.

The improved BP neural network algorithm analyzes the risks in the construction of subway projects, and the feasibility of the intelligent risk identification model is analyzed and demonstrated. This model is actually applied to subway stations, and appropriate risk prevention and control measures are taken according to the identification results, which effectively reduces the occurrence of construction safety risk accidents and safely realizes the goal of safe construction of subway stations.

Data Availability

The data that support the findings of this study are available from the corresponding author upon reasonable request.

Conflicts of Interest

The authors declare that they have no conflicts of interest.

References

- [1] J. Yang, J. Zhang, and H. Wang, "Urban traffic control in software defined internet of things via a multi-agent deep reinforcement learning approach," *IEEE Transactions on Intelligent Transportation Systems*, vol. 4, no. 3, pp. 177–188, 2010.
- [2] H. Liu, B. Liu, H. Zhang, L. Li, X. Qin, and G. Zhang, "Crowd evacuation simulation approach based on navigation knowledge and two-layer control mechanism," *Information Sciences*, vol. 436–437, pp. 247–267, 2018.
- [3] Y. Zou, B. Lin, X. Yang, L. Wu, M. Muneeb Abid, and J. Tang, "Application of the bayesian model averaging in analyzing freeway traffic incident clearance time for emergency management," *Journal of Advanced Transportation*, vol. 2021, no. 4, Article ID 6671983, 9 pages, 2021.
- [4] Y. Sun, "Green and reliable freight routing problem in the road-rail intermodal transportation network with uncertain parameters: a fuzzy goal programming approach," *Journal of Advanced Transportation*, vol. 2020, no. 3, Article ID 7570686, 21 pages, 2020.
- [5] M. Li, H. Yu, and P. Liu, "An automated safety risk recognition mechanism for underground construction at the pre-construction stage based on BIM," *Automation in Construction*, vol. 91, pp. 284–292, 2018.
- [6] L. Yang, X.-R. Wen, X.-L. Wu et al., "Height prediction of water flowing fractured zones based on BP artificial neural network," *Journal of Groundwater Ence and Engineering*, vol. 7, no. 4, pp. 354–359, 2019.
- [7] J. Yang, J. Wen, and B. Jiang, "Blockchain-based sharing and tamper-proof framework of big data networking," *IEEE Network*, vol. 34, no. 4, pp. 62–67, 2020.
- [8] B. Wu, S. Han, J. Xiao, X. Hu, and J. Fan, "Error compensation based on BP neural network for airborne laser ranging," *Optik*, vol. 127, no. 8, pp. 4083–4088, 2016.
- [9] Y.-H. Yuan, S.-H. Tsao, J.-T. Chyou, and S.-B. Tsai, "An empirical study on effects of electronic word-of-mouth and Internet risk avoidance on purchase intention: from the perspective of big data," *Soft Computing*, vol. 24, no. 8, pp. 5713–5728, 2020.
- [10] D. Ma, T. Zhou, J. Chen, S. Qi, M. Ali Shahzad, and Z. Xiao, "Supercritical water heat transfer coefficient prediction analysis based on BP neural network," *Nuclear Engineering and Design*, vol. 320, pp. 400–408, 2017.
- [11] S.-B. Tsai, Y.-Z. Xue, P.-Y. Huang et al., "Establishing a criteria system for green production," *Proceedings of the Institution of Mechanical Engineers, Part B: Journal of Engineering Manufacture*, vol. 229, no. 8, pp. 1395–1406, 2014.
- [12] Z. Cheng and T. Juncheng, "Adaptive combination forecasting model for China's logistics freight volume based on an improved PSO-BP neural network," *Kybernetes*, vol. 44, no. 4, pp. 707–710, 2015.
- [13] C.-H. Chen, F. Song, F.-J. Hwang, and L. Wu, "A probability density function generator based on neural networks," *Physica A: Statistical Mechanics and its Applications*, vol. 541, Article ID 123344, 2020.
- [14] L. Yiming, H. U. Zhuowei, Z. Wenji et al., "Research on spatial characteristics of regional poverty based on BP neural network: a case study of wuling mountain area," *Journal of Geo-Information Science*, vol. 17, no. 1, pp. 69–77, 2015.
- [15] X. Han, X. Xiong, and F. Duan, "A new method for image segmentation based on BP neural network and gravitational search algorithm enhanced by cat chaotic mapping," *Applied Intelligence*, vol. 43, no. 4, pp. 855–873, 2015.
- [16] W. Longkang, R. Tingxiang, N. Baisheng et al., "Development of a spontaneous combustion TARPs system based on BP neural network," *International Journal of Mining Ence & Technology*, vol. 25, no. 5, pp. 803–810, 2015.
- [17] X. H. Zeng, G. H. Li, D. F. Song et al., "Rollover warning algorithm based on genetic algorithm-optimized BP neural network," *Huanan Ligong Daxue Xuebao/Journal of South China University of Technology (Natural Science)*, vol. 45, no. 2, pp. 30–38, 2017.
- [18] L. M. T. Pham, L. T. T. Tran, P. Thipwong, and W. T. Huang, "Dynamic capability and organizational performance," *Journal of Organizational and End User Computing*, vol. 31, no. 2, pp. 1–21, 2019.
- [19] M. Abdel-Basset, R. Mohamed, M. Elhoseny, and V. Chang, "Evaluation framework for smart disaster response systems in uncertainty environment," *Mechanical Systems and Signal Processing*, vol. 145, Article ID 106941, 2020.
- [20] Y. Chen, W. Zheng, W. Li, and Y. Huang, "The robustness and sustainability of port logistics systems for emergency supplies from overseas," *Journal of Advanced Transportation*, vol. 2020, Article ID 8868533, 10 pages, 2020.
- [21] X. Chen, T. Wang, and W. Liang, "General aircraft material demand forecast based on PSO-BP neural network," *International Journal of Control and Automation*, vol. 9, no. 5, pp. 407–418, 2016.

- [22] H. Song and M. Brandt-Pearce, "A 2-D discrete-time model of physical impairments in wavelength-division multiplexing systems," *Journal of Lightwave Technology*, vol. 30, no. 5, pp. 713–726, 2012.
- [23] Y. Cui, X. L. Ma, and Z. Liu, "Application of improved BP neural network with correlation rules in network intrusion detection," *International Journal of Security and Its Applications*, vol. 10, no. 4, pp. 423–430, 2016.
- [24] S. Zhang, J. Lv, X. Yuan et al., "BP neural network with genetic algorithm optimization for prediction of geo-stress state from wellbore pressures," *International Journal of Computational Intelligence & Applications*, vol. 15, no. 3, pp. 80–85, 2016.
- [25] X. Li, Y. Wang, and G. Liu, "Structured medical pathology data hiding information association mining algorithm based on optimized convolutional neural network," *IEEE Access*, vol. 8, no. 1, pp. 1443–1452, 2020.
- [26] Y. Q. Liu, Q. Xu, D. Infield et al., "Fault identification of wind turbine drivetrain using BP neural network based on gravitational search algorithm," *Zhendong Yu Chongji/Journal of Vibration and Shock*, vol. 34, no. 2, pp. 134–137, 2015.
- [27] L. Yongkui, H. Yi, X. Bo et al., "Proactive behavior-based system for controlling safety risks in urban highway construction megaprojects," *Automation in Construction*, vol. 95, pp. 118–128, 2018.
- [28] Y. Tang and M. Elhoseny, "Computer network security evaluation simulation model based on neural network," *Journal of Intelligent and Fuzzy Systems*, vol. 37, no. 3, pp. 3197–3204, 2019.
- [29] C. Caldas, G. Gibson, A. M. Yohe, R. Weerasooriya et al., "Identification of effective management practices and technologies for lessons learned programs in the construction industry," *Journal of Construction Engineering & Management*, vol. 135, no. 6, pp. 531–539, 2015.
- [30] T. Kasproicz, "Quantitative identification of construction risk," *Archives of Civil Engineering*, vol. 63, no. 1, pp. 63–75, 2017.
- [31] T. Zhang, "Application of safety quality hidden danger investigation and management system in subway construction," *Value Engineering*, vol. 38, no. 20, pp. 57–59, 2019.
- [32] Y. Chen, W. Zheng, W. Li, and Y. Huang, "Large group activity security risk assessment and risk early warning based on random forest algorithm," *Pattern Recognition Letters*, vol. 144, pp. 1–5, 2021.
- [33] S. Sultan, "Book review: moving safely: crime and perceived safety in stockholm's subway stations," *International Criminal Justice Review*, vol. 26, no. 1, pp. 49–50, 2016.
- [34] A. Bryson, "Health and safety risks in britain's workplaces: where are they and who controls them?" *Industrial Relations Journal*, vol. 47, no. 5-6, pp. 547–566, 2016.
- [35] Z. Ying, L. Chenshuang, D. Lieyun et al., "Combining association rules mining with complex networks to monitor coupled risks," *Reliability Engineering System Safety*, vol. 186, pp. 194–208, 2019.
- [36] P. Gomba and I. Bradacova, "Critical systems and processes affecting the resilience of subway systems to terrorism risks," *Komunikacie*, vol. 17, no. 1, pp. 22–27, 2015.
- [37] H. S. Lee, H. L. Mun, and S. K. Lee, "Evacuation time at Jongno 3ga subway station considering electric train delays and congestion," *Journal of Transportation Security*, vol. 11, no. 3-4, pp. 137–150, 2018.
- [38] Y. Lv, X. D. Yan, W. Sun, and Z. Y. Gao, "A risk-based method for planning of bus-subway corridor evacuation under hybrid uncertainties," *Reliability Engineering & System Safety*, vol. 139, pp. 188–199, 2015.
- [39] J. Peng, J. Quan, and L. Peng, "It application maturity, management institutional capability and process management capability," *Journal of Organizational and End User Computing*, vol. 31, no. 1, pp. 61–85, 2019.

Research Article

Incentive Contract Design for Supply Chain Enterprise's Pollution Abatement with Carbon Tax

Jing Yu ¹, Chi Zhou ¹, Yixin Wang ¹ and Zhibing Liu ²

¹School of Management, Tianjin University of Technology, Tianjin 300384, China

²Institute of Uncertain Systems, Huanggang Normal University, Hubei 438000, China

Correspondence should be addressed to Chi Zhou; czhou@tjut.edu.cn

Received 20 February 2021; Revised 5 April 2021; Accepted 19 April 2021; Published 29 April 2021

Academic Editor: Aijun Liu

Copyright © 2021 Jing Yu et al. This is an open access article distributed under the Creative Commons Attribution License, which permits unrestricted use, distribution, and reproduction in any medium, provided the original work is properly cited.

This paper applies mechanism design to the supply chain enterprise's pollution abatement problem with carbon tax. To maximize the government's expected utility, an uncertain contract model is presented in the framework of principal-agent theory, where the government's assessment of the supply chain enterprise's carbon emission level is described as an uncertain variable. Afterwards, the equivalent model is provided to obtain the optimal contract for the uncertain pollution abatement problem. The results demonstrate that the supply chain enterprise's optimal output decreases with the carbon emission level. Furthermore, the government's optimal transfer payment decreases with the carbon emission level if the carbon tax is low. In contrast, if the carbon tax is high, the optimal transfer payment increases with the carbon emission level. In addition, an increase in the carbon emission level decreases the optimal utilities of both the government and the supply chain enterprise and also leads to the supply chain enterprise's incremental marginal utility. Finally, we provide a numerical example, which illustrates the effectiveness and practicability of the proposed model.

1. Introduction

The implementation of an environmental governance policy on government agendas around the world has stirred a renewed interest in the optimal mechanism design of pollution abatement. Environmental pollution is caused by the excessive discharge of various industrial pollutants, such as carbon emissions, leading to climate change, air pollution, and water pollution. According to the Global Carbon Budget 2020, the Global Carbon Project's researchers estimate that global carbon emissions in 2019 will increase by 2% (+0.8% to +3.0%) after three years of almost no growth, reaching a new high of 9.9 ± 0.5 GtC. From the report of Climate News Network 2020, almost one-fifth of all the world's carbon emissions come from the supply chain enterprises. According to a McKinsey report on consumer packaged goods (CPG) supply chain enterprises, more than 80% of the overall emissions come from getting a product from the source to the consumer as part of the supply chain. Mitigating environmental pollution will require the government

to adopt substantial abatement mechanisms of industrial pollutants or carbon emissions that can be implemented most cost-effectively by the carbon tax policy [1]. The government's choice of appropriate pollution abatement mechanisms is essential for minimizing the environmental pollution and stimulating the supply chain enterprises to increase productivity, which will further promote economic growth [2]. This paper presents an optimal incentive contract design for an uncertain pollution abatement problem with carbon tax.

The government, as an environmental regulator, usually lacks perfect information on supply chain enterprises' demand for pollution. Because of the influence of such asymmetric information, supply chain enterprises have incentives to misreport their pollution demand if the pollution abatement mechanism is based on such reports. Therefore, many authors (e.g., Kim and Chang [3], Duggan and Roberts [4], and Montero [5]) have designed incentive mechanisms that can induce regulated supply chain enterprises to truthfully reveal their demand. For example, these studies

present mechanisms whereby the regulator provides the supply chain enterprise a menu of contracts; faced with this menu, the supply chain enterprise's dominant strategy is to truthfully report its private information. By applying principal-agent theory, the relationship between the economy and the environment is discussed under asymmetric carbon emission information. However, few studies in the existing literature investigate how the incentive contract is designed in the uncertain pollution abatement problem when carbon tax is considered.

As a representative approach to mitigating environmental pollution, carbon tax discourages the use of fossil fuels by making carbon emissions more costly [6]. Moreover, this policy also facilitates reductions in carbon emissions via fuel choices or technological innovations. In 1990, a carbon tax policy was first introduced in Finland and was subsequently extended to several other countries. For instance, Japan introduced a carbon tax policy in 2012. The use of carbon taxes has shown broadly positive effects in reducing carbon emissions while generating slightly negative impacts on economic growth. In China, an environmental protection tax law was implemented on 1 January 2018. The carbon tax policy has received increasing attention since the launch of the national carbon trading market. Nevertheless, there are few theoretical studies of the impact of carbon emissions and taxes on the optimal incentive contract design.

To study this problem, we construct an optimal contract model in which the government is regarded as the principal and the supply chain enterprise is regarded as the agent. To this end, an uncertain contract model is presented to maximize the expected utility of the government, in which the government's assessment of the supply chain enterprise's carbon emission level is subjective and is described as an uncertain variable. Then, we provide the crisp equivalent model and obtain the optimal solution of this problem. If the government has historical data on the supply chain enterprise's carbon emissions, then the uncertain information about carbon emission level may be rationally described as a random variable. A model can be built to maximize the government expected net profit, and its equivalent deterministic model can be also obtained naturally by applying the probability measure. Meanwhile, the optimal solution of the contract model under stochastic environment can be also obtained. However, in most practical scenarios, historical data are unavailable. The supply chain enterprise's carbon emission level is often difficult to measure directly. In fact, for a supply chain enterprise without historical data on the carbon emission level, the government can ask domain experts to subjectively evaluate the degree of belief about the supply chain enterprise's carbon emissions. Subsequently, the uncertainty distribution of carbon emissions could be estimated by using uncertainty theory.

The main findings of our paper are as follows. First, if a supply chain enterprise's carbon emission level increases, then the supply chain enterprise is less willing to produce output; that is, the optimal output of the enterprise decreases with the carbon emission level. Second, the government's optimal transfer payment decreases with the carbon emission level if the carbon tax is below a certain threshold. In

contrast, if the carbon tax is above this threshold, the government's optimal transfer payment to the supply chain enterprise increases with the carbon emission level. Finally, the optimal utilities of both the government and the enterprise decrease with the carbon emission level.

The remainder of this study is organized as follows. Section 2 reviews the related literature. We present an uncertain contract model in Section 3. Section 4 derives an equivalent model for uncertain pollution abatement problem. Moreover, we obtain the optimal contract for the equivalent model in Section 5. In Section 6, we provide a numerical example to illustrate the effectiveness and practicability of the proposed model. Finally, Section 7 summarizes the main conclusions of this study.

2. Literature Review

This study is mainly related to three streams of literature. The first stream concentrates on the economics of the pollution abatement problem. The second stream explores principal-agent problems associated with pollution abatement. The last research stream addresses the application of uncertainty theory to principal-agent problems.

In the first stream of literature on the economics of the pollution abatement problem, the effect of government policy on the economics of pollution abatement has been investigated by many researchers [7, 8]. Laffont and Tirole [9] study how spot and futures markets for tradeable pollution permits affect the polluters' compliance decisions. The conclusions can be applied to a variety of situations, such as public transportation, demand-side management, bypass in telecommunications, or forward sales by a private monopolist. Moreover, the researchers discuss the negative impact of plain pollution allowance markets on the environmental pollution innovation. Lothe and Myrteit [10] establish a formal model to interpret the issues that arise in the multitask environmental problem of implementing an optimal strategy. In recent years, research and practice in the area of carbon tax policy have continued to grow. For instance, Martin et al. [2] examine the effects of carbon tax on manufacturing plants by using the panel data from the UK production census. Liu et al. [6] summarize an analysis of choice preferences to design the carbon tax policy from the viewpoint of Chinese businesses. Fahimnia et al. [11] establish a supply chain optimization model that combines carbon emissions and economic objectives under the scheme of carbon tax policy. In addition, Klenert and Mattauch [12] study the distributional effects of carbon tax reform while considering that households must consume carbon-intensive goods in the market. In contrast to these papers, we consider the optimal mechanism design in the pollution abatement problem with carbon tax and analyze how carbon tax affects the optimal contract.

This paper also examines numerous studies of principal-agent problems associated with pollution abatement [13]. Helm and Wirl [14] discuss contracting of a principal with an agent if multilateral externalities are present; the example is that of an international climate agreement given private information about the willingness to pay for emissions abatement. By

studying a hierarchical model of environmental regulation and enforcement, Arguedas and Rousseau [15] investigate the national regulator and the monitoring decision made by a local enforcement agency. In addition, Shrestha [16] designs an incentive mechanism in which the regulator provides a menu of linear price-quantity contracts to each firm. Lika et al. [17] study incentive water pricing schemes under asymmetric information by using a principal-agent model. By applying the agency theory and drawing on the organizational culture, Dubey et al. [18] study a theoretical model of reconfigurable manufacturing systems to integrate the top management's beliefs, participation, and environmental performance. However, our work differs from the studies cited above in three aspects. First, the carbon emission level is the private information of the supply chain enterprise. Second, we consider a carbon tax that the supply chain enterprise pays to the government in the pollution abatement problem. Third, we assume that the government's subjective assessment of the supply chain enterprise's carbon emission level is described as an uncertain variable.

The last stream of literature examines the application of uncertainty theory to principal-agent problems. The existing literature characterizes the uncertain information in principal-agent problems as a random variable or a fuzzy variable [19, 20]. However, due to the influence of subjective factors and the lack of historical data, characterizing the information uncertainty as randomness is not entirely reasonable. Therefore, uncertainty theory, an axiomatic approach based on the subjective information, has been proposed, including an uncertain variable, uncertainty distribution, and expected value [21]. Since then, uncertainty theory has attracted considerable attention among researchers in related fields as an important mathematical approach to dealing with information uncertainty. Many researchers apply uncertainty theory to principal-agent problems [22]. For instance, Mu et al. [23] study a principal-agent problem between one enterprise and one rural migrant worker and then establish an uncertain contract model. Zhou et al. [24] establish an uncertain model of principal-agent problem under loss aversion and inequity aversion and analyze how loss aversion and inequity aversion affect the wage structure in optimal contract design. By studying an uncertain principal-agent model, Zhou et al. [25] investigate the effect of referral services on the optimal contract with CPC or CPS payments. In addition, the application of uncertainty theory in supply chain management has been extensively researched in the literature [26, 27]. Similar to the above literature, our work depicts the government's subjective assessment of the supply chain enterprise's carbon emission level by an uncertain variable.

3. Uncertain Pollution Abatement Model

Consider an uncertain pollution abatement problem with two participants: the government (she) and the supply chain enterprise (he). The government is the principal, and the supply chain enterprise is the agent. To induce the supply chain enterprise to truthfully reveal the carbon emission level, the government should design a mechanism to optimize the trade-off between the economic development and environmental protection.

The carbon emission level is the private information of the supply chain enterprise, and the government cannot observe it exactly. The government's subjective assessment of the supply chain enterprise's carbon emission level can be characterized as an uncertain variable ξ in the range of $[a, b]$, where $0 \leq a < b < +\infty$. The uncertain variable ξ has the uncertainty distribution function $\Phi(x)$; it is assumed that $\phi(x)$ is the derivative of $\Phi(x)$, where $\Phi(x)$ and $\phi(x)$ satisfy $(\Phi(x)/\phi(x))/dx \geq 0, \forall x \in [a, b]$. Let $q(x)$ be the output of the supply chain enterprise, where x denotes the carbon emissions he realizes in the production process. The degree of pollution of the environment is $p(x)$, which can be practically measured by air quality, water quality, and biological pollution. $C(q(x), x)$ denotes the supply chain enterprise's production cost at a given level of carbon emissions. Moreover, the transfer payment the government makes to the supply chain enterprise is denoted by $t(x)$, and $G(q(x))$ represents the revenue the government obtains if the supply chain enterprise's output is $q(x)$. In addition, βx is the corresponding carbon tax the supply chain enterprise pays to the government, where β represents the tax rate of the carbon emissions quota. This assumption implies that an increase in carbon emissions increases the carbon tax if the tax rate is unchanged. Thus, the contract that the government designed can be characterized by a mechanism $(q(\cdot), t(\cdot))$.

In the pollution abatement problem, an uncertain contract model is presented to maximize the expected utility of government. The government could induce the supply chain enterprise to truthfully reveal carbon emission level by the optimal incentive contract. To be more specific, several assumptions are listed as follows.

- (3.1) For the supply chain enterprise's production cost function $C(q, x)$, we assume that

$$\begin{aligned} \frac{\partial C(q, x)}{\partial q} &> 0, \\ \frac{\partial C(q, x)}{\partial x} &> 0. \end{aligned} \tag{1}$$

That is, when the carbon emission the supply chain enterprise realizes is constant, the supply chain enterprise's production cost increases as the output q increases; and when the output is constant, the supply chain enterprise's production cost increases as the realized carbon emission level increases. In addition, the cost function also satisfies the following conditions:

$$\begin{aligned} \frac{\partial^2 C(q, x)}{\partial q^2} &> 0, \\ \frac{\partial^2 C(q, x)}{\partial q \partial x} &> 0, \\ \frac{\partial^3 C(q, x)}{\partial q \partial x^2} &\geq 0, \\ \frac{\partial^3 C(q, x)}{\partial q^2 \partial x} &\geq 0. \end{aligned} \tag{2}$$

Referring to some literature [8, 13, 16], we also assume that an increase in the supply chain enterprise's output and carbon emission level will increase the production cost. This assumption means that the supply chain enterprise's output is positively correlated with the production cost due to the law of diminishing marginal profit. Moreover, the enterprise with higher carbon emission level may have a higher production quantity and lower green production technology. An efficient production output and advanced green production technology can help the supply chain enterprise reduce production costs.

- (3.2) The degree of pollution $p(x)$ to the environment is increasing in the realized carbon emission level x ; that is,

$$\frac{dp(x)}{dx} > 0, \quad 0 < p(x) < p_0, \quad \forall x \in [a, b], \quad (3)$$

where p_0 is constant, implying the highest degree of environmental pollution. Clearly, this means that there is an upper bound on the degree of environmental pollution.

- (3.3) The transfer payment $t(x)$ of the government and the output $q(x)$ of the supply chain enterprise are almost everywhere continuously differentiable, and

$$0 \leq t(x) \leq T, \quad \forall x \in [a, b]. \quad (4)$$

- (3.4) The government's revenue function $G(q)$ is an increasing and concave function with the output q ; that is,

$$\begin{aligned} \frac{dG(q)}{dq} &> 0, \\ \frac{d^2G(q)}{dq^2} &\leq 0, \\ G(0) &= 0. \end{aligned} \quad (5)$$

- (3.5) For each contract $(q(x), t(x))$, we assume that

$$\frac{dG(q)}{dq} - \frac{\partial C(q, x)}{\partial q} \geq 0, \quad \forall x \in [a, b]. \quad (6)$$

The government's utility function can be represented by

$$\begin{aligned} V(q(x), t(x), x) &= \lambda(G(q(x)) - t(x) + \beta x) \\ &+ (1 - \lambda)(p_0 - p(x)), \end{aligned} \quad (7)$$

where $\lambda \in (0, 1)$ represents the government's preferences for environment. If λ is close to 0, the government is only concerned with the environment. If λ is close to 1, the government behaves as a pure expected utility-maximizing entity concerned only with the economy. On the right-hand side of equation (7), the first term represents the sum of the revenue and net carbon tax of the transfer payment. The second term also implies the change value of the initial state and the pollution state of the environment. The expected utility of the government can be obtained as follows:

$$\begin{aligned} E[V(q(\xi), t(\xi), \xi)] &= E[\lambda(G(q(\xi)) - t(\xi) + \beta\xi) \\ &+ (1 - \lambda)(p_0 - p(\xi))]. \end{aligned} \quad (8)$$

Since the government cannot exactly assess the carbon emission level of the supply chain enterprise, the carbon emission level cannot be observed. To motivate the supply chain enterprise to truthfully reveal their private information, the incentive-compatible constraint of the supply chain enterprise should be written as follows:

$$t(x) - \beta x - C(q(x), x) \geq t(y) - \beta y - C(q(y), x), \quad \forall x, y \in [a, b]. \quad (9)$$

In addition, the supply chain enterprise has two choices: one is to accept the contract that the government designed; alternatively, the supply chain enterprise can reject the contract. Only if the difference between the transfer payment and the carbon tax is larger than the production cost is it rational for the enterprise to participate in production; that is,

$$U(q(x), t(x), x) = t(x) - \beta x - C(q(x), x) \geq 0, \quad \forall x \in [a, b], \quad (10)$$

which represents the participation constraint of the uncertain contract model.

The uncertain contract model of pollution abatement problem can be written as follows:

$$\begin{aligned} &\max_{\{q(\cdot), t(\cdot)\}} E[V(q(\xi), t(\xi), \xi)] \\ \text{s.t.} \quad &t(x) - \beta x - C(q(x), x) \geq t(y) - \beta y - C(q(y), x), \quad \forall x, y \in [a, b], \\ &t(x) - \beta x - C(q(x), x) \geq 0, \quad \forall x \in [a, b]. \end{aligned} \quad (11)$$

4. Equivalent Model for the Uncertain Pollution Abatement Problem

In this section, the equivalent form of the uncertain pollution abatement model is considered to obtain the optimal solution of the model (11). We first consider the incentive compatibility constraint (9) and then derive the following proposition.

Proposition 1. For any $x \in [a, b]$, the incentive compatibility constraint (9) is equivalent to

$$\begin{cases} \frac{dt(x)}{dx} = \beta + \frac{\partial C(q, x)}{\partial q} \cdot \frac{dq(x)}{dx}, \\ \frac{dq(x)}{dx} < 0. \end{cases} \quad (12)$$

Proof. Let $R(x, y) = t(y) - \beta y - C(q(y), x)$, which represents the utility of the supply chain enterprise obtains with the carbon emission level x but choosing the mechanism $(q(\cdot), t(\cdot))$, where $x \neq y$. Therefore, the incentive compatibility constraint (9) is rewritten as

$$R(x, x) \geq R(x, y), \quad \forall x, y \in [a, b]. \quad (13)$$

For any $x \in [a, b]$, from the first-order condition

$$\left. \frac{\partial R(x, y)}{\partial y} \right|_{y=x} = 0, \quad (14)$$

we obtain that

$$\frac{dt(x)}{dx} = \beta + \frac{\partial C(q(x), x)}{\partial q} \cdot \frac{dq(x)}{dx}, \quad \forall x \in [a, b]. \quad (15)$$

Moreover, the second-order condition should also be satisfied; that is,

$$\left. \frac{\partial^2 R(x, y)}{\partial y^2} \right|_{y=x} < 0, \quad (16)$$

Furthermore, we derive

$$\frac{d^2 t(x)}{dx^2} - \frac{\partial^2 C(q(x), x)}{\partial q^2} \cdot \left(\frac{dq(x)}{dx} \right)^2 - \frac{\partial C(q(x), x)}{\partial q} \cdot \frac{d^2 q(x)}{dx^2} < 0. \quad (17)$$

By differentiating equation (15) with respect to x , we obtain that

$$\begin{aligned} \frac{d^2 t(x)}{dx^2} &= \frac{\partial^2 C(q(x), x)}{\partial q^2} \left(\frac{dq(x)}{dx} \right)^2 + \frac{\partial^2 C(q(x), x)}{\partial q \partial x} \frac{dq(x)}{dx} \\ &+ \frac{\partial C(q(x), x)}{\partial q} \frac{d^2 q(x)}{dx^2}. \end{aligned} \quad (18)$$

Substituting equation (18) into (17) yields that

$$\frac{\partial^2 C(q(x), x)}{\partial q \partial x} \frac{dq(x)}{dx} < 0, \quad \forall x \in [a, b]. \quad (19)$$

Since we have $(\partial^2 C(q, x)/\partial q \partial x) > 0$ by assumption (3.1), it follows that $(dq(x)/dx) < 0$. In addition, equation (15) can be rewritten as

$$\frac{dt(x)}{dx} = \beta + \frac{\partial C(q, x)}{\partial q} \cdot \frac{dq(x)}{dx}. \quad (20)$$

In addition, when $y > x$,

$$\begin{aligned} t(y) - \beta y - (t(x) - \beta x) &= \int_x^y \frac{\partial C(q(\tau), \tau)}{\partial q} \frac{dq(\tau)}{d\tau} d\tau \\ &\leq \int_x^y \frac{\partial C(q(\tau), x)}{\partial q} \frac{dq(\tau)}{d\tau} d\tau \\ &= C(q(y), x) - C(q(x), x), \end{aligned} \quad (21)$$

from $(\partial^2 C(q, x)/\partial q \partial x) > 0$ and $(dq(x)/dx) < 0$.

When $y < x$, inequality (21) also holds. Therefore, the inequality $t(x) - \beta x - C(q(x), x) \geq t(y) - \beta y - C(q(y), x)$ holds for any $x, y \in [a, b]$.

Proposition 1 implies that as the carbon emission level x increases, the regulated polluting supply chain enterprise lowers his output $q(x)$. This observation implies that the optimal output of the regulated polluting supply chain enterprise will decrease with the increase in the carbon emission level.

Next, we discuss the participation constraint (10) and derive the following proposition. \square

Proposition 2. The participation constraint (10) is equivalent to

$$U(q(b), t(b), b) = 0. \quad (22)$$

Proof. Differentiating equation (10) with respect to x yields

$$\frac{dU(q(x), t(x), x)}{dx} = \frac{dt(x)}{dx} - \beta - \frac{\partial C(q(x), x)}{\partial q} \cdot \frac{dq(x)}{dx} - \frac{\partial C(q(x), x)}{\partial x}. \quad (23)$$

From equation (15) and assumption (3.1), we obtain

$$\frac{dU(q(x), t(x), x)}{dx} = -\frac{\partial C(q(x), x)}{\partial x} < 0, \quad (24)$$

which shows that the supply chain enterprise's utility function is decreasing in the carbon emission level; that is, for any $x \in [a, b]$, there exists

$$U(q(x), t(x), x) > U(q(b), t(b), b) \geq 0. \quad (25)$$

Therefore, provided that $U(q(b), t(b), b) = 0$, the participation constraint can be satisfied.

Finally, we further investigate the objective function of the government and obtain the equivalent form as follows. \square

Proposition 3. *The objective function of the government can be rewritten as*

$$E[V(q(\xi), t(\xi), \xi)] = \int_a^b [\lambda(G(q(x)) - t(x) + \beta x) + (1 - \lambda)(p_0 - p(x))] \phi(x) dx. \quad (26)$$

Proof. Differentiating $V(q(\xi), t(\xi), \xi)$ with respect to x yields

$$\begin{aligned} \frac{dV(q(x), t(x), x)}{dx} &= \lambda \left[\frac{dG(q(x))}{dq} \cdot \frac{dq(x)}{dx} - \frac{dt(x)}{dx} + \beta \right] - (1 - \lambda) \frac{dp(x)}{dx} \\ &= \lambda \left[\frac{dG(q(x))}{dq} - \frac{C}{\partial q} \right] \cdot \frac{dq(x)}{dx} - (1 - \lambda) \frac{dp(x)}{dx}. \end{aligned} \quad (27)$$

By assumptions (3.2) and (3.5) and Proposition 1, we obtain

$$\begin{cases} \frac{dG(q(x))}{dq} - \frac{\partial C(q(x), x)}{\partial q} \geq 0, \\ \frac{dp(x)}{dx} > 0, \\ \frac{dq(x)}{dx} < 0, \end{cases} \quad (28)$$

that is, $(dV(q(x), t(x), x)/dx) < 0$. It implies that the government's utility function decreases with the carbon emission level x .

With reference to Liu and Ha [28], the government's expected utility function is presented as

$$\begin{aligned} E[V(q(\xi), t(\xi), \xi)] &= \int_a^b [\lambda(G(q(x)) - t(x) + \beta x) + (1 - \lambda)(p_0 - p(x))] \phi(x) dx. \end{aligned} \quad (29)$$

According to Propositions 1–3, it is clear to prove that model (11) is equivalent to

$$\begin{aligned} \max_{\{q(\cdot), t(\cdot)\}} & \int_a^b [\lambda(G(q(x)) - t(x) + \beta x) + (1 - \lambda)(p_0 - p(x))] \phi(x) dx \\ \frac{dt(x)}{dx} &= \beta + \frac{\partial C(q, x)}{\partial q} \cdot \frac{dq(x)}{dx}, \quad \forall x \in [a, b], \end{aligned} \quad (30)$$

$$\text{s.t. } \frac{dq(x)}{dx} < 0, \quad \forall x \in [a, b],$$

$$t(b) - \beta b - C(q(b), b) = 0.$$

5. Optimal Solution of the Equivalent Model

This section obtains the optimal solution of the equivalent contract model. The following theorem states the main result that there exists an optimal contract of the equivalent model of the uncertain pollution abatement problem.

Theorem 1. *If $(q^*(x), t^*(x))$ is the optimal contract of model (30), then we have*

$$\frac{dG(q^*(x))}{dq} - \frac{\partial C(q^*(x), x)}{\partial q} - \frac{\partial^2 C(q^*(x), x)}{\partial x \partial q} \cdot \frac{\Phi(x)}{\phi(x)} = 0, \quad \square \quad (31)$$

$$t^*(x) = \beta x + C(q^*(x), x) + \int_x^b \frac{\partial C(q^*(\tau), \tau)}{\partial \tau} d\tau. \quad (32)$$

Proof. From $U(q(b), t(b), b) = 0$ and equation (24), we derive that

$$U(q(x), t(x), x) = \int_x^b \frac{\partial C(q(\tau), \tau)}{\partial \tau} d\tau. \quad (33)$$

Furthermore, by equation (10), we have

$$t(x) - \beta x = C(q(x), x) + \int_x^b \frac{\partial C(q(\tau), \tau)}{\partial \tau} d\tau. \quad (34)$$

Let $S = \int_a^b (G(q(x)) - t(x) + \beta x)\phi(x)dx$, and then it follows from equation (34) that

$$S = \int_a^b \left(G(q(x)) - C(q(x), x) - \int_x^b \frac{\partial C(q(\tau), \tau)}{\partial \tau} d\tau \right) \phi(x) dx. \quad (35)$$

Define $Y = \int_a^b \int_x^b (\partial C(q(\tau), \tau) / \partial \tau) d\tau \phi(x) dx$, and then

$$S = \int_a^b (G(q(x)) - C(q(x), x))\phi(x) dx - Y. \quad (36)$$

Since

$$\begin{aligned} Y &= \int_a^b \left(\int_x^b \frac{\partial C(q(\tau), \tau)}{\partial \tau} d\tau \right) \phi(x) dx \\ &= \int_a^b \left(\int_x^b \frac{\partial C(q(\tau), \tau)}{\partial \tau} d\tau \right) d\Phi(x) \\ &= \int_a^b \Phi(x) \frac{\partial C(q(x), x)}{\partial x} dx - \Phi(a) \int_a^b \frac{\partial C(q(\tau), \tau)}{\partial \tau} d\tau \\ &= \int_a^b \Phi(x) \frac{\partial C(q(x), x)}{\partial x} dx, \end{aligned} \quad (37)$$

it is apparent that

$$\begin{aligned} S &= \int_a^b (G(q(x)) - C(q(x), x))\phi(x) dx - \int_a^b \Phi(x) \frac{\partial C(q(x), x)}{\partial x} dx \\ &= \int_a^b \left\{ (G(q(x)) - C(q(x), x))\phi(x) - \Phi(x) \frac{\partial C(q(x), x)}{\partial x} \right\} dx \quad \left[(G(q(x)) - C(q(x), x)) - \frac{\partial C(q(x), x)}{\partial x} \cdot \frac{\Phi(x)}{\phi(x)} \right] \phi(x) dx. \\ &= \int_a^b \end{aligned} \quad (38)$$

Therefore, the government's expected utility function can be rewritten as

$$\begin{aligned} E[V(q(\xi), t(\xi), \xi)] &= \int_a^b \lambda G(q(x))\phi(x) dx - \int_a^b \lambda C(q(x), x)\phi(x) dx \\ &\quad + \int_a^b (1 - \lambda)(p_0 - p(x))\phi(x) dx \\ &\quad - \int_a^b \lambda \Phi(x) \frac{\partial C(q(x), x)}{\partial x} dx. \end{aligned} \quad (39)$$

Let

$$F(q, x) = \lambda \left(G(q(x)) - C(q(x), x) - \frac{\partial C(q(x), x)}{\partial x} \cdot \frac{\Phi(x)}{\phi(x)} \right) + (1 - \lambda)(p_0 - p(x)). \quad (40)$$

By taking the first-order and second-order partial derivative of $F(q, x)$ with respect to x , we obtain

$$\begin{aligned}\frac{\partial F(q, x)}{\partial q} &= \lambda \left[\frac{dG(q(x))}{dq} - \frac{\partial C(q(x), x)}{\partial q} - \frac{\partial^2 C(q(x), x)}{\partial x \partial q} \cdot \frac{\Phi(x)}{\phi(x)} \right], \\ \frac{\partial^2 F(q, x)}{\partial q^2} &= \lambda \left[\frac{d^2 G(q(x))}{dq^2} - \frac{\partial^2 C(q(x), x)}{\partial q^2} - \frac{\partial^3 C(q(x), x)}{\partial x \partial q^2} \cdot \frac{\Phi(x)}{\phi(x)} \right].\end{aligned}\quad (41)$$

According to assumptions (3.1) and (3.4), it is apparent that $(\partial^2 F(q, x)/\partial q^2) \leq 0$; that is, the government's utility function $V(q, t, x)$ is concave in q . Therefore, the optimal output $q^*(x)$ satisfies $(\partial F(q, x)/\partial q)|_{q=q^*(x)} = 0$; that is,

$$\frac{dG(q^*(x))}{dq} - \frac{\partial C(q^*(x), x)}{\partial q} - \frac{\partial^2 C(q^*(x), x)}{\partial x \partial q} \cdot \frac{\Phi(x)}{\phi(x)} = 0. \quad (42)$$

Under such settings, the optimal transfer payment $t^*(x)$ can be written as

$$t^*(x) = \beta x + C(q^*(x), x) + \int_x^b \frac{\partial C(q^*(\tau), \tau)}{\partial \tau} d\tau. \quad (43)$$

In addition, the derivation of equation (42) with respect to x is

$$\begin{aligned}& \left(\frac{d^2 G(q^*(x))}{dq^2} - \frac{\partial^2 C(q^*(x), x)}{\partial q^2} - L(x) \frac{\partial^3 C(q^*(x), x)}{\partial x \partial q^2} \right) \frac{dq^*(x)}{dx} \\ &= \frac{\partial^2 C(q^*(x), x)}{\partial q \partial x} + \frac{\partial^2 C(q^*(x), x)}{\partial q \partial x} \cdot \frac{dL(x)}{dx} + L(x) \frac{\partial^3 C(q^*(x), x)}{\partial q \partial x^2},\end{aligned}\quad (44)$$

where $L(x) = (\Phi(x)/\phi(x))$. From assumptions (3.1) and (3.4), we have $(dq^*(x)/dx) < 0$. Hence, the feasible solution $(q^*(x), t^*(x))$ is the optimal solution of model (30).

By using Theorem 1, we can convert the uncertain pollution abatement problem (11) into an optimal control problem with boundary constraints by substituting equation (34) into the government's objective function. Theorem 1 designs the optimal contract $(q^*(x), t^*(x))$ for the uncertain pollution abatement problem. This implies that the supply chain enterprise has the optimal output and the government

pays the enterprise the optimal transfer payment. The incentive contract $(q^*(x), t^*(x))$ is also the optimal mechanism designed by the government.

Let $u(x) = dq(x)/dx$. By converting the proposed model into the following optimal control problem, we obtain the necessary conditions for the optimal solution by applying Pontryagin's maximum principle. \square

Remark 1. The uncertain pollution abatement problem (11) can be cast as the following optimal control problem:

$$\begin{aligned}& \int_a^b \lambda \left(G(q(x)) - C(q(x), x) - \frac{\partial C(q(x), x)}{\partial x} \cdot \frac{\Phi(x)}{\phi(x)} \right) \phi(x) dx \\ & \max_{u(\cdot)} + \int_a^b (1 - \lambda)(p_0 - p(x)) \phi(x) dx \\ & \frac{dq(x)}{dx} = u(x), \quad \forall x \in [a, b], \\ & \text{s.t. } u(x) < 0, \quad \forall x \in [a, b], \\ & t(b) - \beta b - C(q(b), b) = 0.\end{aligned}\quad (45)$$

In fact, construct the Hamiltonian $H(q(x), u(x), \gamma(x), x)$ as

$$H(q(x), u(x), \gamma(x), x) = \lambda \left(G(q(x)) - C(q(x), x) - \frac{\partial C(q(x), x)}{\partial x} \frac{\Phi(x)}{\phi(x)} \right) \phi(x) + (1 - \lambda)(p_0 - p(x))\phi(x) + \gamma(x)u(x), \tag{46}$$

where $q(x)$ is the state variable, $u(x)$ is the control variable, and $\gamma(x)$ is the adjoint variable. From Pontryagin's maximum principle, the necessary condition of the optimal solution to model (45) is that there exists an adjoint variable $\gamma^*(\cdot)$ such that $(q^*(\cdot), u^*(\cdot))$ satisfies the following:

- (1) $u^*(\cdot)$ maximizes the Hamiltonian function (46); that is,

$$H(q^*(x), u^*(x), \gamma^*(x), x) = \max_{u(x) \geq 0} H(q^*(x), u(x), \gamma^*(x), x). \tag{47}$$

- (2) $q^*(x)$ satisfies the state equation

$$\frac{dq(x)}{dx} = \frac{\partial H}{\partial \gamma}. \tag{48}$$

- (3) $\gamma^*(x)$ satisfies the adjoint equation

$$\frac{d\gamma(x)}{dx} = -\frac{\partial H}{\partial q}. \tag{49}$$

- (4) The terminal constraints are satisfied; that is,

$$\begin{cases} \gamma(a) = 0, \\ t(b) - \beta b - C(q(b), b) = 0. \end{cases} \tag{50}$$

From the above statement, it can be seen from equations (31) and (32) that the optimal contract $(q^*(x), t^*(x))$ can also be obtained by applying Pontryagin's maximum principle. Furthermore, we investigate the effects of carbon emission level on the supply chain enterprise's output and the government's transfer payment in the following proposition.

Proposition 4. *The optimal contract $(q^*(x), t^*(x))$ for model (30) has the following features:*

- (i) $q^*(x)$ is decreasing in x .
- (ii) *If there exist a tax rate β and a carbon emission level x such that $\beta + (\partial C(q^*(x), x)/\partial q^*(x)) (\partial q^*(x)/\partial x) \leq 0$, then $t^*(x)$ is decreasing in x ; if there also exist a tax rate β and a carbon emission level x such that $\beta + (\partial C(q^*(x), x)/\partial q^*(x)) (\partial q^*(x)/\partial x) > 0$, then $t^*(x)$ is increasing in x .*

Proof. Result (i) can be obtained immediately from the proof of Theorem 1.

For result (ii), due to $dq^*(x)/dx < 0$, $\partial C(q^*(x), x)/\partial q^*(x) > 0$ and

$$\frac{dt^*(x)}{dx} = \beta + \frac{\partial C(q^*(x), x)}{\partial q^*(x)} \cdot \frac{dq^*(x)}{dx}, \tag{51}$$

and it is clear that $dt^*(x)/dx < 0$ on the condition that $0 < \beta \leq -(\partial C(q^*(x), x)/\partial q^*(x)) (\partial q^*(x)/\partial x)$. Moreover, it is also obtained that $dt^*(x)/dx > 0$ on the condition that $-(\partial C(q^*(x), x)/\partial q^*(x)) (\partial q^*(x)/\partial x) < \beta < 1$.

Proposition 4 implies that as the realized carbon emission level increases, the supply chain enterprise lowers the output to reduce the pollution emissions. We assumed that the supply chain enterprise's production cost increases with the realized carbon emission level. In this assumption, it is believed that the increase in production cost may result in a reduction in the supply chain enterprise's output. Moreover, an increase in the carbon emission level will also affect the government's transfer payment to the supply chain enterprise. If the tax rate of the carbon emissions quota is below a certain threshold ($0 < \beta \leq -(\partial C(q^*(x), x)/\partial q^*(x)) (\partial q^*(x)/\partial x)$), the government's transfer payment will decrease with the carbon emission level to reduce the pollution emissions. However, if the tax rate of this quota is above this threshold ($-(\partial C(q^*(x), x)/\partial q^*(x)) (\partial q^*(x)/\partial x) < \beta < 1$), the government's transfer payment to the regulated polluting supply chain enterprise will increase with the carbon emission level. This finding leads us to an interesting conclusion that the impacts of the government's transfer payment on carbon emission level have opposite effects under different tax rates. Specifically, an increase in carbon emissions could increase the government's transfer payment given a high tax rate for the carbon emissions quota. When the carbon emission level increases, so do the supply chain enterprise's production cost and carbon tax. Moreover, the regulated polluting supply chain enterprise's utility decreases with the increase in production cost and carbon tax. Then, the government's transfer payment to the supply chain enterprise may increase. The reason is that the government should encourage the supply chain enterprise to participate in production. Furthermore, it also follows from the participation constraint that when the carbon emission level increases further, the incentive for the government to increase the transfer payment becomes stronger.

Additionally, the government collects a carbon tax from the supply chain enterprise. The carbon tax consists of the tax rate of the carbon emission quota and the carbon emission level. Therefore, as the tax rate or the carbon emission level increases, so will the carbon tax, and then the government's transfer payment will decrease. In reality, it is believed that the government often wants to use a carbon tax to control the carbon emission level and improve the utility. According to Proposition 4, a decrease in the carbon emission level will increase the supply chain enterprise's output. However, a decrease in the carbon emission level would decrease the government's transfer payment if the carbon tax is high. The following proposition answers the question of how carbon emissions affect the government and the supply chain enterprise's optimal utilities. \square

Proposition 5. *The optimal utilities $V(q^*(x), t^*(x), x)$ and $U(q^*(x), t^*(x), x)$ of the uncertain pollution abatement model satisfy the following:*

- (i) *The government's optimal utility $V(q^*(x), t^*(x), x)$ is decreasing in the carbon emission level x .*
- (ii) *The supply chain enterprise's optimal utility $U(q^*(x), t^*(x), x)$ is decreasing in the carbon emission level x , and his marginal utility is also increasing in the carbon emission level x .*

Proof. For result (i), by taking the partial derivative of equation (7) with x , we have

$$\frac{\partial V(q^*(x), t^*(x), x)}{\partial x} = \lambda \left(\frac{\partial G(q^*(x))}{\partial q^*(x)} \frac{\partial q^*(x)}{\partial x} - \frac{\partial t^*(x)}{\partial x} + \beta \right) - (1 - \lambda) \frac{\partial p(x)}{\partial x}. \quad (52)$$

According to Proposition 1, it is clear that

$$\begin{aligned} \frac{\partial V(q^*(x), t^*(x), x)}{\partial x} &= \lambda \left(\frac{\partial G(q^*(x))}{\partial q^*(x)} \frac{\partial q^*(x)}{\partial x} - \frac{\partial C(q^*(x), x)}{\partial q^*(x)} \cdot \frac{\partial q^*(x)}{\partial x} \right) - (1 - \lambda) \frac{\partial p(x)}{\partial x} \\ &= \lambda \left(\frac{\partial G(q^*(x))}{\partial q^*(x)} - \frac{\partial C(q^*(x), x)}{\partial q^*(x)} \right) \frac{\partial q^*(x)}{\partial x} - (1 - \lambda) \frac{\partial p(x)}{\partial x}. \end{aligned} \quad (53)$$

From assumptions (3.2) and (3.5), we have $(\partial p(x)/\partial x) > 0$ and $(\partial G(q^*(x))/\partial q^*(x)) - (\partial C(q^*(x), x)/\partial q^*(x)) > 0$.

Furthermore, it follows from Proposition 1 that

$$\frac{\partial V(q^*(x), t^*(x), x)}{\partial x} < 0. \quad (54)$$

For result (ii), by taking the partial derivative of equation (10) with respect to x , we also have

$$\frac{\partial U(q^*(x), t^*(x), x)}{\partial x} = \frac{\partial t^*(x)}{\partial x} - \beta - \frac{\partial C(q^*(x), x)}{\partial x} - \frac{\partial C(q^*(x), x)}{\partial q^*(x)} \frac{\partial q^*(x)}{\partial x}. \quad (55)$$

From Proposition 1, we obtain that

$$\frac{\partial U(q^*(x), t^*(x), x)}{\partial x} = -\frac{\partial C(q^*(x), x)}{\partial x} < 0. \quad (56)$$

Furthermore,

$$\frac{\partial^2 U(q^*(x), t^*(x), x)}{\partial^2 x} = -\frac{\partial^2 C(q^*(x), x)}{\partial x \partial q^*(x)} \frac{\partial q^*(x)}{\partial x}. \quad (57)$$

From assumption (3.1) and Proposition 1, it is apparent that

$$\begin{aligned} \frac{\partial^2 C(q^*(x), x)}{\partial x \partial q^*(x)} &> 0, \\ \frac{\partial q^*(x)}{\partial x} &< 0. \end{aligned} \quad (58)$$

Therefore, we have

$$\frac{\partial^2 U(q^*(x), t^*(x), x)}{\partial^2 x} > 0. \quad (59)$$

This proposition indicates that the government and the supply chain enterprise's optimal utilities will decrease as the carbon emission level increases. Previously, we determined that an increase in carbon emissions increased the government's transfer payment when the carbon tax was high. Although the transfer payment increases, the carbon tax βx also increases and then negatively affects the utility of the supply chain enterprise. Therefore, the above conclusion is reasonable. If the carbon tax βx is constant, the carbon emission level x decreases with the increase in tax rate β . Therefore, the tax rate could control the carbon emission

level. When holding the carbon emission level x constant, an increase in the tax rate will lead to deterioration of the supply chain enterprise's utility. To maintain the participation constraint, the supply chain enterprise would lower the production cost. Based on assumption (3.1), it is observed that the production cost $C(q(x), x)$ decreases as the output $q(x)$ decreases. Thus, an increase in the tax rate will reduce the regulated polluting supply chain enterprise's optimal output. \square

6. Numerical Example

In this section, we provide a numerical example to illustrate the effectiveness of the optimal contract and investigate the

effects of carbon emissions, carbon tax rate, and environmental preference on the optimal contract design. Without loss of generality, we assume that the supply chain enterprise's carbon emission level $\xi = \mathcal{L}(a, b)$ is a linear uncertain variable; that is, the supply chain enterprise's carbon emission level has the minimum value a and the maximum value b .

Assume that the government's revenue function is $G(q(x)) = \ln q(x)$, and the supply chain enterprise's production cost is $C(q, x) = x^2q$. The degree of pollution to the environment is $p(x) = e^x$, and $p_0 = e^b$. Therefore, the government's utility function can be written as

$$V(q(x), t(x), x) = \lambda(\ln q(x) - t(x) + \beta x) + (1 - \lambda)(e^b - e^x), \quad x \in [a, b]. \tag{60}$$

The supply chain enterprise's utility function can be written as

$$U(q(x), t(x), x) = t(x) - \beta x - x^2q(x), \quad x \in [a, b]. \tag{61}$$

The uncertain pollution abatement model is

$$\begin{aligned} & \max_{\{q(\cdot), t(\cdot)\}} E[\lambda(\ln q(x) - t(x) + \beta x) + (1 - \lambda)(e^b - e^x)] \\ \text{s.t.} \quad & t(x) - \beta x - x^2q(x) \geq t(y) - \beta y - x^2q(y), \quad \forall x, y \in [a, b], \\ & t(x) - \beta x - x^2q(x) \geq 0, \quad \forall x \in [a, b]. \end{aligned} \tag{62}$$

According to Propositions 1–3, it follows from equation (30) that model (62) can be described as

$$\begin{aligned} & \max_{\{q(\cdot), t(\cdot)\}} \int_a^b [\lambda(\ln q(x) - t(x) + \beta x) + (1 - \lambda)(e^b - e^x)] \phi(x) dx \\ & \frac{dt(x)}{dx} = \beta + x^2 \frac{dq(x)}{dx}, \quad \forall x \in [a, b], \\ \text{s.t.} \quad & \frac{dq(x)}{dx} < 0, \quad \forall x \in [a, b], \\ & t(b) - \beta b - b^2q(b) = 0. \end{aligned} \tag{63}$$

From equations (31) and (32) in Theorem 1, the optimal contract $(q^*(x), t^*(x))$ to model (63) satisfies

$$\begin{aligned} & \frac{1}{q^*(x)} - x^2 - 2x \frac{\Phi(x)}{\phi(x)} = 0, \\ & t^*(x) = \beta x + x^2q^*(x) + \int_x^b 2\tau q^*(\tau) d\tau. \end{aligned} \tag{64}$$

Since it is clear that

$$\Phi(x) = \begin{cases} 0, & \text{if } x < a, \\ \frac{x - a}{b - a}, & \text{if } a \leq x \leq b, \\ 1, & \text{if } x > b, \end{cases} \tag{65}$$

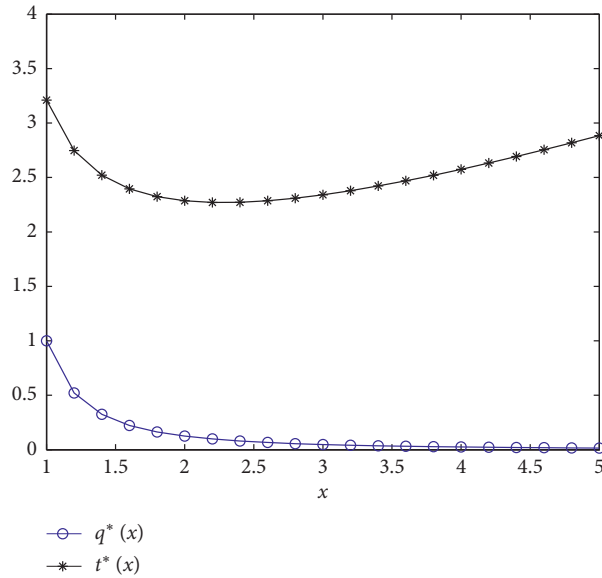


FIGURE 1: Optimal solutions of uncertain pollution abatement model.

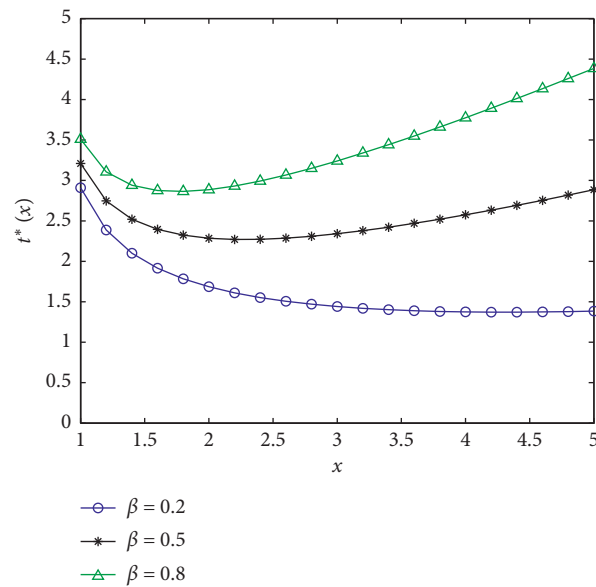


FIGURE 2: Effect of carbon tax rate on optimal transfer payment.

and $(\Phi(x)/\phi(x)) = x - a, \forall x \in [a, b]$, we obtain that

$$q^*(x) = \frac{1}{3x^2 - 2ax}, \tag{66}$$

$$t^*(x) = \beta x + \frac{x}{3x - 2a} + \frac{2}{3} \ln(3b - 2a) - \frac{2}{3} \ln(3x - 2a). \tag{67}$$

In particular, if $a = 1, b = 5$, and $\beta = 0.5$, the optimal contract $(q^*(x), t^*(x))$ obtained from equations (66) and (67) is shown in Figure 1. It can be observed from Figure 1 that the optimal design of the pollution abatement contract generally involves a negative supply chain enterprise's output, and it would be the optimal strategy for the

government to order a reduction in the supply chain enterprise's output when the supply chain enterprise's carbon emission level increases. Moreover, when the supply chain enterprise's carbon emission level is below a certain threshold, the government's transfer payment will decrease with the carbon emission level. When the supply chain enterprise's carbon emission level is above that threshold, the government's transfer payment will increase with the carbon emission level.

Furthermore, we examine the effect of the carbon tax rate on the government's optimal transfer payment. Without loss of generality, we assume that the carbon tax rate β can be chosen from the set $\{0.2, 0.5, 0.8\}$ and that the parameters $a = 1$ and $b = 5$ remain unchanged. From Figure 2, we

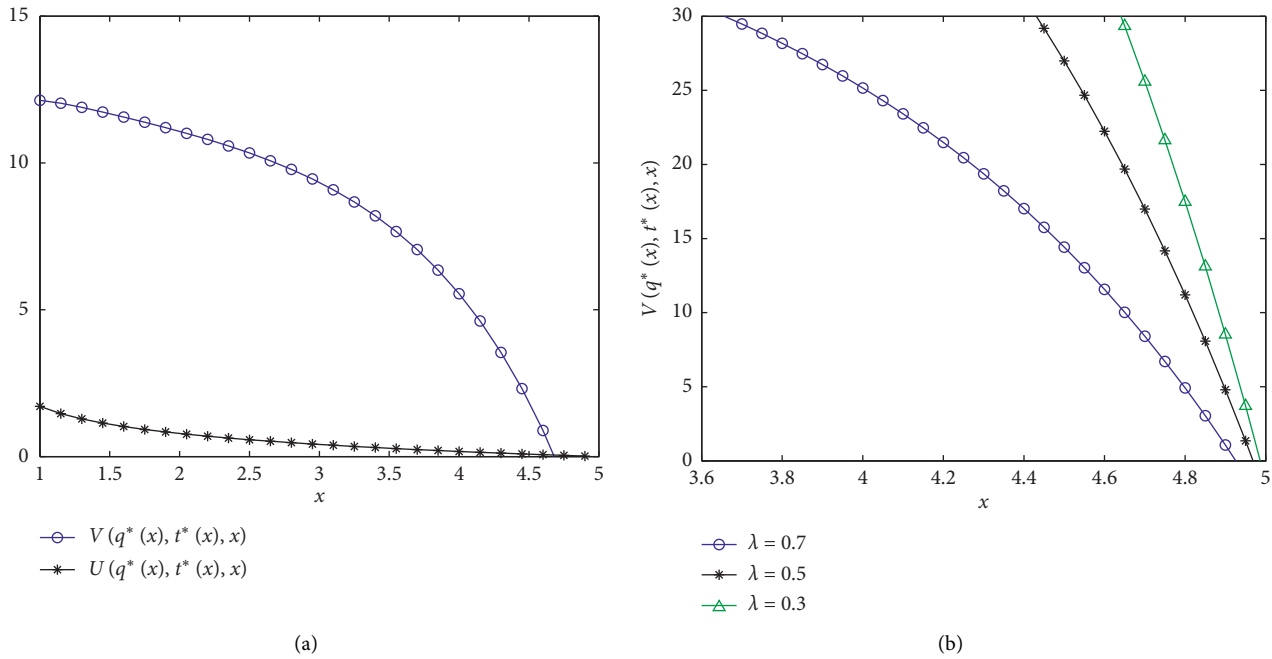


FIGURE 3: Optimal utility of uncertain pollution abatement model. (a) Effect of carbon emission on optimal utility. (b) Effect of environmental preference on government's utility.

observe that the government's transfer payment is decreasing in the carbon emission level if the carbon tax rate is low. When the carbon tax rate increases, the government's transfer payment shows a rising trend as the carbon emission level increases.

Finally, we illustrate the optimal utility of the uncertain pollution abatement model and examine the impacts of carbon emissions and environmental preference on the optimal utility. Suppose that the parameters $a = 1$, $b = 5$, and $\lambda = 0.9$ remain unchanged. Figure 3(a) shows that the optimal utility of the uncertain pollution abatement model decreases with the carbon emission level. However, an increase in the carbon emission level will lead to the government's diminishing marginal utility and the supply chain enterprise's incremental marginal utility. To test and verify the effect of the environmental preference on the government's utility, the environmental preference λ can be chosen from the set $\{0.7, 0.5, 0.3\}$. Accordingly, Figure 3(b) shows that the government's utility will increase as the environmental preference decreases, that is, as the government becomes more concerned with the environment.

7. Conclusion

This paper studies an uncertain contract model for the pollution abatement problem in which the government faces the supply chain enterprise with private carbon emission information. The optimal contract model, in which the government's assessment of the supply chain enterprise's carbon emission level is characterized as an uncertain variable, is presented with the purpose of maximizing the expected utility of the government. The crisp equivalent model for the uncertain contract model is

presented and the optimal solution of the equivalent model is obtained. The results show that the regulated polluting supply chain enterprise's optimal output will decrease if the supply chain enterprise's carbon emission level increases. Additionally, if the carbon tax is below a certain threshold, the government's optimal transfer payment decreases with the carbon emission level. However, we reach an interesting conclusion that the impacts of the government's transfer payment on carbon emission level have opposite effects under different carbon tax rates. The government's optimal transfer payment to the regulated polluting supply chain enterprise increases with the carbon emission level if the carbon tax is above a threshold. In addition, the government and the supply chain enterprise's optimal utilities will strictly decrease as the supply chain enterprise's carbon emission level increases.

In future work, we could incorporate competition into the contract design in the pollution abatement problem. For instance, the government may offer an incentive contract to motivate supply chain enterprises and induce competition among them. Furthermore, it would also be interesting to study the bounded rationality decision in the optimal incentive contracts for the pollution abatement problem.

Data Availability

The data of numerical example used to support the findings of this study are included within the article.

Conflicts of Interest

The authors declare that they have no conflicts of interest.

Acknowledgments

This work was supported by Humanity and Social Science Youth Foundation of Ministry of Education of China (no. 16YJC630159), the National Natural Science Foundation of China (no. 71702129), and China Postdoctoral Science Foundation (no. 2017M6101 60).

References

- [1] S. Pacala and R. Socolow, "Stabilization wedges: solving the climate problem for the next 50 years with current technologies," *Science*, vol. 305, no. 5686, pp. 968–972, 2004.
- [2] R. Martin, L. B. de Preux, and U. J. Wagner, "The impact of a carbon tax on manufacturing: evidence from microdata," *Journal of Public Economics*, vol. 117, no. 1, pp. 1–14, 2014.
- [3] J.-C. Wagner and K.-B. Chang, "An optimal tax/subsidy for output and pollution control under asymmetric information in oligopoly markets," *Journal of Regulatory Economics*, vol. 5, no. 2, pp. 183–197, 1993.
- [4] J. Duggan and J. Roberts, "Implementing the efficient allocation of pollution," *American Economic Review*, vol. 92, no. 4, pp. 1070–1078, 2002.
- [5] J.-P. Montero, "A simple auction mechanism for the optimal allocation of the commons," *American Economic Review*, vol. 98, no. 1, pp. 496–518, 2008.
- [6] X. Liu, C. Wang, D. Niu, S. Suk, and C. Bao, "An analysis of company choice preference to carbon tax policy in China," *Journal of Cleaner Production*, vol. 103, no. 1, pp. 393–400, 2015.
- [7] M. Wang, M. Wang, C. Dang, and S. Wang, "A pareto optimal auction mechanism for carbon emission rights," *Mathematical Problems in Engineering*, vol. 2014, Article ID 438104, 7 pages, 2014.
- [8] Y. Li, Q. Deng, C. Zhou, and L. Feng, "Environmental governance strategies in a two-echelon supply chain with tax and subsidy interactions," *Annals of Operations Research*, vol. 290, no. 1–2, pp. 439–462, 2020.
- [9] J.-J. Laffont and J. Tirole, "Pollution permits and compliance strategies," *Journal of Public Economics*, vol. 62, no. 1–2, pp. 85–125, 1996.
- [10] S. Lothe and I. Myrvtveit, "Compensation systems for green strategy implementation: parametric and non-parametric approaches," *Business Strategy and the Environment*, vol. 12, no. 3, pp. 191–203, 2003.
- [11] B. Fahimnia, J. Sarkis, A. Choudhary, and A. Eshragh, "Tactical supply chain planning under a carbon tax policy scheme: a case study," *International Journal of Production Economics*, vol. 164, no. 1, pp. 206–215, 2015.
- [12] D. Klenert and L. Mattauch, "How to make a carbon tax reform progressive: the role of subsistence consumption," *Economics Letters*, vol. 138, no. 1, pp. 100–103, 2016.
- [13] X. Zhao, Y. Li, F. Xu, and K. Dong, "Sustainable collaborative marketing governance mechanism for remanufactured products with extended producer responsibility," *Journal of Cleaner Production*, vol. 166, no. 1, pp. 1020–1030, 2017.
- [14] C. Helm and F. Wirl, "The principal-agent model with multilateral externalities: an application to climate agreements," *Journal of Environmental Economics and Management*, vol. 67, no. 1, pp. 141–154, 2014.
- [15] C. Arguedas and S. Rousseau, "Emission standards and monitoring strategies in a hierarchical setting," *Environmental and Resource Economics*, vol. 60, no. 3, pp. 395–412, 2015.
- [16] R. K. Shrestha, "Menus of price-quantity contracts for inducing the truth in environmental regulation," *Journal of Environmental Economics and Management*, vol. 83, no. 1, pp. 1–7, 2017.
- [17] A. Lika, F. Galioto, and D. Viaggi, "Water authorities' pricing strategies to recover supply costs in the absence of water metering for irrigated agriculture," *Sustainability*, vol. 9, no. 12, pp. 1–16, 2017.
- [18] R. Dubey, A. Gunasekaran, P. Helo, T. Papadopoulos, S. J. Childe, and B. S. Sahay, "Explaining the impact of reconfigurable manufacturing systems on environmental performance: the role of top management and organizational culture," *Journal of Cleaner Production*, vol. 141, no. 1, pp. 56–66, 2017.
- [19] Q. Song and K. Shi, "A fuzzy waiting time contract for patient's public health care," *Journal of Intelligent & Fuzzy Systems*, vol. 27, no. 2, pp. 1001–1009, 2014.
- [20] H. Zhang and J. Jiang, "Informed principal model and contract in supply chain with demand disruption asymmetric information," *Mathematical Problems in Engineering*, vol. 2016, Article ID 2306583, 12 pages, 2016.
- [21] B. Liu, *Uncertainty Theory*, Springer, Berlin, Germany, 2nd edition, 2007.
- [22] Z. Chen, Y. Lan, and R. Zhao, "Impacts of risk attitude and outside option on compensation contracts under different information structures," *Fuzzy Optimization and Decision Making*, vol. 17, no. 1, pp. 13–47, 2018.
- [23] R. Mu, Y. Lan, and W. Tang, "An uncertain contract model for rural migrant worker's employment problems," *Fuzzy Optimization and Decision Making*, vol. 12, no. 1, pp. 29–39, 2013.
- [24] C. Zhou, J. Peng, Z. Liu, and B. Dong, "Optimal incentive contracts under loss aversion and inequity aversion," *Fuzzy Optimization and Decision Making*, vol. 18, no. 1, pp. 85–102, 2019.
- [25] C. Zhou, G. Xu, and Z. Liu, "Incentive contract design for internet referral services: cost per click vs cost per sale," *Kybernetes*, vol. 49, no. 2, pp. 601–626, 2020.
- [26] C. Zhou, N. Ma, X. Cui, and Z. Liu, "The impact of online referral on brand market strategies with consumer search and spillover effect," *Soft Computing*, vol. 24, no. 4, pp. 2551–2565, 2020.
- [27] Z. Liu, C. Zhou, H. Chen, and R. Zhao, "Impact of cost uncertainty on supply chain competition under different confidence levels," *International Transactions in Operational Research*, vol. 28, no. 3, pp. 1465–1504, 2021.
- [28] Y. Liu and M. Ha, "Expected value of function of uncertain variables," *Journal of Uncertain Systems*, vol. 4, no. 3, pp. 181–186, 2010.

Research Article

The Level of Regional Economic Development, Green Image, and Enterprise Environmental Protection Investment: Empirical Evidence from China

Quanxin Gan ^{1,2}, Liu Yang ³, Jin Liu ⁴, Xiaofan Cheng ⁵, Han Qin ⁵, Jiafu Su ⁶,
and Weiyi Xia ⁷

¹Admissions and Employment Office, Guangxi University of Finance and Economics, Nanning 530003, China

²International College, National Institute of Development Administration, Bangkok 10240, Thailand

³School of International Education, Guangxi University of Finance and Economics, Nanning 530003, China

⁴Guangxi University of Finance and Economics, Nanning 530003, China

⁵MPAcc Center, Guangxi University of Finance and Economics, Nanning 530003, China

⁶National Research Base of Intelligent Manufacturing Service, Chongqing Technology and Business University, Chongqing, China

⁷Fangchenggang College, Guangxi University of Finance and Economics, Nanning 530003, China

Correspondence should be addressed to Liu Yang; liuyang_vinda@hotmail.com and Jiafu Su; jiafu.su@hotmail.com

Received 25 February 2021; Revised 23 March 2021; Accepted 31 March 2021; Published 9 April 2021

Academic Editor: Ming Bao Cheng

Copyright © 2021 Quanxin Gan et al. This is an open access article distributed under the Creative Commons Attribution License, which permits unrestricted use, distribution, and reproduction in any medium, provided the original work is properly cited.

Does green image impact enterprise environmental protection investment? How does the green image affect enterprise environmental protection investment? In order to solve the above problems, this paper uses an empirical analysis to explore the relationship among regional economic development level, green image, and enterprise environmental protection investment based on the empirical data of A-share manufacturing listed companies from 2007 to 2015 in China. The research results show that good green image has a positive role to promote enterprise environmental protection investment, and regional economic development level partially mediates green image and enterprise environmental protection investment. The article confirms that a good green image can send positive signals to stakeholders and increase their loyalty and satisfaction with the enterprise's products or services. The level of regional economic development provides opportunities for the green development of enterprises. With the improvement in the level of regional economic development, stakeholders' awareness of environmental protection has increased, and they have become more sensitive to enterprise environmental protection investment behaviors. The research results also show that the environmental awareness of corporate stakeholders plays an important role in actively fulfilling, and it provides new ideas for companies to conduct production and management in a green-oriented model.

1. Introduction

According to the data of "China's green GDP (green GDP = total GDP - (environmental resources cost + environmental resources protection service fee); the Chinese government has issued the first green GDP accounting research report since 2006) performance evaluation report" in 2018, China's green GDP is growing continuously, and its growth rate has begun to exceed the GDP growth rate of the same period. In 2016, the average

growth rate of China's green GDP economic aggregate reached 7.58%, exceeding the GDP growth rate of the same period by 0.08%. In addition, the average growth rate of per capita green GDP of China's 31 provinces/regions has reached 6.79%. With the advent of the era of green economy, the government, public, and society pay more attention to environmental issues. The environmental awareness of enterprise stakeholders, including consumers, investors, suppliers, and employees, is increasing. Stakeholders exert pressure on enterprises to carry out green production and

management and reduce the impact of enterprises on the environment, which urges enterprises to start integration resources for environmental protection investment to meet the requirements of legitimacy and green demands of stakeholders. Therefore, if an enterprise wants to survive and develop, it needs not only to be successful in finance but also to have an outstanding performance in sustainable development. Only in this way can it obtain competitive advantage and survive and develop. In addition, with the implementation of China's environmental protection strategy, the Chinese government continues to increase its investment in environmental protection. According to the National Bureau of Statistics, from 2001 to 2017, China's investment in environmental pollution control increased by 14% annually, reaching 952.9 billion yuan. However, the average proportion of China's environmental pollution control investment in GDP from 2015 to 2018 is about 1.33%, which is still lower than the international level. It is urgent for enterprises to participate in environmental protection investment. As the emitters of pollutants and consumers of resources, they should take the initiative to undertake the responsibility of environmental protection investment and reduce the degree of environmental pollution. As an investment, enterprise environmental protection investment can successfully eliminate or reduce the negative impact of corporate production and management on the environment [1]. However, because the managers think that the cost and income of environmental protection investment do not match, the enterprises lack the initiative of environmental protection investment.

Most studies believe that enterprises need to carry out environmental protection investment behaviors under strict environmental regulations [2, 3]. For example, Tang et al. [3] take the heavy pollution industry as an example, and the research shows that the scale of enterprise environmental protection investment is seriously insufficient at present. Most enterprises' environmental protection investment is a passive behavior under government regulation, and the relationship between them is U-shaped. Li et al. [4] and Gao and Zhang [5] hold the same view. According to Leiter et al. [6], the relationship between the intensity of environmental regulation and the scale of enterprise environmental protection investment is an inverted U-shaped relationship; when the environmental benefits are greater than the environmental costs, they are positively correlated; if the environmental benefits are less than the environmental costs, they are negatively correlated. From the above research results, we can see that there is a threshold value for the impact of environmental regulation on enterprise environmental protection investment, and environmental regulation is not omnipotent. Therefore, the existing literature also studies the impact of external factors such as consumer behaviors [7–9] and the public [10–12] on enterprise environmental protection investment. Part of the research focuses on the impact of equity concentration [13, 14], environmental management system [15, 16], private benefits of managers [17], and other internal factors [18] on enterprise environmental protection investment. However, there is a lack of research on the mediating effect of

combining the internal and external factors of the organization with the environmental protection investment of enterprises. Through the study of intermediary effect, we can strengthen the correlation between the internal and external factors of the organization and the environmental protection investment of enterprises and help to clarify the focus of promoting enterprises' active environmental protection investment behavior.

This paper will first study the impact of green image on environmental protection investment from the internal perspective. Green image is closely related to the perception of enterprise stakeholders. It can not only transmit the information of enterprise environmental management and decision-making to the public but also provide convenience for the public to evaluate the performance of enterprise environmental responsibility. While striving to create a green image, enterprises also provide the public with information on pollution prevention and control of enterprises, thus affecting the public's cognition of environmental behavior of enterprises [19]. Can green image promote enterprises' positive environmental protection investment behavior to meet the public's environmental protection needs? However, the impact of corporate green image on enterprise environmental protection investment is not necessarily direct. If the stakeholders cannot capture the information of enterprise environmental responsibility performance and put it into action to recognize enterprise environmental protection behaviors, then the enterprise will lack the motivation to carry out environmental protection investment. Therefore, this paper further studies the mediating effect of regional economic development level as a macroeconomic factor between green image and enterprise environmental protection investment from an external perspective.

The contributions of this paper are as follows: firstly, based on the resource-based view, green image is regarded as a scarce and valuable and difficult-to-copy important resource. This paper studies the impact mechanism of corporate voluntary environmental management performance on enterprise environmental protection investment and enriches the research results of resource-based view applied to green investment. Secondly, this paper combines the internal and external factors, emphasizes that the green image plays an indirect role in the enterprise environmental protection investment through the level of regional economic development, which helps to enrich and deepen the research on the motivation of enterprise environmental protection investment, provides new ideas for promoting enterprises to fulfill the accountability of environmental protection, and also provides a better basis for the government to formulate relevant environmental protection policies. Thirdly, in order to promote enterprises to actively invest in environmental protection, the government should improve environmental laws and regulations, and the government ought to enact various policies conducive to enhancing environmental innovation capacity and optimizing industry structure. Finally, the government should further issue specific guidance documents based

on the level of economic development in different regions so as to better improve the company's environmental awareness and take the initiative to carry out environmental governance-related activities.

2. Theoretical Background and Hypotheses

2.1. The Influence of Green Image on the Scale of Enterprise Environmental Protection Investment. When this era based on green economy comes, companies must explore development directions, such as strengthening corporate green brand building, so as to achieve a green image. The green image of an enterprise is an intangible asset of an enterprise. Most scholars believe that the green image of an enterprise is related to the perception of corporate stakeholders [20]. For example, Chen [21] and Chang and Fong [22] believe that green image is a series of consumer perceptions of corporate environmental commitments and environmental issues. Therefore, the corporate green image is also called "corporate green reputation" [23]. From the scholars' definition of the enterprise's green image, the green image is closely related to stakeholders, and stakeholders attention to corporate environmental behavior can effectively promote the enterprise to carry out ISO14001 certification [24], establishing a good green image can be a signal for enterprises to convey environmental commitments to stakeholders [25]. From the perspective of signal transmission, an enterprise can predict the attitude and demand of stakeholders towards its products or services by comparing the changes in product sales before and after the establishment of a green image. In addition, the green image can promote the matching of environmental protection demands of corporate stakeholders with corporate environmental behaviors, increase consumer loyalty and satisfaction with the brand, and increase the likelihood of consumers buying products [26]. In short, enterprises can reduce the cost of communication with consumers, suppliers, and other stakeholders through the green image, thereby gaining greater market development opportunities and stimulating companies to further invest in environmental protection to achieve the goals of legitimacy and maintaining a green image.

The scholars of the resource-based view (BRT) and the advocates of the natural resource-based view (NRBV) all believe that the green image is of strategic significance to the enterprise, and a good green image is an effective way to implement the enterprise's differentiation strategy. The green image forms the uniqueness of the enterprise's products or services from other enterprises and increases the brand recognition, degree of specialization, and the reputation of leading product quality and technology. The differentiation strategy enables companies to gain consumer loyalty to the brand and reduces consumers' sensitivity to product prices, which makes enterprises not need to have low-cost competitive advantages to make profits. An enterprise's green image can only be formed in a relatively long period of time, so it is difficult to imitate [27], which helps companies gain competitive and sustainable development advantages. For example, Chen [21] and Robinson et al. [28] believe that a green image can create new markets for

companies to gain a competitive advantage and protect the natural environment. Porter and Van der Linde [29] believe that a good green image of an enterprise is conducive to gaining the "first-mover advantage," which not only increases the correlation between the green image of an enterprise and its business performance and environmental performance [30] but also increases the correlation between the green image and its core green competitiveness [31]. López-Gamero et al. [32] found that the differentiated competitive advantage of the hotel industry more significantly comes from the marketing of green image shaping; green image increases the competitiveness of the enterprise in the international market and has a positive impact on the financial performance of the enterprise, and thus, environmental protection investment cost of the enterprise can be transformed through operating performance, to further promote enterprise environmental protection investment. Fortune et al. [33] use data from 100 South African listed companies (JSE) from 2010 to 2014 to empirically test the impact of green image on enterprise environmental protection investment. Research shows that green image can stimulate enterprise environmental protection investment, and green image is the driving force for enterprise environmental protection investment. Both BRT theory and NRBV theory believe that enterprises generate competitive advantages through resource bundles [34]. As intangible assets, green image forms a complementary relationship with tangible assets of enterprises, which helps enterprises to implement pollution prevention and control behaviors and achieve the goal of reducing environmental pollution and improving economic performance.

A corporate green image can be used as a means to achieve corporate legitimacy, reputation, and profitability. Establishing a good green image can increase product sales or product prices, improve the enterprise's ability to obtain new resources needed for development, and improve the overall enterprise value, thereby stimulating enterprise environmental protection investment. Based on the above analysis, this article proposes Hypothesis 1.

Hypothesis 1. Green image is positively correlated with the scale of environmental protection investment.

2.2. The Influence of Corporate Green Image on Regional Economic Development Level. The green image of an enterprise can convey environmental commitments and environmental concerns to stakeholders, including consumers, shareholders, competitors, and government departments. The establishment of a green image by an enterprise can release a green signal to the government. The government uses microlevel green signals to judge the implementation of market-based regulatory tools in environmental regulations, such as emission trading [35], environmental tax [36, 37], subsidy policy [38], green credit, and other environmental and economic policy measures to determine the degree of influence and operational efficiency of enterprises' environmental protection behaviors. The government knows the environmental intentions of enterprises through their

commitment to green image construction and gives the government insights into the differences in environmental behavior of companies in different regions, which plays an important role in improving environmental regulations. Environmental regulation is an important tool to effectively promote the coordinated development of regional economy and environment [39]; environmental regulations are an important tool to effectively promote the coordinated development of regional economy and environment. Improving environmental regulations can promote environmental performance in different regions while promoting economic transformation and economic growth. In addition, a good green image is a prerequisite for an enterprise and its products to enter the international market. For example, the green environmental logo representing the enterprise's green image not only indicates that the product quality meets the standards but also that the product's entire life cycle meets the requirements of environmental protection. Another example is the ISO14001 environmental management system certification, which represents the enterprise's green image [21]. The certification is formulated in accordance with international standards. After the certification, it can obtain international recognition, obtain a "green pass" for international trade [40], and integrate into the international market will promote regional economic development. Based on the above analysis, this article proposes Hypothesis 2.

Hypothesis 2. The green image is positively correlated with the level of local economic development.

2.3. The Influence of Regional Economic Development Level on Enterprise Environmental Protection Investment. Market stimulus is particularly important for enterprise environmental protection investment [41]. The level of regional economic development reflects the driving force of the market to a certain extent, among which the level of regional economic development can effectively reflect the level of environmental protection awareness of enterprise stakeholders, and environmental protection awareness is one of the influencing factors for the market to play a pulling role. The green image releases the signal of environmental protection commitment to stakeholders, and the continuous growth of the enterprise needs to be promoted under the awareness of green environmental protection of the stakeholders. Fortune [33] found that only when stakeholders have environmental awareness, can they respond more fully to the enterprise's green demands. When the environmental awareness of stakeholders increases, the demand for corporate products or services can be increased through the green image [42]. With the enhancement of environmental protection awareness, consumers are more willing to buy products with low environmental pollution, and manufacturers are more willing to purchase environmental-friendly raw materials or green products from suppliers at high prices. The environmental protection awareness of stakeholders motivates enterprises to change from traditional models to sustainable development models to create a brand

value [43]. Tang and Li [44], using the K-W test and median test, it is found that, under different economic development levels, the scale of enterprise environmental protection investment is significantly different. Wei et al. [45] show that the level of local economic development is positively related to corporate environmental management, and corporate environmental commitments have a positive regulatory effect on environmental management. Therefore, the higher the level of local economic development, the stronger the environmental awareness of stakeholders, and the more sensitive they are to green images, thereby increasing consumers' loyalty and satisfaction in purchasing environmental-friendly products, increasing the possibility of green supply chains, and promoting the intention of pollution prevention and increase enterprise environmental protection investment. At the same time, in areas with a high level of regional economic development, the stronger the consumption ability of consumers, the more likely to accept the price of environmental protection products higher than the general product price and promote companies to realize environmental investment returns. Based on the above analysis, the green image exerts a positive influence on the scale of enterprise environmental protection investment through the regional economic development level. Therefore, Hypothesis 3 and Hypothesis 4 are proposed. We propose the following theoretical model shown in Figure 1.

Hypothesis 3. The level of local economic development is positively correlated with the scale of enterprise environmental protection investment.

Hypothesis 4. The level of local economic development plays an intermediary role between the green image and the scale of enterprise environmental protection investment.

3. Methodology and Data

3.1. Research Samples and Data Sources. This paper selects A-share manufacturing listed companies in Shanghai and Shenzhen stock markets that made environmental protection investments from 2007 to 2015 as the research sample (because 2007–2015 went through 11th and 12th Five-Year Plan for National Environmental Protection of China, forming a complete cycle). The listed companies that disclose enterprise environmental protection investment data are screened as follows: (1) exclude sample companies with ST and *ST; (2) exclude samples with missing variable indicators. After screening, this article finally obtained 2544 enterprise environmental investment data. The sources of data in this article are as follows: (1) the data on enterprise environmental protection investment mainly come from balance sheets and social responsibility reports and are collected manually; (2) ISO14001 data come from China National Accreditation Service for Conformity Assessment (<http://www.cnas.org.cn>) collected manually; (3) the level of regional economic development comes from the "China Statistical Yearbook"; and (4) other research variables come from the Wind database. In order to overcome the influence of

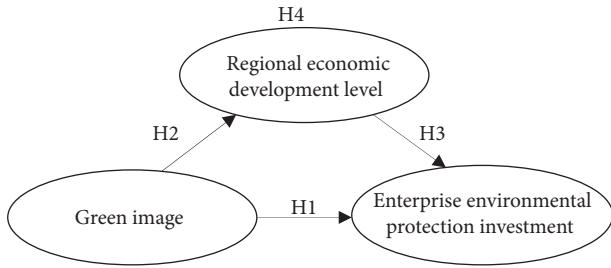


FIGURE 1: Theoretical model.

outliers on the research conclusions, Winsorize processing is performed on continuous variables at 1% and

99% quantiles, and all data processing software is Stata 13.0.

3.2. *Model Setting and Variable Selection.* In order to test the relationship between the green image and the enterprise’s environmental protection investment scale, as well as the intermediary effect of the regional economic development level on the relationship between the green image and the enterprise’s environmental protection investment scale, the sequential test method is adopted to test, and the model is constructed in (1)–(3) [46]. Also, consider the time interval of one period lagging behind the dependent and independent variables in the model, which can better avoid the endogenous problem in the model:

$$EI_{i,t} = \beta_0 + \beta_1 GIM_{i,t-1} + \sum Control_{var} + \sum YEAR + \varepsilon, \tag{1}$$

$$EDL_{i,t-1} = \beta_0 + \beta_1 GIM_{i,t-1} + \sum Control_{var} + \sum YEAR + \varepsilon, \tag{2}$$

$$EI_{i,t} = \beta_0 + \beta_1 GIM_{i,t-1} + \beta_2 EDL_{i,t-1} + \sum Control_{var} + \sum YEAR + \varepsilon. \tag{3}$$

Among them, the scale of enterprise environmental protection investment (EI) ((1) other related expenditures incurred by enterprises for environmental protection are not included, such as environmental monitoring fees, environmental design fees, environmental assessment, and energy assessment fees, plant greening fees, and environmental management fees; (2) indirect expenditure items are not included, such as donating green fund fees; (3) expenditure items that have been expensed are not included, such as pollution discharge and preparation of social responsibility reports (environmental reports), environmental taxes, and pollution discharge fees) is based on the content and structure of enterprise environmental protection investment [3], which divides environmental protection investment into environmental protection products and environmental technology research and development and transformation investment, specifically: environmental protection facilities and systems investment and transformation investment; cleaner production investment; pollution control technology research and development and transformation investment; pollution control equipment and system investment and transformation investment. At present, most scholars’ explanations of EI tend to prevent pollution, and for protecting the environment, enterprises carry out special economic activities while taking into account environmental and social benefits. This article uses “total investment/capital stock” to measure the scale of enterprise environmental protection investment [3].

The green image (GIM) is measured by the ISO14001 environmental management system certification. ISO14001 environmental management system has the characteristics of legality, prevention, sustainability, systematicness, voluntariness, certifiability, and applicability. The certification is formulated in accordance with international standards

and has been internationally recognized, which can better measure the enterprise’s green image [21]. If the enterprise has passed the ISO14001 system certification, it is 1; otherwise, it is 0.

The regional economic development level (EDL) is measured by the regional GDP per capita. Scholars mainly use the absolute value of regional GDP, the growth rate of regional GDP, and regional per capita GDP [47] to measure the level of regional economic development when studying regional economic development issues. In comparison, regional GDP per capita reflects not only the economic development of the region but also the living and consumption level of local residents, so this article uses this indicator as a substitute variable for the level of regional economic development [48]; therefore, this article uses this indicator as a substitute variable for the level of regional economic development.

Following the conventional practice of the existing literature [49–53], this study considered the internal characteristics of the enterprise and external environmental indicators. The corporate profitability (EPS), corporate debt level (LEV), operating cash flow (FLOW), cash holdings (CASH), opportunity cost (OPP), enterprise size (SIZE), equity checks and balances (BALANCE), agency cost (COST), and annual dummy variables (YEAR) were used as control variables. The variable description is shown in Table 1.

Secondly, test model (2) and model (3) in turn. If β_1 in the model (2) is positive and significant and β_2 in the model (3) is positive and significant, it means that the quality of internal control is a significant way to achieve financial performance through corporate environmental investment.

Finally, make further judgments based on the test results of model (3). If β_1 is not significant and β_2 is significant in model

TABLE 1: Research variable description.

Type	Name	Code	Connotation
Explained variable	Scale of enterprise environmental protection investment	EI	New investment in environmental protection in that year/average total assets
Explanatory variable	Green image	GIM	1 if ISO14001 certification, 0 otherwise
	Regional economic development level	EDL	GDP per capita
	Corporate profitability	EPS	Earnings per share
	Corporate debt level	LEV	Asset-liability ratio
	Operating cash flow	FLOW	Ratio of net operating cash flow to average total assets
	Cash holding	CASH	Ratio of year-end monetary funds to average total assets
	Opportunity cost	OPP	Tobin' Q
	Control variable	Enterprise size	SIZE
Equity checks and balances		BALANCE	Shareholding ratio of the second largest shareholder to the fifth largest shareholder
Agency cost		COST	Management expense ratio = management expense/operating income
Annual dummy variable		YEAR	Take 8 dummy variables in 9 years

TABLE 2: Research variable descriptive statistics.

Variables	N	Mean	Std.	Minimum	Maximum
EI	2544	0.01719	0.03419	0.00001	0.20989
GIM	2544	0.52516	0.49946	0	1
EDL	2544	4.38200	2.12003	1.06	9.91
EPS	2544	0.33860	0.49229	-1	2.27
LEV	2544	48.58414	19.64632	7.34	94.13
FLOW	2544	4.85934	7.64966	-18	30
CASH	2544	18.62820	14.56274	1	76
OPP	2544	1.74578	1.37041	0	7.77
SIZE	2544	22.03175	1.18909	19.51	25.86
BALANCE	2544	98.98053	80.70027	1.462915	307.8098
COST	2544	7.49871	4.62989	0.81	27.59

(3), it means that the impact of internal control quality on financial performance is completely achieved through the enterprise's environmental protection investment transmission; if β_1 is significant and β_2 is significant, it indicates that the impact of internal control quality on financial performance is partially passed implementation of corporate environmental protection investment transmission.

4. Empirical Results and Analysis

4.1. Descriptive Statistics. Table 2 lists the descriptive statistical results of the research variables. The maximum value of enterprise environmental protection investment t scale is 0.20989, and the minimum value is 0.00001. There is a large gap between the two, and the scale of enterprise environmental protection investment is relatively small; the average value of green image is 0.52516, which reflects to a certain extent that most sample companies are willing to establish a good corporate green image; the mean of the regional economic development level is higher than the minimum value, and the standard deviation is 2.12003, indicating that there are large differences in the economic development level of the regions where listed companies belong to my country. In terms of other variables, the gap between the maximum

and minimum values of asset-liability ratio, operating cash flow, cash holdings, degree of equity balance, and agency costs is large, and the standard deviation is also large.

4.2. Correlation Analysis. It can be seen from Table 3 that GIM and EI are correlated at the 1% significance level, indicating that green image has a good explanatory power for the scale of enterprise environmental protection investment; EDL is correlated with GIM and EI at the 1% significance level, indicating that there is a good explanatory power between the green image, the level of regional economic development, and the scale of enterprise environmental protection investment. The correlation coefficients among other variables in the model are all lower than 0.5, which indicates that the multiple regression model constructed in this paper will not produce serious multicollinearity problems.

4.3. Multiple Regression Analysis. In the establishment of the multiple regression model, the independent variable lags by one period and the robust standard error method is used in the model estimation to solve the

TABLE 3: Research variable correlation analysis.

Variables	EI	GIM	EDL	EPS	LEV	FLOW	CASH	OPP	SIZE	BALANCE	COST
EI	1										
GIM	0.0619***	1									
EDL	0.0658***	0.2259***	1								
EPS	0.0818***	0.0918***	0.0037	1							
LEV	-0.0663***	-0.0907**	-0.1782***	-0.2641***	1						
FLOW	-0.0083	0.0201	-0.0991***	0.2659***	-0.0954***	1					
CASH	0.0895***	0.0442*	0.0667***	0.3471***	-0.4444***	0.0609***	1				
OPP	0.1026***	-0.0785***	-0.0324	0.2103***	-0.4437***	0.1143***	0.2784***	1			
SIZE	-0.0536***	0.1469***	0.0532***	0.1388***	0.4210***	0.0520***	-0.1741***	-0.4599***	1		
BALANCE	-0.0252	-0.0977***	-0.2461***	0.1132***	0.0471**	0.0253	0.0751***	-0.0329*	0.0439**	1	
COST	0.0776***	-0.0351*	0.1819***	-0.1267***	-0.2090***	-0.1001***	0.087***	0.2435	-0.3278***	-0.1730***	1

Notes. *, **, and *** represent the significance level of 1%, 5%, and 10%, respectively.

TABLE 4: Regression results.

Variables	Model (1) EI	Model (2) EDL	Model (3) EI
GIM	0.005*** (3.29)	0.262*** (3.62)	0.004*** (3.07)
EDL			0.001*** (3.04)
EPS	0.005*** (2.72)	0.166* (1.91)	0.005*** (2.60)
LEV	0.000 (0.92)	-0.011*** (-4.87)	0.000 (1.16)
FLOW	-0.000 (-1.42)	-0.009* (-1.85)	-0.000 (-1.32)
CASH	0.000 (1.40)	0.002 (0.86)	0.000 (1.36)
OPP	0.002* (1.94)	-0.066* (-1.94)	0.002** (2.02)
SIZE	-0.001 (-0.72)	0.020 (0.47)	-0.001 (-0.75)
BALANCE	-0.000 (-0.92)	0.002** (2.51)	-0.000 (-1.06)
COST	0.000** (2.29)	0.035*** (3.99)	0.000** (2.08)
YEAR	Control	Control	Control
Constant	0.015 (0.95)	1.732* (1.87)	0.013 (0.83)
N	2,544	2,544	2,544
R ²	0.031	0.377	0.034
Adj_R ²	0.0243	0.373	0.0271
F	3.782	110.3	4.202
F (p value)	0.0000	0.0000	0.0000

Notes. *, **, and *** represent the significance level of 1%, 5%, and 10%, respectively; *t* value is in parentheses, and results are subject to standard error handling.

heteroscedasticity problem. Table 4 shows the regression results of models (1)–(3). From the regression results of model (1), the green image is positively correlated with the scale of enterprise environmental protection investment at a significant level of 1%, indicating that a good green image can promote the scale of enterprise environmental protection investment, which supports Hypothesis 1 of this article. Except for the corporate profitability (EPS), opportunity cost (OPP), and agency cost (COST), other control variables have no significant relationship with EI. From the regression results of model (2), the green image is positively correlated with the level of regional economic development at the 1% significance level, which supports the Hypothesis 2 of this article. Except EPS, LEV, FLOW, BALANCE, and COST, other control variables have no significant relationship with EDL. In model (3), the level of regional economic development is positively correlated with the scale of enterprises' environmental protection investment at the significance level of 1%, which supports Hypothesis 3 of this paper. It also indicates that the level of local economic development has an intermediate effect in the positive influence of green image on the scale of enterprise environmental protection investment and supports Hypothesis 4 of this article. Except EPS, OPP, and COST, other control variables have no significant relationship with EI.

In model (3), the green image is positively correlated with the scale of enterprise environmental protection investment at the significance level of 1%, indicating that the positive influence of green image on the scale of enterprise environmental protection investment is partly influenced by the level of local economic development.

The proportion of the indirect effect of local economic development level in the total effect is $0.262 \times 0.001 / 0.005 = 5.24\%$.

4.4. Robustness Tests. Firstly, use the natural logarithm (NEI) of the total environmental protection investment to measure the scale of enterprise environmental protection investment and use the market index (market) constructed by Fan et al. and Wang et al. [54, 55] to measure the level of regional economic development. However, considering that the data from 2008 to 2014 are based on 2008, the data calculation and scoring of all aspects of the changes in the marketization of all provinces since 2008 are reperformed. As a result, there is a big difference between the data before 2008 and the data after 2008. Therefore, the ranking of provinces in the market-oriented index is adopted to measure the level of regional economic development. Secondly, in the regression model, replace and increase the control variables that affect the enterprise's environmental investment. For the measurement method of the shareholding structure, replace "shareholding ratio of the second largest shareholder to the fifth largest shareholder (BALANCE)" with "shareholding ratio of the largest shareholder to the fifth largest shareholder (SHARE)." At the same time, we add the corporate performance indicator (ROE) into it. The specific results are shown in Table 5. It can be seen from Table 5 that the green image is significantly positively correlated with the scale of enterprise environmental protection investment, the green image is significantly positively correlated with the market, and both the green image and the market are significantly positively

TABLE 5: Robustness test.

Variables	Use marketization index to measure regional economic development level			Add control variables to the model		
	NEI	Market	NEI	EI	Market	EI
GIM	0.279*** (3.25)	0.571*** (8.33)	0.245*** (2.81)	0.317*** (3.55)	0.584*** (8.12)	0.285*** (3.15)
Market			0.061** (2.46)			0.054** (2.11)
EPS	-0.161 (-0.98)	0.040 (0.30)	-0.163 (-1.00)	-0.802*** (-3.61)	-0.269 (-1.45)	-0.788*** (-3.54)
LEV	-0.001 (-0.41)	-0.010*** (-4.47)	-0.001 (-0.19)	-0.001 (-0.45)	-0.009*** (-3.59)	-0.001 (-0.29)
FLOW	0.552 (1.05)	0.161 (0.38)	0.542 (1.03)	-0.104 (-0.18)	0.048 (0.10)	-0.107 (-0.18)
CASH	0.147 (0.44)	0.831*** (3.38)	0.096 (0.29)	-0.070 (-0.20)	0.673*** (2.63)	-0.107 (-0.31)
Tobin	-0.009 (-0.21)	-0.120*** (-4.06)	-0.001 (-0.03)	0.022 (0.44)	-0.123*** (-3.32)	0.028 (0.58)
SIZE	0.870*** (23.29)	-0.218*** (-7.09)	0.884*** (23.47)	0.930*** (20.37)	-0.237*** (-6.20)	0.942*** (20.56)
AGE	-0.064*** (-6.53)	0.012 (1.64)	-0.065*** (-6.62)	-0.061*** (-5.66)	0.012 (1.46)	-0.062*** (-5.72)
COST				-0.002 (-0.21)	0.006 (0.68)	-0.003 (-0.24)
SHARE				-0.106 (-1.41)	0.063 (1.06)	-0.109 (-1.46)
ROE				0.018*** (3.84)	0.011*** (2.82)	0.018*** (3.72)
YEAR	Control	Control	Control	Control	Control	Control
Constant	-2.455*** (-3.14)	13.001*** (20.04)	-3.246*** (-3.87)	-3.609*** (-3.70)	13.056*** (15.97)	-4.312*** (-4.23)
N	2,728	2,728	2,728	2,616	2,616	2,616
R ²	0.218	0.190	0.220	2,521	2,521	2,521
Adj_R ²	0.213	0.185	0.215	0.221	0.187	0.223
F	53.60	42.92	50.55	0.215	0.181	0.217
F(p-value)	0.0000	0.0000	0.0000	0.0000	0.0000	0.0000

Notes. *, **, and *** represent the significance level of 1%, 5%, and 10% respectively; *t* value is in parentheses, and results are subject to standard error handling.

correlated with enterprise environmental protection investment. It shows that the level of regional economic development plays an intermediary role between the green image and the scale of enterprise environmental protection investment. The above robustness test results show that the hypothesis in this article has been statistically verified, so the research conclusions are more reliable.

5. Conclusions

Based on the resource-based view, stakeholder theory, and signal transmission theory, this article, based on the sample data of A-share manufacturing listed companies from 2007 to 2015, found that a green image can significantly promote the scale of enterprise environmental protection investment. Further research found that the level of regional economic development played a part of the intermediary role in the positive impact of the green image on the scale of enterprise environmental protection investment.

This article studies the driving factors of enterprise environmental protection investment at the microlevel from the internal perspective and also studies the intermediary effect of macroeconomic factors on the relationship between green image and the scale of enterprise environmental protection investment from the external perspective. The results show that a good green image is one of the driving factors of enterprise environmental protection investment scale. Firstly, the green image conveys signals to stakeholders to make their green demands match the environmental protection behaviors of the enterprise, thus increasing the loyalty and satisfaction of stakeholders towards the products or services of the enterprise. Second, the green image is conducive to the formation of the

uniqueness of products or services different from other enterprises and the implementation of differentiation strategy, promote companies to improve competitiveness from the differentiation strategy, gain new market share, and promote the sustainable development of companies. In a word, improving and maintaining a good green image is very important for the sustainable development of companies. Green image is conducive to the legitimacy of companies and the improvement of economic performance, and it is the driving force for companies to make various kinds of environmental investment. Therefore, enterprises should take the initiative to obtain ISO14001 environmental management system certification, green product logo, or actively obtain international and domestic awards related to environmental protection, so as to establish a good green image.

On the contrary, the impact of green image on enterprise environmental protection investment is partly realized through the transmission of regional economic development. Research results show the following: first, the environmental awareness of stakeholders is very important to promote the enterprise take the initiative to perform environmental responsibility. Improving the level of regional economic development is conducive to enhancing the environmental awareness of stakeholders and affecting their consumption concepts, thereby increasing the stakeholders' demand and purchasing power for green goods and services and demand stimulating enterprise environmental protection investment. Second, in the market competition environment, stakeholders are sensitive to the green image established by the enterprise. It is necessary to coordinate environmental regulations and market-based environmental regulatory tools to make up for the shortcomings. Under the premise of ensuring the regional economic development, it

is used as a restraint means to force enterprises to fulfill their environmental fiduciary responsibilities and as an incentive means to encourage enterprises develop and adopt clean energy, clean technology, produce green products, and provide green services.

There are also some limitations to this study. First, this study only explores the mediating roles between the green image and the scale of enterprise environmental protection investment, without considering the moderators. Future research can continue to explore the boundary conditions for the current model. Second, this study only used China's A-share manufacturing listed companies as a sample; thus, the conclusions of the study may not be fully applicable to all companies, and caution should be exercised in the promotion of the conclusions. Future studies can further select samples of other industries to explore. Third, although the research data in this article are sufficient to support the research conclusions, the latest data can still be added to future research to further enhance the representativeness of the conclusions.

Data Availability

The data used to support the findings of this study are included within the article.

Conflicts of Interest

The authors declare that there are no conflicts of interest.

Acknowledgments

This research was supported by the National Social Science Foundation of China (Grant no. 17CGL017), Research on the Performance Evaluation Mechanism of Local Government Ecological Governance Project Expenditure (Grant no. 20BGL001), Guangxi Universities Young and Middle-Aged Teachers Scientific Research Basic Ability Improvement Project (Grant no. 2019KY0648), Major Project of National Social Science Foundation of China (Grant no. 18VHQ013), and High-Level Innovation Team and Outstanding Scholar Program Project of Guangxi Colleges and Universities (Gui Teacher Fan, [2019] No. 52).

References

- [1] L. Yang, H. Qin, Q. Gan et al., "Internal control quality, enterprise environmental protection investment and finance performance: an empirical study of China's a-share heavy pollution industry," *International Journal of Environmental Research and Public Health*, vol. 17, no. 6, p. 6082, 2020.
- [2] J. Su, C. Li, Q. Zeng, J. Yang, and J. Zhang, "A green closed-loop supply chain coordination mechanism based on third-party recycling," *Sustainability*, vol. 11, no. 19, p. 5335, 2019.
- [3] G. P. Tang, L. H. Li, and D. J. Wu, "Environmental regulation, industry attributes and enterprises environmental protection investment," *Accounting Research*, vol. 6, pp. 83–89, 2013.
- [4] Y. E. Li, P. W. Li, and H. L. Dong, "Property right, environmental regulation and enterprise environmental protection investment," *Journal of China University of Geosciences (Social Sciences Edition)*, vol. 18, no. 6, pp. 36–45, 2018.
- [5] J. C. Gao and W. M. Zhang, "The influence of environmental regulation on enterprises environmental investment," *Chinese Agricultural Accounting*, vol. 4, pp. 6–7, 2020.
- [6] A. M. Leiter, A. Parolini, and H. Winner, "Environmental regulation and investment: evidence from European industry data," *Ecological Economics*, vol. 70, no. 4, pp. 759–770, 2011.
- [7] E. Kesidou and P. Demirel, "On the drivers of eco-innovations: empirical evidence from the UK," *Research Policy*, vol. 41, no. 5, pp. 862–870, 2012.
- [8] H. Wang, J. Li, A. Mangmeechai, and J. Su, "Linking perceived policy effectiveness and proenvironmental behavior: the influence of attitude, implementation intention, and knowledge," *International Journal of Environmental Research and Public Health*, vol. 18, no. 6, p. 2910, 2021.
- [9] S. Yi and Q. H. Xue, "Green supply chain management and green innovation—based on the empirical research of Chinese manufacturing enterprises," *Science Research Management*, vol. 6, pp. 103–110, 2016.
- [10] F. Zhou, M. K. Lim, Y. He et al., "End-of-life vehicle (ELV) recycling management: improving performance using an ISM approach," *Journal of Cleaner Production*, vol. 228, pp. 231–243, 2019.
- [11] Y. Su and W. Sun, "Analyzing a closed-loop supply chain considering environmental pollution using the NSGA-II," *IEEE Transactions on Fuzzy Systems*, vol. 27, no. 5, pp. 1066–1074, 2019.
- [12] S. Q. Zheng, G. H. Wan, W. Z. Sun, and D. L. Luo, "Public demands and urban environmental governance," *Management World*, vol. 6, pp. 72–84, 2013.
- [13] C. Mackenzie, W. Rees, and T. Rodionova, "Do responsible investment indices improve corporate social responsibility? FTSE4Good's impact on environmental management," *Corporate Governance: An International Review*, vol. 21, no. 5, pp. 495–512, 2013.
- [14] G. P. Tang and L. H. Li, "Ownership structure, property right nature and corporate environmental investment—empirical evidence from China's A-share listed companies," *Research on Financial and Economic Issues*, vol. 3, pp. 93–100, 2013.
- [15] Y. Xin, S. Suntrayuth, and J. Su, "A comprehensive evaluation method for industrial sewage treatment projects based on the improved entropy-topsis," *Sustainability*, vol. 12, no. 17, p. 6734, 2020.
- [16] J. Long, Z. Sun, P. M. Pardalos, Y. Hong, S. Zhang, and C. Li, "A hybrid multi-objective genetic local search algorithm for the prize-collecting vehicle routing problem," *Information Sciences*, vol. 478, pp. 40–61, 2019.
- [17] J. Su, Y. Yang, and X. Zhang, "Knowledge transfer efficiency measurement with application for open innovation networks," *International Journal of Technology Management*, vol. 81, no. 2, pp. 118–142, 2019.
- [18] J. Jian, B. Li, N. Zhang, and J. Su, "Decision-making and coordination of green closed-loop supply chain with fairness concern," *Journal of Cleaner Production*, vol. 298, p. 126779, 2021.
- [19] M. T. Kacperczyk and H. G. Hong, "The price of sin: the effects of social norms on markets," *Journal of Financial Economics*, vol. 93, no. 1, pp. 15–36, 2009.
- [20] J. Amores-Salvadó, G. M.-D. Castro, and J. E. Navas-López, "Green corporate image: moderating the connection between environmental product innovation and firm performance," *Journal of Cleaner Production*, vol. 83, pp. 356–365, 2014.
- [21] Y.-S. Chen, "The drivers of green brand equity: green brand image, green satisfaction, and green trust," *Journal of Business Ethics*, vol. 93, no. 2, pp. 307–319, 2010.

- [22] N. J. Chang and C. M. Fong, "Green product quality, green corporate image, green customer satisfaction, and green customer loyalty," *African Journal of Business Management*, vol. 13, pp. 2836–2844, 2010.
- [23] M. Kang and S.-U. Yang, "Comparing effects of country reputation and the overall corporate reputations of a country on international consumers' product attitudes and purchase intentions," *Corporate Reputation Review*, vol. 13, no. 1, pp. 52–62, 2010.
- [24] S. F. Zhang and M. L. Bu, "Embedding in global value chains, informal environmental regulations and ISO14001 certification for chinese enterprises," *Finance and Trade Research*, vol. 2, pp. 70–78, 2015.
- [25] T. Hillestad, C. Xie, and S. A. Haugland, "Innovative corporate social responsibility: the founder's role in creating a trustworthy corporate brand through "green innovation"" *Journal of Product & Brand Management*, vol. 19, no. 6, pp. 440–451, 2010.
- [26] H. Lin, S. X. Zeng, H. Y. Ma, G. Y. Qi, and V. W. Y. Tam, "Can political capital drive corporate green innovation? Lessons from China," *Journal of Cleaner Production*, vol. 64, pp. 63–72, 2014.
- [27] R. Yadav, A. Kumar Dokania, and G. Swaroop Pathak, "The influence of green marketing functions in building corporate image," *International Journal of Contemporary Hospitality Management*, vol. 28, no. 10, pp. 2178–2196, 2016.
- [28] M. Robinson, A. Kleffner, and S. Bertels, "Signaling sustainability leadership: empirical evidence of the value of DJSI membership," *Journal of Business Ethics*, vol. 101, no. 3, pp. 493–505, 2011.
- [29] M. Porter and C. Linde, "Green and competitive: ending the stalemate," *Long Range Planning*, vol. 28, pp. 128–129, 1995.
- [30] M. P. Miles and J. G. Covin, "Environmental marketing: a source of reputational, competitive, and financial advantage," *Journal of Business Ethics*, vol. 23, no. 3, pp. 299–311, 2000.
- [31] Y.-S. Chen, "The driver of green innovation and green image - green core competence," *Journal of Business Ethics*, vol. 81, no. 3, pp. 531–543, 2008.
- [32] M. D. López-Gamero, J. F. Molina-Azorín, and E. Claver-Cortés, "The potential of environmental regulation to change managerial perception, environmental management, competitiveness and financial performance," *Journal of Cleaner Production*, vol. 18, no. 10–11, pp. 963–974, 2010.
- [33] G. Fortune, C. C. Ngwakwe, and C. M. Ambe, "Corporate image as a factor that supports corporate green investment practices in johannesburg stock exchange listed companies," *International Journal of Sustainable Economy*, vol. 8, no. 1, pp. 57–75, 2016.
- [34] J. Su, Y. Yu, and Y. Tao, "Measuring knowledge diffusion efficiency in R&D networks," *Knowledge Management Research & Practice*, vol. 16, no. 2, pp. 208–219, 2018.
- [35] D. M. You and J. J. Yuan, "Research on the Impact of Pollutant Emission Trading Policy on Enterprise Environmental Investment," <http://kns.cnkia.net/kcms/detail/11.1874.S.20200702.1738.002.html>.
- [36] X. Wu and Y. Wang, "Environmental taxation, enterprise environmental investment and environmental quality-based on empirical study of China's A share heavy pollution industry," *Tax and Economic Research*, vol. 4, pp. 27–37, 2019.
- [37] X. Y. Liang and Y. Tan, "Can green taxes improve the efficiency of corporate environmental investment?" *Finance and Accounting Monthly*, vol. 16, pp. 9–17, 2020.
- [38] M. H. Lǚ, G. H. Xu, and W. Zhu, "Research on the impact of government subsidies on enterprise environmental protection investment – "Effective" or "work without effort"?" *Communication of Finance and Accounting*, vol. 18, pp. 20–25, 2020.
- [39] B. C. Erbas and D. G. Abler, "Environmental policy with endogenous technology from a game theoretic perspective: the case of the US pulp and paper industry," *Environmental and Resource Economics*, vol. 40, no. 3, pp. 425–444, 2008.
- [40] H. C. Wang and P. L. Wu, "Implement ISO14000 to create a green corporate image," *China Coal*, vol. 27, pp. 49–50, 2001.
- [41] T. Cleff and K. Rennings, "Determinants of environmental product and process innovation-evidence from the manheim innovation panel and a follow up telephone survey," *European Environment*, vol. 9, pp. 191–201, 1999.
- [42] D. Kammerer, "The effects of customer benefit and regulation on environmental product innovation," *Ecological Economics*, vol. 68, no. 8–9, pp. 2285–2295, 2009.
- [43] V. Bathmanathan and C. Hironaka, "Sustainability and business: what is green corporate image?" *International Conference on Advances in Renewable Energy and Technologies*, vol. 32, pp. 1–5, 2016.
- [44] G. P. Tang and L. H. Li, "Research on enterprise environmental protection investment structure and its distribution characteristics empirical evidence from a-share listed companies from 2008 to 2011," *Audit & Economy Research*, vol. 4, pp. 94–103, 2013.
- [45] T. J. Wei, H. Lin, D. Wang, C. Li, and Y. J. Wu, "Research on the impact of corporate environmental commitments on their environmental management," *Industrial Engineering and Management*, vol. 5, pp. 74–79, 2013.
- [46] Z. Wen and B. Ye, "Analyses of mediating effects: the development of methods and models," *Advances in Psychological Science*, vol. 22, no. 5, pp. 731–745, 2014.
- [47] C. H. Lin, "An empirical study on the interactive relationship between environmental protection input and economic development analysis and application," *Journal of Capital Normal University (Natural Science Edition)*, vol. 2, pp. 74–79, 2013.
- [48] Y. Su and Y.-Q. Yu, "Spatial agglomeration of new energy industries on the performance of regional pollution control through spatial econometric analysis," *Science of The Total Environment*, vol. 704, Article ID 135261, 2020.
- [49] L. Yang, D. L. Zhang, and Y. D. Jia, "Public participation, environmental regulation and corporate environmental protection investment based on empirical evidence of our country's A-share heavy pollution industry," *Finance and Accounting Monthly*, vol. 12, pp. 32–40, 2018.
- [50] W. C. Ma and Y. J. Tang, "Provincial environment competition, environmental pollution level and enterprise' environmental protection investment," *Accounting Research*, vol. 8, pp. 72–79, 2018.
- [51] Y. Xiao, C. Li, L. Song, J. Yang, and J. Su, "A multidimensional information fusion-based matching decision method for manufacturing service resource," *IEEE Access*, vol. 9, pp. 39839–39851, 2021.
- [52] J. Su, F. Zhang, S. Chen et al., "Member selection for the collaborative new product innovation teams integrating individual and collaborative attributions," *Complexity*, vol. 2021, Article ID 8897784, 14 pages, 2021.
- [53] Y. M. Guan and X. Sun, "Environmental control, equity structure and corporate environmental investment," *Friends of Accounting*, vol. 16, pp. 54–59, 2018.
- [54] G. Fan, X. L. Wang, and H. P. Zhu, *China's Marketization Index by Provinces-Report on the Relative Process of*

Marketization in Various Regions in 2011 pp. 1–220, Economic Science Publishers, Beijing, China, 1st ed. edition, 2011.

- [55] X. L. Wang, G. Fan, and J. W. Yu, *China's Marketization Index Report by Provinces* pp. 1–323, Social Sciences Literature Publishers, Beijing, China, 1st ed edition, 2017.

Research Article

Competitive Analysis of Operation Mode of Enterprise Value Chain under the Background of Green Economy

Peng Fan ¹, Yifeng Wang,¹ and Yuwei Dong²

¹Xidian University, Xi'an, Shaanxi 710071, China

²Shaanxi Petrochemical Research and Design Institute, Xi'an, Shaanxi 710054, China

Correspondence should be addressed to Peng Fan; pfan@mail.xidian.edu.cn

Received 24 November 2020; Revised 25 February 2021; Accepted 20 March 2021; Published 1 April 2021

Academic Editor: Alessandro Mauro

Copyright © 2021 Peng Fan et al. This is an open access article distributed under the Creative Commons Attribution License, which permits unrestricted use, distribution, and reproduction in any medium, provided the original work is properly cited.

In order to improve the competitive advantage of the supply chain, occupy more market shares, and obtain greater benefits, many companies participate in the competition within or between supply chains. This article mainly introduces the game analysis of enterprise value chain operation mode under the background of green economy. This article mainly introduces the competition of business value chain operation mode under the background of green economy and determines its best-selling price and sales volume. This article first outlines the background of the green economy. Secondly, a competition model between multiple retailers is constructed, and the optimal strategy under the two modes of Cournot competition and Stackelberg competition is studied. Finally, the impact of the green economy coefficient on the maximum sales is analyzed. The experimental results of this article show that the average growth rate of total income after the transformation of the business value chain operation mode of the business under the background of the green economy is 9.03%, which also shows that the green economic policy has ultimate significance and is obviously innovative.

1. Introduction

Nowadays, with the improvement of people's living standard and consumption concept, more and more consumers' pursuit of product demand is becoming diversified and personalized [1], which makes many enterprises face more challenges in management and decision-making. In order to adapt to the new management environment and enhance the competitiveness in the fierce market, the management level of production and sales needs to be continuously improved. Enterprises are the core force of my country's social development. The state has invested a large amount of funds to support the development of the green economy of enterprises. Therefore, the transformation and development of the business value chain operation mode under the background of green economy directly affects the implementation effect of my country's green economy strategy [2]. Chain operation mode is the research object, and it has important practical significance to explore the game analysis of enterprise operation mode.

D'Amato et al. found that in terms of economic and environmental sustainability, the green economy is an "umbrella" concept [3], which includes elements in circular economy and bioeconomy concepts (such as eco-efficiency and renewable energy) and other elements. Particularly circular economy and bioeconomy are centered on resources, while green economy recognizes the fundamental role of all ecological processes in principle. Regarding the social level, the green economy includes more, for example, eco-tourism and education. By comparing the different sustainability strategies advocated by these concepts, it does not advocate its substitutability, but its clarity and reciprocal integration. McAfee discusses the findings based on the synergy and limitations of the concept, which are used to provide a basis for studying the business value chain operating mode and policy implementation in the context of a green economy. This study lacks case verification, no relevant experimental data, and does not constitute convincing [4]. Based on the theory of dynamic capability and value chain, Han et al. takes Angel orange juice and

Huiyuan Juice as examples to carry out empirical research. Through the comparative analysis of new retail enterprises and traditional retail enterprises, he further discusses the influence background of dynamic capabilities of enterprises on value chain reconstruction under the new retail mode. Then, it is further discussed how to apply the dynamic capabilities of enterprises to the value chain reconstruction in the complex and changeable market environment. The starting point of this research is good, but the discussion is too vague and should be studied in light of the actual situation [5]. Loiseau et al. in order to find the selection mechanism of green economy enterprise value chain routines, based on the description of the choice of green economy enterprise value chain routines, proposed and constructed an evolutionary game model. In addition, they also used the model to analyze green strategies for achieving evolutionary stability in routine procedures of economic enterprise value chains. The research is more prominent in the experimental part, but lacks a theoretical description [6]. Su et al., taking the environmental protection green closed-loop supply chain as the research object, a two-stage closed-loop supply chain game model is established. Considering the impact of environmental protection investment on the entire supply chain, the decisions of supply chain participants are different. When manufacturers choose a closed-loop supply chain, different choices will have an impact on the benefits of the entire supply chain. Therefore, this work compares and analyzes the impact of centralized and decentralized decisions on the returns and pricing strategies of each participant. Finally, a decision model of optimized cooperation mechanism considering cost-profit sharing contract is further designed [7].

The overall structure of this article is summarized as follows:

- (i) *Introduction*. It summarizes the domestic and international research status of supply chain enterprise competition, analyzes the significance of this paper, and summarizes the research content, research methods, and technical routes of this paper.
- (ii) *Method Part*. It presents the game theory, fuzzy mathematics theory, and supply chain theory research content of this article.
- (iii) *Experimental Part*. A competition model is constructed between two retailers under the background of green economy, and the optimal strategies are studied under four competition modes.
- (iv) *Analysis Part*. Game analysis of competition between retailers in a green economy environment and game analysis of competition between a single manufacturer and two retailers are carried out.
- (v) *Summary Part*. It summarizes the relationship between the optimal solutions under different competition modes in the green economic environment. In addition, it draws the shortcomings of this article and the expectations for future research.

2. Competitive Methods of Operation Mode of Enterprise Value Chain

2.1. Method of Business Value Chain Operation Mode under the Background of Green Economy

2.1.1. System Theory Analysis. The analysis methods of system theory include the integrity, relevance, and coordination of the system. Taking the main participants of the green economy, governments, enterprises, and consumers as examples, integrity means that if any one of these three parties is abnormal, then the overall green economy will be abnormal [1]. Relevance means that any one of these three parties will be abnormal, and the other two will be abnormal; coordination means that the abnormal relationship of the three parties will cause the tripartite imbalance [8]. Therefore, when discussing issues related to green economy in this article, we must adhere to the method of system theory and establish an economic development model based on the characteristics of tripartite interest balance [9]. This article defines the concept and characteristics of green economy and uses sustainable development theory, ecological economics theory, circular economy theory, low-carbon economy theory, and basic game theory to analyze the status quo of the development of business value chain operation models under the background of China's green economy. Analyzing the problems and their causes, and thus establishing a three-in-one economic development model of government, enterprises and consumers, belongs to the category of system analysis [10].

2.1.2. Combination of Qualitative Analysis and Quantitative Analysis. Economics is characterized by a high degree of abstraction. Many scholars use qualitative analysis methods for research, while natural sciences tend to use quantitative models to analyze problems [11]. In view of the fact that the green economic development theory has the characteristics of both social science and natural science, the method of qualitative analysis and quantitative analysis is comprehensively used in this research [12]. This article mainly uses qualitative research methods for the development status, existing problems, and cause analysis of the enterprise value chain operation mode under the background of my country's green economy. In the process of researching the value chain operation mode of my country's green economy enterprise value chain from the perspective of game theory, it mainly uses qualitative and quantitative research methods [13]. Qualitative research is the foundation, and quantitative research is deepening. The two correspond to each other and complement each other [14].

2.1.3. Comparative Analysis. Through studying the experience of the development of corporate value chain operation mode in foreign countries and various regions of my country under the background of green economy, certain enlightenment can be obtained, so as to put forward countermeasures and suggestions for the development of corporate value chain operation mode under the background of green

economy in my country [15]. Through the comparison of the practical experience of the development of the value chain operation mode of green economy enterprises in some countries and regions, it provides an effective reference for the development of the theory and practice of the enterprise value chain operation mode under the background of my country's green economy [16]. However, due to the different backgrounds of green economy development in various regions, relevant theories must be innovated. This article focuses on the in-depth study of how to promote the healthy development of my country's green economy through game analysis of corporate value chain operating models based on my country's actual national conditions [17].

2.1.4. Theory and Practice. Theory needs to be tested by practice, and practice is the only criterion for testing truth. At the same time, theory also needs to be gradually revised and perfected in the process of exploration in practice [18]. The research on the theory and practice of green economy development in my country's enterprises is still in its infancy. For example, the core concepts and characteristics of green economy have not yet reached a unified standard, and a relatively complete system needs to be tested by practice [19]. This article adopts the method of combining theoretical analysis and practical summary, interspersing part of the data support and practical content in the theoretical discussion process, in order to achieve the effect of integrating theory with practice [20].

2.2. The Cost Control Method of Enterprise Value Chain under the Background of Green Economy. From the perspective of enterprise cost control under the background of green economy, the ultimate goal of enterprises implementing value chain management is to reduce product costs from a strategic perspective, improve corporate competitive advantages, and achieve environmentally friendly and sustainable economic development [20]. Strategic cost management requires companies to give full play to the role of value chain in the cost management process, combine value chain theory, use overall planning analysis methods, tap the potential of cost reduction from a strategic perspective, and create relevant conditions for the adoption of activity-based costing [21]. According to the location where the product runs, it can be divided into internal processes and external processes. From the interaction between the input rate of the enterprise process and the postoperation process, look for a process with low input rate and weak correlation, separate it from the internal business, and try to merge the external business to achieve the goal of reducing the company's operating costs [22, 23].

- (1) Let X represent the collection of products or cost objects, Y represent the set of activity cost drivers associated with the job, x represent the x th product ($x \in X$), y represent the y th activity cost driver, and M_y represent the activity cost of the activity cost driver Sum of Y . N_x represents the sum of operations for the x th product, O_{xy} represents the number of

products x consuming activity cost drivers y (absolute quantity), and P_{xy} represents the percentage of product x consuming activity cost drivers y to the total y activity cost drivers (relative proportion). And x -product is called x -activity cost driver coefficient, referred to as activity cost driver coefficient [24, 25]. This gives the following formula:

$$P_{xy} = \frac{O_{xy}}{\sum_{x=1}^X O_{xy}}, \tag{1}$$

$$\sum_{x=1}^X P_{xy} = 1.$$

In $P_{xy} = O_{xy} / \sum_{x=1}^X O_{xy}$, $\sum_{x=1}^X O_{xy}$ represents the total amount of y -cost drivers, so the sum of the operating costs of product x is

$$N_x = \sum_{y=1}^Y M_y P_{xy}. \tag{2}$$

The cost of all products is

$$N = \sum_{x=1}^X N_x. \tag{3}$$

In order to construct a cost driver optimization model, it is necessary to first determine how to measure the accuracy of cost information and the loss of accuracy after the cost driver is merged [26]. Therefore, the accuracy standard of the merger of the two cost drivers based on the operation is required [27]. Let N_x^{km} denote the cost of product x calculated after merging the activity cost driver k into the activity cost driver m ; the cost of the new cost library after k and m are combined is $M_k + M_m$, and the cost driver coefficient is $\frac{xm}{p}$; then, the following relationship holds:

$$N_x^{km} = \sum_{y=1}^Y M_y P_{xy} + (M_k + M_m) P_{im},$$

$$N_x = \sum_{y=1}^Y M_y P_{xy} = \sum_{y=1}^Y M_y P_{xy} + M_k P_{xk} + M_m P_{xm}. \tag{4}$$

Subtract formula (4) to obtain a formula representing the difference between the product cost calculated after merging the activity cost driver k into m and the product cost before the merger [28], that is, the accuracy loss formula after the two activity cost drivers are combined:

$$N_x^{km} - N = M_k (P_{xm} - P_{xk}). \tag{5}$$

- (2) Suppose C_y is the information cost related to the activity cost driver y . Because the activity cost drivers k and m are combined, the information cost C_k

related to k can be saved. In other words, not all products are exactly the same, and some products are more important to the enterprise strategic or operational importance [23]. Therefore, a weight ω_x is

set for the product x . The model maximizes the difference between the information cost savings and the loss of cost calculation accuracy. The relationship is as follows:

$$\begin{aligned} \text{Max} \quad & \sum_{\text{allpairs}(k,m)} \alpha_{km} \left\{ C_k - \text{SQRT} \left[\sum_{x=1}^X \omega_x (N_x - N_x^{km})^2 \right] \right\} \\ = \text{Max} \quad & \sum_{\text{allpairs}(k,m)} \alpha_{km} \left\{ C_k - M_k \cdot \text{SQRT} \left[\sum_{x=1}^X \omega_x (P_{xk} - P_{xm})^2 \right] \right\}, \end{aligned} \quad (6)$$

where $\alpha_{km} \in \{0, 1\}$ ($k, m = 1, 2, \dots, y$). If k and m are combined, then $\alpha_{km} = 1$; if k does not combine with m , then $\alpha_{km} = 0$. In practice, based on the consideration of the cost-benefit principle, the number of activity cost drivers should not be too large [29]. Therefore, let D be the upper limit of the number of activity cost drivers, and there are constraints:

$$Y - \sum_{\text{allpairs}(k,m)} \alpha_{km} \leq D. \quad (7)$$

The combination of a number of completely related activity cost drivers does not change the accuracy of product activity costs. According to this theory, it is possible to combine the many operating cost drivers of the implementing enterprise according to their quantitative relevance [30]. In this way, it can greatly reduce the number of cost libraries, reduce the workload of identifying, collecting, calculating, and analyzing the drivers of operating costs, reduce corporate costs, and achieve a green economy [31].

manufacturers and retailers determine their own competitive decision-making issues when retailers conduct different competitive behaviors. According to different competitive behaviors, this article assumes that there are three types of competition between retailers as follows:

Mode 1. Cournot competition among retailers

Mode 2. Collusion competition among retailers

Mode 3. Stackelberg competition among retailers

A game model of competition between two manufacturers and two retailers: when establishing a competition model between supply chains, it is assumed that the production and sales in the supply chain are equal. Since the two supply chains are playing a Cournot game, they decide their respective retail sales at the same time. When making decentralized decision-making, the manufacturer in the supply chain is the leader and the retailer is the follower; that is, the Stackelberg game is played in the chain. Finally, the three situations of decentralized-decentralized decision-making (mode 1), centralized-decentralized decision-making (mode 2), and centralized-centralized decision-making (mode 3) are separately established and solved.

2.3. Game Analysis Model. A game model of competition between two retailers: in this model, retailer A and retailer B will determine their own sales at the same time, and neither of these two companies knows each other's sales decisions. Therefore, it is necessary to use the ranking index of the profit function to obtain the first-order derivation of the profit function ranking index of the two retailers one by one for the sales volume of the company, so as to determine the optimal sales volume of each retailer.

Game model of competition among multiple retailers: in this model, all retailers will determine their own sales at the same time, and each retailer does not know the sales strategies of other retailers. Each retailer competes for sales based on the principle of maximizing its own profit. Therefore, it is necessary to use the ranking index of the profit function to find the first-order derivation of the sales volume of the company by the profit function ranking index of each retailer to determine each retailer.

A game model of competition between a single manufacturer and two retailers: a two-level supply chain competition model composed of a single manufacturer and two competing retailers is constructed. This model analyzes how

3. Construction of Competitive Experiments on the Operation Mode of Enterprise Value Chain

3.1. Design of Green Supply Chain Operation System. Before the implementation of the green supply chain, the process of green supply chain management is very complex, which can be divided into the following stages: first, green supply chain planning and then, green supply chain management.

3.1.1. The Start of Green Supply Chain Plan

(1) *Choose the Right Partner.* Before starting the green supply chain management plan, enterprises should first choose the right supply chain management partners. According to the relevant theories of green supply chain management, choosing the right supply chain partners is the basis for the efficient operation of the supply chain. Because the operation mode of green supply chain management is different from the general supply chain

operation mode, there are often obstacles due to the unqualified suppliers. Therefore, the correct selection of suppliers is the basis for the smooth operation of green supply chain.

(2) *Coordinate with Partners.* After selecting the right supply chain partners, we need to coordinate the green supply chain plan with the partners. The start-up of green supply chain may be caused by the environmental, health and safety departments finding out the needs and opportunities of green supply chain management first, and then making suggestions to the top management of enterprises. It may also be caused by the enterprises' awareness of the importance of environmental problems and the opportunities that green supply chain management will bring to enterprises. In order to improve the environmental performance, not only the departments in the core enterprises need to pay attention to the environmental problems, but also the cooperation of the external partners in the green supply chain. Therefore, the core enterprises need to communicate and negotiate with suppliers, customers, and even consumers at the stage of starting the green supply chain, so as to explain the benefits that the implementation of green supply chain management can bring to the enterprises, get partners' attention to environmental issues, reach an agreement with partners, and set overall environmental goals for the supply chain so that enterprises in the supply chain can make specific action plans according to specific goals.

3.1.2. Set Specific Objectives of Green Supply Chain Management. The next stage of green supply chain management is to set management objectives. Due to different motivations of green supply chain operation and dynamic factors of external environment, the objectives are also different. Generally speaking, they mainly include the following aspects:

- (1) Optimize environmental performance
- (2) Cost reduction
- (3) Improve quality
- (4) Expand trademark image

Cost reduction and quality improvement are the same goals set by enterprises under the influence of internal motivation, which seek to improve the quality of products and processes. The focus on trademark image is mainly related to external motivation, but the environmental factors of the goals are very clear.

3.1.3. Selection of Working Objects in Green Supply Chain. Green supply chain management is oriented to the whole supply chain, and the most important thing is to ensure that suppliers comply with various environmental regulations. Due to limited resources or limited supply chain improvement process, in fact, each green supply chain management plan can only focus on a few specific problems or organizations, and most companies need to choose the

working objects of green supply chain management according to the situation.

3.2. Building a Flat Organizational Structure of the Enterprise Value Chain Operation Model. The flat organizational structure can meet changing environmental requirements and further reduce management costs. Streamlining the organizational structure is a process in which the management level continues to decrease and the scope of management continues to expand. The system architecture has gradually changed from a single application (dividing data access directly into a service-based green economic structure) and gradually transformed into a composite organizational structure based on small teams. These team members generally only have about 10 people. This organizational structure pays more attention to the concept of responsibility of each member. Although there are not many people, they can maintain a certain focus within their responsibilities and be responsible for their work and the entire team. For example, the responsibility of search engine optimization team members is to reduce click costs and increase profitability by optimizing links. All they have to do is to focus on their work, and completing the work is the ultimate goal. From the results, this small team brought two more advantages.

On the one hand, when the business system is assigned to a small team by function (or specific business), the scale and complexity of the problem it can handle will be limited. Similarly, the scale and complexity of the architectural problem the team has to face is reduced accordingly, which is achieved precisely through team division to reduce the scale and complexity of the problem. On the other hand, when the number of people decreases, bureaucracy is difficult to develop, and the entire team is more likely to form a positive and autonomous atmosphere.

This division allows the technical team to focus on solving the corresponding business problems, or this is the embodiment of business-driven technology in the organizational structure (or business priority). Because the team size is usually around ten people at this time, there is generally no particularly complicated work, and business design decisions will be digested within the team. Another advantage of this division is that technical personnel, especially the leaders of the technical team, are very familiar with the business. Under this organizational structure, companies divide the organization vertically by business line, and technical support is usually within the business line. The internal members of the team take their work seriously, perform their duties with due diligence, and possess certain innovative capabilities. In a team, there are engineers, product managers, and designers who directly report work problems to the team's supervisor. There is almost no cooperation within the team, and members can act independently among various departments to complete their own tasks. In this way, the team can maintain its own innovation, improve the agility of response to affairs, save human resources, and achieve green economic development.

3.3. Building a Dynamic Cooperative Alliance Operation Model

3.3.1. *Effectively Reduce Marketing Costs.* The cost of dynamic alliance is borne by all parties in the alliance. This corresponds to the fact that other members of the organization provide themselves with a certain amount of free advertising or a certain degree of sales comfort, while the company uses the marketing resources of other parties for free, which of course reduces marketing costs.

3.3.2. *Expand Customer Base.* Through dynamic alliances, companies can make consumers belonging to only one party become their own consumers to a certain extent and at the same time increase the number of potential consumers under the powerful offensive of dynamic alliances, thereby expanding the consumer group of products. Dynamic alliance can only develop further. The influence of each brand can use the other to expand consumer groups and create greater market space.

3.3.3. *Expand Brand Influence.* Even if it is a well-known brand or a strong brand, it is impossible for everyone to be familiar with and like it. Customers with different brand knowledge, different reputations, and different loyalties will have different impressions, feelings, and ratings. In dynamic alliances, use certain brand influence, promotion skills, and other resource advantages to improve the visibility and reputation of related brands, enhance the loyalty of certain brands, and increase the influence of related brands. By forming a dynamic alliance, alliance members can provide other alliance members with a certain degree of advertising comfort on their respective powerful sales terminals and at the same time exchange experience with successful advertising and promotional activities across the country.

3.3.4. *Market Information Exchange, Strengthening Alliance, and Cooperation.* Under the guidance of multi-interest thinking, with the extension and deepening of the franchise company's cooperation period, the alliance members will gradually break the pure business relationship and realize the exchange of market information between the companies in the alliance organization, through the use of operators as collaboration links. It can even communicate through other technical information to maximize market potential, improve market efficiency, and gradually develop from the initial transactional partnership with operators to alliance partnerships with value-added channels within the alliance organization. The efficiency of information utilization by member companies can be improved, and higher benefits are achieved. By using the market information network to communicate with each member company externally, transaction costs can be reduced and the market information network can be improved. More effective information exchange and processing can enable all member companies to fully share the information benefits of the companies in the dynamic alliance and improve market competitiveness.

4. Competitive Analysis of the Operation Mode of Enterprise Value Chain

4.1. *Status Quo of Enterprise Value Chain under the Background of Green Economy.* For the enterprise value chain, starting from the basic value-added activities and auxiliary activities of the value chain, the basic value-added activities of the value chain include marketing, internal logistics, production and operation, and external logistics. The supporting activities include corporate infrastructure. The purpose is to formulate the management system of the organization, implement corporate strategies, and effectively integrate internal resources and market resources through the information management system to provide effective protection for the value creation of the value chain; the purpose of human resource management is that the strategy requires building a highland of talents and cultivating compound talents for enterprises; the purpose of technology development is to continuously summarize cooperation experience and solve cooperation problems, form the enterprise's own marketing skills, and improve its core competitiveness; the purpose of enterprise procurement is to improve combining our own resources and market resources to achieve the purpose of controlling procurement costs by choosing an optimized procurement plan.

4.1.1. *The Status Quo of Enterprise Value Chain System under the Background of Green Economy.* With the phased changes in China's economic development and the deepening of structural adjustments in supply-side reforms, the shortcomings of small- and medium-sized private enterprises have gradually been exposed. The vast majority of enterprises in the industry are facing a shortage of comprehensive resources, lack of talents, lack of intellectual property rights, and work efficiency. The current traditional value chain management system has begun to face the challenges of Internet+ and other emerging value chain systems, such as the low quality of production methods and production lines, and the low value-added benefits of the value chain management system. Although the comprehensive governance structure of small- and medium-sized private enterprises is unreasonable, they still have the advantage of rapid turnaround in terms of mechanism; although the property rights structure of large state-owned enterprises is not dynamic enough, they may accumulate and develop after reform or transformation; listed companies have advantages in financing, but pursuing the profit-seeking mentality of rapid capital return is very easy to cause investment errors. The development status of the enterprise value chain under the background of the green economy, etc., is charted, as shown in Figure 1.

For small- and medium-sized enterprises, the advantage is that they have a flexible management structure, and the disadvantage is that they lack sufficient corporate funds; for large enterprises, the advantage is that they have a huge management structure that can better allocate talents, and the disadvantage is management personnel complexity and long decision-making process; for state-owned enterprises,

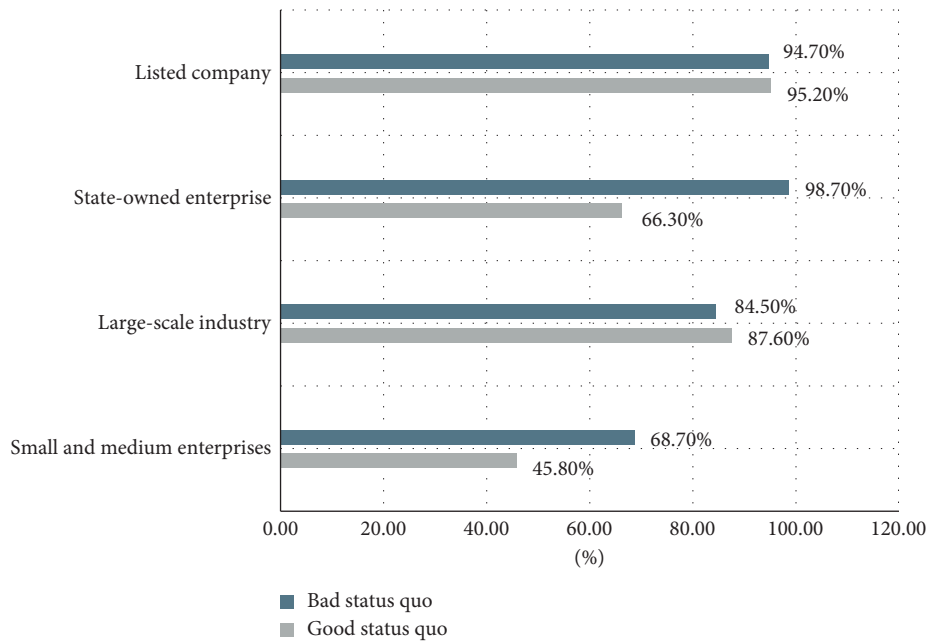


FIGURE 1: Development status of enterprise value chain under the background of green economy.

the advantage is the strong support of national policies and control of many people’s livelihood operations, and the disadvantage is that the management structure is relatively loose, which is not conducive to vertical management; for listed companies, the advantage is that the flow of funds is sufficient. The value chain of the enterprise is adjusted more freely. The disadvantage is the same as that of a large enterprise. The management personnel are complicated, and the decision-making process is longer.

4.1.2. Elements of Enterprise Value Chain and Competitors. Collect and count the elements of the enterprise value chain and competitors. The elements of the enterprise value chain include governance structure, employment mechanism, work efficiency, enterprise scale, enterprise management, business model, logistics support, corporate culture, human resource management, market adaptability, corporate infrastructure, corporate operating qualifications, capital financing capabilities and technology development capabilities, etc.; competitors can be divided into small- and medium-sized enterprises and large-scale enterprises according to the total amount. Draw specific statistics into charts, as shown in Figure 2.

From the comprehensive analysis table of value-added elements of the value chain, it can be concluded that although small- and medium-sized enterprises have simple advantages in terms of property rights structure and flexible management structure, they have comparative advantages in terms of corporate mechanism, work efficiency, and employment system, but in other comprehensive governance structures, there are obvious shortcomings in terms of operation and management, human resources and capital management, and technological development. Large-scale enterprises have

relatively sufficient capital flow and a relatively complete management structure. It is more advantageous to adjust the business value chain operation mode under the background of green economy.

4.2. Business Revenue Analysis under the Background of Green Economy. This article uses relevant databases to inquire about the revenue of my country’s enterprises in the past five years after the adjustment of the value chain operation model under the advocacy of the green economy strategy (the year 2020 has not yet ended, not included) (only representative companies are used as examples, not all included data), including small- and medium-sized enterprises, large-scale enterprises, and state-owned enterprises. The statistical data drawing results of the specific situation are shown in Table 1. Table 1 shows the total income of enterprises under the background of the green economy from 2015 to 2019.

It can be seen from the statistical chart that small- and medium-sized enterprises have achieved good results in compliance with the development strategy of the green economy. The total revenue has been rising steadily, with an average growth rate of 10.50%; state-owned enterprises have been supported by national policies and subsidies, and most of them are subsidized support. The total revenue of the people’s livelihood companies also showed a steady growth trend, with an average growth rate of 12.22%; the revenue of large enterprises occasionally declined in 2017, but the overall growth trend is still growing, with an average growth rate of 4.36%. It can be seen that the transformation of the business value chain operation mode of the enterprise in accordance with the green economic policy advocated by the country is conducive to the steady development of the enterprise, saving costs, and increasing revenue. The average growth rate of overall revenue is 9.03%.

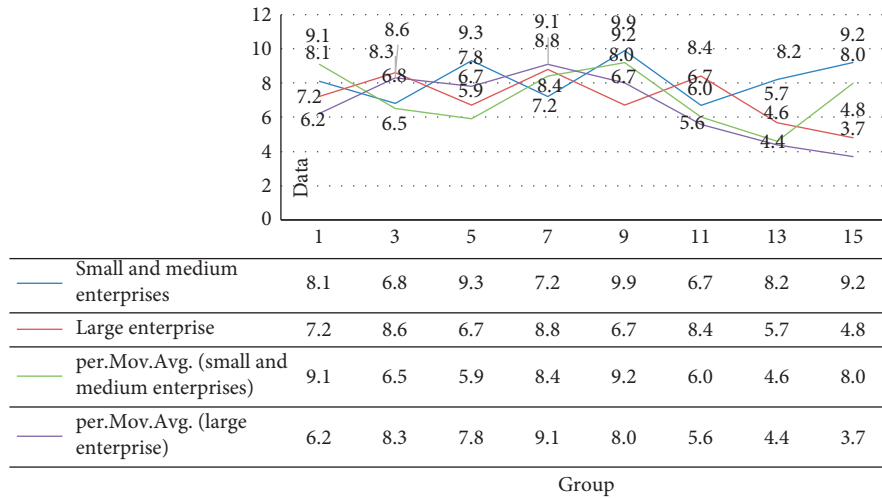


FIGURE 2: Elements of the corporate value chain and competitors.

TABLE 1: Total revenue of enterprises under the background of green economy (unit: ten million).

Small and medium enterprises	4.12	4.23	4.81	5.92	6.07
Large-scale industry	30.31	31.25	29.87	33.56	35.71
State-owned enterprise	8.26	9.34	10.52	12.37	13.06

4.3. Mixed Strategy Game of Enterprise Value Chain Operation Mode under the Background of Green Economy

- (1) Based on the noncooperative game strategy under uniform distribution, the distribution of corporate revenue in the case of different transaction volumes is shown in Figure 3.

It can be seen from Figure 3 that whether it is a small and medium-sized enterprise, a large private enterprise, or a state-owned enterprise, the revenue distribution is relatively even, and the trend is relatively consistent. With the development of the green economy, the total revenue has increased the most from 2018 to 2019. Small and medium enterprises increased by 18.89%; large private enterprises increased by 2.93%; and state-owned enterprises increased by 16.01%.

- (2) Based on the noncooperative game strategy under the normal distribution, the distribution of corporate revenue in the case of different transaction volumes is shown in Figure 4.
- (3) Stability test of mixed strategy game of enterprise value chain operation mode under the background of green economy.

Small- and medium-sized, large-scale enterprises' competitive advantages weaken the costs and high R&D

costs caused by low-end lock-in effects. The two decision-making costs have strong hidden and indirect effects, and the reverse effect on the potential of the domestic value chain of latecomers is not significant, especially in the early and middle stages of the evolutionary game. In view of the obscure contract orientation, it is assumed that hidden costs are not an important consideration for corporate decision-making. However, under long-term cooperation conditions, it will affect the evolution of the game stabilization strategy between the companies. The result is shown in Figure 5.

On the whole, the local stability of the mixed strategy game is relatively strong. The first company compares the expected benefits of overflowing knowledge with the speculative cost plus the penalty for breach of contract and believes that it is worthwhile to negotiate with internal personnel or third-party intelligence agencies to reach an obscure contract, indicating that the first company will choose a breach strategy to acquire technology and products. Knowledge resources are required for upgrading. The second company's initial judgment believes that taking the risk of default to acquire the spillover knowledge of the first company cannot offset the sum of the speculative cost and the penalty for default, and the second company tends to choose a contract-abiding strategy.

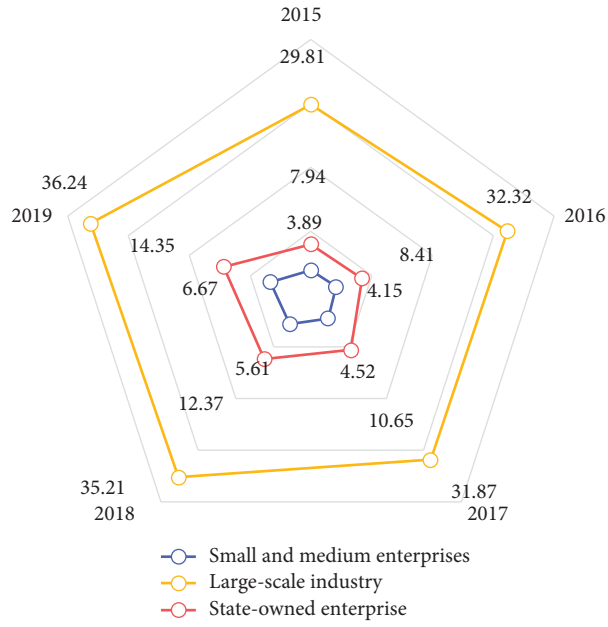


FIGURE 3: Corporate revenue under uniform distribution (unit: ten million).

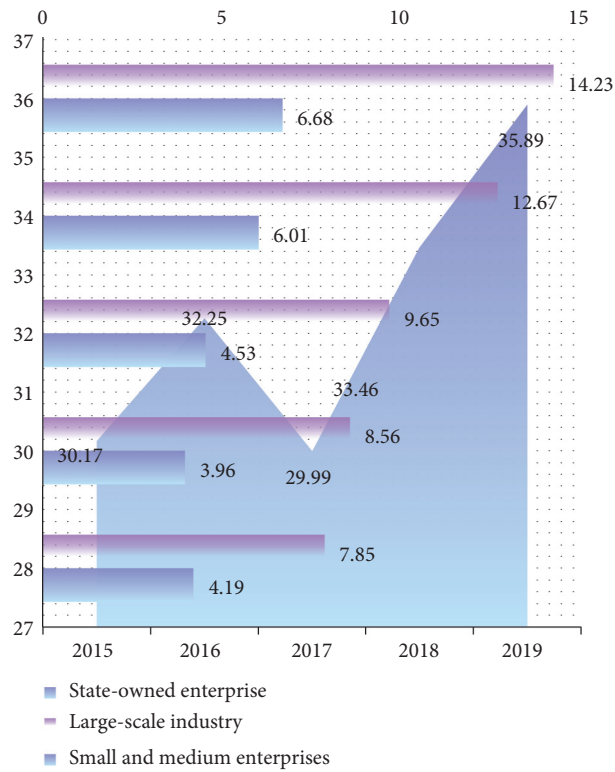


FIGURE 4: Corporate revenue under normal distribution (unit: ten million).

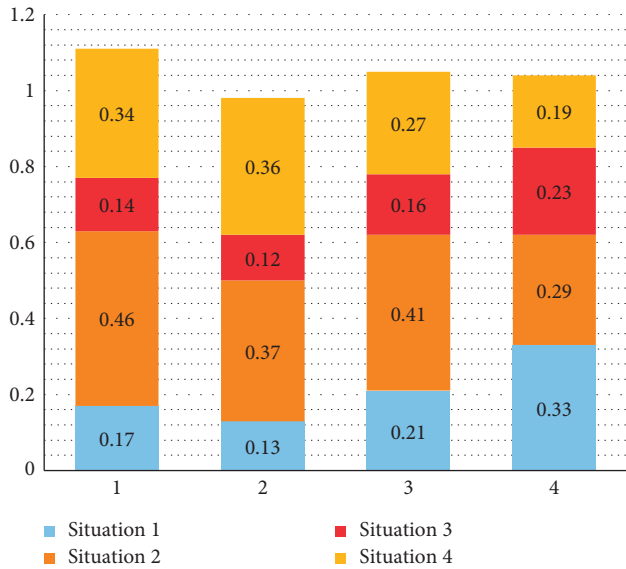


FIGURE 5: Local stability of mixed strategy game.

5. Conclusions

The understanding of environmental problems is constantly deepening, and the theory of solving environmental problems is constantly innovating. The understanding of environmental issues has evolved from the early days of environmental understanding to the theory of sustainable development on a global scale in the 1990s. In recent years, on the basis of the theory of sustainable development, the concept of environmental security has been gradually established and improved, and some theoretical systems have been formed to raise environmental security to a high level of understanding of national security and human survival. Regarding the model of solving environmental problems, the model of “circular economy” has been proposed and started to be established. It is required to use natural resources and environmental capacity in an environmentally friendly way to realize the ecological shift of economic activities. The efficiency of the green economy is an important indicator to measure the quality of current economic development. The theoretical and empirical analysis involved in the efficiency of the green economy still has broad room for expansion in the context of the new era.

At the beginning of the research, this paper summarized the relevant experience of the predecessors and proposed the analysis method of enterprise value chain operation mode under the background of green economy, including system theory analysis method, qualitative analysis and quantitative analysis combination method, comparative analysis method, and theory integration method. A cost control method for enterprise value chain under the background of green economy is proposed, which reduces the cost of enterprise products from a strategic point of view and maximizes the difference between the design activity cost driver coefficient and the information cost savings and the loss of cost calculation accuracy, which also includes the mixed-strategy

game Nash equilibrium. However, there are some shortcomings in this paper. The mastery of theoretical knowledge of supply chain management is relatively preliminary, which will have an impact on the interpretation of knowledge map. Because the overall grasp of supply chain management is not very sufficient, it will make the interpretation of this map more simple. In the future study, we should invest more time to improve theoretical cognition. With the increasing importance of supply chain management, the research of supply chain management is becoming more and more mature. For researchers, it is more and more important to sort out the research context and clarify the research hot-spots efficiently and intuitively.

This article analyzes the business value chain operation mode under the background of green economy. Traditional technology has problems such as low technical content, high resource consumption, and serious environmental pollution, which have become the bottleneck of its development. In order to achieve a balanced development of environment and interest, it is necessary to study the protection of value chain business models under the constraints of green environment. To this end, color textile companies should establish a distinct differentiation strategy, establish function settings, corporate culture, flat organization, and coordinated incentive mechanism structure. At the same time, a strong customer value management system should be relied on to establish a value chain business model with competitive advantages to realize the sustainable development of color textile enterprises.

Data Availability

No data were used to support this study.

Conflicts of Interest

The authors declare that they have no conflicts of interest regarding the publication of this paper.

References

- [1] L. Fabisiak, “Web service usability analysis based on user preferences,” *Journal of Organizational and End User Computing*, vol. 30, no. 4, pp. 1–13, 2018.
- [2] L. Yishu, “Wildlife management in China from the perspective of green economy development,” *Revista Cientifica*, vol. 10, no. 1, pp. 197–205, 2020.
- [3] D. D’Amato, N. Droste, B. Allen et al., “Green, circular, bio economy: a comparative analysis of sustainability avenues,” *Journal of Cleaner Production*, vol. 168, no. Dec.1, pp. 716–734, 2017.
- [4] K. McAfee, “Green economy and carbon markets for conservation and development: a critical view,” *International Environmental Agreements: Politics, Law and Economics*, vol. 16, no. 3, pp. 333–353, 2016.
- [5] B. Han, P. Zhang, H. Kuang, and M. Wan, “Screening of port enterprise value chain routines based on evolution equilibrium,” *Wireless Personal Communications*, vol. 102, no. 2, pp. 861–878, 2018.

- [6] E. Loiseau, L. Saikku, R. Antikainen et al., "Green economy and related concepts: an overview," *Journal of Cleaner Production*, vol. 139, pp. 361–371, 2016.
- [7] J. Su, C. Li, Q. Zeng, J. Yang, and J. Zhang, "A green closed-loop supply chain coordination mechanism based on third-party recycling," *Sustainability*, vol. 11, no. 19, p. 5335, 2019.
- [8] M. Ringel, B. Schlomann, M. Krail, and C. Rohde, "Towards a green economy in Germany? The role of energy efficiency policies," *Applied Energy*, vol. 179, pp. 1293–1303, 2016.
- [9] Å. Lindman and P. Söderholm, "Wind energy and green economy in Europe: measuring policy-induced innovation using patent data," *Applied Energy*, vol. 179, pp. 1351–1359, 2016.
- [10] L. Mundaca, L. Neij, A. Markandya, P. Hennicke, and J. Yan, "Towards a green energy economy? assessing policy choices, strategies and transitional pathways," *Applied Energy*, vol. 179, pp. 1283–1292, 2016.
- [11] N. Gregson, M. Crang, J. Botticello, M. Calestani, and A. Krzywoszynska, "Doing the 'dirty work' of the green economy: resource recovery and migrant labour in the EU," *European Urban and Regional Studies*, vol. 23, no. 4, pp. 541–555, 2016.
- [12] L. Mundaca and A. Markandya, "Assessing regional progress towards a 'green energy economy'," *Applied Energy*, vol. 179, pp. 1372–1394, 2016.
- [13] D. D'Amato, N. Droste, S. Chan, and A. Hofer, "The green economy: pragmatism or revolution? perceptions of young researchers on social ecological transformation," *Environmental Values*, vol. 26, no. 4, pp. 413–435, 2017.
- [14] J. Rifkin, "How the third industrial revolution will create a green economy," *New Perspectives Quarterly*, vol. 33, no. 1, pp. 6–10, 2016.
- [15] W. Dressler, J. De Koning, M. Montefrío, and J. Firn, "Land sharing not sparing in the "green economy": the role of livelihood bricolage in conservation and development in the Philippines," *Geoforum*, vol. 76, pp. 75–89, 2016.
- [16] K. Karakul and Aygülen, "Educating labour force for a green economy and renewable energy jobs in Turkey: a quantitative approach," *Renewable & Sustainable Energy Reviews*, vol. 63, pp. 568–578, 2016.
- [17] S. Amaruzaman, B. Leimona, M. Van Noordwijk, and B. Lusiana, "Discourses on the performance gap of agriculture in a green economy: a Q-methodology study in Indonesia," *International Journal of Biodiversity Science, Ecosystem Services & Management*, vol. 13, no. 1, pp. 233–247, 2017.
- [18] A. Verbeke and W. Yuan, "The impact of "distance" on multinational enterprise subsidiary capabilities," *Multinational Business Review*, vol. 24, no. 2, pp. 168–190, 2016.
- [19] D. Logue, A. Pitsis, S. Pearce, and J. Chelliah, "Social enterprise to social value chain: indigenous entrepreneurship transforming the native food industry in Australia," *Journal of Management & Organization*, vol. 24, no. 2, pp. 1–17, 2017.
- [20] D. J. Flanagan, D. A. Lepisto, and L. F. Ofstein, "Coopetition among nascent craft breweries: a value chain analysis," *Journal of Small Business and Enterprise Development*, vol. 25, no. 1, pp. 2–16, 2018.
- [21] R. Yadav and T. Mahara, "An exploratory study to investigate value chain of Saharanpur wooden carving handicraft cluster," *International Journal of System Assurance Engineering & Management*, vol. 9, no. 1, pp. 147–154, 2018.
- [22] D. Norell, E. Janoch, E. K. Mwesigwa, M. Tolat, M. Lynn, and E. C. Riley, "Value chain development with the extremely poor: evidence and lessons from CARE, Save the Children, and World Vision," *Enterprise Development & Microfinance*, vol. 28, no. 1-2, pp. 44–62, 2017.
- [23] C. Dahl, "The final frontier: E & P low-cost operating model," *The Energy Journal*, vol. 40, no. 3, pp. 263–266, 2019.
- [24] P. Khanna, "A governance operating model for open and distance learning institutions," *Education and Information Technologies*, vol. 24, no. 1, pp. 531–547, 2019.
- [25] Y. C. Ko, C. H. Lo, and S. W. Hsiao, "Interface design optimization by an improved operating model for college students," *Eurasia Journal of Mathematics Ence & Technology Education*, vol. 13, no. 9, pp. 2601–2625, 2017.
- [26] W. Wu, S. An, C.-H. Wu, S.-B. Tsai, and K. Yang, "An empirical study on green environmental system certification affects financing cost of high energy consumption enterprises-taking metallurgical enterprises as an example," *Journal of Cleaner Production*, vol. 244, p. 118848, 2020.
- [27] K. Antoniewicz, M. Jasinski, M. P. Kazmierkowski, and M. Malinowski, "Model predictive control of three-level four-leg flying capacitor converter operating as Shunt Active Power Filter," *IEEE Transactions on Industrial Electronics*, vol. 63, no. 8, pp. 5255–5262, 2016.
- [28] C. Kim, A. Dudin, O. Dudina, and J. Kim, "Queueing system operating in random environment as a model of a cell operation," *Industrial Engineering and Management Systems*, vol. 15, no. 2, pp. 131–142, 2016.
- [29] C. H. Hsueh, I. C. Wu, T. S. Hsu, and J. C. Chen, "An investigation of strength analysis metrics for game-playing programs: a case study in Chinese dark chess," *ICGA Journal*, vol. 40, no. 2, pp. 77–104, 2018.
- [30] I. Ghergulescu and C. H. Muntean, "A novel sensor-based methodology for learner's motivation analysis in game-based learning," *Interacting with Computers*, vol. 26, no. 4, pp. 305–320, 2018.
- [31] D. Lee and K. H. Baik, "Concealment and verification over environmental regulations: a game-theoretic analysis," *Journal of Regulatory Economics*, vol. 51, no. 3, pp. 235–268, 2017.

Research Article

Risk Aversion of Public Service Marketization Based on Fuzzy Analytic Hierarchy Process

Shoubin Qi¹ and Junwen Feng ²

¹School of Intellectual Property NUST, Nanjing University of Science and Technology, Nanjing 210094, Jiangsu, China

²School of Economics and Management NUST, Nanjing University of Science and Technology, Nanjing 210094, Jiangsu, China

Correspondence should be addressed to Junwen Feng; qishoubin@njust.edu.cn

Received 8 December 2020; Revised 23 February 2021; Accepted 19 March 2021; Published 30 March 2021

Academic Editor: Ming Bao Cheng

Copyright © 2021 Shoubin Qi and Junwen Feng. This is an open access article distributed under the Creative Commons Attribution License, which permits unrestricted use, distribution, and reproduction in any medium, provided the original work is properly cited.

With the development of China's economy, people's demand for public services is increasing. While meeting the public better through marketization, it is also easy to lead to some risks. The purpose of this study is to use the fuzzy analytic hierarchy process (FAHP) to evaluate the risk of public service marketization and make effective measures to avoid it. This study selects the Public Gymnasiums in different districts of our city as the research object and selects one as the nationalized public service place and the other as the market-oriented public service place. In this study, the amount of service, service equipment, service supervision status, and people's score under the situation of nationalization and marketization is used as the evaluation indexes of public service marketization. At the same time, combined with the fuzzy analytic hierarchy process (FAHP), the risks to the normal operation of the place after marketization are summarized. The results show that the turnover of the nationalized public service places is about 40 million yuan in the past five years, and the capital flow rate gradually decreases from 1.5%; while the market-oriented turnover reaches the maximum of 90 million yuan, the capital flow rate also rises to 2.21%. However, with the marketization, the scores are high and low. This shows that the marketization of public services leads to the improvement of service items and the increase of service charges. The conclusion is that the marketization of public services will have certain risks, but with the control and fine adjustment of enterprises, it is gradually supported by the public.

1. Introduction

New public management reform has appeared in the world. The marketization of public service is the main one [1]. It breaks the monopoly supply mode of the traditional public service government, introduces the market competition mechanism, and establishes a diversified supply organization with separation of production and supply. The key point of the composite model is the change in the quality and efficiency of public service supply. The marketization of public services has proved a considerable reform practice in improving the quality and efficiency of public services, reducing the financial pressure of the government, improving national satisfaction [2], and promoting the construction of a service-oriented government and a clean and efficient government. The marketization of public service has brought new brilliance and vitality to the

previously stopped public service. The reform plan with market intention has become the common choice of the government's public service reform.

The improved analytic hierarchy process method and fuzzy analytic hierarchy process are combined with qualitative evaluation and quantitative evaluation to comprehensively evaluate the market-oriented risk of public service [3] and lay a solid foundation for risk prevention and control. Moreover, the risk assessment suitable for enterprises is not only to meet the needs of market risk management but also to consider the principle of cost and benefit, improve the level of risk assessment and risk management in the public service market, effectively prevent the mechanization of risk assessment of comprehensive risk, and try to establish a risk caused by the lack of risk assessment after reform [4].

In his research on the marketization of public services, lunt analyzes a neglected factor in the marketization of public services. He examines overseas trade activities in the fields of health and criminal justice. This paper discusses the differences between these departments, their policies, and their driving forces. His focus on contrasting experiences is an opportunity to understand the complex and differentiated operational and structural environments in which this form of “public entrepreneurship” is expressed. The accuracy of his method is not high [5]. Gang and Hanwen think the provision of public services should be both universal, that is, independent of the social or economic status of the recipients, and contextual, that is, able to compensate for different local needs and conditions. Coordinating these two attributes requires various forms of innovation, mainly digital public service innovation. Based on the four-stage model of the United Nations e-government survey, this paper proposes a framework for developing such innovation, and takes transparency, participation, anticipation, personalization, CO creation, situational awareness, and situational intelligence services (including actual cases) as the initial set of innovation. It also outlines the new technology, organizational and policy related government capabilities needed to participate in digital public service innovation [6]. But its approach is not stable [7]. In the study of Rajabi F, fuzzy analytic hierarchy process (FAHP) and fuzzy additive ratio evaluation (ARAS-F) were used to identify and rank the control measures of violence among medical staff. In the first stage, through the review of previous studies, his method identified and extracted the most common violence standards and control programs. In the next phase, he uses the FAHP criteria for priority control measures. Finally, he used the ARAS-F method to give priority to control measures of workplace violence. His method is not practical [8]. Gaber et al.’s research attempts to overcome the lack of reliable estimation of Malaysian users’ willingness to pay for public transport (especially buses) through a fuzzy analytic hierarchy process (FAHP) [9]. This is a breakthrough research. He tries to evaluate the satisfaction factors of bus users based on FAHP and uses the application to find the pattern of WTP characteristics by shortening travel time. Data were collected from public transport users’ intentions in Kuala Lumpur, Malaysia. His method is not convincing [10].

This paper first introduces the concept of public service and the detailed problems encountered in the process of marketization. Then, it also describes the risk aversion of payment methods and risk research methods, including literature induction, questionnaire survey, and quantitative and qualitative analysis. This research mainly uses the fuzzy analytic hierarchy process, which is mainly composed of a fuzzy judgment matrix and analytic hierarchy process. This study takes the public sports facilities in different districts of our city as the research object and, respectively, discusses the development status and the public evaluation under the situation of nationalization and marketization. Combined with the experimental results, this paper analyzes the current situation of public service market-oriented project supervision, the importance of regulatory measures, the

market-oriented business amount analysis, and scoring analysis. So as to avoid the risk of public service marketization, this paper mainly studies the risk aversion of public service marketization based on a fuzzy analytic hierarchy process. First of all, using the method of literature review, this paper gives a brief overview of public service and fuzzy analytic hierarchy process, then establishes the model of this paper combined with the two, and finally analyzes all aspects of public service according to the model.

2. Marketization of Public Service and Fuzzy Analytic Hierarchy Process

2.1. Concept of Public Service. In our country, the main areas of public service are public security service, public sports service, public health service, public education service, public security service, public law service, and public policy service. Because the field of public service is very extensive, we cannot use a unified concept to define the “public service.” At present, the main opinions on “public service” are as follows [11, 12].

First, in our country, public service is one of the contents of “serving the people” that the government often emphasizes. The general attribute of responsibility and work is a common term in all government work to make up for the defects of the market and promote social justice. Second, public service refers to the responsibility, and responsibility of the government led public goods and service departments to produce and supply pure public goods, public goods, mixed public goods, and special folk goods. It refers to the public goods and services produced by the whole society for common consumption and equal enjoyment. Fourth, public service refers to the public goods produced by the government and nongovernmental organizations in the process of handling public business [13].

2.2. Problems in the Process of Public Service Marketization

2.2.1. Lack of Public Responsibility Brought by Marketization. In the process of market-oriented reform, some local governments are more worried about the change of government functions, the reduction of personnel, and the solutions to financial and investment problems [14], but they have not formulated countermeasures and underestimated the potential gap of public responsibility after marketization. We hope to take preventive measures or reduce the responsibility of the government subjectively. Because enterprises and nongovernmental organizations have no obligation to undertake social public responsibility, they sometimes lose public responsibility for the purpose of pursuing interests. Therefore, the government cannot bear the public responsibility; on the contrary, it should formulate the relevant laws and regulations for the management and supervision of enterprises and nongovernmental organizations and bear the corresponding responsibilities [15]. Public service can be marketized, but public responsibility cannot be marketized [16, 17].

2.2.2. Marketization Causes the Loss of State-Owned Assets.

The loss of state-owned assets, reflected in the loss of government finance and state-owned enterprises, will eventually damage the interests of the state. Taking the cooperation between the government and the people as an example, the government uses several public service projects such as infrastructure construction, water supply, and power supply to cooperate with nonstate-owned funds [18], and each party has a certain share. Due to the lack of funds from the state-owned government, the proportion of joint ventures is only offset by the discount of fixed assets, and the nonstate-owned capital actually contributes to the capital [19].

This general marketization method is due to the reformers' lack of necessary knowledge and skills, the lack of perfect supervision and restriction mechanism, and the lack of scientific evaluation methods [20], resulting in the direct loss of state-owned assets (improper behavior of managers) and indirect losses (under evaluation). This kind of situation often occurs in the early stage of marketization, especially the asset loss of small and medium-sized state-owned enterprises with poor efficiency.

2.2.3. Marketization Causes Fairness Problems.

Public services and the security of public services must be fair and just, reflecting social equity to the maximum extent. Public service is not inherent to a few people but must have universal significance. However, the marketization of public services follows the same exchange principle. The services with low payment capacity or no services at all decline and cannot be accessed. The hierarchical situation of public services is formed. On the premise of insufficient total public services, the disadvantaged groups can obtain very few public service goods, which cannot meet their basic living needs [21, 22].

In the market situation, in order to improve profits, producers will choose the service items with high profitability, but the profitability is low, but they may be denied to provide the services that need to be provided. Consumers can choose various types and levels of services [23], but people who live in difficulties have limited ability to pay, so they lose the right to choose [24].

2.3. Risk Aversion of Payment Methods in Public Services.

Government functions must strictly control the scope of user payment for applications. The user's payment is only applicable to the relatively high operating cost and crowded public facilities resources and does not import the user's payment to the project with a lower operating cost.

In order to prevent the complete privatization of public resources, it is necessary to monitor the price of public goods, control the price within a reasonable range, and adopt subsidies to socially disadvantaged groups to ensure the publicity principle of public service supply. This can effectively avoid the risk of this model [25, 26].

In short, in the case of market economy, the supply of public sports must follow the application form of market intention. In this case, the cost is inevitable and is the necessary condition to maintain the public supply. In the

user charging mode, in order to solve the problem of price setting mechanism, the two-part price setting method is relatively advanced. It has the value of practical application and improvement. At the same time, this market-oriented application mode needs to pay attention to the possible risks and strengthen the use of risk management.

2.4. Research Methods of Public Service Marketization Risk

- (1) Literature induction: most of the research results used in the coding part of the theory are obtained from the library and Internet resources. After reading a lot of domestic and foreign public service outsourcing knowledge, they have formed their own unique series of knowledge systems and selected a valuable part for research. The theory and literature summary used in this paper will be obtained through comparison [27, 28].
- (2) Qualitative analysis: the research idea starts from the research results at home and abroad, summarizes the research results of previous scholars, points out the nature of public service outsourcing directly, and puts forward the research framework of this paper, which determines that the decision-making stage, implementation stage, and introduction stage of service outsourcing process are divided into two stages [29]. The corresponding risk avoidance strategies are proposed from three aspects.
- (3) Quantitative analysis method: in the qualitative analysis of public service outsourcing, the risk of public service outsourcing is quantified through a data model, which makes the analysis results more convincing [30].
- (4) Questionnaire survey method: as a case study, through the questionnaire survey of government agencies and the corresponding third-party service consulting agencies, we get valuable data, conduct model analysis, and finally grasp the risk situation of China's public service outsourcing [31].

2.5. Fuzzy Analytic Hierarchy Process

2.5.1. Analytic Hierarchy Process.

Analytic hierarchy process is a systematic and multifunctional decision analysis method with a multilevel structure, which is characterized by the combination of qualitative analysis and quantitative analysis. Enterprise risk assessment and analysis is a complex practical problem. After the application of the analytic hierarchy process, the indicators of multiple complex problems are found, and they are decomposed into target level, benchmark level, index level, and other levels to form a hierarchical evaluation model. By selecting a specific quantitative proportion, all indicators are quantified to the same level, and the judgment matrix is constructed by a pairwise comparison of indicators. Through the individual ranking of each level and the ranking of the whole level, the relative importance of the indicators is determined, and the indicators are analyzed and judged by calculating the weight of

the indicators, and finally, a comprehensive decision is made. The model architecture of the analysis hierarchy process is shown in Figure 1 [32, 33].

2.5.2. Calculation Steps of Analytic Hierarchy Process. The calculation sequence of the analysis hierarchy process is mainly composed of the following contents. The first is to determine the problems of evaluation and analysis, the second is to build a multilevel structure, the third is to form a judgment matrix based on multiple clear hierarchical structures, and the fourth is to implement the hierarchical structure: single sort and whole sort. The specific steps are as follows [34].

The first is to sort out the overall objective of evaluation problems, determine the problems that need decision-making, and clarify the relationship with relevant index elements through comprehensive analysis.

Second, construct a multilevel structure. The multilevel structure model of the analytic hierarchy process is mainly divided into three levels (target, benchmark, and plan). In terms of the number of indicator elements in each level, the target layer is usually uniquely determined, with multiple baseline and planning layers. Indicator elements correspond to indicators at multiple reference levels and indicators at multiple program levels [35, 36].

The third is to form a judgment matrix. After comparing the two indicator elements, assume that there are n indicator elements so that the i and ji target ($i = 1, 2, \dots, n$). The importance degree of the index element is a_{ij} , and the n -order judgment matrix $(a_{ij})_{n \times n}$ is obtained. The determination matrix is the value that compares the importance of index elements at the same level with the importance of corresponding index elements after the previous level. The decision matrix is as follows:

$$A = \begin{bmatrix} a_{11} & a_{12} & \dots & a_{1n} \\ a_{21} & a_{22} & \dots & a_{2n} \\ \dots & \dots & \dots & \dots \\ a_{n1} & a_{n2} & \dots & a_{nn} \end{bmatrix}. \quad (1)$$

In the process of analyzing hierarchy, the importance of judgment matrix is judged by the ratio of 1 to 9. That is, the relative importance indicator can be replaced by a number. Specifically, it can be summarized as simple as 1, and the two indicator elements are equally important. The numbers 3, 5, 7, and 9 are important benchmarks. Among the two index elements compared, the index element (i) of the former is more important than the index element (j) of the latter, and the second is the slightly important and relative element (Important, very important, especially important). If numbers 2, 4, 6, and 8 are displayed, the relative importance of the two compared index elements is expressed in the middle of the adjacent importance. When the importance is reciprocal of each other, it will reflect the opposite value of

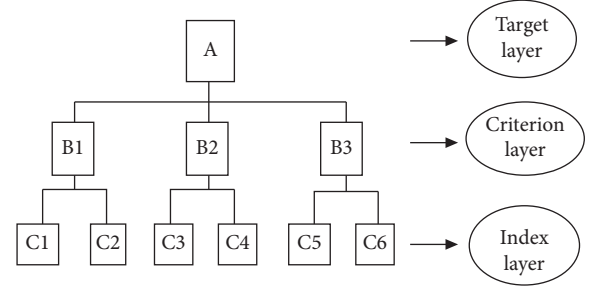


FIGURE 1: Analytic hierarchy process model architecture.

the importance scale. For example, the importance scale used to compare element index i and element index j is a_{ij} , and the importance scale for comparing element index j with element index i is $1/a_{ij}$.

If the index elements of the judgment matrix are determined by the ratio of 1 to 9, the matching index of the judgment matrix needs to be tested:

$$CI = \frac{(\lambda_{\max} - n)}{(n - 1)}. \quad (2)$$

The match index of the determined matrix depends on the value of CI. For the calculation results, the larger the CI value, the greater the matching deviation of the judgment matrix. On the contrary, the smaller the calculated value of CI, the lower the consistency of the decision matrix and the greater the degree. In addition, the calculated value of CI will also be affected by the order of the decision matrix. With the increase of the calculated value of Ci, the influence of deviation will gradually increase. The average random matching index is imported into the decision matrix [37]. Thus, the order of the decision matrix can be prevented from affecting the integrated index CI. The random index is omitted as RI, and its value depends on the order [38].

When judging the matching of the matrix, the order of the matrix is used as a reference. When the matrix is completely matched, the order of the matrix is 1 or 2. If the order of CR is greater than 3, the random matching rate must be calculated in the matching check:

$$CR = \frac{CI}{RI}. \quad (3)$$

The reference standard of the matrix matching test is random matching ratio $CR = 0.1$. When Cr is less than 0.1, it means that the decision matrix has passed the integration test. Otherwise, the decision matrix does not meet the requirements of integration testing. At this point, the judgment value needs to be adjusted to pass the integration test.

The fourth is to solve the hierarchical ranking of weights. There are two kinds of hierarchical sorting: first level sorting and total level sorting. For single rank sorting, the maximum eigenvalue of the determined matrix must be calculated. The maximum eigenvalue has the corresponding eigenvector calculation [39]. The calculation method includes root

detection and multiplication. After sorting the importance of index elements at the same level as the parent level, the total level is sorted based on the sorting results.

2.5.3. *Fuzzy Judgment Matrix.* The weight of the fuzzy judgment matrix is calculated. In the process of fuzzy analysis hierarchy, it is necessary to use a fuzzy decision matrix to calculate the weight. The calculation method of weight:

$$\omega_i = \frac{(\sum_{j=1}^n a_{ij} + (n/2) - 1)}{n(n-1)} \quad (4)$$

When the vector $\omega = (\omega_1, \omega_2, \dots, \omega_n)$ is the sorted vector of fuzzy complementary matrix A , then the matrix W representing the weight of a is $(\omega_{ij})_{n \times n}$, and the values of $\omega_{ij} = \omega_i - \omega_j + 0.5$, i and j are 1, 2, ..., n .

In the process of fuzzy analysis hierarchy, the construction of a fuzzy decision matrix is completed. After checking the consistency of the fuzzy decision matrix, the ranking of single level and total level is calculated according to the same steps as the analysis hierarchy process. The single time method of each level is consistent with the analytic hierarchy process. In this paper, the characteristic root method is used.

- (1) Calculate the total of each column in the fuzzy matrix:

$$a_j = \sum_{i=1}^n a_{ij} \quad (i, j = 1, 2, \dots, n) \quad (5)$$

- (2) The standard fuzzy decision matrix is established. The elements of the fuzzy decision matrix are divided by the sum of the corresponding columns to obtain a new fuzzy decision matrix:

$$b_{ij} = \frac{a_{ij}}{a_j} \quad (i, j = 1, 2, \dots, n) \quad (6)$$

- (3) Get the normalized weight of each indicator element. Specifically, the average value of each row of the standard fuzzy judgment matrix is calculated:

$$b_j = \frac{\sum_{i=1}^n b_{ij}}{n} \quad (i, j = 1, 2, \dots, n) \quad (7)$$

Different from the general analytic hierarchy process, if the fuzzy analytic hierarchy process is adopted, the total ranking weight w is calculated:

$$w_j = \sum_{i=1}^n w_i w_{ij} \quad (8)$$

where w_j represents the j -th index element of the total weight w of the hierarchy; w_i represents the weight of the i -th criterion level relative to the total target level; w_{ij} represents the weight of the j -th element index corresponding to the i -th criterion level.

3. Fuzzy Analytic Hierarchy Process Model of Public Service Marketization

3.1. *Research Object.* Based on the research on the relevant concepts of the market-oriented mode of urban public sports service supply in China, this study takes 18 swimming pools randomly selected from 9 districts (2 swimming pools in each region) as the investigation objects. This paper mainly investigates the current situation of swimming pool operators, coaches, and other related swimming pool practitioners and social sports organizations participating in public sports service.

3.2. Model Construction of Fuzzy Evaluation Method

3.2.1. *Establishment of Evaluation Index System.* Index system is the basis of fuzzy evaluation and the concrete content of things evaluation. Rating elements, such as audio, can be set at multiple levels as needed. The elements of the first level are "price," "mode," etc. Layers can adjust the mode to surround, 3D, and other sides.

3.2.2. *Determination of Evaluation Set.* The evaluation set is different from the evaluation index set. It is mainly based on a variety of analysis problems and makes comments on the evaluation results of each interval according to the needs. Its nature is to provide a framework for the final model processing results. According to the needs of evaluation, the evaluation level is divided into different levels (high, medium, low, very good, good, fair, bad, etc.).

3.2.3. *Determination of Weight.* In the analysis and evaluation, after the indicator system is determined, the importance of these individual indicators must be scored when explaining the items. Because the size of the weight will ultimately have a greater impact on the evaluation results, the determination of the weight is objective, and the weight must be determined as much as possible. There are more in every aspect of the matter. The actual weight coefficient can be flexibly determined according to the characteristics of the evaluated things, but the general principle is that the total weight is 1 regardless of the actual working conditions.

3.2.4. *Comprehensive Evaluation Model.* After obtaining the weight and the evaluation results of a single element, the final result of the two products must correspond to the evaluation set established in the second step if the annotation corresponding to the maximum value is selected according to the principle of maximum membership, the final result of the evaluation.

4. Public Service Marketization and Risk Aversion Analysis

4.1. *Analysis of the Current Situation of Public Service Marketization Project Supervision.* Since 2013, the Chinese government has paid more attention to the cooperation between the government and the people and has issued a

series of documents to standardize and explain the cooperation mode between the government and the people, making up for the lack of legal provisions on the current comprehensive cooperation mode between the government and the people. At the same time, it is also an encouragement to the nongovernmental sectors, which provides a good regulatory environment for participating in the cooperation projects between the government and the people, and improves their trust in the cooperation between the government and the people. The evaluators of this paper are the government and enterprises. Public service has always been dominated by the government. However, after the marketization of public service, the participants have become more and more, which can better reflect the determination of the government to marketize public service and also a kind of trust in enterprises. As shown in Figure 2, the limited number of documents issued by the government for government civilian cooperation projects.

Figure 2 shows the number of regulatory documents issued by the government and different governments at various levels for the government people cooperation projects in the past five years. The model is associated. In addition, the report classified the information published on the relevant websites of the Ministry of Finance and found that the regulatory documents were basically guidelines, with few laws and regulations.

4.2. Analysis of the Importance of Public Service Marketization Supervision Measures. Next, descriptive statistics will be used to analyze the importance of project related regulatory measures and the significance of project construction supervision and supervision measures and draw corresponding analysis conclusions. The descriptive statistics of project construction supervision measures are shown in Table 1.

According to the data in Table 1, the highest average score is the government's supervision of private sector visits. It is not difficult to understand that a high-quality private sector is key to implementing cooperative projects effectively. Because infrastructure projects need a relatively large amount of funds, the supervision of funds during the construction period is, of course, the third under the supervision of the government. To ensure the safety of funds is not only to ensure the smooth completion of the project but also to prevent corruption and not violate the interests of the society. The statistical description of project service supervision measures is shown in Table 2.

According to the data in Table 2, the highest average score is the supervision of service price. Public facilities in order to use public facilities need to pay a certain fee. If the price is too high, it will not only lose the public welfare attribute of the project but also bring a negative impact to the direct experience of consumers using the project, which will damage the social usefulness of the project. The service quality of the project in use can be directly measured whether the private sector provides high-quality services.



FIGURE 2: Broken line chart of the number of normative documents issued by the government for public private partnership projects.

4.3. Analysis of Business Amount of Public Service Marketization. Figure 3 shows the turnover of nationalization and marketization of public services.

Figure 3 reflects the profitability related data indicators after the marketization of public services. From the point of view of net asset ratio and total profit rate, there are few examples of government control of net assets and total profits. After marketization, capital and profits have increased significantly. This shows that marketization makes the real value and market competition more clear.

Figure 4 shows the capital flow ratio of nationalization and privatization of public services.

As can be seen from Figure 4, the debt data indicators of market-oriented public service companies include current ratio, demand ratio, asset liability ratio, and other indicators to objectively reflect the company's ability in the past five years and test whether it has potential possibility. Investigate whether there are tax risks caused by financial risks and capital flow difficulties. The profitability of a business is inseparable from the effective turnover rate of funds used. The closely related debt indicators are the current ratio, which, respectively, represents the ratio of current assets and current assets to current liabilities. A high current ratio means that assets are highly liquid but not too high. If it is too high, it will occupy more funds, affect the capital turnover rate, and the profitability will decline.

The appropriate benchmark for current ratios is 2 and for current ratios is 1. In order to measure the capacity of an enterprise, it is necessary to combine the indicators of current ratio and demand ratio. From the changes of the current ratio and current ratio of public service companies in the past five years from 2015 to 2019, both sides have moved

TABLE 1: Descriptive statistics of the importance degree of project construction supervision measures.

	Number of samples	Minimum value	Maximum	Average value	Standard deviation
Entry criteria	74	1	5	4.28	0.948
Construction safety	74	1	5	3.69	0.901
Project progress	74	1	5	3.73	1.021
Construction quality	74	2	5	4.26	0.735
Capital security	74	1	5	3.99	1.017

TABLE 2: Descriptive statistics of importance degree of project service supervision measures.

	Number of samples	Minimum value	Maximum	Average value	Standard deviation
Service quality	74	1	5	3.99	0.934
Service price	74	2	5	4.13	0.891
Operating costs	74	1	5	3.84	1.121
Scope of services	74	1	5	3.71	1.207

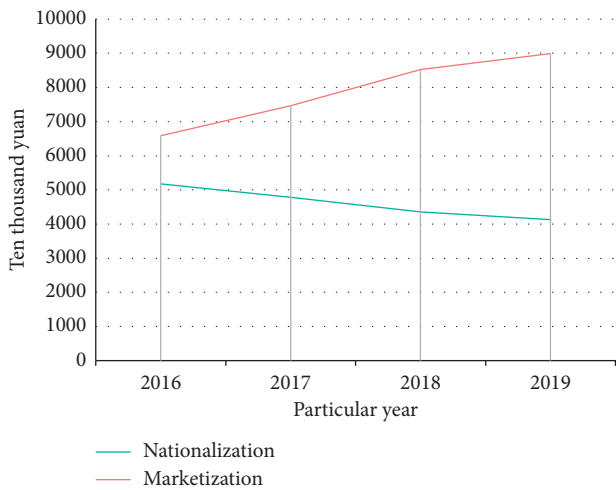


FIGURE 3: Turnover of nationalization and marketization of public services.

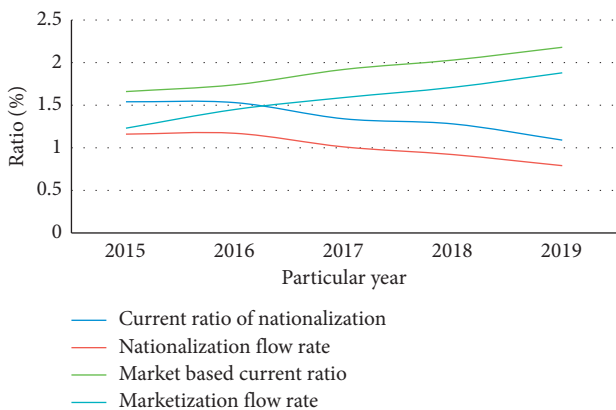


FIGURE 4: Capital flow ratio of nationalization and privatization of public services.

in a relatively stable range. After 2017, the current ratio has increased significantly, close to the reference value of 2, and the demand ratio has also increased significantly compared with 2018, reflecting the trend of these two indicators. The

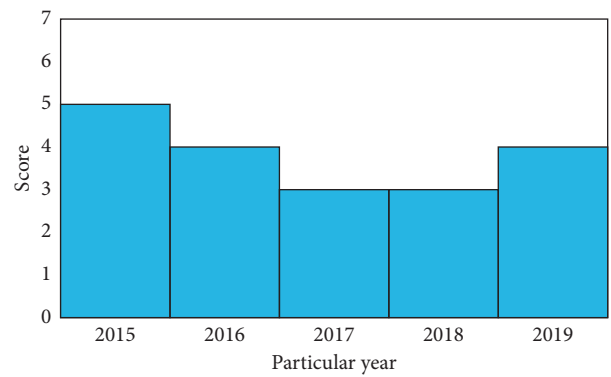


FIGURE 5: Public service marketization score.

situation and index trend are basically the same, the liquidity of assets is strongly guaranteed, and the company is able to repay its debts. There is no tax risk caused by the company's capital flow difficulties.

4.4. *Public Service Analysis Score.* Figure 5 shows the public service marketization score.

As can be seen from Figure 5, after the marketization of public services, at first, the public had a high evaluation of the measure, but as time went on, people were dissatisfied with the measure, and the score dropped. It is because the amount of service caused by marketization has increased a lot compared with the previous period, which has been resisted by many people. After that, the phenomenon of improvement shows that the market-oriented public service is improving step by step and moving towards the direction of being more accepted and loved by the people.

5. Conclusion

This paper mainly studies the risk aversion of public service marketization based on the Fuzzy Analytic Hierarchy Process (FAHP). It uses the methods of literature review, fuzzy analytic hierarchy process (FAHP), and mathematical model and establishes the risk aversion model of public service marketization. Finally, it analyzes the current

situation of public service marketization risk in China and distinguishes the risks according to the degree of influence. The research of this paper is mainly through the reform of public service marketization, adjusting government functions, and improving the level of public service optimization governance.

This paper analyzes the marketization of public service from the perspective of government propaganda and discusses the realization and separation of the public service marketization reform plan publicized by the government. This paper discusses the relevant theories and historical process of marketization of public service. Secondly, by comparing the previous public service supply mode with the multiagent supply mode of market intention, this paper analyzes the realization of government propaganda through marketization, mainly including the optimization of market-oriented reform scheme. We should allocate resources, relieve government pressure, break government monopoly, adjust government functions, introduce market mechanisms, improve service efficiency, strengthen citizen participation, and promote the realization of democracy.

The risk of public service marketization is not certain but a dynamic process accompanied by environmental changes. From the government's market-oriented choice to the implementation and supervision of enterprises, and finally, to the evaluation of market-oriented quality, there are various risks in each stage, the types of various risks and the impact on the market-oriented quality of public services. The analysis and comparison of these risk factors and the subsequent risk aversion are the basis of decision-making. In this stage, the marketization of public service should start from reality, improve the system of paying attention to public satisfaction, cultivate and develop social organizations, expand the scope of a public service purchase, improve the supervision and evaluation mechanism of public service marketization, effectively improve the government's optimal governance, avoid risks to the maximum extent, and promote the marketization of public service into standardization and scientific development.

Data Availability

The data underlying the results presented in the study are available within the manuscript.

Conflicts of Interest

The authors declare that they have no conflicts of interest.

References

- [1] J. Chen, X. Wang, and Z. Chu, "Capacity sharing, product differentiation and welfare," *Economic Research-Ekonomska Istraživanja*, vol. 33, no. 1, pp. 107–123, 2020.
- [2] H. Kim, "Investigating the mediating role of social networking service usage on the big five personality traits and on the job satisfaction of Korean workers," *Journal of Organizational and End User Computing*, vol. 31, no. 1, pp. 110–123, 2019.
- [3] Y. T. Chen, C. H. Chen, S. Wu, and C. C. Lo, "A two-step approach for classifying music genre on the strength of AHP weighted musical features," *Mathematics*, vol. 7, no. 1, p. 19, 2019.
- [4] Y.-H. Yuan, S.-H. Tsao, J.-T. Chyou, and S.-B. Tsai, "An empirical study on effects of electronic word-of-mouth and Internet risk avoidance on purchase intention: from the perspective of big data," *Soft Computing*, vol. 24, no. 8, pp. 5713–5728, 2020.
- [5] N. Lunt, "The entrepreneurial state: service exports in healthcare and criminal justice," *Journal of International & Comparative Social Policy*, vol. 33, no. 1, pp. 1–18, 2017.
- [6] L. Gang and Z. Hanwen, "An ontology constructing technology oriented on massive social security policy documents," *Cognitive Systems Research*, vol. 60, pp. 97–105, 2020.
- [7] J. Bertot, E. Estevez, and T. Janowski, "Universal and contextualized public services: digital public service innovation framework," *Government Information Quarterly*, vol. 33, no. 2, pp. 211–222, 2016.
- [8] F. Rajabi, M. Jahangiri, F. Bagherifard, S. Banaee, and P. Farhadi, "Strategies for controlling violence against health care workers: application of fuzzy analytical hierarchy process and fuzzy additive ratio assessment," *Journal of Nursing Management*, vol. 28, no. 4, pp. 777–786, 2020.
- [9] T. Gaber, S. Abdelwahab, M. Elhoseny, and A. E. Hassanien, "Trust-based secure clustering in WSN-based intelligent transportation systems," *Computer Networks*, vol. 146, pp. 151–158, 2018.
- [10] S. J. Hashem, B. Peyman, and Y. Nur, "The combination of a fuzzy analytical hierarchy process and the taguchi method to evaluate the Malaysian users' willingness to pay for public transportation," *Symmetry*, vol. 8, no. 9, pp. 1–17, 2016.
- [11] M. B. Hansen and A. C. Lindholst, "Marketization revisited," *International Journal of Public Sector Management*, vol. 29, no. 5, pp. 398–408, 2016.
- [12] L. Li and R. C. K. Chan, "Contesting China's engagement with neoliberal urbanism," *Asian Education and Development Studies*, vol. 6, no. 1, pp. 44–56, 2017.
- [13] L. T. Christensen, "Passenger rail SOEs as domestic institutional market actors," *International Journal of Public Sector Management*, vol. 31, no. 2, pp. 128–141, 2018.
- [14] J.-Y. Yeh and C.-H. Chen, "A machine learning approach to predict the success of crowdfunding fintech project," *Journal of Enterprise Information Management*, vol. 28, no. 5, pp. 924–944, 2020.
- [15] S.-B. Tsai, R. Saito, Y.-C. Lin et al., "Discussing measurement criteria and competitive strategies of green suppliers from a Green law Perspective," *Proceedings of the Institution of Mechanical Engineers, Part B: Journal of Engineering Manufacture*, vol. 229, no. S1, pp. 135–145, 2015.
- [16] J. Ohlsson and H. Sjøvaag, "Protectionism vs. Non-interventionism: two approaches to media diversity in commercial terrestrial television regulation," *Javnost—The Public*, vol. 26, no. 1, pp. 70–88, 2018.
- [17] M. Gabrielle, T. Lundström, M. Sallns et al., "Big business in a thin market: understanding the privatization of residential care for children and youth in Sweden," *Social Policy & Administration*, vol. 50, no. 7, pp. 805–823, 2016.
- [18] Z. Lv, B. Hu, and H. Lv, "Infrastructure monitoring and operation for smart cities based on IoT system," *IEEE Transactions on Industrial Informatics*, vol. 16, no. 3, pp. 1957–1962, 2020.
- [19] B. Jantz, T. Klenk, F. Larsen et al., "Marketization and varieties of accountability relationships in employment services:

- comparing Denmark, Germany, and great britain,” *Administration & Society*, vol. 14, no. 3, pp. 501–520, 2016.
- [20] Y. Tang and M. Elhoseny, “Computer network security evaluation simulation model based on neural network,” *Journal of Intelligent & Fuzzy Systems*, vol. 37, no. 3, p. 3197, 2019.
- [21] K. Kateřina and J. Havlíková, “Current developments in social care services for older adults in the Czech republic: trends towards deinstitutionalization and marketization,” *Journal of Social Service Research*, vol. 42, no. 2, pp. 180–198, 2016.
- [22] T. Kotkas, “From official supervision to self-monitoring: privatizing supervision of private social care services in Finland,” *Social Policy & Administration*, vol. 50, no. 5, pp. 599–613, 2016.
- [23] L. Fabisiak, “Web service usability analysis based on user preferences,” *Journal of Organizational and End User Computing*, vol. 30, no. 4, pp. 1–13, 2018.
- [24] S. Wang, “Innovation of tourism public service mechanism of wisdom tourism based on neural network,” *Boletin Tecnico/ Technical Bulletin*, vol. 55, no. 20, pp. 82–89, 2017.
- [25] R. Engelbrecht-Wiggans and E. Katok, “A direct test of risk aversion and regret in first price sealed-bid auctions,” *Decision Analysis*, vol. 6, no. 2, pp. 75–86, 2016.
- [26] S. Opper, V. Nee, and H. J. Holm, “Risk aversion and guanxi activities: a behavioral analysis of CEOs in China,” *Academy of Management Journal*, vol. 60, no. 4, pp. 1504–1530, 2017.
- [27] M. Berardi, “Endogenous time-varying risk aversion and asset returns,” *Journal of Evolutionary Economics*, vol. 26, no. 3, pp. 581–601, 2016.
- [28] L. Eeckhoudt, L. Liu, and J. Meyer, “Restricted increases in risk aversion and their application,” *Economic Theory*, vol. 64, no. 1, pp. 1–21, 2017.
- [29] C.-L. Wei and C.-T. Ho, “Exploring signaling roles of service providers’ reputation and competence in influencing perceptions of service quality and outsourcing intentions,” *Journal of Organizational and End User Computing*, vol. 31, no. 1, pp. 86–109, 2019.
- [30] M. Carey, “Journey’s end? From residual service to newer forms of pathology, risk aversion and abandonment in social work with older people,” *Journal of Social Work*, vol. 16, no. 3, pp. 344–361, 2016.
- [31] K.-H. Lee and S. S. Hyun, “A model of value-creating practices, trusting beliefs, and online tourist community behaviors,” *International Journal of Contemporary Hospitality Management*, vol. 28, no. 9, pp. 1868–1894, 2016.
- [32] S. Oh, J. Rhodes, and R. Strong, “Impact of cost uncertainty on pricing decisions under risk aversion,” *European Journal of Operational Research*, vol. 253, no. 1, pp. 144–153, 2016.
- [33] T. O’Donoghue and J. Somerville, “Modeling risk aversion in economics,” *Journal of Economic Perspectives*, vol. 32, no. 2, pp. 91–114, 2018.
- [34] Z. Chang, S. Song, Y. Zhang, J.-Y. Ding, R. Zhang, and R. Chiong, “Distributionally robust single machine scheduling with risk aversion,” *European Journal of Operational Research*, vol. 256, no. 1, pp. 261–274, 2017.
- [35] S. Nicholson-Crotty, J. Nicholson-Crotty, and S. Fernandez, “Performance and management in the public sector: testing a model of relative risk aversion,” *Public Administration Review*, vol. 77, no. 4, pp. 603–614, 2017.
- [36] M. Yazdi, “Retracted article: an extension of the fuzzy improved risk graph and fuzzy analytical hierarchy process for determination of chemical complex safety integrity levels,” *International Journal of Occupational Safety and Ergonomics*, vol. 25, no. 4, pp. 551–561, 2019.
- [37] A. Liu, Y. Xiao, H. Lu, S. B. sai, and W. Song, “A fuzzy three-stage integrated multi-criteria decision-making approach based on customer needs for sustainable supplier selection,” *Journal of Cleaner Production*, vol. 239, no. 5, p. 118043, 2019.
- [38] F. Salehian, J. Razmi, and F. Jolai, “A hybrid ranking approach based on fuzzy analytical hierarchy process and data envelopment analysis: road maintenance and transport organization of Iran,” *Journal of Intelligent & Fuzzy Systems*, vol. 34, no. 4, pp. 2373–2383, 2018.
- [39] B. Cao, J. Zhao, P. Yang et al., “Multiobjective feature selection for microarray data via distributed parallel algorithms,” *Future Generation Computer Systems*, vol. 100, pp. 952–981, 2019.

Research Article

Construction of Control Rights Allocation Index of Listed Companies Based on Neural Network and Machine Learning

Tao Zhang^{1,2} and Yuxiang Peng¹ 

¹School of Economics and Management, Xi'an University of Technology, Xi'an 710048, Shaanxi, China

²Business School, Gansu University of Political Science and Law, Lanzhou 730070, Gansu, China

Correspondence should be addressed to Yuxiang Peng; 1180511013@stu.xaut.edu.cn

Received 17 December 2020; Revised 20 February 2021; Accepted 9 March 2021; Published 22 March 2021

Academic Editor: Ming Bao Cheng

Copyright © 2021 Tao Zhang and Yuxiang Peng. This is an open access article distributed under the Creative Commons Attribution License, which permits unrestricted use, distribution, and reproduction in any medium, provided the original work is properly cited.

Control power is a core issue that every listed company pays great attention to. The company's shareholding structure directly affects the allocation of control rights. Therefore, the shareholding structure of listed companies is analyzed, and various factors related to the allocation of company control rights are discussed. It is very important to build indicators of control allocation of listed companies and improve the governance model of listed companies. Based on this, this article proposes to use neural networks and machine learning techniques to build related models and solve related problems. This article takes the control allocation index of listed companies on the SSE and SZSE platforms under good securities' market conditions as the research object and takes the stock holding allocation of listed companies as a reference for the control allocation index. Combine sliding removal technology and approximate entropy with sample entropy, select the sliding window and sliding step size as 21 data, keep the sliding window unchanged, and calculate the approximate entropy and sample entropy of the sequence after removing 21 data for each sliding value to analyze the correlation between the rate of return, complexity, and effectiveness. The results of the study show that the mean and median of the majority shareholder's equity pledge behavior are 0.249 and 0, respectively, and the mean and median of the majority shareholder's equity pledge ratio are 0.147 and 0, respectively, indicating that 24.9% of the companies in the sample have major shareholder equity. Pledge is limited by sample data, and the proportion of major shareholders' equity pledge is moderate, which means that there is a certain gap in the quality of internal control between companies.

1. Introduction

Since the reform and opening up, our country's market economy has developed rapidly, but there is still a big gap between the stock market and developed countries, which is mainly reflected in the company's shareholding structure and company management and governance. This reflects that there is a big problem with the control allocation index of listed companies. Some personnel hold large-scale management rights in a small number of shares and are subject to improper management or sanctions during this period, reducing related profits. Faced with these problems, this paper studies the research results related to financial management and, on this basis, conducts the research on the corporate control allocation index.

Most researchers take investment as their main research direction. For example, Zhou Min's research found that the introduction of nonexecutive directors is conducive to improving the independence of the board of directors, curbing managerial conservatism, supervising the company's excessive investment behavior, and promoting innovative output [1, 2]. Ying believes that, in the form of centralized power, nonexecutive directors, as the spokesperson for the interests of major shareholders, have stronger supervisory motivation and ability and have a significant "supervisory effect" on enterprise innovation output [3]. Pan pointed out that nonexecutive directors often work in parent companies or affiliated companies, and they know the company better than part-time independent directors, and they have rich industry experience and a good relationship

network. They cannot only provide professional consulting and advice to companies but also provide companies with more external resources to promote the transformation of innovation output results [4]. Xiaofang and Zhao believe that, in the form of relatively centralized power, the conflict of interest between the controlling shareholder and other major shareholders is more serious, and the “same bed and different dreams” in the process of promoting the transformation of innovation output are not conducive to the innovation output of enterprises [5]. Based on the panel data of 153 companies listed on the Board of Directors of the Growth Enterprise Market (GEM) in 2020, Zhang and Erasmus’s research analyzes the status quo of the ownership structure and company performance and explores the mechanism of the company’s ownership structure on the company [6].

From the perspective of enterprise life cycle heterogeneity, Lusk et al. believe that the feedback between executive incentives and corporate performance presents different effects at different stages [7]. In terms of corporate innovation investment, Gupta et al.’s effective innovation activities can help companies gain competitive advantages and benefits, especially for high-tech companies that rely on emerging technologies to make their fortunes, and stable innovation investment is the source of life to ensure their development. For nonhigh-tech enterprises, innovation investment is not the decisive factor for their development [8, 9]. Dalla et al. proposed that the level of executive incentives can affect the decision-making of corporate innovation activities to a certain extent. The increase in executive compensation makes the executives more enthusiastic about innovation activities and the greater the intensity of corporate innovation investment [10]. Ding et al. believe that the more concentrated the equity, the more effective it is to control the behavior of executives and ensure that executives invest more funds in innovative activities. At the same time, according to the supervision theory, the concentration of equity can increase the restraint on executives’ decision-making and avoid the pursuit of executives. Private interests harm the efficiency of enterprises and ensure that executives make reasonable decisions and innovative activities to enhance corporate performance [11]. Shouqing et al.’s research shows that when equity concentration meets certain conditions, the relationship between salary incentives and corporate performance can be revealed, but no adjustment of equity concentration has been found [12].

This article first summarizes the current status of management control allocation schemes at home and abroad, compares the characteristics of the implementation of the management control allocation index at home and abroad, and draws a conclusion. Secondly, it uses control allocation theory and enterprise manager theory. Classical theory provides a more comprehensive and detailed analysis of the management control assignment index and believes that the implementation of the management control assignment plan is feasible. Third, the establishment of an optimal allocation model of equity. The concept of “agent state” is proposed, and the ownership structure and agency cost are connected through the agency state. The ownership structure determines the agency state, and the agency state

determines the agency cost. Based on this, an optimal allocation model of equity from the perspective of controlling agency costs is established. From the perspective of improving company performance, a general model of optimal allocation of equity is established, and combined with the control of agency costs; a decision analysis table for optimal allocation of equity is formulated. Finally, the model established in this paper is tested with the case of the domestic management control allocation plan, and the results show that the model has a certain degree of scientificity and guidance.

2. Allocation Index Model under the Neural Network and Machine Learning Method

2.1. Control-Type Division Method Based on the Control Right Realization Coefficient. Control power is the basis of property rights for deepening reform, and deepening reform is a rational choice to consolidate control power [13]. The reform is not to give up control, but to ensure control in the process of reducing state-owned shares and giving priority to ensuring the dominant position of the state-owned economy in major issues [14]. Based on Berle’s classification of control rights and the estimation of the optimal control rights threshold, the control types after the mixed ownership reform are divided into three interval types:

- (1) Weak type: the controlling shareholder’s direct shareholding ratio is less than 20%, meaning weak control; state-owned enterprises have a tendency to privatize, and the nonstate-owned capital has a certain degree of control over the decision-making of state-owned enterprises, which can easily lead to malicious embezzlement of state-owned assets [15].
- (2) Semistrong type: the controlling shareholder’s shareholding is concentrated in the 20%–50% range, and the controlling shareholder has weaker control [16]. The controlling shareholder of a semistrong company has strong control, but the controlling shareholder of a semistrong company has volatility [17]. Still, large state-owned enterprises in the region may lose control due to the ambiguity of property rights transactions [18].
- (3) Strong: the controlling shareholder holds more than 50% of the shares, the state-owned enterprises in the region are highly concentrated, and the participation of the nonstate-owned capital is insufficient [19]. According to the principle of the division of control types by controlling shareholders, it is believed that the mixed reform is centered on the main line of “guaranteeing control rights,” continuously optimizing the structure of equity checks and balances, and ultimately achieving the goal of mutual promotion of the private capital [20].

2.2. Control Power-Realization Coefficient Validity Function. According to the control realization coefficient, the effectiveness of controlling shareholders’ control over the

enterprise is defined as the validity of the control realization coefficient [21]. The control right realization coefficient (Z) is mainly determined by the controlling shareholder's shareholding ratio ($A1$) and the control right threshold (P^{**}) [22]. This coefficient can effectively measure the validity of the control right allocation after the mixed ownership reform [23]. At the same time, using the more commonly used contingency chart in qualitative analysis, the three intervals of the threshold of control rights are combined with the three types of controlling shareholder's shareholding ratio, and the matching and combination of the control rights realization coefficient types are analyzed to obtain the control rights [24]. According to the actual control types of the controlling shareholders of state-owned enterprises after the mixed ownership reform, they are reclassified into the following three types:

- (1) Invalid control type: C2, E2, F, G2, H, and I areas. This type of state-owned enterprise has control power realization coefficient $Z < 1$, the controlling shareholder cannot effectively control the major issues of the enterprise, and the control right will increase the risk of state-owned assets and private ownership [25]. Among them, the C2 area belongs to the strong type of controlling shareholder control [26]. At this time, the company's equity is highly concentrated, and the participation of the private capital is also relatively large [27]. There is no benign balance between the state-owned capital and non-state-owned capital, and state-owned enterprises fail to protect their control rights; E2 and F areas belong to the semistrong type of control types. At this time, the company's equity is relatively concentrated, but the nonstate capital has too much power to speak, but the control chain fails to play its actual role; In G2, H, and I areas, the control type of the controlling shareholder is weak. Although the company's shareholding structure is relatively dispersed at this time, the nonstate-owned capital is still in the most advantageous position.
- (2) Effective control type: In D, E1, and G1 areas, the controlling shareholder of this type of Chinese state-owned enterprise has a significant advantage in the operation of the enterprise. The control realization coefficient is $Z1$, and the enterprise ownership structure is relatively reasonable, which can effectively prevent problems such as "one share dominance" and controlling shareholder abuse of control. Under such a well-balanced shareholding structure, state-owned enterprises cannot only expand the voice of the private capital and effectively release the vitality of state-owned enterprises but also guarantee control rights to prevent the loss of state-owned assets. Among them, the D and E1 areas belong to the semistrong control type. The shareholding structure of enterprises in this area is relatively concentrated, and the state-owned capital and nonstate-owned capital form a good check and balance effect, creating a more fair competition

environment for enterprises. The G1 area is a weak type of control. The company's shareholding structure in this area is relatively decentralized. Effective reduction of state-owned stocks will be further realized without affecting control, the process of mixed ownership reform will be accelerated, and state-owned enterprises will be satisfied with the requirements for equity diversification.

- (3) Excess control type: In A, B, and C1 areas, although such state-owned enterprises have the control rights realization coefficient Z , the control rights of controlling shareholders obviously overflow, which is manifested in the obvious phenomenon of "one share dominance" of the state-owned capital; the state-owned capital has a high degree of autonomy and strong government intervention ability. The shareholding ratio of the controlling shareholders of the companies in the A, B, and C1 regions is strong, and the process of reforming the integration and win-win situation of the state-owned capital and private capital has been greatly hindered.

2.3. Grey Absolute Proximity Correlation Model under Neural Network and Machine Learning. When carrying out multi-factor evaluation, weights are usually used to reflect the importance of index factors, and common weighting methods are analyzed to make up for the shortcomings of single weighting methods. Therefore, the use of combined weighting methods for research in this paper is reliable and advanced.

2.3.1. Fuzzy Weight. Based on the influencing factor index system constructed above, the scoring results are weighted and averaged to obtain the fuzzy complementary matrix of each influencing factor $R = (r_{ij})_{n \times n}$, and according to the formula,

$$f_{ij} = \frac{r_i - r_j}{2(n-1)} + 0.5. \quad (1)$$

Calculate the weights of primary and secondary indicators w_i^1 and w_i^3 :

$$w_i^k = \frac{1}{n} - \frac{1}{2\alpha} + \frac{\sum_{j=1}^n r_{ij}}{n\alpha}, \quad (i, k = 1, 2, \dots, n), \quad (2)$$

$$w_i^2 = w_i^1 \times (w_{i1}^2, w_{i2}^2, \dots, w_{ij}^2)^T.$$

Among them,

$$r_i = \sum_{j=1}^n r_{ij}, \quad (i, j, \dots, n), \quad (3)$$

$$\alpha = \frac{(n-1)}{2}.$$

2.3.2. Entropy Method to Determine Weights. Based on the data obtained from questionnaire surveys, the average value of the top five industry results is selected to construct an

index evaluation matrix $P = (P_{ij})_{n \times k}$; among them, $i = 1, 2, \dots, n$ and $j = 1, 2, \dots, k$, and carry out dimensionless processing for each index, and calculate the weight of the first and second index h_i^1 and h_i^2 according to the following formula:

$$p_{ij}'' = \frac{P_{ij}'}{\sum_{i=1}^n P_{ij}'} \quad (i = 1, 2, \dots, n, j = 1, 2, \dots, k),$$

$$e_j = -\frac{1}{\ln k} \sum_{i=1}^n p_{ij}'' \ln p_{ij}'', \quad (i = 1, 2, \dots, n, j = 1, 2, \dots, k),$$

$$h_i = \frac{(1 - e_j)}{\sum_{j=1}^k (1 - e_j)}, \quad (j = 1, 2, \dots, k). \quad (4)$$

Finally, combine the weight w_i and h_i according to the following formula to get the first and second index combination weight t_i and the ranking of organizational innovation factors:

$$t_i = \frac{w_i h_i}{\sum_{i=1}^n w_i h_i}, \quad (i = 1, 2, \dots, n), \quad (5)$$

$$f(x) = \frac{1}{Nh} \sum_{i=1}^N k \left(\frac{X_i - x}{h} \right).$$

It can be seen from the above formula that the primary indicators that affect organizational innovation are mainly technology, knowledge, organizational structure, and strategic characteristics; secondary indicators are mainly organizational learning, knowledge flow, and information technology. At the same time, in order to explore the logical relationship of the main influencing factors, select the first 80% of the secondary indicators as the main influencing factors and further analyze the influence mechanism between the factors.

2.3.3. Analysis of the Impact Mechanism of Organizational Innovation. The Interpretive Structure Model (ISM) construction of ISM can be used to analyze complex systems and visually express the logical relationship between factors, thereby constructing ISM to explore the hierarchical relationship between factors. By issuing questionnaires to universities and experts in various industries, the value of element C is 1 or 0, indicating whether the element C_i pair C_j has a direct impact, and the threshold is set to 80% to determine the correlation between factors, and the adjacency matrix C is established based on the correlation; on this basis, using MATLAB programming to perform multiple Boolean operations makes

$$M = (C + I)^k = (C + I)^{k-1} \neq (C + I)^{k-2} \neq \dots$$

$$\neq (C + I) (k \leq n - 1), \quad (6)$$

$$h_t = \tanh(w_c x_t + u_c (r_t \Theta h_{t-1}) + b_c),$$

$$h_t = z_t \Theta h_{t-1} + (1 - z_t) \Theta h_t.$$

The reachable matrix M is obtained, and the hierarchical division is carried out according to the reachable set = common set, and finally, the explanatory structure model of the influence factors is obtained. From the analysis of the model's path of influence, the processes that influence organizational innovation originate from information technology, market environment, and economic policy, and by acting on organizational structure and strategy and cultural and leadership qualities, it manifests itself in the flow of knowledge, organizational learning, and collaborative openness. The total number of shares is $T = \sum_{i=1}^N S_i$, and the shareholding ratio of the i th shareholder is $P_i = S_i/T$. The calculation formula of the control degree α of the Cubbin-Leech model under the resolution of major issues is

$$\alpha = \Pr(M' > 0) = \Phi\left(\frac{P_1 T}{\sigma_y}\right) = \Phi\left(\frac{P_1 T}{\sqrt{\theta \sum_{i=2}^N S_i^2}}\right) \quad (7)$$

$$= \Phi\left(\frac{P_1 T}{\sqrt{\theta(H - P_1^2)}}\right).$$

For the calculation of the shareholding ratio of other shareholders, refer to the extreme concentration method, that is, assuming the number of other shareholders as 10,000 to divide the remaining shares equally, you can get

$$H = H_{10} + 10000 \times \left(\frac{1 - A_{10}}{10000}\right)^2, \quad (8)$$

$$\sigma_t = \frac{\sqrt{(1/n) \sum_{i=1}^n (FI_{it} - FI_{it})^2}}{FI_{it}}, \quad (9)$$

$$u_{(j|i)} = w_{ij} A_i. \quad (10)$$

Combining formula (10) can obtain the control degree α of the controlling shareholder of the listed company. Conversely, if you directly limit the controlling shareholder's degree of control over the company α (α should be large enough, such as $\alpha = 95\%$ or 99%), you can calculate the minimum shareholding ratio required to control the company's decision-making, that is, optimal control weight threshold P^{**} , and the calculation formula is

$$P^{**} = Z_\alpha \sqrt{\theta \times \frac{H}{1 + Z_\alpha^2 \theta}}, \quad (11)$$

$$\ln\left(\frac{FI_{it}}{FI_{it} - 1}\right) = \alpha + \beta \ln FI_{it} - 1 + v_i + \mathfrak{F}_t.$$

Among them, Z_α is a normal discrete variable with predefined control rights. Then, define the control right realization coefficient as

$$Z = \frac{A_1}{P_{99\%}}, \quad (12)$$

$$\ln\left(\frac{FI_{it}}{FI_{it} - 1}\right) = \alpha + \beta \ln FI_{it} - 1 + \phi X_{it} - 1 + v_i + \tau_t.$$

3. Construction of the Allocation Rights' Control Index of Listed Companies

3.1. Data Sources of Experimental Samples. The sample data selected in this article are the equity information of listed companies on the Shanghai Securities Platform (SSE) and Shenzhen Constituent Stocks Platform (SZSE) to reflect the allocation of control rights. The data span is from January 1, 2014 to December 31, 2020. Transaction information data between SSE uses big data to optimize business ecology, adjust organizational structure, and realize securities' trading. Its self-developed C2M-personalized customization platform and digital cloud service platform form a virtuous circle ecosystem to facilitate securities' transactions for listed companies. Therefore, in this article, we will take as an example the composition of control of listed companies on the SSE and SZSE platforms to illustrate the impact mechanism of the assignment of control in the age of big data. The data source is Google Data Analysis.

3.2. Research Index Selection and Research Steps. According to the implementation goals and steps of the adjustment of control rights allocation, the process of adjustment of control rights allocation can be divided into three time periods: the trial period (May 9, 2017~September 9, 2017), the comprehensive control rights allocation adjustment period (2017) (September 12, 2018~September 29, 2018), and the critical period for the adjustment of control right allocation (after October 9, 2018). Therefore, the selected data is divided into four time periods: preadjustment phase, pilot phase, full implementation phase, and critical phase.

In order to initially understand the effectiveness and complexity of the Chinese stock market before and after the adjustment of the control allocation, first of all, descriptive statistics are performed on the selected SSE and SZSE return rate series. The sample size of the two series is 854. The sample size is 327, and the sample size after the adjustment of the control configuration is 394, as shown in Table 1.

The Kurtosis values of SSE and SZSE before and after the adjustment of control rights allocation are both greater than 3, and the skewness value is greater than 0, indicating the instability of stock market returns. At the same time, combining the J-B test value and the return value h is equal to 1; it can be determined that the return rate sequence rejects the assumption of a normal distribution. This shows that the distribution of stock market returns cannot be reasonably explained by the efficient market hypothesis, and its volatility does not follow periodic or completely random walks, which can preliminarily reflect the impact of the adjustment of the allocation of control rights on the effectiveness of the stock market.

4. Dynamic Analysis of the Effectiveness and Complexity of Control Rights Allocation Based on Neural Networks and Machine Learning

4.1. Relationship between Effectiveness and Complexity. This part mainly studies the optimal allocation of the equity structure from both theoretical and empirical aspects. In theoretical research, the impact of different equity concentration and equity checks and balances on the company's supervision mechanism, the exercise of shareholder power, and the company's takeover of the market is discussed, which theoretically proves the necessity of the optimization of the equity structure and the existence of the optimal equity structure problem.

In order to explore the dynamic changes of the effectiveness and complexity of the stock market by the adjustment of control rights allocation, this paper analyzes the dynamic values of the approximate entropy and sample entropy of the SSE and SZSE annual return series from 2014 to 2020, as shown in Figure 1. It can be seen that the SSE and SZSE are on the rise, indicating that the complexity of the stock market is increasing. As a result, the stock market is getting closer to the random state, the randomness of the stock price gradually increases, the predictability of the stock price decreases, and the effectiveness of the stock market is also has been promoted. At the same time, the approximate entropy or sample entropy of different sequences has similar changes, and there are local differences between the approximate entropy and sample entropy of the same sequence.

As shown in Table 2, the change characteristics of the entropy value of the SSE and SZSE stock market sequences can be obtained. The mean and median of the pledge of major shareholders' equity are 0.249 and 0, respectively, and the mean and median of the percentage of major shareholders' equity pledges are 0.147 and 0, respectively, indicating that 24.9% of the companies in the sample have pledged major shareholders' equity, which is restricted. In relation to sample data, the majority shareholder's equity pledge ratio is moderate, which means that there is a certain gap in the quality of internal control between companies. In 2017, Pilot Notices, Guidance, and Control Measures were issued to adjust the distribution of control of listed companies, formal initiation and implementation of adjustment of the distribution of control, and "not tradeable with the same share" "same rights" for stocks that can be traded with stocks. The operating mechanism of the stock market gradually improves the effectiveness of the market, which is manifested in the fact that the fluctuation of stock prices is closer to the supply and demand of the market so that the

TABLE 1: Sample size after adjustment of control configuration.

Time	Stock index	Mean	Skewness	Kurtosis	J-B value
Early stage of share reform	SSE	1.19	1.24	0.58	0.97
	SZSE	3.53	1.01	1.9	2.68
Late share reform	SSE	5.62	5.53	3.93	5.54
	SZSE	4.62	2.41	3.41	2.2
Full time period	SSE	1.68	1.59	1.87	1.21
	SZSE	4.68	3.61	2.28	3.07

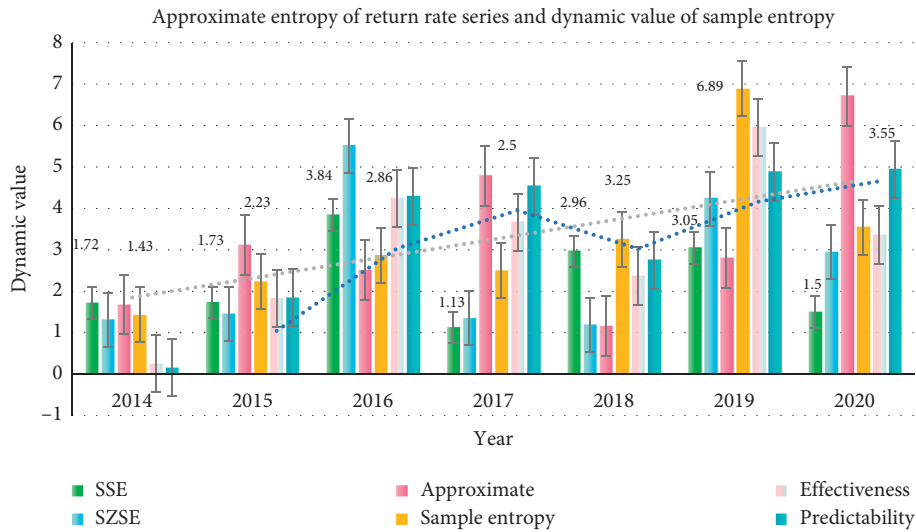


FIGURE 1: Approximate entropy of return rate series and dynamic value of sample entropy.

TABLE 2: The change characteristics of the entropy value of the SSE and SZSE stock market.

Year	SSE	SZSE	Approximate	Sample entropy	Effectiveness	Predictability
2014	1.72	1.31	1.68	1.43	0.26	0.16
2015	1.73	1.46	3.12	2.23	1.83	1.85
2016	3.84	5.51	2.51	2.86	4.24	4.29
2017	1.13	1.35	4.79	2.5	3.67	4.54
2018	2.96	1.19	1.17	3.25	2.37	2.75
2019	3.05	4.23	2.81	6.89	5.95	4.88
2020	1.5	2.94	6.7	3.55	3.36	4.94

formation of stock prices is getting closer and closer to randomness, and the entropy of the sequence sample reaches the local maximum in that year.

As shown in Figure 2, from 2014 to 2020, the sample entropy of the sequence showed a slight increase. This is mainly due to the fact that, in June 2014, the China Securities Regulatory Commission imposed a certain restriction on illegal manipulation of additional new shares, reducing artificial speculation or behaviors such as insider manipulation that interfered with the normal operation of the stock market and have increased the randomness of stock prices or yields, and the effectiveness of the stock market has also been slightly improved. After 2015, the China Securities Regulatory Commission continued to intensify its crackdown on illegal acts of manipulating the stock market, which provided support for capital market pricing to more closely reflect changes in the market supply and demand.

As shown in Table 3, the overall stability of the stock market from 2014 to 2020 reflects the increasing benefits brought about by the allocation of control rights of listed companies. It also verifies that, in 2016, government departments have successively issued the opening and stability of the stock market, protecting public investment and activating. There are several opinions and regulations on the vitality of the stock market and the improvement of the effectiveness of the stock market. The sample entropy of the series in that year has continued to increase, and the effectiveness of the stock market has improved to a certain extent.

As shown in Figure 3, in 2018 and 2019, the entropy of sequence samples showed a downward trend and reached a local minimum in 2019. This is mainly due to multiple capital violations and manipulations in 2018, with the majority of public investors and their strong “herd effect”

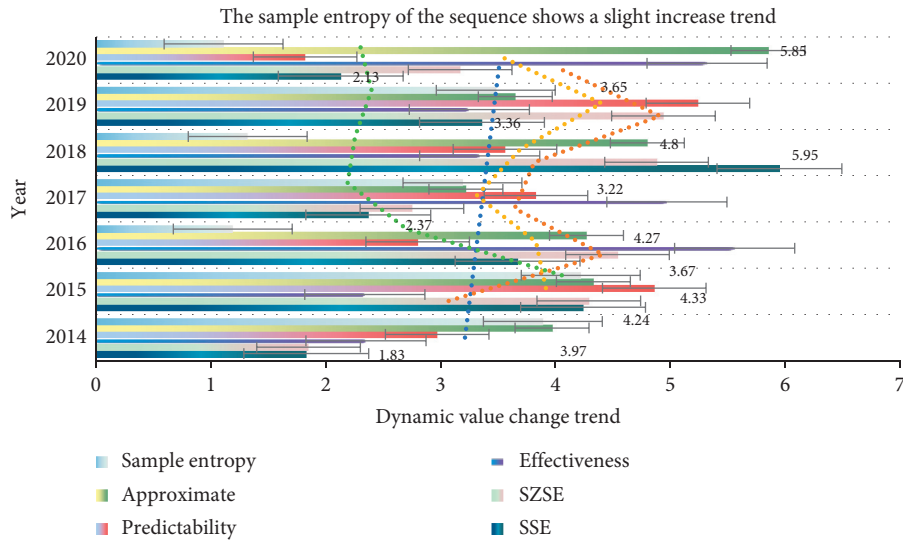


FIGURE 2: The sample entropy of the sequence shows a slight increase trend.

TABLE 3: Sequence sample entropy reaches the local value.

Year	SSE	SZSE	Approximate	Sample entropy	Effectiveness	Predictability
2014	1.83	1.85	3.97	3.89	2.35	2.97
2015	4.24	4.29	4.33	4.22	2.34	4.86
2016	3.67	4.54	4.27	1.19	5.56	2.8
2017	2.37	2.75	3.22	3.19	4.97	3.83
2018	5.95	4.88	4.8	1.32	3.34	3.56
2019	6.36	4.94	3.65	3.48	3.25	5.24
2020	8.13	5.17	5.85	4.11	5.32	6.82

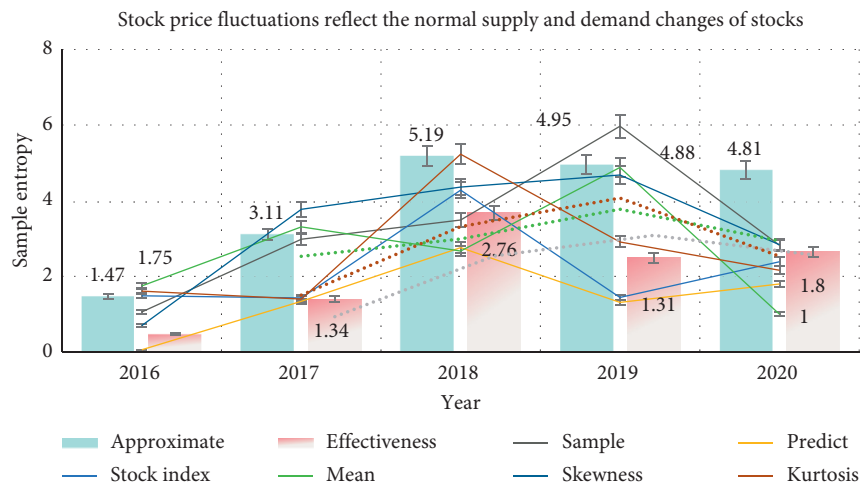


FIGURE 3: Stock price fluctuations reflect the normal supply and demand changes of stocks.

psychology, making stock price fluctuations unable to reflect the normal supply and demand changes of stocks. Although the China Securities Regulatory Commission issued a notice in May 2019 to further strengthen the education of investors and strengthen market supervision and management to regulate the normal operation of the capital market, as the

opening up of China’s stock market continues to increase, it is in contact with the international capital market increasingly closer and is more sensitive to the international market. As a result, the US subprime mortgage crisis and the US stock market crash that year spread rapidly to the Chinese stock market. In addition, the Chinese stock market is still in

the development stage and has its own shortcomings. Under the interaction of policy and environmental factors, although the government has introduced favorable measures for the market, the further improvement of the effectiveness of the stock market is still restricted.

As shown in Figure 4, from the analysis of the changes in the sequence approximate entropy and sample entropy from 2014 to 2020, the entropy values in 2017 when the adjustment of the control rights configuration is initiated have reached the local maximum, indicating that the adjustment of the control rights configuration has an impact on development and improvement. The operating mechanism of the stock market plays a great role in promoting. The changes in stock prices more randomly reflect the changes in the market supply and demand, and the effectiveness of the stock market has been improved. In 2020, the government will continue to introduce measures to stabilize the market and stabilize growth. Many good news to enhance market confidence have strengthened the confidence of investment participants, and finally, the value of the sequence sample entropy in 2020 has rebounded slightly.

4.2. Correlation between the Rate of Return and the Effectiveness and Complexity of the Allocation of Control Rights of Listed Companies. In order to examine the relationship between the adjustment of the allocation of control rights and the return rate, complexity, and effectiveness of the stock market, the sliding removal technique and the approximate entropy are combined with the sample entropy. The sliding window and sliding step size are both 21 data, and the sliding window is unchanged, and the approximate entropy and sample entropy of the sequence after removing 21 data in each sliding are calculated to analyze the correlation between the rate of return, complexity, and effectiveness.

As shown in Figure 5, there is a significant reverse relationship between the SSE and SZSE return rate sequences and their complexity (approximate entropy and sample entropy), that is, the complexity of the stock market becomes smaller as the return rate increases mainly because, with the initiation and implementation of the adjustment of the allocation of control rights, the institutional obstacles that are not conducive to the normal pricing mechanism of the stock market and the optimization of the function of resource allocation have been greatly improved, and the problem of the “nontradable” stocks of listed companies unable to be listed and circulated has been solved which makes the relationship between stock transactions and stock price fluctuations more in line with the operating laws of the market, reflecting that the randomness of stock price fluctuations has also increased and the predictability has been weakened. The fluctuations are getting closer and closer to random walks; thus, investors expect that the rate of return will also decrease.

As shown in Table 4, the efficiency of the stock market in developed market economies that are free and open is relatively high. The formation of stock prices is basically determined by the supply and demand relationship in the

market. The formation process of stock prices shows greater randomness and regularity. Compliance is almost nonexistent; on the contrary, countries with higher market intervention or control have lower stock market effectiveness and greater regularity in stock price changes, and the formation of stock prices has certain regularity, indicating that the stock market is affected by various influences of non-market factors. With the initiation of the adjustment of the allocation of control rights, policy interventions and controls have gradually decreased, and the degree of openness of the stock market has gradually increased. Stock pricing mechanisms tend to improve. The effectiveness of the stock market should be fully reflected in changes in stock prices. The approximate entropy and sample entropy of the sequence should theoretically show a relatively larger value, its dynamic structure characteristics have become more complex, and the stock market system has shown changes in complexity.

As shown in Table 5, the centralized equity structure often manifests as the company’s controlling shareholder’s monopoly on board members, and directors’ supervision of management is often trapped in their own situation. Therefore, the board of directors’ supervision mechanism under this equity structure is more weak. The decentralized shareholding structure often shows that the membership of the board of directors is more complicated. This type of shareholding structure also leads to a weaker board of directors’ supervision mechanism, and the directors lack the motivation to monitor the management. A moderate shareholding structure is often manifested; in that, board members are sent by several major shareholders, forming a balance of mutual checks and balances. Under this type of shareholding structure, board members will maintain their respective positions through more supervision of the management. The interests of shareholders represented may result in a win-win situation for several major shareholders.

As shown in Figure 6, the centralized equity structure is not conducive to the governance role of the company’s takeover market because the centralized equity structure causes stock selling in the circulating stock market and does not pose a threat to the company’s takeover. The decentralized shareholding structure makes companies easy to be acquired. In countries such as the United Kingdom and the United States, where shareholding is dispersed, active corporate takeover markets have greatly promoted and improved corporate governance. The appropriate ownership structure is more difficult for external receivers to successfully acquire because large shareholders within the company can easily unite to prevent acquisitions. According to the current “one share, one vote” system, the centralized shareholding structure often leads to a mere formality in the convening of general meetings. The controlling shareholders completely manipulate the voting results, and the majority of small and medium shareholders generally give up the exercise of shareholder power. The decentralized shareholding structure makes most shareholders have no enthusiasm to exercise shareholder rights, which will cause serious insider control problems, and most shareholders will be easily manipulated by management. In

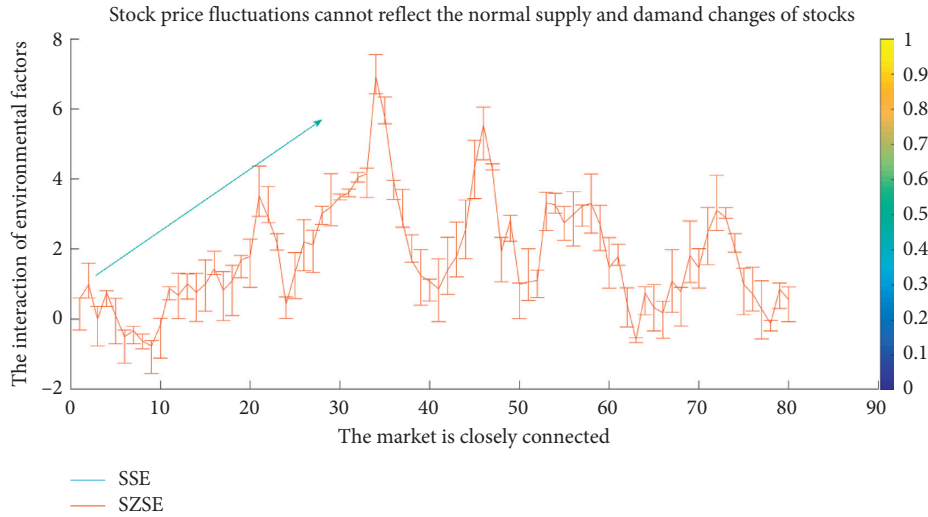


FIGURE 4: Stock price fluctuations cannot reflect the normal supply and demand changes of stocks.

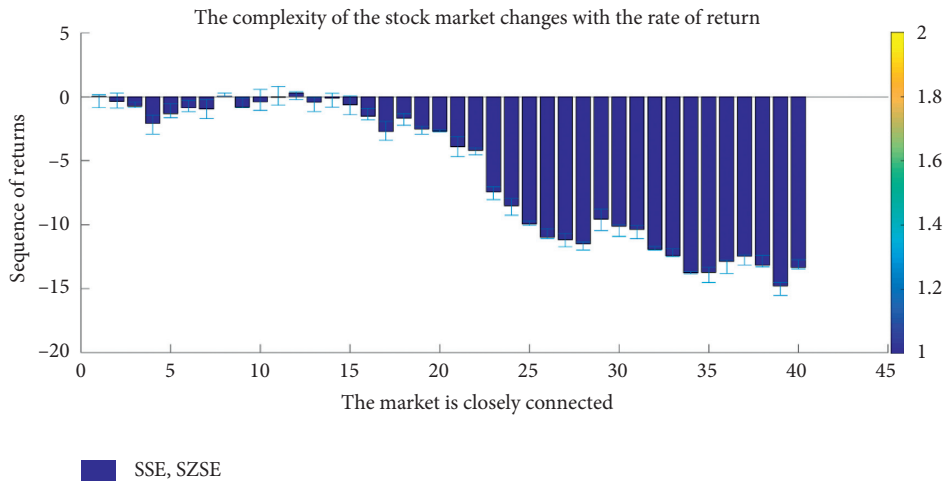


FIGURE 5: The complexity of the stock market changes with the rate of return.

TABLE 4: The randomness of stock price formation.

Item	Cost	Corporate	Performance	Sequence	Approximate	S-entropy
SSE	3.11	2.98	1.4	1.34	1.43	3.31
SZSE	5.19	3.49	3.68	2.76	4.28	2.67
Approximate	4.95	5.97	2.49	1.31	1.44	4.88
Sample	4.81	2.82	2.65	1.8	2.39	1
Effectiveness	6.21	1.68	3.91	5.79	3.55	5.07
Predict	4.09	2.48	6.47	3.98	4.35	6.73

TABLE 5: Performance of the concentrated ownership structure.

Item	Theory	Effectiveness	Structure optimization	Equity concentration	Shareholder power	Monitoring mechanism
Management	0.1	0.51	1.57	0.51	0.08	1.85
Allocation	1.6	2.76	1.81	2.84	3.38	2.95
Equity	5.56	2.75	5.89	2.73	3.77	5.59
Configuration	2.41	5.46	2.28	3.07	5.89	4.36
Scientific	4.6	3.06	3.21	2.77	4.37	4.92
Guiding	1.2	1.94	2.92	5.84	2.88	2.41

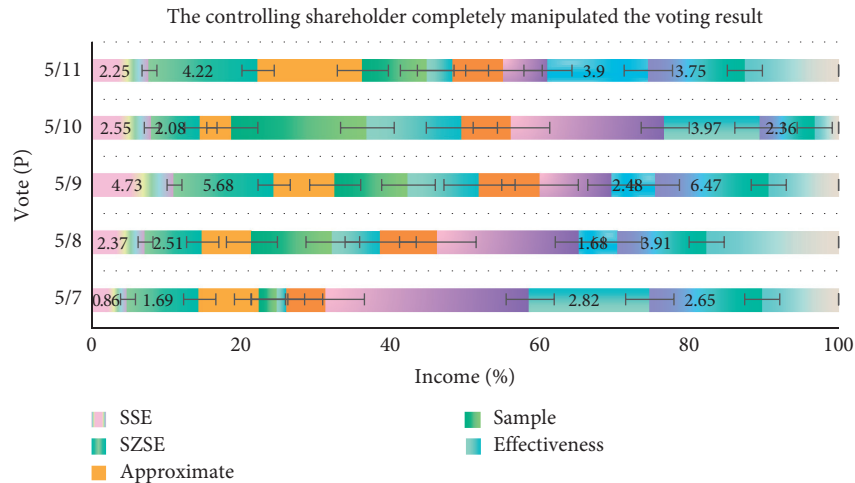


FIGURE 6: The controlling shareholder completely manipulated the voting result.

a moderate shareholding structure, several large shareholders generally send their representatives to participate in the general meeting of shareholders and exercise voting rights. Relatively speaking, under this ownership structure, the exercise of shareholder rights represents the interests of more shareholders.

As shown in Figure 7, in the absence of the guidance of the optimal allocation model of equity, the general law of equity allocation in the management buyout of listed companies in our country further verifies whether the previous empirical conclusions are valid and scientific. This represents a preacquisition note by observation. It turns out that this is during a proper increase in stock concentration acquisitions. The result of the actual investigation is that, after the implementation of the management buyout, there was a high degree of equity concentration. There were no changes in the equity concentration of two companies, and only three companies had their equity concentration decreased.

According to the results of the previous empirical research, it can be seen that increasing the degree of equity checks and balances does not necessarily promote the improvement of company performance; only when the degree of equity checks and balances is lower than the increase, this should reduce the degree of equity checks and balances of these listed companies; otherwise, it may not be conducive to the improvement of company performance. As shown in Table 6, if the degree of equity checks and balances of these listed companies is increased, it may cause a decrease in company performance. In order to further verify this inference, we once again investigated the return on total assets. The code is referred to as the return on total assets. Note that the performance of each company has been significantly reduced. Therefore, we believe that the increase in equity checks and balances may be one of the main reasons for this result.

As shown in Figure 8, many control rights allocation models are based on agency costs. Most of these models assume that an enterprise's income is asymmetry in information among insiders. The former can occupy all the income that is not paid to the latter. Under this assumption, it is concluded that due to the limitation of the managers' own funds and the protection of their own interests by external investors, this has led to more use of liabilities in management buyouts. Secondly, the managers adopt more dual securities, which are both equity and debt. In terms of rights, there are residual claims and fixed claims. In many debt contracts signed with managers, some investors often attach some conditions for converting debts into equity, which not only guarantees the minimum rate of return for investors but also enables investors to obtain high returns. Through the above investigation of the equity allocation of management buyouts of listed companies in our country, the effectiveness of the previous empirical conclusions is basically verified. Therefore, the equity optimization allocation model designed in this article has certain scientific and guiding significance for the equity allocation in our country's management buyouts.

As shown in Figure 9, the model established in this article is universal, and it is this universality that makes it not entirely suitable for all types of companies. In the empirical study, through the curve relationship between cost and corporate performance and the general model of the learning model and the allocation of stock optimization, this provides useful guidance for the management to optimize the allocation of the company's equity structure after the acquisition. In fact, it is unrealistic to expect to establish an optimal model of the equity structure suitable for all types of enterprises. The significance of the model established in this article is to provide a way to find an optimal allocation model of equity, that is, the concentration of equity and the balance of equity. Combine land and use curve estimation method to establish an optimal allocation

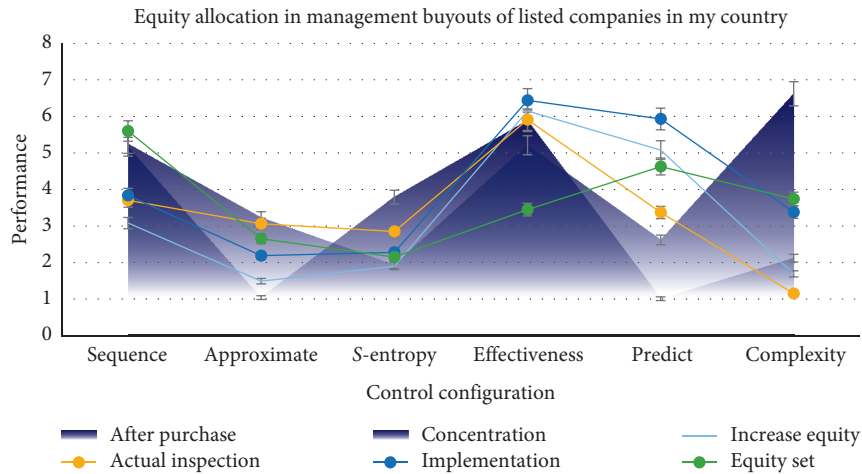


FIGURE 7: Equity allocation in management buyouts of listed companies in our country.

TABLE 6: Promote the improvement of company performance.

Item	After purchase	Increase equity	Concentration	Actual inspection	Implementation	Equity set
Sequence	5.17	3.08	5.25	3.7	3.84	5.6
Approximate	1.04	1.49	3.23	3.06	2.19	2.65
S-entropy	3.79	1.9	1.93	2.85	2.28	2.15
Effectiveness	5.88	6.15	5.21	5.91	6.44	3.45
Predict	1.01	5.08	2.62	3.37	5.93	4.63
Complexity	2.12	1.69	6.62	1.15	3.38	3.74

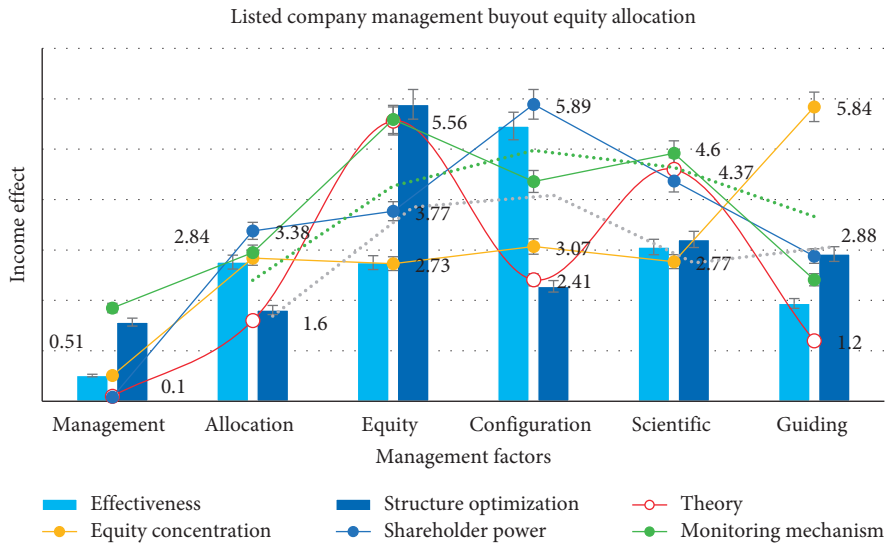


FIGURE 8: Listed company management buyout equity allocation.

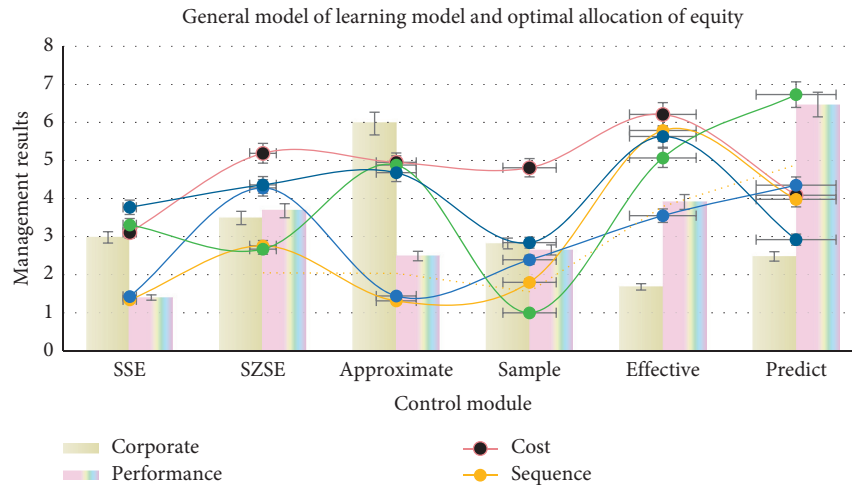


FIGURE 9: General model of learning model and optimal allocation of equity.

model of the equity structure. At the end of this part, case analysis is used to test the designed equity optimization allocation model, and the results show that the model is scientific and effective.

5. Conclusions

This paper uses the theory of complexity entropy to measure and analyze the approximate entropy and sample entropy of stock market returns from the perspective of the adjustment of control rights allocation and system thinking. The main conclusions are as follows. (1) According to the definition of randomness, the hypothesis of market efficiency, and the theory of approximate entropy and sample entropy, it is proved that the value and randomness state of the approximate entropy and sample entropy of the stock market can reflect the logical relationship between the complexity and effectiveness of the stock market and prove the randomness and effectiveness of the stock market. (2) By measuring the dynamic values of the approximate entropy and sample entropy of the stock market return sequence during the year and the control allocation adjustment stage and analyzing the change characteristics of the sequence complexity, it shows that the randomness of the stock market after the control allocation adjustment has been enhanced. Effectiveness has been improved, and it presents greater complexity. (3) The complexity of the stock market sequence from before the adjustment of control rights allocation to after the adjustment of control rights allocation shows an overall increasing trend. The sample entropy is more accurate than the approximate entropy in the sensitivity of the detection data.

From the perspective of the dynamic changes in the complexity of the stock market before and after the adjustment of control rights allocation and the relationship between its return rate and its complexity, although the effectiveness of the stock market after the adjustment of control rights allocation has improved to a certain extent, the increase is small. Therefore, the allocation of control of the

company needs to be further improved, and the ability to allocate resources needs to be optimized. The author believes that, under the premise of ensuring the normal and stable operation of the stock market, we should continue to implement market reforms, establish a sound regulatory system, improve the speed and efficiency of effective information dissemination and ultimately achieve further enhancement of the effectiveness of the stock market, and form a reasonable and complete listing. The formation mechanism of corporate control rights maximizes the efficiency of resource allocation optimization in the capital market and promotes the healthy development of the stock market in accordance with its own laws.

Although this article has done a lot of work on research, there are still some deficiencies in the article due to my level and time constraints. For example, in the economic interpretation of the management control allocation index, a deep economic foundation is required, and this article does not do enough in this respect. Another example is when investigating the case of management control allocation plan, only the information of the management control allocation index of listed companies is public, which leads to a small number of case samples, and this article only selects the sample company control allocation index before comparing the performance indicators of one year with that of the control right allocation index, the rationality of which is questionable. Future research in this field should pay more attention to corporate governance issues. You can use the China Corporate Governance Evaluation Index to investigate whether the company after the implementation of the control allocation plan is developing in a positive way in corporate governance and whether it is a successful experience or failed. The lessons will help the subsequent enterprises to formulate management control allocation plans.

Data Availability

The data that support the findings of this study are available from the corresponding author upon reasonable request.

Conflicts of Interest

There are no potential competing interests in our paper.

Acknowledgments

There is no funding was received for this article.

References

- [1] M. Zhou, "On the disclosure of internal control information of listed companies," *Enterprise Technology Development*, Academic Edition, vol. 37, no. 2, pp. 114–116, Cambridge, MA, USA, 2018.
- [2] Q. Qu, K.-Y. Chen, Y.-M. Wei, Y. Liu, S.-B. Tsai, and W. Dong, "Using hybrid model to evaluate performance of innovation and technology professionals in marine logistics industry," *Mathematical Problems in Engineering*, vol. 2015, Article ID 361275, 8 pages, 2015.
- [3] H. Ying, "Research on the measurement and influencing factors of commercial bank's capital mismatch-take listed banks for example," *International Core Journal of Engineering*, vol. 5, no. 9, pp. 221–226, 2019.
- [4] T. Pan, "Research on the influence of macroeconomic policy uncertainty on cash dividend level of enterprises-based on the empirical analysis of listed companies in China's main board and small and medium-sized board," *World Scientific Research Journal*, vol. 6, no. 5, pp. 95–111, 2020.
- [5] Xiaofang and Y. Zhao, "Research on the impact of government subsidies on the development capabilities of listed companies—based on the perspective of equity concentration of renewable energy companies," *Journal of Inner Mongolia University of Finance and Economics (Comprehensive Edition)*, vol. 17, no. 4, pp. 25–28, 2019.
- [6] Q. Zhang and P. Erasmus, "Study on the relationship between ownership structure and corporate performance: evidence from Chinese companies listed on the GEM board," *International Business & Economics Research Journal (IBER)*, vol. 15, no. 2, pp. 27–39, 2016.
- [7] E. J. Lusk, M. Halperin, and B. D. Zhang, "The balanced scorecard: suggestions for rebalancing," *Problems and Perspectives in Management*, vol. 4, no. 2, pp. 100–114, 2017.
- [8] P. P. Gupta, H. Sami, and H. Zhou, "Do companies with effective internal controls over financial reporting benefit from sarbanes-oxley sections 302 and 404?" *Journal of Accounting, Auditing & Finance*, vol. 33, no. 2, pp. 200–227, 2018.
- [9] U. Mishra, J. Tijerina-Aguilera, S. Tiwari, and E. C.-B. Leopoldo, "Retailer's joint ordering, pricing, and preservation technology investment policies for a deteriorating item under permissible delay in payments," *Mathematical Problems in Engineering*, vol. 2018, Article ID 6962417, 14 pages, 2018.
- [10] L. Dalla Valle, M. E. De Giuli, C. Tarantola, and C. Manelli, "Default probability estimation via pair copula constructions," *European Journal of Operational Research*, vol. 249, no. 1, pp. 298–311, 2016.
- [11] C. Ding, Z. Zhao, X. Zhu et al., "Application of neural network in intelligent fire alarm system," *Sensors and Microsystems*, vol. 37, no. 1, pp. 154–156, 2018.
- [12] W. Shouqing, W. U. Di, P. Wei et al., "Allocation of control rights between governments and companies in urban development PPP projects," *Journal of Tsinghua University (Science and Technology)*, vol. 57, no. 4, pp. 369–375, 2017.
- [13] P. Boeing, "The allocation and effectiveness of China's R&D subsidies-evidence from listed firms," *Research Policy*, vol. 45, no. 9, pp. 1774–1789, 2016.
- [14] L. Yang-Bok, "A study on introducing dual class stock into the Korean commercial code," *Business Law Review*, vol. 31, no. 2, pp. 91–118, 2017.
- [15] L. Hu and N. Li, "Research on the construction of machine learning platform under big data technology," *Computer Knowledge and Technology*, vol. 15, no. 10, pp. 157–159, 2019.
- [16] A. J.-P. Tixier, M. R. Hollowell, B. Rajagopalan, and D. Bowman, "Application of machine learning to construction injury prediction," *Automation in Construction*, vol. 69, no. 8, pp. 102–114, 2016.
- [17] O. Weisman, M. Chetouani, C. Saint-Georges et al., "Dynamics of non-verbal vocalizations and hormones during father-infant interaction," *IEEE Transactions on Affective Computing*, vol. 7, no. 4, pp. 337–345, 2017.
- [18] M. Kawamura, T. Suzuki, and K. Kobayashi, "Construction of a dividual model using a reinforcement learning based Bayesian network," *IEEJ Transactions on Electronics, Information and Systems*, vol. 137, no. 2, pp. 288–293, 2017.
- [19] J. Kim and S. Park, "Field applicability of a machine learning-based tensile force estimation for pre-stressed concrete bridges using an embedded elasto-magnetic sensor," *Structural Health Monitoring*, vol. 19, no. 1, pp. 281–292, 2020.
- [20] Y. Zhou, S. Zheng, and G. Zhang, "Machine learning-based optimal design of a phase change material integrated renewable system with on-site PV, radiative cooling and hybrid ventilations—study of modelling and application in five climatic regions," *Energy*, vol. 192, no. 1, pp. 1–21, 2020.
- [21] G. Liu, J. H. Nzige, and K. Li, "Trending topics and themes in offsite construction(OSC) research," *Construction Innovation*, vol. 19, no. 3, pp. 343–366, 2019.
- [22] K. Tangirala, N. Herndon, and D. Caragea, "A comparative analysis between k -mers and community detection-based features for the task of protein classification," *IEEE Transactions on NanoBioscience*, vol. 15, no. 2, pp. 84–92, 2016.
- [23] H. Sun, "Research on the construction of electronic resources of university library based on text similarity," *Intelligent Computers and Applications*, vol. 8, no. 5, pp. 155–158, 2018.
- [24] X. Ma, X. Yuan, and Y. Sun, "Application of wavelet neural network in the mine deformation monitoring," *Mine Measurement*, vol. 44, no. 6, pp. 44–47, 2016.
- [25] B. Liu, L. Jin, and Y. Liu, "Study on application problems of DRGs performance evaluation indicators in the evaluation in the specific hospital," *Chinese Health Industry*, vol. 15, no. 10, pp. 29–31, 2018.
- [26] K. Henchi, M. Fafard, M. Talbot et al., "Application of artificial neural networks to the identification and detection of the damage in bridges," *Revue Européenne des Éléments Finis*, vol. 7, no. 3, pp. 257–272, 2016.
- [27] L. X. Weiyang, "The application of deep convolution neural network to building extraction in remote sensing images," *World Scientific Research Journal*, vol. 6, no. 3, pp. 136–144, 2020.

Research Article

Particle Swarm Optimization Algorithm in Numerical Simulation of Saturated Rock Slope Slip

Bowen Liu ¹, Zhenwei Wang ², and Xiaoyong Zhong ³

¹School of Energy and Mining Engineering, China University of Mining and Technology, Beijing 100083, China

²School of Civil Engineering, North China University of Technology, Beijing 100144, China

³Hulunbuir Dongming Mining Co., Ltd., Hulunbuir 021500, Inner Mongolia, China

Correspondence should be addressed to Bowen Liu; bqt1800101016@student.cumtb.edu.cn and Zhenwei Wang; kingzw627@163.com

Received 17 December 2020; Revised 13 January 2021; Accepted 22 February 2021; Published 17 March 2021

Academic Editor: Sang-Bing Tsai

Copyright © 2021 Bowen Liu et al. This is an open access article distributed under the Creative Commons Attribution License, which permits unrestricted use, distribution, and reproduction in any medium, provided the original work is properly cited.

With the continuous popularization and development of highway traffic in mountainous areas, the number of rock slopes is also increasing. In order to improve the stability of rock slope and reduce the harm caused by slope slip, this paper carries out numerical simulation of rock slope sliding based on particle swarm optimization algorithm. Firstly, this paper combines the differential evolution algorithm and simplex method to improve the global and local search ability of particle swarm optimization (PSO) algorithm and analyzes the performance of the algorithm. ABAQUS software is used to simulate rock slope sliding, the finite element method is used to analyze the stability of rock slope, and LS-DYNA program is used to simulate rockfall impact rock slope. During the numerical simulation, the improved algorithm is used to analyze all the data. Experimental data show that the improved PSO algorithm converges after nearly 100 iterations and the convergence speed and optimization accuracy are high. In the numerical simulation, the average failure probability of the left and right sides of the main section at the top, middle, and foot of the slope is 0.0820 and 0.0723, 0.0772 and 0.0492, and 0.0837 and 0.0677, respectively, indicating that the overall instability probability of the left side of the rock slope is higher than that of the right side. The rock slope with the same direction through joint is mainly affected by the joint at the toe of the slope, the rock slope with reverse through joint is mainly affected by the joint in the slope, and the sliding occurs from the middle to both ends. In addition, with the increase of the size and height of rockfall, the total energy of rock slope is also increasing, and the possibility and degree of rock slope sliding are higher. This shows that the improved particle swarm optimization algorithm can effectively analyze some factors affecting slope slip in numerical simulation of saturated rock slope slip.

1. Introduction

1.1. Background Significance. In mountainous areas, because of the development of traffic and economy, the construction of roads and buildings, there are a large number of rock slopes with potential safety hazards. The stability of rock slope has a direct impact on the safety of traffic and residents in nearby areas. Once landslide disaster occurs, it will bring huge economic losses and security threats [1, 2]. Therefore, it is necessary to detect and predict the slip of rock slope in real time. Numerical simulation of slip of rock slope can effectively analyze the stability of rock slope, but it requires a large amount of calculation in data analysis. Particle swarm

optimization algorithm has the advantages of simple operation and fast convergence speed, which can improve the efficiency of analysis [3, 4]. Therefore, this paper proposes an improved algorithm based on particle swarm optimization algorithm and applies it to the numerical simulation of slope sliding, which provides a new idea for solving the engineering problem of rock slope stability.

1.2. Related Work. Particle swarm optimization (PSO) is widely used in many fields because of its advantages of simple operation and fast convergence speed. Mohamadi proposed a multiobjective stochastic programming model to

establish an earthquake response plan integrating pre-disaster and postdisaster decision-making. Aiming at this model, he proposed a new multiobjective particle swarm optimization algorithm and designed binary particle swarm optimization algorithm and continuous particle swarm optimization algorithm based on genotype sound pattern to deal with binary position and other continuous decision variables. Zhang et al. proposed a chaos multiobjective particle swarm optimization algorithm based on particle swarm optimization algorithm and invasive weed algorithm and evaluated the performance of the method through four common two-objective problems [5]. Their improvement of particle swarm optimization algorithm provides a reference for this study, but, after the improvement of the algorithm, they did not carry out more comparative analysis to prove the effectiveness of the improvement.

The problem of rock slope sliding has always been the focus of engineering. Wang et al. studied the sliding failure of jointed rock slope caused by mechanical degradation of rock mass under dry wet cycle [6]. According to the mechanical parameters of reservoir limestone under different drying and wetting cycles, he used the discrete element method to analyze the slippage failure mode of the North-South slope of the Yellow River in the Three Gorges Reservoir area. Zhuang et al. studied the sliding mechanism of Earth rock slope by using transparent soil technology and considered the influence of rock joint roughness coefficient, soil angle, rock angle, and soil layer thickness on slope stability [7]. He also used particle image velocimetry and laser speckle technology to obtain the deformation characteristics of rock and soil slope. Although their research on rock slope slip is effective, there are still some deficiencies in the technology of predicting the occurrence time of rock slope slip.

1.3. Innovative Points in This Paper. In order to conduct more accurate numerical simulation of rock slope slip, improve the stability of rock slope, and reduce the economic and life hazards brought by rock slope sliding, this paper analyzes the rock slope sliding based on particle swarm optimization algorithm. The innovation points of this study are as follows: (1) based on the differential evolution algorithm and simplex method, the standard particle swarm optimization algorithm is improved, which improves the global and local search ability of the particle swarm optimization algorithm in the early and late iterations [8]. It is found that the proposed algorithm has faster convergence speed and higher optimization accuracy. (2) ABAQUS software is used for numerical simulation of rock slope sliding, and finite element method is used for analysis. The top, middle, and foot of slope are selected as feature points. It is found that the failure probability of the left side of the rock slope model is higher than that of the right side. (3) LS-DYNA program was used to construct the slope model of rockfall impact rock, and numerical simulation was carried out. It was found that the size and height of rockfall were proportional to the possibility of slope slip.

2. Particle Swarm Optimization Algorithm and Sliding Analysis of Saturated Rock Slope

2.1. Particle Swarm Optimization Algorithm

2.1.1. Mathematical Model and Process. The particle swarm optimization (PSO) algorithm simulates the foraging behavior of birds, taking birds as potential optimal solutions, that is, particles [9]. Because the mass and volume of the birds are ignored, the number of parameters is small and easy to operate. Local and global optimal values are found through population iterative optimization [10]. Assuming that there are m particles in the solution space, the expressions of the position and velocity of the i -th particle in the n -dimensional space are shown in the following formulae:

$$P_i = (p_{i1}, p_{i2}, \dots, p_{iN}), \quad (1)$$

$$V_i = (v_{i1}, v_{i2}, \dots, v_{iN}), \quad (2)$$

where $i = 1, 2, \dots, M$. The historical optimal position of the particle is H_{best} and the global optimal position is G_{best} . Formulae (1) and (2) are improved by introducing inertia weight and learning factor. The position and speed of particles are updated as shown in the following formulae:

$$P_i^{e+1} = P_i^e + V_i^{e+1}, \quad (3)$$

$$V_i^{e+1} = \omega V_i^e + s_1 r_1 (H_{\text{best}} - P_i^e) + s_2 r_2 (G_{\text{best}} - P_i^e), \quad (4)$$

where ω is the inertia weight, e is the current iteration number, s_1, s_2 are the learning factor, and r_1, r_2 are the random number between $[0, 1]$. ωV_i^e is the inertial motion of the previous generation of particles, $s_1 r_1 (H_{\text{best}} - P_i^e)$ is the particle's own position, $s_2 r_2 (G_{\text{best}} - P_i^e)$ represents the group information sharing, and the three parts restrain each other to achieve balance. The dynamic value of inertia weight ω is shown in the following formula:

$$\omega(e) = \omega_{\text{max}} - \frac{e}{\max ie} (\omega_{\text{max}} - \omega_{\text{min}}). \quad (5)$$

The running process of particle swarm optimization algorithm is as follows:

As shown in Figure 1, the parameters of the particle swarm are initialized first, and then the fitness value of each particle is calculated. The third step is to calculate the historical optimal value and the global optimal value of the particle to determine whether the particle speed is less than or beyond the speed constraint, and, if so, set it to the maximum or minimum speed. The fourth step is to determine whether the termination conditions are met. If not, the fitness value of particles is recalculated, the position and velocity of particles are updated, and the following steps are repeated.

2.1.2. Influence of Algorithm Parameter Setting. The parameters of PSO algorithm directly affect the performance of PSO algorithm, so we must consider it again when choosing

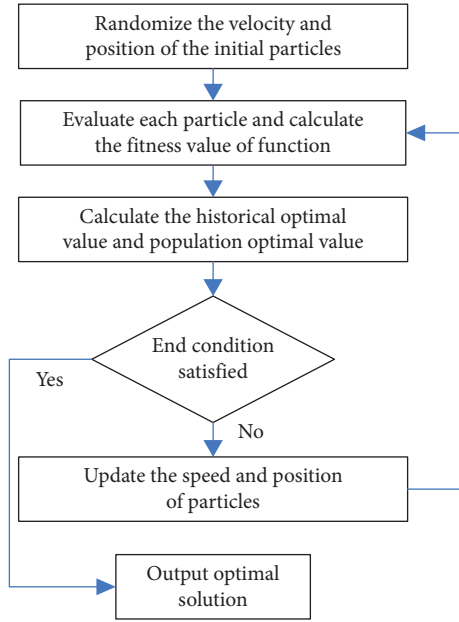


FIGURE 1: Flow chart of particle swarm optimization algorithm.

parameters, in order to improve the convergence speed of the algorithm and find the global optimal solution. Inertia weight can balance the local and global distribution of particle swarm optimization search ability [11]. In order to ensure the global search ability at the beginning of the iteration and the local search ability at the later stage of the iteration, the inertia weight should be gradually reduced with the increase of iteration times.

The two learning factors affect the degree of historical optimization and global optimization of particles, respectively, so the local and global search can be adjusted to balance their capabilities [12]. Small learning factors tend to fall into local optimality, while large learning factors tend to ignore the optimal solution even though they accelerate the convergence speed.

The number of particles affects particle swarm search. Too many particles will improve the information sharing ability between particles, but it will also increase the search time. Too few particles will reduce the communication, leading to the algorithm falling into local optimization. The maximum flight speed of the particle determines the moving distance of the particle and the search ability of the algorithm [13]. The faster the speed, the stronger the search ability, but it is easy to miss the optimal solution. The slower the reading, the stronger the development ability, but it is easy to fall into local optimum. In addition, the range of particles, the termination condition, and fitness function of the algorithm will also affect the optimization results, which need to be determined according to the specific situation of the problem.

2.1.3. Convergence Analysis and Deficiency. If the current position, historical optimal position, and global optimal position of a particle are the same, then the particle cannot approach the optimal position because its inertia weight

and speed are not zero, so the algorithm cannot converge [14]. If the inertia weight and velocity are very close to zero, the particles can approach the optimal position, but the diversity of the population will be affected [15]. Because almost all particles will gather in the same optimal position, the optimization will be stagnant and unable to find the global optimal value. It is not advisable for particles to keep the initialization speed and iterate until the end of the algorithm, because the historical optimal and global optimal of particles cannot work, which will reduce the adaptability of the algorithm. This also shows that if the algorithm does not find the global optimal solution before convergence, premature convergence will occur.

The particle iterative optimization of the PSO algorithm inevitably has the defect of only optimizing a part. The local optimal solution will cause the particle to stop searching and communicating with other particles. This will affect the diversity of the population and the optimization results, resulting in the final optimal solution which is not ideal.

2.2. Improved Method of Particle Swarm Optimization Algorithm

2.2.1. Improvement of Inertia Weight. The traditional PSO algorithm uses the inertia weight decreasing strategy to realize the dynamic change of inertia weight, but this method cannot reflect the dynamic search process of particle swarm optimization, and it is easy to lead to the local optimization of the algorithm. Therefore, a sine adjustment strategy with random disturbance appears. Adding sine adjusted inertia weight before and after the search can accelerate the convergence speed of the algorithm [16]. The inertia weight is adjusted according to the following formula:

$$\omega = \omega_1 \times \left[1 - \sin\left(\frac{\pi t}{e_{\max}}\right) \right] + r \times \omega_2 \times \sin\left(\frac{\pi t}{e_{\max}}\right), \quad (6)$$

where r is a random number, e_{\max} is the maximum number of iterations, and ω_1, ω_2 are the initial inertia weight and the final inertia weight, respectively. After the inertia weight is adjusted according to formula (6), the inertia weight is close to the initial value in the initial iteration of the algorithm, so the global search ability of the algorithm is strong, but the local search ability is weak. In the later stage of iteration, the inertia weight will be close to the final value, which can improve the local search ability and search accuracy.

PSO algorithms with different inertia weights have different balance points in global and local search capabilities [17]. The improved PSO algorithm process of inertia weight increases the threshold and the maximum number of iterations on the basis of the standard PSO algorithm process. When updating the velocity and position of particles, the inertia weight is determined first. When choosing the value of inertia weight, the decreasing strategy is no longer used, but the sine adjustment strategy of random disturbance is adopted.

2.2.2. Improvement of Learning Factors. In the standard PSO algorithm, the value range of two learning factors s_1, s_2 is generally $[0, 2]$ [18]. When solving complex optimization problems, particles at the beginning of iteration are easy to gather together, resulting in the algorithm falling into local optimal value. The dynamic learning factor can help the algorithm avoid local optimization and avoid premature convergence under the premise of accelerating the convergence speed. At the beginning of iteration, if s_1 is larger and s_2 is smaller, the ability of particles of learning themselves can be strengthened and a large number of particles can be avoided. At the later stage of iteration, if s_1 is smaller and s_2 is larger, it can enhance the ability of particles of learning groups and quickly and accurately finding the global optimal solution [19].

The value of learning factor is determined on the basis of formulae (3) and (4). At that time, the values of the two learning factors were as follows:

$$\begin{aligned} s_1 &= 0.6 \times u \begin{pmatrix} e_{\max} - e \\ e_{\max} \end{pmatrix}, \\ s_2 &= 0.4 + 0.1 \times r. \end{aligned} \quad (7)$$

When $e > 0.6 \times e_{\max}$, the values of the two learning factors are as follows:

$$\begin{aligned} s_1 &= 0.4 + 0.1 \times u, \\ s_2 &= 0.6 \times u \begin{pmatrix} e \\ e_{\max} \end{pmatrix}, \end{aligned} \quad (8)$$

where u is a random number. This improvement can improve the convergence speed of the algorithm at the beginning of the iteration and the accuracy of the solution in the late iteration. Based on the standard PSO algorithm, the improved PSO algorithm process also increases the threshold and the maximum number of iterations. When updating the velocity and position of particles, the two learning factors are determined first. Instead of fixed values, the dynamic changes of learning factors are realized by adding random numbers according to the maximum iterations of particles.

2.2.3. Improvement of Differential Evolution Algorithm.

The differential evolution (DE) algorithm performs random search based on population differences [17]. Firstly, the initial population is generated randomly and evenly, and m individuals are randomly generated in N -dimensional space. Then, three individuals x_{v1}, x_{v2}, x_{v3} are randomly selected from the feasible solutions for mutation operation. The mutation individuals are shown in the following formula:

$$b_{ij}(k) = x_{v1j} + F(x_{v2j} - x_{v3j}). \quad (9)$$

where F is the scaling factor. In order to increase the diversity of feasible solutions, cross operation is carried out, as shown in the following formula:

$$c_{ij}(k+1) = \begin{cases} b_{ij}(k), & \text{if } \text{rand}(0, 1) \leq p \text{ or } j = \text{rand}(1, n), \\ x_{ij}(k), & \text{if } \text{rand}(0, 1) > p \text{ or } j \neq \text{rand}(1, n), \end{cases} \quad (10)$$

where p is the crossover probability and the value range is $[0, 1]$. Then, select and update the target individual, as shown in the following formula:

$$x_i(k+1) = \begin{cases} c_i(k+1), & \text{if } f(c_i(k+1)) < f(c_i(k)), \\ x_i(k), & \text{if } f(c_i(k+1)) \geq f(c_i(k)). \end{cases} \quad (11)$$

The mutation, crossover, and selection operations are repeated until the convergence accuracy of the algorithm meets the requirements or the iteration times meet the termination conditions. The DE algorithm is used to improve the PSO algorithm. In the specific operation, the mutation, crossover, and selection operations in DE algorithm are used to mutate the historical optimal position of particles, so as to maintain the diversity of particles and avoid the weakening of global search ability in the late iteration stage and the emergence of premature scene. In order to judge the aggregation degree of particles, the particle aggregation factor is introduced into the basic PSO algorithm, as shown in the following formula:

$$d(e) = \frac{\min(y(p_g(e)), \bar{y})}{\max(y(p_g(e)), \bar{y})}, \quad (12)$$

where $y(p_g(e))$ is the fitness value of the historical optimal position, e is the current iteration number, and \bar{y} is the average of the current fitness of the particle. The value range of aggregation factor is $(0, 1]$, and the value is directly proportional to the degree of aggregation. In other words, the smaller the value, the lower the aggregation degree of particles and the greater the diversity of particle swarm [20, 21].

Improved PSO algorithm flow based on DE algorithm on the basis of standard PSO algorithm, after calculating the historical optimal position and fitness value, the calculation of aggregation factor, and mutation operation of historical optimal position are added, and then the position and speed of particles are updated according to aggregation factor and mutation operation. In this way, the diversity of particles can be maintained throughout the iteration process, the global search ability can be improved, and the optimization results can be optimized.

2.3. Sliding of Saturated Rock Slope

2.3.1. Monitoring Technology of Saturated Rock Slope Slip.

The geophysical methods for slope monitoring include radioactive measurement method, seismic exploration method, ground penetrating radar, and acoustic emission technology [22]. The radioactive measurement method can determine the geological form of slope slip by monitoring radon and its daughters in rock slope. It has the advantages of simplicity and economy, but the results are easily affected

by many factors and the accuracy is not high. In order to excite seismic wave, seismic exploration company uses reflection and refraction signal of seismic wave to judge the nature and shape of rock. Ground penetrating radar (GPR) is similar to seismic exploration, which uses the reflected signal of electromagnetic wave to find the position of slope slip. Through the monitoring of two closely connected acoustic emission probes, acoustic emission technology can judge the position of slope sliding and the time of slope sliding according to the intensity of acoustic emission.

The surface deformation morphology monitoring methods for slope monitoring include digital close range photogrammetry, global positioning system, geographic information system, and remote sensing and telemetry system [23]. Digital close range photogrammetry compares the pictures of the same position in different time periods and then uses computer processing technology to sort out and analyze the data to determine the relevant value of slip. The global positioning system (GPS) can locate and monitor the rock slope from multiple angles and in all directions and has the advantages of high accuracy and efficiency. The digital map of GIS can explore, analyze, and process huge geographic data. It can not only analyze the stability of rock, but also predict the stability of potential rock slope slip area. Remote sensing system uses remote sensing sensor device to survey and monitor large area of landform and geological disasters.

The deep deformation morphology detection methods for slope monitoring mainly include inclinometer technology, strain tube monitoring technology, and time domain reflection technology [24]. The inclinometer uses the movement law of the pendulum under the action of gravity, measures the relevant angle and horizontal displacement data, calculates the deformation trend and depth, and has high measurement accuracy. The strain tube monitoring technology can judge the deep displacement of the slope by monitoring the resistance change of the resistance strain gauge embedded in the strain tube in the slope body. Time domain reflectometry (TDR) is used to collect and analyze the reflected and projected signals of electromagnetic wave to monitor the stability of slope.

2.3.2. Stability Analysis of Saturated Rock Slope. The Swedish circular arc method considers that the ratio of the shear strength of the whole slip surface to the actual shear stress is the stability safety factor, which has the advantages of easy implementation and practical application [25]. In a homogeneous cohesive rock slope, l is a slip arc, and its center and radius are o, r , respectively. The antisliding moment $c \cdot l \cdot R$ on the slip arc and the reaction force caused by the self-weight of the sliding rock are N_R . When the internal friction angle between reaction force and rock is 0 , the stability safety factor is shown in the following formula:

$$F_s = \frac{N_R}{N_s} = \frac{c \cdot l \cdot R}{wk}. \quad (13)$$

Among them, the rotational moment $N_s = wk$, w is the self-weight of the sliding rock, and k is the horizontal

distance from the vertical line of the rock center to the center of the circle.

The Bishop method takes into account the effect of interslice forces, assuming that the vertical shear forces on both sides of the soil strip are the same, but the direction is opposite. The total normal force and tangential resistance at the bottom of soil strip are z_i, t_i , respectively. The equilibrium condition of vertical force of each soil strip is shown in the following formula:

$$w_i + q_i - q_{i+1} - z_i \cos \alpha_i - t_i \sin \alpha_i = 0, \quad (14)$$

where w_i is the self-weight and q_i is the tangential interstrip force. The tangential resistance at the bottom of the soil strip is shown in the following formula:

$$t_i = \frac{c'_i g_i}{F_s} + \frac{N_i - \mu g_i}{F_s} ad\phi'. \quad (15)$$

In limit equilibrium, the overall moment equilibrium condition is shown in the following formula:

$$\sum w_i q_i + \sum v_i e_i - \sum t_i r = 0, \quad (16)$$

where v is the horizontal force. The stability safety factor under Bishop method is shown in the following formula:

$$F_s = \frac{\sum (1/m_{ai}) [c'_i g_i + (w_i - \mu_i g_i) ad\phi']}{\sum w_i \sin \alpha_i + \sum v_i (e_i/r)}. \quad (17)$$

2.3.3. Numerical Analysis Method of Saturated Rock Slope.

The numerical analysis method mainly depends on the constitutive relation of materials to analyze the slip of rock slope, which can solve the slip field and stress field of the slope and can also simulate the specific process of the slip. The commonly used numerical analysis methods include finite element method, discrete element method, fast Lagrangian method, and boundary element method [26]. In the finite element method, the wireless element problem is discretized into a finite element problem, and then it is solved. The function equation is established and analyzed. The application of finite element method in slope mainly includes finite element arc search method and finite element strength reduction method. This method has the advantages of strong applicability and high authenticity of stress calculation, but the workload of calculation is very large and it is easy to make mistakes.

The discrete element method (DEM) discretizes the research object into rigid units and uses the central difference method to solve the motion equation. The result is the motion state of the research object. This method can solve the problem of large displacement of rock mass and simulate the process of rock sliding. The principle of the fast Lagrangian method is consistent with that of the discrete element method, but, compared with the discrete element method, it can be applied to the nonlinear solution of various boundary conditions and constitutive models. Although the solution speed is fast, the accuracy is not high.

The boundary element method transforms the partial differential equation into the boundary integral equation

and then discretizes it into an algebraic equation with only boundary nodes to solve the unknown variables. The algorithm can reduce the dimension of the problem, so it greatly reduces the calculation workload and improves the efficiency. But, when dealing with nonlinear problems, the performance is poor. Sometimes, the results are complex and not clear enough.

3. Experiments on Numerical Simulation of Rock Slope Sliding Based on PSO Algorithm

3.1. Improvement of Particle Swarm Optimization Algorithm. Although the improved PSO algorithm based on DE algorithm mentioned in Chapter 2 can improve the global search ability, it needs a strong local search ability in the later stage of iteration. Simplex method has a small amount of computation. It has the advantages of strong local search ability and fast convergence speed, but poor convergence characteristics. It is difficult to achieve good optimization results only by using simplex method when solving complex functions with higher dimensions. Therefore, on the basis of optimizing the global search capability based on DE algorithm, this paper also uses the simplex method to optimize the local search capability of PSO algorithm.

The flow of the improved algorithm is as follows: firstly, the parameters of particle swarm are initialized, and then the fitness value of each particle is calculated. The second step is to calculate the historical optimal value and global optimal value of particles and update the position and velocity of particles. The third step is to calculate the aggregation factor of particles. If it is greater than 0.1, the DE algorithm is used for mutation, crossover, and selection to update the historical optimal position of particles. In the fourth step, after the fitness values of particles are arranged in ascending order, the first few particles are selected to form a simplex, and simplex search is carried out to update the historical optimal position of particles. The fifth step is to judge whether the termination condition is satisfied. If it is satisfied, the algorithm will be terminated. If not, it will return to the second step to repeat the search.

3.2. Stage Analysis of Rock Slope Sliding. The first is the elastic deformation stage, the rock slope under the load force of instantaneous deformation. Then, in the initial deformation stage, the structural planes and pores in the rock body are gradually closed under the action of sliding force, resulting in elastic aftereffect deformation. The third stage is isokinetic deformation stage, in which the material of rock slope shows viscous damage or creep damage, and the deformation develops at constant speed. The fourth stage is the accelerated deformation stage. Plastic damage and viscous damage appear simultaneously in the rock slope, and the deformation speed will accelerate with time. The last stage is the instability stage, the deformation of the slope presents a steep increase and failure situation, the cracks in the slope spread to the maximum, and the duration of the instability stage is relatively short.

3.3. Numerical Simulation of Rock Slope Slip. The slip of rock slope was simulated numerically by ABAQUS software, the stability of rock slope was analyzed by finite element method, and all data were analyzed by the improved PSO algorithm in this paper. The Mohr-Coulomb model of ABAQUS software can simulate the main characteristics of rock and can be used to analyze transversely isotropic rock slope. The finite element analysis model of rock slope has a slope height of 45 m and a slope angle of 40°. The physical property parameters of the material are the common sandy mudstone with density of 2.44 g/cm³, elastic modulus of 1.21×10^4 mpa, and porosity of 5.42%. After confirming the model data and material parameters, the model was established by ABAQUS software. The top, middle, and foot of the slope are selected as feature points to judge whether the slope is sliding.

In order to analyze the effect of rockfall impact on rock slope slip, LS-DYNA program is used to simulate rock slope with rockfall impact. Assuming that the rock slope under impact has uniform texture and fixed boundary, the rockfall in the simulated value is a rigid cube, and then the rockfall drop model is established.

4. Discussion on Results of Numerical Simulation Analysis

4.1. Performance of the Improved Algorithm in This Paper. The convergence performance of improved algorithm (TP-PSO), standard PSO algorithm, and improved PSO algorithm based on DE algorithm (DE-PSO) is compared and analyzed.

As shown in Figure 2, the improved PSO algorithm converges after nearly 100 iterations, and the improved PSO algorithm based on DE algorithm converges after 150 iterations, while the standard PSO algorithm shows a slow convergence trend. Therefore, in terms of convergence speed, the improved PSO algorithm is better than the improved PSO algorithm based on DE and the standard PSO algorithm.

The performance of the algorithm is also reflected in the optimization effect. Therefore, the optimization results of the test function under different algorithms are compared. The optimal value results obtained by the three algorithms are as follows:

As shown in Table 1, the optimization results of TP-PSO algorithm in four functions are 3.5712, 0.0572, 5.0417, and 2.2401. In different test functions, the optimal values obtained by different algorithms are not consistent, and they are greatly different due to the characteristics of the function itself.

As shown in Figure 3, the minimum optimization result of TP-PSO algorithm is 0.0572 and the maximum is 5.0417. The minimum optimization result of DE-PSO algorithm is 0.0275 and the maximum is 15.3622. The minimum and maximum results of PSO algorithm are 2.8083 and 19.7796, respectively. This shows that the accuracy of TP-PSO algorithm is higher than that of DE-PSO algorithm and PSO algorithm.

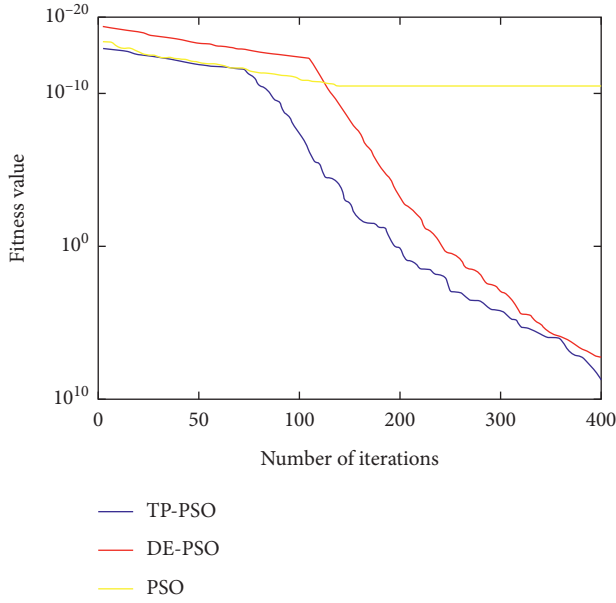


FIGURE 2: Convergence curve of the algorithm.

TABLE 1: Optimal values of different algorithms.

Algorithm	Function 1	Function 2	Function 3	Function 4
TP-PSO	3.7512	0.0572	5.0417	2.2401
DE-PSO	2.0458	15.3622	9.1219	0.0275
PSO	2.8083	3.6157	19.7796	19.4803

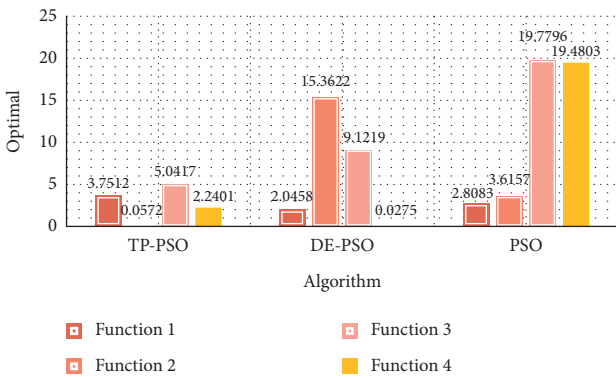


FIGURE 3: Comparison of optimal values of different algorithms.

4.2. Numerical Simulation Results of Rock Slope Slip. In this paper, the stability of rock slope is analyzed by numerical simulation of finite element method. Three main sections of the top, middle, and foot of the slope are selected to calculate the instability probability of the left and right sides of each main section. The results are as follows:

As shown in Table 2, the maximum failure probability of the left and right sides of the main section at the top of the slope is 0.1789 and 0.1816, and the minimum probability of instability is 0.0021 and 0.0059. However, in most cases, the instability probability of the left side is slightly higher than that of the right side, and it is impossible to judge which side

TABLE 2: Instability probability of main section at the top of slope.

X_i (m)	$\mu_A(x)$ left	P left	$\mu_A(x)$ right	P right
0	1	0.1789	1	0.1816
1	0.9272	0.1473	0.8924	0.1489
2	0.8815	0.1279	0.7718	0.1147
3	0.8251	0.1056	0.6675	0.0873
4	0.7762	0.0857	0.5781	0.0671
5	0.7264	0.0653	0.5004	0.0481
6	0.6835	0.0510	0.4332	0.0328
7	0.6399	0.0347	0.3753	0.0226
8	0.5907	0.0213	0.3267	0.0142
9	0.5346	0.0021	0.2750	0.0059

has the higher instability probability only by the maximum and minimum value.

As shown in Figure 4, in the main section at the top of the slope, the average instability probability on the left is 0.0820, and the average instability probability on the right is 0.0723. This shows that, in general, the instability probability of the left side is slightly higher than that of the right side. Therefore, for the top of slope, more attention should be paid to the generation of left side slope slip.

Then, the stability of the main section in the middle of the slope is analyzed, and the instability probability of the left and right sides of the main section is calculated.

As shown in Table 3, the maximum instability probability of the left and right sides of the main section in the slope is 0.1557 and 0.1353, and the minimum instability probability is 0.0111 and 0.0029. The variation trend of instability probability of the left and right sides of the main section in the slope is as follows:

As shown in Figure 5, in the main section of the middle slope, the average instability probability on the left side is 0.0772, and that on the right side is 0.0492. This shows that, in general, the instability probability of the left side is higher than that of the right side. Therefore, it is necessary to pay more attention to the left side slope slip for the middle slope.

Then, the stability of the main section at the toe of the slope is analyzed, and the instability probability of the left and right sides of the main section of the toe is calculated.

As shown in Table 4, the maximum failure probability of the left and right sides of the main section at the toe of the slope is 0.1755 and 0.1784, and the minimum probability of instability is 0.0115 and 0.0063. The variation trend of the instability probability of the left and right sides of the main section of the slope toe is as follows:

As shown in Figure 6, in the main section of slope toe, the average instability probability on the left side is 0.0837, and that on the right side is 0.0677. This shows that, in general, the instability probability of the left side is higher than that of the right side. Therefore, for the toe of slope, it is necessary to pay more attention to the left side slope slip.

To sum up, in the three main sections of the top, middle, and toe of the slope, the trend of the instability probability of the top and foot of the slope is similar, and the instability probability of the left side is higher than that of the right side. Although the left side of the slope is higher than the right side, it is relatively stable.

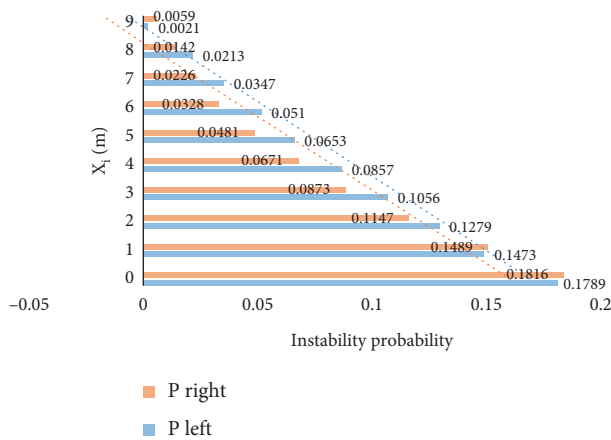


FIGURE 4: Variation trend of instability probability of main section at the top of slope.

TABLE 3: Instability probability of main section in middle slope.

X_i (m)	$\mu_A(x)$ left	P left	$\mu_A(x)$ right	P right
0	1	0.1557	1	0.1353
1	0.9538	0.1489	0.8516	0.1082
2	0.8979	0.1158	0.6963	0.0793
3	0.8452	0.0963	0.5692	0.0574
4	0.7956	0.0785	0.4653	0.0408
5	0.7484	0.0621	0.3804	0.0284
6	0.7051	0.0478	0.3112	0.0191
7	0.6637	0.0347	0.2549	0.0127
8	0.6226	0.0215	0.2081	0.0074
9	0.5860	0.0111	0.1688	0.0029

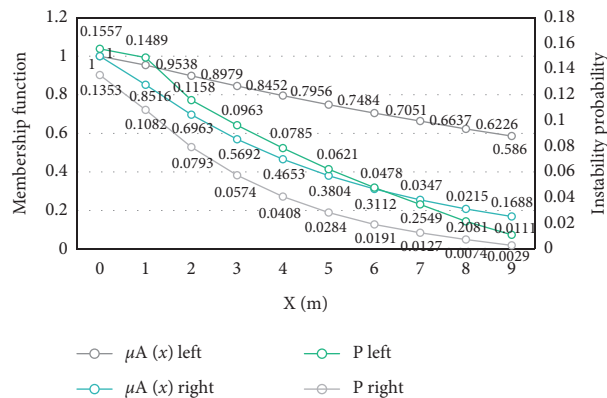


FIGURE 5: Variation trend of instability probability of main section in middle slope.

4.3. Influencing Factors of Rock Slope Slip

4.3.1. *Influence of Rock through Joint.* The influence of joint on rock slope slip is analyzed from the same direction through joint and reverse through joint. The same joint parameters are used in the experiment, 5 joints are set in the same direction and 5 joints in the reverse direction, respectively. Starting from the foot of the rock, 5 reference points were selected on average to observe and calculate the

TABLE 4: Instability probability of main section of slope toe.

X_i (m)	$\mu_A(x)$ left	P left	$\mu_A(x)$ right	P right
0	1	0.1755	1	0.1784
1	0.9391	0.1519	0.8672	0.1427
2	0.8815	0.1279	0.7512	0.1108
3	0.8272	0.1058	0.6507	0.0847
4	0.7762	0.0857	0.5626	0.0408
5	0.7284	0.0675	0.4884	0.0463
6	0.6835	0.0511	0.4231	0.0325
7	0.6414	0.0364	0.3666	0.0215
8	0.6019	0.0232	0.3176	0.0129
9	0.5648	0.0115	0.2752	0.0063

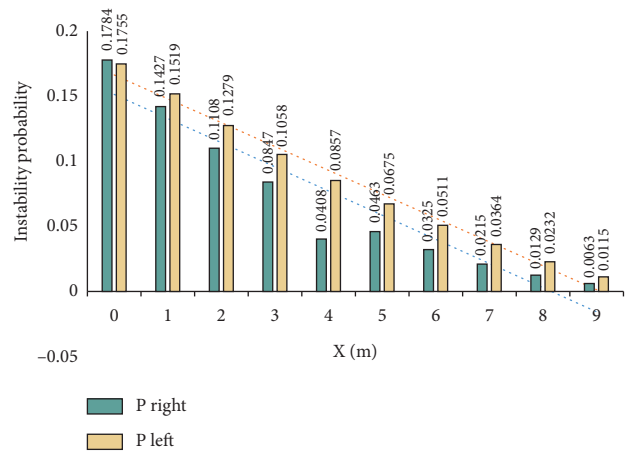


FIGURE 6: Variation trend of instability probability of main section at slope toe.

displacement of the upper and lower sides and the left and right sides of the reference points.

As shown in Table 5, in the same direction through joint, reference point no. 1 has the largest displacement at the upper and lower sides, which are -5.992 cm and -4.481 cm, respectively; in the reverse through joint, the largest displacement at the upper and lower sides is reference point 3, which is -5.782 cm and -7.626 cm, respectively.

As shown in Figure 7, the relative displacement of no. 1 reference point is the largest, which is 1.511 cm, and the relative displacement of no. 5 reference point is the smallest, which is 0.122 cm. This shows that the rock slope with the same direction through joint is mainly affected by the joint at the toe of the slope and the sliding occurs from bottom to top.

As shown in Figure 8, the relative displacement of no. 3 reference point is the largest, which is 1.656 cm, while the relative displacement of no. 1 reference point is the smallest, which is 0.401 cm. This shows that the rock slope with reverse through joints is mainly affected by the joints in the slope and the sliding occurs from the middle to both ends.

4.3.2. *Impact of Rockfall.* The influence of rockfall on rock sliding can be analyzed from the impact position, height, and size of rockfall. This study analyzes the height and size of

TABLE 5: Displacement of reference point.

Reference point	Displacement in the same direction			Reverse displacement		
	Upside	Downside	Relative	Left side	Right side	Relative
1	-5.992	-4.481	1.511	-4.523	-4.122	0.401
2	-5.331	-4.476	0.855	-5.210	-4.258	0.952
3	-4.235	-3.993	0.242	-6.982	-5.326	1.656
4	-3.426	-3.019	0.407	-4.731	-3.877	0.854
5	-2.223	-2.101	0.122	-3.906	-3.019	0.887

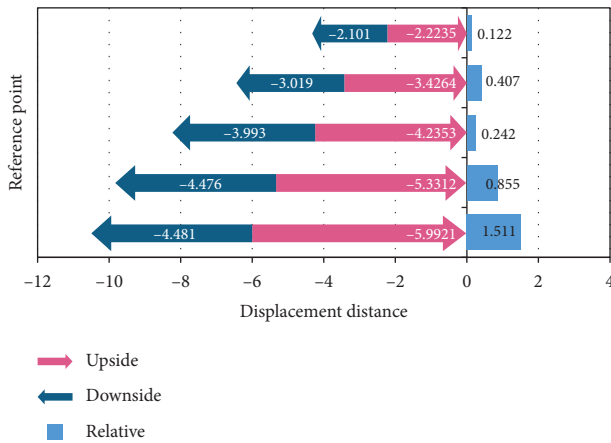


FIGURE 7: Displacement of reference point through joint in the same direction.

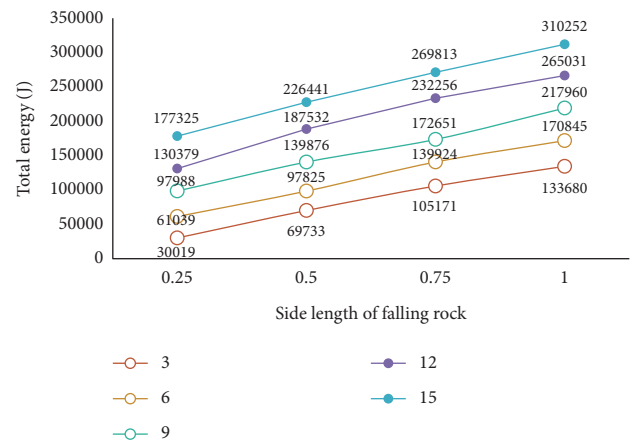


FIGURE 9: Total energy of rock slope.

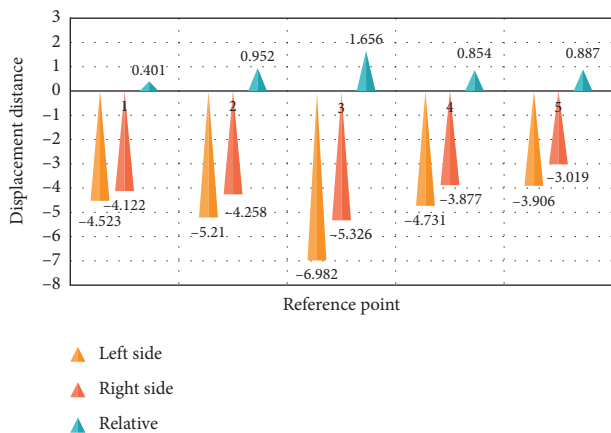


FIGURE 8: Displacement of reference point of reverse through joint.

rockfall and unifies the material and impact position of rockfall. The total energy of rock slope is analyzed by selecting cubic rockfall with side length of 0.25 m, 0.5 m, 0.75 m, and 1 m, respectively, from the height of 3 m, 6 m, 9 m, 12 m, and 15 m.

As shown in Figure 9, the total energy of a rockfall with a side length of 0.25 m impacting the rock slope at 3 m is the minimum, which is 30019 J. When the rockfall with a side length of 1 m impacts the rock slope at 15 m, the maximum energy is 310252 J. The difference between the minimum and the maximum is about 10 times. With the increase of the size and height of rockfall, the total energy of rock slope is also increasing, and the possibility and degree of rock slope sliding are higher.

5. Conclusions

Particle swarm optimization (PSO) algorithm is bound to fall into local optimization due to its continuous iterative optimization. In this paper, based on DE algorithm and simplex method, the particle swarm optimization algorithm is improved, which improves the global search ability in the initial iteration stage and the local search ability in the late iteration stage. Through comparative analysis, it is found that the algorithm in this paper has faster convergence speed and higher optimization accuracy.

The traditional algorithm is always difficult to improve the analysis efficiency because of the large amount of calculation in the analysis of data of rock slope. The improved algorithm can effectively solve this problem. The stability of rock slope is analyzed by finite element method, and all simulation data are analyzed by improved PSO algorithm. In the sliding model of rock slope constructed in this paper, the instability probability of the left side is higher than that of the right side, and the sliding is more likely to occur. The rock slope with the same direction through joint is mainly affected by the joint at the toe of the slope, and the rock slope with reverse through joint is mainly affected by the joint in the slope, and the sliding occurs from the middle to both ends. In addition, the size and height of rockfall will directly affect the possibility of rock slope sliding.

Due to the limited time and knowledge, there are some deficiencies in this study. The first is the defect of the numerical simulation method itself. There is a big difference between the numerical simulation in the laboratory and the actual situation, so it is difficult to achieve complete

reduction. Secondly, when analyzing the factors affecting slope slip, the condition of unbroken joints and irregular rockfall is not taken into account. These shortcomings in the future research work need to be improved as far as possible, in order to improve the reliability of the data.

Data Availability

No data were used to support this study.

Conflicts of Interest

The authors declare that they have no conflicts of interest.

Acknowledgments

This work was supported by the General Programs of the National Natural Science Foundation of China (Grant no. 51774184).

References

- [1] D. P. Deng, L. H. Zhao, and L. Li, "Limit equilibrium analysis for rock slope stability using basic Hoek–Brown strength criterion," *Journal of Central South University*, vol. 1, no. 09, pp. 230–239, 2017.
- [2] Y. Deng, "A threat assessment model under uncertain environment," *Mathematical Problems in Engineering*, vol. 2015, Article ID 878024, 12 pages, 2015.
- [3] A. Ketabi and M. H. Fini, "Adaptive underfrequency load shedding using particle swarm optimization algorithm," *Journal of Applied Research & Technology*, vol. 15, no. 1, pp. 54–60, 2018.
- [4] R. Mohammadi, S. M. T. F. Ghomi, and F. Jolai, "Pre-positioning emergency supplies for earthquake response: a new multi-objective particle swarm optimization algorithm," *Applied Mathematical Modelling*, vol. 40, no. 9–10, pp. 5183–5199, 2016.
- [5] X. Zhang, X. Wang, Y. Niu, and G. Cui, "A novel multi-objective particle swarm optimization algorithm based on invasive weed optimization," *Journal of Computational and Theoretical Nanoscience*, vol. 13, no. 6, pp. 3902–3908, 2016.
- [6] L. Wang, B. Huang, Z. Zhang, Z. Dai, P. Zhao, and M. Hu, "The analysis of slippage failure of the HuangNanBei slope under dry-wet cycles in the three gorges reservoir region, China," *Geomatics, Natural Hazards and Risk*, vol. 11, no. 1, pp. 1233–1249, 2020.
- [7] W. Zhuang, L. I. Chi, and D. Xuan-Ming, "Application of transparent soil model tests to study the soil-rock interfacial sliding mechanism," *Journal of Mountain Science*, vol. 16, no. 04, pp. 214–222, 2019.
- [8] M. Wang and Q. Tian, "Dynamic heat supply prediction using support vector regression optimized by particle swarm optimization algorithm," *Mathematical Problems In Engineering*, vol. 2016, Article ID 3968324, 10 pages, 2016.
- [9] A. Rana and D. Sharma, "Mobile ad-hoc clustering using inclusive particle swarm optimization algorithm," *International Journal of Electronics and Information Engineering*, vol. 8, no. 1, pp. 1–8, 2018.
- [10] M. A. Tawhid and K. B. Dsouza, "Hybrid binary dragonfly enhanced particle swarm optimization algorithm for solving feature selection problems," *Mathematical Foundations of Computing*, vol. 1, no. 2, pp. 181–200, 2018.
- [11] G. Guan, Q. Yang, W. Gu, W. Jiang, and Y. Lin, "Ship inner shell optimization based on the improved particle swarm optimization algorithm," *Advances in Engineering Software*, vol. 123, pp. 104–116, 2018.
- [12] H. Ouyang, Y. Quan, L. Gao et al., "Global hierarchical path planning of mobile robot based on hybrid genetic particle swarm optimization algorithm," *Zhengzhou Daxue Xuebao/ Journal of Zhengzhou University*, vol. 41, no. 4, pp. 34–40, 2020.
- [13] M. Alimardani and M. Almasi, "Investigating the application of particle swarm optimization algorithm in the neural network to increase the accuracy of breast cancer prediction," *International Journal of Computer Trends and Technology*, vol. 68, no. 4, pp. 65–72, 2020.
- [14] Y. Sun and Y. Gao, "An efficient modified particle swarm optimization algorithm for solving mixed-integer nonlinear programming problems," *International Journal of Computational Intelligence Systems*, vol. 12, no. 2, p. 530, 2019.
- [15] J. K. Arthur, E. K. Boahen, F. Doh et al., "Firewall rule anomaly detection and resolution using particle swarm optimization algorithm," *International Journal of Computer Applications*, vol. 178, no. 33, pp. 975–8887, 2019.
- [16] D. Wu, Y. Liu, K. Zhou, K. Li, and J. Li, "A multi-objective particle swarm optimization algorithm based ON human social behavior for environmental economics dispatch problems," *Environmental Engineering and Management Journal*, vol. 18, no. 7, pp. 1599–1607, 2019.
- [17] G. Chinnadurai and H. Ranganathan, "Curvature based 2 wheels self supporting robot based on the particle swarm optimization algorithm," *International Journal of Computing & Information Technology*, vol. 11, no. 1, pp. 37–43, 2019.
- [18] N. R. Zhou, A. W. Luo, and W. P. Zou, "Secure and robust watermark scheme based on multiple transforms and particle swarm optimization algorithm," *Multimedia Tools and Applications*, vol. 78, no. 2, pp. 2507–2523, 2019.
- [19] D. Li, K. Li, J. Liang, and A. Ouyang, "A hybrid particle swarm optimization algorithm for load balancing of MDS on heterogeneous computing systems," *Neurocomputing*, vol. 330, pp. 380–393, 2019.
- [20] J. Liu, Y. Guo, S. Zha et al., "Multi station assembly sequence planning based on improved particle swarm optimization algorithm," *Jisuanji Jicheng Zhizao Xitong/Computer Integrated Manufacturing Systems, CIMS*, vol. 24, no. 11, pp. 2701–2711, 2018.
- [21] J. Guan and L. Jia, "A multi-objective particle swarm optimization algorithm for solving human resource allocation problem," *IPPTA: Quarterly Journal of Indian Pulp and Paper Technical Association*, vol. 30, no. 8, pp. 144–149, 2018.
- [22] K. Y. Yang, C. X. Chen, K. Z. Xia et al., "Research on sliding failure mechanism of gently inclined bedding compound rock mass slope under hydraulic drive," *Zhongguo Gonglu Xuebao/ China Journal of Highway and Transport*, vol. 31, no. 2, pp. 144–153, 2018.
- [23] L. Xinrong, H. Chunmei, H. Chunmei, L. Xingwang, L. Gang, and Z. Bin, "Study on the safety factors of the bedding rock slope under dynamic loading," *Journal of Engineering Science and Technology Review*, vol. 2016, no. 3, pp. 161–175, 2016.
- [24] Z. Li, H. U. Zheng, L. Wenlian et al., "Plastic limit analysis of open-pit mine jointed rock slope considering translation-rotation mechanisms," *Yanshilixue Yu Gongcheng Xuebao/ Chinese Journal of Rock Mechanics and Engineering*, vol. 37, no. s2, pp. 4056–4068, 2018.
- [25] C. Wen, X. Jiang, H. Yang et al., "Influence of slope conditions on seismic displacement modes of gravity retaining wall,"

Journal of Vibration, Measurement & Diagnosis, vol. 37, no. 4, pp. 763–768, 2017.

- [26] D. Mercier, J. Coquin, T. Feuillet et al., “Are Icelandic rock-slope failures paraglacial? Age evaluation of seventeen rock-slope failures in the Skagafjörður area, based on geomorphological stacking, radiocarbon dating and tephrochronology,” *Geomorphology*, vol. 296, pp. 45–58, 2017.

Research Article

Evolutionary Game Research on the Impact of Environmental Regulation on Overcapacity in Coal Industry

Bo Fan,^{1,2} Tingting Guo ,² Ruzhi Xu ,² and Wenquan Dong³

¹School of Earth Sciences and Resources, China University of Geosciences (Beijing), Beijing 100191, China

²School of Finance, Qilu University of Technology, Jinan, Shandong 250100, China

³Department of Industrial and Systems Engineering, The University of Tennessee, Knoxville, TN 37996, USA

Correspondence should be addressed to Ruzhi Xu; xrz@qlu.edu.cn

Received 2 February 2021; Revised 26 February 2021; Accepted 5 March 2021; Published 17 March 2021

Academic Editor: Ming Bao Cheng

Copyright © 2021 Bo Fan et al. This is an open access article distributed under the Creative Commons Attribution License, which permits unrestricted use, distribution, and reproduction in any medium, provided the original work is properly cited.

Currently, the world is facing two significant challenges: low-carbon development and overcapacity. Government departments must reexamine their development strategy of energy industry. Implementing environmental regulatory policies and technological innovation can help alleviate coal industry's overcapacity, while sustainable development requires joint actions of governments, enterprises, and the market. Based on the evolutionary game theory, this study constructs a tripartite evolutionary game model of local government, power industry, and coal enterprise. Under the premise of bounded rationality, the evolution path of each player in the game under the market incentive environmental regulation is analyzed, and the influence of the change of parameters of each player on the result is numerically simulated. The study found that strengthening environmental regulation by local governments is an inevitable choice to promote the transformation and upgrading of coal industry and power industry. In addition, reducing law enforcement costs and technological innovation costs are the fundamental point of the coordinated development of the three parties. Technological innovation in the power industry will reduce the probability of coal companies' choosing clean production strategies, while seeking low-cost clean production technology and financial support is the key to coal companies' optimization of production capacity.

1. Introduction

Environmental protection has always been the focus of all countries' attention, and many countries are pursuing more stringent environmental regulations to achieve green and low-carbon development. The Kyoto Protocol and the Paris Agreement signed by many countries aim to control greenhouse gas emissions; however, economic growth is inevitably accompanied by substantial increase in power generation [1]. Due to its low prices and large reserves, coal is widely used in energy-intensive industries such as power generation and heating. However, a large amount of carbon dioxide is emitted during coal mining and use. About 40% of global greenhouse gas emissions come from coal consumption [2]. Many countries and regions have called for a suspension of coal mining [3] and sought new ways of clean production, such as increasing the proportion of renewable

energy and clean energy in power generation [4, 5]. However, with relatively high cost of promoting and utilizing renewable energy and the low feasibility in the short term [6], the emission reduction targets for complete decarbonization of the power sectors in many countries remain unachievable. On the other hand, although countries like China, the United States, and other major energy consumers have restricted coal mining to meet their increasing demand for electricity, coal-fired power remains dominant in most developing countries [7, 8]. Notably, as an essential resource for the industrial economic development, the scale of coal trading is still enormous; meanwhile, the scale of the coal industry's backward production capacity is gradually expanding as well. Since coal overcapacity causes a waste of investment and destroys the ecological environment and seriously endangers human society's sustainable development [9], how to use coal resources reasonably while

protecting the environment is a significant problem that needs to be solved urgently.

Overcapacity is a common problem [10]. Take China, which ranks first in energy consumption, as an example. The 2016 Central Economic Work Conference listed “de-capacity” as the first of the five major structural reform tasks, and various coal de-capacity policies have been introduced since then. However, in 2019, China’s coal overcapacity scale has reached 210GW-260GW [11], which meant that the coal overcapacity remained relatively serious. The Chinese government must strengthen its environmental regulations and supervision of high-polluting industries such as coal and electricity before reaching the “threshold” that the ecological environment can withstand [12] so that to realize its promise of extremely challenging emission reduction to peak carbon dioxide emissions in 2030. Although environmental regulations are conducive to improving the utilization rate of energy companies and adjusting overcapacity [13], existing environmental regulations may become rigid under different socioeconomic conditions [14], let alone that it takes a long time before the backward production capacity is eliminated from market. Therefore, specific implementation of environmental regulations by local governments is the key to optimizing the production capacity structure and improving the ecological environment. The rules and regulations promulgated by the government can help speeding up the elimination of “zombie companies” in the coal industry and accelerate the pace of de-capacity [15]. Since coal industry and power industry belong to an industrial symbiosis system, under the influence of environmental regulations and other policies, the power sector is in a critical period of transformation and upgrading, which will lead to a sharp decline of the demand for coal in the future [16]. If the coal industry does not carry out green innovation in time, it will inevitably run adrift of the market needs. On the other hand, many studies have proved that for countries such as China, India, and Russia, where coal occupies a fundamental position in energy, as well as regions where coal occupies a significant proportion of the energy mix (such as the European Union), the key to energy transition is to promote clean and efficient coal use [17–19]. In summary, resolving coal overcapacity is a process of dynamic equilibrium that requires the cooperation of government, coal companies, and power industry, which will help optimize the industrial structure while ensuring the quality of capacity reduction and better achieving green and low-carbon development.

When studying the evolution of overcapacity under environmental regulations, time, changes in supervision efforts, and the learning capabilities of interest bodies need to be taken into consideration [20]. Therefore, given the assumptions of bounded rationality and decision-making dynamics in the evolutionary game theory, many scholars have explored the impact of environmental regulations on enterprise innovation and overcapacity by constructing evolutionary game models. As the primary consumers of coal companies, power industry is closely related to coal industry and both are affected by environmental regulations.

Furthermore, the coal purchase plan and power generation technology innovation in the power industry also affect coal companies’ production capacity. However, the existing related researches, which mainly focus on the game between the central government, local governments, and coal enterprises [21–23], lack the investigation of external factors such as the market supply and demand environment [24]. In this respect, this paper uses evolutionary game theory to contemplate the intensity of carbon emission reduction and coal market demand after technological upgrading in the coal and power industries, and studies the behavioral strategy relationship and dynamic evolution mechanism among the three-party game players of the local government, power industry, and coal enterprises under different constraint scenarios so as to provide a theoretical reference for the government to regulate and control related policy systems and help coal companies to break through the dilemma of overcapacity with the goal of low-carbon development.

Compared with existing researches, this study mainly makes contributions on the following aspects:

- (1) This study not only contemplates the game between regulatory agencies and enterprises but also takes the primary consumers of coal, namely, the power industry, as one of the main players in the game and constructs a three-party evolutionary game model (different from [20, 21]) to analyze how the tripartite game’s leading players coordinate to promote the transformation and upgrading of high-polluting coal industries and power industries under the premise of bounded rationality.
- (2) Existing researches do not incorporate environmental taxes and market factors into the game model. This paper takes the market-incentive environmental regulations adopted by China, a major coal consumer, as an example. Through numerical simulation of initial strategy selection, environmental taxes, and government subsidies and penalties, as well as costs and performance of innovation, we analyze the influence of different environmental regulations and other factors on the evolution path of coal enterprises and the power industry.
- (3) According to the results of the evolutionary game analysis, the key factors affecting the stability of the evolutionary game are found. It is concluded that local governments may strengthen environmental regulations and solve overcapacity by promoting technological innovation of enterprises (different from [25–27]), specifically, by increasing environmental taxes and increasing subsidies and penalties simultaneously, and the effect of strengthening penalties is particularly significant. When the amount of coal saved by technological innovation reaches a certain threshold, the power industry will actively carry out technological innovation. Although the power industry is a close strategic partner of coal companies, the power industry’s

technological innovation strategies will have a negative incentive for coal companies' cleaner production. Therefore, reducing the cost of technological innovation is the key to promoting the coordinated development of coal and power industries.

The rest of this paper is organized as follows: Section 2 reviews relevant literature; Section 3 constructs a tripartite evolutionary game model of local government, power industry, and coal enterprises; Section 4 analyzes the evolutionary stability of individual game player and the game system; Section 5 carries out numerical simulations to verify and analyze the research conclusions; Section 6 summarizes the research results of this study and puts forward corresponding policy recommendations.

2. Literature Review

This paper aims to study the impact of environmental regulations on the overcapacity of the coal industry and conduct a quantitative analysis through evolutionary game theory. The literature related to this study mainly relates to the impact of environmental regulations on enterprise innovation and overcapacity, the causes and solutions of overcapacity, which are reviewed on the following aspects.

The first aspect considers the impact of environmental regulations on corporate innovation and overcapacity. Innovation involves complex interaction between an enterprise and its environment. Shao et al. [28] believed that the impact of environmental regulatory policies on enterprise innovation can be roughly divided into four aspects: technological innovation, product innovation, institutional innovation, and ecological innovation. According to the "Porter Hypothesis," reasonable environmental regulations will stimulate enterprises to carry out technological innovation and achieve a win-win situation of improving enterprise competitiveness and reducing emissions [29]. Without mandatory requirement of environmental policy, due to the externality of innovation, the marginal cost of technological innovation of enterprises in the short term is much higher than the marginal benefit, which would impede enterprises from carrying out technological innovation due to lack of sufficient motivation [30]. Based on the "Porter Hypothesis," scholars have concluded that there is a U-shaped relationship between the intensity of environmental regulation and overcapacity, and a significant inverted U-shaped relationship with enterprise technological innovation [31], that is, before reaching a certain threshold, higher environmental regulations will improve the technological innovation capabilities of enterprises and alleviate overcapacity. For example, improving environmental regulation can increase the utilization rate of industrial capacity [32], accelerate the exit of "zombie companies" in the coal industry, and promote the governance of energy companies' capacity issues [15]. By an empirical analysis of 12 resource-based industries in China, Li et al. [33] pointed out that environmental regulations have a significant role in promoting technological innovation in the lagging period of resource-based industries. Ren et al.

[34] divided China's environmental regulations into three types: command-controlled, market-incentive, and voluntary-consciousness. Command-controlled regulations refer to the government's enactment of environmental laws and policies to enforce emission reduction; market-incentive regulations refer to the use of economic means such as the collection of sewage charges, emission taxes, etc., to limit corporate pollution emissions; voluntary-consciousness regulations refer to citizens actively supervising corporate emissions and protecting the environment. And different types of environmental regulations have different impacts on enterprise innovation. Chen et al. [35] pointed out that mandatory emission reduction is the main reason for the overcapacity in the southeast coastal area of China. Pan et al. [36] found that technological innovation can improve energy efficiency. In the long run, compared with command-controlled environmental regulations, market-incentive environmental regulations have more incentives and long-term effects on technological innovation and significantly improve energy efficiency. In addition, carbon tax has a positive effect on energy saving and emission reduction and can restrain energy consumption [37].

We can see that most of the literature focuses on the comparison of the policy effects of different types of environmental regulations, and this paper studies the impact of specific types of environmental regulations on the overcapacity of specific industries, which is mainly manifested through enterprise technological innovation.

The second aspect considers the causes and solutions of overcapacity. Generally speaking, the factors that cause overcapacity are related to both supply and demand: overheated investment on the supply side, uncertainty in demand, reduced exports, information asymmetry, etc. In addition, the government's regulatory failure will also promote overcapacity [32, 38]. Coal overcapacity has many impacts on economic development and the environment, such as a sharp decline in coal prices, which may cause loss or even bankruptcy of a great number of companies [39], and unreasonable allocation of economic resources, which thereby hinders investment on renewable energy. Scholars have found that although China's current de-capacity policy has achieved some results to a certain degree, there are still drawbacks. Shi et al. [40] pointed out that China's blind coal reduction policy cannot solve the fundamental problem. It is necessary to consider regional heterogeneity, and it would be more reasonable to use market tools to regulate and control capacity. Following a SWOT analysis on the safety and environmental laws and regulations of China and the United States, Dzonzi-Undi and Li [41] pointed out that a series of policies related to coal production safety and environmental protection formulated by China have insignificant effects on promoting safe production, environmental protection investment, and technology research and development, and only reduced the number of deaths. Regarding specific measures to resolve overcapacity, Zhang et al. [42] pointed out that eliminating backward units and regulating power generation prices can help improve energy efficiency. The implementing of environmental regulation policies are conducted by the central government and local

governments, where the central government is the target maker, and the local governments have actual control over the specific implementation of the target [43]. However, due to the pursuit of different interests, the effect of local governments in improving overcapacity policies is better than that of the central government [44], and the influence of local governments on carbon emission reduction is more significant than that of enterprises [45]. The government can use policy means to coordinate multi-interest bodies [46], which shows that local governments play an important role in capacity control and environmental protection.

The above literature on resolving overcapacity mostly focuses on the research of strategies between regulatory agencies. This paper focuses on the interaction between regulatory agencies and enterprises, as well as between enterprises and enterprises. We take the environmental regulation policies implemented in China as an example, assuming that local governments must implement the central government's relevant regulations on environmental regulation and mainly adopt market-incentive environmental regulations and adjust their regulatory intensity according to actual conditions.

To sum up, the key to resolving overcapacity lies in the close and reasonable arrangements of the government, enterprises, and consumers. Researches nowadays focus on the policy effects of government departments' implementation of environmental regulations on corporate overcapacity and do not place market factors in the same research framework. On the contrary, this study incorporates environmental taxes, government subsidies, and penalties, as well as innovation performance into the model. Through the three-party evolutionary game analysis of local government, power industry, and coal enterprises, we provide a reference for resolving the problem of coal overcapacity and the establishment of a market-oriented overcapacity early warning mechanism. The research differences between this study and other papers are shown in Table 1.

3. Problem Analysis and Model Construction

3.1. Problem Analysis and Model Assumptions. Overcapacity leads to a decline in coal prices, which increases global coal demand again. Faced with huge environmental pressure, if not strictly controlled, such a situation will fall into a vicious circle, according to which, as the executor of environmental regulations and policies, local governments must adjust the intensity of regulations. The implementation of environmental regulations has brought a considerable impact on coal-fired power plants, and the power industry is closely related to coal companies whose overcapacity is mostly affected by the amount of coal used in the power industry. Both players are susceptible to environmental protection policies. Based on the logical relationship diagram shown in Figure 1, this study explains the game between local governments, coal companies, and power industry players under market-incentive environmental regulations.

Figure 1 shows that the implementation of environmental regulations by local governments will impact the coal companies and power industries. The transformation and upgrading of thermal power plants to increase clean energy use will reduce the demand for coal and the operating income of coal companies. As coal enterprises are affected by environmental regulations, to make up for the loss of income and meet future sustainable development, the probability of choosing cleaner production will increase, and coal production capacity will be in a more reasonable range. Conversely, if power plants maintain the original coal demand, the probability of coal companies choosing cleaner production will also decrease, which will exacerbate coal overcapacity.

Based on the above analysis, before constructing an evolutionary game model among local governments, power industry, and coal companies, the following assumptions are made:

- (1) There are 3 players in the evolutionary game model, assuming the local government as player 1, the power industry as player 2, and coal companies as player 3, and all three are bounded rational decision-makers.
- (2) The "Environmental Protection Tax Law of PRC" came into effect on January 1, 2018, levying environmental protection taxes on air pollutants, water pollutants, solid pollutants, and noise. The damage to the ecological environment by the power industry and coal companies is prominently manifested in air pollution and water pollution [54]. The tax rate of air pollutants is 1.2 RMB to 12 RMB per pollution equivalent while the tax rate of water pollutants is 1.4 RMB to 14 RMB per pollution equivalent. Local governments can levy environmental taxes 1–10 times the minimum standard. Therefore, it is assumed that each region's environmental tax standard is 1.2–14 RMB per pollution equivalent, which is set as B . When local governments strengthen environmental regulations, the cost paid is C_1 . Local governments mainly impose environmental taxes on coal-fired power companies by levying B /per pollution equivalent standards, take financial or administrative penalties P for polluting companies that do not innovate in technology or maintain current production capacity, and subsidize S for companies that upgrade their technology to seek cleaner production, so as to force coal companies and the power industry to conduct clean production, alleviate the problem of overcapacity, and protect the local environment. According to the actual situation, it is assumed that $C_1 < P - S$. Technological innovation by either the power industry or coal companies can bring additional environmental benefits R to the local area. If both parties choose technological innovation, the local government's environmental benefits will be $2R$. There is a principal-agent relationship between the central government and local governments. When energy governance intensifies conflict of interest, local governments will choose to

TABLE 1: Papers that are most related to our research.

Literature	Government department	Power industry	Coal industry	Environmental regulation	Technological innovation
[29]				✓	✓
[47]				✓	✓
[48]		✓	✓	✓	✓
[49]		✓	✓	✓	✓
[50]	✓	✓	✓		✓
[51]	✓			✓	✓
[22]	✓			✓	✓
[52]	✓	✓		✓	✓
[53]			✓	✓	✓
This paper	✓	✓	✓	✓	✓

Source: authors' compilation.

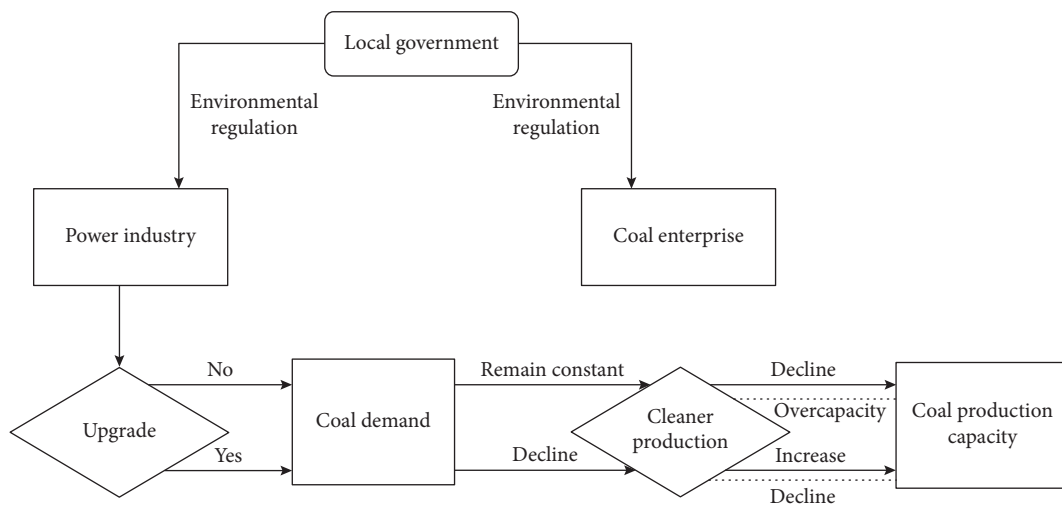


FIGURE 1: Logical relationship diagram of the three-party evolutionary game.

continue relatively loose environmental regulatory arrangements to seek a balance between environmental regulations and the economic benefits of local industries. It is assumed here that local governments only impose environmental taxes on power industry and coal companies. When the local environmental pollution is severe, or coal overcapacity protrudes, the local government will be held accountable by the higher-level competent authority, and the corresponding administrative penalty F , and $F > C_1$. In summary, the strategy set of local governments is (strengthening regulations, maintaining current regulations), $B \in [1.2, 14]$.

- (3) Nowadays, the proportion of coal power remains high in China's power industry, accounting for about 70%. Hydropower development has slowed down while clean energy power generation such as wind power and photovoltaics has developed rapidly; however, the proportion of its total installed capacity is still small [55] and coal-fired thermal power units still rely mainly on load reduction. Besides, starting from January 1, 2020, China has abolished the coal-electricity linkage mechanism, allowing the market

to set part of coal-fired power generation prices, which affects the profits of the power industry. With the improvement of environmental regulations, the amount of coal used in the power industry decreases, and the demand for clean energy is gradually increasing. The power industry chooses technological innovation to transform, upgrade, and adjust the structure of energy use. In this respect, the amount of coal saved is Q , the cost paid for technological innovation is C_2 , the increase in income after technological innovation is I_2 , and the initial emissions of power industry are G_2 . If the power industry carries out technological innovations, the emission reductions $t_2 G_2$ can be brought about, and the environmental taxes and fees that can be saved are $Bt_2 G_2$. However, if the cost of technological innovation is too high, the cost of environmental compliance is accordingly too low, or the cost gap between the use of coal and new energy is too small, then the power industry is likely to maintain the current coal consumption. Therefore, the power industry strategy set is (technical innovation, remaining unchanged), $t_2 \in (0, 1)$.

(4) Affected by environmental regulations, low-carbon environmental protection requirements have become increasingly stringent. The cost of environmental compliance for coal companies has increased so much that if coal companies maintain their existing capacity, hedging risks will be challenging. Considering that the transformation and upgrading of the power industry will exacerbate the overcapacity issue, coal enterprises seek ways to clean and efficient use of coal with a cost of C_3 and the increase in revenue from cleaner production of I_3 . Assuming that the current emissions of coal enterprises are G_3 , and the emission reduction that cleaner production can bring is t_3G_3 , the environmental tax savings would be Bt_3G_3 . However, when coal companies' cost of pollutant discharge is lower than the cost of cleaner production, or the power industry maintains the current demand for coal, companies will choose to maintain unchanged. As China's coal industry is in a buyer's market, if the coal company fails to adjust the production capacity after the technological innovation of the power company, it will cause overcapacity, and the price in this case is U_0 ; if the coal enterprise conducts clean production, the coal price is U_1 , $U_0 < U_1$. Therefore, the possible strategic

combination of coal companies is cleaner production, remaining unchanged.

Assuming that under bounded rationality, the probabilities that local governments choose to strengthen environmental regulation and maintain the current intensity are x and $1 - x$, respectively; the probabilities that the power industry chooses technological innovation and remains unchanged are y and $1 - y$, respectively; the probabilities that coal companies choose cleaner production and remain unchanged are z and $1 - z$, respectively, $x, y, z \in [0, 1]$.

3.2. Payoff Matrix of the Tripartite Evolutionary Game. According to the above assumptions, the payoff matrix of the three parties, namely, local government, power industry, and coal enterprise is so obtained (Table 2).

4. Evolutionary Game Model Solving and Stability Analysis

4.1. Stability Analysis of Local Government. Assuming that the expected profit when the local government chooses the strategy of "strengthening regulation" is U_x , the expected profit when the local government chooses the strategy of "maintaining the current regulation" is U_{1-x} , and the average expected profit is \bar{U}_1 , we can obtain

$$\begin{cases} U_x = yz[2R - B(t_2G_2 + t_3G_3) - 2S - C_1] + y(1-z)[R - Bt_2G_2 - S + P - C_1] \\ \quad + (1-y)z[R - Bt_3G_3 + P - S - C_1] + (1-y)(1-z)[2P - C_1], \\ U_{1-x} = yz[2R - B(t_2G_2 + t_3G_3)] + y(1-z)[R - Bt_2G_2] \\ \quad + (1-y)z[R - Bt_3G_3] + (1-y)(1-z)(-F), \\ \bar{U}_1 = xU_x + (1-x)U_{1-x}. \end{cases} \quad (1)$$

The replication dynamic equation of the local government strategy selection is

$$F(x) = \frac{dx}{dt} = (1-x)x[-C_1 + 2P + F(y-1)(z-1) - (P+S)(y+z)]. \quad (2)$$

Taking the derivative of $F(x)$,

$$\frac{dF(x)}{dx} = (1-2x)[-C_1 + 2P + F(y-1)(z-1) - (P+S)(y+z)]. \quad (3)$$

Let $F(x) = 0$, we can get $x = 0$, $x = 1$, $y = -([C_1 - F - 2P + (F + P + S)z]) / (F + P + S - Fz) = y^*$, according to the stability theorem of differential equations, if the probability that the local government chooses to strengthen environmental regulation is in a stable state, it must meet the conditions that $F(x) = 0$ and $d(F(x))/dx < 0$. When $y = y^*$, we can get $F(x) \equiv 0$, any value of x is an evolutionary stable strategy of the local government, and the local government

strategy does not change with time. When $y \neq y^*$, there will be two situations that result:

- (1) When $C_1 - F - 2P + (F + P + S)z < 0$, we can get $y^* > 0$. For any y in the interval $[0, 1]$, when $y > y^*$, we can get $dF(x)/dx|_{x=1} > 0$ and $dF(x)/dx|_{x=0} < 0$. Thus, $x = 0$ is the steady state. When $y < y^*$, we can get $dF(x)/dx|_{x=1} < 0$ and $dF(x)/dx|_{x=0} > 0$. Thus, $x = 1$ is the steady state.
- (2) When $C_1 - F - 2P + (F + P + S)z > 0$, we can get $y^* < 0$. Because $y \in [0, 1]$, then $y > y^*$ is held, we can get $dF(x)/dx|_{x=1} > 0$ and $dF(x)/dx|_{x=0} < 0$. Thus, $x = 0$ is the steady state. Figure 2 shows the evolution of local government strategies.

Proposition 1. *The probability that the local government chooses the strategy of "strengthening environmental regulation" is positively related to the penalty amount imposed by the superior authority on the local government, the punishment income from strengthening environmental regulation, and the cost of strengthening environmental regulation, and is*

TABLE 2: Payoff matrix.

Local government	Power industry	Coal enterprises	
		Cleaner production (z)	Remain unchanged ($1 - z$)
Strengthen regulations (x)	Technical innovation (y)	$\begin{bmatrix} 2R - B(t_2G_2 + t_3G_3) - 2S - C_1 \\ I_2 + S + QU_1 + Bt_2G_2 - C_2 \\ I_3 + S - QU_1 + Bt_3G_3 - C_3 \end{bmatrix}$	$\begin{bmatrix} R - Bt_2G_2 - S + P - C_1 \\ I_2 + S + QU_0 + Bt_2G_2 - C_2 \\ -QU_0 - P \end{bmatrix}$
	Remain unchanged ($1 - y$)	$\begin{bmatrix} R - Bt_3G_3 + P - S - C_1 \\ -P \\ I_3 + S + Bt_3G_3 - C_3 \end{bmatrix}$	$\begin{bmatrix} 2P - C_1 \\ -P \\ -P \end{bmatrix}$
Maintain current regulations ($1 - x$)	Technical innovation (y)	$\begin{bmatrix} 2R - B(t_2G_2 + t_3G_3) \\ I_2 + QU_1 + Bt_2G_2 - C_2 \\ I_3 - QU_1 + Bt_3G_3 - C_3 \end{bmatrix}$	$\begin{bmatrix} R - Bt_2G_2 \\ I_2 + QU_0 + Bt_2G_2 - C_2 \\ -QU_0 \end{bmatrix}$
	Remain unchanged ($1 - y$)	$\begin{bmatrix} R - Bt_3G_3 \\ 0 \\ I_3 + Bt_3G_3 - C_3 \end{bmatrix}$	$\begin{bmatrix} -F \\ 0 \\ 0 \end{bmatrix}$

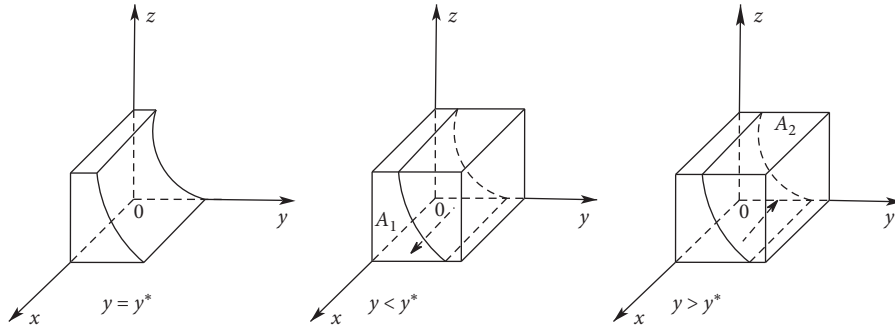


FIGURE 2: Phase diagram of strategy evolution of the local government.

negatively related to the cost of strengthening environmental regulations and the number of subsidies to enterprises.

Proof. Figure 2 shows that the probability of local governments adopting the strategies of “strengthening environmental regulations” and “maintaining current regulation” is the volume of space A_1 and A_2 , respectively, calculated as

$$\begin{aligned}
 V_{A_1} &= \int_0^1 \int_0^1 [-C_1 - F - 2P + (F + P + S)z] dx dz \\
 &= \frac{[-2C_1 + F + 3P - S - (F + 2(P + S))y]}{2}, \quad (4)
 \end{aligned}$$

$$V_{A_2} = 1 - V_{A_1}.$$

□

According to the expression of V_{A_1} when the local government adopts the strategy of “strengthening environmental regulation,” the first-order partial derivative of

each element can be obtained: $dV_{A_1}/dF > 0$, $dV_{A_1}/dP > 0$, $dV_{A_1}/dC_1 < 0$, $dV_{A_1}/dS < 0$. In summary, the increase in penalties imposed by higher-level authorities on local governments, the increase in revenue from fines coming with strengthening environmental regulations, or the reduction in the cost of strengthening environmental regulations and the reduction of subsidies can all increase the probability of local governments’ strengthening of environmental regulations.

Proposition 2. *The probability that the local government chooses the strategy of “strengthening environmental regulation” is negatively related to the probability that the power industry chooses “technical innovation” and the probability that coal companies choose “cleaner production.”*

Proof. When $z < -([C_1 - F - 2P + (F + P + S)y]) / (F + P + S - Fy)$ and $y < y^*$, we can get $dF(x)/dx|_{x=1} < 0$, thus, $x = 1$ is the steady state; otherwise, $x = 0$ is the steady state. Therefore, with the gradual increase in y and z , the evolutionary stabilization strategy of local governments will be

reduced from $x = 1$ (strengthening environmental regulations) to $x = 0$ (maintaining current regulations).

The probability that the local government chooses the strategy of “strengthening environmental regulation” will decrease with the increase of the probability that the power industry chooses the strategy of “technological innovation” and the probability that coal companies choose “cleaner production.” It shows that the active technological innovation of pollutant companies may slow down the process of

local governments’ strengthening of environmental regulations. \square

4.2. Stability Analysis of the Power Industry. Assuming that the expected profit when the power industry chooses the “technical innovation” strategy is U_y , the expected profit when the power industry chooses the “remain unchanged” strategy is U_{1-y} , and the average expected profit is \bar{U}_2 , we can obtain

$$\begin{cases} U_y = xz(I_2 + S + QU_1 + Bt_2G_2 - C_2) + x(1-z)(I_2 + S + QU_0 + Bt_2G_2 - C_2) \\ \quad + (1-x)z(I_2 + QU_1 + Bt_2G_2 - C_2) + (1-x)(1-z)(I_2 + QU_0 + Bt_2G_2 - C_2), \\ U_{1-y} = xz(-P) + x(1-z)(-P), \\ \bar{U}_2 = yU_y + (1-y)U_{1-y}. \end{cases} \quad (5)$$

The replication dynamic equation of the power industry strategy selection is

$$F(y) = \frac{dy}{dt} = (1-y)y[-C_2 + I_2 + BG_2t_2 + (P+S)x + Q(U_0(1-z) + U_1z)]. \quad (6)$$

Taking the derivative of $F(y)$,

$$\frac{dF(y)}{dy} = (1-2y)[-C_2 + I_2 + BG_2t_2 + (P+S)x + Q(U_0(1-z) + U_1z)]. \quad (7)$$

Let $F(y) = 0$, we can get $y = 0$, $y = 1$, $z = [-C_2 + I_2 + BG_2t_2 + QU_0 + (P+S)x]/Q(U_0 - U_1) = z^*$, according to the stability theorem of differential equations, if the probability of choosing technological innovation in the power industry is stable, it must meet the conditions that $F(y) = 0$ and $d(F(y))/dy < 0$. When $z = z^*$, we can get $F(y) \equiv 0$, any value of y is an evolutionary stable strategy of the power industry, and the strategy of the power industry does not change over time. When $z \neq z^*$, there are two situations that result:

- (1) When $-C_2 + I_2 + BG_2t_2 + QU_0 + (P+S)x < 0$, we can get $z^* > 0$. For any z in the interval $[0, 1]$, when $z > z^*$, we can get $dF(y)/dy|_{y=1} < 0$ and $dF(y)/dy|_{y=0} > 0$. Thus, $y = 1$ is the steady state. When $z < z^*$, we can get $dF(y)/dy|_{y=1} > 0$ and $dF(y)/dy|_{y=0} < 0$. Thus, $y = 0$ is the steady state.
- (2) When $-C_2 + I_2 + BG_2t_2 + QU_0 + (P+S)x > 0$, we can get $z^* < 0$. Because $z \in [0, 1]$, then $z > z^*$ is held, we can get $dF(y)/dy|_{y=1} < 0$ and $dF(y)/dy|_{y=0} > 0$. Thus, $y = 1$ is the steady state. The strategy evolution diagram of power industry is shown in Figure 3.

Proposition 3. *The probability that the power industry chooses the “technological innovation” strategy is positively*

related to the increase in revenue brought by technological innovation in the power industry, government subsidies and penalties, the environmental taxes that can be saved, and the increase in the cost of saving coal, and is negatively related to technology research and development costs.

Proof. Figure 3 shows that the probability that the power industry adopts “remaining unchanged” and “technological innovation” strategies are the volumes of B_1 and B_2 , respectively, calculated as

$$\begin{aligned} V_{B_1} &= \int_0^1 \int_0^1 \frac{[-C_2 + I_2 + BG_2t_2 + QU_0 + (P+S)x]}{Q(U_0 - U_1)} dx dy \\ &= \frac{[-2C_2 + 2I_2 + P + S + 2BG_2t_2 + 2QU_0]}{2Q(U_0 - U_1)}, \end{aligned} \quad (8)$$

$$V_{B_2} = 1 - V_{B_1} = \frac{[-2C_2 + 2I_2 + P + S + 2BG_2t_2 + 2QU_1]}{2Q(U_1 - U_0)}.$$

\square

According to the expression of V_{B_2} , when the power industry adopts the strategy of “technical innovation,” the first-order partial derivative of each element can be obtained: $dV_{B_2}/dC_2 < 0$, $dV_{B_2}/dI_2 > 0$, $dV_{B_2}/dP > 0$, $dV_{B_2}/dS > 0$, $dV_{B_2}/dBG_2t_2 > 0$, $dV_{B_2}/dQU_1 > 0$. In summary, it can be seen that the increase in benefits after technological improvement in the power industry, the increase in government subsidies and penalties, the increase in environmental taxes and fees that can be saved, and the increase in the cost of saving coal, or the reduction of technology research and development costs in the power industry can all promote the power industry’s acceleration of technological innovation.

Proposition 4. *The probability that the power industry chooses the “technological innovation” strategy is positively related to the probability that the local government chooses “strengthen environmental regulation” and the probability that coal companies choose “cleaner production.”*

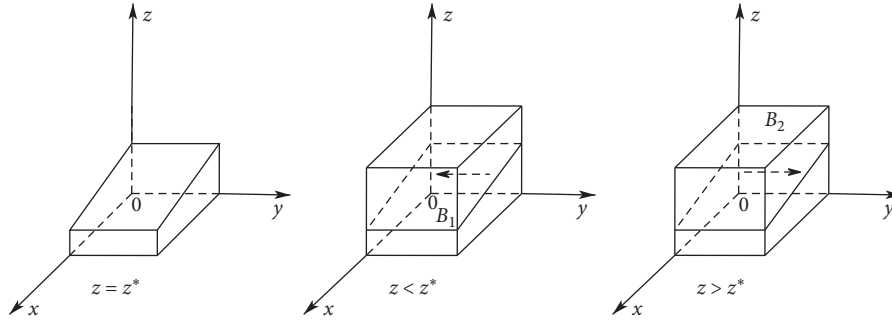


FIGURE 3: Phase diagram of strategy evolution of the power industry.

Proof. The proving process is the same as Proposition 2. The probability of the power industry choosing the strategy of “technological innovation” increases with the increase of the local government choosing the strategy of “strengthening environmental regulation” and the probability of coal enterprises choosing the strategy of “cleaner production,” suggesting that the local government’s strengthening of environmental regulations can promote the technical innovation of the power industry, and the power industry technology innovation needs the government’s strict regulation. The impact of coal companies’ strategic

choices on the power industry is further reflected in coal price fluctuation, and the promotion of cleaner production by coal companies can help the power industry in technological innovation. \square

4.3. Stability Analysis of Coal Enterprise. Assuming that the expected profit when the coal company chooses the “cleaner production” strategy is U_z , the expected profit when the coal company chooses the “remain unchanged” strategy is U_{1-z} , and the average expected profit is \bar{U}_3 , we can obtain

$$\begin{cases} U_z = xy(I_3 + S - QU_1 + Bt_3G_3 - C_3) + x(1 - y)(I_3 + S + Bt_3G_3 - C_3) \\ \quad + (1 - x)y(I_3 - QU_1 + Bt_3G_3 - C_3) + (1 - x)(1 - y)(I_3 + Bt_3G_3 - C_3), \\ U_{1-z} = xy(-QU_0 - P) + x(1 - y)(-P) + (1 - x)y(-QU_0), \\ \bar{U}_3 = zU_z + (1 - z)U_{1-z}. \end{cases} \quad (9)$$

The replication dynamic equation of coal enterprise strategy selection is

$$F(z) = \frac{dz}{dt} = (1 - z)z[I_3 - C_3 + BG_3t_3 + (P + S)x + Q(U_0 - U_1)y]. \quad (10)$$

Taking the derivative of $F(z)$,

$$\frac{dF(z)}{dz} = (1 - 2z)[I_3 - C_3 + BG_3t_3 + (P + S)x + Q(U_0 - U_1)y]. \quad (11)$$

Let $F(z) = 0$, we can get $z = 0$, $z = 1$, $x = [C_3 - I_3 - BG_3t_3 + Q(U_1 - U_0)y] / (P + S) = x^*$. According to the stability theorem of differential equations, if the probability of selecting cleaner production in the coal enterprise is stable, it must meet the conditions that $F(z) = 0$ and $d(F(z))/dz < 0$. When $x = x^*$, $F(z) \equiv 0$, any value of z is the evolutionary stable strategy of coal enterprises, and the strategy of coal enterprises does not change with time. When $x \neq x^*$, there are two situations that result:

- (1) When $C_3 - I_3 - BG_3t_3 + Q(U_1 - U_0)y > 0$, we can get $x^* > 0$. For any x in the interval $[0, 1]$, when $x > x^*$, we can get $dF(z)/dz|_{z=1} < 0$ and $dF(z)/dz|_{z=0} > 0$. Thus, $z = 1$ is the steady state. When $x < x^*$, we can get $dF(z)/dz|_{z=1} > 0$ and $dF(z)/dz|_{z=0} < 0$. Thus, $z = 0$ is the steady state.
- (2) When $C_3 - I_3 - BG_3t_3 + Q(U_1 - U_0)y < 0$, we can get $x^* < 0$. Because $x \in [0, 1]$, then $x > x^*$ is held, we can get $dF(z)/dz|_{z=1} < 0$ and $dF(z)/dz|_{z=0} > 0$. Thus, $z = 1$ is the steady state. The strategy evolution diagram of the coal enterprise is shown in Figure 4.

Proposition 5. The probability that coal companies choose “cleaner production” is positively related to the increase in revenue brought about by cleaner production, government subsidies and penalties, and the environmental taxes and fees that can be saved, and is negatively related to the decrease in coal sales revenue and the cost of clean production inputs.

Proof. Figure 4 shows that the probability of coal enterprises adopting “remain unchanged” and “cleaner production” strategies are the volumes of D_1 and D_2 respectively, calculated as

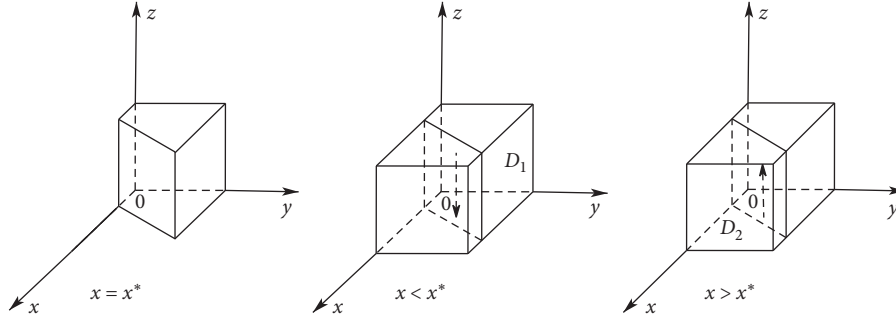


FIGURE 4: Phase diagram of strategy evolution of coal enterprises.

$$\begin{aligned}
 V_{D_1} &= \int_0^1 \int_0^1 \frac{[C_3 - I_3 - BG_3 t_3 + Q(U_1 - U_0)y]}{(P + S)} dy dz \\
 &= \frac{[2C_3 - 2I_3 - 2BG_3 t_3 + Q(U_1 - U_0)]}{2(P + S)}, \\
 V_{D_2} &= 1 - V_{D_1} = \frac{[-2C_3 + 2I_3 + 2(P + S) + 2BG_3 t_3 - Q(U_1 - U_0)]}{2(P + S)}. \quad (12)
 \end{aligned}$$

According to the expression of V_{D_2} , when the coal enterprise adopts “cleaner production” strategy, the first-order partial derivative of each factor can be obtained: $dV_{D_2}/dC_3 < 0$, $dV_{D_2}/dI_3 > 0$, $dV_{D_2}/dP > 0$, $dV_{D_2}/dS > 0$, $dV_{D_2}/dBG_3 t_3 > 0$, $dV_{D_2}/d(Q(U_1 - U_0)) < 0$. In summary, it can be seen that increasing the benefits of clean production of coal enterprises, increasing government subsidies and penalties, increasing the environmental taxes and fees that can be saved, and reducing the difference in coal sales revenue of coal enterprises or reducing the cost of clean production can all promote coal enterprises’ speeding up of clean production. \square

Proposition 6. *The probability that coal companies choose “cleaner production” strategy is positively correlated with the probability that the local government chooses “strengthening environmental regulation.” However, it is negatively*

correlated with the probability that the power industry chooses the strategy of “technical innovation.”

Proof. The proving process is the same as Proposition 2.

The probability that coal companies choose a “cleaner production” strategy increases with the increase in the probability of local governments choosing “strengthening regulation” strategy, indicating that subject to the measures taken by the local government to improve environmental regulation, coal companies must seek transformation and upgrading actively. The probability that coal companies choose the “cleaner production” strategy decreases with the increase of the probability when the power industry chooses “technological innovation” strategy. This conclusion contradicts our analysis in the previous problem description because as the demand for coal in the power industry has drastically reduced after technological upgrades, the income of coal companies from coal sales has also plummeted, which is far from covering the cost of clean production; thus, companies have insufficient motivation for independent innovation and will eventually choose to maintain the status quo. \square

4.4. Stability Analysis of Tripartite Evolutionary Game System.

It can be seen from the above that formulas (2), (6), and (10) constitute a three-dimensional continuous dynamic system:

$$\begin{cases}
 F(x) = (1-x)x[-C_1 + 2P + F(y-1)(z-1) - (P+S)(y+z)], \\
 F(y) = (1-y)y[-C_2 + I_2 + BG_2 t_2 + (P+S)x + Q(U_0(1-z) + U_1 z)], \\
 F(z) = (1-z)z[I_3 - C_3 + BG_3 t_3 + (P+S)x + Q(U_0 - U_1)y].
 \end{cases} \quad (13)$$

Let $F(x) = 0, F(y) = 0, F(z) = 0$, we can get 9 system equilibrium points: $E_1(0, 0, 0)$, $E_2(0, 1, 0)$, $E_3(0, 0, 1)$, $E_4(1, 0, 0)$, $E_5(1, 0, 1)$, $E_6(1, 1, 0)$, $E_7(0, 1, 1)$, $E_8(1, 1, 1)$, and $E_9(x^*, y^*, z^*)$ is the solution of formula (9).

$$\begin{cases}
 [-C_1 + 2P + F(y-1)(z-1) - (P+S)(y+z)] = 0 \\
 [I_2 - C_2 + BG_2 t_2 + (P+S)x + Q(U_0(1-z) + U_1 z)] = 0 \\
 [I_3 - C_3 + BG_3 t_3 + (P+S)x + Q(U_0 - U_1)y] = 0.
 \end{cases} \quad (14)$$

According to Selten’s research, only when X is a strict Nash equilibrium, the strategy combination X is gradually stable in a multi-agent evolutionary game dynamic replication system [56]. The strict Nash equilibrium is a pure strategy Nash equilibrium. Therefore, the asymptotically stable state must be evolutionary stable strategies (ESS), and it must be a pure strategy Nash equilibrium. $E_9(x^*, y^*, z^*)$ is a nonstrict Nash equilibrium and does not meet the evolutionary stability criterion of the multi-agent model [22]. Therefore, we only need to discuss the asymptotic stability of the eight pure strategy equilibrium points of E_{1-8} for the

abovementioned dynamic replication system. To simplify the calculation, let $A = P + S$, $D = I_2 - C_2 + BG_2t_2$, $E = Q(U_0 - U_1)$, and $H = I_3 - C_3 + BG_3t_3$, we can see that $A > 0$ and $E < 0$.

By using the replication dynamic equation, the *Jacobian matrix* of the tripartite game can be obtained as

$$J = \begin{bmatrix} (2x - 1)(C_1 - 2P - F(y - 1)(z - 1) + A(y + z)) & x(x - 1)(A - F(z - 1)) & x(x - 1)(A - F(y - 1)) \\ y(1 - y)A & (-D - Ax + Ez - QU_0)(2y - 1) & y(y - 1)E \\ z(1 - z)A & z(1 - z)E & (-H - Ax - Ey)(2z - 1) \end{bmatrix}. \tag{15}$$

According to the first theorem of Lyapunov [57], all the eigenvalues of the *Jacobian matrix* corresponding to the asymptotically ESS must be less than 0. Taking the equilibrium point $E_1(0, 0, 0)$ as an example to discuss its asymptotic stability, the characteristic value of the *Jacobian matrix* at $E_1(0, 0, 0)$ of the dynamic replication system is: $\lambda_1 = -C_1 + F + 2P$, $\lambda_2 = D + QU_0$, $\lambda_3 = H$. Since $F > C_1$, thus, $\lambda_1 > 0$, E_1 is an unstable point. Similarly, the gradual stability of the remaining 7 equilibrium points can be judged, and the results are shown in Table 3.

choose cleaner production, they still fail to change the power industry's strategic choices.

Scenario 1. When $D + A + QU_0 < 0$ and $H + A < 0$, that is, when the cost of innovation in the power industry is higher than the sum of the increase in revenue brought about by innovation and the savings in coal purchase costs and pollution discharge cost, and government subsidies and punishments, as well as when the clean production cost is higher than the sum of the benefits brought about by clean production, the government subsidies and punishments, and the saved pollution discharge cost, as shown in Table 3, there is only one stable point $E_4(1, 0, 0)$ in the dynamic replication system, which corresponds to the strategic set of (strengthening environmental regulation, remaining unchanged, remaining unchanged). In this case, the failure to promote the technological innovation of coal power enterprises by local government's strengthened environmental regulation is a situation that should be avoided in policy-making.

Scenario 3. When $D + A + QU_0 > 0$ and $H + A + E < 0$, that is, when the cost of innovation in the power industry is lower than the sum of the increase in revenue brought about by innovation and the savings in coal purchase costs and pollution discharge cost, and government subsidies and punishments, as well as when the clean production cost is higher than the sum of the benefits brought about by cleaner production, government subsidies, and punishments, the saved pollution discharge cost, and reduced coal sales revenue. It can be seen from Table 3 that there is only one stable point $E_6(1, 1, 0)$ in the dynamic replication system, which corresponds to the strategic set of (strengthening environmental regulations, technical innovation, remaining unchanged). In this case, even if local governments strengthen environmental regulations and reduce coal consumption in the downstream power industry, it is still the optimal strategy for coal companies to maintain the status quo to bring in more benefits.

Scenario 2. When $D + A + QU_1 < 0$ and $H + A > 0$, that is, when the cost of innovation in the power industry is higher than the sum of the increase in revenue brought about by innovation and the savings in coal purchase costs and pollution discharge cost, and government subsidies and punishments, as well as when the clean production cost is lower than the sum of the benefits brought about by clean production, the government subsidies and punishments, and the saved pollution cost, as shown in Table 3, there is only one stable point $E_5(1, 0, 1)$ in the dynamic replication system, which corresponds to the strategic set of (strengthening environmental regulations, remaining unchanged, cleaner production). In this case, because power industry cannot afford the high cost of technological innovation, even though local governments choose to strengthen environmental regulations and coal companies

Scenario 4. When $D + QU_1 > 0$ and $H + E > 0$, that is, when the cost of innovation in the power industry is lower than the sum of the increase in revenue brought about by innovation and the savings in coal purchase costs and pollution discharge cost, as well as when the clean production cost is lower than the sum of the benefits brought about by cleaner production, saved pollution discharge costs, and reduced coal sales revenue, as shown in Table 3, there is only one stable point $E_7(0, 1, 1)$ in the dynamic replication system, which corresponds to the strategic set of (maintaining current regulations, technical innovation, cleaner production). In this case, even if the local government still maintains the current environmental regulations, when the benefits of innovation can cover the cost of innovation, coal companies and the power industry will spontaneously choose to carry out technological innovation.

Based on the research hypothesis, the equilibrium points of Scenarios 1–4 are $E_4(1, 0, 0)$, $E_5(1, 0, 1)$, $E_6(1, 1, 0)$, and $E_7(0, 1, 1)$. For equilibrium point $E_4(1, 0, 0)$, local governments have adopted measures to strengthen environmental regulation, but they have still failed to change the current production status of coal-fired power companies and have no research value. For the equilibrium point $E_7(0, 1, 1)$, the

TABLE 3: Local stability analysis results.

Equilibrium point	Eigenvalues			Asymptotically stable
	λ_1	λ_2	λ_3	
$E_1(0, 0, 0)$	$-C_1 + F + 2P$	$D + QU_0$	H	Unstable point
$E_2(0, 1, 0)$	$-C_1 + P - S$	$-D - QU_0$	$H + E$	Unstable point
$E_3(0, 0, 1)$	$-C_1 + P - S$	$D + QU_1$	$-H$	Unstable point
$E_4(1, 0, 0)$	$C_1 - F - 2P$	$D + A + QU_0$	$H + A$	Condition 1
$E_5(1, 0, 1)$	$C_1 - P + S$	$D + A + QU_1$	$-H - A$	Condition 2
$E_6(1, 1, 0)$	$C_1 - P + S$	$-D - A - QU_0$	$H + A + E$	Condition 3
$E_7(0, 1, 1)$	$-C_1 - 2S$	$-D - QU_1$	$-H - E$	Condition 4
$E_8(1, 1, 1)$	$C_1 + 2S$	$-D - A - QU_1$	$-H - A - E$	Unstable point

Condition 1: $D + A + QU_0 < 0, H + A < 0$
Condition 2: $D + A + QU_1 < 0, H + A > 0$
Condition 3: $D + A + QU_0 > 0, H + A + E < 0$
Condition 4: $D + QU_1 > 0, H + E > 0$

government chooses to remain unchanged, but the cost of enterprise technological innovation is much higher than the income in the short run. According to the Prisoner's Dilemma, "remaining unchanged" is the absolute dominant strategy of the power industry and coal companies. No coal company and power industry will unilaterally choose technological innovation; so in reality, this equilibrium point does not exist and should be discarded. In summary, $E_5(1, 0, 1)$ and $E_6(1, 1, 0)$ are the possible equilibrium points of the three-dimensional dynamic system. Under certain conditions, the strengthening of environmental regulations by local governments can enable the power industry to choose technological innovation or enable coal companies for clean production, which will help resolve overcapacity and improve environmental quality.

5. Simulation Analysis

By referring to relevant statistical indicators in the "China Environmental Statistical Yearbook" and "China Environment Yearbook" (<https://www.yearbookchina.com>), we assign values to the model, and use MATLAB software to perform simulation analysis to verify the validity of evolutionary stability analysis.

The difference between the cost of technological innovation and the benefits brought about by innovation has a significant impact on the stability of the equilibrium point. The system is in a dynamic process in which each entity continuously adjusts the game strategy. Through effective adjustment of relevant parameters, the three-party game players can be observed considering how to reach the optimal strategy. According to the model hypothesis and the interaction relationship between the two more ideal evolutionary steady-state constraints of Scenarios 2 and 3, we assign values to the system parameters. To simplify the calculation, assume that the amount of steam coal that can be saved by power plant A after technological innovation is 1, the coal price $U_0 = 2.6$, and $U_1 = 3$. For Scenario 2, the remaining parameter assignments are: $C_1 = 3, P = 10, S = 3, F = 5, C_2 = 45, I_2 = 15, B = 14, G_2 = G_3 = 1, t_2 = t_3 = 0.3, I_3 = 15$, and $C_3 = 30$; For Scenario 3, the remaining parameter assignments are: $C_1 = 3, P = 10,$

$S = 3, F = 5, C_2 = 30, I_2 = 15, B = 14, G_2 = G_3 = 1, t_2 = t_3 = 0.3, I_3 = 15$, and $C_3 = 45$. For the sake of generality, assume that the probability of initial game strategy choice of local government, power industry, and coal company are respectively $x = 0.5, y = 0.4$, and $z = 0.4$; in the short term, the innovation income of coal companies and the power industry is a fixed value. On this basis, this study mainly analyzes the impact of initial strategy selection, environmental taxes, local government subsidies and punishments, and changes in the cost of the technological innovation of the power industry and coal companies on the evolution process and results of the three-dimensional dynamic system.

5.1. The Impact of Initial Strategy Choice on the Stability of Game Strategy. Local governments, power industry, and coal companies are in the same dynamic system. Changes in one player's game strategy will have a corresponding impact on the other two players' strategic choices. To analyze the impact of strategy selection on the evolutionary game process and results, on the basis of the initial values, keeping the remaining parameters unchanged, four groups of values are set: $x = 0.5, y = z = 0.4; x = 0.8, y = z = 0.4; x = 0.5, y = 0.8, z = 0.4;$ and $x = 0.5, y = z = 0.8$. The simulation result is shown in Figure 5.

It can be seen from Figure 5 that under the conditions of Scenario 2, as the probability of the power industry choosing technological innovation strategies increases, the evolution rate of coal companies gradually slows down, which further verifies Proposition 6. When the advantage of thermal power generation weakens and technological innovation in the power industry shifts to other energy resources, the operating income of coal companies will drop sharply. Even if the government grants certain subsidies, they cannot cover the costs of clean production. How to save costs and seek low-cost innovation is one of the challenges faced by coal companies. Whether in Scenarios 2 or 3, lower y and z will push the local government to stabilize and strengthen environmental regulations, which further verifies Proposition 2. With the increase of x , the stability of the evolution rate of coal enterprises under Scenario 2 and the power industry under Scenario 3 has increased significantly, which means

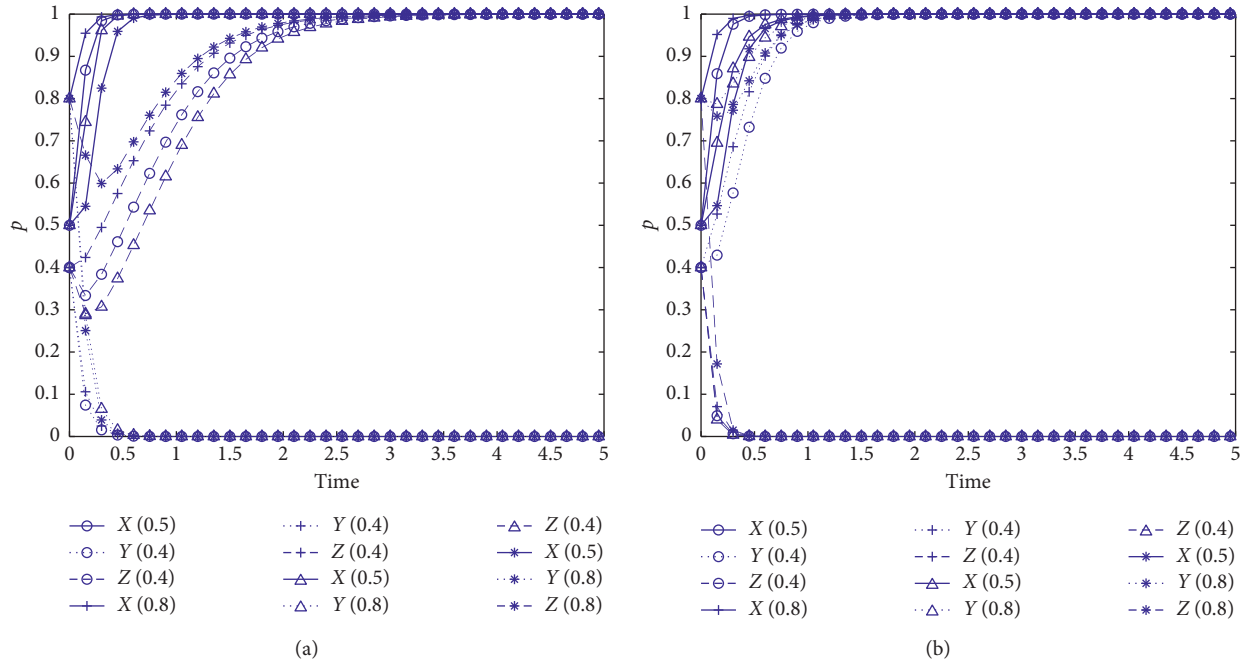


FIGURE 5: Evolution path under different initial strategies. (a) Scenario 2. (b) Scenario 3.

that local governments’ strengthening of environmental regulations has a significant policy effect and reveals the indispensable role of local governments in promoting industrial upgrading.

5.2. The Impact of Environmental Tax on the Stability of Game Strategy. Coal and power companies are regarded as high polluting industries and are sensitive to environmental taxes. Environmental taxes of different levels have different impacts on the power industry and coal companies’ strategic choices. Therefore, to analyze environmental taxes’ impact on the evolutionary game process and results, based on the initial values, we keep the remaining parameters unchanged, set three groups of values: $B = 14$; $B = 7$; and $B = 1.2$. The simulation result is shown in Figure 6.

It can be seen from Figure 6 that under Scenario 2, only when the environmental tax standard (B) reaches the maximum value, the coal companies’ strategic choice tends to be a stable state of cleaner production. And as B drops to the minimum value within the constraints, the coal companies’ strategic choices have changed from cleaner production to remaining unchanged. Similarly, under Scenario 3, the larger the B , the shorter the evolution time required for the power industry to reach a stable state of technological innovation. The above analysis further verifies Propositions 3 and 5. Under the lower environmental tax, the power industry has insufficient motivation to break through the original technology; a higher environmental tax can promote clean production for coal enterprises. We can conclude that the adoption of the highest environmental tax by local governments is essential to reduce the production capacity of coal companies and optimize the energy use structure of

the power industry. Levying a carbon tax can reduce carbon emissions. However, due to the diverse and heavy tax burdens of the coal industry, the normal operations of coal enterprises may be affected considering reality. Besides, environmental taxes will also hinder investment in renewable energy [58]. Therefore, local governments should make reasonable adjustments to environmental taxes based on actual local conditions and seek a balance between corporate innovation and environmental protection.

5.3. The Impact of Government Subsidy and Punishment Intensity on the Stability of Game Strategy. Most local governments strengthen environmental regulations and encourage coal power companies to carry out technological innovation by issuing administrative orders and formulating supporting subsidies and punishments. To analyze the influence of government subsidies and punishments on the evolutionary game process and results, based on the initial values, we keep the remaining parameters unchanged and set four groups of simulation values: $P = 10, S = 3$; $P = 10, S = 0, P = 0, S = 3$; and $P = 0, S = 0$. The simulation result is shown in Figure 7.

It can be seen from Figure 7 that under Scenario 2 when the government subsidies and penalties become more and more powerful, the probability of coal companies choosing cleaner production increases significantly; under Scenario 3, increasing subsidies and penalties can speed up the evolution rate of technological innovation in the power industry. No matter under Scenarios 2 or 3, the local government only issues subsidies or only adopts punitive measures, and the impact on the power industry and coal companies’ strategic choices is not as practical as the simultaneous use of

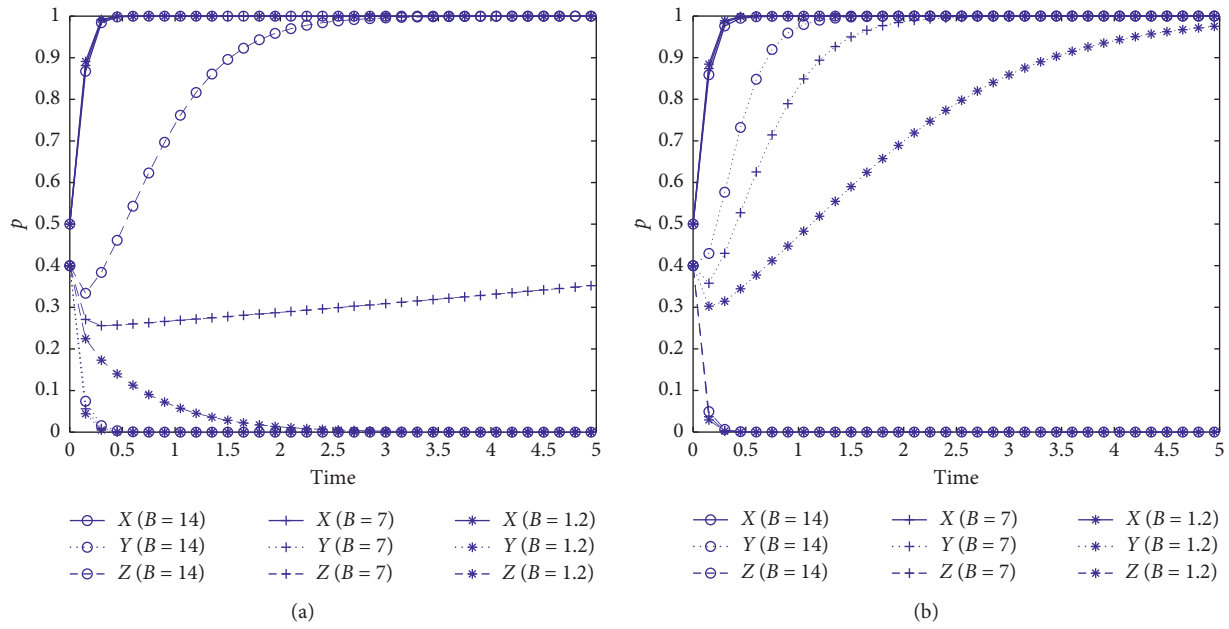


FIGURE 6: Evolution path under different environmental tax standards. (a) Scenario 2. (b) Scenario 3.

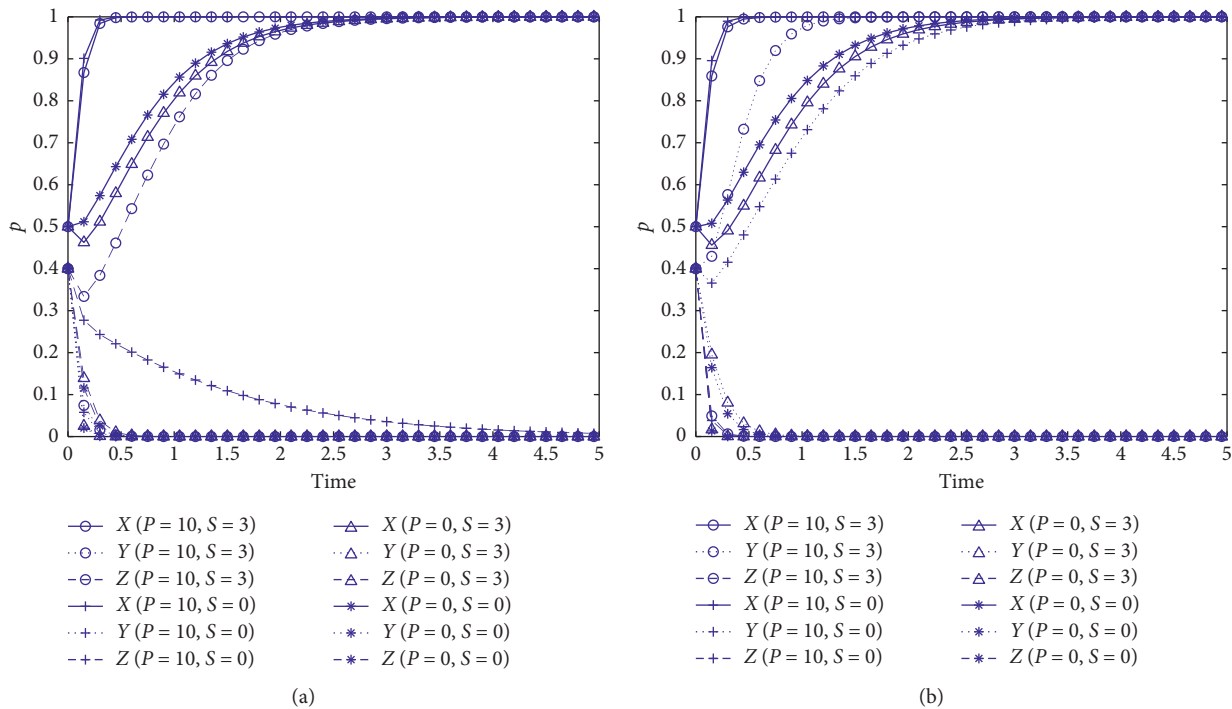


FIGURE 7: Evolutionary paths under different levels of subsidies and penalties. (a) Scenario 2. (b) Scenario 3.

subsidies and punishments; the effect of adopting the subsidy policy only is not as good as the policy of adopting penalties only; penalizing enterprises that violate the regulations alone can significantly increase the rate of evolution of local governments. When local governments do not take any subsidies and impose penalties ($P = 0, S = 0$), coal and power companies choose to keep the existing technology

unchanged. Even if the local government eventually tends to strengthen the stable state of environmental regulation, due to the decline in revenue, the evolution and stability of the local government will be extended. The above analysis also further verifies Propositions 1, 3, and 5. It can be seen that the local governments adopt a two-pronged approach to increase environmental taxes, subsidies, and punishments,

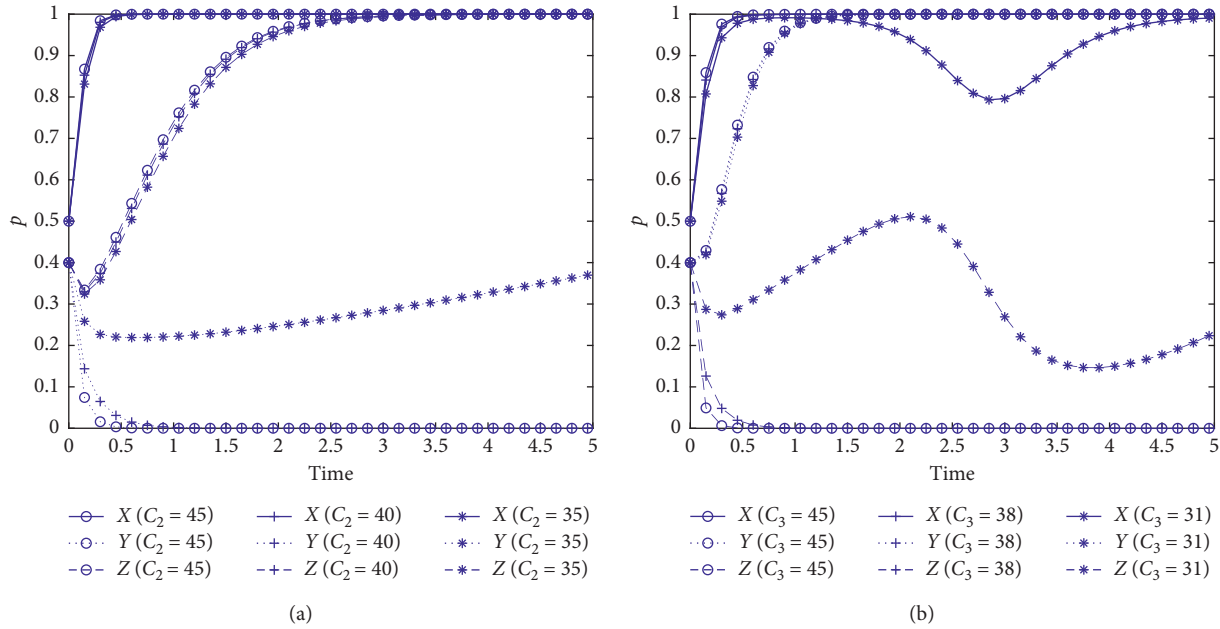


FIGURE 8: Evolutionary paths under different technological innovation costs. (a) Scenario 2. (b) Scenario 3.

and strictly supervise the coal and power industries, which will promote the transformation and upgrading of the coal power industry.

5.4. The Impact of Technological Innovation Cost on the Stability of Game Strategy. The cost of technological innovation in the coal-fired power industry is high. Except for large state-owned enterprises, most small and medium-sized enterprises cannot afford considerable costs in the short term; therefore, they lack technological innovation motivation. To analyze the impact of technological innovation costs on the evolutionary game process and results, based on the initial values, we keep the remaining parameters unchanged and set two groups of values: $C_2 = 45, C_2 = 40, C_2 = 35$; $C_3 = 45, C_3 = 38, C_3 = 31$. The simulation result is shown in Figure 8.

It can be seen from Figure 8 that under Scenario 2, with the gradual decrease of C_2 , the power industry's strategic choices no longer tend to be stable, but display a trend toward technological innovation strategies. Under Scenario 3, with the decrease of C_3 , the strategic choices of coal companies fluctuate sharply and are no longer stable in a passive state that remains unchanged. Moreover, when coal enterprises' innovation cost reduces to a certain level, local governments and coal enterprises' strategic choices are distributed symmetrically. The above analysis further verifies Propositions 3 and 5. It can be seen that the cost of innovation is a crucial factor affecting the transformation and upgrading of enterprises. Most companies use financing channels like loan to plan for technological upgrades. However, given that financial institutions nowadays do not know much about the operating characteristics of coal and electricity companies, existing financial products lack applicability and high financing costs. Besides, the lack of

collateral for small and medium-sized coal enterprises makes it difficult to meet the financing needs for technological innovation, which further restrains enterprise innovation motivation.

5.5. The Impact of Coal Saving on the Stability of Game Strategy. With the strategic transformation of the power industry, the demand for thermal power will continue to decline. The strategic choices of coal companies are bound to change to cater to the market. The coal saving Q brought about by technological innovation in the power industry is used to describe coal companies' sensitivity to the power industry strategy. Based on the initial values, we keep the remaining parameters unchanged and set three groups of values: $Q = 1; Q = 2.5; Q = 4.5$. The simulation result is shown in Figure 9.

It can be seen from Figure 9 that under Scenario 2, with the increase of Q , the evolution rate of coal enterprises' choice of cleaner production slows down. In the short term, the decline in coal enterprises' operating income is an essential factor affecting cleaner production. Technology upgrades have saved coal consumption for the power industry. As the demand for coal has fallen sharply, the power industry's choice of maintaining the same strategy has slowed down and even reversed. While under Scenario 3, the impact of coal sales volume on coal enterprises' evolution is not significant for the reason that coal enterprises are more likely unable to bear the innovation costs of cleaner production actively. The above analysis further verifies Propositions 3 and 5, which shows that coal companies are susceptible to technological upgrades in the power industry. The reduction in coal market demand will further aggravate coal overcapacity. Coal companies follow market demand as an inevitable choice for sustainable development.

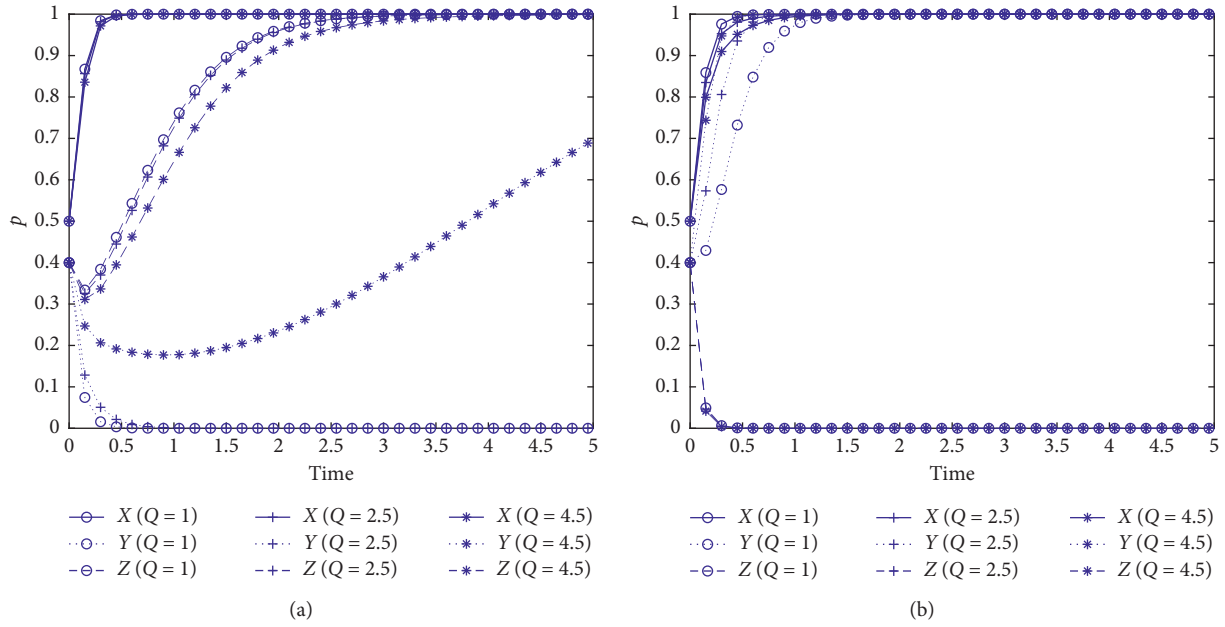


FIGURE 9: Evolution paths at different coal saving rates. (a) Scenario 2. (b) Scenario 3.

6. Conclusions

Based on the evolutionary game theory, this paper analyzes the evolutionary game process between local government, power industry, and coal enterprises through modeling. We analyze both the stability of a single player and the overall system, and conduct numerical simulations by adjusting factors such as the initial strategy choice of the game player, environmental taxes, government subsidies and punishments, technological innovation costs, and coal demand to explore the specific evolution path of a coal company's overcapacity under market-incentive environmental regulations. The numerical simulation analysis in this study further verifies the inferences of the stability analysis, summarizes the results of several simulations, and draws specific conclusions as follows:

- (1) The actions of local governments, concurrently increasing subsidies and punishments or increasing environmental taxes, can enable coal and power companies to reach an evolutionarily stable state faster, and the simultaneous implementation of both will help to further shorten the evolution time. Increasing government subsidies to energy companies can alleviate overcapacity to a certain extent (different from [59, 60]), but it is not as effective as taking punishment measures. If coal-fired power companies actively choose technological innovation, local governments will not change the current regulatory policies. Under this condition, the benefits of companies after innovation are far greater than the costs. In reality, this situation is difficult to exist in the early stages of technological innovation. It also shows that increasing environmental regulation is an inevitable choice for local governments to help enterprises transform and upgrade and resolve overcapacity.
- (2) The cost of enterprise technological innovation is a key factor affecting the stability of evolution. When the cost of innovation is lower, enterprises tend to choose technological innovation. Therefore, in technological innovation and capacity reduction of coal power enterprises, financial support should be increased. The government provides many subsidies to thermal power plants every year. Although subsidies may lead to inefficient use of resources [61], appropriate subsidies are necessary to transform the coal and power industries.
- (3) From the perspective of initial strategic choices, the strategic choices of local governments have a profound impact on the evolution and stability of coal-fired power companies. Reducing the cost of implementing environmental regulations and increasing the penalties for overcapacity can shorten the evolution time for local governments to strengthen environmental regulations, which will help realize the coordinated development of the three parties ultimately. Technological innovation in the power industry will reduce the operating income of coal companies and delay the evolutionary stability time for them to choose cleaner production. The increase in revenue and the reduction in both parties' costs are an essential prerequisite for coal companies and power industry's collaborative innovation.
- (4) The amount of coal saved after technological innovation is the focus of attracting power industry adjustment strategies. A certain level of coal saving will promote the power industry to carry out technological innovation actively. It also shows that with the continuous upgrading of power generation technology in the power industry, renewable energy

and clean energy will continue to swallow the coal market. The importance of clean coal production has become more prominent.

According to the above research conclusions, the following policy implications can be drawn:

- (1) When local governments implement specific environmental regulations and policies, there are often certain deviations related to their interests, which may result in the phenomenon that the coal industry can hardly reach the goal of reducing the production capacity. The central government must strengthen the supervision on local governments, and local governments must use their information advantages to rationally and timely regulate local environmental regulations. Overcapacity reduction is a task that every department should pay attention to. Taking a series of measures to reduce the cost of government environmental regulations can effectively promote local governments to strengthen their attention to overcapacity reduction tasks. On the other hand, the follow-up work to reduce overcapacity also requires the government to take supporting measures to speed up the process of transformation and upgrading of coal power enterprises by adhering to the principle of combining market forces with government support.
- (2) Economic development cannot be completely separated from the support of the coal industry; in other words, coal companies must assess the situation and improve their competitiveness through active clean production to meet the needs of the power industry and other consumers, accelerate the withdrawal of outdated production capacity, and improve de-capacity mechanism by arranging properly the resettlement of assets, debts, and employees. The business of coal and power companies involves vast investment, and their technological innovation costs and difficulties are also high. Coal mining companies should actively enhance their research to promote clean production technologies such as unharmed coal and intelligent mining to reduce subsequent operating costs and cater to green and era requirements of low-carbon development. In addition, given that many small and medium-sized coal companies do not have the economic strength to increase investment in clean production, planning mergers and acquisitions with other high-quality coal companies may be a good choice for their future development.
- (3) The existing differentiated industrial lending policies in the coal industry have given great support to high-quality companies, forcing “zombie companies” to withdraw from the market voluntarily. However, this has also made it more difficult for some small and medium-sized coal companies with good credit to obtain financing, thus making it difficult for them to put clean production into action. Therefore, it is

necessary to optimize the existing big data platforms such as the China (Taiyuan) Coal Trading Center and improve the credit ratings for coal companies. Financial institutions should meet the financial needs of high-quality coal companies and innovate inclusive financial products so as to achieve the goal of “structural reduction of production capacity and optimization of production capacity.”

This study has certain limitations: Firstly, local governments, power industry, and coal companies are in a complex system that many factors affect their strategic choices, and this study is not comprehensive enough to consider the influencing factors in the tripartite game process. Secondly, due to the limitations of data acquisition and the ideality of parameter assignment, we only carried out numerical simulations at the industry level. In the next step, we will conduct more profound research in combination with actual cases.

Data Availability

The data used to support the findings of this study in Section 5 “Simulation Analysis” are included within the paper.

Conflicts of Interest

The authors declare that they have no conflicts of interest.

Acknowledgments

This study was supported by Major Scientific and Technological Innovation Projects in Shandong Province (Project no. 2018CXGC0703).

References

- [1] B. Atems and C. Hotaling, “The effect of renewable and nonrenewable electricity generation on economic growth,” *Energy Policy*, vol. 112, pp. 111–118, 2018.
- [2] W. Li, P. L. Younger, Y. Cheng et al., “Addressing the CO₂ emissions of the world’s largest coal producer and consumer: lessons from the Haishiwan Coalfield, China,” *Energy*, vol. 80, pp. 400–413, 2015.
- [3] M. Blondeel and T. Van de Graaf, “Toward a global coal mining moratorium? A comparative analysis of coal mining policies in the USA, China, India and Australia,” *Climatic Change*, vol. 150, no. 1–2, pp. 89–101, 2018.
- [4] J. Stich, S. Ramachandran, T. Hamacher, and U. Stimming, “Techno-economic estimation of the power generation potential from biomass residues in Southeast Asia,” *Energy*, vol. 135, pp. 930–942, 2017.
- [5] C. Zhu, R. Fan, and J. Lin, “The impact of renewable portfolio standard on retail electricity market: a system dynamics model of tripartite evolutionary game,” *Energy Policy*, vol. 136, 2020.
- [6] A. Aslani and K.-F. V. Wong, “Analysis of renewable energy development to power generation in the United States,” *Renewable Energy*, vol. 63, pp. 153–161, 2014.
- [7] J. P. C. Bento, N. Szczygiel, and V. Moutinho, “Fossil fuel power generation and economic growth in Poland,” *Energy*

- Sources, Part B: Economics, Planning, and Policy, vol. 12, no. 10, pp. 930–935, 2017.
- [8] R. Zaman, C. Hofer, and T. Brudermann, “One step ahead, two steps backwards: energy transitions and coal in developing countries,” in *Proceedings of the 2018 International Conference and Utility Exhibition on Green Energy for Sustainable Development (ICUE)*, Phuket, Thailand, October 2018.
 - [9] A. Gupta and D. Spears, “Health externalities of India’s expansion of coal plants: evidence from a national panel of 40,000 households,” *Journal of Environmental Economics and Management*, vol. 86, pp. 262–276, 2017.
 - [10] S. Moret, F. Babonneau, M. Bierlaire, and F. Maréchal, “Overcapacity in European power systems: analysis and robust optimization approach,” *Applied Energy*, vol. 259, 2020.
 - [11] Y. Feng, S. Wang, Y. Sha, Q. Ding, J. Yuan, and X. Guo, “Coal power overcapacity in China: province-level estimates and policy implications,” *Resources, Conservation and Recycling*, vol. 137, pp. 89–100, 2018.
 - [12] F. Wang, L. Feng, J. Li, and L. Wang, “Environmental regulation, tenure length of officials, and green innovation of enterprises,” *International Journal of Environmental Research and Public Health*, vol. 17, no. 7, 2020.
 - [13] W. Du, F. Wang, and M. Li, “Effects of environmental regulation on capacity utilization: evidence from energy enterprises in China,” *Ecological Indicators*, vol. 113, 2020.
 - [14] V. Koziuk, Y. Hayda, O. Dluhopolskyi, and Y. Klapkiv, “Stringency of environmental regulations vs. global competitiveness: empirical analysis,” *Economics & Sociology*, vol. 12, no. 4, pp. 278–298, 2019.
 - [15] W. Du and M. Li, “Can environmental regulation promote the governance of excess capacity in China’s energy sector? The market exit of zombie enterprises,” *Journal of Cleaner Production*, vol. 207, pp. 306–316, 2019.
 - [16] J. Yuan, P. Li, Y. Wang et al., “Coal power overcapacity and investment bubble in China during 2015–2020,” *Energy Policy*, vol. 97, pp. 136–144, 2016.
 - [17] E. Hille, W. Althammer, and H. Diederich, “Environmental regulation and innovation in renewable energy technologies: does the policy instrument matter?” *Technological Forecasting and Social Change*, vol. 153, 2020.
 - [18] W. van der Gaast, K. Begg, and A. Flamos, “Promoting sustainable energy technology transfers to developing countries through the CDM,” *Applied Energy*, vol. 86, no. 2, pp. 230–236, 2009.
 - [19] K. Kavouridis and N. Koukouzas, “Coal and sustainable energy supply challenges and barriers,” *Energy Policy*, vol. 36, no. 2, pp. 693–703, 2008.
 - [20] Y. Ma, Z. Zhang, J. Jang, and J. Qu, “Overcapacity investment and supervision fluctuation: an evolutionary game approach,” *Applied Economics Letters*, vol. 27, no. 3, pp. 221–227, 2019.
 - [21] K. Jiang, D. You, R. Merrill, and Z. Li, “Implementation of a multi-agent environmental regulation strategy under Chinese fiscal decentralization: an evolutionary game theoretical approach,” *Journal of Cleaner Production*, vol. 214, pp. 902–915, 2019.
 - [22] J. Sheng, W. Zhou, and B. Zhu, “The coordination of stakeholder interests in environmental regulation: lessons from China’s environmental regulation policies from the perspective of the evolutionary game theory,” *Journal of Cleaner Production*, vol. 249, 2020.
 - [23] F. Pan, B. Xi, and L. Wang, “Environmental regulation strategy analysis of local government based on evolutionary game theory,” in *Proceedings of the 2014 International Conference on Management Science & Engineering 21th Annual Conference Proceedings*, pp. 1957–1964, Helsinki, Finland, August 2014.
 - [24] Y. Zhang, M. Zhang, Y. Liu, and R. Nie, “Enterprise investment, local government intervention and coal overcapacity: the case of China,” *Energy Policy*, vol. 101, pp. 162–169, 2017.
 - [25] A. B. Jaffe and R. N. Stavins, “Dynamic incentives of environmental regulations: the effects of alternative policy instruments on technology diffusion,” *Journal of Environmental Economics and Management*, vol. 29, no. 3, pp. S43–S63, 1995.
 - [26] B. Shi, C. Feng, M. Qiu, and A. Ekeland, “Innovation suppression and migration effect: the unintentional consequences of environmental regulation,” *China Economic Review*, vol. 49, pp. 1–23, 2018.
 - [27] B. Yuan and Q. Xiang, “Environmental regulation, industrial innovation and green development of Chinese manufacturing: based on an extended CDM model,” *Journal of Cleaner Production*, vol. 176, pp. 895–908, 2018.
 - [28] S. Shao, Z. Hu, J. Cao, L. Yang, and D. Guan, “Environmental regulation and enterprise innovation: a review,” *Business Strategy and the Environment*, vol. 29, no. 3, pp. 1465–1478, 2020.
 - [29] M. E. Porter and C. V. D. Linde, “Toward a new conception of the environment-competitiveness relationship,” *Journal of Economic Perspectives*, vol. 9, no. 4, pp. 97–118, 1995.
 - [30] M. Yi, X. Fang, L. Wen, F. Guang, and Y. Zhang, “The heterogeneous effects of different environmental policy instruments on green technology innovation,” *International Journal of Environmental Research and Public Health*, vol. 16, no. 23, 2019.
 - [31] M. Gong, Z. You, L. Wang, and J. Cheng, “Environmental regulation, trade comparative advantage, and the manufacturing industry’s green transformation and upgrading,” *International Journal of Environmental Research and Public Health*, vol. 17, no. 8, 2020.
 - [32] B. Yu and C. Shen, “Environmental regulation and industrial capacity utilization: an empirical study of China,” *Journal of Cleaner Production*, vol. 246, 2020.
 - [33] W. Li, H. Sun, D. K. Tran, and F. Taghizadeh-Hesary, “The impact of environmental regulation on technological innovation of resource-based industries,” *Sustainability*, vol. 12, no. 17, 2020.
 - [34] S. Ren, X. Li, B. Yuan, D. Li, and X. Chen, “The effects of three types of environmental regulation on eco-efficiency: a cross-region analysis in China,” *Journal of Cleaner Production*, vol. 173, pp. 245–255, 2018.
 - [35] Z. Chen, X. Zhang, and G. Ni, “Decomposing capacity utilization under carbon dioxide emissions reduction constraints in data envelopment analysis: an application to Chinese regions,” *Energy Policy*, vol. 139, 2020.
 - [36] X. Pan, B. Ai, C. Li, X. Pan, and Y. Yan, “Dynamic relationship among environmental regulation, technological innovation and energy efficiency based on large scale provincial panel data in China,” *Technological Forecasting and Social Change*, vol. 144, pp. 428–435, 2019.
 - [37] X. Li and X. Yao, “Can energy supply-side and demand-side policies for energy saving and emission reduction be synergistic? A simulated study on China’s coal capacity cut and carbon tax,” *Energy Policy*, vol. 138, 2020.
 - [38] S. K. Lee and S. Jang, “Re-examining the overcapacity of the US lodging industry,” *International Journal of Hospitality Management*, vol. 31, no. 4, pp. 1050–1058, 2012.

- [39] Y. Ju and X. Wang, "Understanding the capacity utilization rate and overcapacity of China's coal industry and inter-provincial heterogeneity," *IEEE Access*, vol. 7, pp. 111375–111386, 2019.
- [40] X. Shi, B. Rioux, and P. Galkin, "Unintended consequences of China's coal capacity cut policy," *Energy Policy*, vol. 113, pp. 478–486, 2018.
- [41] J. Dzonzi-Undi and S. Li, "SWOT analysis of safety and environmental regulation for China and USA: its effect and influence on sustainable development of the coal industry," *Environmental Earth Sciences*, vol. 74, no. 8, pp. 6395–6406, 2015.
- [42] M. Zhang, T. Lv, Y. Zhao, and J. Pan, "Effectiveness of clean development policies on coal-fired power generation: an empirical study in China," *Environmental Science and Pollution Research*, vol. 27, no. 13, pp. 14654–14667, 2020.
- [43] Y. Zhang, J. Orbie, and S. Delputte, "China's climate change policy: central-local governmental interaction," *Environmental Policy and Governance*, vol. 30, no. 3, pp. 128–140, 2020.
- [44] M. Liu, M. Chen, and G. He, "The origin and prospect of billion-ton coal production capacity in China," *Resources, Conservation and Recycling*, vol. 125, pp. 70–85, 2017.
- [45] X. Yao, X. Zhang, and Z. Guo, "The tug of war between local government and enterprises in reducing China's carbon dioxide emissions intensity," *Science of the Total Environment*, vol. 710, Article ID 136140, 2020.
- [46] C. Dong, Y. Qi, and G. Nemet, "A government approach to address coal overcapacity in China," *Journal of Cleaner Production*, vol. 278, 2021.
- [47] P. del Río González, "The empirical analysis of the determinants for environmental technological change: a research agenda," *Ecological Economics*, vol. 68, no. 3, pp. 861–878, 2009.
- [48] G.-B. Bi, W. Song, P. Zhou, and L. Liang, "Does environmental regulation affect energy efficiency in China's thermal power generation? Empirical evidence from a slacks-based DEA model," *Energy Policy*, vol. 66, pp. 537–546, 2014.
- [49] H. Wang and T. Nakata, "Analysis of the market penetration of clean coal technologies and its impacts in China's electricity sector," *Energy Policy*, vol. 37, no. 1, pp. 338–351, 2009.
- [50] A. P. Chikkatur, A. D. Sagar, and T. L. Sankar, "Sustainable development of the Indian coal sector," *Energy*, vol. 34, no. 8, pp. 942–953, 2009.
- [51] R. Ramanathan, Q. He, A. Black, A. Ghobadian, and D. Gallear, "Environmental regulations, innovation and firm performance: a revisit of the Porter hypothesis," *Journal of Cleaner Production*, vol. 155, pp. 79–92, 2017.
- [52] L. Gan, G. S. Eskeland, and H. H. Kolshus, "Green electricity market development: lessons from Europe and the US," *Energy Policy*, vol. 35, no. 1, pp. 144–155, 2007.
- [53] X. Qian, D. Wang, J. Wang, and S. Chen, "Resource curse, environmental regulation and transformation of coal-mining cities in China," *Resources Policy*, 2019.
- [54] Y. Li, P. Yang, and H. Wang, "Collecting coal-fired power environmental tax to promote wind power development and environmental improvement," *Acta Scientifica Malaysia*, vol. 2, no. 1, pp. 5–8, 2018.
- [55] L. Pingkuo, P. Huan, and W. Zhiwei, "Orderly-synergistic development of power generation industry: a China's case study based on evolutionary game model," *Energy*, vol. 211, 2020.
- [56] R. Selten, "A note on evolutionarily stable strategies in asymmetric animal conflicts," *Journal of Theoretical Biology*, vol. 84, no. 1, pp. 93–101, 1980.
- [57] A. M. Liapunov, *Stability of Motion*, Academic Press, New York, NY, USA, 1966.
- [58] H. Sánchez-Beltrán, C. D. M. Rodríguez, J. C. B. Triviño, P. L. Iglesias-Rey, J. S. Valderrama, and F. J. Martínez-Solano, "Characterization of modular deposits for urban drainage networks using CFD techniques," *Procedia Engineering*, vol. 186, pp. 84–92, 2017.
- [59] H. Zhang, Y. Zheng, U. A. Ozturk, and S. Li, "The impact of subsidies on overcapacity: a comparison of wind and solar energy companies in China," *Energy*, vol. 94, pp. 821–827, 2016.
- [60] Z. Zhu and H. Liao, "Do subsidies improve the financial performance of renewable energy companies? Evidence from China," *Natural Hazards*, vol. 95, no. 1-2, pp. 241–256, 2018.
- [61] A. Karaev, V. Ponkratov, A. Masterov, E. Kireeva, and M. Volkova, "Cross-country analysis of the comparative efficiency of government support for coal and lignite production," *International Journal of Energy Economics and Policy*, vol. 10, no. 5, pp. 220–227, 2020.

Research Article

Application of Computer Technology in Optimal Design of Overall Structure of Special Machinery

Caiping Guo 

School of Mechanical and Electrical Engineering, Jiaozuo University, Jiaozuo 454003, Henan, China

Correspondence should be addressed to Caiping Guo; guocaiping@jzu.edu.cn

Received 24 December 2020; Revised 26 January 2021; Accepted 6 February 2021; Published 23 February 2021

Academic Editor: Ming Bao Cheng

Copyright © 2021 Caiping Guo. This is an open access article distributed under the Creative Commons Attribution License, which permits unrestricted use, distribution, and reproduction in any medium, provided the original work is properly cited.

With the transformation and upgrading of my country's industrial structure, the level of manufacturing automation has gradually improved. According to research, the design of mechanical products is mostly completed by improvement or innovation on the basis of existing design knowledge. Knowledge reuse is a technique to ensure the maximization of design resource utilization by reusing design knowledge. This article applies knowledge reuse technology to the development and design of mechanical products. By integrating the technical logic of the functional analysis system with the development of quality functions, the transformation of customer demand information and product function design is realized, and the task of the product design plan analysis phase is completed. This paper uses the finite element analysis software ANSYS to explore a new nonlinear finite element modeling method and conducts simulation experiments. At the same time, this paper improves the genetic algorithm, which effectively improves the optimization efficiency and completes the parameter optimization under multiobjective and multistructure conditions. From the experimental results, it takes 328.64 seconds for the basic genetic algorithm to search for the optimal solution of the complex problem. The improved time is shortened to 86.31 seconds, and the efficiency is increased by 73.74%. This shows that the improved genetic algorithm has better robustness and can find the optimal solution in a shorter calculation time. For complex problems such as the optimization of the overall structure of special machinery, the improved genetic algorithm obviously helps to improve the optimization efficiency and improves the effectiveness and pertinence of product design schemes.

1. Introduction

The advancement of science has gradually made intelligent manufacturing the mainstream of the development of manufacturing industries in various countries, and computers have also provided a lot of technical support for this. For example, intelligent detection based on computer neural network can help special machinery to better realize fault diagnosis and structural optimization; data induction based on analogy reasoning can help people establish a comprehensive machinery manufacturing knowledge system; intelligent optimization based on genetic algorithm is also special indispensable technology in mechanical design. In the current research, people still need to continuously improve computer intelligence technology to better improve the rationality of mechanical structure optimization.

Abroad, research on computational intelligence and structural optimization has accumulated a lot of excellent results. Moreira tried to use genetic calculation and simulated annealing to solve the problem of structural optimization. He and his team studied the performance of two random search methods and applied them to the optimization of pin-connected steel structures. From the research results, genetic algorithm and simulated annealing can indeed play a very good role in structural optimization. If they can be embedded in a single parameter algorithm, better performance can be achieved through a hybrid scheme [1]. Reynolds proposed a new reverse adaptive method for automatically generating solutions to initial design and redesign problems. He carried out inverse adaptive analysis of the initial finite element problem and refined the low-stress area of the finite element mesh according to element

subdivision. After that, he deleted all low-stress subdivision elements and repeated the process continuously. This method can effectively improve some of the shortcomings in the existing optimization scheme, but there is still a lot of room for improvement in the efficiency of optimization [2]. Motta and his team developed an efficient calculation tool for robust structural optimization. Due to the combination of multiobjective optimization, normal boundary intersection, and normalized normal constraints, this integrated tool can effectively obtain the best solution for robust design optimization. Of course, the tool needs more experiments to ensure the stability of its calculations [3].

Although domestic research on computer technology in structural optimization design started relatively late, it has developed very rapidly. Qu et al. proposed a reasoning method of fuzzy design knowledge, which can refer to the relevant detailed information of product design in a certain order in the reasoning process of product parameters. The prerequisite for this purpose is to establish a hierarchical model to express the product design, processing, and technology on the basis of meeting the product design accuracy requirements [4]. Bijuan et al. conducted research on the parameter analysis and optimization of the damping structure of the tubular transition layer of agricultural machinery. He introduced the concept of transition layer on the basis of the traditional constrained damping structure, combined with computer technology, and proposed a new type of tubular damping structure. From the experimental results, the optimized agricultural machinery can better deal with the severe vibration and impact that may occur during the work process, but the stability of the tubular structure needs to be appropriately improved [5].

Through reading materials and market research, this article understands the problems encountered in the current mechanical product design process and analyzes it. It is concluded that the application research of knowledge reuse technology has brought progress to the design and development of mechanical products and the development of manufacturing enterprises, which means using the idea of functional analysis system technology and quality function deployment technology to successfully complete the transformation between customer demand information and structural design parameters and focus on the process of using multilevel classification technology to generate design plans and discuss the basic elements of multilevel decomposition. Classification method, indexing process, and matching reasoning form the complete idea of applying knowledge reuse technology to generate design scheme.

Introduction systematically introduces the research overview of the overall structure optimization design of special machinery and expounds the current main problems in the overall structure optimization design of special machinery and the main work and research content of this article. Section 2 explains intelligent optimization design technology and method of mechanical structure and introduces structural intelligent optimization, genetic algorithm, data mining technology, ANSYS-based optimization technology, and penalty function constraints. Section 3 includes data preprocessing part, detailed description of the

corresponding method of simulation experiment in this paper, and the establishment of experimental model. Section 4 mainly introduces the establishment of a special machine model based on ANSYS and intelligence and conducts related experiments to optimize the implementation strategy. Section 5, Summary and Prospects, summarizes the work done in this article, states the innovation and effectiveness of the method proposed in this article, and proposes the next research direction.

2. Technology and Method of Intelligent Optimal Design of Mechanical Structure

2.1. Structural Intelligent Optimization. The intelligent optimization design of the structure is essentially an optimization process; that is, a solution is determined in the solution space of the mechanical design to make the objective function obtain the minimum value under the condition of satisfying the state variable constraints [6]. The more complex the mechanical design is, the more constraints and variables it contains. Not only that, but some constraints are even discrete and difficult to describe quantitatively. In the process of structural optimization, the final evaluation standard for the quality of the design plan will be reflected in the way of evaluation function [7]. If there is only a single optimization goal, then the optimization process will be relatively simple. But in actual work, there may be two or more optimization goals that have contradictory relationships with each other. At this time, it is necessary to integrate multiple methods such as multiobjective fuzzy optimization, evaluation function method, and goal planning method to optimize the overall structure [8].

Traditional optimization algorithms include mathematical programming method, optimal criterion method, and so on. These classic optimization methods are limited by various conditions, so they can be used in a limited range, and it is difficult to meet the optimization of special machinery structures in complex environments [9]. For this reason, it is necessary to introduce computer technology into intelligent optimization methods, imitate the evolution and development process of nature, and combine logic, mathematics, and science to realize project design and optimization. In the process of searching for the optimal solution, the most representative one is genetic algorithm (GA). In addition, simulated annealing (SA), fuzzy systems, and artificial neural networks (ANN) are common search optimization techniques at this stage [10, 11].

2.2. Genetic Algorithm. The essence of genetic algorithm is to simulate the laws of biological heredity and evolution in the natural environment and obtain a highly adaptive algorithm that can search for global probability [12]. The genetic algorithm strictly follows the natural law of survival of the fittest in the calculation process. In each genetic process, only the group with effective information can iterate to the next round. After multiple iterations of calculation, the operations of selection, crossover, and mutation are continuously performed on individuals, until the optimal solution that satisfies the conditions is obtained [13].

2.2.1. Basic Genetic Algorithm. The most basic genetic algorithm operation process must first clarify the objective function, variable, variable search range, and search precision of the problem, then determine the length of each design variable code, and then code the variable [14]. In the process of population initialization, an initial population containing a certain number of individuals can be randomly generated according to the selected coding method; namely,

$$\text{pop}i(t), t = 1, 2, 3, \dots, n. \quad (1)$$

Here, t represents the initial population number, which is used to evaluate and select the fitness value of individuals to complete genetic processes such as crossover and mutation. It can reflect the pros and cons of all individuals in the form of a function, and its expression satisfies

$$f_i = \text{fitness}(\text{pop}i(t)), \quad (2)$$

where f_i means to select highly adaptable individuals from the group to form a new group. In the genetic process, the process of selection can also be seen as a process of replication, that is, selecting excellent individuals with strong adaptability from the population and forming them into a new population [15]. It is necessary to comprehensively consider the fitness value when selecting operators. Normally, the calculated selection probability of each individual satisfies the formula

$$P_i = \frac{f_i}{\sum_{i=1}^n f_i}. \quad (3)$$

Combining formula (3), when selecting outstanding individuals from the current group $\text{pop}i(t)$ to inherit to the next generation, the new group constituted satisfies

$$\text{newpop}(t+1) = \{\text{pop}q(t), q = 1, 2, 3, \dots, n\}, \quad (4)$$

where $\text{newpop}(t+1)$ represents the probability obtained by the crossover method. The crossover process refers to randomly selecting two parents of individuals, and then according to the determined crossover method and probability, part of the individual genes of the parents are crossed to form two brand new offspring individuals [16]. Generally speaking, there are one-point intersection, two-point intersection, and multipoint intersection.

The process of mutation is to reverse the value of a certain gene in the chromosome. Generally speaking, it is to call 0 and 1 in the binary string. If the mutated parent individual is [01100110], when the fourth point is mutated, then the mutated offspring individual is [01110110]. The main role of mutation operator in the genetic process is to enhance the diversity of individuals in the entire population. The more significant the differences between individuals, the lower the probability of local optimization [17].

2.2.2. Improved Genetic Algorithm. The basic genetic algorithm can solve most simple optimization problems, but there are still some shortcomings in the face of complex multiobjective optimization. In order to meet the requirement of designing and optimizing the overall structure of

special machinery in this paper, genetic algorithm needs to be improved appropriately. Generally speaking, the improvement methods of genetic algorithms are mainly divided into improved coding methods, adding advanced operators, and combining other search algorithms.

Binary encoding is one of the commonly used encoding methods in genetic algorithms. Suppose ceil represents rounding to positive infinity, perk represents coding accuracy, and $[\text{low}, \text{up}]$ represents the search range of variables under restricted conditions; then the length calculation formula satisfies

$$l = \text{ceil} \left[\log_2 \left(\frac{\text{up} - \text{low}}{\text{perk}} + 1 \right) + 1 \right]. \quad (5)$$

The actual precision perk' of the string satisfies the formula

$$\text{perk}' = \frac{\text{up} - \text{low}}{2^l - 1}. \quad (6)$$

On the whole, binary coding is simple to operate and has better global search capabilities, but due to the mapping error of continuous function discretization, it cannot directly reflect the structural characteristics of the problem [18]. In order to improve the search efficiency of genetic algorithm, this paper improves it to a segmented coding method. The characteristic of segmented coding is to use two different coding schemes to divide the algorithm into preliminary search and final search. In the early stage of calculation, the genetic algorithm can perform a rough search of the whole world and first confirm the possible range of the optimal solution. In the later stage, gray coding is used to perform a more detailed search to achieve precise search in a small area.

2.2.3. Advantages of Genetic Algorithm. Compared with traditional methods, the superiority of genetic algorithms is mainly manifested in first, and under the action of genetic operators, genetic algorithms have strong search capabilities and can find the global optimal solution of the problem with a large probability. The inherent parallelism can effectively handle large-scale optimization problems. Genetic algorithm has a good global search ability, can quickly search out all solutions in the solution space without falling into the trap of rapid decline of local optimal solutions; and using its inherent parallelism, it can easily perform distributed computing to speed up the solution. However, the local search ability of genetic algorithm is poor, which makes the pure genetic algorithm more time-consuming and the search efficiency is lower in the later stage of evolution. In practical applications, genetic algorithms are prone to premature convergence. Which selection method should be adopted to keep good individuals and maintain the diversity of the group has always been a difficult problem in genetic algorithms.

2.3. Data Mining Technology. The basis of data mining is realized on the basis of metadata definition, modeling, and multidimensional data modeling. Its essence is to mine

useful data from a large amount of data according to its related laws [19]. Simply put, it is to find the characteristics of the data through statistics and machine learning on the basis of data samples and use icons to describe them and establish their knowledge description model. With the help of models, people can dig out the value and relevance behind the information.

Data mining technology can be very helpful to the optimization design of the structure. In actual work, data can be classified, summarized, and clustered according to optimization objects and constraints and finally confirmed its association rules [20]. In the machinery manufacturing industry, data mining technology is often used for fault diagnosis of parts and components, and resource optimization is achieved by analyzing the production process.

2.4. Optimization Technology Based on ANSYS. ANSYS is a finite element analysis software, which is often used in computer engineering aids to solve various linear and nonlinear problems [21]. ANSYS not only has an excellent modeling level but also can effectively achieve problem solving, nonlinear analysis, and system optimization. Using ANSYS to optimize design can help users determine the optimal design plan, use ANSYS's topology optimization module to optimize the shape of the model, or confirm the best distribution of materials [22].

The optimization analysis technology based on ANSYS is usually divided into three categories; the most common is the optimization technology based on parametric design language. This optimization method can not only effectively form finite element modeling but also further realize parametric analysis and solution, so it can play a very good effect in the secondary development and optimization design of mechanical structure.

2.5. Penalty Function Constraint. Optimization problems are usually accompanied by certain constraints. The penalty function method is a constraint processing method that is often used in the solution of constraint optimization problems using intelligent algorithms [23]. As an indirect processing method, the penalty function will form a new function with the constraint term together with the objective function after imposing a certain penalty on the constraint function. Commonly used penalty functions include external point penalty function, differentiable penalty function, and multiplier method, which can also be directly divided into internal penalty function method and external penalty function method [24].

The operating idea of the external point penalty function method is to define the constraints outside the feasible region through the penalty effect, and, in the search process, it gradually moves from the outside of the feasible region to the boundary until the optimal solution that meets the requirements is found. The basic idea of the differentiable penalty function method is to approximate a nondifferentiable precise penalty function through a differentiable function. The basic idea of the multiplier method is to introduce some undetermined coefficients into the constraint function to form a

new unconstrained augmentation objective function with the original objective function and finally make unconstrained augmentation by continuously modifying the multiplier vector of the constraint function. The optimal solution of the wide objective function is equal to the optimal solution of the original problem [25]. Because the parameter model studied in this paper is relatively complicated, when optimizing the parameter structure, this paper uses the advantages of computers in data storage and analysis, combined with the use of historical adaptive DE, and improves the intelligence of optimization [26].

3. Optimization Experiment of Mechanical Structure Based on Computer Technology

3.1. Experimental Background. Although special machinery is not manufactured and used as frequently as daily necessities, it is an essential part of the national development strategy. As a high-level weapon machine, the structural optimization and design process of artillery will inevitably involve a lot of optimization goals and constraints. This includes, but is not limited to, the overall structure of the artillery, the links of the various components of the artillery system, and finite element dynamics analysis. In order to optimize the overall structure of the artillery, it is necessary to combine genetic algorithms, data mining, ANSYS optimization, and penalty functions in computer technology.

3.2. Experimental Model Establishment. The establishment of a mathematical model of structural optimization is a very important part of using mathematical methods to solve structural optimization problems in practical engineering. In the field of special machinery manufacturing, the mathematical model of structural optimization design needs to meet the constraints of a series of equilibrium conditions to maximize the rigidity of the structure, the least flexibility, the least total weight, or the least material cost. From the perspective of abstract mathematical form, the mathematical model of structural optimization mainly includes design variables, constraint conditions, and objective functions. Towing artillery is a complicated mechanical structure. In the modeling process, it is necessary to establish a corresponding finite element model based on its structural characteristics. This article divides it into four parts: recoil part, landing part, rotating part, and fixed part.

3.3. Experiment Process. The overall idea of the experiment is as follows. First, we determine the parameter variables and their design space and establish a parameterized finite element model on this basis. Then, the parameterized model is used for finite element analysis to obtain the objective function value and the constraint value, thereby establishing the implicit correspondence between the objective function and the constraint function and the current design variables. Finally, the intelligent optimization algorithm is used to optimize the overall structure of the artillery, and the optimization results are given.

In order to further examine the search efficiency of the improved genetic algorithm and its influence on structural optimization, this paper records the operating parameters of the basic genetic algorithm and compares them with the improved algorithm. When dealing with constrained optimization problems, this paper also compares the constraint capabilities of several common penalty functions, which reflects the excellent constraint processing capabilities of the multiplier method.

4. Application of Computer Technology in Optimal Design of Overall Structure of Special Machinery

4.1. Establishment of Special Machinery Model Based on ANSYS

4.1.1. Application of Special Machinery Parameterized Model in Structural Optimization. Parameterization is to use a set of design parameters to agree on the relationship of the structure size when the structure shape is basically fixed and then change the structure shape through size drive. Unlike traditional design methods, parametric design can store the entire involved process and design a family of models that are similar in shape and function instead of a single model. It is precisely because of the parametric modeling technology that the transmission of data changes between different levels has the uniqueness and immediacy. On the whole, parametric technology has a very wide application background and important significance in the design of special machinery products and systems.

When building the overall structure model of the artillery, it is not only necessary to determine the multi-objective function and constrain the design but also to select variables based on requirements. Table 1 shows the variable ranges of various variables in the structural model. It can be seen from Table 1 that when designing variable spaces, the results of historical data analysis give priority variables as much space as possible. For nonpriority variables, you can refer to the priority basic model and give it a data fluctuation range of about 30%. Among them, the data of M8 and M9 will directly affect the situation of the gun tail colliding with the ground when the firing angle range is large. It is impossible to judge whether the structure itself interferes. Therefore, the interference check function must be added when the new group is optimized; that is, the maximum between recoil displacement and M8 and M9 is a constraint that the new group must meet.

After selecting the optimized variables based on historical data, this paper analyzes the sensitivity of each parameter to the stability of the overall structure, the weight of the whole gun, the stress of the frame, and the muzzle disturbance. Figure 1 is a statistical graph of parameter sensitivity of the overall structure of the model.

It can be seen from Figure 1 that the parameters that have a greater impact on the stability of the model structure are M2, M3, M4, M7, and M14. The parameters that have a greater impact on muzzle disturbance are M3, M4, and M14. When M3 increases by 10%, the muzzle disturbance of the

TABLE 1: Variable range of various variables in structural model.

Design variable	M1	M2	M3	M4	M5	M6	M7
Design upper limit	125	350	5200	650	1400	600	1000
Design lower limit	0	150	2000	200	1100	400	500
Design variable	M8	M9	M10	M11	M12	M13	M14
Design upper limit	1200	1200	460	550	8	8	680
Design lower limit	600	-400	200	350	2	2	420

artillery increases from 2780 to 3227, and the rate of disturbance increases as high as 16.08%. The parameters that have a greater impact on the total mass of the artillery are M3, M10, and M12. It can be seen that in the optimization, the upper and lower limits of the above parameters should be given sufficient width, and the interference of the structure should be considered, and the interference check of the final feasible design plan should be done.

4.1.2. Intelligently Optimized Implementation Strategy. In the process of structural optimization, the specific optimization steps are as follows. (1) Extract valuable data from past models to form a source database and perform equivalent processing on all parameter data in it to eliminate structural differences caused by performance differences. (2) Determine the variable range of all parameters and ensure that each parameter will not interfere or conflict with each other. At the same time, confirm the structural design variables and various constraints. (3) Form an optimized mathematical model and determine the objective function and penalty function as the basic model of genetic algorithm. (4) Parameterize the finite element model, encode the chromosome, analyze the finite element of different design parameters, and confirm the correspondence between the various data in the structure. (5) Complete genetic calculation through selection, crossover, and mutation operations and find the optimal solution through genetic algorithm to achieve system optimization. Figure 2 shows the changes of various parameters of the model after intelligent optimization.

It can be seen from Figure 2 that the optimized overall structure has a certain change from the beginning. For example, the height of the live wire is reduced from 900 mm to 600 mm, the length of the frame is changed from 3600 to 3000, and the wall thickness of the frame is changed from 5 to 3. After further understanding the dynamic performance curve of the optimized model, it can be determined that the dynamic performance of the model meets the requirements of use, that is, meets the requirements of accuracy and stability. Through subsequent optimization and adjustment of parts, the final optimization plan can be realized.

4.2. Realization of Mechanical Structure Optimization Based on Genetic Algorithm

4.2.1. Improved Genetic Algorithm and ANSYS Collaborative Research. In actual work, it is difficult to establish an accurate mathematical model for large complex structures. Therefore, special finite element analysis tools are required for analysis and calculation. Improved genetic algorithm and

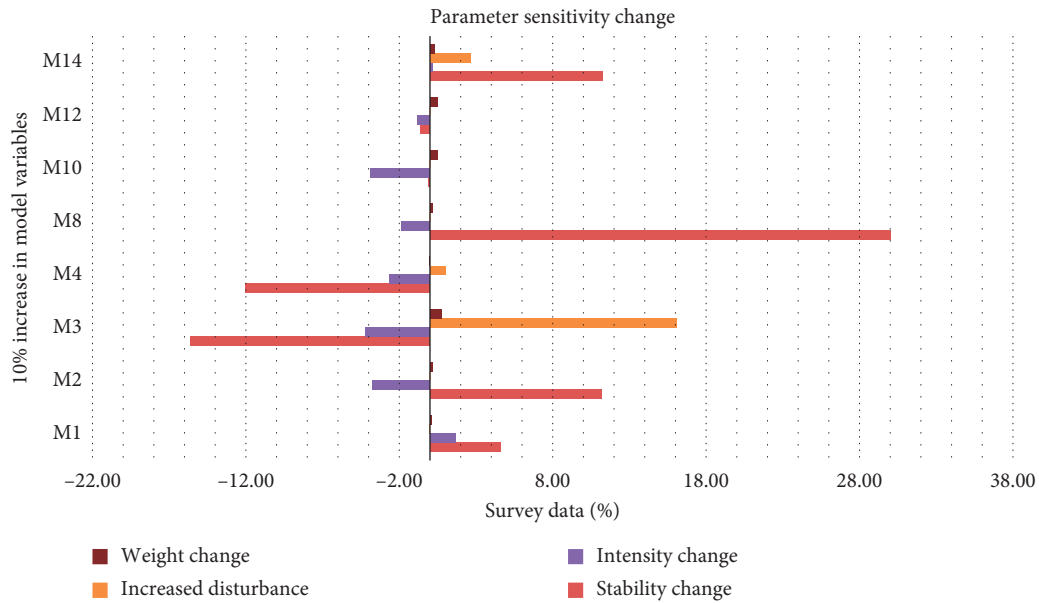


FIGURE 1: Parameter sensitivity statistical graph of the overall structure of the model.

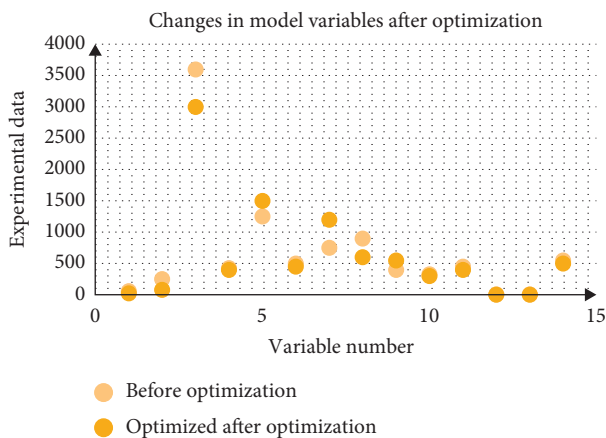


FIGURE 2: Changes in various parameters of the model after intelligent optimization.

ANSYS for collaborative calculation can not only effectively ensure the correct rate of calculation but also reduce some difficulties that may be encountered in the programming process and more efficiently achieve structural optimization design. Figure 3 is a comparison diagram of optimization results between the basic genetic algorithm and the improved genetic algorithm. Among them, A1–A5 represent the number of population sizes in five test functions, and B1–B5 represent the number of optimal solutions obtained by five test functions in 100 optimization calculations.

It can be seen from Figure 3 that when solving simple optimization problems such as Project 1 and Project 3, the basic genetic algorithm can also search for the optimal solution with a greater probability. But when faced with a highly discrete multiobjective optimization problem, it is difficult to determine the optimal solution in the global search of the basic genetic algorithm. And for the improved genetic algorithm, even in the face of complex optimization

tasks, the probability of obtaining the optimal solution can be maintained above 90%. After further understanding the optimization, it can be found that for simple items 1 and 3, there is no obvious difference in the calculation time before and after the genetic algorithm improvement. However, as the calculation difficulty increases, the efficiency improvement of the improved genetic algorithm will become more obvious. In Project 5, the basic genetic algorithm took 328.64 seconds, while the improved time was only 86.31 seconds, which increased the efficiency by 73.74%. Overall, the improved genetic algorithm has better robustness and can find the optimal solution in a shorter calculation time. For complex problems such as the optimization of the overall structure of special machinery, the improved genetic algorithm can obviously greatly help improve the optimization efficiency.

4.2.2. Modeling Stability Analysis Based on Penalty Function.

In the process of using genetic algorithm to optimize the overall structure of special machinery, more variables and constraints will appear. For this reason, it is necessary to introduce a penalty function as a constraint function to ensure that the genetic algorithm can better achieve system optimization. Figure 4 is a comparison of three different forms of penalty function constraints. Among them, M1–M4 represent the number of times that the constraint conditions are met when the four types of test functions are calculated 100 times. N1–N4 represent the number of times the optimal solution is obtained when the four types of test functions are calculated 100 times.

It can be seen from Figure 4 that in a total of 400 optimization calculations, the three penalty functions meet the constraint conditions relatively well, and the multiplier method still has a slight advantage in comparison. However, when comparing the number of times to obtain the optimal solution,

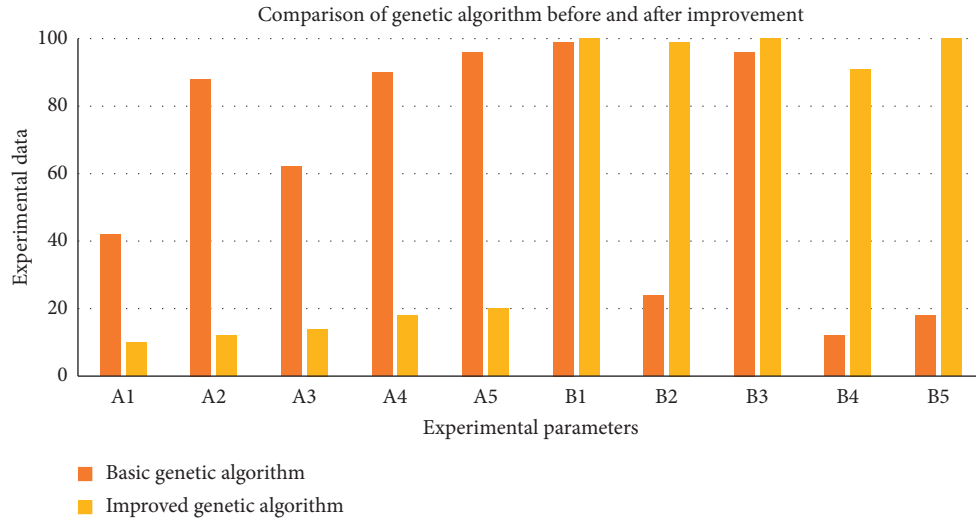


FIGURE 3: Comparison chart of optimization results of basic genetic algorithm and improved genetic algorithm.

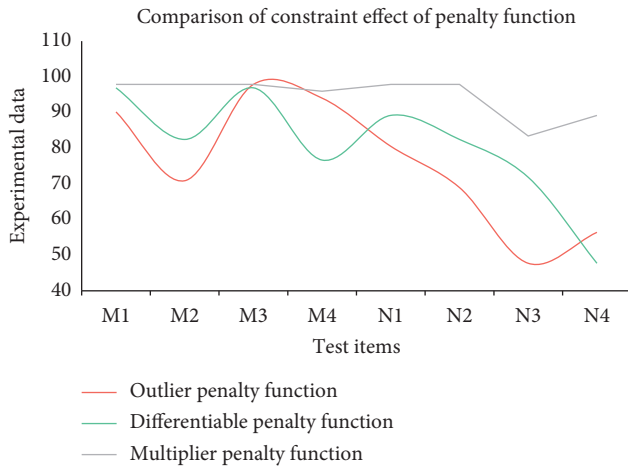


FIGURE 4: Comparison of constraint effects of three different penalty functions.

it can be found that the multiplier method has significantly better performance than the exterior point penalty function and the differentiable penalty function. On the whole, using the multiplier method to constrain the overall structure of special machinery can achieve better results.

4.3. Finite Element Analysis Based on Ansys. APDL parametric modeling is used to establish a finite element analysis model from bottom to top. Its mechanical behavior is based on the principle of no pressure, and only the pulling force is considered. The anchor rod and the raft are connected by a common node to ensure their deformation coordination under load. The specific results are shown in Table 2.

From Figure 5, we can see that the fitness change is very small after the 150th generation of evolution, and there is basically no change in fitness after the 250th generation. The change in the weight of the whole gun changes greatly before the 120th generation. After the change is small, there is basically no change after the 250th generation. It can be seen

TABLE 2: Overall structure weight change data sheet.

Number of evolutions	0	50	100	150	200	250	300
A	2.90	3.41	3.84	4.41	4.25	4.59	4.71
B	2.92	3.56	4.20	4.01	4.33	4.52	4.53
C	2.85	3.31	4.13	4.45	4.27	4.59	4.51
D	3.40	3.73	3.93	4.19	4.46	4.77	4.75
E	3.29	3.53	3.96	4.08	4.43	4.59	4.71

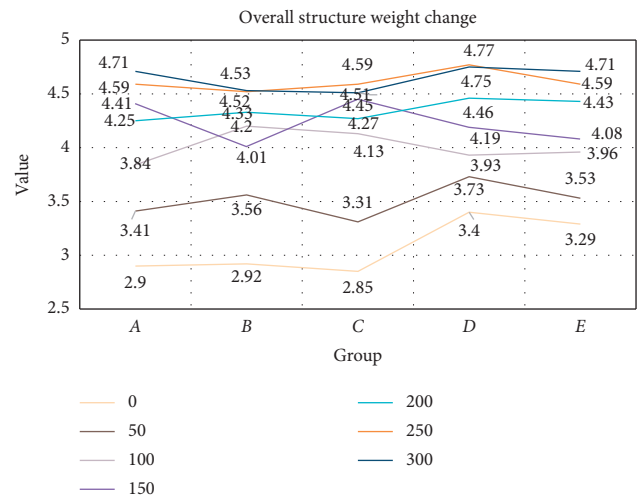


FIGURE 5: Analysis chart of overall structure weight change.

from the above trends that the evolution 300 has made the optimization mature, and the optimization results have basically reached the optimal value. The optimization effect of increasing the evolution algebra is not great.

5. Conclusions

This paper analyzes the special machinery model based on ANSYS. In this paper, a mathematical model is established around the overall structure of the artillery. In the determination of multiple objective functions and constraint

design, genetic algorithms are introduced to improve various problems in the optimization process. When confirming the optimized variables and variable ranges, a data fluctuation range of about 30% was given to nonfinite variables. After understanding the parameter sensitivity of the overall structure of the artillery, the parameters that have a greater impact on performance were optimized. Because the artillery parameter model is more complicated, when optimizing the parameter structure, this article uses the advantages of the computer in data storage and analysis, combined with the past historical data to improve the intelligence of the optimization. In this paper, the overall optimization design of the artillery model is carried out according to the scientific and intelligent optimization steps, and the random election method is used to ensure the diversity of the population in the genetic process. From the experimental results, the adjustment of various parameters in the model makes the model more in line with dynamic performance in terms of accuracy and stability.

In this paper, the optimal design of mechanical structure is realized based on genetic algorithm. As a finite element analysis software, the combination of ANSYS and genetic algorithm can effectively promote the overall structure optimization of special machinery. In the experiment, this paper found that the basic genetic algorithm can solve most simple objective optimization tasks, but there are still many shortcomings in the face of multiobjective tasks with high discrete variables. Because this paper has improved the genetic algorithm, from the experimental data, the improved genetic algorithm can greatly improve the optimization calculation efficiency on the basis of ensuring the optimization accuracy and has higher robustness. This paper compares the constraint performance of the three types of penalty functions: external point penalty function, differentiable penalty function, and multiplier method. From the final result, the multiplier method has better performance in two types of tests: satisfying the constraints and obtaining the optimal solution.

With the advent of the era of automation, how companies can keep up with the rapid development of the market and correctly grasp the direction of product development and design is the key to winning this opportunity. Through the study of knowledge reuse, this paper has realized the purpose of shortening the development cycle and satisfying the needs of customers to the greatest extent. It proposes a method to realize the scientific analysis of market demand information through the integration of quality function deployment technology and functional system analysis technology. The transformation of demand information and functional parameter design and a method for calculating transformation weights are proposed, which provide important weight coefficients for the product instance matching stage. This paper uses multilevel example decomposition to achieve the decomposition of the target design scheme and uses the subspace algorithm to classify the existing design examples. And it is proposed to complete the calculation process of matching the target design scheme with the existing design examples.

Data Availability

The data used to support the findings of this study are available from the corresponding author upon reasonable request.

Conflicts of Interest

The authors declare that they have no conflicts of interest.

References

- [1] H. S. Moreira, J. Lucas de Souza Silva, M. V. Gomes dos Reis, D. de Bastos Mesquita, B. H. Kikumoto de Paula, and M. G. Villalva, "Experimental comparative study of photovoltaic models for uniform and partially shading conditions," *Renewable Energy*, vol. 164, no. 3, pp. 58–73, 2021.
- [2] D. Reynolds, J. Mcconnachie, P. Bettess et al., "Reverse adaptivity—a new evolutionary tool for structural optimization," *International Journal for Numerical Methods in Engineering*, vol. 45, no. 5, pp. 529–552, 2015.
- [3] R. D. S. Motta, S. M. B. Afonso, P. R. Lyra, and R. B. Willmersdorf, "Development of a computational efficient tool for robust structural optimization," *Engineering Computations*, vol. 32, no. 2, pp. 258–288, 2015.
- [4] X. Qu, G. Xu, X. Fan, and X. Bi, "Intelligent optimization methods for the design of an overhead travelling crane," *Chinese Journal of Mechanical Engineering*, vol. 28, no. 1, pp. 187–196, 2015.
- [5] Y. Bijuan, S. Dagang, Z. Wenjun et al., "Parameter analysis and optimization of tubular transitional layer damping structure for agricultural machinery," *Transactions of the Chinese Society of Agricultural Engineering*, vol. 31, no. 22, pp. 56–62, 2015.
- [6] C. Wang, Z. G. Zhao, T. Zhang et al., "Structure optimization and its validation for compound power-split e-CVT," *China Journal of Highway & Transport*, vol. 28, no. 3, pp. 117–126, 2015.
- [7] H. A. Pham, "Reduction of function evaluation in differential evolution using nearest neighbor comparison," *Vietnam Journal of Computer Science*, vol. 2, no. 2, pp. 121–131, 2015.
- [8] R. Acedo-Hernández, M. Toril, S. Luna-Ramírez, and C. Úbeda, "A PCI planning algorithm for jointly reducing reference signal collisions in LTE uplink and downlink," *Computer Networks*, vol. 119, pp. 112–123, 2017.
- [9] L. Yang, S. Liu, S. Tsoka, and L. G. Papageorgiou, "Mathematical programming for piecewise linear regression analysis," *Expert Systems with Applications*, vol. 44, pp. 156–167, 2016.
- [10] G. Müller and R. Brendel, "Simulated annealing of porous silicon," *Physica Status Solidi (A)*, vol. 182, no. 1, pp. 313–318, 2015.
- [11] A. K. Jain, J. Mao, and K. M. Mohiuddin, "Artificial neural networks: a tutorial," *Computer*, vol. 29, no. 3, pp. 31–44, 2015.
- [12] B. A. Norman, "A genetic algorithm methodology for complex scheduling problems," *Naval Research Logs*, vol. 46, no. 2, pp. 199–211, 2015.
- [13] G. A. Rauwolf and V. L. Coverstone-Carroll, "Near-optimal low-thrust orbit transfers generated by a genetic algorithm," *Journal of Spacecraft & Rockets*, vol. 33, no. 6, pp. 859–862, 2015.
- [14] G. M. Morris, D. S. Goodsell, R. S. Halliday et al., "Automated docking using a Lamarckian genetic algorithm and an

- empirical binding free energy function,” *Journal of Computational Chemistry*, vol. 19, no. 14, pp. 1639–1662, 2015.
- [15] J. A. Niesse and H. R. Mayne, “Global optimization of atomic and molecular clusters using the space-fixed modified genetic algorithm method,” *Journal of Computational Chemistry*, vol. 18, no. 9, pp. 1233–1244, 2015.
- [16] R. Tavakkoli-Moghaddam, J. Safari, and F. Sassani, “Reliability optimization of series-parallel systems with a choice of redundancy strategies using a genetic algorithm,” *Reliability Engineering & System Safety*, vol. 93, no. 4, pp. 550–556, 2017.
- [17] R. Kumar Sahu and V. Vikas Thakare, “Optimization of symmetric linear phase low pass FIR filter using genetic algorithm,” *Acta Radiologica*, vol. 45, no. 6, pp. 679–688, 2015.
- [18] J.-P. Heo, Y. Lee, J. He, S.-F. Chang, and S.-E. Yoon, “Spherical hashing: binary code embedding with hyperspheres,” *IEEE Transactions on Pattern Analysis and Machine Intelligence*, vol. 37, no. 11, pp. 2304–2316, 2015.
- [19] D. A. Adeniyi, Z. Wei, and Y. Yongquan, “Automated web usage data mining and recommendation system using K-nearest neighbor (KNN) classification method,” *Applied Computing and Informatics*, vol. 12, no. 1, pp. 90–108, 2016.
- [20] A. Buczak and E. Guven, “A survey of data mining and machine learning methods for cyber security intrusion detection,” *IEEE Communications Surveys & Tutorials*, vol. 18, no. 2, pp. 1153–1176, 2017.
- [21] G. Hattori and A. L. Serpa, “Contact stiffness estimation in ANSYS using simplified models and artificial neural networks,” *Finite Elements in Analysis and Design*, vol. 97, pp. 43–53, 2015.
- [22] S. Kato, T. Takagi, and M. Kawahara, “A finite element analysis of mach reflection by using the Boussinesq equation,” *International Journal for Numerical Methods in Fluids*, vol. 28, no. 4, pp. 617–631, 2015.
- [23] A. Panda and S. Pani, “A symbiotic organisms search algorithm with adaptive penalty function to solve multi-objective constrained optimization problems,” *Applied Soft Computing*, vol. 46, no. C, pp. 344–360, 2016.
- [24] M. Brzoza-Brzezina, M. Kolasa, and K. Makarski, “A penalty function approach to occasionally binding credit constraints,” *Economic Modelling*, vol. 51, pp. 315–327, 2015.
- [25] B. C. Fabien, “An extended penalty function approach to the numerical solution of constrained optimal control problems,” *Optimal Control Applications & Methods*, vol. 17, no. 5, pp. 341–355, 2015.
- [26] Y. J. Song, D. Q. Wu, A. W. Mohamed, X. B. Zhou, B. Zhang, and W. Deng, “Enhanced success history adaptive DE for parameter optimization of photovoltaic models,” *Complexity*, vol. 2020, Article ID 6660115, 22 pages, 2020.

Research Article

Parallel Processing Method of Inertial Aerobics Multisensor Data Fusion

Hongda Zhang  and Ting Zhang

Physical Education Department, Hunan Institute of Technology, Hengyang 421000, Hunan, China

Correspondence should be addressed to Hongda Zhang; houda1985@hnit.edu.cn

Received 17 December 2020; Revised 18 January 2021; Accepted 6 February 2021; Published 22 February 2021

Academic Editor: Sang-Bing Tsai

Copyright © 2021 Hongda Zhang and Ting Zhang. This is an open access article distributed under the Creative Commons Attribution License, which permits unrestricted use, distribution, and reproduction in any medium, provided the original work is properly cited.

Aerobics is one of the main contents of physical education, which has a positive role in promoting the health of young people. This paper mainly studies the parallel processing method of inertial aerobics multisensor data fusion. In this paper, an aerobics exercise system is designed, which uses digital filter to remove the noise generated in the process of exercise. In this paper, Kalman filter is used to filter the pulse error of accelerometer, and the data structure of unidirectional link is used to achieve the effect of sliding window, which can reduce the memory cost to the greatest extent. In this paper, the region of moving object is determined by horizontal and vertical projection of binary symmetric difference image. At the same time, the optimal feature combination is selected from the reduced features by feature subset selection, and the classification algorithm is used as the evaluation function in the optimization process. Finally, the collected data are tested, analyzed, and sorted out. The experimental data show that, after calibrating the sensor data, the static x -axis and y -axis data are about 0 g, and the z -axis data are about 1 g, which is closer to the real value. The results show that the attitude data collected by the inertial sensor can be stably transmitted to the software of the computer wirelessly for attitude reconstruction, and the recognition of each attitude and parameter has reached a high accuracy.

1. Introduction

Calisthenics is one of the main contents of physical education in high schools, which has a positive role in promoting the health of teenagers. It is of great significance to carry out good calisthenics in high schools for the popularization and development of calisthenics. In three-dimensional space, the motion of an object may cause a change in its attitude. In some control areas, it is very important to determine the attitude information of the object at a certain moment.

As a key technology, attitude detection technology plays an important role in some traditional fields. Inertial motion information includes acceleration and angular velocity information, which are ubiquitous in daily life. Our actions and behaviors will generate specific inertial information. Therefore, by effectively processing acceleration information, we can extract corresponding motion information from it. This infers the intention of the performer of the action.

Inertial sensors are increasingly used in data fusion and parallel processing. Vitale C et al. proposed the criticality of MEMS testing and calibration, and related researches have gradually increased. MEMS testing methods mainly include zero-point drift method and Allan variance method. The zero-point drift method is based on the basic working principle of MEMS devices and collects the output of the device at the static zero position. To determine the zero drift value, this method is relatively simple and intuitive, but it is easy to be affected by the initial alignment error [1]. Aceto et al. proposed that the evolving nature of mobile network traffic makes machine learning solutions based on manual and expert-created functions unable to keep up with their development speed. These limitations paved the way for the use of deep learning as a feasible strategy for designing traffic classifiers based on automatically extracted features, reflecting complex patterns extracted from multiple aspects of traffic properties, implicitly in a “multimodal” manner carrying information [2]. Martinelli A et al. analyzed the

visual inertial sensor fusion problem of two kinds of agents in cooperation and proved that the sensor fusion problem is equivalent to a simple polynomial equation system, which consists of multiple linear equations and three quadratic polynomial equations composition. The analytical solution of this polynomial equation system can be easily obtained by using algebraic methods. They provided an analytical solution to the vision-inertial sensor fusion problem for the two agents. The factors considered in their research content are not comprehensive [3]. Wang et al. proposed a robust and tightly coupled global positioning system integration scheme based on wavelet, which aims to improve the overall positioning accuracy during signal interruption. They proposed a tightly coupled GPS/BDS/INS integration scheme based on robust wavelet and introduced GPS/BDS double-difference (DD) carrier phase and pseudorange measurements to construct a 27-state tightly coupled GPS/BDS/INS integral equation. Their research lacks innovation [4].

Based on the study of the traditional hybrid and multilevel data fusion processing structure, this paper first proposes a new form of serial hybrid data fusion processing structure, which has both distributed and centralized fusion processing structure. Aiming at the multitarget tracking of nonlinear and non-Gaussian systems, this paper proposes an improved marginalized particle probability hypothesis density filtering method, which solves the problem of target missing in multitarget tracking. Aiming at multitarget tracking with low sensor detection probability, a smoother solution of probability hypothesis density is proposed, which reduces the target tracking miss rate and false follow rate under low sensor detection probability [5].

2. Data Fusion and Parallel Processing

2.1. Aerobics. The healthy development of the body will then lead to the improvement of the psychological and mental state. For example, in the students' intense schoolwork, aerobics can let people lay down the burden of tension and enjoy the pleasant beauty of the body through its unique sense of movement. Sports not only promote the development of human right brain to improve learning and memory ability but also stimulate the development of people's ability to recognize three-dimensional space and physical coordination. Aerobics can fully satisfy the coordinated development of the left and right brain and fully develop the potential of the brain [6].

2.2. Inertial Sensors. In the Cartesian coordinate system, if $(x(t), y(t))$ is used to represent the position of the target at time t , its trajectory can be approximated by a polynomial:

$$x(t) = a_0 + a_1t + a_2t^2 + \dots + a_nt^n, \quad (1)$$

$$y(t) = b_0 + b_1t + b_2t^2 + \dots + b_nt^n. \quad (2)$$

In the formula, n is the order of the motion model, and its size reflects the characteristics of the target motion. Since, in the Kalman filter formula, the noise of the system is required to be white noise, a shaping filter needs to be added

to the input of the target dynamic system, its input is white noise, and the output characteristics should be the same as $F(t)$ [7]. In general, the differential equation of the shaping filter can be expressed as

$$\sum_{i=0}^m a_i(t) \frac{d^i}{dt^i} F(t) = \sum_{j=0}^l b_j(t) \frac{d^j}{dt^j} u(t). \quad (3)$$

In the formula, $u(t)$ is the unit white noise.

Each sensor node sends the angular velocity, acceleration, and magnetic field strength data to the base station, which collects and transmits the data to the host computer. The information interaction between nodes and base stations is based on wireless communication. Multiple nodes send data to the base station at the same time, which is prone to signal collision and data loss. In order to ensure the integrity of data in wireless transmission and improve the efficiency of data transmission, the system defines the star topology structure with base station as the center and realizes the network protocol based on time division multiplexing. Because the components of each sensor node and base station are difficult to be strictly consistent, and there is clock deviation between different nodes, clock synchronization is required [8, 9].

Kalman filter mainly includes two stages: prediction and update; in the prediction stage, the Kalman filter obtains the estimation of the current state variables (including uncertainty) and enters the update stage of the filter when the next measurement value is available. Combining the estimated value of the previous time and the measured value of the current time, the weighted average method is used to update the previous estimated value. Higher certainty means greater weight. Because of its recursion, only the current measurement value, the state estimation value of the previous moment, and the corresponding uncertainty matrix are used, and the real-time performance of the algorithm can be guaranteed [10]. For the gyroscope, the state equation of the Kalman filter is composed of the gyroscope's measurement error $\Delta\theta$ and the offset error $\Delta\delta$:

$$\begin{bmatrix} \Delta\theta_{k+1} \\ \Delta\delta_{k+1} \end{bmatrix} = \begin{bmatrix} 1 & T \\ 0 & 1 \end{bmatrix} \begin{bmatrix} \Delta\theta_k \\ \Delta\delta_k \end{bmatrix} + \begin{bmatrix} T \\ 1 \end{bmatrix} \mu. \quad (4)$$

Among them, μ is the measurement error of the gyroscope.

The error covariance equation can be expressed by the following formula:

$$\hat{P}_k = A_{k-1} P_{k-1} A_{k-1}^T + Q. \quad (5)$$

After the standing phase is detected, the accelerometer's measurement of gravity can be used to complete the correction of the system state. The correction process can be written as

$$x_k = \hat{x}_k + K_k (a_k - Hg), \quad (6)$$

$$P_k = (I_{7 \times 7} - K_k H_k) \hat{P}_k. \quad (7)$$

Among them, K_k is the Kalman filter gain, which can be obtained by the following formula:

$$K_k = \hat{P}_k H_k^T (H_k \hat{P}_k H_k^T + R)^{-1}. \quad (8)$$

Kalman filter continuously updates the sensor error model and makes corrections, so the quadratic integration error caused by sensor deviation is minimized [11].

2.3. Data Fusion. The advantages of multisource data fusion are shown in Figure 1. Specifically, it includes enhancing the survivability of the system, improving the credibility, expanding the space coverage, extending the time coverage, reducing the ambiguity of information, improving the detection performance, improving the spatial resolution, increasing the number of measurement spaces, and the characteristics of low cost, light weight, and less space occupation [12].

The function model of level 6 of data fusion system is shown in Figure 2. Data fusion system can be divided into three fusion units and one management unit from the functional process. Inertial sensors usually collect different physical information. The data from the corresponding data processing and calculation to control the movement of the upper virtual character model are packaged and processed according to the agreement with the upper computer; then the sensor data are obtained through the micro control unit, and then the preprocessed data are sent to the upper computer by the wireless module in real time to drive the control upper virtual figure model [13, 14].

By simultaneously interpreting the static and dynamic properties of different sensors, different sensor data can be obtained with different frequency-domain characteristics. The measured sensor signal is transformed from time domain to frequency domain, and its specific noise characteristics are obtained. According to whether the sensor signal contains high-frequency noise or low-frequency noise, the specific filter in the complementary filter is selected to remove the corresponding noise. Finally, the effective signal of the whole frequency band is obtained by adding multiple filtering signals, and the whole process of denoising and fusion is completed [15]. Assuming that there are two sensors in the attitude detection system and their output values contain low-frequency noise and high-frequency noise, respectively, the attitudes in frequency domain are $C_1(s)$ and $C_2(s)$, respectively [16]. If the real attitude is $C(s)$, there exists the following relationship:

$$\begin{cases} C_1(s) = C(s) + \mu_L(s), \\ C_2(s) = C(s) + \mu_H(s). \end{cases} \quad (9)$$

The state equation of moving target in rectangular coordinate system is as follows:

$$x(k+1) = F(k)x(k) + \Gamma(k)v(k). \quad (10)$$

In the formula, $x(k) \in R^{n \times 1}$ is the target state vector at time k . Kalman filter algorithm can effectively estimate the target state from noisy measurement data, which generally includes two stages: state prediction stage and state correction stage [17]. In the state prediction stage, the state equation is mainly used to determine the predicted value of the state vector. The expression is as follows:

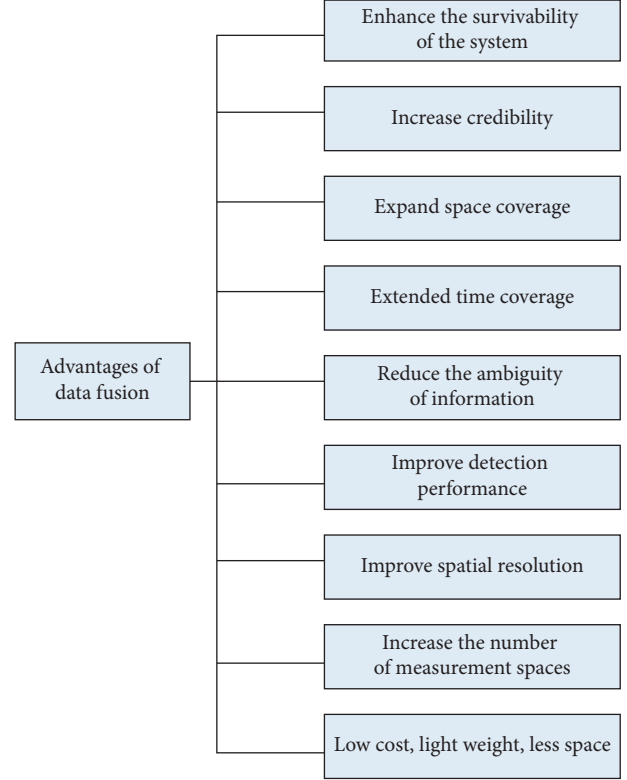


FIGURE 1: Advantages of multisource data fusion.

$$\hat{x}(k|k-1) = F(k-1)\hat{x}(k-1|k-1) + \Gamma(k-1)v(k-1). \quad (11)$$

In the state correction stage, the observation equation is used to determine the predicted value of the observation vector. The specific formula is

$$\hat{z}(k|k-1) = H(k)\hat{x}(k|k-1) + w(k). \quad (12)$$

Calculate the word vector output by the BiGRU layer. The purpose of the BiGRU layer is mainly to extract the deep features of the text from the input text vector. The BiGRU model can be regarded as consisting of two parts: forward GRU and reverse GRU, which is simplified here as 11. After feature extraction at the BiGRU layer, the relationship between contexts can be learned more fully and semantic coding can be performed. The specific calculation formula is shown in equation (11).

$$h_{ijt} = \text{BiGRU}(c_{ijt}), \quad t \in [1, m]. \quad (13)$$

Calculate the probability weight that each word vector should be assigned. This step is mainly to assign corresponding probability weights to different word vectors, further extract text features, and highlight the key information of the text. In the text, different words play different roles in the text sentiment classification. Place adverbial and time adverbial are of little importance to text sentiment classification, while adjectives with emotional color are very important to text sentiment classification. In order to highlight the importance of different words to the sentiment

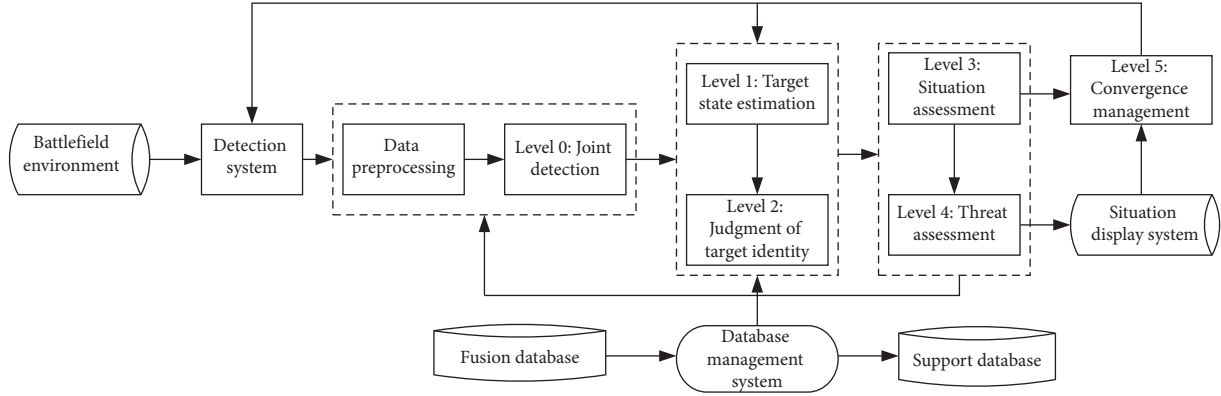


FIGURE 2: The 6-level functional model of the data fusion system.

classification of the entire text, the attention mechanism layer is introduced in the BiGRU-Attention model. The input of the attention mechanism layer is the output vector h_{ijt} processed by the activation of the BiGRU neural network layer in the previous layer. The weight coefficient of the attention mechanism layer is specifically calculated by the following formulas:

$$u_{ijt} = \tanh(w_w h_{ijt} + b_w), \quad (14)$$

$$a_{ijt} = \frac{\exp(u_{ijt}^T u_w)}{\sum_t \exp(u_{ijt}^T u_w)}, \quad (15)$$

$$s_{ijt} = \sum_{i=1}^n a_{ijt} h_{ijt}. \quad (16)$$

Among them, h_{ijt} is the output vector of the previous BiGRU neural network layer, w_w is the weight coefficient, b_w is the bias coefficient, and u_w is the randomly initialized attention matrix. The attention mechanism matrix is the cumulative sum of the product of the different probability weights assigned by the attention mechanism and the state of each hidden layer, and the softmax function is used for normalization.

2.4. Parallel Processing. According to its connectivity and control strategy, parallel interconnection network can be divided into static network and dynamic network. Static network is used to establish point-to-point links, and its network structure does not change in the process of processing tasks. In other words, static network has fixed connection between processing nodes, so static network is also called direct network. Dynamic network, which realizes the communication between nodes through switching channels, can dynamically connect channels to meet the communication needs of user programs, which is the biggest difference between it and static network. Dynamic network can be divided into shared bus, cross switch, and multilevel network. Its routing is realized

through a group of switches, so it is also called indirect network [18, 19].

Due to the limitation of image acquisition methods and the influence of various interference factors in the transmission process, the image sequence collected and transmitted by the high-speed image sequence moving target detection system is inevitably contaminated by various noises. The block diagram of the data acquisition terminal is shown in Figure 3. It mainly includes power supply circuit, main control chip, acceleration and angular velocity sensor, magnetic sensor, and wireless radio frequency module [20].

Suppose that the output of a three-axis gyroscope is (w_x, w_y, w_z) , respectively representing the angular velocity of the gyroscope rotating around its own x -, y -, and z -axes. Combine the three parameters into a quaternion ${}^s w$, and the specific expression is as follows:

$${}^s w = (0, w_x, w_y, w_z). \quad (17)$$

The feature extraction is realized by using binary symmetric difference image. ${}^E_s q$ represents the posture quaternion of the target object relative to the ground coordinate system, and the derivative of ${}^E_s q$ can be obtained by the following formula [21]:

$${}^E_s \dot{q} = \frac{1}{2} {}^E_s q {}^s \omega. \quad (18)$$

Therefore, $q(t)$ can be obtained by integrating $\dot{q}(t)$, and discretization can be obtained:

$${}^E_s q(t + \Delta t) = {}^E_s q(t) + {}^E_s \dot{q}(t) \Delta t. \quad (19)$$

2.5. Main Methods of Multisensor Data Fusion

2.5.1. Bayesian Theory. Bayesian theory belongs to one of many classical statistical reasoning methods. It is active in all aspects of data fusion applications and is committed to solving multisource data fusion problems. However, as a probabilistic method, Bayesian theory often has many shortcomings in practical applications. Bayesian theory mainly uses conditional probability in probability statistics

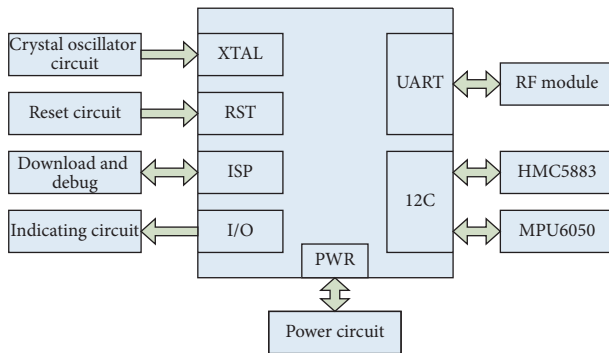


FIGURE 3: Block diagram of the data acquisition end.

to complete the reasoning of the fusion result. The entire fusion process needs to determine the prior probability and likelihood function of the system, and, for the two types of “uncertain” and “unknown,” Bayesian theory is still unable to provide an effective representation method for the common basic concepts in data fusion.

2.5.2. Kalman Filter. In data fusion, the Kalman filter-based data fusion method is usually used for low-level multisensor data fusion processing that requires high real-time performance. The data fusion method based on Kalman filter mainly recursively processes the statistical characteristics of the system measurement model and then obtains the optimal fusion and data estimation of the system. This method can provide the only optimal estimation for the data fusion system that conforms to the linear dynamic model and the error satisfies the Gaussian distribution. Using Kalman filter for data fusion processing, the system does not need to perform a large amount of calculation processing and has high real-time performance. This method is suitable for dealing with dynamic and low-level data fusion problems.

2.5.3. Fuzzy Theory. Fuzzy theory uses fuzzy sets to describe the membership relationship of general sets. In the description process, the membership relationship of elements to sets is expressed as any digit in the interval $[0,1]$. In the practical application of fuzzy theory, it is mainly to select the membership function of the fuzzy set to which the problem belongs and use this function to quantitatively express the fuzzy function and fuzzy measure.

2.5.4. Neural Network Method. Neural network can simulate nonlinear mapping under complex system and has strong fault tolerance, good adaptability, and strong self-learning ability. This performance is a must-have for multisensor fusion system. Therefore, neural networks are widely used in various fields of multisensor data fusion. The processing process of neural network in multisource information fusion is similar to the verification process of “uncertainty” in the process of logical reasoning. The neural network performs classification by the similarity of samples and assigns the classification

results by the weight of the network. This method is similar to the preprocessing process of sample data in the fusion system.

2.5.5. Decision Theory Method. Decision theory is based on the mature development of probability theory. As an important branch of operations research and the theoretical basis of decision analysis, decision theory uses quantitative methods to query or select the optimal decision plan based on information fusion and evaluation criteria. According to the sampling data provided by the sensors and the evaluation criteria of the fusion center, the quantitative method is used to find the optimal decision-making plan.

3. Application Experiment of Inertial Sensor in Aerobics

3.1. Design of Aerobics Sports System. The overall block diagram of the system is shown in Figure 4. High-performance Bluetooth chip CC2541 plus MPU6050 component as the main step counting system hardware, complete acceleration data processing and step count, and real-time transmission to the mobile phone Bluetooth device terminal display can realize the effective detection of human movement step number. MPU6050 detects and collects the three-axis acceleration of human movement. CC2541 reads and processes acceleration data through I2C interface, Uses a digital filter to remove noise, and then sets reasonable thresholds of acceleration rising edge and falling edge for step detection, which is then transmitted to the mobile phone APP for display through wireless Bluetooth [22].

3.2. Experimental Parameters. In the IDNet data set, because some testers only collected a small amount of data or the data were confused due to mobile phone hardware problems, only 35 people’s gait data were selected for the experiment in this chapter [23]. The specific distribution of the data is shown in Table 1.

3.3. Data Preprocessing. The object of the inertial aerobics motion sensor is the human body, and the human activity is relatively slow in general, so the frame number collected by the sensor in the process of human motion capture is relatively low. At the same time, the sensitivity of MEMS sensor is very high. In this paper, Kalman filter is used to filter the pulse error of accelerometer. Since the system has high requirements for sensor delay rate, it is appropriate to set the length of window A to 5 [24].

3.4. Whole Body Motion Capture Test. The platform used in the test is Intel Core i5 processor, the operating system is Windows 7, and the graphics card is GTX1060. The USB interface is USB 3.0, and the wearable circuit uses a 3.7 V lithium battery. The data refresh frequency during the test is 40 Hz. First connect the 10 nodes organically through the CAN bus, and then insert the wireless receiving USB module into the USB interface of the PC and turn on the upper

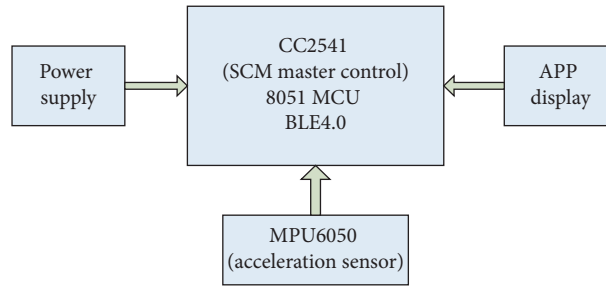


FIGURE 4: The overall block diagram of the system.

TABLE 1: IDNet data set.

Data set name	Number of training data set samples	Number of test data set samples	Number of categories
IDNet	2100	3500	35

TABLE 2: Multinode motion capture system parameter comparison.

Comparison item	This paper's design system	Notion
Number of nodes	10	17
Maximum capture angular velocity	± 2000 dps	± 2000 dps
Accelerometer measuring range	± 2 g	± 8 g
Data refresh frequency	40 Hz	96 Hz
Data transmission method	2.4 G	2.4 G
Dynamic measurement range	360°	360°
Calibration steps	1	3
Accuracy of pitch and roll angle	0.01°	0.02°
Heading angle accuracy	1°	1°

computer, and finally start the power of the wireless transmitting Hub module [25]. The multinode motion capture system parameter comparison is shown in Table 2.

3.5. Implementation of Sliding Window. In this paper, the data structure of unidirectional link is used to achieve the effect of sliding window, which can reduce the memory cost to the greatest extent, where each node records the sensor sampling value at the current time. Taking the three-axis acceleration sensor signal as an example, each node contains three pieces of data, which are each axis of the three-axis acceleration signal. Since we adopt a unidirectional link structure, the pointer p points to the oldest node in the link and updates the value of the node. Therefore, the node becomes the latest node in the link [26].

3.6. Extraction of Moving Target Regions. In this paper, the region of moving object is determined by horizontal and vertical projection of binary symmetric difference image. Due to the block processing method, the reference frame data reading, background motion compensation, and moving target region extraction of different subblock images can be carried out simultaneously. In the process of background motion compensation, the gradient information is used for matching block prediction to determine the subblocks that do not participate in the

motion vector parameter estimation. Only the subblocks need to be marked. After the motion vector is determined, the background motion compensation is performed [27].

3.7. Feature Extraction. Firstly, the time-domain and frequency-domain features are extracted, and the optimal feature combination is selected from the feature space by combining principal component analysis (PCA) with feature subset selection. PCA removes similar dimensions by calculating the correlation between different dimensions, so as to reduce redundant features. Through feature subset selection, the optimal feature combination is selected from the features after dimension reduction, and the classification algorithm is used as the evaluation function in the optimization process, so that the feature combination most consistent with the classification algorithm can be selected [28].

3.8. Statistical Analysis. The collected data were tested, analyzed, and sorted out. Excel software was used to record the pretest data and posttest data of students, and a database was established. Then, SPSS 23.0 software was used to count the data of pretest and posttest, and the effectiveness of the experiment was tested with independent-sample t . The measured data were statistically analyzed.

4. Data Fusion Parallel Processing Analysis

4.1. Data Preprocessing Effect Analysis. In the scene of fitness action recognition, compared with the recognition of human daily behavior, fitness action has a big feature; that is, it will not change the state of exercise easily. Therefore, we can postprocess the recognition results and revise the results according to the characteristics of fitness movement in the process of recognition. In order to obtain the information contained in the continuous time signal, the appropriate sampling frequency should be determined first to prevent frequency overlap phenomenon; second, the appropriate sample length should be selected to prevent energy leakage. The comparison of gyroscope data before and after the mean filter is shown in Table 3 and Figure 5. After low-pass filtering and recursive average filtering, the burr of gyroscope data is reduced and the data become smoother than before, which is conducive to the subsequent algorithm.

For biological systems, sensory perception provides necessary information for understanding the external world, and the knowledge and laws formed by the accumulation of information in turn guide the process of understanding. Place the accelerometer sensor on a horizontal table, and calibrate the accelerometer sensor by the six-position calibration method. The comparison of the output data before and after calibration is shown in Figure 6. As can be seen from the above figure, after the accelerometer data are calibrated by the six-position calibration method, the accelerometer data change significantly. The x -axis and y -axis data at rest are around 0 g, and the z -axis data are around 1 g, and the data change. It is more stable, its existing error is effectively eliminated, and it is closer to the true value. Usually the preprocessing steps of the original data include the following: denoising, zero-speed update, position correction, windowing, and so on. In order to reduce the computational complexity of the classification model, these preprocessed data are then entered into the next module, and the motion features are extracted through the feature extraction algorithm, usually in the time domain and frequency domain for feature extraction, and finally a sample library is formed. There will be a training set and a validation set in the library, which are used for model training and movement status recognition and classification.

4.2. Comparison of Aerobics Skill Test Results. Aerobics skill test results are shown in Table 4. The results showed that there was no significant difference between the experimental group and the control group ($P > 0.05$). Therefore, it can be proved that the samples of the experimental group and the control group are from the same level, the students' Calisthenics technical level is equivalent, and the samples are representative and meet the experimental requirements. Before the experiment, through the independent-sample t -test of two samples of healthy physical fitness indexes, it is concluded that, in the body composition test items, namely, BMI index, there is no significant difference between the experimental group and the control group, $P > 0.05$; in the muscle strength and muscle endurance fitness test items,

namely, sit ups and 800-meter run, there is no significant difference between the experimental group and the control group, $P > 0.05$. Therefore, it can be proved that the samples of the experimental group and the control group in this experiment come from the same level, the levels of various indicators of students' health and physical fitness are similar, and the samples are representative and meet the experimental requirements.

The student factors that affect the formation of teaching ability of aerobics major undergraduates in physical education colleges and universities are composed of four factors: the level of aerobics special theoretical knowledge, the level of aerobics special technology, the students' self-awareness, and the motivation of learning aerobics. Theory is the basis of guiding practice. The formation of aerobics special teaching ability needs to be based on rich scientific teaching theory and aerobics professional theoretical knowledge and grasp the knowledge that can reflect the objective law and has internal relationship with specific activity objects. In the organization and referee of the event, the preparation, organization, and management of the event and the learning of the referee rules can not only be on paper. In addition to understanding the general rules of the event process, also mastering the arrangement and organization methods of the common or major events in the event and experiencing in the event can be trained and mastered. Although students now have more experience in participating in competition adjudication outside school, due to the fact that different students have different enthusiasm levels, the opportunity to get exercise is different, and the content of each referee is not the same, so not often experience will lead to poor executive ability.

4.3. Data Fusion Results. PCA processing not only reduces the dimensionality of the feature space but also, more importantly, removes the influence of redundant information on classification and recognition, making it easier to find different features of the data and discover hidden patterns in the data. PCA dimensionality reduction only deletes redundant information based on the correlation between features. The resulting dimensionality reduction features can only ensure that the correlation between features is small and achieves the effect of initially reducing the dimension of features. The search for the superior feature subset narrows the scope.

The optimal feature subset refers to the feature subset that can best represent different actions. Its intuitive effect is to use this subset to model classifiers to achieve the highest recognition rate. The distribution of eigenvalues is shown in Figure 7. It can be seen from the figure that the filter method has nothing to do with the learning algorithm used in the system. It only evaluates the quality of the feature subset through the statistical performance of the subset, which has the characteristic of fast speed. However, due to the difference of the learning algorithm, the feature subset obtained by the evaluation is quite different from the optimal subset of the specific learning algorithm. The wrapper method ensures that the selected subset pair is the optimal subset of the

TABLE 3: Comparison of gyroscope data before and after the average filter.

Time	1	2	3	4	5	6	7	8	9	10	11	12	13	14	15
Before filtering	20.6	29.3	34.5	25.6	17.3	34.8	21.8	37.5	17.4	36.2	38.6	23.4	37.1	18.5	22.4
After filtering	41.4	43.7	47.2	51.3	37.2	31.2	46.6	47.5	36.6	48.6	26.8	45.3	30.2	22.1	42.1

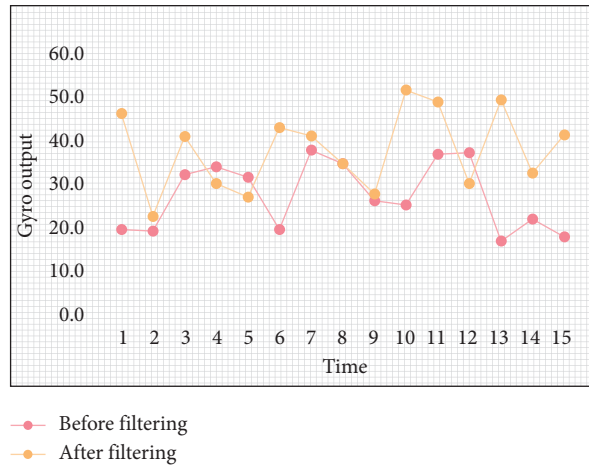


FIGURE 5: Comparison of gyroscope data before and after the average filter.

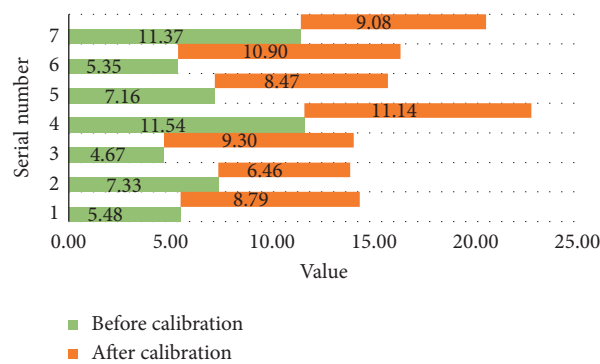


FIGURE 6: Comparison of output data before and after calibration.

TABLE 4: Aerobics skills test results.

Test items	Experimental group (60) Mean \pm standard deviation	Control group (60) Mean \pm standard deviation	t	P
Aerobics skills	81.80 \pm 3.85	81.98 \pm 4.14	-0.25	>0.05

learning algorithm by taking the real training accuracy rate of the subset pair learning algorithm as the evaluation criterion, which has the advantage of small deviation. However, due to the model training and verification of the feature set in the evaluation process, it needs a large amount of calculation and is not suitable for the scenario with too large data set.

4.4. Parallel Computing. A huge computing job can be divided into relatively independent computing tasks. These computing tasks are evenly distributed to each computing

node. After the calculation task of each node is completed, the management node will reschedule and allocate the task to summarize the results. The parallel processing results are shown in Figure 8. LSTM model can fully extract the temporal features between gait features. Based on LSTM model, we can learn the change rules of gait features, increase the performance of the model, and improve the prediction accuracy. The accuracy rate in the experiment reaches 96.85%. BiGRU has better performance than LSTM. Its model can make full use of the context information of gait features and improve the classification accuracy. The experimental accuracy reaches 97.28%. After the attention

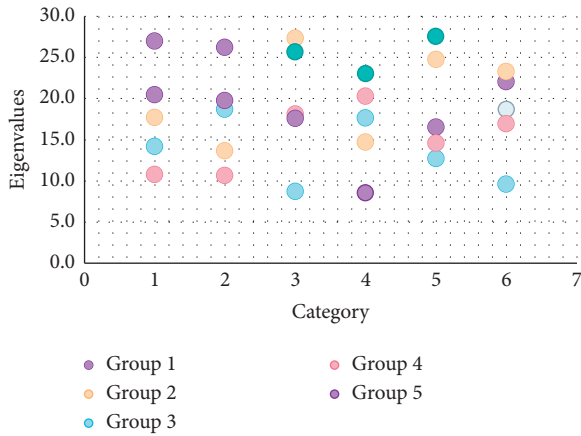


FIGURE 7: Eigenvalue distribution.

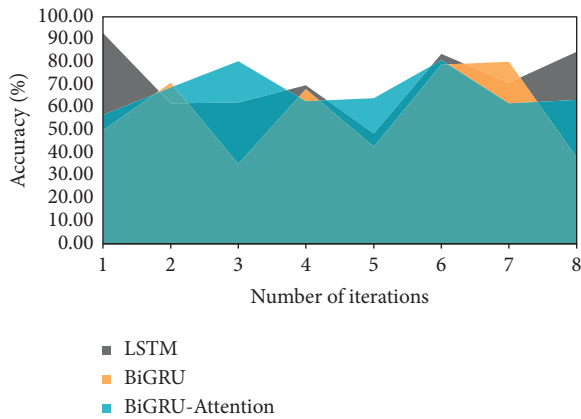


FIGURE 8: Parallel processing results.

layer is added to BiGRU model, the experimental results are improved, which shows that attention mechanism can pay attention to more important sequence information and further improve the accuracy of the model. It can play an optimization role in the training process of the model, and the experimental result reaches 97.64%.

Each action collector will place the inertial sensor in different positions, so the initial attitude obtained will be different, which will lead to the deviation of the initial calibration of the initial action. Since the rotation increment of the same skeleton is a fixed value, this paper uses the rotation increment to drive the human model, solves the sensitive problem of inertial sensor fixation, and uses adaptive linear interpolation to process the data, so as to solve the discontinuous problem of attitude data and achieve the ideal effect. In this system, the calibration methods designed for the three sensors can effectively reduce the error contained in the sensor data and improve the accuracy of the sensor measurement value. However, the calibration method cannot completely eliminate the measurement error of sensor, especially that the output value of accelerometer and gyroscope still fluctuates, which will affect the measurement accuracy and stability of the system.

It can be seen from Figure 8 that the classic fusion rules cannot effectively deal with evidences that deviate from each

other to a large degree, and the fusion results obtained are quite different from the facts; while the LSTM method cannot make correct decisions after the evidence has accumulated to a certain extent, the two-way GRU method can. It has a certain fusion effect for evidences that deviate from each other to a certain degree, but it takes a long time; meanwhile Sun Quan’s method is suspected of being faulty when dealing with evidences that deviate from each other, and it is easy to put the results of fusion into the limit. Compared with the above methods, the evidence theory fusion algorithm based on the compatibility coefficient proposed in this paper, from a global perspective, comprehensively considers the information with a greater degree of mutual support between the evidences and a higher degree of credibility. For the conflict between two pieces of evidence with a larger degree of deviation, the fusion result is more reliable and efficient.

5. Conclusions

The main research content of this paper is the parallel processing method of inertial aerobics multisensor data fusion. In aerobics gesture recognition, the main collection is the human leg and arm movement information, so the sensor is attached to the forearm and calf of the subject, respectively. In the process of collecting limb signal data, due to the drift of the gyroscope sensor, it is necessary to filter the sensor signal. Experiments show that Kalman filter can complete sensor data fusion, reduce the interference of noise signals in attitude calculation, and improve the accuracy of attitude calculation.

In order to improve the connection between information fusion technology and people’s daily life, so that the application range of information fusion algorithms is wider and more efficient, many scholars are committed to researching and mining fusion algorithms with stronger applicability and higher fusion efficiency. Significant progress has been made. Based on the data fusion algorithm, this paper conducts in-depth research and exploration on the theory, fusion results, and fusion efficiency of the algorithm. The following innovations are proposed on the theoretical basis: after studying the homogeneous multisensor and heterogeneous multisensor fusion algorithm, a fusion algorithm based on fuzzy adaptive trust value and a weighted correction based on compatibility coefficient are successively proposed. The fusion algorithm mainly introduces the basic theory, basic function model and architecture of data fusion, and the level of fusion. This article compares the advantages and disadvantages of several typical data fusion algorithms, introduces correlation coefficient-based fusion methods, and evidence-based fusion methods and conducts in-depth research on them.

Aiming at the problem of high fusion complexity caused by traditional data fusion models that cannot effectively filter out errors and redundant data, this paper proposes a relative gradient fusion model that introduces median filtering and derivative functions to effectively perform data pre-processing. On this basis, this paper proposes a new evidence theory fusion method based on the compatibility coefficient.

This algorithm, in terms of the weight distribution of conflicting evidence, starts from the overall situation and assigns higher weight to the evidence with high reliability to the greatest extent. The impact of high-reliability evidence on the results is improved. At the same time, by assigning a lower weight value, the impact of less-reliable evidence is minimized and the credibility of decision-making is improved. In this paper, the sample base for data fusion is small, so the relative spatial distance can be used. Analysis of the algorithm shows that the method in this paper may not be applicable to the fusion of large sample data. In future research, targeted research can be made.

Data Availability

The data that support the findings of this study are available from the corresponding author upon reasonable request.

Conflicts of Interest

The authors declare that they have no conflicts of interest.

References

- [1] C. Vitale, V. Agosti, D. Avella et al., "Effect of Global Postural Rehabilitation program on spatiotemporal gait parameters of parkinsonian patients: a three-dimensional motion analysis study," *Neurological Sciences*, vol. 33, no. 6, pp. 1337–1343, 2012.
- [2] G. Aceto, D. Ciuonzo, A. Montieri et al., "MIMETIC: mobile encrypted traffic classification using multimodal deep learning," *Computer Networks*, vol. 165, no. 24, pp. 106944.1–106944.12, 2019.
- [3] A. Martinelli, A. Oliva, and B. Mourrain, "Cooperative visual-inertial sensor fusion: the analytic solution," *IEEE Robotics and Automation Letters*, vol. 4, no. 2, pp. 453–460, 2019.
- [4] J. Wang, H. Han, X. Meng, L. Yao, and Z. Li, "Robust wavelet-based inertial sensor error mitigation for tightly coupled GPS/BDS/INS integration during signal outages," *Survey Review*, vol. 49, no. 357, pp. 419–427, 2017.
- [5] K. Li, P. Gao, and L. Wang, "Analysis and improvement of attitude output accuracy in rotation inertial navigation system," *Mathematical Problems in Engineering*, vol. 2015, Article ID 768174, 10 pages, 2015.
- [6] J. Collet, M. Cerny, L. Delporte et al., "Effect of the placement of the inertial sensor on the human motion detection," *Lekar A Technika*, vol. 44, no. 4, pp. 21–24, 2017.
- [7] A. Choi, H. Jung, H. Kim, and J. H. Mun, "Predicting center of gravity displacement during walking using a single inertial sensor and deep learning technique," *Journal of Medical Imaging and Health Informatics*, vol. 10, no. 6, pp. 1436–1443, 2020.
- [8] C. J. Lee and J. K. Lee, "Relative position estimation using kalman filter based on inertial sensor signals considering soft tissue artifacts of human body segments," *Journal of Sensor Science and Technology*, vol. 29, no. 4, pp. 237–242, 2020.
- [9] G.-H. Kim, J. Lee, J. Lee, P.-Y. Lee, H. S. Kim, and H. Lee, "GPS and inertial sensor-based navigation alignment algorithm for initial state alignment of AUV in real sea," *Journal of Korea Robotics Society*, vol. 15, no. 1, pp. 16–23, 2020.
- [10] Y. Guo, D. Tao, W. Liu, and J. Cheng, "Multiview cauchy estimator feature embedding for depth and inertial sensor-based human action recognition," *IEEE Transactions on Systems, Man, and Cybernetics: Systems*, vol. 47, no. 4, pp. 617–627, 2017.
- [11] M. Varga, C. Ladd, S. Ma, J. Holbery, and G. Tröster, "On-skin liquid metal inertial sensor," *Lab on a Chip*, vol. 17, no. 19, pp. 3272–3278, 2017.
- [12] S. Guerrier, R. Molinari, and J. Balamuta, "Discussion on maximum likelihood-based methods for inertial sensor calibration," *IEEE Sensors Journal*, vol. 16, no. 14, pp. 5522–5523, 2016.
- [13] S.-L. Han, M.-J. Xie, C.-C. Chien, Y.-C. Cheng, and C.-W. Tsao, "Using MEMS-based inertial sensor with ankle foot orthosis for telerehabilitation and its clinical evaluation in brain injuries and total knee replacement patients," *Microsystem Technologies*, vol. 22, no. 3, pp. 625–634, 2016.
- [14] G. S. Abarca-Jiménez, M. A. Reyes-Barranca, S. Mendoza-Acevedo, J. E. Munguía-Cervantes, and M. A. Alemán-Arce, "Electromechanical modeling and simulation by the Euler-Lagrange method of a MEMS inertial sensor using a FGMS as a transducer," *Microsystem Technologies*, vol. 22, no. 4, pp. 767–775, 2016.
- [15] J. Yao, C. Huang, and D. Li, "Research on a novel ferrofluid inertial sensor with levitating nonmagnetic rod," *IEEE Sensors Journal*, vol. 16, no. 5, pp. 1130–1135, 2016.
- [16] W. Jiang, B. Wei, X. Qin, J. Zhan, and Tang, "Yongchuan, sensor data fusion based on a new conflict measure," *Mathematical Problems in Engineering*, vol. 2016, Article ID 5769061, 11 pages, 2016.
- [17] K. J. Kim, V. Agrawal, I. Gaunaurd, R. S. Gailey, and C. L. Bennett, "Missing sample recovery for wireless inertial sensor-based human movement acquisition," *IEEE Transactions on Neural Systems and Rehabilitation Engineering*, vol. 24, no. 11, pp. 1191–1198, 2016.
- [18] C. Nüesch, P. Ismailidis, L. Hegglin et al., "Unterschiede im Gangbild zwischen Patienten mit Gonarthrose und gesunden gemessen mit Inertialsensoren - einfluss der Ganggeschwindigkeit," *Sports Orthopaedics and Traumatology*, vol. 36, no. 2, pp. 203–204, 2020.
- [19] P. Kumar, S. Mukherjee, R. Saini, P. Kaushik, P. P. Roy, and D. P. Dogra, "Multimodal gait recognition with inertial sensor data and video using evolutionary algorithm," *IEEE Transactions on Fuzzy Systems*, vol. 27, no. 5, pp. 956–965, 2019.
- [20] F. Mokaya, H. Y. Noh, R. Lucas, and P. Zhang, "MyoVibe," *ACM Transactions on Sensor Networks*, vol. 14, no. 1, pp. 1–26, 2018.
- [21] S. Guo and H. Ang, "Modal optimization of inertial sensor structure for helicopter," *Nanjing Hangkong Hangtian Daxue Xuebao/Journal of Nanjing University of Aeronautics and Astronautics*, vol. 50, no. 2, pp. 200–206, 2018.
- [22] P. Zhang, R. Chen, Y. Li et al., "A localization database establishment method based on crowdsourcing inertial sensor data and quality assessment criteria," *IEEE Internet of Things Journal*, vol. 5, no. 6, pp. 4764–4777, 2018.
- [23] J. J. Balamuta, R. Molinari, S. Guerrier, and W. Yang, "A computationally efficient framework for automatic inertial sensor calibration," *IEEE Sensors Journal*, vol. 18, no. 4, pp. 1636–1646, 2018.
- [24] M.-A. Alvaro, G.-M. Alejandro, C.-V. A. Ignacio, and C. V. A. Ignacio, "Kinematic analysis BY gender IN different jump tests based ON a smartphone inertial sensor," *Revista Brasileira de Medicina do Esporte*, vol. 24, no. 4, pp. 263–267, 2018.
- [25] W. Yao, "Application of motion capture system based on MEMS inertial sensor in martial arts competition," *Journal of Mechanical Engineering Research and Developments*, vol. 40, no. 1, pp. 7–13, 2017.

- [26] J. Wen, X. Yang, S. Xu et al., "Walking ability assessment system for Parkinson's patients based on inertial sensor," *Zhongguo Yi Liao Qi Xie Za Zhi*, vol. 41, no. 6, pp. 415–418, 2017.
- [27] S. Lim, A. Case, and C. D'Souza, "Comparative analysis of inertial sensor to optical motion capture system performance in push-pull exertion postures," *Proceedings of the Human Factors and Ergonomics Society Annual Meeting*, vol. 60, no. 1, pp. 970–974, 2016.
- [28] S. Guerrier, R. Molinari, and Y. Stebler, "Wavelet-based improvements for inertial sensor error modeling," *IEEE Transactions on Instrumentation & Measurement*, vol. 65, no. 99, pp. 2693–2700, 2016.

Research Article

Decision-Making Behavior of Fertilizer Application of Grain Growers in Heilongjiang Province from the Perspective of Risk Preference and Risk Perception

Xin Li and Jie Shang 

College of Economy and Management, Northeast Forestry University, Harbin 150040, China

Correspondence should be addressed to Jie Shang; hello_o_o@nefu.edu.cn

Received 7 December 2020; Revised 21 January 2021; Accepted 8 February 2021; Published 20 February 2021

Academic Editor: Sang-Bing Tsai

Copyright © 2021 Xin Li and Jie Shang. This is an open access article distributed under the Creative Commons Attribution License, which permits unrestricted use, distribution, and reproduction in any medium, provided the original work is properly cited.

Heilongjiang Province, as a major grain-planting province in China, under the condition of limited production level and cognitive level, the food and agriculture industry often adopts the “high input-high output” production model to achieve grain yield and increase production. As one of the important material input elements in agricultural production, chemical fertilizer plays an irreplaceable role in increasing crop output and farmers’ income. The reduced application of chemical fertilizer can improve the soil and water source, improve the production environment from the internal agricultural production, and ensure the quality and safety of agricultural products from the source, which is beneficial to the sustainable development of agriculture in China. In this paper, Probit model is used to analyze the risk preference and risk perception of grain farmers in Heilongjiang Province. The results showed that high degree of risk preference had a negative effect on decision behavior of fertilizer application, while high natural risk perception had a positive effect on fertilizer application behavior of grain farmers. At the same time, the results showed that the cultivated land area owned by farmers, the total income of agricultural production, the training of fertilizer technology, and the cognition of the impact of fertilizer on the environment all had significant effects on the chemical fertilizer application behavior of grain farmers. Finally, according to the results of this study, some feasible suggestions are put forward.

1. Introduction and Literature Review

Agriculture is a typical risk industry. In the process of agricultural production and agricultural products management, farmers will face uncertainty from nature, market, agricultural system, and so on [1]. As one of the main material input factors to provide nutrients and efficacy of crops, chemical fertilizers play an irreplaceable role in improving the yield and quality of agricultural products [2]. According to the experience of agricultural development in the world, the application of chemical fertilizer has played an important role in meeting the demand for agricultural products and achieving agricultural modernization and agricultural sustainable development [3, 4]. According to a large number of research data, under the dual constraints of natural risk and market risk, farmers tend to increase the input of chemical fertilizer and pesticides to ensure the

quality and yield of agricultural products. Excessive application of chemical fertilizer is common among Chinese farmers, and excessive chemical input has caused serious environmental problems, which has become the bottleneck constraint of sustainable development of agriculture in China [5–7].

In the aspect of farmers’ fertilization behavior, some scholars mainly studied it from the perspective of family characteristics and farmers’ characteristics. They find that the number of household labor force, the age of household head, education level, gender of household head, nonagricultural income, farmers’ concern about the environment, and so on have an impact on farmers’ fertilization behavior [8–10]. When agriculture faces the risk of natural disasters, the risk decision-making behavior of farmers under uncertainty is affected by its risk characteristics. The risk decision-making behavior of farmers is a function of risk preference and risk

perception [11]. Roumasset and Scott put forward farmers as “risk averse”; farmers’ risk preference and risk perception will directly affect farmers’ fertilization behavior [12, 13]. Farmers’ risk decision-making behavior is affected by the degree of risk preference, which shows that farmers with higher risk aversion are more likely to take risk resistance behavior to reduce losses [14]. Huanguang et al. explaining farmers’ overfertilization behavior from the perspective of farmers’ risk aversion believe that the risk characteristics of farmers are an important factor affecting the amount of fertilizer used by farmers. Farmers with high degree of risk aversion are more inclined to use fertilizer to reduce losses and reduce production uncertainty [15]. Research by Roydatul Zikria and Arie Damayanti showed that agricultural extension can significantly reduce the amount of chemical fertilizers used in Indonesian rice cultivation; the risk preference of farmers has a significant negative impact on fertilizer overuse. Lusk and Coble revealed that perception plays an important role in farmers’ risk decision-making behavior research, and risk perception is even more important than risk preference [16]. Patil and Veetil indicated that, in developing countries, covariate production risk is one of the main characteristics of the agricultural sector, and farmers’ risk attitudes play a crucial role in designing and determining risk mitigation mechanisms [17]. Camacho-Cuena and Requate designed experiments to examine the effect of collective penalty, immediate penalty, and tax subsidy schemes on agricultural pollution abatement for farmers with different risk preferences. The results show that if farmers are risk averse, tax subsidies can effectively alleviate the problem of excessive emission reduction [18]. Qiu et al. obtained farmers’ risk preference index using experimental economics and found that risk preference has different influence on farmers’ adoption of conservation tillage technology under different risk perception [19–21]. To sum up, fertilization behavior as one of the important behaviors to ensure farmers’ production benefits is affected by their risk preference and risk perception.

Heilongjiang Province is an important agricultural production area in China. It has abundant agricultural production resources. However, its agricultural infrastructure construction is not perfect, and its ability to resist natural disasters is relatively weak. Therefore, the agricultural production high risk characteristic is obvious. Selecting grain farmers in Heilongjiang Province as the research object of this paper has a certain representative role and practical significance in promoting China’s agricultural development. Through reading the literature, it is found that there are few studies on the influence of risk preference and risk perception on farmers’ fertilizer behavior decision-making. Therefore, this paper selects Heilongjiang Province as a sample area, takes risk preference and risk perception as the research entry point, studies farmers’ chemical fertilizer application decision-making behavior, and simulates the possible influence of farmers’ risk preference on fertilizer application behavior decision-making of grain farmers. From the point of view of risk preference and risk perception, this paper puts forward some ideas and countermeasures to optimize the fertilizer behavior of grain farmers, guide grain farmers to fertilize

scientifically and reasonably, and achieve the purpose of reducing ecological environment pollution and realizing sustainable development of agriculture.

2. Theoretical Logic and Model Setting

2.1. Theoretical Logic. The cognition and preference of grain farmers to risks in production have the general attribute of farmers’ behavior. Farmers’ decision-making on chemical fertilizer application behavior will directly affect farmers’ own interests and the quality and safety of agricultural products, but under the influence of their subjective judgment, the decisions of different farmers must be different. Based on Expected Utility Theory and Risk-Return Theory, this paper draws on the analysis of Lusk and Coble to establish a theoretical model of the relationship among risk preference, risk perception, and fertilization behavior of grain farmers [16]. This paper assumes that grain farmers are risk averse, and grain farmers believe that appropriate increase in fertilizer application can protect their own revenue function. In order to study the effect of risk perception and risk preference on chemical fertilizer application decision-making behavior of grain farmers, the utility function of grain farmers is $U(W)$, where W is wealth. The expected value of incremental application of chemical fertilizer is expressed by random variable Z . C is defined as the risk premium of incremental fertilization behavior of grain farmers; that is, the utility of incremental fertilizer and loss of C amount of uncertainty currency have no difference. Thus, the following equation holds:

$$E[U(W + Z)] = U[W + E(Z) - C], \quad (1)$$

$$E(Z) = a, \quad (2)$$

$$\text{var}(Z) = \sigma^2. \quad (3)$$

In formulas (2) and (3), a is positive, which means that the average effect of increasing fertilizer application on grain farmers’ income is positive. σ^2 is the variance of random variable Z , which represents farmer’s perception of agricultural risk. The higher the perceived risk of grain farmers, the greater the σ^2 .

Suppose the utility function $U(\cdot)$ is a continuous second derivative function. The utility function $U(W + E(Z) - C)$ is a first-order Taylor expansion at $[W + E(Z)]$. The results are as follows:

$$U[W + E(Z) - C] \approx U[W + E(Z)] - \frac{\partial U}{\partial W} \cdot C. \quad (4)$$

The utility function $U(W + E(Z))$ is used to carry out the first-order Taylor expansion and the second-order Taylor expansion at $[W + E(Z)]$. The results are as follows:

$$\begin{aligned} U(W + Z) &\approx U[W + E(Z)] + \frac{\partial U}{\partial W} \cdot [Y - E(Z)] \\ &+ 0.5 \cdot \frac{\partial^2 U}{\partial W^2} \cdot [Y - E(Z)]^2. \end{aligned} \quad (5)$$

According to equation (5), and $E[Z - E(Z)] = 0$, the expected result of utility function $U(W + Z)$ is as follows:

$$E[U(W + Z)] \approx E\{U[W + E(Z)]\} + 0.5 \cdot \frac{\partial^2 U}{\partial W^2} \cdot \sigma^2. \quad (6)$$

Let $U' = (\partial U / \partial W)$, $U'' = (\partial^2 U / \partial W^2)$, which can be solved by equations (4) and (6):

$$C \approx -\frac{1}{2} \left(\frac{U''}{U'} \right) \sigma^2 = \frac{1}{2} \cdot C(W) \cdot \sigma^2, \quad (7)$$

where $C(W)$ in equation (7) is Arrow–Pratt absolute risk aversion coefficient. The increase of $C(W)$ means that the degree of risk aversion increases.

2.2. Model Setting. In order to investigate the influence of risk preference and risk perception on fertilizer application behavior of grain farmers in Heilongjiang Province, Y was made to represent the decision result of farmers' choice of fertilizer application. According to the benefit effect of different chemical fertilizer application decisions, this paper will reduce chemical fertilizer application, keep chemical fertilizer application unchanged, and increase chemical fertilizer use from low to high. Because the dependent variable is an ordered classification variable, this paper uses the ordered Probit model for empirical estimation. The general form of the model can be expressed as follows:

$$Y = \beta_0 + \beta_1 RF + \beta_2 RC + \beta_3 X + \varepsilon. \quad (8)$$

In the model, the explained variable Y is the latent variable, and $\beta_0, \beta_1, \beta_2$, and β_3 are estimated coefficients. ε is the residual term, subject to normal distribution, and the variance is σ^2 , that is, $\varepsilon \sim N(0, \sigma^2)$. RF and RC are the core explanatory variables, RF is the risk preference index, and RC is the risk perception. X is the vector of control variables, including grain farmers families' characteristics, policy promotion, and other variables.

3. Data Sources and Descriptive Statistics

3.1. Data Sources. The data used in this paper is from a multistage stratified sampling survey of grain farmers in Heilongjiang Province in November 2018. First of all, because Heilongjiang Province is the main grain producing area in China, the main research object is to select grain growers. Secondly, according to the level of economic development and geographical distribution stratified sampling, 3 sample counties were selected. Two sample townships were selected from each district in the same way. Finally, considering the production behavior of grain farmers with different scale of operation may be different, in each sample county, random scale households and nonscale households. The survey interviewed 152 grain farmers and collected 137 valid questionnaires. Table 1 displays the definition of each variable and the descriptive statistical results of 137 grain farmers surveyed.

3.2. Descriptive Statistical Analysis of Variables

3.2.1. Fertilization Behavior. The explained variable in this paper is the change behavior of chemical fertilizer application rate of grain farmers in Heilongjiang Province, which is an orderly classified variable, reduces the assignment value of chemical fertilizer application rate to 0, keeps the constant assignment value of chemical fertilizer application rate to 1, and increases the assignment amount of chemical fertilizer application rate to 2. The statistical results are shown in Figure 1, 16.79% of the grain farmers chose to reduce the amount of chemical fertilizer, 48.18% of the farmers chose to keep the amount of chemical fertilizer unchanged, and 35.03% of the farmers chose to increase the amount of chemical fertilizer. Thus, it can be seen that most grain farmers in Heilongjiang Province basically keep the level of chemical fertilizer application unchanged.

3.2.2. Risk Preference. The risk preference of grain farmers is obtained by using the method of risk preference measure, as shown in Table 2. Use the investment preference to measure the risk preference. Raise questions about the investigated grain farmers: if you have one thousand yuan to invest, you will receive five possible returns, which one do you prefer? According to the different answers of grain farmers, the risk preference is positioned. The results are as follows: if the farmers choose the option of 1000 yuan, they are very risk averse. If farmers choose the option of grain may be 900 yuan or 1600 yuan, the probability of the two benefits is the same; it is more risk averse. If the income of grain farmers may be 800 yuan or 2000 yuan, the probability of the two kinds of income is the same; it is a general risk type. If the grain farmers choose the option to gain 400 yuan or 3000 yuan, the probability of obtaining the two kinds of income is the same; it is the risk type. If the income of grain farmers may be 0 yuan or 4000 yuan, the two kinds of income gain the same probability; it is a very preference for risk. The results show that the average risk preference of grain farmers in Heilongjiang Province is 2.31, the standard deviation is 1.14, and the overall risk type is close, showing the type of risk avoidance.

3.2.3. Risk Perception. This paper explores the influencing factors of fertilization behavior decision-making in agricultural production of grain farmers and therefore does not consider factors such as social risks that farmers may face. Choose only consider the agricultural natural risks that may occur in the production process as the research point of this paper risk perception factors, the survey results are shown in Table 3. The risk perception of grain farmers is measured by the following question: "Do you expect the environment for agricultural production to deteriorate in the future?" When farmers expect "the future agricultural production environment will become worse," it means that farmers perceive the existence of agricultural natural risk. On the contrary, it means that farmers do not perceive agricultural natural risk. The results show that 40.88% of the 137 grain farmers think that the agricultural production environment will become

TABLE 1: Name, meaning, and statistical characteristics of variables.

Variable Name	Variable meaning and assignment	Mean	Standard deviation	Minimum	Maximum
	Fertilizer application behavior of farmers				
Behavior	Reduce the amount of fertilizer application = 0 The amount of chemical fertilizer application remained unchanged = 1. Increase the amount of chemical fertilizer = 2.	1.18	0.70	0	2
	Risk preference				
RF	Very averse to risk = 1, more risk averse = 2, general preference risk = 3, comparative preference for risk = 4, and very risk averse = 5	2.31	1.14	1	5
	Risk perception				
RC	Do you feel that the future agricultural production environment will become worse? No = 0, yes = 1	0.41	0.49	0	1
	Age of head of household				
Age	Unit: years old	41.55	7.34	26	61
	Education level				
Education level	Primary school and below = 1, middle school = 2, high school or technical secondary school = 3, and college or above = 4	2.23	0.60	1	4
	Engaged in agricultural planting time				
Time	Unit: years	16.42	8.52	2	40
	The number of households participating in agricultural production				
Number	Unit: person	2.12	0.88	1	8
	Families own arable land; unit: Mu				
Area		194.24	204.05	20	1385
	Annual family income; unit: 10000 yuan				
Income		17.12	17.16	2	98
	Have you received chemical fertilizer training? No = 0, yes = 1				
Train		0.37	0.48	0	1
	The effect of chemical fertilizer on agricultural ecological environment				
Cognition	No effect = 0, slight effect = 1, general effect = 2, large impact = 3, and severe impact = 4	1.99	1.13	0	4
	Are you willing to reduce fertilization if the government provides fertilizer subsidies?				
Policy	No = 0, yes = 1	0.55	0.50	0	1

Mu is the unit of land measurement in China, equivalent to about 666.67 square meters.

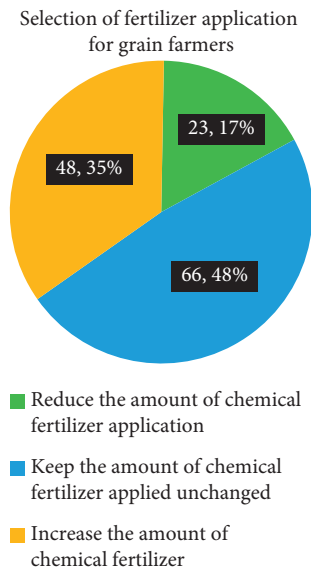


FIGURE 1: Selection of fertilizer application behavior of grain farmers.

worse in the future, and 59.12% of the grain farmers expect the agricultural production environment to not deteriorate in the future; that is to say, more than half of the farmers are optimistic about the possible agricultural natural risks in the future.

3.2.4. Other Control Variables. In this paper, the main control variables are the householder characteristics, production and management characteristics, and subsidy policies of the investigated grain farmers.

The main characteristics of heads of grain farmers include the age of heads of households, education, experience of heads of households, whether heads of households have received fertilizer-related technical training, and heads of household fertilizer pollution awareness as control variables. According to the statistics of the survey results, the average age of the farmers surveyed is 42 years, the average education level is junior high school level, and the average number of years of agricultural planting of the head of household is 16.42 years. It can be seen that farmers have rich planting experience. 37% of the grain farmers have received training in fertilizer-related technologies; the results are shown in Figure 2. The surveyed grain farmers generally believed that the environmental impact of chemical fertilizer pollution was general.

The production and management characteristics of grain farmers mainly include investigating the number of farmers engaged in agricultural production, planting scale, and family annual income level. The average number of farmers engaged in agricultural production is 2, the average family planting scale is 194 mu, and the largest planting scale is about 1385 mu. The average income of the sample family farming was 170,000 yuan.

TABLE 2: Risk preference measures.

Question	Answer options	Types of risk preference	Frequency
If you have 1000 yuan to invest, you will receive five possible returns. Which one do you prefer?	Income 1000 yuan	Very risk averse	41
	The income may be 900 yuan or 1600 yuan	More risk averse	40
	The income may be 800 yuan or 2000 yuan	General risk type	35
	The income may be 400 yuan or 3000 yuan	Risk preference	15
	The income may be 0 yuan or 4000 yuan	Very risk oriented	6

TABLE 3: Risk perception measures.

Question	Answer options	Frequency
Do you expect the agricultural production environment to become worse in the future?	Yes	56
	No	81

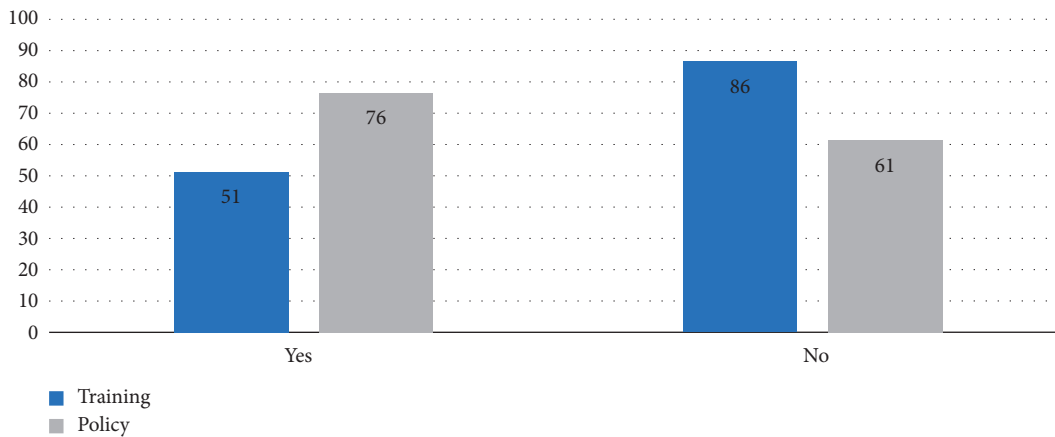


FIGURE 2: Situation of farmers receiving fertilization technology training and policy incentive selection.

In order to investigate the change of fertilization decision of grain farmers under the condition of government subsidies, the question was raised: “Does the government choose to reduce fertilizer application?” According to the results of the survey, 55% of farmers are willing to reduce the amount of fertilizer application under the condition that the government provides fertilizer subsidies; the results are shown in Figure 2.

4. Analysis of Empirical Results

According to the output of Stata 15 software, the Probit regression analysis of survey data was carried out. The running results of the model are shown in Table 4. The fitting degree of the pseudo- R^2 interpretation model is closer to 1, which means that the fitting degree of the model is better. From the results of model estimation, the value of pseudo- R^2 is 0.7315, which is at a high level. Therefore, the model fitted well, and most of the variables have an impact on farmer’s decision-making of fertilization behavior.

4.1. Impact of Risk Preference. According to the results of the effect of risk preference in Table 2 on the fertilization behavior of grain farmers in Heilongjiang Province, this factor was significant at the significance level of 1% and was negative, with a coefficient of 1.88; that is, grain farmers with high risk preference tend to choose to reduce fertilizer application behavior decision. Chemical fertilizer is an important agricultural product to ensure the yield of modern agriculture. Proper application of chemical fertilizer can effectively reduce the possibility of crop yield reduction and increase loss. According to previous relevant studies, risk preference has a significant impact on farmers’ fertilizer behavior, and some of the results show that farmers with low risk preference are more inclined to choose to increase fertilizer application in order to avoid the natural risk of agriculture. This study also verifies the validity of this conclusion.

4.2. Impact of Risk Perception. The effect of risk perception on fertilizer application behavior of grain farmers in Heilongjiang Province was analyzed in Table 2. The results

TABLE 4: Model estimation results.

Variable name	Coef.	Std. Err.	z	$P > z $	95% Conf. interval	
RF	-1.880***	0.578	-3.25	0.001	-3.014	-0.746
RC	1.573*	0.835	1.88	0.060	-0.065	3.210
Age	-0.027	0.064	-0.42	0.673	-0.151	0.098
Education level	0.546	0.642	0.85	0.395	-0.712	1.804
Time	-0.123	0.076	-1.61	0.108	-0.272	0.027
Number	0.234	0.405	0.58	0.563	-0.560	1.028
Area	0.017**	0.007	2.44	0.015	0.003	0.031
Income	-0.167**	0.071	-2.35	0.019	-0.306	-0.028
Train	-2.043***	0.786	-2.60	0.009	-3.583	-0.503
Cognition	-1.136**	0.480	-2.37	0.018	-2.078	-0.195
Policy	-0.906	0.748	-1.21	0.226	-2.373	0.560
_Cons	12.714	4.364	2.91	0.004	4.160	21.268

Log likelihood = -16.642974

Number of obs = 137
LR chi2 (11) = 90.70
Prob > chi2 = 0.0000
Pseudo-R² = 0.7315

***, **, *, respectively, represent 1%, 5%, and 10% of the statistics of the level.

showed that the factor was significant at 10% significance level and had a positive effect with a coefficient of 1.573; that is to say, grain farmers with high risk perception tended to choose to increase chemical fertilizer application behavior decision. Thus, it can be seen that the natural risk has a great influence on the fertilizer behavior of grain farmers. In the absence of effective natural risk aversion methods, grain farmers will usually choose to use a certain amount of chemical fertilizer to avoid the risk after perceiving the natural risk, but the result of this kind of behavior decision often leads to excessive fertilizer.

4.3. Impact of Other Variables. Observing the results of other control variables in Table 2, we can see that the training factor of fertilization technology is significant at the significance level of 1%, and the influence direction is negative, which indicates that farmers who have been trained in fertilization technology are more inclined to choose the decision of reducing fertilizer application behavior. After fertilization technology training of grain farmers, they may choose more reasonable fertilization behavior to ensure their own production income, rather than relying on fertilizer to ensure grain yield. Cultivated area, total income of family agriculture, and knowledge of environmental impact of fertilization were significant at the significant level of 5%. The influence direction of cultivated land area was positive, which indicated that grain farmers with larger cultivated land were inclined to increase fertilizer application. The influence direction of total agricultural production income and fertilization on environmental impact cognition was negative, indicating that grain farmers with high household income tended to choose to reduce fertilizer application behavior. Grain farmers themselves believe that the severity of fertilization on the environment impels grain farmers to make the opposite fertilization behavior; that is to say, the more serious the impact of chemical fertilizer on environment, the more grain farmers are willing to choose to reduce fertilizer application behavior decision. In the model, the age

of the householder, the length of time the householder engaged in farming, and the subsidy policy had a negative effect on the fertilization behavior of the grain farmer. The education level of the head of household and the number of farmers have positive effects on the fertilization behavior of grain farmers, but the results are not significant.

5. Conclusions and Suggestions

In this paper, a questionnaire survey was conducted among grain farmers in Heilongjiang Province. The Probit empirical model was used to analyze the influence mechanism of risk preference and risk perception on fertilizer application behavior decision of grain farmers. The results showed that the high risk preference of grain farmers had a negative effect on the decision-making behavior of chemical fertilizer application, and the high degree of natural risk perception had a positive effect on the chemical fertilizer application behavior of grain farmers. At the same time, the results showed that the cultivated land area owned by farmers, the total income of agricultural production, the training of fertilizer technology, and the cognition of the impact of fertilizer on the environment all had significant effects on the chemical fertilizer application behavior of grain farmers.

With the increasing diversification and high standardization of food demand by Chinese consumers, food quality, food safety, environmental protection, and other aspects of demand, agrochemical residues have been widely concerned. The high use and low efficiency of agricultural chemical fertilizer in China have brought a series of environmental problems, which has become an important factor of hindering the sustainable development of agriculture and threatening the quality and safety of agricultural products. Therefore, the above conclusions have certain policy significance. First, the characteristics of strong risk aversion and relying on natural risk perception to predict fertilization behavior were used to guide grain farmers to learn and use

new technologies such as conservation tillage. The sustainable development of agriculture can be promoted by improving the ability of grain farmers to resist agricultural natural risks through advanced farming techniques. Secondly, because grain farmers as a whole have received low level of training in fertilizer technology, by increasing the training of fertilizer application technology to grain farmers, the knowledge of scientific fertilizer application is improved, and through the scientific proportion of more effective selection of chemical fertilizer application amount, excessive fertilizer application phenomenon is avoided. Third, the relevant departments should strengthen the popularization of science and publicity on the impact of chemical fertilizer application on the living environment, production environment, and food safety and enhance the awareness of the impact of chemical fertilizer application on grain farmers which can effectively improve the chemical fertilizer application choice of grain farmers and achieve the purpose of grain farmers choosing to reduce chemical fertilizer application behavior.

Data Availability

The data that support the findings of this study are available from the corresponding author upon reasonable request.

Conflicts of Interest

The authors declare no conflicts of interest.

Authors' Contributions

All authors have seen the manuscript and approved to submit it.

Acknowledgments

This work was financially supported by the National Natural Science Foundation Project on "Farmers' Behavior of Fertilizer Application and Agricultural Non-Point Source Pollution Control: Impact Mechanism and Policy Simulation Research" (71573036), National Social Science Foundation: Research on the Coupling of Blockchain Technology and Supply Chain Governance of Agricultural Ecological Products (20FGLB059), Study on the Behavior Response and Incentive Mechanism of Farmers' Low Carbon Agricultural Technology Adoption in Heilongjiang Province (2572019BM01), and Research on Performance Evaluation and Mechanism Construction of Circular Agriculture Development of Agricultural Enterprises in Heilongjiang Province (18GLD301).

References

- [1] M. Li, C. Zhou, and L. Lian, "Risk assessment of agricultural flood and drought disasters in China based on entropy information diffusion theory," *Journal of Natural Resources*, vol. 32, no. 4, pp. 620–631, 2017.
- [2] S. Ma and H. Ye, "Research on China's food security based on the effective supply of cultivated land resources at home and abroad," *Agricultural Economic Issues*, vol. 36, no. 6, pp. 9–19, 2015.
- [3] J. Wang, W. Ma, R. Jiang et al., "Integrated management of nutrient resources and food security in China," *Resource Science*, no. 3, pp. 415–422, 2008.
- [4] X. Xie and J. Zhu, "Analysis of regional differences in influencing factors of cultivated land quality and Research on improvement approaches-taking Xinzheng City, Henan Province as an example," *China Land Science*, vol. 31, no. 6, pp. 70–78, 2017.
- [5] K. Li and D. Ma, "Research on Farmers' behavior and decision-making mechanism of fertilizer reduction in ecologically vulnerable areas: a case study of 421 farmers in 4 counties of Shanxi Province," *Journal of Nanjing Agricultural University (Social Science Edition)*, no. 5, pp. 138–145, 2018.
- [6] C. Chao, Y. Wang, and Q. Zhai, "Risk preference, risk perception and pesticide application behavior of peach farmers," *Journal of Jiangxi Agricultural University (Social Science Edition)*, vol. 18, no. 4, pp. 472–480, 2019.
- [7] X. Cheng, X. Jia, J. Huang et al., "Effects of agricultural technology training on farmers' nitrogen application behavior: an empirical study based on maize production in shouguang city, shandong province," *Agricultural Technology Economy*, no. 9, pp. 4–10, 2012.
- [8] Q. Gong, X. Mu, and Z. Tian, "Analysis on Influencing Factors of farmers' risk perception and avoidance ability of excessive fertilization-based on a questionnaire survey of 284 farmers in Jiangnan Plain," *China Rural Economy*, no. 10, pp. 66–76, 2010.
- [9] J. Ma and X. Cai, "Analysis of farmers' willingness to reduce nitrogen application rate and its influencing factors-taking North China Plain as an example," *China Rural Economy*, no. 9, pp. 9–16, 2007.
- [10] Y. Jiang, R. Lei, X. Guo et al., "Spatial variability of soil nitrogen and its influencing factors in Jiangxi Province," *Resources and Environment of the Yangtze River Basin*, 2018.
- [11] J. W. Pratt, "Risk aversion in the small and in the large," *Econometrica*, vol. 32, no. 1/2, pp. 122–136, 1964.
- [12] J. A. Roumasset, *Rice and Risk: Decision-Making Among Low-Income Farmers*, North-Holland Press, no. 98, Amsterdam, Netherlands, 1976.
- [13] J. C. Scott, *The Moral Economy of the Peasant: Rebellion and Subsistence in Southeast Asia*, Yale University Press, London, UK, 1977.
- [14] Z. He, L. Hu, and Q. Lu, "Influence of farmers' risk preference and risk cognition on willingness to adopt water-saving irrigation technology," *Resource Science*, vol. 40, no. 4, pp. 797–808, 2018.
- [15] Q. Huanguang, H. Luan, L. Jin et al., "Impact of risk aversion on Farmers' excessive fertilizer application behavior," *China Rural Economy*, no. 3, pp. 85–96, 2014.
- [16] J. L. Lusk and K. H. Coble, "Risk perceptions, risk preference, and acceptance of risky food," *American Journal of Agricultural Economics*, vol. 87, no. 2, p. 393, 2005.
- [17] V. Patil and P. C. Veetil, "Experimental evidence of risk attitude of farmers from risk-preference elicitation in India," *International Association of Agricultural Economists*, 2018.
- [18] E. Camacho-Cuena and T. Requate, "The regulation of non-point source pollution and risk preferences: an experimental approach," *Ecological Economics*, vol. 73, no. 1727, pp. 179–187, 2012.
- [19] H. Qiu, L. Su, Y. Zhang et al., "Risk preference, risk perception and farmers' adoption of conservation tillage technology," *China Rural Economy*, no. 7, pp. 59–79, 2020.

- [20] Y. Li, J. Fu, P. Li et al., "A review of experimental research on risk preference," *Science and Technology and Management*, no. 5, pp. 34–37, 2009.
- [21] C. A. Holt and S. K. Laury, "Risk aversion and incentive effects," *American Economic Review*, vol. 92, no. 5, pp. 1644–1655, 2002.

Research Article

Neural Network Optimization Method and Its Application in Information Processing

Pin Wang,¹ Peng Wang ,² and En Fan³

¹School of Mechanical and Electrical Engineering, Shenzhen Polytechnic, Shenzhen 518055, Guangdong, China

²Garden Center, South China Botanical Garden, Chinese Academy of Sciences, Guangzhou 510650, Guangdong, China

³Department of Computer Science and Engineering, Shaoxing University, Shaoxing 312000, Zhejiang, China

Correspondence should be addressed to Peng Wang; sdhzdtpw@126.com

Received 3 December 2020; Revised 31 December 2020; Accepted 22 January 2021; Published 8 February 2021

Academic Editor: Sang-Bing Tsai

Copyright © 2021 Pin Wang et al. This is an open access article distributed under the Creative Commons Attribution License, which permits unrestricted use, distribution, and reproduction in any medium, provided the original work is properly cited.

Neural network theory is the basis of massive information parallel processing and large-scale parallel computing. Neural network is not only a highly nonlinear dynamic system but also an adaptive organization system, which can be used to describe the intelligent behavior of cognition, decision-making, and control. The purpose of this paper is to explore the optimization method of neural network and its application in information processing. This paper uses the characteristic of SOM feature map neural network to preserve the topological order to estimate the direction of arrival of the array signal. For the estimation of the direction of arrival of single-source signals in array signal processing, this paper establishes a uniform linear array and arbitrary array models based on the distance difference vector to detect DOA. The relationship between the DDOA vector and the direction of arrival angle is regarded as a mapping from the DDOA space to the AOA space. For this mapping, through derivation and analysis, it is found that there is a similar topological distribution between the two variables of the sampled signal. In this paper, the network is trained by uniformly distributed simulated source signals, and then the trained network is used to perform AOA estimation effect tests on simulated noiseless signals, simulated Gaussian noise signals, and measured signals of sound sources in the lake. Neural network and multisignal classification algorithms are compared. This paper proposes a DOA estimation method using two-layer SOM neural network and theoretically verifies the reliability of the method. Experimental research shows that when the signal-to-noise ratio drops from 20 dB to 1 dB in the experiment with Gaussian noise, the absolute error of the AOA prediction is small and the fluctuation is not large, indicating that the prediction effect of the SOM network optimization method established in this paper does not vary. The signal-to-noise ratio drops and decreases, and it has a strong ability to adapt to noise.

1. Introduction

In the information society, the increase in information generation is getting bigger [1]. To make information available in a timely manner to serve the development of the national economy, science and technology, and defense industry, it is necessary to collect, process, transmit, store, and make decisions on information data. Theoretical innovation and implementation are carried out to meet the needs of the social development situation. Therefore, neural networks have extremely extensive research significance and application value in information science fields such as communications, radar, sonar, electronic measuring instruments, biomedical engineering, vibration engineering,

seismic prospecting, and image processing. This article focuses on the study of neural network optimization methods and their applications in intelligent information processing.

Based on the research of neural network optimization method and its information processing, many foreign scholars have studied it and achieved good results. For example, Al Mamun MA has developed a new method of image restoration using neural network technology, which overcomes to a certain extent the above shortcomings of traditional methods. In addition, neural networks have also been widely used in image edge detection, image segmentation, and image compression [2]. Hamza MF proposed a BP algorithm to train RBF weights. The BP algorithm with additional momentum factor can improve the training

coefficient of the network and avoid the occurrence of oscillations, which improves the training rate of the network [3]. Tom B proposed an RBF-PLSR model based on genetic clustering. This model uses the clustering analysis of genetic algorithm to determine the number of hidden layer nodes and the center of hidden nodes in the RBF network, and the PLSR method is used to determine the network's right to connect [4, 5].

In my country, an adaptive linear component model is proposed. They also made Adaline into hardware and successfully applied it to offset the echo and noise in communications. Quan proposed the error back-propagation algorithm, the BP algorithm, which in principle solves the problem of the multilayer neural network training method, which makes the neural network have strong computing power and greatly increases the vitality of the artificial neural network [6]. Cheng uses mathematical theory to prove the fundamental limitation of single-layer perceptron in computing. However, for multilayer neural networks with hidden layers, an effective learning algorithm has not yet been found [7].

In this paper, the problem of single-signal source azimuth detection under uniform linear sensor array and arbitrary array is studied, and the direction-of-arrival detection array model is established, respectively. In the case of a uniform linear array, this paper establishes a two-layer SOM neural network. First, explain the theoretical basis of this neural network, that is, the homotopological structure between the input vector and the output result. For this reason, we separately analyzed the topological structure of the DDOA vector and the predicted value of the AOA in the case of a uniform linear array. Through derivation and simulation data, we can see that the two do have similar topological structures, which led us to establish the SOM neural network system. It can be applied to AOA prediction problems based on DDOA. Finally, simulation experiments and lake water experiments verify the practical feasibility of this method.

2. Neural Network Optimization Method and Its Research in Information Processing

2.1. Array Optimization and Orientation Based on DDOA and SOM Neural Network. Signal and information processing mainly includes three main processes: information acquisition, information processing, and information transmission [8, 9]. The array signal processing can be regarded as an important branch of modern data signal processing. Its main research object is the signal transmitted in the form of spatial transmission wave. It receives the wave signal through a sensor array with a certain spatial distribution and performs information on the received signal extract. This paper mainly studies the algorithm of the sensor array to detect the sound wave's azimuth, namely, the direction of arrival (DOA).

2.1.1. Array Signal Model. Array signal processing is often based on a strict mathematical theoretical model based on a series of assumptions about the observed signal. The objects

explored in this article are all two-dimensional spatial signal problems. These assumptions stem from the abstraction and generalization of the observed signal and noise.

- (1) Narrowband signal: when the bandwidth of the spatial source signal is much smaller than its center frequency, we call this spatial source signal a narrowband signal; that is, the general requirement is met.

$$\frac{W_B}{f_o} < \frac{1}{10}, \quad (1)$$

where W_B is the signal bandwidth and f_o is the signal center frequency. A single-frequency signal with a center frequency of f_o can be used to simulate a narrowband signal. The sine signal as we know it is a typical narrowband signal. The analog signals used in this article are all single-frequency sine signals.

- (2) Array signal processing model: suppose that there is a sensor array in the plane, in which M sensor array elements with arbitrary directivity are arranged, and K narrowband plane waves are distributed in this plane. The center frequencies of these plane waves are all w_o and the wavelength is λ , and suppose that $M > K$ (that is, the number of array elements is greater than the number of incident signals). The signal output received by the k -th element at time t is the sum of K plane waves; namely,

$$x_k(t) = \sum_{i=1}^K a_k(\theta_i) s_i(t - \tau_k(\theta_i)), \quad (2)$$

where $a_k(\theta_i)$ is the sound pressure response coefficient of element k to source i , $s_i(t - \tau_k(\theta_i))$ is the signal wavefront of source i , and $\tau_k(\theta_i)$ is the relative value of element k to the reference element time delay. According to the assumption of narrowband waves, the time delay only affects the wavefront by the phase change, so

$$s_i(t - \tau_k(\theta_i)) \approx s_i(t) e^{-jw_0\tau_k(\theta_i)}. \quad (3)$$

Therefore, formula (2) can be rewritten as

$$x_k(t) = \sum_{i=1}^K a_k(\theta_i) s_i(t) e^{-jw_0\tau_k(\theta_i)}. \quad (4)$$

Write the output of M sensors in vector form; the model becomes

$$x(t) = \sum_{i=1}^K a(\theta_i) s_i(t). \quad (5)$$

Among them,

$$a(\theta_i) = \left[a_1(\theta_i) e^{-jw_0\tau_1(\theta_i)}, a_2(\theta_i) e^{-jw_0\tau_2(\theta_i)}, \dots, a_M(\theta_i) e^{-jw_0\tau_3(\theta_i)} \right]. \quad (6)$$

It is called the direction vector of the incoming wave direction 0.

Let $A(\theta) = [a(\theta_1), a(\theta_1), \dots, a(\theta_1)], s(t) = [s_1(t), s_1(t), \dots, s_1(t)]^T$. The other measurement noise is $n(t)$; then the above array model can be expressed as

$$x(t) = A(\theta)s(t) + n(t). \quad (7)$$

Among them, $x(t), n(t) \in C^K$, and $A(\theta) \in C^{M \times K}$ is the direction matrix of the array model.

2.1.2. Subspace Decomposition Based on Eigendecomposition of Array Covariance Matrix. The DOA estimation problem is the estimation of the direction of arrival angle and the parameter $\theta_i (i = 1, 2, \dots, K)$ in natural space, which requires the covariance information between the different elements of the array for analysis. For this, first calculate the spatial covariance matrix output by the array:

$$R = E[x(t)x^H(t)], \quad (8)$$

where $E\{\cdot\}$ represents statistical expectation; let

$$E[s(t)s^H(t)] = R_s, \quad (9)$$

$$E[n(t)n^H(t)] = \sigma^2 I. \quad (10)$$

It is the covariance matrix of noise. It is assumed that the noise received by all elements has a common variance, and σ^2 is also the noise power. From equations (9) and (10), we can get

$$R = AR_s A^H + \sigma^2 I. \quad (11)$$

It can be proved that R is a nonsingular matrix and a positive definite Hermitian square matrix; that is, $R^H = R$. Therefore, the singular value decomposition of R can be performed to achieve diagonalization, and the eigendecomposition can be written as follows:

$$R = U \Lambda U^H, \quad (12)$$

where U is the transformation unitary matrix, so that matrix R is diagonalized into a real-valued matrix $\Lambda = \text{diag}(\lambda_1, \lambda_2, \dots, \lambda_M)$, and the eigenvalues are ordered as follows:

$$\lambda_1 \geq \lambda_2 \geq \dots \geq \lambda_M > 0. \quad (13)$$

From equation (13), it can be seen that any vector orthogonal to A is an eigenvector of matrix R belonging to the eigenvalue σ^2 .

2.1.3. RBF Neural Network Estimates the Direction of Arrival.

RBF neural network is a method that can perform curve fitting or interpolation in high-dimensional space. If the relationship between the input space and the output space is regarded as a mapping, this mapping can be regarded as defined in the high-dimensional space. A hypersurface of the input data and a designed RBF neural network are equivalent to the height fitting of this hypersurface. It establishes an

approximate hypersurface by interpolating the input data points [10, 11].

The sensor array is equivalent to a mapping from the DOA space ($\{\theta = [\theta_1, \theta_2, \dots, \theta_K]\}$) to the sensor array output space ($\{s = [s_1, s_2, \dots, s_M]\}$), a mapping $G: R^K \rightarrow C^M$:

$$s_m = \sum_{k=1}^K a_k e^{j((m\omega_0 d \sin \theta_k/c) + a_k)}, \quad m = 1, 2, \dots, M, \quad (14)$$

where K is the number of source signals, M is the number of elements of the uniform linear array, a_k is the complex amplitude of the k -th signal, α is the initial phase, ω_0 is the signal center frequency, d is the element spacing, and c is the propagation speed of the source signal [12, 13].

When the number of information sources has been estimated as K , the function of the neural network on this problem is equivalent to the inverse problem of the above mapping, that is, the inverse mapping $F: C^M \rightarrow R^K$. To obtain this mapping, it is necessary to establish a neural network structure in which the preprocessed data based on the incident signal is used as the network input, and the corresponding DOA is used as the network output after the hidden layer activation function is applied. The whole process is a targeted training process, and the process of fitting the mapping with the RBF neural network is equivalent to an interpolation process.

2.2. Estimation of Direction of Arrival of Uniform Linear Array SOM Neural Network

2.2.1. Kohonen Self-Organizing Neural Network. A SOM neural network consists of two layers: the input layer and the competition layer (also called the output layer). The number of nodes in the input layer is equal to the dimension of the input vector, and the neurons in the competing layer are usually arranged in a rectangle or hexagon on a two-dimensional plane. The output node j and the input node are connected by weights:

$$w_j = [\omega_{j1}, \omega_{j2}, \dots, \omega_{jm}]^T. \quad (15)$$

The training steps of the Kohonen SOM neural network used in this article are as follows: the first step is network initialization [14, 15]. Normalize the input vector x to \hat{x} such that $\|(\hat{x})\| = 1$:

$$\hat{x} = \frac{x}{\|x\|} = \frac{x}{[\sum_{i=1}^m (x_i)^2]^{1/2}}, \quad (16)$$

where $x = [x_1, x_2, \dots, x_m]^T$ is the training sample vector of the network. Initialize the network weight $w_j (j = 1, 2, \dots, K)$ to be the same as the partially normalized input vector \hat{x} .

The second step is to calculate the Euclidean distance between the input vector \hat{x} and the corresponding weight vector w_j of each competing layer neuron to obtain the

winning neuron ω_c [16, 17]. The selection principle of the winning neuron is as follows:

$$\|\hat{x} - t\omega_c\| = \min_j \|\hat{x} - t\omega_j\|. \quad (17)$$

The third step is to adjust the weight of the winning neuron ω_c and its neighborhood ω_j . The adjustment method is as follows:

$$\omega_{ji}(t+1) = \omega_{ji}(t) + \eta(t)[\hat{x}_i - \omega_{ji}(t)], \quad j \in U_c(t). \quad (18)$$

Among them, $\eta(t)$ is the learning rate function, which decreases with the number of iteration steps t [18, 19]. The function $U_c(t)$ is the neighborhood function; here is the Gaussian function:

$$U_c(t) = \exp\left(\frac{\|r_j - r_c\|^2}{2\sigma^2}\right)\eta(t), \quad (19)$$

where r is the position of the neurons in the competition layer on a two-dimensional plane and σ is the smoothing factor, which is a normal number.

2.2.2. DOA Estimation Model Based on SOM Neural Network. Build a two-layer SOM neural network. The first layer of SOM neural network is the sorting layer, which maps the input training data into a two-dimensional space. According to the activation of neuron nodes on the first two-dimensional grid, the output of the corresponding neuron node in the second grid is defined by the following rules:

- (1) If the neuron node j is activated by only one training sample vector and the signal position corresponding to this sample is $(x_{k_i}, y_{k_i}) (i = 1, 2, \dots, n_j)$, then the output of the corresponding node of the second layer of grid is the direction angle of this signal [20, 21], namely,

$$\theta_j = \arctan \frac{y_i}{x_i - M(r/2)}. \quad (20)$$

- (2) If the neuron node j is activated by more than one training sample vector, that is, $n_j > 1$, and the signal positions corresponding to these samples are $(x_{k_i}, y_{k_i}) (i = 1, 2, \dots, n_j)$, then the output of the corresponding node of the second layer of grid is the average value of the direction angle of these signals [22, 23], namely,

$$\theta_j = \frac{1}{n_j} \sum_{i=1}^{n_j} \arctan \frac{y_{k_i}}{x_{k_i} - M(r/2)}. \quad (21)$$

- (3) If the neuron node j has never been activated by any training sample vector, the corresponding output neuron node is regarded as an invalid node. When this node is activated by a new input vector, the output value is defined as the output direction angle of the valid node closest to this node.

2.2.3. Method Reliability Analysis. The establishment process of the two-layer SOM neural network we proposed above shows that the topological order of AOA is similar to the topological distribution of DDOA vectors. In other words, when the Euclidean distance between two DDOA vectors is small, the Euclidean distance of the corresponding AOA value must also be small. This is the theoretical basis for our proposed method, and we will conduct a detailed analysis on this nature.

Suppose that the DDOA vectors of two adjacent source signals are d and $d_1 = d + \Delta d$, and the corresponding AOA values are θ and $\theta_1 = \theta + \Delta\theta$, respectively. The DDOA increment and AOA increment are

$$\begin{aligned} \Delta d &= [\Delta d_{0,1}, \Delta d_{1,2}, \dots, \Delta d_{M-1,M}]^T, \\ \Delta\theta &= \theta_1 - \theta, \end{aligned} \quad (22)$$

where $\Delta d_{i,j+1} = d_{i,j+1}^1 - d_{i,j+1}$; obviously the function $d_{i,j+1}$ at the point $(x, y) \in R^2$ is differentiable, which shows that the DDOA vector d and the AOA value θ have a consistent trend [24, 25]. In other words, when the DDOA vectors of two source signals are similar, their arrival direction angles AOA must also be similar. Therefore, the topological orders and distributions of DDOA vector and AOA are basically the same.

2.3. Genetic Clustering Method. In cluster analysis, the K-means clustering method is a clustering method that is often used. Generally, when determining the structure of the RBF network, this method is used to determine the number of hidden layer nodes of the network and the center of the node.

2.3.1. Chromosome Coding and Population Initialization. In order to accelerate the speed of convergence, we use real number coding [26]. For samples with m -dimensional dimensions, if the number of classes to be classified is n , the centers of n classes are encoded, and the dimensions of each center are m -dimensional; then the length of the chromosome is $n \times m$. In this way, a chromosome represents a complete classification strategy. Initialize the preset number of chromosomes to get the initial population.

2.3.2. Determination of Fitness Function and Selection of Fitness. For each chromosome, according to the classification information carried on it, according to the idea of distance classification, the classification of each sample in the original data can be determined, and the distance between the sample and its category center (here is Euclidean distance) can also be determined [27, 28]. After determining the classification of the sample, the sum of the distances within the class can be calculated:

$$F = \sum_{i=1}^k \sum_{j=1}^{n_i} \|x_j - C_i\|. \quad (23)$$

At the same time, the sum of the distances between classes can also be found:

$$Q = \frac{1}{2} \sum_{i=1}^k \sum_{j=1, j \neq i}^k \|C_i - C_j\|, \quad (24)$$

where F is the sum of distances within classes, Q is the sum of distances between classes, k is the number of classes in the classification, n_i is the number of samples belonging to the i -th class, x_j is the j -th sample of the i -th class, and C_i is the center of the i -th class.

3. Neural Network Optimization Method and Its Experimental Research in Information Processing

3.1. Underwater Experimental Research in the Lake. The underwater experiment is carried out in the lake. The average depth of the lake water is 50 meters to 60 meters. The area of open water is more than 300 meters * 1200 meters, and the water body is relatively stable and suitable for DOA estimation experiments. The experimental equipment used this time is a uniform linear array composed of 4 acoustic pressure hydrophones with an array spacing of 0.472 meters.

3.2. Experimental Methods and Data Collection

3.2.1. No Noise. In order to verify the effectiveness of the two-layer SOM neural network established in this paper for arbitrary array conditions, we conducted a simulation experiment of detecting the direction of acoustic signals with arbitrary sensor arrays underwater. Assuming that the sensor array contains 4 sensors, the frequency of a single sound source signal is $f = 2$ kHz, the propagation speed of the sound signal in water is $c = 1500$ m/s, and the distance between two adjacent sensors is $\Delta_i = 0.375$, which is the wavelength half. The positions of the four sensor array elements are $(x_1 = 0, y_1 = 0)$, $(x_2 = 0.3, y_2 = 0.225)$, $(x_3 = 0.5, y_3 = -0.0922)$, and $(x_4 = 0.6, y_4 = 0.2692)$. In order to obtain the training vector, we uniformly collect 60×30 points from the rectangular area $[-20, 20] \times [0, 20] \in R^2$ as the emission positions of 1800 simulated sound source signals, which can calculate 1800 DDOA vectors r , and input them into the network as training vectors of the network.

Calculate the value of $R_{\max}(x, y)$:

$$R_{\max}(x, y) = \max R(x, y, \Delta x, \Delta y), \quad (x, y) \in [-100, 100] \times [-100, 100]. \quad (25)$$

Except for the few points near the origin $(0, 0)$, the function $R_{\max}(x, y)$ at most of the remaining points has a common upper bound, which belongs to the second case.

3.2.2. Noise. In practice, the signal data collected by the sensor array is often noisy, and the energy of noise is generally large. The signal-to-noise ratio between signal and

noise often reaches very low values, even below 0 dB; that is, the signal is overwhelmed by environmental noise that is much stronger than its strength. When the signal-to-noise ratio is particularly small, people usually perform a denoising filtering process artificially in advance to make the filtered signal-to-noise ratio at least above 0 dB. Therefore, a good model that can be applied to practice must be applicable to noisy environments.

3.3. Performing Genetic Clustering on Standardized Training Sample Data. The number of preselected clustering categories is in the interval between 1/7 and 1/4 of the total number of samples (in order to facilitate the training of the network, too few or too many categories will result in poor training effects), take the population number as 30, the crossover rate is 75%, and the mutation rate is 5%. The fitness function is selected so that the ratio of the interclass distance to the intraclass distance increases with the increase of the fitness function, and a convergent solution can be obtained in about 50 generations. In the interval class, the number of classes is changed one by one until the fitness function is minimized. The number of categories at this time is the number of hidden nodes in the RBF network, and the center of each category is the center of the node.

4. Neural Network Optimization Method and Its Experimental Research Analysis in Information Processing

4.1. Noise-Free Simulation Experiment. To test the performance of the network, we select six sets of source signals with different distances from the origin, that is, six sets of points as the test. The distances to the origin of the coordinates are 8 meters, 16 meters, 20 meters, 30 meters, 50 meters, and 100 meters. Each group contains 21 simulated signals with different AOA values. Calculate the DDOA vectors corresponding to these simulated signal emission points, and then input these vectors as test vectors into the trained two-layer SOM neural network. The output of the network is the corresponding AOA predicted value. The experimental results are shown in Figure 1.

The absolute error value of the AOA prediction result is shown in Figure 1. It can be seen that not only can the SOM network trained with the near-field simulation signal (the signal position is within the area $[0, 21] \times [0, 21]$) perform the training in the near-field (4 m, 8 m, and 12 m) but also the AOA prediction effect of the test signal is good. Except for individual points, the AOA prediction accuracy of the test signal (16 m, 32 m, and 64 m) in the far field is also very high, and the error is basically controlled in the interval $[-0.4^0, 0.4^0]$, the error is smaller than the near field, the effect is better, and the error fluctuation is smaller.

To illustrate the effectiveness and scalability of this method in predicting AOA, we set up an RBF neural network for comparison. The RBF neural network established here uses the DDOA vector of the same simulation signal (within the area $[0, 20] \times [0, 20]$) as the input vector of the

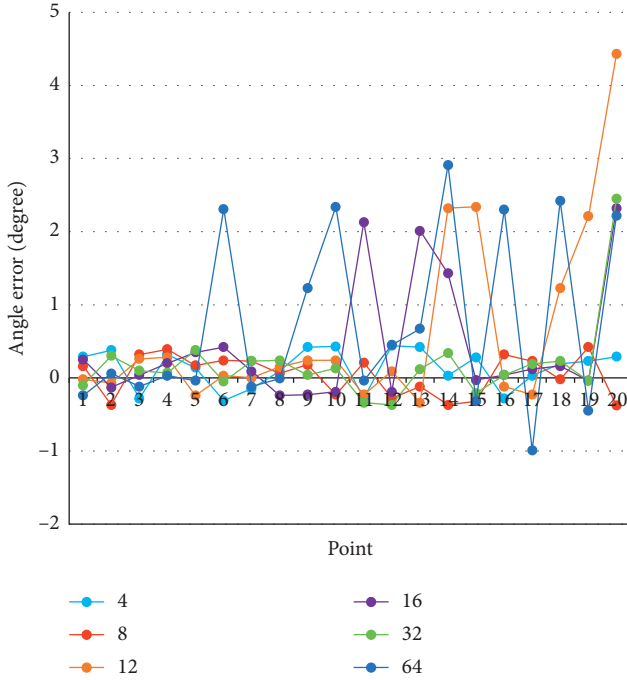


FIGURE 1: Absolute error of AOA predicted value of source signal at different distances using SOM neural network.

network training and the corresponding AOA value as the target output of the network training.

As shown in Table 1 and Figure 2, the average of the absolute value of the AOA prediction error of the noise-free signal in the simulation experiment is approximately 0.1° to 0.4° , the minimum is 0.122° , and the maximum is only 0.242° , and most of the test signals (accounting for the absolute value of the prediction error of the number of test signals (70%~80%)) are less than 0.1° .

To illustrate the effectiveness and scalability of this method in predicting AOA, we set up an RBF neural network for comparison. The RBF neural network established here uses the DDOA vector of the same simulation signal (within the area $[0, 20] [0, 20]$) as the input vector for network training, and the corresponding AOA value is used as the target output of the network training. Experimental results are shown in Table 2.

As shown in Figure 3, the two networks both use the same 20 simulated signals as test signals. The transmission positions of the tested signals are evenly distributed between 2 meters and 40 meters from the origin, including the training area, that is, within 20 meters. It can be seen from Figure 4 that the prediction effect of the RBF neural network in the training area is similar to that of the SOM neural network, but the prediction effect outside the training area is poor, while the SOM neural network shows strong adaptability to distance changes. This shows that the RBF neural network will be affected by the distance factor, because its training principle is to use the idea of interpolation to fit the mapping relationship, which makes the error larger when the test data exceeds the training range.

TABLE 1: SOM neural network prediction results of noise-free signal AOA.

Distance	4	8	12	16	32	64
Average error	0.215	0.124	0.147	0.105	0.109	0.152
Pr (err < 0.3°)	0.763	0.862	0.901	0.986	0.853	0.901
Pr (err < 0.2°)	0.782	0.816	0.792	0.827	0.879	0.815

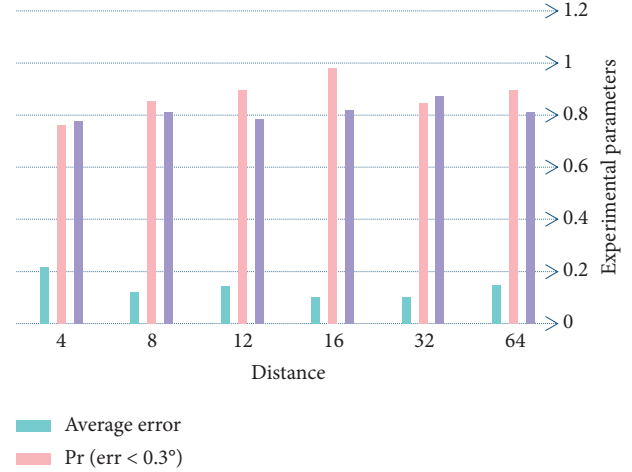


FIGURE 2: SOM neural network prediction results of noise-free signal AOA.

TABLE 2: Comparison of AOA errors predicted by SOM neural network and RBF neural network.

x	0	5	10	15	20	25	30	35	40
BRF	0.43	-0.05	0.08	-0.16	0.09	6.25	15.64	16.28	17.89
SOM	-0.08	0.04	-0.11	0.03	0.08	0.13	0.01	0.04	0.02

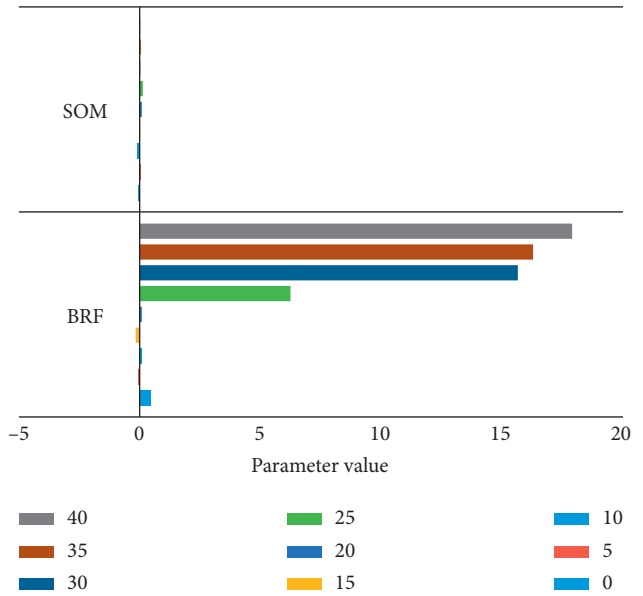


FIGURE 3: Comparison of AOA errors predicted by SOM neural network and RBF neural network.

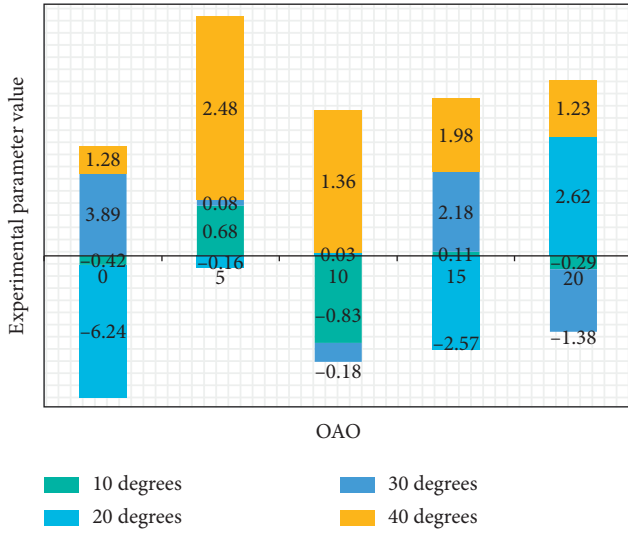


FIGURE 4: SOM neural network predicts AOA resulting in the case of additional Gaussian noise.

4.2. *Simulation Experiment with Gaussian Noise.* In practical applications, the signal received by the sensor array is often noisy. So here we use the signal containing Gaussian white noise to test the abovementioned SOM neural network, and the test results are shown in Table 3.

It can be seen from Figure 4 that when the signal-to-noise ratio drops from 20 dB to 1 dB, the absolute error of the AOA prediction is small and the fluctuations are not large; that is, when the signal-to-noise ratio is greater than 1 dB, we establish that the prediction effect of the SOM network does not decrease with the decrease of the signal-to-noise ratio, and it has strong adaptability to noise.

4.3. *Experimental Analysis of Underwater Experiment Results in the Lake.* During the experiment, the hydrophone array was placed at a depth of 3.7 meters below the surface of the water to be fixed. The sound source to be measured is produced by a transducer. Here, the transducer is placed at a depth consistent with the depth of the hydrophone, and the sound wave frequency is 2 KHz. The position and direction of the sound source are changed by changing the position of the transducer. When the transducer is at a certain position, the hydrophone array receives the signal, considering the speed of the sound signal in the water and the time difference of the signal after noise reduction, and we can get the DDOA vector. Input the DDOA vector into the pretrained SOM neural network to get the estimated value of AOA. The estimated results are shown in Table 4.

As shown in Figure 5, the results of the noise-free signal test show that this method is ideal for both near-field signals and far-field signals; the test results for signals containing Gaussian white noise reflect the high prediction accuracy of this method under low signal-to-noise ratios. Further, the applicability of this method in actual experiments can be seen from the results of lake water field experiments.

This paper uses the two-layer SOM neural network proposed earlier and inputs the DDOA vector consistent

TABLE 3: SOM neural network predicts AOA resulting in the case of additional Gaussian noise.

AOA (degrees)	0	5	10	15	20
10	-0.42	0.68	-0.83	0.11	-0.29
20	-6.24	-0.16	0.03	-2.57	2.62
30	3.89	0.08	-0.18	2.18	-1.38
40	1.28	2.48	1.36	1.98	1.23

TABLE 4: AOA prediction results of the experiment in the lake.

Actual AOA	Sound distance (m)	Forecast AOA	Absolute error
85	900	78.5	7.4
55	500	47.3	3.8
25	200	26.2	5.2

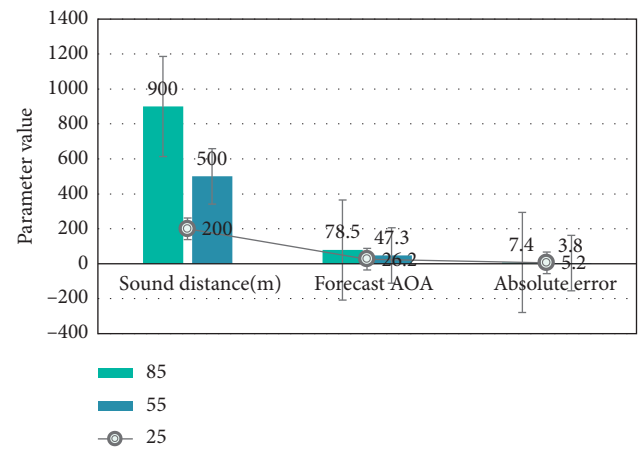


FIGURE 5: AOA prediction results of the experiment in the lake.

with the previous simulation experiment as training data into the network to train the network. Assuming that similar DDOA vectors also correspond to similar signal emission positions, the signal emission positions are also estimated according to the aforementioned three neuron activation situations and principles. The test signal emission points are selected as 20 points in the area where the simulation signal used for training the network is located, and they are evenly distributed along the curve. The test results are shown in Table 5.

The test result is shown in Figure 6, the actual position point number is consistent with the abscissa, and the corresponding network estimated position is marked with a number. It can be seen that, except for a few points, the estimated deviation is small, and the other deviations are still large. Therefore, the hypothesis is not true, and this two-layer SOM neural network is not suitable for the estimation of signal transmission position.

4.4. *Comparison and Analysis of Results.* The category center of K-means clustering method is generated based on a limited number of iterations, while the category center of genetic clustering is generated by global search. Therefore, in terms of the clustering effect and the robustness of the

TABLE 5: Using SOM neural network to predict signal position results.

X	0	5	10	15	20
Real	3.68	5.18	6.63	8.46	17.36
Estimation	4.95	6.32	7.13	10.47	15.36

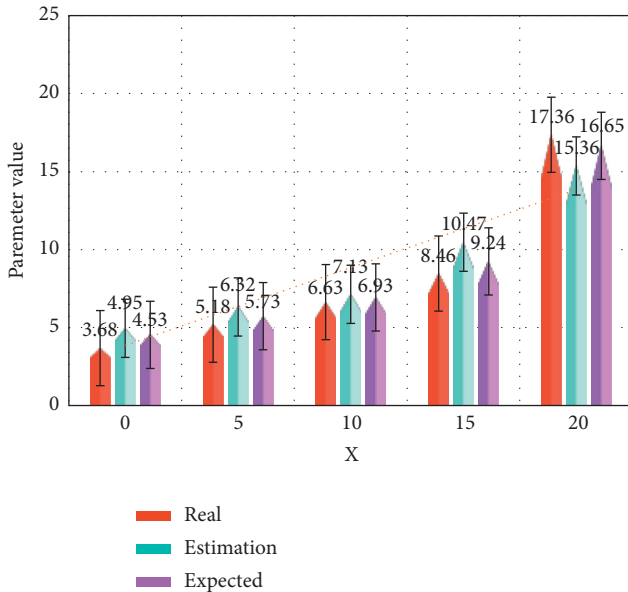


FIGURE 6: Using SOM neural network to predict signal position results.

category center, genetic clustering algorithm is better than k-means clustering method in these two points. Table 6 lists the ratio of the sum of the interclass distances to the sum of intraclass distances obtained by using these two methods, respectively, that is, the fitness function.

It can be seen from Figure 7 that, compared to the K-means clustering method, the genetic clustering method has obvious advantages in the “cohesion effect” of the cluster center. Especially for RBF networks, the “cohesion effect” of the center often has a greater impact on the performance of the network, so although from the perspective of purely physical or chemical clustering analysis, genetic clustering is not necessarily superior to K-means method, in terms of the effect of RBF network learning, genetic clustering has greater advantages compared to K-means clustering.

4.5. Influence of the Number of Neuron Nodes on the Prediction Effect. In order to study the influence of the number of neuron nodes in the network on the prediction effect, simulation experiments were carried out on 6 different neuron node distribution modes. The absolute value of the absolute error of the experimental results is then averaged, as shown in Table 7.

As shown in Figure 8, it can be seen that the network prediction effect using the signal on the circle as the training

TABLE 6: Comparison of genetic clustering and K-means clustering methods.

Number of categories	Fitness	
	K-means clustering method	Genetic clustering method
4	3.26	4.61
5	3.52	4.78
6	3.78	4.98
7	3.62	5.18
8	3.29	4.72

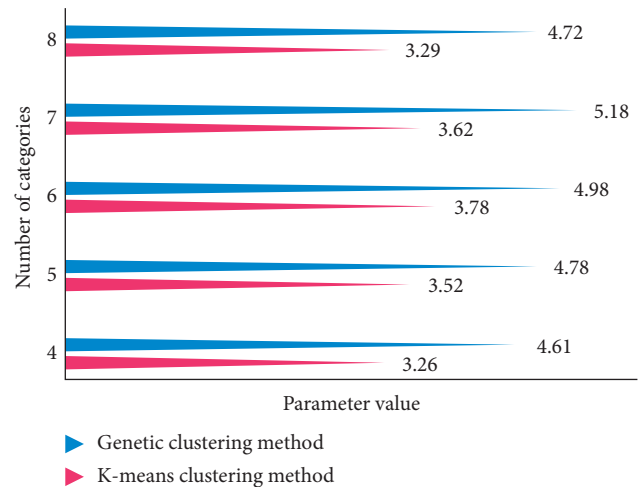


FIGURE 7: Comparison of genetic clustering and K-means clustering methods.

TABLE 7: Average absolute value of AOA prediction error under different neuron node arrangements.

Node arrangement	20 × 20	25 × 25	30 × 30	35 × 35	40 × 40	45 × 45
Rectangular domain	0.72	0.61	0.57	0.48	0.55	0.62
Circle	0.51	0.56	0.42	0.37	0.33	0.41

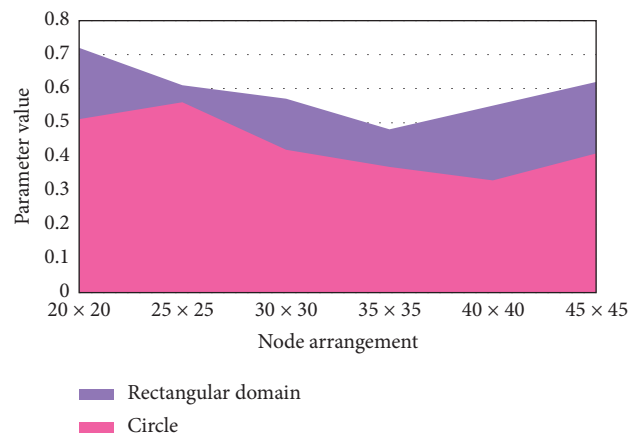


FIGURE 8: Average absolute value of AOA prediction error under different neuron node arrangements.

data is better than that of the signal training network in the rectangular area. The prediction accuracy of the network with a neuron node distribution of 40×40 is relatively better than that of other node distributions. This distribution is an $n \times n$ square matrix arrangement, which is slightly smaller in number than the number of training samples. It can also be seen that the prediction effect of the network is not better as the number of neuron nodes increases.

5. Conclusions

In this paper, a two-layer SOM neural network is used to study the AOA prediction problem based on DDOA vectors under arbitrary arrays in theory and simulation experiments. This network is equivalent to a classifier, through the classification of DDOA vectors to achieve the classification of AOA values, so as to achieve the purpose of predicting AOA. The established two-layer SOM neural network is further discussed, and the feasible situation of applying the network for prediction is given. First, clarify the features used for prediction and form the input vector, and the predicted object is used as the output of the network.

This method is verified through simulation experiments and actual lake experiments. From the experimental results, it can be seen that the neural network trained in advance through simulation data can detect the direction of arrival of the source signal without noise, Gaussian white noise, and real noise environment, and the angle estimation effect is good. Finally, we further compare the prediction effect of this method with the classic MUSIC algorithm and RBF neural network method. The experimental results show that the performance of this network is excellent and can be considered for practice.

This paper applies SOM neural network to the estimation of the direction of arrival of array signals. It is found through research that the DDOA vector and AOA in the array signal have similar topological distributions. Based on this, the SOM neural network is connected with the topological order to establish a two-layer SOM neural network to estimate the direction of arrival of the array signal. While the method has a theoretical basis, it also shows high estimation accuracy in both simulation experiments and lake water experiments.

Data Availability

The data that support the findings of this study are available from the corresponding author upon reasonable request.

Conflicts of Interest

The authors declare that they have no conflicts of interest regarding the publication of the research article.

Acknowledgments

This work was supported by the National Natural Science Foundation of China under Grant 61703280.


References

- [1] X. Li, Y. Wang, and G. Liu, "Structured medical pathology data hiding information mining algorithm based on optimized convolutional neural network," *IEEE access*, vol. 8, no. 1, pp. 1443–1452, 2020.
- [2] M. A. A. Mamun, M. A. Hannan, A. Hussain, and H. Basri, "Theoretical model and implementation of a real time intelligent bin status monitoring system using rule based decision algorithms," *Expert Systems with Applications*, vol. 48, pp. 76–88, 2016.
- [3] M. F. Hamza, H. J. Yap, and I. A. Choudhury, "Recent advances on the use of meta-heuristic optimization algorithms to optimize the type-2 fuzzy logic systems in intelligent control," *Neural Computing and Applications*, vol. 28, no. 5, pp. 1–21, 2015.
- [4] B. Tom and S. Alexei, "Conditional random fields for pattern recognition applied to structured data," *Algorithms*, vol. 8, no. 3, pp. 466–483, 2015.
- [5] Y. Chen, W. Zheng, W. Li, and Y. Huang, "The robustness and sustainability of port logistics systems for emergency supplies from overseas," *Journal of Advanced Transportation*, vol. 2020, Article ID 8868533, 10 pages, 2020.
- [6] W. Quan, "Intelligent information processing," *Computing in Science & Engineering*, vol. 21, no. 6, pp. 4–5, 2019.
- [7] X. Q. Cheng, X. W. Liu, J. H. Li et al., "Data optimization of traffic video vehicle detector based on cloud platform," *Jiaotong Yunshu Xitong Gongcheng Yu Xinxin/Journal of Transportation Systems Engineering and Information Technology*, vol. 15, no. 2, pp. 76–80, 2015.
- [8] S. Wei, Z. Xiaorui, P. Srinivas et al., "A self-adaptive dynamic recognition model for fatigue driving based on multi-source information and two levels of fusion," *Sensors*, vol. 15, no. 9, pp. 24191–24213, 2015.
- [9] M. Niu, S. Sun, J. Wu, and Y. Zhang, "Short-term wind speed hybrid forecasting model based on bias correcting study and its application," *Mathematical Problems in Engineering*, vol. 2015, no. 10, 13 pages, 2015.
- [10] X. Song, X. Li, and W. Zhang, "Key parameters estimation and adaptive warning strategy for rear-end collision of vehicle," *Mathematical Problems in Engineering*, vol. 2015, no. 20, 20 pages, Article ID 328029, 2015.
- [11] M. El-Banna, "A novel approach for classifying imbalance welding data: mahalanobis genetic algorithm (MGA)," *International Journal of Advanced Manufacturing Technology*, vol. 77, no. 1–4, pp. 407–425, 2015.
- [12] J. P. Amezcua-Sanchez and H. Adeli, "Signal processing techniques for vibration-based health monitoring of smart structures," *Archives of Computational Methods in Engineering*, vol. 23, no. 1, pp. 1–15, 2016.
- [13] C. Li, X. An, and R. Li, "A chaos embedded GSA-SVM hybrid system for classification," *Neural Computing and Applications*, vol. 26, no. 3, pp. 713–721, 2014.
- [14] A. Abboud, F. Iutzeler, R. Couillet, M. Debbah, and H. Siguerdidjane, "Distributed production-sharing optimization and application to power grid networks," *IEEE Transactions on Signal and Information Processing Over Networks*, vol. 2, no. 1, pp. 16–28, 2016.
- [15] X. Xu, D. Cao, Y. Zhou et al., "Application of neural network algorithm in fault diagnosis of mechanical intelligence," *Mechanical Systems and Signal Processing*, vol. 141, no. Jul, pp. 106625.1–106625.13, 2020.

- [16] H. Xiao, B. Biggio, B. Nelson, H. Xiao, C. Eckert, and F. Roli, "Support vector machines under adversarial label contamination," *Neurocomputing*, vol. 160, no. jul.21, pp. 53–62, 2015.
- [17] G. Kan, C. Yao, Q. Li et al., "Improving event-based rainfall-runoff simulation using an ensemble artificial neural network based hybrid data-driven model," *Stochastic Environmental Research & Risk Assessment*, vol. 29, no. 5, pp. 1345–1370, 2015.
- [18] S. Cuomo, G. De Pietro, R. Farina, A. Galletti, and G. Sannino, "A novel O (n) numerical scheme for ECG signal denoising," *Procedia Computer Science*, vol. 51, no. 1, pp. 775–784, 2015.
- [19] H. Guo, G. Dai, J. Fan, Y. Wu, F. Shen, and Y. Hu, "A mobile sensing system for UrbanPM2.5Monitoring with adaptive resolution," *Journal of Sensors*, vol. 2016, no. 9, 15 pages, Article ID 7901245, 2016.
- [20] Q. Liu, J. Liu, R. Sang et al., "Fast neural network training on FPGA using quasi-Newton optimization method," *IEEE Transactions on Very Large Scale Integration (VLSI) Systems*, vol. 26, no. 99, pp. 1575–1579, 2018.
- [21] R. M. S. F. Almeida and V. P. De Freitas, "An insulation thickness optimization methodology for school buildings rehabilitation combining artificial neural networks and life cycle cost," *Journal of Civil Engineering and Management*, vol. 22, no. 7, pp. 915–923, 2016.
- [22] A. S. Soma, T. Kubota, and H. Mizuno, "Optimization of causative factors using logistic regression and artificial neural network models for landslide susceptibility assessment in Ujung Loe Watershed, South Sulawesi Indonesia," *Journal of Mountain Science*, vol. 16, no. 2, pp. 383–401, 2019.
- [23] S. C. Miao, J. H. Yang, X. H. Wang et al., "Blade pattern optimization of the hydraulic turbine based onneural network and genetic algorithm," *Hangkong Dongli Xuebao/Journal of Aerospace Power*, vol. 30, no. 8, pp. 1918–1925, 2015.
- [24] Z. Junsheng, Y. Gu, and Z. Feng, "Optimization of processing parameters of power spinning for bushing based on neural network and genetic algorithms," *Journal of Bjing Institute of Technology*, vol. 28, no. 3, pp. 228–238, 2019.
- [25] N. Melzi, L. Khaouane, S. Hanini, M. Laidi, Y. Ammi, and H. Zentou, "Optimization methodology of artificial neural network models for predicting molecular diffusion coefficients for polar and non-polar binary gases," *Journal of Applied Mechanics and Technical Physics*, vol. 61, no. 2, pp. 207–216, 2020.
- [26] N. Chen, B. Rong, X. Zhang, and M. Kadoch, "Scalable and flexible massive MIMO precoding for 5G H-cran," *IEEE Wireless Communications*, vol. 24, no. 1, pp. 46–52, 2017.
- [27] R. Noorossana, A. Zadbood, F. Zandi et al., "An interactive artificial neural networks approach to multiresponse optimization," *International Journal of Advanced Manufacturing Technology*, vol. 76, no. 5–8, pp. 765–777, 2015.
- [28] D. Sánchez, P. Melin, and O. Castillo, "Optimization of modular granular neural networks using a firefly algorithm for human recognition," *Engineering Applications of Artificial Intelligence*, vol. 64, no. sep, pp. 172–186, 2017.

Research Article

Offline and Online Channel Selection of Low-Carbon Supply Chain under Carbon Trading Market

Qiang Han ¹, Zhenlong Yang,¹ Zheng Zhang,¹ and Liang Shen²

¹School of Management Science and Engineering, Shandong University of Finance and Economics, Jinan 250014, China

²School of Public Finance and Taxation, Shandong University of Finance and Economics, Jinan 250014, China

Correspondence should be addressed to Qiang Han; qiang.han@sdufe.edu.cn

Received 18 November 2020; Revised 10 December 2020; Accepted 15 December 2020; Published 5 January 2021

Academic Editor: Ming Bao Cheng

Copyright © 2021 Qiang Han et al. This is an open access article distributed under the Creative Commons Attribution License, which permits unrestricted use, distribution, and reproduction in any medium, provided the original work is properly cited.

This paper investigates the low-carbon product manufacturer's different decision behavior in the offline traditional retail channel and online e-commerce channel when the carbon trading market has been established. The low-carbon product manufacturer is both in the carbon trading market and product market. In the former market, the manufacturer can gain profits by selling its emission quota. In the latter market, the manufacturer has two sales channel options, the traditional offline retailer and the online e-commerce platform. These two channels make two supply chains, the manufacturer-led offline one and the e-commerce platform-led online one. This paper combines the carbon trading market with the product market, formulates different Stackelberg game models, compares the manufacturer's decision under two channels and the impact of channels on the carbon emission, does sensitivity analysis, and verifies the conclusions with numerical examples. Our findings are (1) the establishment of the carbon market will help the manufacturer reduce its carbon emission, especially for those sensitive to the carbon price and those with too much emissions; (2) whether the manufacturer turns to the online channel depends on the consumers' sensitivity to the sales service, and consumers' attention will guide the way to the online mode; (3) which mode is conducive to carbon emission reduction relies on the product type: the e-commerce platform does well for daily necessities of mass production while the traditional channel is better for experience goods.

1. Introduction

Traditionally, the manufacturer used to sell products through the offline retail channel. Up to this day, with the rapid development of information and Internet technology, the birth of Amazon, Jingdong, and other e-commerce platforms opens up a more convenient option [1], which is transforming the consumers' shopping style with rapid momentum. In contrast with the traditional offline mode, the online one features convenient access to the product distinctively and the low cost to promote it. The manufacturer has to pay the sales revenue proportionally to the e-commerce platform when selling through it. The income ratio for the platform in the whole sales revenue is called the commission rate.

While the manufacturer provides consumers with various products, it also does with carbon emission, which will

lead to an unpredictable influence on the globe. Data from NASA showed that the carbon dioxide level had reached the highest in the past 650,000 years (<https://climate.nasa.gov/>). So, consumers, with their increase in low-carbon awareness, are preferring low-carbon products. A poll from Accenture said that 72% of the respondents are willing to purchase low-carbon products and pay a higher price (<https://www.businessnewsdaily.com/15087-consumers-want-sustainable-products.html>). As a result, the manufacturer will invest more to carry out carbon emission reduction transformation and produce many low-carbon products. Thus, the manufacturer producing low-carbon products along with its upstream and downstream enterprises forms low-carbon supply chains [2].

To address the carbon emission problem, governments have tried many measures to promote low-carbon products. The EU initiated the carbon trading mechanism

(<https://www.thebalance.com/carbon-emissions-trading-3305652>), which gets accepted widely because of its marketization property and has been applied in China [3], Australia [4], New Zealand [5], and Europe [6]. The concept of carbon trading was originated from the UN Framework Convention on Climate Change and the Kyoto Protocol. The latter regards market mechanism as a new way to solve the problem of greenhouse gas emission reduction; that is, carbon emission right is regarded as one common commodity, and manufacturers are encouraged to save carbon emission quota through technological progress, which can be exchanged with other manufacturers. Carbon trading can internalize their original external cost, thus forming a forced mechanism to promote manufacturers to carry out emission reduction innovation.

The current research studies on carbon trading mostly focus on the traditional offline channel [7, 8]. However, the e-commerce of the online channel is a more and more potential option for manufacturers to sell their products. Since manufacturers' ultimate goal is profit, they will weigh whether they can profit from the carbon trading market and which channel is more beneficial between the offline and online mode. We aim to answer the following questions:

- (1) Under what conditions can manufacturers be profitable in the carbon trading market?
- (2) Under what conditions can manufacturers turn to the online mode?
- (3) What effects of the offline mode and online mode have on manufacturers' carbon emission?

Our study contributes to the related research by analyzing the supply chain decision after putting the manufacturer into both the carbon trading market and the low-carbon product market and applying the carbon trading into the online e-commerce supply chain mode. We formulate two Stackelberg game models to describe the low-carbon product manufacturer's decision behavior and compare the effect of different factors on its channel selection and carbon emission reduction. Results show that the carbon trading mechanism provides the manufacturer with a flexible carbon emission decision option and can guide it to reduce emissions consciously and effectively. However, the manufacturer's condition to gain profits is that the carbon market scale is located in a specific interval. From the view of channel selection, the commission rate plays an important role. It is concluded by combining the carbon trading and channel selection that which mode is conducive to the emission reduction depends on the product property sold by the manufacturer.

The rest of this paper is organized as follows. In Section 2, we review the related literature. In Section 3, we elaborate on the problem and give the necessary mathematical expression. Then, after low-carbon supply chain decision models are built in Section 4, we compare the results of different models and do managerial insights and sensitivity analysis in Section 5. In Section 6, we do numerical examples. And lastly, conclusions are made in Section 7.

2. Literature Review

Our research is closely related to two streams: carbon trading and supply chain channel selection.

2.1. Carbon Trading. Carbon trading is human beings' active strategy to deal with global climate change. Simulation results of Cheng et al. [9] showed the success of the carbon trading system to achieve emission reduction goal. The region starting the carbon trading system has reduced more carbon emission distinctively, which can also maintain sustainable economic development at the same time [10]. This was achieved by improving technology efficiency and transforming industry structure [3, 11, 12].

However, Liu et al. [13] and Jiang et al. [14] thought there are still some challenges for the carbon trading market, for example, incomplete mechanism, inaccurate quota allocation, and the absence of real-time carbon price. Caparrós et al. [15] found that the emission trading system, though designed in its original intention to encourage manufacturers to reduce carbon emission by new technology, might result in manufacturers' production reduction. Jaraite and Di Maria [6] concluded based on Lithuanian data that EU's emission trading system did not help reduce emission at all.

Later, carbon emission in the supply chain was taken into research. Cheng et al. [16], after building the supply chain cooperative decision model combining carbon trading and carbon tax, showed that highly intense carbon policy does not mean manufacturers' emission reduction and low-carbon production increase. Chen et al. [17] investigated how to regulate carbon trading in the case of uncertainty with stochastic programming. Benjaafar et al. [7] integrated carbon emission concern into the operation decision about procurement, production, and inventory management and studied the effect of the cooperation between multiple companies on emission reduction. Pang et al. [18] studied the influence of carbon price and consumers' environmental protection awareness on carbon emission in the supply chain and found clean manufacturers' unit carbon emission increased with the carbon trading price while other manufacturers stood opposite. Wang and Wu [19] considered the carbon trading behavior in the closed-loop supply chain and revealed that product recycle helped reduce carbon emission but high initial carbon emission did not. Xu et al. [20] studied decision and coordination in the dual-channel supply chain under cap-and-trade, suggesting that governments should achieve coordinated development of economy and environment by starting carbon trading. Xu et al. [8] explored the emission reduction decision in the make-to-order supply chain and concluded that manufacturers could adopt green technology to reduce unit carbon emission and the optimal production would not be affected by the increase in carbon price.

2.2. Supply Chain Channel Selection. Product sales can be divided into single channel, multichannel, and omnichannel [21]. However, dual-channel, one mode among multichannels, is mostly focused. Dual-channel means the

addition of direct sales or other channel besides the traditional retail, in which consumers determine their purchase channel based on the product price and service level [22–24]. After considering the supply chain with the traditional retail channel and direct online channel, in which the manufacturer provides customized product online while provides standard products offline, Batarfi et al. [25] found that the customized product sales through the extra online channel could increase its profit but also bring conflict. Yoo and Lee [26] discovered that the online channel did not bring much lower price and much higher consumers' welfare necessarily. Bernstein et al. [27] also found that new channel did not mean better returns when analyzing the feasibility for the retailers in the transition from offline sales to mixed modes.

There are two special ones, BOPS (buy online and pick up in store) and O2O (online to offline) in the dual-channel mode. Gao and Su [28] argued not all goods suit the BOPS mode, even for regular customers, but it can attract much more new customers. Gallino and Moreno [29] found that the BOPS mode would lead to the decrease in online sales and the increase in store sales. Chen et al. [30] analyzed the pricing strategy of the offline mode and online mode in the mixed dual-channel and the influence of supply chain power structure on pricing.

In different modes, it is vital whether consumers accept them. Jia [31] investigated two e-commerce modes, self-owned platform and others-owned platform, and came to a conclusion that the channel service level and the sensitivity of consumers to channel service would influence the supply chain decision. Li et al. [32] compared the relation between direct online sales and brand stores and revealed that if the brand store was established first, the manufacturer might introduce the direct online mode; otherwise, it might not. Zhang et al. [33] showed that the optimal channel is pure offline mode, dual-channel mode, and pure online mode, respectively, corresponding to consumers' acceptance degree of the online mode, low, medium, and high. Lu and Niu [34] found that the channel acceptance played an important role in affecting equilibrium price when then the traditional retail channel and e-commerce channel were compared.

Based on the above literature review, most research about carbon trading focuses on the offline supply chain channel, while the e-commerce is rarely touched. However, the online sale has been trending. So, we should extend the carbon trading from the offline mode to online one. From the view of channel selection, the offline mode, together with the online mode, will result in the free rider problem with high probability, which will decrease the supply chain profit [35]. And, multiple channels are easy to cause channel conflict [36]. In the supply chain under the carbon trading market, the manufacturer, as the primary source of carbon emission, will take into account the revenue from carbon emission and product sales together. Thus, this paper investigates the channel selection problem between the offline and online modes from the manufacturer's perspective and analyzes which channel is conducive to carbon emission reduction under the carbon trading background.

3. Problem Description and Basic Relations

3.1. Problem Description. Suppose there is a low-carbon product manufacturer located in the region where has started a carbon trading system. So, the manufacturer is contained in the carbon trading market and product market.

The manufacturer brings carbon emissions during production. Then, it will make process improvements to reduce emissions. Afterward, the manufacturer can attract consumers preferring low-carbon products and sell its carbon emission quota to gain profit in the carbon trading market.

The manufacturer can sell its product through the traditional offline retail channel or online e-commerce platform channel. What is different from the offline mode is that the manufacturer has to pay some proportional sales revenue to the platform as the feedback for providing the sales channel in the online mode [37]. The ratio of the income for the platform in the whole sales revenue is called commission rate.

Therefore, we will investigate two supply chains, the supply chain consisting of one low-carbon manufacturer and one retailer and that consisting of one low-carbon manufacturer and one e-commerce platform (abbreviated as the platform if no ambiguity exists). In different channels, the manufacturer has contrasting status [38]: it is the leader in the product-oriented offline mode while it is the follower in the channel-oriented online one [39]. The manufacturer's profit comes from carbon trading and product sales.

3.2. Mathematical Notations and Relations of the Supply Chain. In this subsection, we provide mathematical notations and relations corresponding to the supply chain member. Some notations are listed in Table 1, which will be used frequently in this paper.

(i) Manufacturer

The manufacturer sells its product at the unit price of P to consumers in the e-commerce platform and wholesale price of P_w in the offline mode to the retailer.

It is obvious that $E < \hat{E}$. According to Nair and Narasimhan's research [40], the manufacturer's cost for process improvements is functioned as

$$C_m(E) = \alpha(\hat{E} - E)^2. \quad (1)$$

(ii) E-commerce platform

According to Wu's research [41], the platform's cost to serve consumers can be formulated as

$$C_p(L_p) = \beta L_p^2. \quad (2)$$

(iii) Retailer

To gain much revenue, the retailer will try its best to sell products. Then, its sales cost can be expressed as [41]

TABLE 1: Mathematical notations.

Notations	Meaning
C	The manufacturer's unit production cost
P_w	Unit offline wholesale price
P	Unit online retail price
P_r	Unit offline retail price
P_c	Carbon price in the carbon trading market
\bar{E}	The manufacturer's carbon emission before process improvements
E	The manufacturer's carbon emission after process improvements
α ($\alpha > 0$)	Elastic coefficient of carbon emission reduction cost
β ($\beta > 0$)	Elastic coefficient of service cost
γ ($\gamma > 0$)	Promotion effort level coefficient
θ ($0 < \theta < 1$)	Commission rate
L_p	The platform's sales service level
L_r	The retailer's promotion effort level
Q	Product market scale, a large enough positive number
d_1	Sensitivity coefficient to the product price
d_2	Sensitivity coefficient to the product service
Φ	Carbon market scale
φ	Sensitivity coefficient to the carbon price

$$C_r(L_r) = \gamma L_r^2. \quad (3)$$

As well known, more cost has to be invested in the offline service than the online one because of the channel difference in the amount of target audience and the convenience of promotion. Therefore, we suppose $\gamma > \beta$.

3.3. *Demand Functions for Different Markets.* Demand functions of different markets are given as follows:

(i) Offline channel product market

In the offline mode, the product demand is dominated by the product price and retailer's service. The demand function of the product can be formulated as [37, 39]

$$q_1(P_r, L_r) = Q - d_1 P_r + d_2 L_r. \quad (4)$$

To let the following gaming process hold, we suppose $4d_1\gamma > d_2^2$, $4d_1\beta > d_2^2$.

(ii) Online channel product market

In the online mode, the product demand is dominated by the product price and platform's service. The demand function can be expressed as [37, 39]

$$q_2(P, L_p) = Q - d_1 P + d_2 L_p. \quad (5)$$

(iii) Carbon trading market

The carbon emission reduction can increase the low-carbon product sales after consumers' environmental awareness rises and helps the manufacturer profit from the carbon trading market. As

the trading is concerned, carbon emission quota can be treated as common products. Similar to the inverse demand function of common products that of P_c with the carbon emission can be functioned as [7]

$$P_c(E) = \Phi - \varphi E, \quad (6)$$

where φ is used to measure the influence of emissions on the carbon price. Positive P_c means that the manufacturer can gain profit because of its low-carbon emission, while negative P_c indicates that the manufacturer has to pay cost for its high emission. Obviously, we have $\Phi - \varphi \bar{E} < 0$. Otherwise, manufacturers with too much emissions cannot be punished so that they do not have initiative to reduce them, which is contrary to the original intention of opening the carbon trading market.

Also, let e_c denote the carbon emission per unit product. Then,

$$e_c = \frac{E}{q}, \quad (7)$$

where q is the product demand. The smaller e_c is, the better the low-carbon level of the product is.

4. Supply Chain Decision Models under Carbon Trading Market

In this section, we formulate two supply chain game models corresponding to the manufacturer's sales channels.

4.1. *Model I: Offline Channel.* In the traditional offline supply chain channel, the product demand function is

$$q_1(P_r, L_r) = Q - d_1P_r + d_2L_r. \quad (8)$$

The manufacturer's profit from product market is

$$\begin{aligned} I_{m1p}(P_w, P_r, L_r) &= (P_w - C)q_1 \\ &= (P_w - C)(Q - d_1P_r + d_2L_r). \end{aligned} \quad (9)$$

The manufacturer's profit from carbon trading market is

$$I_{m1c}(E) = P_cE - C_m(E). \quad (10)$$

Thus, the manufacturer's total profit is

$$\begin{aligned} \Pi_{m1}(P_w, P_r, L_r, E) &= I_{m1p} + I_{m1c} \\ &= (P_w - C)(Q - d_1P_r + d_2L_r) \\ &\quad + (\Phi - \varphi E)E - \alpha(\hat{E} - tE)^2. \end{aligned} \quad (11)$$

The retailer's profit is

$$\begin{aligned} \Pi_{r1}(P_w, P_r, L_r) &= (P_r - P_w)q_1 - C_r(L_r) \\ &= (P_r - P_w)(Q - d_1P_r + d_2L_r) - \gamma L_r^2, \end{aligned} \quad (12)$$

and the supply chain's profit is

$$\begin{aligned} \Pi_1(P_r, L_r, E) &= \Pi_{m1}(P_w, P_r, L_r, E) + \Pi_{r1}(P_w, P_r, L_r) \\ &= (P_r - C)(Q - d_1P_r + d_2L_r) \\ &\quad + (\Phi - \varphi E)E - \alpha(\hat{E} - tE)^2 - \gamma L_r^2. \end{aligned} \quad (13)$$

During the gaming process, the manufacturer and the retailer form a Stackelberg game, with the former as the leader and the latter as the follower. The manufacturer determines its wholesale price P_w and carbon emission level E ; then, the retailer determines its retail price P_r and service level L_r . Their gaming problem can be formulated as

$$\begin{aligned} \max_{P_w, E} \quad & \Pi_{m1}(P_w, P_r, L_r, E) = (P_w - C)(Q - d_1P_r + d_2L_r) \\ & + (\Phi - \varphi E)E - \alpha(\hat{E} - tE)^2 \\ \text{s.t.} \quad & \max_{P_r, L_r} \Pi_{r1}(P_w, P_r, L_r) = (P_r - P_w)(Q - d_1P_r + d_2L_r) \\ & - \gamma L_r^2. \end{aligned} \quad (14)$$

Thus, the optimal decision of this model is obtained as in Conclusion 1.

Conclusion 1. When the manufacturer sells its low-carbon product through the offline channel, the optimal decision is

$$\begin{aligned} P_w^* &= \frac{C}{2} + \frac{Q}{2d_1}, \\ E_1^* &= \frac{2\hat{E}\alpha + \Phi}{2(\alpha + \varphi)}, \\ P_r^* &= \frac{C}{2} + \frac{Q}{2d_1} + \frac{(Q - Cd_1)\gamma}{4d_1\gamma - d_2^2}, \\ L_r^* &= \frac{d_2(Q - Cd_1)}{8d_1\gamma - 2d_2^2}, \\ \Pi_{m1}^* &= \frac{(Q - Cd_1)^2\gamma}{2(4d_1\gamma - d_2^2)} + \frac{\Phi^2 + 4\alpha\hat{E}(\Phi - \varphi\hat{E})}{4(\alpha + \varphi)}, \\ \Pi_{r1}^* &= \frac{(Q - Cd_1)^2\gamma}{4(4d_1\gamma - d_2^2)}, \\ \Pi_1 &= \frac{3(Q - Cd_1)^2\gamma}{4(4d_1\gamma - d_2^2)} + \frac{\Phi^2 + 4\alpha\hat{E}(\Phi - \varphi\hat{E})}{4(\alpha + \varphi)}, \\ q_1 &= (Q - Cd_1)d_1\gamma. \end{aligned} \quad (15)$$

See Appendix A for the proof of Conclusion 1.

4.2. *Model II: Online Channel.* In the online e-commerce supply chain channel, the product demand function is

$$q_2(P, L_p) = Q - d_1P + d_2L_p. \quad (16)$$

The manufacturer's profit from the product market is

$$\begin{aligned} I_{m2p}(P, L_p) &= (P - \theta P - C)q_2 \\ &= (P - \theta P - C)(Q - d_1P + d_2L_p), \quad 0 < \theta < 1. \end{aligned} \quad (17)$$

The manufacturer's profit from the carbon trading market is

$$I_{m2c}(E) = P_c E - C_m(E). \quad (18)$$

Thus, the manufacturer's total profit is

$$\begin{aligned} \Pi_{m2}(P, L_p, E) &= I_{m2p} + I_{m2c} \\ &= (P - \theta P - C)(Q - d_1P + d_2L_p) \\ &\quad + (\Phi - \varphi E)E - \alpha(\widehat{E} - tE)^2. \end{aligned} \quad (19)$$

The e-commerce platform's profit is

$$\Pi_{p2}(P, L_p) = \theta Pq - C_p(L_p) = \theta P(Q - d_1P + d_2L_p) - \beta L_p^2, \quad (20)$$

and the supply chain's profit is

$$\begin{aligned} \Pi_2(P, L_p, E) &= \Pi_{m2}(P, L_p, E) + \Pi_{p2}(P, L_p) \\ &= (P - C)(Q - d_1P + d_2L_p) \\ &\quad + (\Phi - \varphi E)E - \alpha(\widehat{E} - tE)^2 - \beta L_p^2. \end{aligned} \quad (21)$$

Their decision process forms a Stackelberg game, with the platform as the leader and the manufacturer as the follower, in which the platform gives its service level L first and then the manufacturer decides its sale price P and carbon emission level E . Their gaming problem can be formulated as

$$\begin{aligned} \max_{P, E} \quad & \Pi_{m2}(P, L_p, E) = (P - \theta P - C)(Q - d_1P + d_2L_p) \\ & + (\Phi - \varphi E)E - \alpha(\widehat{E} - tE)^2 \\ \text{s.t.} \quad & \max_{L_p} \Pi_{p2}(P, L_p) = \theta Pq - C_p(L_p) \\ & = \theta P(Q - d_1P + d_2L_p) - \beta L_p^2. \end{aligned} \quad (22)$$

Similar to the proof of Conclusion 1, we have the following conclusion.

Conclusion 2. When the manufacturer sells its low-carbon product through the online e-commerce platform channel, the optimal decision is

$$\begin{aligned} P^* &= \frac{4Q\beta(1-\theta) + C(4d_1\beta - d_2^2\theta)}{2(1-\theta)(4d_1\beta - d_2^2\theta)} = \frac{2Q\beta}{4d_1\beta - d_2^2\theta} + \frac{C}{2(1-\theta)}, \\ E_2^* &= \frac{2\widehat{E}\alpha + \Phi}{2(\alpha + \varphi)}, \\ L_p^* &= \frac{d_2Q\theta}{4d_1\beta - d_2^2\theta}, \\ \Pi_{m2}^* &= \frac{d_1[4Q\beta(1-\theta) - C(4d_1\beta - d_2^2\theta)]^2}{4(1-\theta)(4d_1\beta - d_2^2\theta)^2} + \frac{\Phi^2 + 4\alpha\widehat{E}(\Phi - \varphi\widehat{E})}{4(\alpha + \varphi)}, \\ \Pi_{p2}^* &= \frac{\theta[4Q^2\beta(1-\theta)^2 - C^2d_1(4d_1\beta - d_2^2\theta)]}{4(1-\theta)^2(4d_1\beta - d_2^2\theta)}, \\ \Pi_2 &= \frac{4Q^2\beta^2d_1(1-\theta)}{(4d_1\beta - d_2^2\theta)^2} + \frac{d_1C^2(1-2\theta)}{4(1-\theta)^2} + \frac{(Q\theta - 2d_1C)Q\beta}{4d_1\beta - d_2^2\theta} + \frac{\Phi^2 + 4\alpha\widehat{E}(\Phi - \varphi\widehat{E})}{4(\alpha + \varphi)}, \\ q_2 &= \frac{2d_1\beta}{(4d_1\beta - d_2^2\theta) + (1-\theta)d_2^2}Q - \frac{Cd_1}{2(1-\theta)}. \end{aligned} \quad (23)$$

5. Result Analysis and Managerial Insights

Conclusion 3. The manufacturer has the same emission reduction level in Model I as in Model II.

It is shown from Conclusion 3 that the production, only related to the manufacturer who assumes the emission reduction cost and obtains the carbon trading revenue by itself, is not associated with the offline retailer in the traditional supply chain and the online platform in the e-commerce supply chain. Therefore, the carbon emission reduction level is only decided by the manufacturer, and the product sale will be crucial in the manufacturer's decision.

Conclusion 4. The establishment of the carbon market helps the manufacturer reduce its emission. The amount of emission reduction increases with \hat{E} and φ while decreases with Φ and α .

See Appendix B for the proof of Conclusion 4.

Conclusion 4 tells us that the establishment of the carbon trading market for manufacturers is feasible and conducive to emission reduction. The market mechanism creates a suitable environment for manufacturers to actively reduce emissions; this mechanism will drive the manufacturer with large initial carbon emission to reduce much more emission for getting more trading space; manufacturers sensitive to the carbon price also tend to reduce more emission so that it does not have to cost much to get emission permit and can earn revenue by selling its emission quota. In fact, there are also factors against emission reduction. When the current carbon market scale is rising, it means that the corresponding industry is facing many difficulties in reducing emissions. As a result, this manufacturer's emission will rise more or less. If the elastic coefficient of carbon emission reduction cost increases, it suggests that the current unit emission reduction cost has increased so that excessive emission reduction will make the manufacturer's cost go up.

Conclusion 5. The manufacturer has negative profit in the carbon market if

$$0 < \frac{\Phi}{\hat{E}} < 2\alpha \left(\sqrt{\frac{1+\varphi}{\alpha}} - 1 \right), \quad (24)$$

and positive if

$$2\alpha \left(\sqrt{\frac{1+\varphi}{\alpha}} - 1 \right) < \frac{\Phi}{\hat{E}} < \varphi. \quad (25)$$

See Appendix C for the proof of Conclusion 5.

Conclusion 5 indicates that if the carbon market scale is too small and there is not enough demand to encourage carbon trading, the manufacturer cannot sell its carbon emission quota and get profitable from the carbon market. Therefore, the manufacturer's condition to obtain profit is the carbon market must rise to a critical scale, which is $2\alpha \left(\sqrt{\frac{1+\varphi}{\alpha}} - 1 \right)$ times of the manufacturer's emission. Only above this critical scale dose, the manufacturer has the desire to reduce emission. This critical scale multiple is decided by the elastic coefficient of carbon emission

reduction cost α and the sensitivity coefficient to the carbon price φ .

Conclusion 6. In the e-commerce mode, the product price P^* , the platform's service level L_p^* and profit Π_2^* , and the supply chain's profit Π_2 all increase with the commission rate θ . The manufacturer's profit rises with the increase in the commission rate if $d_2^2 < 2d_1\beta$ and rises up then falls down if $d_2^2 > 2d_1\beta$.

See Appendix D for the proof of Conclusion 6.

Conclusion 6 shows that if occupying a higher proportion of profit in the supply chain, the platform can help add its profit and have subsequent desire to improve its service level to attract more consumers, which is conducive to the rise of the supply chain's profit. However, this affects the manufacturer's profit. When the platform's elastic coefficient of service cost β is relatively small ($d_2^2 > 2d_1\beta$), the manufacturer still has space to increase profit, but most profits are eventually been possessed by the platform with the rise of commission rate. It also can be known from the proof that the difference between d_2^2 and $2d_1\beta$ decides the manufacturer's space to increase profit. If this difference is really large, the manufacturer has enough space to maintain growth; otherwise, the space will be narrow. If β is quite large ($d_2^2 < 2d_1\beta$), the platform will try to grab profit in the supply chain to offset its cost for improving the service level, which makes the manufacturer's profit fall down with the increase in the commission rate.

The manufacturer will raise product price to secure its profit, expecting that the loss caused by unfair profit allocation could be made up by high price and sales. This demonstrates the manufacturer's awkward situation under the case led by the platform; after the price is raised, the supply chain's whole profit rises, but its own part is still on the decrease.

It follows from the above conclusion that when θ is close to 1, the product price P will approach infinity. This is produced because the platform excessively occupies the sales income while the manufacturer tends to increase the price for expected profit. This will results in the negative q_2 . Thus, to ensure the research practical, we reset the range of θ . Since

$$q_2 = \frac{2d_1\beta}{(4d_1\beta - d_2^2) + (1 - \theta)d_2^2} Q - \frac{Cd_1}{2(1 - \theta)} > 0, \quad (26)$$

we have the following conclusion.

Conclusion 7. $0 < \theta < \max\{((4Q\beta - Cd_1\beta)/(4Q\beta - Cd_2^2)), 1\}$.

Conclusion 8. In the product market, the manufacturer has more profit than the e-commerce platform if

$$0 < \theta < \frac{4d_1\beta - 2\sqrt{d_1\beta(4d_1\beta - d_2^2)}}{d_2^2}, \quad (27)$$

and the platform has more if

$$\frac{4d_1\beta - 2\sqrt{d_1\beta(4d_1\beta - d_2^2)}}{d_2^2} < \theta < 1. \quad (28)$$

See Appendix E for the proof of Conclusion 8.

Conclusion 9. The manufacturer's criterion to sell online is as follows:

- (1) $\theta \in (0, \min\{\theta_2, 1\})$, if $d_2^2 < 2d_1\gamma$.
- (2) $\theta \in (\theta_1, \min\{\theta_2, 1\})$, if $d_2^2 \geq 2d_1\gamma$, where

$$\theta_1 = \frac{8d_1\beta[(\beta + \gamma)d_2^2 - 4d_1\beta\gamma] - \sqrt{\Delta}}{2\gamma d_2^4},$$

$$\theta_2 = \frac{8d_1\beta[(\beta + \gamma)d_2^2 - 4d_1\beta\gamma] + \sqrt{\Delta}}{2\gamma d_2^4},$$

$$\Delta = 64d_1^2\beta^2[(\beta + \gamma)d_2^2 - 4d_1\beta\gamma]^2 - 32d_1d_2^4\beta^2\gamma(d_2^2 - 2d_1\gamma). \quad (29)$$

See Appendix F for the proof of Conclusion 9.

Conclusion 9 implies that whether the manufacturer selects the online e-commerce mode depends on the sensitivity coefficient to the product price and that to the product service. The change of these two coefficients will affect the suitable commission interval for the manufacturer's channel decision. When the sensitivity coefficient to the product service is small, the service level affects the sales little, so the effect of the platform on the revenue is small. The manufacturer's expectation to gain more profit than offline and occupy more sales revenue can be achieved when the commission rate is low. Conversely, if the service level affects sales greatly, the platform should be expected to provide better service for attracting more consumers. However, the essential condition for the platform willing to cooperate is obtaining much more revenue. Therefore, the commission rate should be raised in this case.

Conclusion 10. The manufacturer's carbon emission per unit product through the online channel is lower than that through the offline one if

$$\gamma < \frac{1}{2d_1}. \quad (30)$$

The manufacturer's carbon emission per unit product through the offline channel is lower than that through the online one if

$$\gamma > \frac{2\beta}{4d_1\beta - d_2^2}. \quad (31)$$

The manufacturer's carbon emission per unit product through the offline channel is first lower and then higher than that through the online one if

$$\frac{1}{2d_1} \leq \gamma \leq \frac{2\beta}{4d_1\beta - d_2^2}. \quad (32)$$

See Appendix G for the proof of Conclusion 10.

Conclusion 10 reveals that the online mode does not necessarily result in better carbon emission per unit product than the offline one. It depends. If both γ and β are small, the e-commerce platform can sell more products. These are products with low sales cost, for example, goods involving daily life. If $\gamma > (2\beta/(4d_1\beta - d_2^2))$, the proof shows that the offline sales have surpassed the online one greatly. This corresponds to goods needing much offline experience. If $(1/(2d_1)) \leq \gamma \leq (2\beta/(4d_1\beta - d_2^2))$, the online product sales is first lower then higher than the offline one with the increase in the commission rate in the e-commerce platform mode. This demonstrates that for goods in between, we can rely on the platform's advantage in customer acquisition, improving the service level after the commission rate rises, to stimulate consumers' demand for the low-carbon product. In this way, the platform's advantage is put to fair use, which can play a positive role in reducing carbon emission.

6. Numerical Examples

In this section, we elaborate on the above conclusions with numerical examples. Suppose $Q = 100000$, $C = 3$, $\bar{E} = 35$, $\Phi = 300$, $\phi = 10$, $\alpha = 5$, $\beta = 2$, $\gamma = 5$, $\theta = 0.4$, $d_1 = 2$, and $d_2 = 3$.

6.1. Carbon Emission Reduction Analysis. The manufacturer's carbon emission reduction relation affected by other factors is shown in Figure 1.

It can be known from Figure 1 that the manufacturer's amount of carbon emission reduction monotonously increases with the initial emission amount and the sensitivity coefficient to the carbon price and monotonously decreases with the carbon market scale and the elastic coefficient of carbon emission reduction cost. The factors influencing the manufacturer's emission reduction behavior include two types, internal and external. Internal factors are initial emission amount and elastic coefficient of carbon emission reduction cost, while the external ones are carbon market scale and sensitivity coefficient to the carbon price. In fact, there is always one factor conducive to emission reduction and one adverse to that, no matter for internal factors and external ones. Once the initial emission amount and carbon market scale are settled down, the significant influencing factors turn to be the sensitivity coefficient to the carbon price (external and conducive to) and elastic coefficient of carbon emission reduction cost (internal and adverse to). Therefore, the governmental supervision department should promote manufacturers' sensitivity to carbon price by moderately strengthening carbon emission control, which can guide manufacturers actively to speeding up emission reduction. Meanwhile, government subsidies and other measures that lower manufacturers' emission reduction cost are also useful in boosting their initiative.

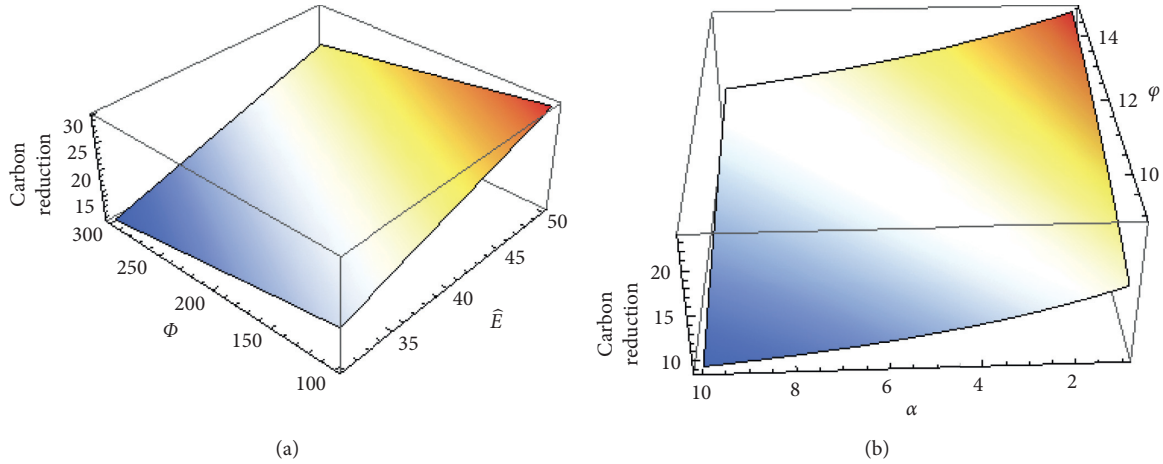


FIGURE 1: The manufacturer’s carbon emission reduction: (a) change with Φ and \hat{E} ; (b) change with α and ϕ .

6.2. *Analysis on the Manufacturer’s Profit from Carbon Market.* The manufacturer’s profit change in the carbon market affected by other factors is depicted in Figure 2.

After making Figure 2(a) with (Φ/\hat{E}) as the independent variable, we can find that the manufacturer’s profit from the carbon market is 0 when $(\Phi/\hat{E}) = 7.32$, negative when $(\Phi/\hat{E}) < 7.32$, and positive only when $(\Phi/\hat{E}) > 7.32$. However, the constraint, $(\Phi/\hat{E}) < \phi = 10$, actually leaves very narrow space for the manufacturer to gain positive profit, which is demonstrated more distinctively in Figure 2(b). Based on the current parameters’ value, only the blue area above the green plane is where the manufacturer will be active in the carbon trading market. Flexibly, we could expand the manufacturer’s profit area by enlarging the sensitivity coefficient to the carbon price. Consistent with the analysis in Section 6.1, this highlights the significance of strengthening carbon emission control by governmental supervision departments because the governmental supervision to promote the manufacturer’s sensitivity to carbon price is a “kill two birds with one stone” strategy, not only stimulating the emission reduction but also further helping the manufacturer gain profit, which will form a virtuous circle.

6.3. *Profit Analysis of Manufacturer and E-Commerce Platform in Online Mode.* The influence of the commission rate on the e-commerce supply chain and its members is displayed in Figure 3.

As can be seen from Figure 3, with the increase in the commission rate, the manufacturer’s profit experiences a significant decline after a slight rise, while profits of the platform and the supply chain rise obviously (Figure 3(a)). During the cooperation between multiple parties, the platform relies on its leading status to set the commission rate. When the platform raises the commission rate to add its profit, the good result is that enough funds can ensure its ability to improve the service level (Figure 3(b)), but the bad result is that this move lowers the manufacturer’s profit, so the latter has to defend its interest by trying to raise the product price (Figure 3(c)). The rise of product price is the

adverse factor for product sales; however, consumers clearly prefer the utility produced by better service level, so the sales can still mount up even though the manufacturer raises the price (Figure 3(d)). This also reflects how important the sales service is in the e-commerce supply chain, which is critical to attract consumers. The reason that the increase in the manufacturer’s profit is not easy to detect at the beginning, combing the proof of Conclusion 6, lies in that d_2^2 and $2d_1\beta$ satisfy $d_2^2 > 2d_1\beta$, but the difference between d_2^2 and $2d_1\beta$ is too small, which squeezes the manufacturer’s space to increase profit so that brief profit rise is soon ruined by the increase in the commission rate.

6.4. *Analysis on Whether the Manufacturer Selects Online Mode.* Based on the given parameters’ value, we make Figure 4(a), showing the change of the manufacturer’s profit in the online mode and offline mode with the commission rate. In Figure 4(a), $d_2^2 < 2d_1\gamma$ holds. In order to contrast, we reset $\beta = 3.4$ and $d_2 = 5$ so that $d_2^2 \geq 2d_1\gamma$ holds, and we make Figure 4(b) similarly.

It can be seen from Figure 4(a) that if $d_2^2 < 2d_1\gamma$, the manufacturer gets much more profit from the online mode than offline mode when $0 < \theta < 0.81$. Figure 4(b) demonstrates that if $d_2^2 \geq 2d_1\gamma$, this case holds when $0.30 < \theta < 1$. Relatively speaking, when the effect of the service level on the sales is not large (Figure 4(a)), the manufacturer’s profit experiences continual fall after slight rise with the increase in commission rate, which is consistent with Figure 3(a). Figure 3(a) tells that the critical point of commission rate is 0.6. The manufacturer has more profit than the platform when the commission rate is smaller than 0.6; on the contrary when that is larger than 0.6. Thus, after the commission rate goes beyond 0.6, although the manufacturer’s profit starts smaller than the platform, its profit is still higher than the offline mode until the commission rate reaches 0.81. When the effect of the service level on the sales is large (Figure 4(b)), $d_2^2 \geq 2d_1\gamma$, and the difference between d_2^2 and $2d_1\beta$ is big, the manufacturer is given enough space to raise profit. As can be seen, the increasing interval has been extended to $\theta < 0.9$.

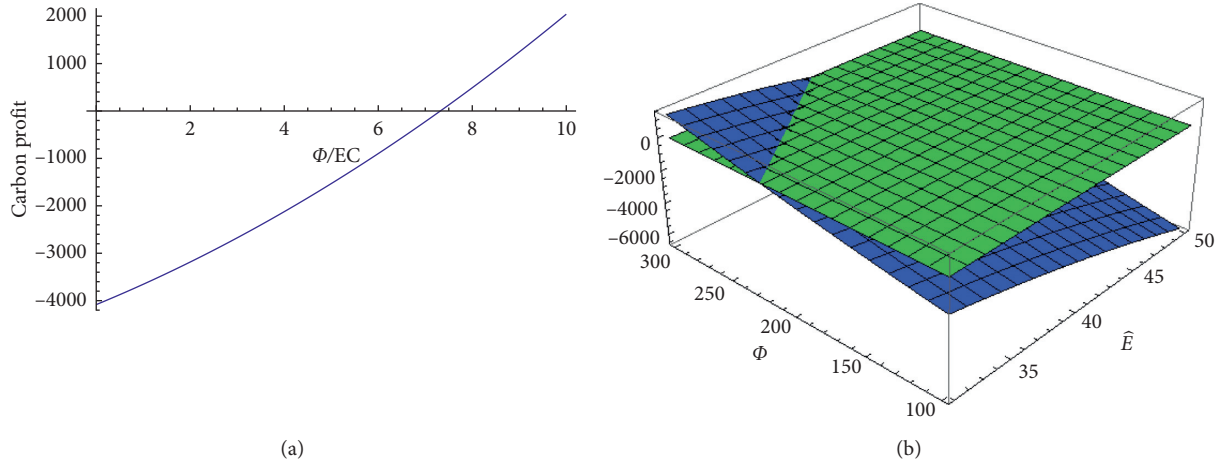


FIGURE 2: The manufacturer's profit from the carbon market: (a) change with (Φ/ϕ) ; (b) change with Φ and \hat{E} .

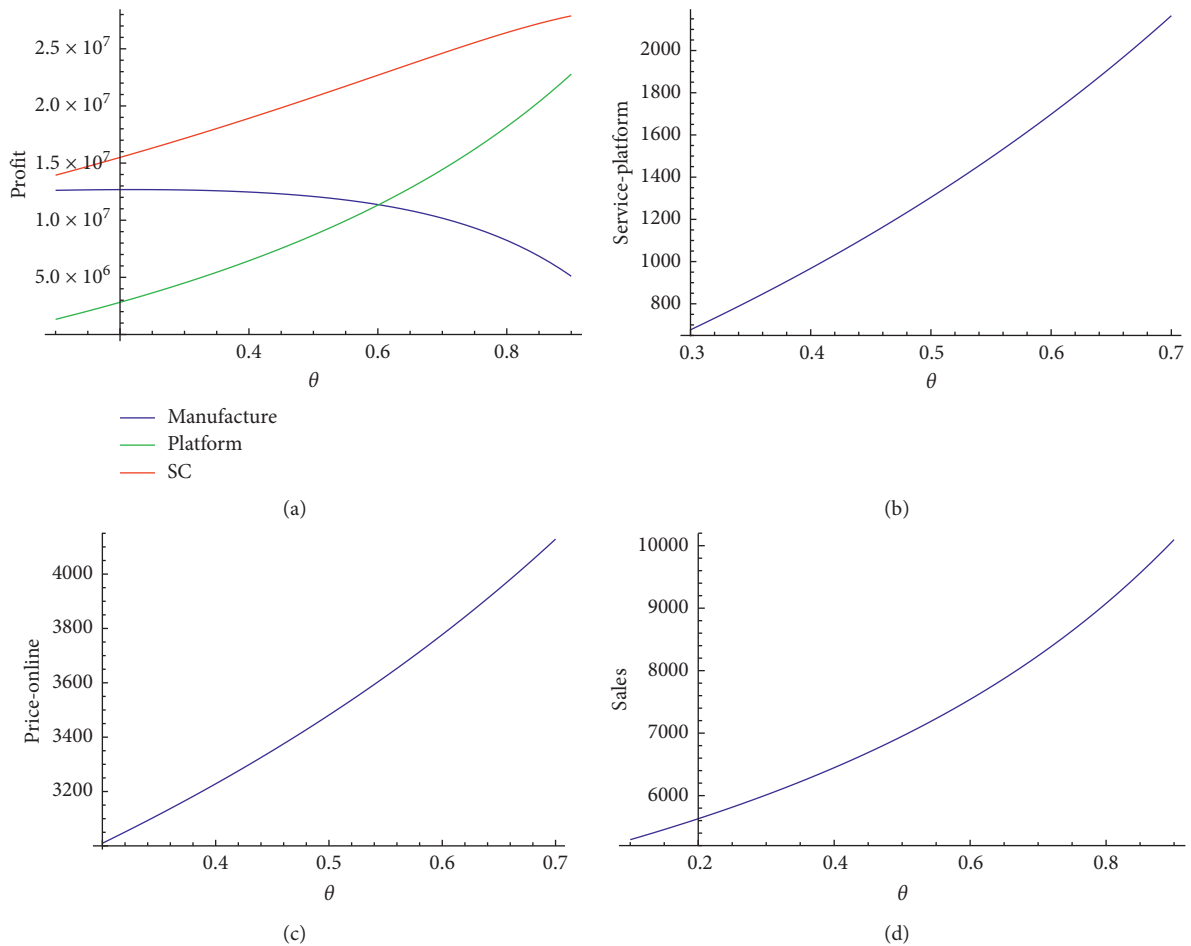


FIGURE 3: Changes of the supply chain's decision with θ in the online mode: (a) change in profits; (b) change in the platform's service level; (c) change in product price; (d) change in product sales.

6.5. Analysis on Carbon Emission per Unit Product of Online and Offline Mode. Based on the parameters' value set at the beginning of Section 6, we make Figure 5(a) showing the change of the manufacturer's carbon emission per unit

product of the online and offline mode with the commission rate, in which $\gamma > (2\beta / (4d_1\beta - d_2^2))$ holds. For further comparison, we provide two more group values of β , γ , and d_2 . One is $\beta = 0.15$, $\gamma = 0.2$, and $d_2 = 1$ so that $\gamma < (1 / (2d_1))$

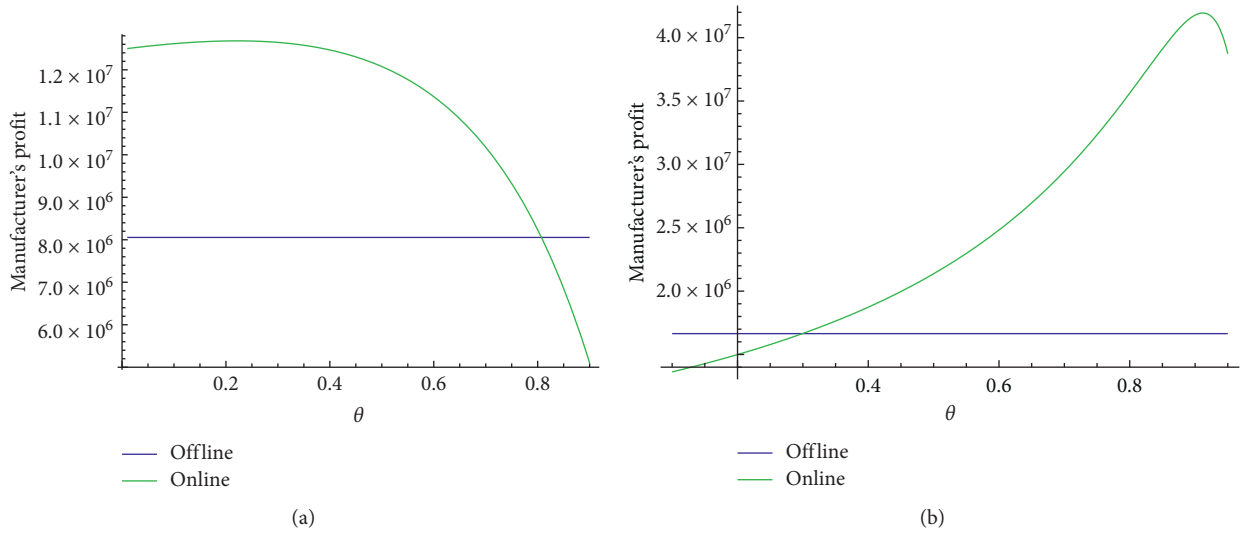


FIGURE 4: The manufacturer's profit in the online and offline mode: (a) case 1: $d_2^2 < 2d_1\gamma$; (b) case 2: $d_2^2 \geq 2d_1\gamma$.

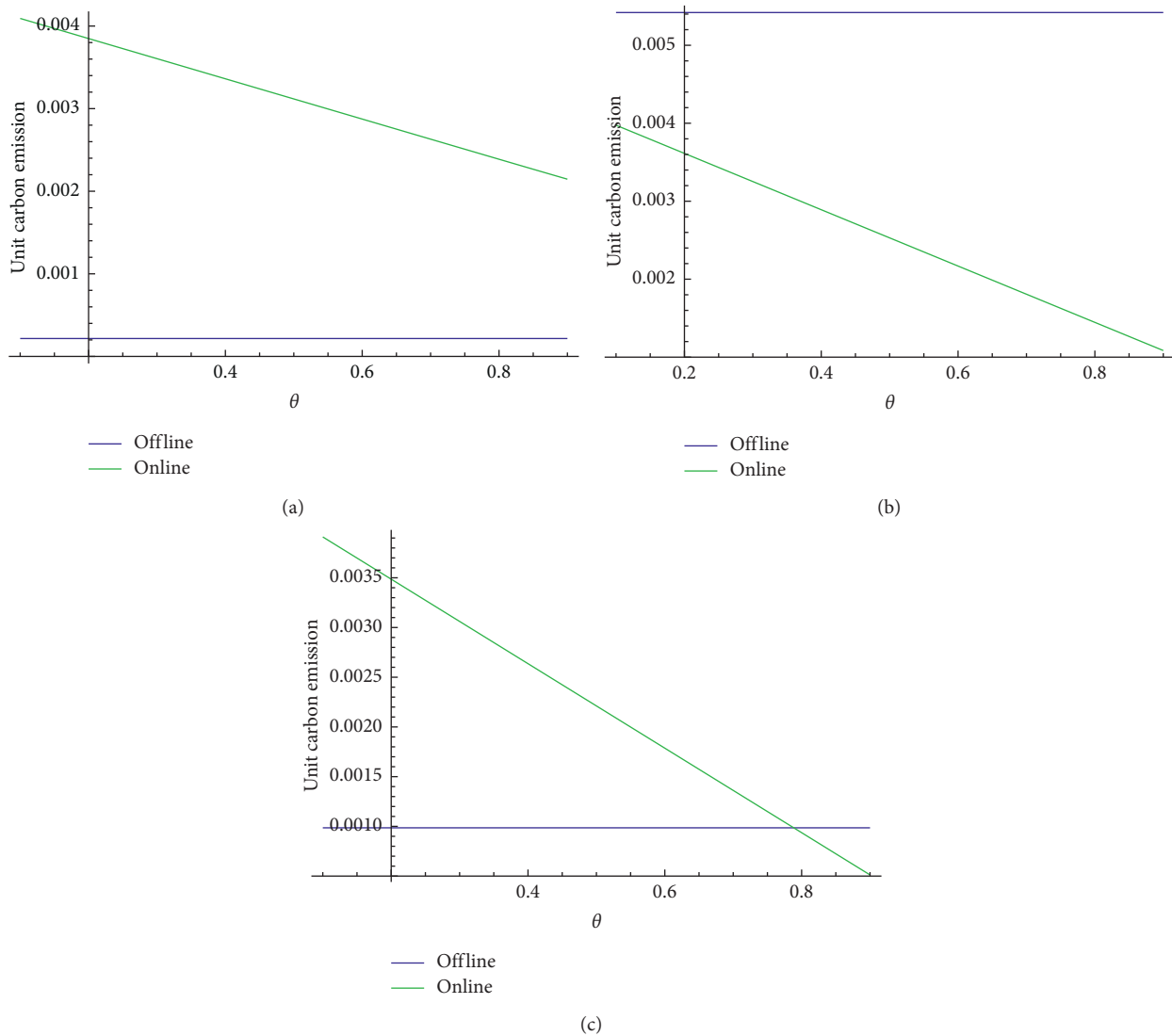


FIGURE 5: Carbon emission per unit product in the online and offline mode: (a) case 1: $\gamma > (2\beta / (4d_1\beta - d_2^2))$; (b) case 2: $\gamma < (1/2d_1)$; (c) case 3: $(1/2d_1) \leq \gamma \leq (2\beta / (4d_1\beta - d_2^2))$.

is satisfied, and then we make Figure 5(b); another is $\beta = 1$, $\gamma = 1.1$, and $d_2 = 2.8$, meeting $(1/(2d_1)) \leq \gamma \leq (2\beta/(4d_1\beta - d_2^2))$, and we make Figure 5(c).

Figure 5(a) demonstrates that under the condition $\gamma > (2\beta/(4d_1\beta - d_2^2))$, the offline mode produces lower carbon emission per unit product. As mentioned earlier, this case corresponds to products relying on offline experiences and needing much promotion efforts. The online channel, although convenient, is not omnipotent and not suitable for all kinds of product sales. Figure 5(b) depicts the case for products with low sales cost, in which both the elastic coefficient of service cost in the online mode and the promotion effort level coefficient in the offline mode become smaller, so the influence of the service on sales falls down. The e-commerce is applicable for selling this kind of goods. The sudden rise of Pinduoduo is similar to this situation. In Figure 5(c), the supply chains have large space to adjust their carbon emissions per unit product. The online mode has the same carbon emission per unit product as the offline one when $\theta = 0.79$, before which the offline mode has lower unit emission and after which the online mode shows its advantages.

However, all these three figures imply that, no matter what the case is, the platform will provide good service with the rise of the commission rate to attract consumers and raise product sales. The platform's behavior has led to good results so that the online mode could cause a continual decrease in unit emission. Therefore, we can adjust the supply chain to the state as we expect by changing the commission rate between the manufacturer and the e-commerce platform properly.

7. Conclusions

This research investigates the low-carbon product manufacturer's supply chain channel decision between the online and offline mode when there is a carbon trading market. The offline supply chain mode consists of one manufacturer and one retailer, in which the former is the leader. In comparison, the online one compromises one manufacturer and one e-commerce platform, with the former being the follower. The manufacturer could get profitable by selling its low-carbon products in the product market and trading its carbon quota to cover its emission reduction cost in the carbon market. We reach the following conclusions with practical value.

First, the carbon market establishment is conducive to the manufacturer's carbon emission reduction, especially for those sensitive to the carbon price and those with many emissions currently. The carbon market trading mechanism could motivate manufacturers much to reduce carbon emission. However, some industries with a large carbon emission base and some manufacturers with a high elastic coefficient of carbon emission reduction cost are still facing many challenges. Governments should provide subsidies moderately to increase their initiative. Furthermore, to be more conducive to emission reduction, the manufacturers' necessary condition to be profitable from the carbon market is that the carbon market scale should not be too small. Thus,

it comes to that carbon trading market mechanism is not universally applicable. Only in proper carbon market scale interval can manufacturers be motivated.

Second, when manufacturers select the supply chain sales channel between the online mode and offline mode, they have to, on the one hand, experience the status change and, on the other hand, weigh their profit gain or loss. In the online mode, the commission rate represents the manufacturer's power in the supply chain. A low commission rate makes the manufacturer have more profit than the platform, while a high one benefits the platform. As manufacturers are concerned, whether they could select the online mode to gain more profit depends on the property of products they are producing. If consumers are not sensitive to the sales service, manufacturers must fight for a low commission rate; otherwise, if consumers take the service level seriously, the e-commerce platform should provide better service. High-quality service from the platform could help the supply chain gain more profit as a whole. Hence, even though the commission rate has risen to a little high level, the manufacturer can still enter the online mode.

Third, which channel is conducive to carbon emission reduction between the online and offline mode depends on the product type. For daily goods from large-scale mass production, the platform can make full use of its convenience to sell more products, making the online mode help reduce emissions. For goods needing experiencing in person, the offline channel works better than the online one. For products between these above two types, the platform can raise the commission rate properly. After getting more profits, it will improve its service level, making the online supply chain mode conducive to reducing emissions in the same way.

However, there are still some limitations in our models to be further addressed. If consumers prefer low-carbon products, the low-carbon level of products might affect their purchase desire, which affects the product demand in the end [42]. Then, to what extent will this influence the demand and would this change the supply chain member's decision behavior? This research will combine the product market and the carbon trading market better.

Appendix

A. Proof of Conclusion 1

We get the optimal decision of this model by the backward induction method. In expression (12), the Hessian matrix of Π_{r1} with respect to P_r and L_r is

$$H_1 = \begin{bmatrix} \frac{\partial^2 \Pi_{r1}}{\partial P_r^2} & \frac{\partial^2 \Pi_{r1}}{\partial P_r \partial L_r} \\ \frac{\partial^2 \Pi_{r1}}{\partial L_r \partial P_r} & \frac{\partial^2 \Pi_{r1}}{\partial L_r^2} \end{bmatrix} = \begin{bmatrix} -2d_1 & d_2 \\ d_2 & -2\gamma \end{bmatrix}. \quad (\text{A.1})$$

It is easy to see H_1 is the negative definite matrix.

Let $(\partial \Pi_{r1} / \partial P_r) = 0$ and $(\partial \Pi_{r1} / \partial L_r) = 0$. Solve these simultaneous equations, and then we can obtain the reaction functions of P_r and L_r as follows:

$$P_r^* = \frac{2Q\gamma + (2d_1\gamma - d_2^2)P_w}{4d_1\gamma - d_2^2}, \quad (A.2)$$

$$L_r^* = \frac{d_2(Q - d_1P_w)}{4d_1\gamma - d_2^2}.$$

Substitute them into expression (11) and let $(\partial \Pi_{m1} / \partial P_w) = 0$ and $(\partial \Pi_{m1} / \partial E) = 0$; then, we can reach the manufacturer's optimal wholesale price and carbon emission level.

B. Proof of Conclusion 4

(i) It follows from Conclusions 1 and 2 that the manufacturer's emissions in two modes are

$$E_1^* = E_2^* = \frac{2\hat{E}\alpha + \Phi}{2(\alpha + \varphi)}. \quad (B.1)$$

Then, its carbon emission reduction is

$$\Delta E = \hat{E} - \frac{2\hat{E}\alpha + \Phi}{2(\alpha + \varphi)} = \frac{2\hat{E}\varphi - \Phi}{2(\alpha + \varphi)}. \quad (B.2)$$

Based on the hypothesis in Section 3, $\varphi\hat{E} - \Phi > 0$.

Thus, $\Delta E > 0$; that is, $E_1^* = E_2^* < \hat{E}$.

(ii) It is derived easily from the expression of ΔE that it increases monotonously with \hat{E} and φ and decreases monotonously with Φ and α .

C. Proof of Conclusion 5

According to the above conclusions, the manufacturer's profit in the carbon market is

$$I_{m1c}^* = I_{m2c}^* = \frac{\Phi^2 + 4\alpha\hat{E}(\Phi - \varphi\hat{E})}{4(\alpha + \varphi)}. \quad (C.1)$$

We take the numerator of this fraction as the function of Φ ,

$$f(\Phi) = \Phi^2 + 4\alpha\hat{E}(\Phi - \varphi\hat{E}). \quad (C.2)$$

Then, $f(\Phi)$ is a parabola pointing upward with two intercepts on the Φ axis, $\Phi_1 = -2\alpha\hat{E}(\sqrt{((1 + \varphi)/\alpha)} + 1)$ and $\Phi_2 = 2\alpha\hat{E}(\sqrt{((1 + \varphi)/\alpha)} - 1)$.

Because $\Phi < 0$, we have that the manufacturer's profit in the carbon market is negative if $0 < (\Phi/\hat{E}) < 2\alpha(\sqrt{((1 + \varphi)/\alpha)} - 1)$ and positive if $(\Phi/\hat{E}) > 2\alpha(\sqrt{((1 + \varphi)/\alpha)} - 1)$.

Moreover, in the carbon market, $\Phi - \varphi\hat{E} < 0$. This conclusion holds.

D. Proof of Conclusion 6

(i) $P^* = (2Q\beta/(4d_1\beta - d_2^2\theta)) + (C/(2(1 - \theta)))$.

It is obvious that both $(2Q\beta/(4d_1\beta - d_2^2\theta))$ and $(C/(2(1 - \theta)))$ increase with θ .

Thus, P increases with θ .

(ii) $L_p^* = (d_2Q\theta/(4d_1\beta - d_2^2\theta))$.

Since $4d_1\beta - d_2^2\theta > 0$, it is obvious that L_p^* increases with θ .

(iii) $\Pi_{p2}^* = ((\theta[4Q^2\beta(1 - \theta)^2 - C^2d_1(4d_1\beta - d_2^2\theta)]/(4(1 - \theta)^2(4d_1\beta - d_2^2\theta))) + \theta[(Q^2\beta/(4d_1\beta - d_2^2\theta)) - (C^2d_1/(4(1 - \theta)^2))]$.

Because Q is a large enough positive number, we only consider terms with Q^2 , that is, $(Q^2\beta\theta/(4d_1\beta - d_2^2\theta))$, which increases with θ .

(iv) The manufacturer's total profit

$$\Pi_{m2}^* = ((d_1[4Q\beta(1 - \theta) - C(4d_1\beta - d_2^2\theta)]^2)/(4(1 - \theta)(4d_1\beta - d_2^2\theta)^2)) + ((\Phi^2 + 4\alpha\hat{E}(\Phi - \varphi\hat{E}))/4(\alpha + \varphi)).$$

We represent the manufacturer's profit in the product market as

$$\Pi_{m21}^* = \frac{d_1[4Q\beta(1 - \theta) - C(4d_1\beta - d_2^2\theta)]^2}{4(1 - \theta)(4d_1\beta - d_2^2\theta)^2}. \quad (D.1)$$

Then,

$$\begin{aligned} \Pi_{m21}^* &= \frac{d_1[4Q\beta(1 - \theta) - C(4d_1\beta - d_2^2\theta)]^2}{4(1 - \theta)(4d_1\beta - d_2^2\theta)^2} \\ &= d_1 \left[\frac{4Q^2\beta^2(1 - \theta)}{(4d_1\beta - d_2^2\theta)^2} - \frac{2CQ\beta}{4d_1\beta - d_2^2\theta} + \frac{C^2}{4(1 - \theta)} \right]. \end{aligned} \quad (D.2)$$

Because Q is a large enough positive number, we only consider terms with Q^2 , that is, $((4Q^2\beta^2(1 - \theta))/(4d_1\beta - d_2^2\theta)^2)$.

Let $f(\theta) = ((\beta^2(1 - \theta))/(4d_1\beta - d_2^2\theta^2))$, then

$$\frac{df(\theta)}{d\theta} = -\frac{\beta^2[(4d_1\beta - d_2^2) - (1 - \theta)d_2^2]}{(4d_1\beta - d_2^2)^3}. \quad (D.3)$$

Because when $d_2^2 < 2d_1\beta$, $(df(\theta)/d\theta) < 0$, $(4d_1\beta - d_2^2) - (1 - \theta)d_2^2 \in (4d_1\beta - 2d_2^2, 4d_1\beta - d_2^2)$, meaning that Π_{m2}^* decreases with θ ; when $d_2^2 > 2d_1\beta$,

$$(4d_1\beta - d_2^2) - (1 - \theta)d_2^2 \in (4d_1\beta - 2d_2^2, 0) \cup [0, 4d_1\beta - d_2^2), \quad (\text{D.4})$$

indicating that Π_{m2}^* first increases and then decreases with θ .

(v) The supply chain's profit

$$\begin{aligned} \Pi_2 &= \frac{4Q^2\beta^2d_1(1-\theta)}{(4d_1\beta - d_2^2\theta)^2} + \frac{d_1C^2(1-2\theta)}{4(1-\theta)^2} + \frac{(Q\theta - 2d_1C)Q\beta}{4d_1\beta - d_2^2\theta} + \frac{\Phi^2 + 4\alpha\widehat{E}(\Phi - \varphi\widehat{E})}{4(\alpha + \varphi)} \\ &= \frac{4Q^2\beta^2d_1(1-\theta) + (Q\theta - 2d_1C)Q\beta(4d_1\beta - d_2^2\theta)}{(4d_1\beta - d_2^2\theta)^2} + \frac{d_1C^2(1-2\theta)}{4(1-\theta)^2} + \frac{\Phi^2 + 4\alpha\widehat{E}(\Phi - \varphi\widehat{E})}{4(\alpha + \varphi)} \\ &= \frac{4d_1\beta - d_2^2\theta^2}{(4d_1\beta - d_2^2\theta)^2}Q^2\beta + \frac{2Cd_1d_2^2\theta - 8Cd_1^2\beta}{(4d_1\beta - d_2^2\theta)^2}Q\beta + \frac{d_1C^2(1-2\theta)}{4(1-\theta)^2} + \frac{\Phi^2 + 4\alpha\widehat{E}(\Phi - \varphi\widehat{E})}{4(\alpha + \varphi)}. \end{aligned} \quad (\text{D.5})$$

Let $f(\theta) = ((4d_1\beta - d_2^2\theta^2)/(4d_1\beta - d_2^2\theta)^2)$, then

$$\frac{df(\theta)}{d\theta} = \frac{8d_1d_2^2\beta(1-\theta)}{(4d_1\beta - d_2^2\theta)^3} > 0. \quad (\text{D.6})$$

Since Q is a large enough positive number, Π_2 increases with θ .

E. Proof of Conclusion 8

The manufacturer's profit in the product market is

$$I_{m2p}^* = \frac{d_1[4Q\beta(1-\theta) - C(4d_1\beta - d_2^2\theta)]^2}{4(1-\theta)(4d_1\beta - d_2^2\theta)^2}. \quad (\text{E.1})$$

The platform's profit in the product market is

$$\Pi_{p2}^* = \frac{\theta[4Q^2\beta(1-\theta)^2 - C^2d_1(4d_1\beta - d_2^2\theta)]}{4(1-\theta)^2(4d_1\beta - d_2^2\theta)}. \quad (\text{E.2})$$

Since Q is a large enough positive number, we only compare terms of Q with the highest power (square) during the comparison of their profit difference in the product market. We denote them by \widehat{I}_{m2p}^* and $\widehat{\Pi}_{p2}^*$, respectively; then,

$$\begin{aligned} \widehat{I}_{m2p}^* &= \frac{16d_1Q^2\beta^2(1-\theta)^2}{4(1-\theta)(4d_1\beta - d_2^2\theta)^2} \\ &= \frac{4d_1\beta(1-\theta)}{(4d_1\beta - d_2^2\theta)\theta} \cdot \frac{Q^2\beta\theta}{4d_1\beta - d_2^2\theta}, \\ \widehat{\Pi}_{p2}^* &= \frac{Q^2\beta\theta}{4d_1\beta - d_2^2\theta}. \end{aligned} \quad (\text{E.3})$$

The necessary condition for $\widehat{I}_{m2p}^* < \widehat{\Pi}_{p2}^*$ is that

$$d_2^2\theta^2 - 8d_1\beta\theta + 4d_1\beta < 0. \quad (\text{E.4})$$

Solve the follow equation with respect to θ

$$d_2^2\theta^2 - 8d_1\beta\theta + 4d_1\beta = 0. \quad (\text{E.5})$$

Then, we have $\theta = ((4d_1\beta \pm 2\sqrt{d_1\beta(4d_1\beta - d_2^2)})/d_2^2)$. Therefore, $\widehat{I}_{m2p} < \widehat{\Pi}_{p2}$ if

$$\frac{4d_1\beta - 2\sqrt{d_1\beta(4d_1\beta - d_2^2)}}{d_2^2} < \theta < \frac{4d_1\beta + 2\sqrt{d_1\beta(4d_1\beta - d_2^2)}}{d_2^2}. \quad (\text{E.6})$$

However,

$$\frac{4d_1\beta + 2\sqrt{d_1\beta(4d_1\beta - d_2^2)}}{d_2^2} > 1. \quad (\text{E.7})$$

Thus, $\widehat{I}_{m2p}^* < \widehat{\Pi}_{p2}^*$ if $((4d_1\beta - 2\sqrt{d_1\beta(4d_1\beta - d_2^2)})/d_2^2) < \theta < 1$.

F. Proof of Conclusion 9

It follows from the above conclusions that

$$\begin{aligned} \Pi_{m1}^* &= \frac{(Q - Cd_1)^2\gamma}{2(4d_1\gamma - d_2^2)} + \frac{\Phi^2 + 4\alpha\widehat{E}(\Phi - \varphi\widehat{E})}{4(\alpha + \varphi)}, \\ \Pi_{m2}^* &= \frac{d_1[4Q\beta(1-\theta) - C(4d_1\beta - d_2^2\theta)]^2}{4(1-\theta)(4d_1\beta - d_2^2\theta)^2} \\ &\quad + \frac{\Phi^2 + 4\alpha\widehat{E}(\Phi - \varphi\widehat{E})}{4(\alpha + \varphi)}, \end{aligned} \quad (\text{F.1})$$

Π_{m1}^* and Π_{m2}^* have the same profit in the carbon trading market, so we only compare their profits in the product market. And, since Q is a large enough positive number, we

only compare terms of Q with the highest power (square). We denote them by $\widehat{\Pi}_{m1}$ and $\widehat{\Pi}_{m2}$, respectively; then,

$$\begin{aligned} \widehat{\Pi}_{m1}^* &= \frac{Q^2\gamma}{2(4d_1\gamma - d_2^2)}, \\ \widehat{\Pi}_{m2}^* &= \frac{16d_1Q^2\beta^2(1-\theta)^2}{4(1-\theta)(4d_1\beta - d_2^2\theta)^2}. \end{aligned} \tag{F.2}$$

Further,

$$\begin{aligned} \widehat{\Pi}_{m2}^* &= \frac{16d_1Q^2\beta^2(1-\theta)^2}{4(1-\theta)(4d_1\beta - d_2^2\theta)^2} = \frac{4d_1\beta(1-\theta)}{(4d_1\beta - d_2^2\theta)\theta} \cdot \frac{Q^2\beta\theta}{4d_1\beta - d_2^2\theta} \\ &= \frac{4d_1Q^2\beta^2(1-\theta)}{(4d_1\beta - d_2^2\theta)^2} = \frac{Q^2\gamma}{2(4d_1\gamma - d_2^2)} \cdot \frac{8d_1\beta^2(1-\theta)(4d_1\gamma - d_2^2)}{\gamma(4d_1\beta - d_2^2\theta)^2} \\ &= \widehat{\Pi}_{m1}^* \times \frac{8d_1\beta^2(1-\theta)(4d_1\gamma - d_2^2)}{\gamma(4d_1\beta - d_2^2\theta)^2}. \end{aligned} \tag{F.3}$$

The necessary condition to gain more profit in the online mode is

$$\frac{8d_1\beta^2(1-\theta)(4d_1\gamma - d_2^2)}{\gamma(4d_1\beta - d_2^2\theta)^2} > 1. \tag{F.4}$$

After simplifying the inequality, we have

$$\gamma d_2^4 \theta^2 - 8d_1\beta[(\beta + \gamma)d_2^2 - 4d_1\beta\gamma]\theta + 8d_1\beta^2(d_2^2 - 2d_1\gamma) < 0. \tag{F.5}$$

Let

$$\begin{aligned} f(\theta) &= \gamma d_2^4 \theta^2 - 8d_1\beta(\beta + \gamma)\left(d_2^2 - 4d_1\frac{\beta\gamma}{\beta + \gamma}\right)\theta \\ &\quad + 8d_1\beta^2(d_2^2 - 2d_1\gamma). \end{aligned} \tag{F.6}$$

Then, it is a parabola with respect to θ , going upward. It is obvious that $4d_1(\beta\gamma/(\beta + \gamma)) < 2d_1\gamma$.

(i) if $d_2^2 < 4d_1(\beta\gamma/(\beta + \gamma)) < 2d_1\gamma$

In this case, the axis of symmetry of $f(\theta)$ is negative, its intercept on the vertical axis is negative, and among its two intercepts on the horizontal axis, one is positive and another is negative. Thus,

$$\theta \in [0, \min\{\theta_2, 1\}]. \tag{F.7}$$

(ii) If $4d_1(\beta\gamma/(\beta + \gamma)) < d_2^2 < 2d_1\gamma$

In this case, the axis of symmetry of $f(\theta)$ is positive, its intercept on the vertical axis is negative, and

among its two intercepts on the horizontal axis, one is positive and another is negative. Thus,

$$\theta \in [0, \min\{\theta_2, 1\}]. \tag{F.8}$$

(iii) if $4d_1(\beta\gamma/(\beta + \gamma)) < 2d_1\gamma < d_2^2$

In this case,

$$\begin{aligned} \Delta &= 64d_1^2\beta^2[(\beta + \gamma)d_2^2 - 4d_1\beta\gamma]^2 - 32d_1d_2^4\beta^2\gamma(d_2^2 - 2d_1\gamma) \\ &= 32d_1\beta^2\left\{2d_1[(\beta + \gamma)d_2^2 - 4d_1\beta\gamma]^2 - d_2^4\gamma(d_2^2 - 2d_1\gamma)\right\}. \end{aligned} \tag{F.9}$$

Let

$$\Delta_1 = 2d_1[(\beta + \gamma)d_2^2 - 4d_1\beta\gamma]^2 - d_2^4\gamma(d_2^2 - 2d_1\gamma). \tag{F.10}$$

Then,

$$\begin{aligned} \Delta_1 &= 2d_1[(\beta + \gamma)d_2^2 - 4d_1\beta\gamma]^2 - d_2^4\gamma(d_2^2 - 2d_1\gamma) \\ &= 2d_1[\beta(d_2^2 - 2d_1\gamma) + \gamma(d_2^2 - 2d_1\beta)]^2 - d_2^4\gamma(d_2^2 - 2d_1\gamma) \\ &= 2d_1\beta^2(d_2^2 - 2d_1\gamma)^2 + \gamma[4d_1\beta(d_2^2 - 2d_1\beta) \\ &\quad - d_2^4](d_2^2 - 2d_1\gamma) + 2d_1\gamma^2(d_2^2 - 2d_1\beta)^2. \end{aligned} \tag{F.11}$$

Hence, Δ_1 is a parabola with respect to $(d_2^2 - 2d_1\gamma)$, going upward. Its axis of symmetry is

$$\begin{aligned} & -\frac{\gamma[4d_1\beta(d_2^2 - 2d_1\beta) - d_2^4]}{4d_1\beta^2} \\ & = \frac{\gamma}{4d_1\beta^2} \left[(d_2^2 - 2d_1\beta)^2 + 4(d_1\beta)^2 \right] > 0. \end{aligned} \quad (\text{F.12})$$

The discriminant of the quadratic equation corresponding to this parabola is

$$\begin{aligned} \Delta_2 & = \gamma^2 [4d_1\beta(d_2^2 - 2d_1\beta) - d_2^4]^2 - 16d_1^2\beta^2\gamma^2(d_2^2 - 2d_1\beta)^2 \\ & = d_2^8\gamma^2 - 8d_1d_2^4\beta\gamma^2(d_2^2 - 2d_1\beta) \\ & = d_2^4\gamma^2(d_2^2 - 4d_1\beta)^2 > 0, \end{aligned} \quad (\text{F.13})$$

which means that Δ_1 has two intersections on the horizontal axis. It is easy to obtain the smaller one is

$$d_2^2 - 2d_1\gamma = 4d_1\gamma. \quad (\text{F.14})$$

However, $d_2^2 < 4d_1\gamma$; that is, $d_2^2 - 2d_1\gamma < 2d_1\gamma$. Therefore, within the range, Δ_1 is always positive; that is, $\Delta > 0$. It follows that $f(\theta)$ has two intersections on the horizontal axis. And, both the axis of symmetry and intercept on the vertical axis of $f(\theta)$ are positive. Its two intercepts on the horizontal axis are positive. Here, $d_2^2 \leq 4d_1\gamma$, so $d_2^2\gamma \leq 4d_1\gamma^2$. Then,

$$\begin{aligned} & 8d_1\beta[(\beta + \gamma)d_2^2 - 4d_1\beta\gamma] - 2\gamma d_2^4 \\ & = 2\gamma d_2^2(4d_1\beta - d_2^2) - 8d_1\beta^2(4d_1\gamma - d_2^2) \\ & < 8d_1\gamma^2(4d_1\beta - d_2^2) - 8d_1\beta^2(4d_1\gamma - d_2^2) \\ & = 8d_1(\gamma - \beta)[4d_1\beta\gamma - d_2^2(\gamma + \beta)] \\ & < 0, \end{aligned} \quad (\text{F.15})$$

and $8d_1\beta[(\beta + \gamma)d_2^2 - 4d_1\beta\gamma] < 2\gamma d_2^4$, namely, $\theta_1 < 1$. Thus, $\theta \in [\theta_1, \min\{\theta_2, 1\}]$. Based on the above analysis, Conclusion 9 holds.

G. Proof of Conclusion 10

It follows from Conclusion 1 and 2 that the online channel produces the same carbon emission as the offline one. We only need to compare the demand in these two modes.

$$\begin{aligned} q_1 & = (Q - Cd_1)d_1\gamma = Qd_1\gamma - Cd_1^2\gamma, \\ q_2 & = \frac{2\beta}{4d_1\beta - \theta d_2^2} Qd_1 - \frac{Cd_1}{2(1 - \theta)}, \\ \frac{2\beta}{4d_1\beta - \theta d_2^2} & \in \left(\frac{1}{2d_1}, \frac{2\beta}{4d_1\beta - d_2^2} \right), \quad 0 < \theta < 1. \end{aligned} \quad (\text{G.1})$$

Based on the fact that Q is a large enough positive number, after comparing the expression of q_1 and q_2 , we have

$$\begin{aligned} q_1 & < q_2, \quad \text{if } \gamma < \frac{1}{2d_1}, \\ q_1 & > q_2, \quad \text{if } \gamma > \frac{2\beta}{4d_1\beta - d_2^2}, \end{aligned} \quad (\text{G.2})$$

$q_1 > q_2$ in the beginning and then $q_1 < q_2$ if $(1/2d_1) \leq \gamma \leq (2\beta/(4d_1\beta - d_2^2))$. Thus, Conclusion 10 holds.

Data Availability

The data used to support the findings of this research are included within this paper.

Conflicts of Interest

The authors declare that they have no conflicts of interest.

Acknowledgments

This paper was supported financially by the Philosophy and Social Science Project of Shandong Province (19BJCJ12).

References

- [1] Y. Wang, Z. Yu, and L. Shen, "Study on the decision-making and coordination of an e-commerce supply chain with manufacturer fairness concerns," *International Journal of Production Research*, vol. 57, no. 9, pp. 2788–2808, 2019.
- [2] Y. Wang, R. Fan, L. Shen, and W. Miller, "Recycling decisions of low-carbon e-commerce closed-loop supply chain under government subsidy mechanism and altruistic preference," *Journal of Cleaner Production*, vol. 259, Article ID 120883, 2020.
- [3] D. Zhou, X. Liang, Y. Zhou, and K. Tang, "Does emission trading boost carbon productivity? Evidence from China's pilot emission trading scheme," *International Journal of Environmental Research and Public Health*, vol. 17, no. 15, p. 5522, 2020.
- [4] D. Nong, S. Meng, and M. Siriwardana, "An assessment of a proposed ETS in Australia by using the MONASH-Green model," *Energy Policy*, vol. 108, pp. 281–291, 2017.
- [5] I. Diaz-Rainey and D. J. Tulloch, "Carbon pricing and system linking: lessons from the New Zealand emissions trading scheme," *Energy Economics*, vol. 73, pp. 66–79, 2018.
- [6] J. Jaraite and C. Di Maria, "Did the EU ETS make a difference? An empirical assessment using Lithuanian firm-level data," *Energy Journal*, vol. 37, no. 1, pp. 1–23, 2016.
- [7] S. Benjaafar, Y. Li, and M. Daskin, "Carbon footprint and the management of supply chains: insights from simple models," *IEEE Transactions on Automation Science and Engineering*, vol. 10, no. 1, pp. 99–116, 2013.
- [8] X. Xu, P. He, H. Xu, and Q. Zhang, "Supply chain coordination with green technology under cap-and-trade regulation," *International Journal of Production Economics*, vol. 183, pp. 433–442, 2017.
- [9] B. Cheng, H. Dai, P. Wang, D. Zhao, and T. Masui, "Impacts of carbon trading scheme on air pollutant emissions in Guangdong province of China," *Energy for Sustainable Development*, vol. 27, pp. 174–185, 2015.
- [10] C. Springer, S. Evans, J. Lin, and D. Roland-Holst, "Low carbon growth in China: the role of emissions trading in a

- transitioning economy,” *Applied Energy*, vol. 235, pp. 1118–1125, 2019.
- [11] Y. Hu, S. Ren, Y. Wang, and X. Chen, “Can carbon emission trading scheme achieve energy conservation and emission reduction? Evidence from the industrial sector in China,” *Energy Economics*, vol. 85, Article ID 104590, 2020.
- [12] Y. Zhang, S. Li, T. Luo, and J. Gao, “The effect of emission trading policy on carbon emission reduction: evidence from an integrated study of pilot regions in China,” *Journal of Cleaner Production*, vol. 265, Article ID 121843, 2020.
- [13] L. Liu, C. Chen, Y. Zhao, and E. Zhao, “China’s carbon-emissions trading: overview, challenges and future,” *Renewable and Sustainable Energy Reviews*, vol. 49, pp. 254–266, 2015.
- [14] J. Jiang, D. Xie, B. Ye, B. Shen, and Z. Chen, “Research on China’s cap-and-trade carbon emission trading scheme: overview and outlook,” *Applied Energy*, vol. 178, pp. 902–917, 2016.
- [15] A. Caparrós, J.-C. Péreau, and T. Tazdaït, “Emission trading and international competition: the impact of labor market rigidity on technology adoption and output,” *Energy Policy*, vol. 55, pp. 36–43, 2013.
- [16] Y. Cheng, D. Mu, and Y. Zhang, “Mixed carbon policies based on cooperation of carbon emission reduction in supply chain,” *Discrete Dynamics in Nature and Society*, vol. 2017, Article ID 4379124, 11 pages, 2017.
- [17] W. T. Chen, Y. P. Li, G. H. Huang, X. Chen, and Y. F. Li, “A two-stage inexact-stochastic programming model for planning carbon dioxide emission trading under uncertainty,” *Applied Energy*, vol. 87, no. 3, pp. 1033–1047, 2010.
- [18] Q. Pang, M. Li, T. Yang, and Y. Shen, “Supply chain coordination with carbon trading price and consumers’ environmental awareness dependent demand,” *Mathematical Problems in Engineering*, vol. 2018, Article ID 8749251, 11 pages, 2018.
- [19] Z. Wang and Q. Wu, “Carbon emission reduction and product collection decisions in the closed-loop supply chain with cap-and-trade regulation,” *International Journal of Production Research*, vol. 2020, Article ID 1762943, 2020.
- [20] L. Xu, C. Wang, and J. Zhao, “Decision and coordination in the dual-channel supply chain considering cap-and-trade regulation,” *Journal of Cleaner Production*, vol. 197, pp. 551–561, 2018.
- [21] L. Liu, L. Feng, B. Xu, and W. Deng, “Operation strategies for an omni-channel supply chain: who is better off taking on the online channel and offline service?” *Electronic Commerce Research and Applications*, vol. 39, Article ID 100918, 2020.
- [22] A. Dumrongsir, M. Fan, A. Jain, and K. Moinszadeh, “A supply chain model with direct and retail channels,” *European Journal of Operational Research*, vol. 187, no. 3, pp. 691–718, 2008.
- [23] P. He, Y. He, and H. Xu, “Channel structure and pricing in a dual-channel closed-loop supply chain with government subsidy,” *International Journal of Production Economics*, vol. 213, pp. 108–123, 2019.
- [24] Y. He, H. Huang, and D. Li, “Inventory and pricing decisions for a dual-channel supply chain with deteriorating products,” *Operational Research*, vol. 20, no. 3, pp. 1461–1503, 2020.
- [25] R. Batarfi, M. Y. Jaber, and S. Zaroni, “Dual-channel supply chain: a strategy to maximize profit,” *Applied Mathematical Modelling*, vol. 40, no. 21–22, pp. 9454–9473, 2016.
- [26] W. S. Yoo and E. Lee, “Internet channel entry: a strategic analysis of mixed channel structures,” *Marketing Science*, vol. 30, no. 1, pp. 29–41, 2011.
- [27] F. Bernstein, J.-S. Song, and X. Zheng, ““Bricks-and-mortar” vs. “clicks-and-mortar”: an equilibrium analysis,” *European Journal of Operational Research*, vol. 187, no. 3, pp. 671–690, 2008.
- [28] F. Gao and X. Su, “Omnichannel retail operations with buy-online-and-pick-up-in-store,” *Management Science*, vol. 63, no. 8, pp. 2478–2492, 2017.
- [29] S. Gallino and A. Moreno, “Integration of online and offline channels in retail: the impact of sharing reliable inventory availability information,” *Management Science*, vol. 60, no. 6, pp. 1434–1451, 2014.
- [30] X. Chen, X. Wang, and X. Jiang, “The impact of power structure on the retail service supply chain with an O2O mixed channel,” *Journal of the Operational Research Society*, vol. 67, no. 2, pp. 294–301, 2016.
- [31] X. Jia, “Decision-making of online channels under three power structures,” *Measurement & Control*, vol. 53, no. 3–4, pp. 296–310, 2020.
- [32] H. Li, K. Leng, Q. Qing, and S. X. Zhu, “Strategic interplay between store brand introduction and online direct channel introduction,” *Transportation Research Part E: Logistics and Transportation Review*, vol. 118, pp. 272–290, 2018.
- [33] P. Zhang, Y. He, and C. Shi, “Retailer’s channel structure choice: online channel, offline channel, or dual channels?” *International Journal of Production Economics*, vol. 191, pp. 37–50, 2017.
- [34] Q. Lu and N. Liu, “Pricing games of mixed conventional and e-commerce distribution channels,” *Computers & Industrial Engineering*, vol. 64, no. 1, pp. 122–132, 2013.
- [35] X. Pu, L. Gong, and X. Han, “Consumer free riding: coordinating sales effort in a dual-channel supply chain,” *Electronic Commerce Research and Applications*, vol. 22, pp. 1–12, 2017.
- [36] A. A. Tsay and N. Agrawal, “Channel conflict and coordination in the E-commerce age,” *Production and Operations Management*, vol. 13, no. 1, pp. 93–110, 2004.
- [37] Q. Han and Y. Wang, “Decision and coordination in a low-carbon e-supply chain considering the manufacturer’s carbon emission reduction behavior,” *Sustainability*, vol. 10, no. 5, p. 1686, 2018.
- [38] Q. Li and B. Li, “Dual-channel supply chain equilibrium problems regarding retail services and fairness concerns,” *Applied Mathematical Modelling*, vol. 40, no. 15–16, pp. 7349–7367, 2016.
- [39] Q. Han, Y. Wang, L. Shen, and W. Dong, “Decision and coordination of low-carbon e-commerce supply chain with government carbon subsidies and fairness concerns,” *Complexity*, vol. 2020, Article ID 1974942, 19 pages, 2020.
- [40] A. Nair and R. Narasimhan, “Dynamics of competing with quality- and advertising-based goodwill,” *European Journal of Operational Research*, vol. 175, no. 1, pp. 462–474, 2006.
- [41] C.-H. Wu, “Price and service competition between new and remanufactured products in a two-echelon supply chain,” *International Journal of Production Economics*, vol. 140, no. 1, pp. 496–507, 2012.
- [42] P. He, Y. He, C. Shi, H. Xu, and L. Zhou, “Cost-sharing contract design in a low-carbon service supply chain,” *Computers & Industrial Engineering*, vol. 139, Article ID 106160, 2020.

Research Article

Decisions of E-Commerce Supply Chain under Consumer Returns and Different Power Structures

Liang Shen,¹ Runjie Fan,¹ and Yuyan Wang^{1,2}

¹School of Public Finance and Taxation, Shandong University of Finance and Economics, Jinan, Shandong 250014, China

²School of Management Science and Engineering, Shandong University of Finance and Economics, Jinan, Shandong 250014, China

Correspondence should be addressed to Yuyan Wang; wangyuyan1224@126.com

Received 22 September 2020; Revised 8 October 2020; Accepted 24 October 2020; Published 16 November 2020

Academic Editor: Ming Bao Cheng

Copyright © 2020 Liang Shen et al. This is an open access article distributed under the Creative Commons Attribution License, which permits unrestricted use, distribution, and reproduction in any medium, provided the original work is properly cited.

Considering the growing phenomenon of consumer returns and channel power struggles in e-commerce supply chains (ESCs), the ESC model is constructed and its equilibrium solutions are calculated and compared. Further, the consumer utility function is constructed to explore the impact of returns and dominant enterprises on consumer utility. Based on this, the “return cost-sharing and commission readjusting” contract is designed to maximize both ESC and consumer utility. Finally, the paper validates and further analyzes conclusions through numerical simulation. The main conclusions are as follows: higher return rates and return handling costs will reduce market demand and ESC profits, while higher salvage value of returned products will have a positive impact on ESC, but the above factors will not affect the online service level under decentralized decisions. The impact of consumer’s service quality preferences on manufacturer’s profits and e-commerce platform’s profit is determined by channel power structure. The impact of return rate on consumer utility depends on two factors: the decision-making model and the hidden cost of consumer returns.

1. Introduction

With the high growth of the network economy, more and more products are sold through online channels, which has led to the formation of the e-commerce supply chain (ESC). In recent years, the e-commerce platform (as e-platform) has emerged as a reliable information center and trading platform in ESC. Through the e-platform, products are sold directly by manufacturers to consumers, which broadens the direct sales model in ESC. This direct sales model brings multiple benefits to manufacturers. On the one hand, due to the low entry barriers and price advantages of e-platforms, manufacturers’ operational costs can be reduced and their scale is no longer limited by space [1, 2]. On the other hand, e-platforms enable manufacturers to reach a larger number of customer segments [3] and make them obtain consumer feedback and adjust their corporate strategies timely [4, 5], which ultimately brings increased economic benefits to manufacturers. For consumers, the rapid development of

ESC increases their shopping flexibility [6], expands their shopping options [7], and reduces their travel time and cost [8]. As a result, more and more manufacturers are entering e-platforms and more and more consumers are buying online. FTI consulting forecasts e-commerce sales to exceed \$1 trillion in 2027 [9], which means that ESC has not only economic and operational advantages but also broad growth prospects.

However, the development of ESC has exacerbated consumer returns. Customer returns have always been a serious problem for traditional supply chains [10, 11], while online sales have higher return rates than offline store sales [12–14]. Invesp infographics statistics show that the return rate for brick-and-mortar stores is 8.89%, while online order products have a return rate of more than 30% [15]. More seriously, return rates will be higher in the aftermath of major promotions, such as “Black Friday” in US and “Double Eleven” in China [16]. The above phenomenon is partly because online shoppers cannot access products,

which increases the inaccuracy of their predictions for product value. Alternatively, the e-commerce sales environment is very complex, where false information and fake reviews can induce consumers to make incorrect choices. Additionally, the return regulations for commodities have become the primary consideration when consumers shopping online [17–19]. As a result, most e-platforms and manufacturers deliver return services. The delivery of return services can enable manufacturers, especially fashion manufacturers, to keep abreast of customer feedback and form a competitive advantage [20, 21], alleviating consumers' concerns about valuation uncertainty [22], and increase consumer willingness to buy instantly [23, 24] and the likelihood of repeat purchases on the platform in the future [25, 26]. However, serious consumer returns will inevitably result in loss of profits for manufacturers, influencing pricing and other decisions of ESC participants, and bring greater risks for the management of ESC operations. Therefore, incorporating consumer returns into ESC's decision-making and exploring its impact on ESC members and systems is a very realistic study that needs to be developed.

In addition, manufacturers introducing online direct sales channels will face competition from e-platforms for channel power. Unlike dual-channel supply chains where manufacturers set up online sales channels, in ESC, both manufacturers and e-platforms have channel power [27]. Nowadays, the power of e-platforms is growing, and the phenomenon of the transfer of the dominant power from manufacturers to e-platforms has emerged in ESC. For well-known manufacturers (e.g., Apple, P&G, and Galanz), they still manage to maintain their ESC dominance. However, for some small- and medium-sized manufacturers, they are already at a disadvantage in cooperating with some powerful e-platforms (e.g., Amazon, JD, and Taobao) because such platforms have formed a large user base and have well-developed entry rules. Different channel power structures will certainly have an impact on ESCs' decisions and profits and further influence consumer return behavior and purchase utility. Which channel power structure is more conducive to the stable operation of the ESC? How do ESC participants in different channel power structures make decisions to maximize their profits? Do consumer returns affect ESC or consumer utility differently under different channel power structures? The existing research does not provide clear answers to these questions. Therefore, this paper explores the optimal solution to ESC under different channel power structures and draws conclusions on the impact of channel power structure on ESC efficiency and consumer utility.

In the ESC, the increase in returns and the instability of dominant enterprise have become issues that every ESC member has to face when they make decisions. To clarify these issues, the article researches the following aspects:

- (1) Considering consumer returns and channel power, what are the optimal decisions for each ESC member? What is the impact of returns on ESC?

- (2) How does the channel power structure of ESC affect the decisions of ESC members? Under different channel powers, do the returns-related variables and consumer preferences affect ESC differently? Which channel power structure is most profitable for members and ESC?
- (3) Many consumers are addicted to returning goods, is the behavior of returning goods beneficial to consumers themselves? How do return rates and consumer's service quality preferences affect consumer utility? What are the differences in consumer utility under different channel powers?
- (4) How can return handling costs and commissions be incorporated into the ESC coordination process? How to design a new contract to maximize ESC efficiency and consumer utility?

Based on the serious consumer returns of ESCs and considering the different channel power structures, the paper examines the impact of channel structures and consumer returns on ESC. Moreover, the paper establishes an extended model of consumer utility, studies the impact of return rates and consumer's service quality preferences on consumer utility, and seeks a balance between system performance and consumer utility. Finally, the return handling costs and commissions are considered, and new coordination mechanisms are designed to optimize ESC profits and maximize consumer utility. The main contributions are listed as follows:

- (1) The paper considers the independent e-platform as an ESC decision-maker and examines the influence of return-related variables on the e-platform's service level. Meanwhile, the influence of consumers' service quality preference on ESC and market demand is addressed. The study finds that, regardless of the channel power structure, the return rate does not affect the e-platform's service level (different from [28]). Increasing consumer service preferences will promote sales prices and service level (unlike [29]) and increase market demand and ESC profitability (unlike [30]). Differently, the effect of consumer service preferences on the profitability of manufacturer and e-platform depends on the channel power of ESC. Additionally, the paper on salvage value and return handling cost of returned products is not limited to the choice of return strategy and pricing (unlike [11, 31, 32]). The impact of salvage value and return handling costs on the e-platform's service level, market demand and return volume, ESC members, and system profits is also discussed.
- (2) In the context of consumer returns, the paper explores the impact of channel structures on ESC. Some conclusions are similar to the studies of Wang et al. [33] and Han and Wang [34], but several previously unavailable findings are found. First, the dominant manufacturer brings higher product market demand, which is facilitated by higher service level at this time. At the same time, the dominant

manufacturer also leads to a benign increase in consumer returns. Moreover, increased consumer's service quality preferences, regardless of the power structure, lead to higher profits for the manufacturer, but e-platform cannot always profit from consumer service preferences. When manufacturer dominates ESC, although the e-platform increased service investment due to the increase in consumer's service quality preferences, it could not profit from it.

- (3) In the paper, an extension model of consumer utility is constructed, and the effects of return rates, channel power structures, and consumer service preferences on consumer utility are explored. The conclusions differ from the existing literature, such as Yan et al., [35]; Zhang et al. [36]; Yan et al. [35]; and Ma et al., [16]. The paper found that return behavior does not always improve consumer utility. The impact of the return rate on consumer utility depends on two factors: the decision-making mode and the consumer's hidden cost of returns. Moreover, the study compares consumer utility under different power structures and finds that centralized decisions can maximize consumer utility. The influence of channel power and consumer service preference on consumer utility depends on consumer price preference and return rate.
- (4) Unlike the coordination mechanisms studied in previous literature, for ESCs with consumer returns, the study uses both commissions and return handling costs as adjustment tools to design a new "return cost-sharing and commission readjusting" contract. The contract maximizes ESC efficiency and consumer utility, which offers a new approach to the design of the ESC coordination mechanism.

The remainder of the study is designed below. The relevant literature is reviewed in Section 2. ESC model is described in Section 3. Section 4 presents and analyzes equilibrium solutions under different models. Section 5 constructs an extension model of consumer utility. Section 6 designs the "return cost-sharing and commission readjusting" contract to maximize system efficiency and consumer utility. Numerical analysis is given in Section 7 from different perspectives. Finally, Section 8 summarizes the paper and depicts management insights.

2. Literature Review

The paper aims to examine how ESC members under different power structures make decisions and coordinate when there is significant consumer return behavior in the e-commerce market. The study allows for a literature review of the three streams of consumer returns, channel power structure, and coordination mechanisms.

The first stream is consumer returns in supply chains. Currently, most of the relevant literature focuses on the study of consumer returns in traditional supply chains [37–39]. There are some scholars who have included manufacturers' or retailers' online sales channels in their

exploration of consumer returns. For example, Li et al. [40] discussed how consumer returns affect return policies, product quality, and pricing of the online direct sales manufacturer. Based on retailers' online sales channels and consumer returns, Balakrishnan et al. [41] examined the effects of consumers' transition from offline to online browsing on online pricing and profits. Considering the return policy, Batarfi et al. [42] demonstrated that a dual-channel strategy is more beneficial to chains. Ji et al. [43] paid attention to consumers' choice of return channels and investigated the return strategies in the dual-channel supply chain. Taleizadeh et al. [44] showed that consumer return decisions depend on the refund amount and product quality. Targeting cross-channel returns in dual-channel supply chains, Radhi and Zhang [45] and Radhi and Zhang [3] studied how the return phenomenon affects product pricing and sourcing, while He et al. [46] obtained ordering and pricing strategies for new and renovated products. Further, the issue of consumer returns has been incorporated into the research of ESCs where e-platforms are covered. For example, Ma et al. [16] found the extent to which return policies affect pricing and profits in relation to retailers' unit purchase costs and market return rates. Cao et al. [32] accounted for the channel choice of whether retailers should enter e-platforms and found that the choice mainly depends on the e-platform's annual service fee. From the above literature, few scholars have considered consumer returns in ESC. Although some scholars consider online sales channels, most of these channels are controlled by manufacturers or retailers and no e-platform is included. Among them, Ma et al. [16] defined an independent e-platform, but they are targeted at the choice of return policies, which differs significantly from the research direction of this study.

The second stream is the channel power structure in supply chains. Currently, channel structure's impact on channel management [47, 48], pricing [8, 49], and system performance [50, 51] has been fully explored in supply chains. The study highlights a review of the literature on power structures in ESCs. In ESC's channel power study, most of the literature considers manufacturers' online sales channels. For example, Taleizadeh et al. [30] developed a two-echelon ESC composed of two manufacturers and retailers, where both manufacturers have online sales channels. This study showed that the channel power structure determines the maximum profit of ESC. Similarly, Zhao et al. [52] examined how channel power affects system profits, but they assumed that only one manufacturer had the online sales channel. This study found that leading manufacturers opening the online sales channel will lose their own profits. Focusing on the power struggle between manufacturers and retailers, Ke et al. [53] and Chun and Park [54] examined how channel structures affect pricing strategies and manufacturers' marketing strategies, respectively. There are a few pieces of literature that consider retailers' online sales channels. For example, Chen et al. [55] constructed an O₂O hybrid dual-channel model and investigated how channel power affects pricing and financial performance. Basak et al. [56] explored how showrooming affects traditional and online retailers under different power

structures. However, in previous literature, they do not regard the independent e-platform as a decision-making subject, much less consider the channel power struggle between e-platforms and manufacturers. More relevant to this study, Wang et al. [27] and Liu and Ke [57] researched the impact of power structures between manufacturers and e-platforms on product pricing, but neither of them considered the serious consumer returns in ESC.

The third stream is the coordination mechanism in supply chains. For supply chains with consumer returns, Xu et al. [58] considered different return periods and proposed differentiated repurchase contracts to achieve supply chain coordination. Heydari and Ghasemi [59] designed revenue-sharing contracts and realized risk sharing and profit growth for reverse supply chain members based on the uncertainty of return product quality. Wang et al. [38] explored how suppliers can coordinate supply chains with returns through options pricing. Further, addressing the more complex issue of returns in the online channel, Yan and Pei [60] constructed an O₂O competition model and developed revenue-sharing contracts to resolve the conflict of returns policies in dual-channel supply chain. Focusing on loss-averse consumer returns, Gu et al. [61] used revenue and cost-sharing contracts to achieve dual-channel fresh agricultural product ESC coordination and captured Pareto improvement areas for suppliers and e-tailers under coordinated conditions. Recognizing the infringement of suppliers' online sales channels on retailers' offline sales, Li and Jiang [22] studied the return strategy and realized a dual-channel supply chain coordination through the two-part tariff contract. The above literature provides the basis for this paper, but they cannot achieve ESC coordination with independent e-platforms.

For supply chains with online channels, Liu et al. [62] mitigated courier capacity overload through option covenants in the supply chain of online retailers. Song and He [63] studied the coordination mechanism of fresh ESC and showed that the cost-sharing contract for preservation efforts will lead to lower demand, but the cost-sharing revenue-sharing contract can effectively coordinate ESC. Amrouche et al. [64] considered online retailers and analyzed the effectiveness of different cooperation mechanisms (minimum pricing strategy, omnichannel price, and revenue-sharing cooperation) in different ESC environments. However, this literature does not integrate e-platforms into coordinated studies of ESC. Incorporating e-platforms into the decision-making process of ESC, Dong et al. [65] found that the revenue-sharing pacts can coordinate ESC in demand determination situations, but transfer payments are required. Zhang et al. [66] found that revenue-sharing pacts allow the leader-follower structure in e-commerce logistics systems to be coordinated. Similarly, Zhong et al. [67] demonstrated that revenue-sharing pacts allow optimizing the profitability of three-echelon logistics service supply chains. In contrast to the coordination mechanisms mentioned above, carbon cost sharing is used to achieve low-carbon ESC coordination in Han and Wang [34]. These papers provide a great deal of research for ESC coordination but do not address the unique profitability mode of e-platforms, that is, charging commissions, which is the core

of the coordination mechanism in this paper. The research of Wang et al. [33] and Wang et al. [68] needs to be highlighted. They used commissions as an adjustment tool, established cost-sharing joint commission contracts, and coordinated ESCs with fairness concerns and altruistic concerns. However, they did not study the flood of consumer returns in the ESC.

It can be seen from the above literature that the previous research only considers one or more of the below factors, such as online sales channels, channel power, customer returns, service level, and coordination contract. The paper synthesizes the above factors and examines the effect of consumer returns on ESC and consumer utility under different channel powers. Additionally, product pricing and e-platform service inputs under different power structures are decided, and an ESC coordination contract is designed in the return environment. The specific differences between this paper and other studies are summarized in Table 1.

3. Model Description

In this study, an ESC consisting of a manufacturer (called he) and an e-platform (called she) is proposed. In the Taobao (<http://www.taobao.com>) platform's basic operating mode, consumers' purchase and return information is conveyed and confirmed through the platform, but the actual delivery and return logistics do not go through the platform. Thus, the model is constructed as follows. In ESC, the manufacturer releases the product information through e-platform, from which products can be directly sold to consumers. For consumers, when they want to perform a return, they can apply for a return through e-platform and return products directly to the manufacturer. After that, the manufacturer who received the returned product will refund the full payment to the consumer. Such a sales and return model is used extensively in JD (not self-managed), Amazon (FBM), and Pinduoduo. At the same time, the operational model is in line with the operational framework of existing research [32, 69, 70]. The model structure is shown in Figure 1.

When a manufacturer enters an independent e-platform, it not only defrays fixed fees such as fixed technical fees and deposits but also pays commissions based on sales volume. Moreover, commissions will vary depending on the brand and type of product. Of course, the services provided by the e-platform for manufacturers will also be different depending on the commission. These services mainly include the quantity and time of advertising for products, the quality of service for quick returns and exchanges, booths in online stores, sales agency operation, storage services, logistics services, payment services, after-sales service, and credit maintenance. It can be seen from the above information that the research for commissions is more meaningful than that for the fixed fee paid by the manufacturer. Therefore, models are simplified in this paper to better analyze e-platform's service level. That is, fixed costs are ignored, while the unit commission is used as a parameter. The notations and assumptions used in the paper are shown in Table 2.

TABLE 1: Papers that are most related to our research.

Author	Online sales channels	Channel power	Customer returns	Service level	Coordination contract
Yan and Pei [60]	√		√		√
Gu et al. [61]	√		√		√
Xu et al. [37]			√		√
Radhi and Zhang [45]	√	√	√		
Radhi and Zhang [3]	√		√		
He et al. [46]	√		√		
Wang et al. [38]			√		√
Zhang et al. [8]	√		√		√
Ma et al. [16]	√ (e-platform is included)		√		
Li and Jiang [22]	√		√		√
Taleizadeh et al. [30]	√	√			
Zhao et al. [52]	√	√			
Ke et al. [53]	√	√			
Wang et al. [27]	√ (e-platform is included)	√		√	
Chun and Park [54]	√	√			
Liu and Ke [57]	√ (e-platform is included)	√			
Wang et al. [33]	√ (e-platform is included)			√	√
Han and Wang [34]	√ (e-platform is included)			√	√
Wang et al. [68]	√ (e-platform is included)			√	√
This paper	√ (e-platform is included)	√	√	√	√

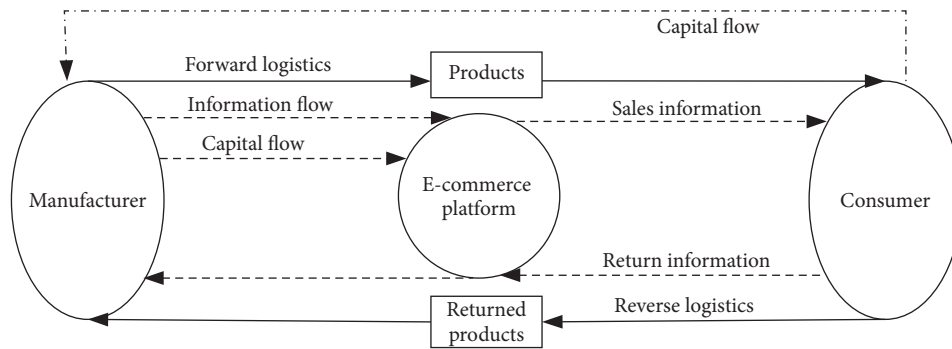


FIGURE 1: The model structure of ESC.

4. Model Formulation and Equilibrium Solutions

4.1. *A Benchmark: Centralized Model.* In this section, centralized decision-making is presented as a benchmark. Under this model, manufacturer and e-platform make decisions to maximize ESC profits. ESC's decision function is

$$\max_{p,s} \pi = pD + (w - h)\epsilon Q - cQ - ks^2. \quad (1)$$

According to equation (1), Hessian matrix of $\pi(p, s)$ is derived as $H = \begin{bmatrix} \partial^2 \pi / \partial^2 p & \partial^2 \pi / \partial p \partial s \\ \partial^2 \pi / \partial s \partial p & \partial^2 \pi / \partial^2 s \end{bmatrix} = \begin{bmatrix} -2\beta & \gamma \\ \gamma & -k \end{bmatrix}$. Since $2k\beta - \gamma^2 > 0$, the optimal solution of $\pi(p, s)$ exists. The equilibrium solutions can be obtained by $\partial\pi/\partial p = 0$ and $\partial\pi/\partial s = 0$, as shown in Table 3.

4.2. *Decentralized Models.* Due to the accelerated development of network economy and communication technology, channel power of e-platforms is growing. In recent years, a transfer in ESC dominance from manufacturers to

e-platforms has been observed. Currently, there are two different channel power structures in the ESC: ESC with dominant manufacturer and ESC with dominant e-platform. These channel power structures are modeled and analyzed as follows:

Manufacturer's profit:

$$\pi_m = (p - \rho)D + (w - h)\epsilon Q - cQ. \quad (2)$$

E-platform's profit:

$$\pi_e = \rho D - ks^2. \quad (3)$$

System profit of ESC:

$$\pi = pD + (w - h)\epsilon Q - cQ - ks^2. \quad (4)$$

4.2.1. *Decentralized Model with Dominant Manufacturer.* If the manufacturer is more powerful, he will dominate ESC and become the leader (first mover in decision-

TABLE 2: Notations description.

Notations	Description
p	The sales price of products (decision variable for manufacturer).
c	The unit production cost of products.
ρ	The unit commission paid by manufacturer.
ε	The consumer return rate. According to Ma et al. [16], $0 < \varepsilon < 1$.
h	The return handling cost of the manufacturer. Referring to Xia et al. [71], assuming $h < w$, it means that it is profitable for the manufacturer to process customer returns.
w	The average salvage value of the returned products, which can be obtained through remanufacturing or secondary market sales. Based on Chen and Chen [11], $w < c$.
s	The service level of e-platform (decision variable for e-platform). According to Shen et al. [72] and Li et al. [73], the service investment cost can be described as $C(s) = ks^2$, where $k(k > 0)$ is the elasticity coefficient of service investment cost.
D	The market demand for products. Similar to Xie et al. [74] and Li et al. [75], this study assumes that the demand function is $D = \alpha - \beta p + \gamma s$, in which $\alpha(\alpha > 0)$ represents the maximum demand in the potential market and $\beta(\beta > 0)$ and $\gamma(\gamma > 0)$ indicate consumers' price preferences and consumers' service quality preferences, respectively. Moreover, $\alpha(1 - \varepsilon) > \beta > \gamma > 0$, which means that it is profitable for manufacturers to enter the market and consumers' preference for sales price over their preference for service level.
Q	The actual sales of products. According to Radhi and Zhang [45] and Reimann [76], the study presumes that the actual sales volume of product is $Q = D/(1 - \varepsilon)$.
R	Volume of returns by consumers, and $R = Q - D = (\varepsilon D)/(1 - \varepsilon)$.
e, m	e represents the e-platform and m represents the manufacturer.
c^*, m^*, e^*	c^* stands for centralized decision-making, m^* stands for decentralized decision-making by manufacturer, and e^* stands for decentralized decision-making led by e-platform.
π_i^n	Profit of decision-maker i under n , $i = e, m$, $n = c^*, m^*, e^*$.
π^n	Total profit of ESC system under n , $n = c^*, m^*, e^*$.
Remarks	<p>(1) Based on Chang and Yeh [77] and Scheriau, [78], the return handling cost is covered by manufacturer, and manufacturer implements a full refund policy for consumers.</p> <p>(2) During the actual operation of ESC, return orders are generally not counted as manufacturer sales. Therefore, the e-platform calculates sales based on completed and nonreturned orders.</p> <p>(3) According to Wang et al. [79], the commission is set up earlier than the ESC decision. The commission appears as an exogenous variable in the paper.</p> <p>(4) To make the study meaningful, assume $2k\beta - \gamma^2 > 0$.</p>

making) in working with smaller e-platforms. In this situation, both manufacturer and e-platform, as an independent economy, make decisions to maximize their own benefits. Based on this, manufacturer-led Stackelberg is formed; that is, manufacturer first determines p according to the market demand. e-platform then decides s .

Equilibrium solutions can be solved by the backward induction method. Due to $\partial^2 \pi_e / \partial s^2 = -2k < 0$, π_e is a concave function of s . By $\partial \pi_e / \partial s = 0$, s^{m^*} can be obtained. Substituting s^{m^*} into π_m , since $\partial^2 \pi_m / \partial p^2 = -2\beta < 0$, π_m is a concave function of p . Solving $\partial \pi_m / \partial p = 0$, p^{m^*} can be solved. Then, the equilibrium solutions of the model can be obtained, as shown in Table 3.

4.2.2. Decentralized Model with Dominant E-Platform.

When large third-party e-platforms (Tmall, JD, Amazon, etc.) form ESCs with small- or medium-sized manufacturers, e-platforms generally dominate ESCs. In the decision-making process, e-platform takes the lead in deciding s , followed by manufacturer in deciding p . Based on backward induction method (the solution is the same as 4.2.1), the optimal decisions can be obtained in Table 3.

4.3. Comparative Analysis. In this section, the comparative analysis of models is presented for two purposes. On the one

hand, the impact of changes in return-related parameters on ESC decisions and profits can be obtained. On the other hand, the impact of the channel power structure on ESC and the volume of returns can also be explored. Comparing and analyzing equilibrium solutions, Conclusions 1–5 can be obtained.

Conclusion 1

- (1) p^{c^*} , p^{m^*} , and p^{e^*} are positively related to ε ; D^{c^*} , D^{m^*} , and D^{e^*} are negatively related to ε ; R^{c^*} , R^{m^*} , and R^{e^*} are positively related to ε ; $\pi_m^{m^*}$, $\pi_e^{m^*}$, $\pi_m^{e^*}$, $\pi_e^{e^*}$, π^{c^*} , π^{m^*} , and π^{e^*} are negatively related to ε .
- (2) s^{c^*} is negatively related to ε , but s^{m^*} and s^{e^*} are independent of ε .

See Appendix A for proof.

According to Conclusion 1, one has the following:

- (1) In ESC, higher product return rates result in higher sales prices, lower market demand, and higher volume of returns, which ultimately results in lower profits for manufacturer, e-platform, and ESC system. This is because the increase in the return rate causes higher return handling fees for the manufacturer, which results in higher total operating costs for him. To compensate for lost

TABLE 3: Optimal solution of different models.

	Centralized model	Manufacturer dominant ESC	E-platform dominant ESC
Sales price	$p^c = 2k\alpha(1-\epsilon) - (2k\beta - \gamma^2)(w\epsilon - h\epsilon - c)/(4k\beta - \gamma^2)(1-\epsilon)$	$p^{ms} = (2\alpha k + \gamma^2\rho)(1-\epsilon) - 2k\beta(w\epsilon + \epsilon\rho - h\epsilon - \rho - c)/4k\beta(1-\epsilon)$	$p^{es} = (4\alpha k + \gamma^2\rho)(1-\epsilon) - 4k\beta(w\epsilon + \epsilon\rho - h\epsilon - \rho - c)/8k\beta(1-\epsilon)$
Service level	$s^{c*} = \gamma[\alpha(1-\epsilon) + \beta(w\epsilon - h\epsilon - c)]/(4k\beta - \gamma^2)(1-\epsilon)$	$s^{ms*} = \gamma\rho/2k$	$s^{es*} = \gamma\rho/4k$
Market demand	$D^c = 2k\beta[\alpha(1-\epsilon) + \beta(w\epsilon - h\epsilon - c)]/(4k\beta - \gamma^2)(1-\epsilon)$	$D^{ms} = (2\alpha k + \gamma^2\rho)(1-\epsilon) + 2k\beta(w\epsilon + \epsilon\rho - h\epsilon - \rho - c)/4k(1-\epsilon)$	$D^{es} = (4\alpha k + \gamma^2\rho)(1-\epsilon) + 4k\beta(w\epsilon + \epsilon\rho - h\epsilon - \rho - c)/8k(1-\epsilon)$
Volume of returns	$R^c = 2k\beta\epsilon[\alpha(1-\epsilon) + \beta(w\epsilon - h\epsilon - c)]/(4k\beta - \gamma^2)(1-\epsilon)^2$	$R^{ms} = (2\alpha k + \gamma^2\rho)(1-\epsilon)\epsilon + 2k\beta\epsilon(w\epsilon + \epsilon\rho - h\epsilon - \rho - c)/4k(1-\epsilon)^2$	$R^{es} = (4\alpha k + \gamma^2\rho)(1-\epsilon)\epsilon + 4\beta k\epsilon(w\epsilon + \epsilon\rho - h\epsilon - \rho - c)/8k(1-\epsilon)^2$
Manufacturer's profit	---	$\pi_m^{ms} = [(2\alpha k + \gamma^2\rho)(1-\epsilon) + 2k\beta(w\epsilon + \epsilon\rho - h\epsilon - \rho - c)]^2/16k^2\beta(1-\epsilon)^2$	$\pi_m^{es} = [(\gamma^2\rho + 4\alpha k)(1-\epsilon) + 4k\beta(w\epsilon + \epsilon\rho - h\epsilon - \rho - c)]^2/64k^2\beta(1-\epsilon)^2$
E-platform's profit	---	$\pi_e^{ms} = \alpha\rho(1-\epsilon) + \beta\rho(w\epsilon + \epsilon\rho - h\epsilon - \rho - c)/2(1-\epsilon)$	$\pi_e^{es} = (8\alpha k\rho + \gamma^2\rho^2)(1-\epsilon) + 8\beta k\rho(w\epsilon + \epsilon\rho - h\epsilon - \rho - c)/16k(1-\epsilon)$
System profit of ESC	$\pi^c = k[\alpha(1-\epsilon) + \beta(w\epsilon - h\epsilon - c)]^2/(4k\beta - \gamma^2)(1-\epsilon)^2$	$\pi^{ms} = [(2\alpha k + \gamma^2\rho)(1-\epsilon) + 2k\beta(w\epsilon + \epsilon\rho - h\epsilon - \rho - c)]^2/16k^2\beta(1-\epsilon)^2 + \alpha\rho(1-\epsilon) + \beta\rho(w\epsilon + \epsilon\rho - h\epsilon - \rho - c)/2(1-\epsilon)$	$\pi^{es} = [(\gamma^2\rho + 4\alpha k)(1-\epsilon) + 4k\beta(w\epsilon + \epsilon\rho - h\epsilon - \rho - c)]^2/64k^2\beta(1-\epsilon)^2 + (8\alpha k\rho + \gamma^2\rho^2)(1-\epsilon) + 8\beta k\rho(w\epsilon + \epsilon\rho - h\epsilon - \rho - c)/16k(1-\epsilon)$

profits from increased costs, the first response from the manufacturer is to increase the products' sales price. This behavior will lead some price-sensitive consumers to switch to other homogeneous products, thereby reducing market demand. At this point, the change direction of the volume of returns is not consistent with the market demand but showing an upward trend. This indicates that the increase in returns is primarily caused by higher return rates, which is a vicious increase in returns. In addition, while the manufacturer attempted to increase sales prices to increase profits, the additional profits generated do not cover profit losses due to declining market demand, which ultimately leads to lower manufacturer profits. Meanwhile, due to the e-platform's profit determined by the market demand, the decrease in demand also makes the e-platform profit decline.

- (2) Under decentralized models, the return rate does not affect service level. This is because the e-platform's service level under decentralized models is determined by the level of commission, which is established when manufacturer enters e-platform and is not affected by the decision results. Under the centralized model, the service level declines with higher return rates, because e-platform and manufacturer make decisions to maximize system profits at this point. When the product return rate increases, the ESC system, in order to minimize losses, will reduce the service cost of the e-platform, which will lead to a lower service level.

Conclusion 2. Optimal decisions are affected by the returned product's average salvage value of w as follows:

- (1) p^{c*} , p^{m*} , and p^{e*} are negatively related to w ; D^{c*} , D^{m*} , and D^{e*} are positively related to w ; R^{c*} , R^{m*} , and R^{e*} are positively related to w ; π_m^{m*} , π_e^{m*} , π_m^{e*} , π_e^{e*} , π^{c*} , π^{m*} , and π^{e*} are positively related to w .
- (2) s^{c*} is positively related to w , but s^{m*} and s^{e*} are independent of w .

The proof is similar to Conclusion 1.

According to Conclusion 2, one has the following:

- (1) In ESC, higher salvage value of returned products results in lower sales prices, higher market demand, and volume of returns, which ultimately results in higher profits for manufacturer, e-platform, and ESC system. This is because of the lower salvage value; the greater the profit loss caused by the return behavior to the manufacturer, the higher the sales price to compensate for the manufacturer's profit loss. Conversely, the higher the salvage value, the more the manufacturers cut prices to expand sales volumes. With a stable return rate, an increase in market demand will also lead to an uptick in the volume of returns, but this benign rise of returns will

not reduce manufacturer profits. Meanwhile, both manufacturers and e-platforms will be more profitable due to the increase in the actual sales of products.

- (2) Under decentralized models, the returned product's salvage value has no impact on the service level of e-platform. Differently, the service level increases with increasing salvage value in the centralized model. This is because, in the actual ESC operation, the commission is made in advance of the decision-making, and e-platform has no motivation to increase service inputs in the decision-making process. But when e-platforms work closely with manufacturers to reach centralized decisions, they make decisions to maximize ESC profits. At this point, the higher salvage value of the returned products brings higher profits to ESC, and the ESC system has an incentive to improve the service level.

Conclusion 3. Optimal decisions are affected by the return handling cost h as follows:

- (1) p^{c*} , p^{m*} , and p^{e*} are positively related to h ; D^{c*} , D^{m*} , and D^{e*} are negatively related to h ; R^{c*} , R^{m*} , and R^{e*} are negatively related to h ; π_m^{m*} , π_e^{m*} , π_m^{e*} , π_e^{e*} , π^{c*} , π^{m*} , and π^{e*} are negatively related to h .
- (2) s^{c*} is negatively related to h , but s^{m*} and s^{e*} are independent of h .

The proof is similar to Conclusion 1.

According to Conclusion 3, one has the following:

- (1) In ESC, higher return handling cost leads to higher sales prices, lower market demand, and volume of returns, which ultimately results in lower profits for manufacturer, e-platform, and ESC system. This shows that when the return handling cost is higher, manufacturer will transfer part of the return handling cost to consumers by raising sales price, which is unfavorable to consumers. This "cost transfer" phenomenon will cause a reduction in market demand, which will lead to a nonbenign reduction in the volume of returns. Further, lower market demand will also lead to lower profits for ESC members.
- (2) Under decentralized models, the return handling costs have no impact on the service level of e-platform. Differently, the service level decreases with increasing the return handling costs in the centralized model. This is the same as the genesis of Conclusions 1 and 2; that is, the service level is only affected by commissions, which are designated in advance of decisions. However, under centralized decision-making, ESCs will reduce the service level to avoid further profit loss due to lower market demand and higher production operating costs in ESC.

Conclusion 4. Optimal decisions are affected by the consumers' service quality preferences γ as follows:

- (1) $p^{c*}, p^{m*}, p^{e*}, s^{m*}, s^{e*}, s^{c*}, D^{c*}, D^{m*}, D^{e*}, R^{c*}, R^{m*}, R^{e*}, \pi^{c*}, \pi^{m*},$ and π^{e*} are positively related to γ . Meanwhile, $(\partial s^{c*}/\partial\gamma) > (\partial s^{m*}/\partial\gamma) > (\partial s^{e*}/\partial\gamma)$.
- (2) π_m^{m*} and π_m^{e*} are positively correlated with γ , and $(\partial\pi_m^{m*}/\partial\gamma) > (\partial\pi_m^{e*}/\partial\gamma)$; π_e^{e*} is positively correlated with γ , but π_e^{m*} is not affected by γ .

The proof is similar to Conclusion 1.

According to Conclusion 4, one has the following:

- (1) Regardless of decision-making models, increased consumers' service quality preferences will result in the increased sales price, service level, market demand, and volume of returns, ultimately increasing the profitability of the ESC. This is due to the direct link between consumers' service quality preferences and the e-platform's user scale. Thus, e-platform improving her service level can increase the likelihood of consumers buying through e-platform. Further, the increase in market demand caused a positive growth in the volume of returns. At the same time, increased consumer service sensitivity makes consumers relatively less price-sensitive, so the manufacturer will raise sales prices to capture additional revenue. Ultimately, the profitability of the ESC system has been enhanced by the expansion of market demand and increased sales prices. Additionally, the service level on centralized decision-making is the most sensitive to the market response, which is the same as previous conclusions. It should be noted that the service level when manufacturers dominate ESC is more catering to consumers' service quality preferences than that when e-platforms dominate ESC. This is because ESC dominators prefer to ask followers to make efforts to improve supply chain performance, rather than to increase their own input. As a result, the dominant manufacturer will require the e-platform to increase service investments in response to increased consumers' service quality preferences. And when the e-platform dominates ESC, she prefers to attract consumers by asking the manufacturer to cut sales prices.
- (2) Under both channel power structures, the improvement in consumers' service preferences can boost manufacturer's profit, and higher profit growth for manufacturer is obtained when he dominates ESC. However, for the e-platform, she cannot profit from consumers' service quality preferences when the manufacturer dominates ESC. Only when the e-platform has channel dominance can she increase revenue from increased consumer's service preferences. Combined with Conclusion 4 (1), it can be found that the following e-platform increases her service investment, but in allocating the

additional profits from the increased consumer's service preferences, she can only receive the part equivalent to her increased service cost, which cannot achieve the profit increase for the following e-platform. For the manufacturer, he can profit from consumer's service quality preferences under both power structures. This is because the manufacturer does not need to put up money for increased service level but benefits from increased market demand. Of course, the larger the manufacturer's channel power, the greater his profit from increased consumer's service quality preferences.

Conclusion 5. The results of the equilibrium solution comparison are as follows:

- (1) $p^{c*} > p^{m*} > p^{e*}, s^{c*} > s^{m*} > s^{e*}, \pi_m^{m*} > \pi_m^{e*},$ and $\pi_e^{m*} < \pi_e^{e*}.$
- (2) $D^{m*} > D^{e*}, R^{m*} > R^{e*},$ and $\pi^{c*} > \pi^{m*} > \pi^{e*}.$

See Appendix B for proof.

According to Conclusion 5, one has the following:

- (1) Product's price and e-platform's service level are highest in centralized decision-making and lowest under decentralized decision-making with dominant e-platform. That is in accordance with previous findings [33, 34] that the dominant manufacturers will use priority decision-making power to make decisions that maximize their own benefits. The manufacturer can use his dominance to raise sales price and force e-platform to improve service level. Similarly, when e-platform dominates ESC, e-platform will decrease the service level to reduce her operating costs. Not only that, but she will also induce manufacturer to cut sales prices, ultimately achieving the goal of expanding the customer base and increasing profits.

In summary, the dominant enterprise, whether it is the manufacturer or the e-platform, will have a decision-making advantage in cooperation, which can increase their own profits. Therefore, ESC participants are reluctant to lose dominant power, which will result in a power struggle between them and even further lead to the breakdown of partnership and the disruption of ESC. As an example, China's liquor e-platform, Jiuxian (<http://www.jiuxian.com>), offered Maotai Liquor at below-market prices without permission, prompting dissatisfaction among Maotai manufacturers, who eventually stopped selling their products on Jiuxian (http://it.southcn.com/9/2014-03/29/content_96281574.htm). Apparently, the strife between Maotai manufacturers and Jiuxian stems from the struggle for dominant power.

- (2) Market demand and the volume of returns are higher in the manufacturer-dominated decentralized model. The increased service level is an important

reason for higher market demand when the manufacturer dominates ESC. Meanwhile, when product return rates are stable, elevated demand will increase the volume of returns, but this benign increase in returns has no negative impact on either ESC members or system profits. Therefore, the system is more profitable when the manufacturer dominates ESC. Additionally, the centralized model prevents double marginal effects, so the system profit reaches the highest under this model.

5. Extension: Consumer Utility Analysis

We have also noticed that more and more consumers are forming return habits [16]. Is the act of returns necessarily beneficial to consumer themselves? Do ESC's different decision-making models and power structures affect consumer utility? How does the e-platform's service level affect consumer utility? To address the above issues, an extended model of consumer utility is proposed in this paper.

Suppose that when the customer determines to purchase the product, he will first make a judgment about the product's basic utility θv , and then he needs to pay p^{i*} ($i = c, m, e$) through the e-platform for the product, where θ ($0 \leq \theta \leq 1$) represents the probability of suitable products and v ($v \geq 0$) is per-unit-of-product valuation, which is

$$U^{i*} = \theta v - p^{i*} + \varepsilon(1 - \theta)(p^{i*} - t) + (1 - \varepsilon)(1 - \theta)g + \gamma s^{i*}, \quad i = c, m, e. \quad (5)$$

In this paper, as a simplified model, it is assumed that consumers will choose to return the product when they think it is not suitable; namely,

$$U^{i*} = (1 - \varepsilon)v - p^{i*} + \varepsilon(p^{i*} - t) + \gamma s^{i*}, \quad i = c, m, e. \quad (6)$$

By comparing the consumer utility under the above decision-making models, the following conclusions can be obtained.

Conclusion 6. The impact of the return rate ε on consumer utility depends on the decision mode and consumer's return cost t (the consumer's return cost thresholds for centralized model, manufacturer-led decentralized model, and e-platform-led decentralized model are t_0^{i*} , $i = c, m, e$).

- (1) Under centralized model, when $t < t_0^{c*}$, the consumer utility first grows and then declines as ε increases, with the maximum consumer utility obtained at $\varepsilon = \varepsilon_0$, where $t_0^{c*} = [2k\alpha - (2k\beta - \gamma^2)(h + v - w) - 2k\beta v](1 - \varepsilon)^2 - (c + h - w)\beta\gamma^2 / (4k\beta - \gamma^2)(1 - \varepsilon)^2$. When $t > t_0^{c*}$, the consumer utility decreases with the increase of ε .
- (2) Under decentralized model, when $t < t_0^{i*}$, the consumer utility increases with ε . When $t > t_0^{i*}$, the consumer utility decreases with ε , where $t_0^{m*} = \gamma^2\rho + 2k[\alpha + \beta(w + \rho - h - 2v)]/4k\beta$ and $t_0^{e*} = \gamma^2\rho + 4k[\alpha + \beta(-h - 2v + w + \rho)]/8k\beta$.

consistent with the assumptions of Zhang et al. [21] and Yan et al. [35].

The service level affects consumer utility by affecting the consumer shopping experience [80, 81]. Therefore, drawing on Yan et al. [35], the positive impact of service level on consumer utility is γs .

Meanwhile, returns will incur implicit costs to consumers, including psychological costs of consumer waiting times for online shopping, price losses resulting from missed promotions, time costs for repurchasing, and so on. Following Wang and Huang [82] and Zhang et al. [83], the paper assumes that t ($t \geq 0$) is the unit implicit cost of the consumer's return (hereafter called consumer return cost).

Based on assumptions in Section 3, the manufacturer will provide a full refund to consumers who file a return request and will bear the corresponding return costs. In the hypothesis of Ma et al. [16], there are two parts to the consumer utility created by unsuitable products: the first part is the refund $\varepsilon(1 - \theta)p^{i*}$ generated by the returned goods and the other part is the residual value $(1 - \varepsilon)(1 - \theta)g$ of the unreturned goods (where g represents the average revenue gained from the resale of the unsuitable goods and $0 < g < v$). At this point, the consumer return cost is expressed as $\varepsilon(1 - \theta)t$ in the utility function, and the consumer utility is

$$(3) \quad t_0^{c*} > t_0^{m*} > t_0^{e*}.$$

See Appendix C for proof.

According to Conclusion 6, one has the following:

- (1) Under the centralized model, if consumer return cost is low, consumer's utility first rises and then falls as return rate increases. On one hand, it is shown that return behavior is not always beneficial to consumers in the context of centralized decision-making achieved by ESC. Consumers can only profit from return behavior if the return rate is below a defined level. On the other hand, this indicates that consumers have an incentive not to engage in malicious returns. And when the ESC achieves coordination, consumers will voluntarily maintain the return rate at a certain level to maximize their own utility. If consumer return cost is higher, the return behavior will reduce the consumer's utility. At this point, ESC members should ensure the authenticity of product descriptions on the platform and guarantee product quality to minimize consumer returns, which can reduce the loss of customer utility.
- (2) Under decentralized models, when consumer return cost is low, consumer utility is positively related to product return rate, and conversely, consumer utility is negatively related to return rate. Returns can increase consumers' fault tolerance when purchasing

goods and give them shopping security. However, when the consumer return cost is high, consumers will suffer a loss of utility from their return behavior. As an example, during China's Double 11 Shopping Festival, the Taobao will offer a 7-day no-excuse return service and freight insurance. However, many consumers still feel a loss of utility from returns, which is due to the high consumer return cost at that time. On the one hand, the dramatic increase in orders during the Double 11 period has caused logistics delays, exacerbating the hidden costs of consumer logistics waiting. On the other hand, after the return of the product, consumers can no longer enjoy the Double 11 promotional activities, which also increases the return cost of consumers.

- (3) Consumers are most likely to benefit from returns when decisions are made centrally, and consumers are more likely to benefit from returns in decentralized decision where manufacturer dominates ESC than where e-platform dominates ESC. This is because ESC is most efficient under the centralized model, where members respond quickly to consumer returns and the service reaches the highest. In addition, consumers are more likely to profit from returns when manufacturers dominate ESCs compared to e-platforms, which is caused by higher service levels at this time.

Conclusion 7. When $2\beta + \varepsilon - 1 > 0$, U^{m*} , U^{e*} , and U^{c*} are positively related to γ . When $2\beta + \varepsilon - 1 < 0$, U^{m*} , U^{e*} , and U^{c*} are negatively related to γ .

The proof is similar to Conclusion 6.

On the one hand, if the product return is low, higher consumer's service quality preferences will enhance consumer utility when consumers have a high price preference. This reflects a positive link between the two types of consumer preferences, and an ESC with a lower return rate should meet consumer demands in terms of both price and service. Additionally, when the volume of returns is high, increased consumer's service quality preferences can have a positive impact on consumer utility even if consumers have lower price preferences. This is because ESC has a full refund policy; consumers who return goods cannot get a utility boost from the price, only from the service in the purchase. At this point, the higher the consumer's service quality preference, the greater the consumer utility.

Conclusion 8. $U^{c*} > \max\{U^{m*}, U^{e*}\}$. When $2\beta + \varepsilon - 1 > 0$, $U^{m*} > U^{e*}$.

The proof is similar to Conclusion 5.

Consumer utility is highest under the centralized model, while consumer utility under different channel powers of decentralized models depends on both consumers' price preferences and return rate. This is because under the centralized model, ESC members work together to enhance the consumer's shopping experience to compensate for the utility loss. For decentralized models, when return rate is stable and consumer's price preference

is high, greater consumer utility is obtained when manufacturer dominates ESC. This is due to higher return prices (selling prices) in the manufacturer-dominated ESC model, which allows consumers to derive more utility from the act of returns. When consumer's price preference is stable and return rate is high, greater consumer utility is obtained when manufacturer dominates ESC. This is because the benefits for returning consumers are mainly derived from the service of the e-platform, while service level is higher when manufacturer dominates ESC by Conclusions 4 and 5.

It can be concluded from Conclusions 1–8 that centralized decision-making can simultaneously maximize ESC efficiency and consumer utility. However, centralized decision-making needs to be achieved through the coordination mechanism. Therefore, in Section 6 of this paper, the return handling costs and commissions are considered, and new coordination mechanisms are designed to optimize ESC profits and maximize consumer utility.

6. Coordination Mechanism

In this section, the "return cost-sharing and commission readjusting" contract is designed to deliver Pareto improvements in decentralized decisions. The concept of contract is that the manufacturer pays higher commissions to the e-platform to cement the ESC partnership and increase the e-platform's profitability. Meanwhile, the e-platform proactively shares a portion of manufacturers' return handling costs to reduce the financial pressure on manufacturers from consumer returns. In the "return cost-sharing and commission readjusting" contract, assume that manufacturer pays commission \bar{p} and e-platform shares the return processing costs in proportion u .

Manufacturer profit function:

$$\bar{\pi}_m = pD - \bar{p}D + w\varepsilon Q - cQ - (1-u)h\varepsilon Q. \quad (7)$$

E-platform profit function:

$$\bar{\pi}_e = \bar{p}D - ks^2 - uh\varepsilon Q. \quad (8)$$

Conclusion 9. Under the "return cost-sharing and commission readjusting" contract, if (\bar{p}, u) satisfies
$$\begin{cases} \bar{p} = (1-\varphi)p + (1-\varphi)(w\varepsilon - c)/1 - \varepsilon + \varphi ks^2/D, \\ u = (1-\varphi) \end{cases}, \quad 0 < \varphi < 1,$$

the contract can achieve ESC coordination, in which φ is the coordination factor, which indicates the bargaining power of manufacturer. The larger φ , the more the profit manufacturer shares after coordination and the less the profit e-platform shares and vice versa.

See Appendix D for proof.

To ensure the effectiveness of coordination, the feasible conditions of the compact are explored as follows:

- (1) Under the decentralized model with the dominant manufacturer, the condition for acceptance of "return cost-sharing and commission readjusting"

contract by manufacturer and e-platform is as follows: the profit of both parties after coordination is not less than their profit before coordination; that is, $\bar{\pi}_m \geq \pi_m^{m*}, \bar{\pi}_e \geq \pi_e^{e*}$ must be guaranteed. The collation gives that the effective range of φ is $(\pi_m^{m*}/\pi^{c*}) \leq \varphi \leq 1 - (\pi_e^{e*}/\pi^{c*})$. So φ meets

$$\varphi \in \left[\frac{(4k\beta - \gamma^2)[(\gamma^2\rho + 2k\alpha)(1 - \varepsilon) + 2k\beta(w\varepsilon + \rho\varepsilon - h\varepsilon - c - \rho)]^2}{16k^3\beta[\alpha(1 - \varepsilon) + \beta(w\varepsilon - h\varepsilon - c)]^2}, 1 - \frac{(4k\beta - \gamma^2)(1 - \varepsilon)\rho[\alpha(1 - \varepsilon) + \beta(w\varepsilon + \rho\varepsilon - h\varepsilon - c - \rho)]}{2k[\alpha(1 - \varepsilon) + \beta(w\varepsilon - h\varepsilon - c)]^2} \right]. \quad (9)$$

$$\varphi \in \left[\frac{[(\gamma^2\rho + 4k\alpha)(1 - \varepsilon) + 4k\beta(w\varepsilon + \rho\varepsilon - h\varepsilon - c - \rho)]^2(4k\beta - \gamma^2)}{64k^3\beta[\alpha(1 - \varepsilon) + \beta(w\varepsilon - h\varepsilon - c)]^2}, 1 - \frac{(\rho^2\gamma^2 + 8k\alpha\rho)(1 - \varepsilon) + 8k\beta\rho(w\varepsilon + \rho\varepsilon - h\varepsilon - c - \rho)(4k\beta - \gamma^2)(1 - \varepsilon)}{16k^2[\alpha(1 - \varepsilon) + \beta(w\varepsilon - h\varepsilon - c)]^2} \right]. \quad (10)$$

Proposition 1. u is negatively correlated with φ .
The proof is similar to Conclusion 1.

Under the coordination mechanism, as u increases, the proportion φ of the system profits shared by manufacturer will decrease, and the proportion $1 - \varphi$ of the system profits shared by e-platform will increase. That is, the higher the return handling costs borne by the e-platform, the higher her share of the ESC profits. Therefore, by using the contract of “return cost-sharing and commission readjusting,” the e-platform’s initiative and enthusiasm to share the manufacturer’s return handling costs will be greatly improved, and the e-platform’s commitment to return costs has increased her own profits. For manufacturer, the e-platform’s behavior of sharing the return cost eases the financial burden on the manufacturer, which strengthens his willingness to cooperate with e-platform. The above fully illustrate the practicality of the “joint commission return cost-sharing” contract.

7. Numerical Analysis

7.1. Numerical Analysis of Models

7.1.1. Numerical Analysis of Optimal Decisions. To further analyze equilibrium solutions, numerical examples are used in this section. Based on Shen and Wang [84] and Wang et al. [68], this paper assumes that $\alpha = 500$, $\beta = 1$, $\gamma = 0.5$, $k = 0.5$, $c = 100$, $w = 60$, $h = 10$, and $\rho = 20$. This subsection discusses the effect of return rate on ESC decisions and profit, taking ε as the dependent variable and $\varepsilon \in [0.2, 0.8]$. The results for different models are presented in Figures 2–4.

(2) Under decentralized decision-making with dominant e-platform, coordinated profits of ESC participants are no less than their precoordination profits; that is, $\bar{\pi}_m \geq \pi_m^{e*}, \bar{\pi}_e \geq \pi_e^{e*}$ must be guaranteed. The collation gives that the effective range of φ is $(\pi_m^{e*}/\pi^{c*}) \leq \varphi \leq 1 - (\pi_e^{e*}/\pi^{c*})$. So φ also meets

Conclusions 1–5 can be verified by Figures 2–4, and the following conclusions can also be drawn:

- (1) As the return rate increases, sales price, market demand, the volume of returns, and profits for manufacturer, e-platform, and system change more and more rapidly. This is because when the return rate increases, the manufacturer compensates for lost profits by raising sales price. The higher the return rate, the more the profit that needs to be made up through higher prices, but the fewer the consumers that are bearing the higher prices. This causes the sales price to rise sharply, which results in a steep decline in market demand. Ultimately, this vicious cycle leads to a drastic increase in lost profits for the manufacturer, the e-platforms, and the ESC system.
- (2) Compared to decentralized decisions, the slightly higher sales price but much higher service level under the centralized model leads to market demand and ESC profits reach highest under centralized decisions. Furthermore, as the return rate rises, the gap between centralized and decentralized decisions on demand and ESC profits gradually shrinks, which is caused by consumer returns shrinking the profit space of ESC.

From the conclusions and numerical simulation results, it can also be concluded that the manufacturer-led decentralized decision is better than e-platform-led decentralized decision. That is, the power structure dominated by e-platform under decentralized decision is not conducive to the operation of ESC. But in reality, there are many powerful e-platforms with channel power, such as Amazon (<http://www.amazon.com>), ebay (<http://www.ebay.com>), and Tmall

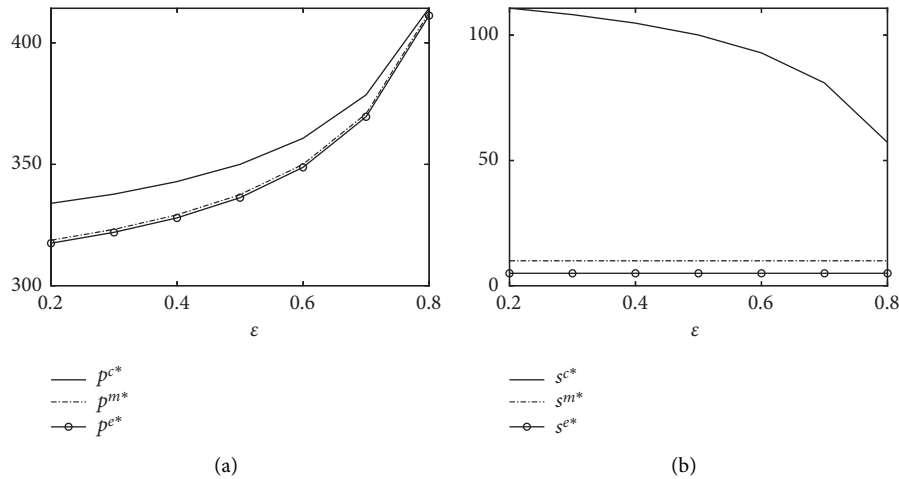


FIGURE 2: Changes in Decision Variables with ϵ . (a) Changes in sales price. (b) Changes in service level.

(<http://www.Tmall.com>). The reasons for this situation are as follows.

The rapidly developing Internet economy has gradually made e-platforms because of reliable information centers and trading platforms. Currently, many powerful e-platforms have formed a loyal customer base, which becomes their advantage in the channel competition. In addition, the role of e-platforms is gradually coming to the fore as manufacturers can greatly reduce the intermediate costs of sales through e-platforms for direct sales. For manufacturers, most of them cannot afford to build their own online sales channels due to high costs and long construction cycles, so they have to choose to enter e-platforms to cater to online consumers.

However, the increased dominance of e-platform is detrimental to ESC's long-term growth. Therefore, the following manufacturers should enhance their channel power through certain strategies, such as enhancing their brand power, building a good corporate image, strengthening communication with e-platforms, and seeking ways to grasp market information. From Conclusion 5, when the manufacturer takes control of the channel, the volume of product returns is higher, although the system operates more efficiently. Therefore, for manufacturers in control of the channel, improving quality management systems, enhancing product compatibility and ease of use, and working to reduce the volume of product returns are urgent issues to be addressed.

Meanwhile, the study also finds that higher return rates can set off a vicious cycle that hurts both consumers and ESCs. Therefore, manufacturers and e-platforms need to cooperate closely to ensure that product return rates are kept within a low range. For manufacturers, on the one hand, they need to control the production, storage, and transportation of their products more carefully to prevent product quality problems. On the other hand, they also need to stabilize sales prices within a reasonable range to meet consumers' price preferences. For e-platforms, they need to enhance service levels to improve consumer utility during shopping and return process. As an example, e-platforms such as Tmall and JD provide protection services such as

“lightning delivery” and “online dispute resolution platform for transactions.”

7.1.2. Numerical Analysis of Consumer Utility.

Considering consumer utility, assume that $\alpha = 400$, $\beta = 1$, $\gamma = 2$, $k = 2$, $c = 100$, $w = 60$, $h = 10$, $\rho = 20$, $v = 150$, and $\epsilon \in [0.2, 0.8]$. With $t = 50$ and $t = 100$, respectively, consumer utility varies with return rate as shown in Figure 5.

Further, assume $\alpha = 500$, $k = 2$, $c = 100$, $w = 60$, $h = 10$, $\rho = 20$, $v = 1000$, and $t = 20$, taking γ as the dependent variable and $\gamma \in [0.1, 0.3]$. Suppose $2\beta + \epsilon - 1 < 0$ (taking $\beta = 0.3$; $\epsilon = 0.1$) and $2\beta + \epsilon - 1 > 0$ (taking $\beta = 1$; $\epsilon = 0.1$), respectively; consumer utility varies with consumer's service quality preferences as shown in Figure 6.

Conclusions 6–8 are validated in Figures 5 and 6, and it can be seen that consumer utility is influenced by the consumers' return costs and the consumers' service quality sensitivity. Consumer utility is more significantly influenced by consumers' service quality sensitivity when manufacturer dominates ESC. Moreover, consumer utility is consistently highest under centralized model, and the gap of consumer utility between centralized model and decentralized models is large. Thus, centralized decision-making is beneficial for both ESCs and consumers.

7.2. Numerical Analysis of the Coordination Mechanism.

Assuming $\alpha = 500$, $\beta = 1$, $\gamma = 0.5$, $k = 0.5$, $c = 30$, $w = 60$, $h = 10$, $\rho = 20$, and $\epsilon = 0.3$, the following results can be obtained by calculation:

- (1) Under the decentralized model with the dominant manufacturer, before coordination of “return cost-sharing and commission readjusting,” the commission is $\rho = 20$, manufacturer's profit is $\pi_m^{m*} = 53725$, and e-platform's profit is $\pi_e^{m*} = 4586$. After coordination, the range of change in commission, manufacturer's profit, and e-platform's profit is $\bar{\rho} \in (53.67, 78.03)$, $\pi_m^{m*} \in (53659, 60202)$, and $\pi_e^{m*} \in (5235, 11779)$,

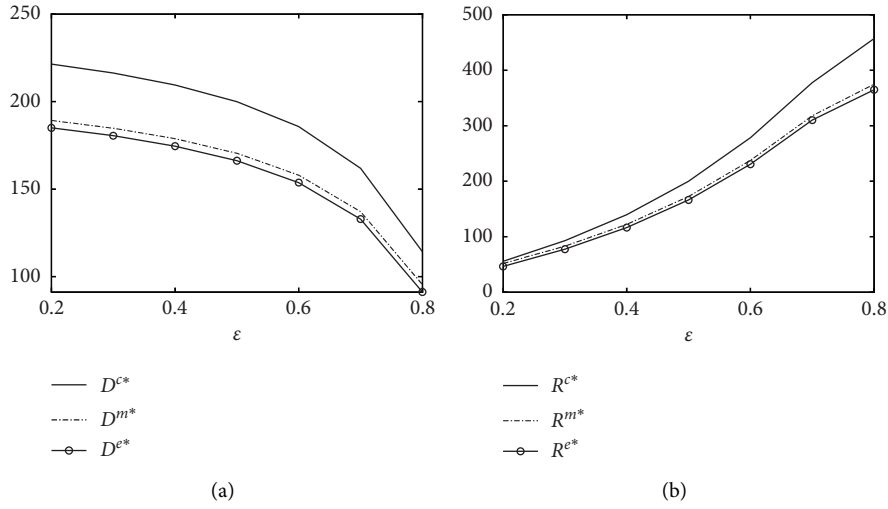


FIGURE 3: Changes in market demand and volume of returns with ϵ . (a) Changes in market demand. (b) Changes in volume of returns.

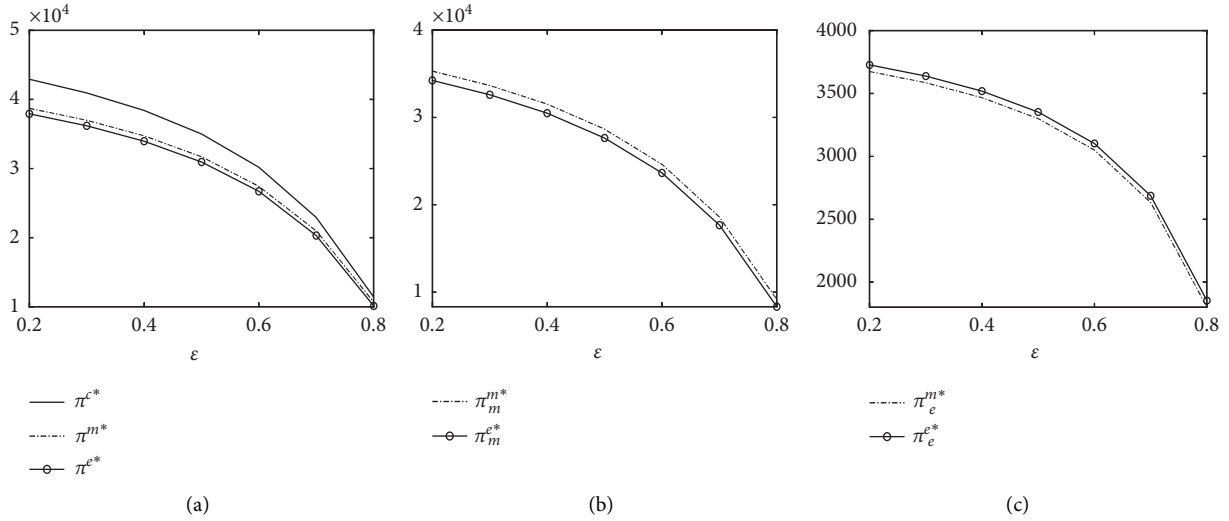


FIGURE 4: Changes in profits with ϵ . (a) Changes in ESC's profit. (b) Changes in manufacturer's profit. (c) Changes in E-platform profit.

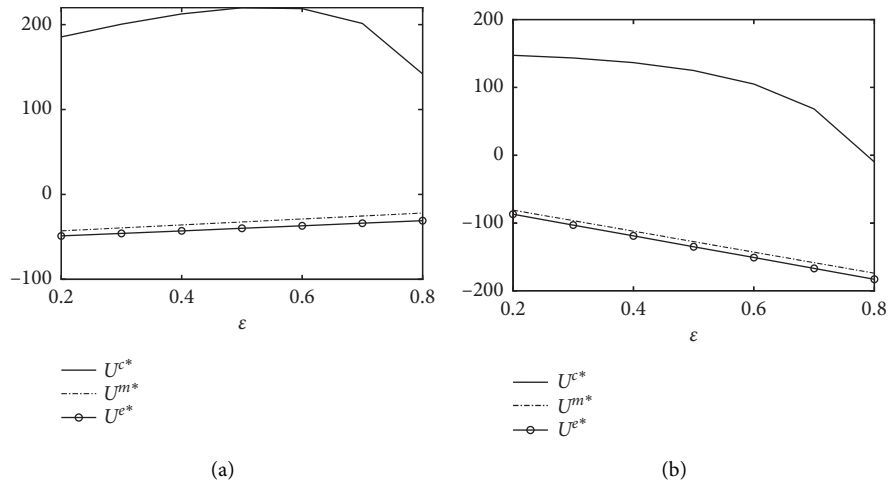


FIGURE 5: Changes in consumer utility with ϵ . (a) $t = 50$. (b) $t = 100$.

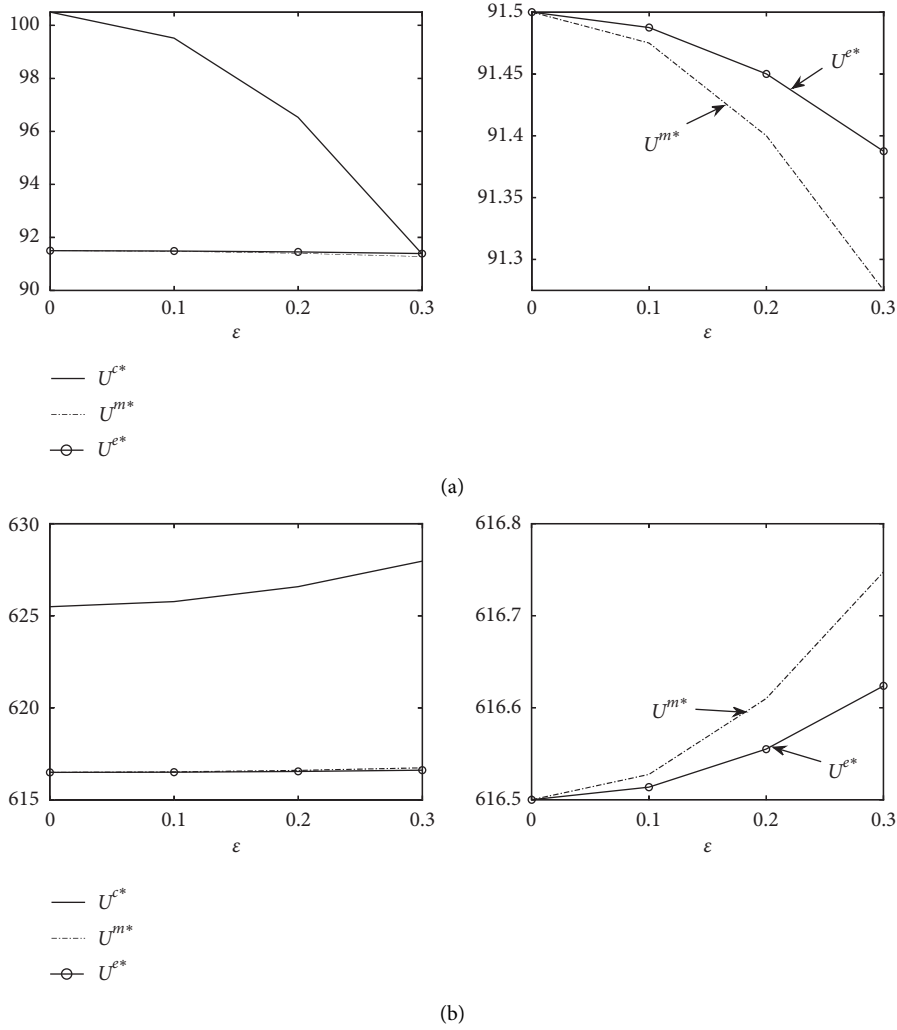


FIGURE 6: Changes in consumer utility with γ . (a) $2\beta + \epsilon - 1 < 0$ ($\beta = 0.3; \epsilon = 0.1$). (b) $2\beta + \epsilon - 1 > 0$ ($\beta = 1; \epsilon = 0.1$).

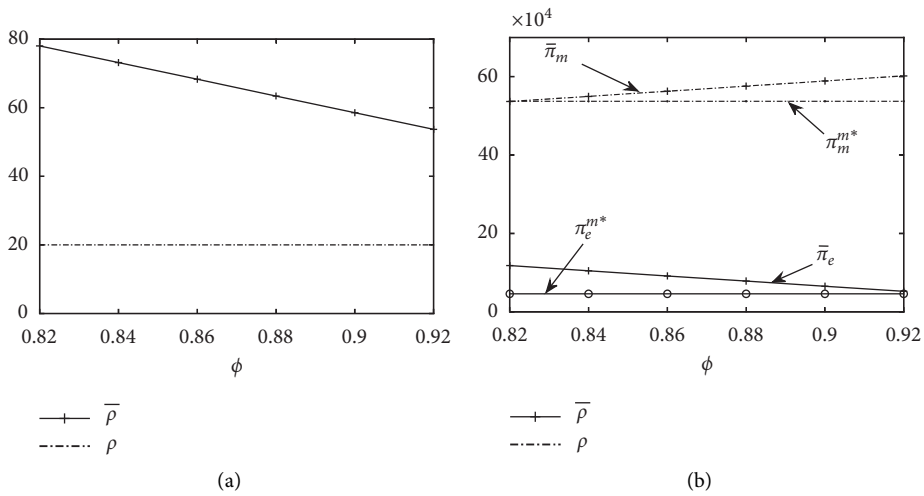


FIGURE 7: Comparison before and after coordination with dominant manufacturer. (a) Changes in commission. (b) Changes in profits.

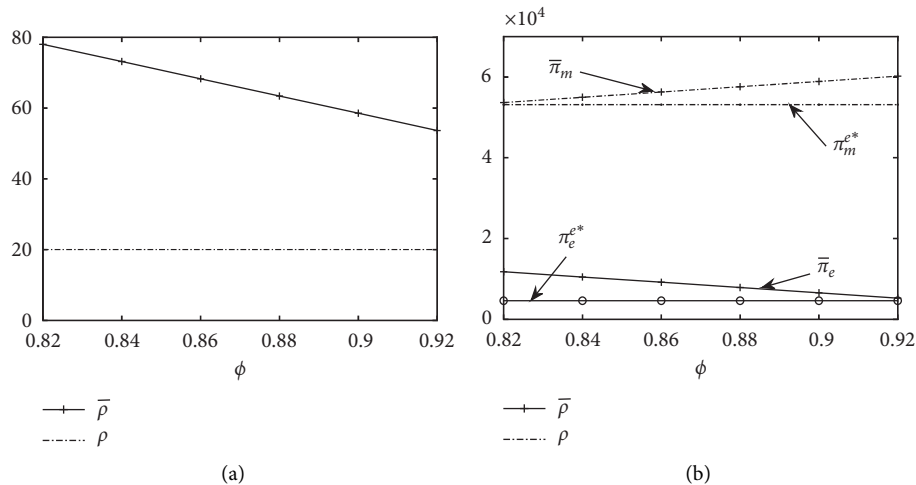


FIGURE 8: Comparison before and after coordination with dominant E-platform. (a) Changes in commission. (b) Changes in profits.

respectively. As the coordination coefficient ϕ ($\phi \in (0.82, 0.92)$) increases, the change in commission and member profits before and after coordination is shown in Figure 7.

- (2) Under the decentralized model with dominant e-platform, before coordination, commission, manufacturer's profit, and e-platform's profit are $\rho = 20$, $\pi_m^{e*} = 53147$, and $\pi_e^{e*} = 4598$, respectively. After coordination, the range of change in commission, manufacturer's profit, and e-platform's profit is $\bar{\rho} \in (53.67, 78.03)$, $\pi_m^{m*} \in (53659, 60202)$, and $\pi_e^{m*} \in (5235, 11779)$, respectively. As the coordination coefficient ϕ ($\phi \in (0.82, 0.92)$) increases, the change in commission and member profits before and after coordination is shown in Figure 8.

The following conclusions can be drawn from Figures 7 and 8.

As coordination factor ϕ increases, the commissions paid by manufacturer to e-platform, although gradually decreasing, are always higher than that before coordination. By adjusting commissions, ESC achieves a redistribution of profits, which demonstrates the feasibility of using commissions as a profit adjustment tool for coordination mechanisms. In addition, the profits of the e-platform after coordination, while decreasing with the increase of ϕ , are always higher than her profits before coordination. Likewise, manufacturers have earned higher profits through coordination.

8. Conclusions

Considering the serious return problems of ESCs and considering the different channel power structures, ESC composed of a manufacturer and an e-platform is constructed. The paper examines the impact of channel structures and consumer returns on ESC. Moreover, this paper

establishes an extended model of consumer utility, studies the impact of return rates and consumer service preferences on consumer utility, and seeks a balance between system performance and consumer utility. Finally, the return handling cost and commissions are considered, and new coordination mechanisms are designed to optimize ESC profits and maximize consumer utility. The main conclusions are listed as follows:

- (1) Consumer return rates, salvage value of returned products, and return handling cost all have significant impacts on ESC. In ESC, higher product return rates result in higher sales prices, lower market demand, and higher volume of returns, which ultimately results in lower profits for manufacturer, e-platform, and ESC system. Second, the higher the salvage value, the lower the sales price, the greater the market demand, and the more profitable the ESC. Additionally, higher return handling costs can result in higher sales price and lower market demand, which adversely affects ESC.
- (2) In centralized decision-making, the service level is inversely proportional to consumer return rates and the return handling costs and proportional to the salvage value of returned products. Under decentralized decisions, return rate does not affect service level of e-platform (different from [28]). Increasing consumers' service preferences will promote product prices and service level (unlike [29]) and increase market demand and ESC profitability (unlike [30]). Moreover, the effect of consumers' service preferences on the manufacturer's profits and the e-platform's profit depends on the channel power structures. Under both channel power structures, an increase in consumers' service quality preferences can increase manufacturer's profit, and the increase in profits is greater when manufacturer dominates ESC. However, for the e-platform, she cannot profit

from consumers' service quality preferences when the manufacturer dominates ESC.

- (3) Under different power structures, the profits of the dominant enterprise are higher than the following enterprise. This is because the dominant enterprises will use priority decision-making power to make decisions that maximize their own benefits. Additionally, when the manufacturer dominates ESC, market demand and system profit are relatively high because the dominant manufacturer forces the e-platform to increase service level.
- (4) The impact of the return rate on consumer utility depends on two factors: the decision-making mode and the consumers' hidden cost of returns. Under centralized decision-making, ESC efficiency optimization and consumer utility maximization can be achieved simultaneously. Under the different channel powers of decentralized decision-making, the impact of channel structure and consumer's service quality preference on consumer utility is determined by consumer's price preference and return rate. When return rate is stable and consumer's price preference is high, consumer's service quality preference will have a positive impact on consumer utility. At this time, the consumer utility is higher when the manufacturer dominates ESC.
- (5) For ESCs with consumer returns, the paper uses both commissions and return handling costs as adjustment tools to design a new "return cost-sharing and commission readjusting" contract. The more e-platform pays for the handling costs, the higher the profit she earns after coordination. The contract maximizes ESC efficiency and consumer utility.

Through the conclusions of the paper, the following management insights can be presented:

- (1) For manufacturers, the first step is to invest more in the technology for handling returned products to reduce the unit cost of returns, which not only meets environmental requirements but also increases the profitability of ESC. Second, manufacturers need to control the production, storage, and transportation of their products more carefully to prevent product quality problems, which can increase their channel power. Moreover, whether or not manufacturers dominate ESCs, they should not compensate for their lost profits by increasing sales prices, because this approach leads to a decrease in market demand, resulting in greater profit loss and a vicious cycle.
- (2) For e-platforms, first, their service level should not be completely limited by the size of the commissions but should cater to consumer's service quality preferences to increase platform traffic and revenue. Particularly for products with high return rates, improvements in the service levels can have a significant impact on the increase in consumer utility. Second, when e-platforms dominate ESCs, they should not require manufacturers to significantly

reduce their prices to attract consumers (a common phenomenon during online shopping festivals). On the contrary, e-platforms should strengthen cooperation with manufacturers, which can not only enhance their own and manufacturers' profits but also increase the utility of platform users, forming a win-win situation.

However, the paper only examines a single-stage ESC composed of a manufacturer and an e-platform. In real life, manufacturers often remanufacture and resell their returned products after receiving them, while consumers can also resell used products directly through the platform. How these behaviors affect ESC decisions and consumer utility and how coordination mechanisms can be designed to accommodate more complex operational situations will be explored in subsequent research.

Appendix

A. Proof of Conclusion 1

Proof. Under centralized model,

$$\frac{\partial p^{c*}}{\partial \varepsilon} = \frac{(c+h-w)(2k\beta-\gamma^2)}{(4k\beta-\gamma^2)(1-\varepsilon)^2} > 0,$$

$$\frac{\partial s^{c*}}{\partial \varepsilon} = \frac{(c+h-w)\beta\gamma}{(4k\beta-\gamma^2)(1-\varepsilon)^2} < 0,$$

$$\frac{\partial D^{c*}}{\partial \varepsilon} = \frac{2k(c+h-w)\beta^2}{(4k\beta-\gamma^2)(1-\varepsilon)^2} < 0,$$

$$\frac{\partial R^{c*}}{\partial \varepsilon} = \frac{2k\beta[\alpha(1-\varepsilon) + 2\beta\varepsilon(w-h) - \beta c(1+\varepsilon)]}{(4k\beta-\gamma^2)(1-\varepsilon)^3} > 0,$$

$$\frac{\partial \pi^{c*}}{\partial \varepsilon} = \frac{2k\beta(c+h-w)[\alpha(1-\varepsilon) + \beta\varepsilon(w-h) - \beta c]}{(4k\beta-\gamma^2)(1-\varepsilon)^3} < 0. \quad (A.1)$$

The same can be proved,

$$\begin{aligned} (\partial p^{m*}/\partial \varepsilon) > 0, \quad (\partial s^{m*}/\partial \varepsilon) = 0, \quad (\partial D^{m*}/\partial \varepsilon) < 0, \\ (\partial R^{m*}/\partial \varepsilon) > 0, \quad (\partial \pi_m^{m*}/\partial \varepsilon) < 0, \quad (\partial \pi_e^{m*}/\partial \varepsilon) < 0, \quad (\partial \pi^{m*}/\partial \varepsilon) < 0; \\ (\partial p^{e*}/\partial \varepsilon) > 0, \quad (\partial s^{e*}/\partial \varepsilon) = 0, \quad (\partial D^{e*}/\partial \varepsilon) < 0, \quad (\partial R^{e*}/\partial \varepsilon) > 0, \\ (\partial \pi_m^{e*}/\partial \varepsilon) < 0, \quad (\partial \pi_e^{e*}/\partial \varepsilon) < 0, \quad \text{and} \quad (\partial \pi^{e*}/\partial \varepsilon) < 0. \quad \square \end{aligned}$$

B. Proof of Conclusion 5

Proof

$$\begin{aligned} (1) \quad p^{c*} - p^{m*} &= (2k\gamma^2\alpha + \gamma^4\rho - 2k\gamma^2\beta\rho - 8k^2\beta^2\rho)(1-\varepsilon) \\ &+ 2k\gamma^2\beta\varepsilon(w-h) - 2k\gamma^2\beta c/4k\beta(4k\beta-\gamma^2)(1-\varepsilon) > 0, \\ p^{m*}/p^{e*} &= 2\gamma^2\rho(1-\varepsilon) + 4k[\alpha(1-\varepsilon) - \beta(w\varepsilon + \rho\varepsilon - h\varepsilon - c - \rho)]/\gamma^2\rho(1-\varepsilon) + 4k[\alpha(1-\varepsilon) - \beta(w\varepsilon + \rho\varepsilon - h\varepsilon - c - \rho)] > 1; \\ \text{therefore, } p^{c*} &> p^{m*} > p^{e*}. \end{aligned}$$

The same can be proved, $s^{c*} > s^{m*} > s^{e*}$.

(2) $D^{c*} - D^{m*} = (2k\gamma^2\alpha + 8k^2\beta^2\rho + \gamma^4\rho - 6k\gamma^2\beta\rho)(1 - \varepsilon) + 2k\gamma^2\beta\varepsilon(w - h) - 2k\gamma^2\beta c/4k(4k\beta - \gamma^2)(1 - \varepsilon) > 0$,
 $D^{m*} - D^{e*} = (\gamma^2\rho/8k) > 0$; therefore, $D^{c*} > D^{m*} > D^{e*}$.

The same can be proved, $R^{c*} > R^{m*} > R^{e*}$, $\pi_m^{m*} > \pi_m^{e*}$,
 $\pi_e^{m*} < \pi_e^{e*}$, $\pi^{c*} > \pi^{m*} > \pi^{e*}$. \square

C. Proof of Conclusion 6

Proof. (1) Under centralized model,

$$\frac{\partial U^{c*}}{\partial \varepsilon} = \frac{[2k\alpha - (2k\beta - \gamma^2)(h + t + v - w) - 2k\beta(t + v)](1 - \varepsilon)^2 - \gamma^2\beta(c + h - w)}{(4k\beta - \gamma^2)(1 - \varepsilon)^2}, \quad (C.1)$$

when

$$t_0^{c*} < \frac{[2k\alpha - (2k\beta - \gamma^2)(h + v - w) - 2k\beta v](1 - \varepsilon)^2 - (c + h - w)\beta\gamma^2}{(4k\beta - \gamma^2)(1 - \varepsilon)^2}. \quad (C.2)$$

By solving $(\partial U^{c*}/\partial \varepsilon) = 0$,

$$\varepsilon_0 = \frac{2k\alpha - (h + t + v - w)(2k\beta - \gamma^2) - (t + v)2k\beta + \sqrt{\beta\gamma^2(c + h - w)(2k\alpha - (h + t + v - w)(2k\beta - \gamma^2) - (t + v)2k\beta)}}{2k(\alpha - (h + 2t + 2v - w)\beta) + (h + t + v - w)\gamma^2} \quad (C.3)$$

can be obtained.

When

$$t_0^{c*} > \frac{[2k\alpha - (2k\beta - \gamma^2)(h + v - w) - 2k\beta v](1 - \varepsilon)^2 - (c + h - w)\beta\gamma^2}{(4k\beta - \gamma^2)(1 - \varepsilon)^2}, \quad (C.4)$$

$(\partial U^{c*}/\partial \varepsilon) < 0$.

(2) Under decentralized model,

$$\frac{\partial U^{m*}}{\partial \varepsilon} = \frac{2k[\alpha - \beta(h + 2t + 2v - w - \rho)] + \gamma^2\rho}{4k\beta} \quad (C.5)$$

when

$$t_0^{m*} < \frac{\gamma^2\rho + 2k[\alpha + \beta(w + \rho - h - 2v)]}{4k\beta} \quad (C.6)$$

$$\frac{\partial U^{m*}}{\partial \varepsilon} > 0.$$

when

$$t_0^{m*} > \frac{\gamma^2\rho + 2k[\alpha + \beta(w + \rho - h - 2v)]}{4k\beta},$$

$$\frac{\partial U^{m*}}{\partial \varepsilon} < 0, \quad (C.7)$$

$$\frac{\partial U^{e*}}{\partial \varepsilon} = \frac{4k[\alpha - \beta(h + 2t + 2v - w - \rho)]\gamma^2\rho}{8k\beta}$$

when

$$t_0^{e*} < \frac{\gamma^2\rho + 4k[\alpha + \beta(-h - 2v + w + \rho)]}{8k\beta}, \quad (C.8)$$

$$\frac{\partial U^{e*}}{\partial \varepsilon} > 0$$

when

$$t_0^{e*} > \frac{\gamma^2\rho + 4k[\alpha + \beta(-h - 2v + w + \rho)]}{8k\beta}, \quad (C.9)$$

$$\frac{\partial U^{e*}}{\partial \varepsilon} < 0.$$

(3) $t_0^{m*} - t_0^{e*} = (\gamma^2\rho/8k\beta) > 0$. Similarly, $t_0^{c*} - t_0^{m*} > 0$.
Therefore, $t_0^{c*} > t_0^{m*} > t_0^{e*}$. \square

D. Proof of Conclusion 9

Proof. Under the “return cost-sharing and commission readjusting” contract, when (\bar{p}, u) satisfies

$$\begin{cases} \bar{p} = (1 - \varphi)p + \frac{(1 - \varphi)(w\varepsilon - c)}{1 - \varepsilon} + \frac{\varphi ks^2}{D}, & 0 < \varphi < 1, \\ u = (1 - \varphi) \end{cases} \quad (D.1)$$

whether the manufacturer dominates ESC or the e-platform dominates ESC, both subjects make decisions to maximize their own profits. At this point,

$$\begin{aligned}\bar{\pi}_m &= pD - \bar{p}D + w\epsilon Q - cQ - (1-u)h\epsilon Q = \varphi\pi, \\ \bar{\pi}_e &= \bar{p}D - ks^2 - u h\epsilon Q = (1-\varphi)\pi.\end{aligned}\quad (\text{D.2})$$

It can be seen that the decision functions of manufacturer and e-platform under both power structures are affine functions of system profit. Therefore, ESC coordination can be achieved. \square

Data Availability

No data were used in our study.

Conflicts of Interest

The authors declare that they have no conflicts of interest.

Acknowledgments

This paper was supported by the National Natural Science Foundation of China (no. 71971129) and Shandong Province Higher Education Youth Innovation and Technology Support Program (no. 2019RWG017).

References

- [1] G. Hua, S. Wang, and T. C. E. Cheng, "Price and lead time decisions in dual-channel supply chains," *European Journal of Operational Research*, vol. 205, no. 1, pp. 113–126, 2010.
- [2] J. Zhang, P. W. Farris, J. W. Irvin, T. Kushwaha, T. J. Steenburgh, and B. A. Weitz, "Crafting integrated multichannel retailing strategies," *Journal of Interactive Marketing*, vol. 24, no. 2, pp. 168–180, 2010.
- [3] M. Radhi and G. Zhang, "Optimal cross-channel return policy in dual-channel retailing systems," *International Journal of Production Economics*, vol. 210, pp. 184–198, 2019.
- [4] R. Yan, "Product categories, returns policy and pricing strategy for e-marketers," *Journal of Product & Brand Management*, vol. 18, no. 6, pp. 452–460, 2009.
- [5] T.-M. Choi and S. Guo, "Responsive supply in fashion mass customisation systems with consumer returns," *International Journal of Production Research*, vol. 56, no. 10, pp. 3409–3422, 2017.
- [6] W. Y. Chiang and G. E. Monahan, "Managing inventories in a two-echelon dual-channel supply chain," *European Journal of Operational Research*, vol. 162, no. 2, pp. 325–341, 2005.
- [7] W.-y. K. Chiang, D. Chhajed, and J. D. Hess, "Direct marketing, indirect profits: a strategic analysis of dual-channel supply-chain design," *Management Science*, vol. 49, no. 1, pp. 1–20, 2003.
- [8] Z. Zhang, S. Liu, and B. Niu, "Coordination mechanism of dual-channel closed-loop supply chains considering product quality and return," *Journal of Cleaner Production*, vol. 248, Article ID 119273, 2019.
- [9] E. Moriarty, "Getting out from under all those ecommerce returns," June 2018, <http://multichannelmerchant.com/blog/getting-out-from-under-all-those-ecommerce-returns/>.
- [10] B. McWilliams, "Money-back guarantees: helping the low-quality retailer," *Management Science*, vol. 58, no. 8, pp. 1521–1524, 2012.
- [11] B. Chen and J. Chen, "Compete in price or service?-A study of personalized pricing and money back guarantees," *Journal of Retailing*, vol. 93, no. 2, pp. 154–171, 2017.
- [12] D. Vlachos and R. Dekker, "Return handling options and order quantities for single period products," *European Journal of Operational Research*, vol. 151, no. 1, pp. 38–52, 2003.
- [13] V. D. R. Guide, G. C. Souza, L. N. Van Wassenhove, and J. D. Blackburn, "Time value of commercial product returns," *Management Science*, vol. 52, no. 8, pp. 1200–1214, 2006.
- [14] A. C. de Araújo, E. M. Matsuoka, J. E. Ung, A. Massote, and M. Sampaio, "An exploratory study on the returns management process in an online retailer," *International Journal of Logistics Research and Applications*, vol. 21, no. 3, pp. 345–362, 2017.
- [15] S. Rudolph, "E-commerce product return statistics and trends," 2016, <https://www.business2community.com/infographics/e-commerce-product-return-statistics-trends-infographic-01505394#hUm45j2iCV31tvsl.97>.
- [16] W. Ma, C. Zhao, H. Ke, and Z. Chen, "Retailer's return policy in the presence of P2P secondary market," *Electronic Commerce Research and Applications*, vol. 39, Article ID 100899, 2019.
- [17] N. N. Bechwati and W. S. Siegal, "The impact of the prechoice process on product returns," *Journal of Marketing Research*, vol. 42, no. 3, pp. 358–367, 2005.
- [18] X. Su, "Consumer returns policies and supply chain performance," *Manufacturing & Service Operations Management*, vol. 11, no. 4, pp. 595–612, 2009.
- [19] S.-P. Jeng, "Increasing customer purchase intention through product return policies: the pivotal impacts of retailer brand familiarity and product categories," *Journal of Retailing and Consumer Services*, vol. 39, pp. 182–189, 2017.
- [20] A. Sorescu and S. M. Sorescu, "Customer satisfaction and long-term stock returns," *Journal of Marketing*, vol. 80, no. 5, pp. 110–115, 2016.
- [21] G. Zhang, J. Shang, and P. Yildirim, "Optimal pricing for group buying with network effects," *Omega*, vol. 63, pp. 69–82, 2016.
- [22] B. Li and Y. Jiang, "Impacts of returns policy under supplier encroachment with risk-averse retailer," *Journal of Retailing and Consumer Services*, vol. 47, pp. 104–115, 2019.
- [23] T. Suwelack, J. Hogreve, and W. D. Hoyer, "Understanding money-back guarantees: cognitive, affective, and behavioral outcomes," *Journal of Retailing*, vol. 87, no. 4, pp. 462–478, 2011.
- [24] Z. Pei, A. Paswan, and R. Yan, "E-tailer's return policy, consumer's perception of return policy fairness and purchase intention," *Journal of Retailing and Consumer Services*, vol. 21, no. 3, pp. 249–257, 2014.
- [25] R. Ramanathan, "An empirical analysis on the influence of risk on relationships between handling of product returns and customer loyalty in E-commerce," *International Journal of Production Economics*, vol. 130, no. 2, pp. 255–261, 2011.
- [26] J. D. Shulman, A. T. Coughlan, and R. C. Savaskan, "Managing consumer returns in a competitive environment," *Management Science*, vol. 57, no. 2, pp. 347–362, 2011.
- [27] Y. Wang, Z. Yu, L. Shen, Y. Ge, and J. Li, "Different dominant models and fairness concern of E-supply chain," *Complexity*, vol. 2018, Article ID 8616595, 13 pages, 2018.
- [28] Q. Li, M. Shi, and Y. Huang, "A dynamic price game model in a low-carbon, closed-loop supply chain considering return rates and fairness concern behaviors," *International Journal of Environmental Research and Public Health*, vol. 16, no. 11, p. 1978, 2019.

- [29] L. Kong, Z. Liu, Y. Pan, J. Xie, and G. Yang, "Pricing and service decision of dual-channel operations in an O2O closed-loop supply chain," *Industrial Management & Data Systems*, vol. 117, no. 8, pp. 1567–1588, 2017.
- [30] A. A. Taleizadeh, F. Akhavanizadeh, and J. Ansarifard, "Pricing and quality level decisions of substitutable products in online and traditional selling channels: game-theoretical approaches," *International Transactions in Operational Research*, vol. 26, no. 5, pp. 1718–1751, 2017.
- [31] W. Feng and H. Chen, "Bricks and clicks: decisions in an O₂O supply chain considering product returns," *IEEE Access*, vol. 7, pp. 180292–180304, 2019.
- [32] K. Cao, Y. Xu, J. Cao, B. Xu, and J. Wang, "Whether a retailer should enter an e-commerce platform taking into account consumer returns," *International Transactions in Operational Research*, vol. 27, no. 6, pp. 2878–2898, 2020.
- [33] Y. Wang, Z. Yu, and L. Shen, "Study on the decision-making and coordination of an e-commerce supply chain with manufacturer fairness concerns," *International Journal of Production Research*, vol. 57, no. 9, pp. 2788–2808, 2018.
- [34] Q. Han and Y. Wang, "Decision and coordination in a low-carbon E-supply chain considering the manufacturer's carbon emission reduction behavior," *Sustainability*, vol. 10, no. 5, p. 1686, 2018.
- [35] B. Yan, Z. Chen, X. Wang, and Z. Jin, "Influence of logistic service level on multichannel decision of a two-echelon supply chain," *International Journal of Production Research*, vol. 58, no. 11, pp. 3304–3329, 2019.
- [36] J. Zhang, H. Li, R. Yan, and C. Johnston, "Examining the signaling effect of E-tailers' return policies," *Journal of Computer Information Systems*, vol. 57, no. 3, pp. 191–200, 2016.
- [37] L. Xu, Y. Li, K. Govindan, and X. Yue, "Return policy and supply chain coordination with network-externality effect," *International Journal of Production Research*, vol. 56, no. 10, pp. 3714–3732, 2018.
- [38] C. Wang, J. Chen, L. Wang, and J. Luo, "Supply chain coordination with put option contracts and customer returns," *Journal of the Operational Research Society*, vol. 71, no. 6, pp. 1003–1019, 2019.
- [39] A. Borenich, Y. Dickbauer, M. Reimann, and G. C. Souza, "Should a manufacturer sell refurbished returns on the secondary market to incentivize retailers to reduce consumer returns?" *European Journal of Operational Research*, vol. 282, no. 2, pp. 569–579, 2019.
- [40] Y. Li, L. Xu, and D. Li, "Examining relationships between the return policy, product quality, and pricing strategy in online direct selling," *International Journal of Production Economics*, vol. 144, no. 2, pp. 451–460, 2013.
- [41] A. Balakrishnan, S. Sundaresan, and B. Zhang, "Browse-and-Switch: retail-online competition under value uncertainty," *Production and Operations Management*, vol. 23, no. 7, pp. 1129–1145, 2013.
- [42] R. Batarfi, M. Y. Jaber, and S. M. Aljazzar, "A profit maximization for a reverse logistics dual-channel supply chain with a return policy," *Computers & Industrial Engineering*, vol. 106, pp. 58–82, 2017.
- [43] G. Ji, S. Han, and K. H. Tan, "False failure returns: optimal pricing and return policies in a dual-channel supply chain," *Journal of Systems Science and Systems Engineering*, vol. 27, no. 3, pp. 292–321, 2018.
- [44] A. A. Taleizadeh, S. R. Beydokhti, and L. E. C. Barrón, "Joint determination of the optimal selling price, refund policy and quality level for complementary products in online purchasing," *European J. of Industrial Engineering*, vol. 12, no. 3, p. 332, 2018.
- [45] M. Radhi and G. Zhang, "Pricing policies for a dual-channel retailer with cross-channel returns," *Computers & Industrial Engineering*, vol. 119, pp. 63–75, 2018.
- [46] Y. He, Q. Xu, and P. Wu, "Omnichannel retail operations with refurbished consumer returns," *International Journal of Production Research*, vol. 58, no. 1, pp. 271–290, 2019.
- [47] L. Fan, T. L. Friesz, T. Yao, and X. Chen, "Strategic pricing and production planning using a Stackelberg differential game with unknown demand parameters," *IEEE Transactions on Engineering Management*, vol. 60, no. 3, pp. 581–591, 2013.
- [48] S. Kolay and G. Shaffer, "Contract design with a dominant retailer and a competitive fringe," *Management Science*, vol. 59, no. 9, pp. 2111–2116, 2013.
- [49] Z. Luo, X. Chen, J. Chen, and X. Wang, "Optimal pricing policies for differentiated brands under different supply chain power structures," *European Journal of Operational Research*, vol. 259, no. 2, pp. 437–451, 2017.
- [50] H. Huang, H. Ke, and L. Wang, "Equilibrium analysis of pricing competition and cooperation in supply chain with one common manufacturer and duopoly retailers," *International Journal of Production Economics*, vol. 178, pp. 12–21, 2016.
- [51] W. Ma, R. Cheng, and H. Ke, "Impacts of power structure on supply chain with a store brand," *Asia-Pacific Journal of Operational Research*, vol. 35, no. 4, Article ID 1850020, 2018.
- [52] J. Zhao, X. Hou, Y. Guo, and J. Wei, "Pricing policies for complementary products in a dual-channel supply chain," *Applied Mathematical Modelling*, vol. 49, pp. 437–451, 2017.
- [53] H. Ke, H. Huang, and X. Gao, "Pricing decision problem in dual-channel supply chain based on experts' belief degrees," *Soft Computing*, vol. 22, no. 17, pp. 5683–5698, 2017.
- [54] S.-H. Chun and S. Y. Park, *Hybrid Marketing Channel Strategies of a Manufacturer in a Supply Chain: Game Theoretical and Numerical Approaches*, Information Technology and Management, vol. 20, no. 4, pp. 187–202, 2019.
- [55] X. Chen, X. Wang, and X. Jiang, "The impact of power structure on the retail service supply chain with an O2O mixed channel," *Journal of the Operational Research Society*, vol. 67, no. 2, pp. 294–301, 2016.
- [56] S. Basak, P. Basu, B. Avittathur, and S. Sikdar, "A game theoretic analysis of multichannel retail in the context of "showrooming"" *Decision Support Systems*, vol. 103, pp. 34–45, 2017.
- [57] J. Liu and H. Ke, "Firms' pricing strategies under different decision sequences in dual-format online retailing," *Soft Computing*, vol. 24, no. 10, pp. 7811–7826, 2019.
- [58] L. Xu, Y. Li, K. Govindan, and X. Xu, "Consumer returns policies with endogenous deadline and supply chain coordination," *European Journal of Operational Research*, vol. 242, no. 1, pp. 88–99, 2015.
- [59] J. Heydari and M. Ghasemi, "A revenue sharing contract for reverse supply chain coordination under stochastic quality of returned products and uncertain remanufacturing capacity," *Journal of Cleaner Production*, vol. 197, pp. 607–615, 2018.
- [60] R. Yan and Z. Pei, "Return policies and O₂O coordination in the e-tailing age," *Journal of Retailing and Consumer Services*, vol. 50, pp. 314–321, 2018.
- [61] B. Guo, Y. Fu, and Y. Li, "Fresh-keeping effort and channel performance in a fresh product supply chain with loss-averse consumers' returns," *Mathematical Problems in Engineering*, vol. 2018, Article ID 4717094, 20 pages, 2018.
- [62] X. Liu, Q. Gou, L. Alwan, and L. Liang, "Option contracts: a solution for overloading problems in the delivery service

- supply chain,” *Journal of the Operational Research Society*, vol. 67, no. 2, pp. 187–197, 2016.
- [63] Z. Song and S. He, “Contract coordination of new fresh produce three-layer supply chain,” *Industrial Management & Data Systems*, vol. 119, no. 1, pp. 148–169, 2018.
- [64] N. Amrouche, Z. Pei, and R. Yan, “Mobile channel and channel coordination under different supply chain contexts,” *Industrial Marketing Management*, vol. 84, pp. 165–182, 2019.
- [65] J. Dong, Z. Hu, and C. Liang, “E-commerce supply chain coordination under demand influenced by historical sales rate,” in *Proceedings of the 2017 3rd International Conference on Information Management (ICIM)*, Chengdu, China, April 2017.
- [66] M. Zhang, Y. Fu, Z. Zhao, S. Pratap, and G. Q. Huang, “Game theoretic analysis of horizontal carrier coordination with revenue sharing in E-commerce logistics,” *International Journal of Production Research*, vol. 57, no. 5, pp. 1524–1551, 2018.
- [67] Y. Zhong, F. Guo, Z. Wang, and H. Tang, “Coordination analysis of revenue sharing in E-commerce logistics service supply chain with cooperative distribution,” *SAGE Open*, vol. 9, no. 3, 2019.
- [68] Y. Wang, R. Fan, L. Shen, and W. Miller, “Recycling decisions of low-carbon E-commerce closed-loop supply chain under government subsidy mechanism and altruistic preference,” *Journal of Cleaner Production*, vol. 259, p. 120883, 2020b.
- [69] Y. Akcay, T. Boyac, and D. Zhang, “Selling with money-back guarantees: the impact on prices, quantities, and retail profitability,” *Production and Operations Management*, vol. 22, no. 4, pp. 777–791, 2013.
- [70] J. Chen and R. Grewal, “Competing in a supply chain via full-refund and no-refund customer returns policies,” *International Journal of Production Economics*, vol. 146, no. 1, pp. 246–258, 2013.
- [71] Y. Xia, T. Xiao, and G. P. Zhang, “The impact of product returns and retailer’s service investment on manufacturer’s channel strategies,” *Decision Sciences*, vol. 48, no. 5, pp. 918–955, 2016.
- [72] B. Shen, R. Qian, and T.-M. Choi, “Selling luxury fashion online with social influences considerations: demand changes and supply chain coordination,” *International Journal of Production Economics*, vol. 185, pp. 89–99, 2017.
- [73] Q. Li, X. Chen, and Y. Huang, “The stability and complexity analysis of a low-carbon supply chain considering fairness concern behavior and sales service,” *International Journal of Environmental Research and Public Health*, vol. 16, no. 15, p. 2711, 2019.
- [74] J. Xie, L. Liang, L. Liu, and P. Ieromonachou, “Coordination contracts of dual-channel with cooperation advertising in closed-loop supply chains,” *International Journal of Production Economics*, vol. 183, pp. 528–538, 2017.
- [75] Q. Li, T. Xiao, and Y. Qiu, “Price and carbon emission reduction decisions and revenue-sharing contract considering fairness concerns,” *Journal of Cleaner Production*, vol. 190, pp. 303–314, 2018.
- [76] M. Reimann, “Accurate response with refurbished consumer returns,” *Decision Sciences*, vol. 47, no. 1, pp. 31–59, 2015.
- [77] S.-Y. Chang and T.-Y. Yeh, “A two-echelon supply chain of a returnable product with fuzzy demand,” *Applied Mathematical Modelling*, vol. 37, no. 6, pp. 4305–4315, 2013.
- [78] S. Scheriau, “Philips–consumer returned products,” Master’s thesis, University of Graz, Graz, Austria, 2016.
- [79] Y. Wang, R. Fan, L. Shen, and M. Jin, “Decisions and coordination of green e-commerce supply chain considering green manufacturer’s fairness concerns,” *International Journal of Production Research*, pp. 1–19, 2020a.
- [80] P.-L. To, C. Liao, and T.-H. Lin, “Shopping motivations on Internet: a study based on utilitarian and hedonic value,” *Technovation*, vol. 27, no. 12, pp. 774–787, 2007.
- [81] F. Kawaf and S. Tagg, “The construction of online shopping experience: a repertory grid approach,” *Computers in Human Behavior*, vol. 72, pp. 222–232, 2017.
- [82] J. Wang and X. Huang, “The optimal carbon reduction and return strategies under carbon tax policy,” *Sustainability*, vol. 10, no. 7, p. 2471, 2018.
- [83] R. Zhang, J. Li, Z. Huang, and B. Liu, “Return strategies and online product customization in a dual-channel supply chain,” *Sustainability*, vol. 11, no. 12, p. 3482, 2019.
- [84] L. Shen and Y. Wang, “Supervision mechanism for pollution behavior of Chinese enterprises based on haze governance,” *Journal of Cleaner Production*, vol. 197, pp. 571–582, 2018.